INFECTIOUS AGENT-INDUCED CHRONIC IMMUNE ACTIVATION: CAUSES, PHENOTYPES, AND CONSEQUENCES

EDITED BY: Pierre Corbeau, Nicholas Funderburg, John Zaunders and Caroline Petitdemange

PUBLISHED IN: Frontiers in Immunology

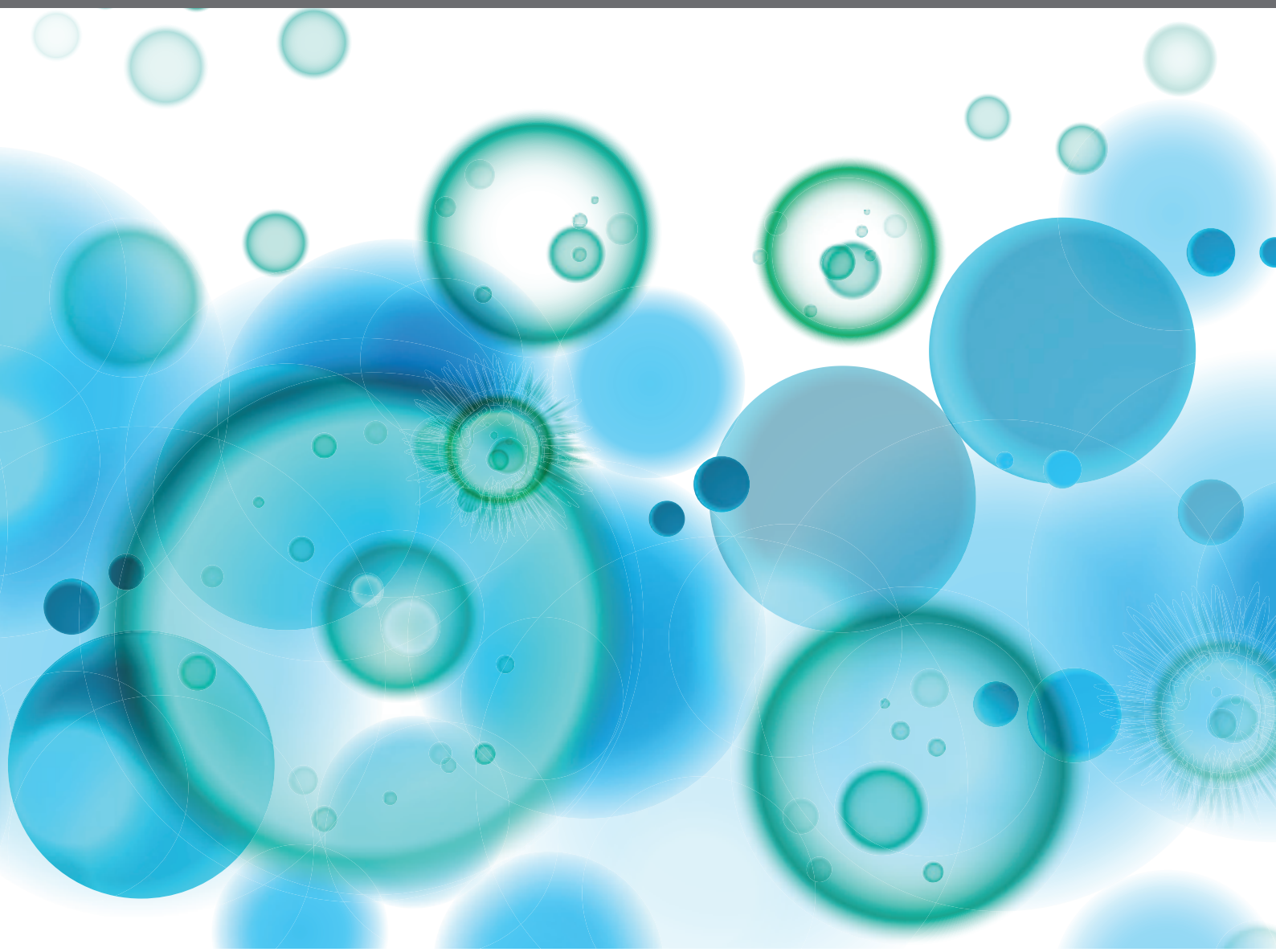

frontiers Research Topics

frontiers

ISSN 1664-8714
ISBN 978-2-88974-230-1
DOI 10.3389/978-2-88974-230-1

About Frontiers

Frontiers is more than just an open-access publisher of scholarly articles: it is a pioneering approach to the world of academia, radically improving the way scholarly research is managed. The grand vision of Frontiers is a world where all people have an equal opportunity to seek, share and generate knowledge. Frontiers provides immediate and permanent online open access to all its publications, but this alone is not enough to realize our grand goals.

Frontiers Journal Series

The Frontiers Journal Series is a multi-tier and interdisciplinary set of open-access, online journals, promising a paradigm shift from the current review, selection and dissemination processes in academic publishing. All Frontiers journals are driven by researchers for researchers; therefore, they constitute a service to the scholarly community. At the same time, the Frontiers Journal Series operates on a revolutionary invention, the tiered publishing system, initially addressing specific communities of scholars, and gradually climbing up to broader public understanding, thus serving the interests of the lay society, too.

Dedication to Quality

Each Frontiers article is a landmark of the highest quality, thanks to genuinely collaborative interactions between authors and review editors, who include some of the world's best academicians. Research must be certified by peers before entering a stream of knowledge that may eventually reach the public - and shape society; therefore, Frontiers only applies the most rigorous and unbiased reviews.
Frontiers revolutionizes research publishing by freely delivering the most outstanding research, evaluated with no bias from both the academic and social point of view. By applying the most advanced information technologies, Frontiers is catapulting scholarly publishing into a new generation.

What are Frontiers Research Topics?

Frontiers Research Topics are very popular trademarks of the Frontiers Journals Series: they are collections of at least ten articles, all centered on a particular subject. With their unique mix of varied contributions from Original Research to Review Articles, Frontiers Research Topics unify the most influential researchers, the latest key findings and historical advances in a hot research area! Find out more on how to host your own Frontiers Research Topic or contribute to one as an author by contacting the Frontiers Editorial Office: frontiersin.org/about/contact

INFECTIOUS AGENT-INDUCED CHRONIC IMMUNE ACTIVATION: CAUSES, PHENOTYPES, AND CONSEQUENCES

Topic Editors:
Pierre Corbeau, Université de Montpellier, Italy
Nicholas Funderburg, The Ohio State University, United States
John Zaunders, St Vincent's Hospital Sydney, Australia
Caroline Petitdemange, Institut Pasteur, France

Citation: Corbeau, P., Funderburg, N., Zaunders, J., Petitdemange, C., eds. (2022). Infectious Agent-Induced Chronic Immune Activation: Causes, Phenotypes, and Consequences. Lausanne: Frontiers Media SA. doi: 10.3389/978-2-88974-230-1

Table of Contents

frontiers in Immunology

EDITORIAL
published: 10 December 2021
doi: 10.3389/fimmu.2021.740556

Editorial: Infectious Agent-Induced Chronic Immune Activation: Causes, Phenotypes, and Consequences

Caroline Petitdemange[1†], *Nicholas Funderburg*[2†], *John Zaunders*[3†] *and Pierre Corbeau*[4*]

[1] Institut Pasteur, HIV Inflammation and Persistence Unit, Paris, France, [2] School of Health and Rehabilitation Sciences, Ohio State University, Columbus, OH, United States, [3] St Vincent's Centre for Applied Medical Research, St Vincent's Hospital, Sydney, NSW, Australia, [4] CHU de Nîmes, Institut de Génétique Humaine CNRS-Université de Montpellier, UMR9002, Montpellier, France

Keywords: inflammation, comorbidity, pathogen, immune cell, immune system

Editorial on the Research Topic

Infectious Agent-Induced Chronic Immune Activation: Causes, Phenotypes, and Consequences

SUMMARY

Persistent immune activation and dysfunction induced by infectious agents may contribute to long term comorbid conditions in individuals exposed to these pathogens. Even during successful antimicrobial treatment, increased levels of inflammation and immune cell activation and inappropriate immune cell migration and retention in tissue sites may contribute to tissue damage and end organ disease (e.g., atherosclerosis or liver or kidney damage). Understanding why some populations infected with a pathogen are able to regulate their immune responses and limit their inflammatory consequences, while other individuals may have exacerbated and persistent immune responses even during suppressive therapy, may provide insights for development of complementary immune-modulatory therapies that may reduce inflammation and morbidity and mortality in these groups. The Research Topic highlights some of these issues.

Any infection induces the activation of the human immune system *via* various mechanisms. The problem is that although some forms of this immune activation are beneficial for the eradication of the microbial agent, others may be toxic, not only in the short term but also in the long term. It is therefore important to understand these pathogenic pathways, inasmuch as they may persist even under efficient antimicrobial therapy.

THE WAYS AN INFECTIOUS AGENT MAY TRIGGER THE IMMUNE SYSTEM

Some microbial components may activate the complement and/or the coagulation system and thereby start an inflammatory reaction. Phagocytic cells will be recruited into infected tissues, and activated to engulf the infectious agent in order to neutralize it. In the meantime, immune and non-immune cells detect the presence of pathogen-associated molecular patterns, triggering a danger signal that also fuels inflammation and promoting the initiation of the adaptive immune response, ideally, resulting in a cellular and humoral immune response targeting specific microbial antigens. Natural killer cells and cytotoxic T cells will identify infected cells and destroy them. All of these

OPEN ACCESS

Edited and reviewed by:
Betsy J. Barnes, Feinstein Institute for Medical Research, United States

***Correspondence:**
Pierre Corbeau
pierre.corbeau@igh.cnrs.fr

[†]*These authors have contributed equally to this work*

Specialty section:
This article was submitted to Viral Immunology, a section of the journal Frontiers in Immunology

Received: *13 July 2021*
Accepted: *22 November 2021*
Published: *10 December 2021*

Citation:
Petitdemange C, Funderburg N, Zaunders J and Corbeau P (2021) Editorial: Infectious Agent-Induced Chronic Immune Activation: Causes, Phenotypes, and Consequences. Front. Immunol. 12:740556. doi: 10.3389/fimmu.2021.740556

types of immune activation may contribute to the elimination of the invader. Yet, besides these desirable effects, the microbial agent may also cause side effects with potential pathogenic consequences (**Figure 1**).

First, many infectious agents have developed the means to evade defenses and subsequently promote immune dysfunction. A master of this gameplay is the human cytomegalovirus (HCMV). HCMV downregulates the density of HLA classes I and II at the surface of the cells it infects (1) and interferes with their ability to present antigens (2), reducing thereby CD4+ T cell and CD8+ T cell specific responses. To prevent the attack by natural killer cells as a consequence of HLA I downregulation, the virus encodes a nonfunctional class I MHC homolog as a decoy (3). Other homologs encoded by HCMV are chemokine receptor and Fc receptor homologs acting as sinks for local chemokines and antibodies, respectively (4, 5). HCMV also inhibits macrophage motility by downregulating chemokine receptors, inducing the production of macrophage migration inhibitory factor, and acting directly on macrophage cytoskeleton functionality (6). In addition, this herpesvirus reduces complement activation by inducing natural complement inhibitors (7), and inflammation by coding for a viral form of the anti-inflammatory cytokine IL-10 (8). Finally, HCMV reduces the ability of T cells to proliferate and to secrete IL-2 and IFN-γ (9). The infectious agent itself will benefit from the immune deficiency it has induced, but other infections may also be thereby boosted, promoting a cycle of more infections and more immune activation and dysfunction.

Second, infections may indirectly activate the immune system *via* metabolic disorders. Thus, Human Immunodeficiency Virus (HIV) infection increases the level of oxidized LDL able to activate monocytes *via* Lectin-like oxidized LDL receptor-1 (10). Proinflammatory lipid classes and species (including ceramides and saturated fatty acids), the levels of which are altered by HIV-1 and antiretroviral therapy (ART), may also promote inflammation and cardiometabolic complications (11, 12). Infections may also indirectly activate the immune system through microbial disorders. For instance, influenza virus has been shown to favor bacterial species in the gut lumen (13). In addition to modifying the microbiota, HIV facilitates the translocation of microbial components from the gut lumen into the circulation by depleting Th17 cells in the gut-associated lymphoid tissue and by causing a local inflammation (14). The same is true for HCMV, known to infect gut epithelial cells and to provoke microbial translocation (15).

Third, some infectious agents may perpetuate immune activation by altering immune suppressor cell function. As an example, HIV has been reported to create a quantitative and probably qualitative deficiency in regulatory T cells (16).

Fourth, microbial components often directly activate immune cells. HIV is again a good example of this; HIV RNA stimulates plasmacytoid dendritic cells *via* TLR7 (17), and HIV DNA triggers CD4+ T cell pyroptosis and the release of inflammatory cytokines (18). The external envelope glycoprotein Gp120 (19) and the accessory protein Vpr (20) activate monocytes/macrophages, whereas the transmembrane envelope glycoprotein Gp40 promotes T cell activation by interacting with the T cell receptor (21). Moreover, the transactivator protein Tat has been reported to induce oxidative stress *via* NFkB in B cells (22).

Finally, even though microbial antigen-driven B cell and T cell activation is intended to be beneficial, protracted activation will result in immune senescence, decreased potential to respond to other stimuli, and immune deficiency.

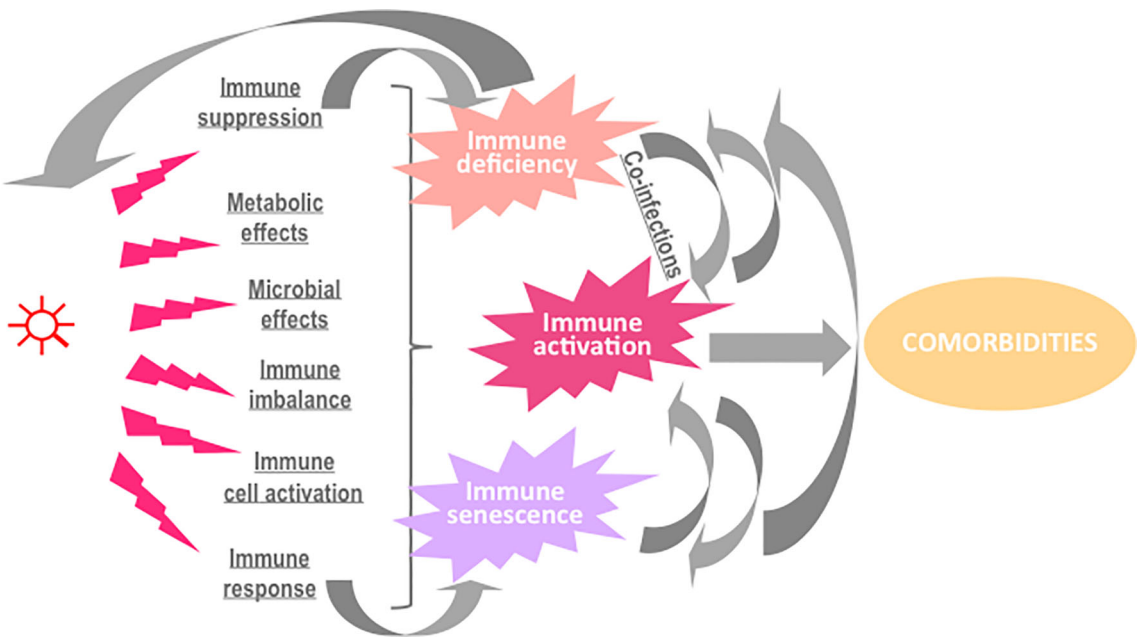

FIGURE 1 | Potential causes and consequences of immune activation in the course of an infection.

Concerning the infectious agents for which we have therapeutic possibilities, the treatment of these pathogens will reduce the levels of immune activation. Yet, even virologically efficient drugs may not abolish all of the immune activation, as it has been abundantly proven for HIV infection (23).

From the point of view of benefit to the microbial agent, triggering a global and generalized activation of the immune system may be paradoxically desirable, if it is able to ultimately evade the storm of the activated immune system and co-exist with chronic activation and the resulting senescence. Yet again, HIV provides an example, whereby it evades antibody responses by constant generation of envelope variants (24), which can act as neoantigens, and continually drive germinal center reactions associated with generation of newly activated CD4 target cells (25).

In this Research Topic, the role of residual microbial load, microbial translocation, and adipose tissue alterations will be addressed.

Younas et al. have identified a particular profile of immune activation in people living with HIV-1 (PLHIV) presenting residual viral load under ART. This profile is characterized by CD4+ T cell, monocyte, and endothelial activation. These data reinforce the hypothesis that low-level viremia could drive a specific form of immune activation in virologic responders. Many studies using the single copy assay of plasma viremia have shown that most patients have persistent plasma viremia in the range of 1-10 copies/ml despite being classified as fully suppressed by standard clinical monitoring assays (26).

However, there now appears to be a spectrum of activity of the HIV proviral reservoir in patients fully suppressed on ART. A new highly sensitive assay using circulating CD4 T cells has shown that there is a 3 $\log_{10}$ range of the level of intracellular HIV RNA transcripts within different patients' CD4 T cells (27), that has not been stopped by ART. Patients at the higher end of this range are those that can have plasma viral load blips (27), consistent with previous results that higher levels of intracellular unspliced HIV-1 RNA in PBMC from patients on ART correlated with shorter time to HIV-1 recrudescence after treatment interruption (28).

Another cause of immune activation is explored by Isnard et al., Mak et al., and Ancona et al., microbial translocation due to loss of gastrointestinal barrier integrity, as a result of HIV infection. Isnard et al. review the mechanisms of immune activation related to fungal translocation in HIV infection. They discuss the different markers of fungal translocation, in particular, β-D Glucan, a major cell wall component of most fungi, linked to disease progression and inflammation in treated and nontreated patients. They also discuss specific strategies that could be critical to reduce the contribution of fungal translation to inflammation in PLHIV.

Mak et al. aimed to directly quantitatively measure, *in vivo*, the loss of gastrointestinal barrier integrity using the technique of confocal endomicroscopy. In contrast to what was expected, they were unable to document a clear weakness in integrity of the epithelial barrier in HIV+ patients on ART, even those who commenced therapy relatively late in disease, compared to HIV-uninfected controls. Even though this was a relatively small study, it should have shown any obvious defect in gut permeability that should have been as widespread as currently believed for PLHIV, according to the literature.

Ancona et al. aimed to measure not only longitudinal changes in markers of microbial translocation and gut microbiota in PLHIV commencing ART for 24 months, but also direct analysis of microbial flora in blood. They found chronic elevation of the plasma marker of microbial translocation, sCD14, but a clinical index of gut permeability, the ratio of lactulose and mannitol in urinary excretion, showed a similar range compared to the level reported in healthy controls and treated coeliac patients, from the literature. Similarly, the level of fecal calprotectin, another clinical marker of gut permeability, after ART appeared to be within the normal range from the literature. However, while their patients' gut microbiota showed that they maintained an apparent gut dysbiosis, as reported in many other studies, the blood microbiota suggested selective translocation of microbes, with a higher plasma abundance of the *Proteobacteria* phylum compared to intestinal abundance.

Finally, Bourgeois et al. have reviewed the role of adipose tissue in HIV-driven immune activation. The loss of muscle and fat tissue mass during untreated HIV-1 infection and then the emergence of ART-related lipodystrophy led to intensive study of adipose tissue in PLHIV. Proteins encoded by HIV-1 may directly affect adipocytes, in addition to the indirect effect of CD4 T cell infection. The lymphatic vasculature is an important part of adipose tissue, therefore the inability of ART to completely eradicate HIV-1 infection can lead to low-grade inflammation in adipose tissue, similar to obesity, with resulting co-morbidities.

Overall, low level chronic activation of the immune system in PLHIV is probably partly due to the inability of current ART to completely suppress HIV transcriptional activity and the resulting extremely low level plasma viremia, reflecting residual production of HIV-1 proteins, and even complete virions, in various tissues.

This is in addition to the compromise of immune defenses, particularly in the gastrointestinal tract, leading to the low level of systemic stimulation by the increased presence of microbial products. Other important frontline barrier systems probably also require more focused study in this regard, particularly HIV persistence in the respiratory tract (29, 30), changes in skin, such as acne following commencement of ART (31), and perturbations in the CNS (32).

THE FORMS OF MICROBIAL-INDUCED IMMUNE ACTIVATION

All types of immune activation have been reported in the course of infections. For the sole example of HIV, CD4+ T cell, CD8+ T cell, B cell, NK cell, dendritic cell, monocyte/macrophage, polymorphonuclear cell, complement activation, and inflammation have been observed in non-treated as well as in ART-treated patients (23).

In this Research Topic, the types of immune activation in severe COVID-19 and HIV-associated immune reconstitution inflammatory syndrome, respectively, are reviewed by Seddiki

and French. They find that there are significant parallels in the two conditions, and the link appears to be amplified activation of monocytes/macrophages associated with aberrant pro-inflammatory T and B cell adaptive responses.

THE CONSEQUENCES OF MICROBIAL-INDUCED IMMUNE ACTIVATION

In addition to fueling non-transmissible chronic diseases, persisting immune activation may be deleterious for the immune system itself, as it may induce immune senescence and immune deficiency. The link between immune activation and non-immune restoration is explored in the work by Shive et al. A combination of persisting elevated levels of pro-inflammatory IP-10 and reduced levels of anti-inflammatory TGF-ß1 is associated with lower CD4 cell count reconstitution in PLHIV on ART, with controlled plasma viremia.

Immune activation may also impact the capability of mounting a specific immune response. Several studies explored the link between COVID-19 severity and the development of an efficient humoral immunity with contradictory results. Moreover, the question of antibodies as beneficial, neutral or harmful in SARS-CoV-2 infection remains controversial. Feng et al. assessed SARS-Cov-2 seroprevalence in 84 hospitalized patients. They observed that the antibody response against three important antigens (RBD, N and S) dynamically changed over time to reach a peak 3-4 weeks after symptom onset with a response lasting for an average of 112 days. They found that these responses were higher in patients with a severe condition.

MICROBIAL-INDUCED IMMUNE ACTIVATION AND THERAPEUTIC INTERVENTION

Antimicrobial therapy may reduce immune activation and its deleterious consequences. This is the case for naïve CD4+ lymphopenia induced by HCV which is reduced by direct-acting antiviral drugs, as shown by Auma et al. resulting in at least partial or full restoration of circulating naïve CD4 T cells numbers. The importance of the size of the pool of these cells for control of future infections has recently been suggested as the cause of the age-related loss of control of SARS-CoV-2 infection in older patients (33).

This is also the case for ART which diminishes HIV-driven immune activation. Yet, there are differences between ART regimens, and potentially between 1-, 2- and 3-drug regimens as discussed by van Welzen et al.

By contrast certain antimicrobial therapies may worsen immune activation. An example thereof is given by Fu et al. They report that although PEG-IFNα-2b has early antiviral effects, it later exerts an immune activation effect inducing an upregulation of $CD24^{+}CD38^{hi}$ B cells driving an immuno-suppressive program and reducing anti-virus therapeutic effects. They show that the expansion of $CD24^{+}CD38^{hi}$ B cells correlated negatively with therapeutic effects. In this context they also found CD24 to be a suitable marker to target $CD24^{+}CD38^{hi}$ cells, and demonstrate the possibility to interrupt the immunosuppressive state using an anti-CD24 antibody.

Last, Kircheis et al. propose a therapeutic strategy targeting directly the immune activation in COVID-19. Indeed, they present the proinflammatory transcription factor NF-κB as a possible therapeutic target for treatment of the cytokine storm associated with the severe forms of COVID-19. The authors used different models, *in vitro* human macrophages, H5N1 infected BALB/c mice and LPS-induced cytokines in BALB/c mice to test VL-01, a proteasome inhibitor. They demonstrated the efficacy of this inhibitor *in vitro* and in mice to significantly reduce the release of pro-inflammatory cytokines (IL-1, IL-6, TNF-α) and chemokines (MIP-1, CXCL1).

AUTHOR CONTRIBUTIONS

All authors listed have made a substantial, direct, and intellectual contribution to the work and approved it for publication.

FUNDING

PC was supported by MSDAvenir (DS-2016-0010).

REFERENCES

1. Barnes PD, Grundy JE. Down Regulation of the Class I HLA Heterodimer and β2-Microglobulin on the Surface of Cells Infected With Cytomegalovirus. *J Gen Virol* (1992) 73:2395. doi: 10.1099/0022-1317-73-9-2395
2. Ahn K, Angulo A, Ghazal P, Peterson PA, Yang Y, Früh K. Human Cytomegalovirus Inhibits Antigen Presentation by a Sequential Multistep Process. *Proc Natl Acad Sci USA* (1996) 93:10990–5. doi: 10.1073/pnas.93.20.10990
3. Reyburn HT, Mandelboim O, Valés-Gómez M, Davis DM, Pazmany L, Strominger JL. The Class I MHC Homologue of Human Cytomegalovirus Inhibits Attack by Natural Killer Cells. *Nature* (1997) 386:514–7. doi: 10.1038/386514a0
4. Neote K, DiGregorio D, Mak JY, Horuk R, Schall TJ. Molecular Cloning, Functional Expression, and Signaling Characteristics of a C-C Chemokine Receptor. *Cell* (1993) 72:415–25. doi: 10.1016/0092-8674(93)90118-A
5. Atalay R, Zimmermann A, Wagner M, Borst E, Benz C, Messerle M, et al. Identification and Expression of Human Cytomegalovirus Transcription Units Coding for Two Distinct Fcgamma Receptor Homologs. *J Virol* (2003) 76:8596–608. doi: 10.1128/JVI.76.17.8596-8608.2002
6. Frascaroli G, Varani S, Blankenhorn N, Pretsch R, Bacher M, Leng L, et al. Human Cytomegalovirus Paralyzes Macrophage Motility Through Down-Regulation of Chemokine Receptors, Reorganization of the Cytoskeleton, and Release of Macrophage Migration Inhibitory Factor. *J Immunol* (2009) 182:477–88. doi: 10.4049/jimmunol.182.1.477
7. Spiller OB, Hanna SM, Devine DV, Tufaro F. Neutralization of Cytomegalovirus Virions: The Role of Complement. *J Infect Dis* (1997) 176:339–47. doi: 10.1086/514050
8. Kotenko SV, Saccani S, Izotova LS, Mirochnitchenko OV, Pestka S. Human Cytomegalovirus Harbors Its Own Unique IL-10 Homolog (cmvIL-10). *Proc Natl Acad Sci USA* (2000) 97:1695–700. doi: 10.1073/pnas.97.4.1695

9. Sester U, Presser D, Dirks J, Gärtner BC, Köhler H, Sester M. PD-1 Expression and IL-2 Loss of Cytomegalovirus- Specific T Cells Correlates With Viremia and Reversible Functional Anergy. *Am J Transplant* (2008) 8:1486–97. doi: 10.1111/j.1600-6143.2008.02279.x
10. Zidar DA, Juchnowski S, Ferrari B, Clagett B, Pilch-Cooper HA, Rose S, et al. (2015) 69.2:154–60.
11. Zhao W, Wang X, Deik AA, Hanna DB, Wang T, Haberlen SA, et al. Elevated Plasma Ceramides Are Associated With Antiretroviral Therapy Use and Progression of Carotid Artery Atherosclerosis in HIV Infection. *Circulation* (2019) 139:2003–11. doi: 10.1161/CIRCULATIONAHA.118.037487
12. Bowman ER, Cameron CM, Richardson B, Kulkarni M, Gabriel J, Cichon MJ, et al. Macrophage Maturation From Blood Monocytes Is Altered in People With HIV, and Is Linked to Serum Lipid Profiles and Activation Indices: A Model for Studying Atherogenic Mechanisms. *PLoS Pathog* (2020) 16: e1008869. doi: 10.1371/journal.ppat.1008869
13. Sencio V, Barthelemy A, Tavares LP, Machado MG, Soulard D, Cuinat C, et al. Gut Dysbiosis During Influenza Contributes to Pulmonary Pneumococcal Superinfection Through Altered Short-Chain Fatty Acid Production. *Cell Rep* (2020) 30:2934–47. doi: 10.1016/j.celrep.2020.02.013
14. Hunt PW. Th17, Gut, and HIV: Therapeutic Implications.Curr Opin HIV AIDS. *Curr Opin HIV AIDS* (2010) 5:189–93. doi: 10.1097/COH.0b013e32833647d9
15. Maidji E, Somsouk M, Rivera JM, Hunt PW, Stoddart CA. Replication of CMV in the Gut of HIV-Infected Individuals and Epithelial Barrier Dysfunction. *PLoS Pathog* (2017) 13:e1006202. doi: 10.1371/journal.ppat.1006202
16. Chevalier MF, Weiss L. The Split Personality of Regulatory T Cells in HIV Infection. *Blood* (2013) 121:29–37. doi: 10.1182/blood-2012-07-409755
17. Beignon A-S, McKenna K, Skoberne M, Manches O, DaSilva I, Kavanagh DG, et al. Endocytosis of HIV-1 Activates Plasmacytoid Dendritic Cells *via* Toll-Like Receptor-Viral RNA Interactions. *J Clin Invest* (2005) 115:3265–75. doi: 10.1172/JCI26032
18. Doitsh G, Cavrois M, Lassen KG, Zepeda O, Yang Z, Santiago ML, et al. Abortive HIV Infection Mediates CD4 T Cell Depletion and Inflammation in Human Lymphoid Tissue. *Cell* (2010) 143:789–801. doi: 10.1016/j.cell.2010.11.001
19. Planès R, Serrero M, Leghmari K, BenMohamed L, Bahraoui B. HIV-1 Envelope Glycoproteins Induce the Production of TNF-α and IL-10 in Human Monocytes by Activating Calcium Pathway. *Sci Rep* (2018) 8 (1):17215. doi: 10.1038/s41598-018-35478-1
20. Varin A, Decrion AZ, Sabbah E, Quivy V, Sire J, Van Lint C, et al. Synthetic Vpr Protein Activates Activator Protein-1, C-Jun N-Terminal Kinase, and NF-kappaB and Stimulates HIV-1 Transcription in Promonocytic Cells and Primary Macrophages. *J Biol Chem* (2005) 280:42557–67. doi: 10.1074/jbc.M502211200
21. Yakovian O, Schwarzer R, Sajman J, Neve-Oz Y, Razvag Y, Herrmann A, et al. Gp41 Dynamically Interacts With the TCR in the Immune Synapse and Promotes Early T Cell Activation. *Sci Rep* (2018) 8:9747. doi: 10.1038/s41598-018-28114-5
22. El-Amine R, Germini D, Zakharova VV, Tsfasman T, Sheval EV, Louzada RAN, et al. HIV-1 Tat Protein Induces DNA Damage in Human Peripheral Blood B-Lymphocytes *via* Mitochondrial ROS Production. *Redox Biol* (2018) 15:97–108. doi: 10.1016/j.redox.2017.11.024
23. Younas M, Psomas C, Reynes J, Corbeau P. Immune Activation in the Course of HIV-1 Infection: Causes, Phenotypes and Persistence Under Therapy. *HIV Med* (2016) 17:89–105. doi: 10.1111/hiv.12310
24. Richman DD, Wrin T, Little SJ, Petropoulos CJ. Rapid Evolution of the Neutralizing Antibody Response to HIV Type 1 Infection. *Proc Natl Acad Sci USA* (2003) 100:4144–9. doi: 10.1073/pnas.0630530100
25. Zaunders J, Xu Y, Kent SJ, Koelsch KK, Kelleher AD. Divergent Expression of CXCR5 and CCR5 on CD4(+) T Cells and the Paradoxical Accumulation of T Follicular Helper Cells During HIV Infection. *Front Immunol* (2017) 8:495. doi: 10.3389/fimmu.2017.00495
26. Palmer S, Maldarelli F, Wiegand A, Bernstein B, Hanna GJ, Brun SC, et al. Low-Level Viremia Persists for at Least 7 Years in Patients on Suppressive Antiretroviral Therapy. *Proc Natl Acad Sci USA* (2008) 105:3879–84. doi: 10.1073/pnas.0800050105
27. Suzuki K, Levert A, Yeung J, Starr M, Cameron J, Williams R, et al. HIV-1 Viral Blips Are Associated With Repeated and Increasingly High Levels of Cell-Associated HIV-1 RNA Transcriptional Activity. *AIDS* (2021) 35 (13):2095–103. doi: 10.1097/QAD.0000000000003001
28. Pasternak AO, Grijsen ML, Wit FW, Bakker M, Jurriaans S, Prins JM, et al. Cell-Associated HIV-1 RNA Predicts Viral Rebound and Disease Progression After Discontinuation of Temporary Early ART. *JCI Insight* (2020) 5(6): e134196. doi: 10.1172/jci.insight.134196
29. Costiniuk CT, Salahuddin S, Farnos O, Olivenstein R, Pagliuzza A, Orlova M, et al. HIV Persistence in Mucosal CD4+ T Cells Within the Lungs of Adults Receiving Long-Term Suppressive Antiretroviral Therapy. *AIDS* (2018) 32:2279–89. doi: 10.1097/QAD.0000000000001962
30. Cribbs SK, Lennox J, Caliendo AM, Brown LA, Guidot DM. Healthy HIV-1-Infected Individuals on Highly Active Antiretroviral Therapy Harbor HIV-1 in Their Alveolar Macrophages. *AIDS Res Hum Retroviruses* (2015) 31:64–70. doi: 10.1089/aid.2014.0133
31. Scott C, Staughton RC, Bunker CJ, Asboe D. Acne Vulgaris and Acne Rosacea as Part of Immune Reconstitution Disease in HIV-1 Infected Patients Starting Antiretroviral Therapy. *Int J STD AIDS* (2008) 19:493–5. doi: 10.1258/ijsa.2008.008026
32. Hellmuth J, Valcour V, Spudich S. CNS Reservoirs for HIV: Implications for Eradication. *J Virus Erad* (2015) 1:67–71. doi: 10.1016/S2055-6640(20)30489-1
33. Sette A, Crotty S. Adaptive Immunity to SARS-CoV-2 and COVID-19. *Cell* (2021) 184:861–80. doi: 10.1016/j.cell.2021.01.007

Conflict of Interest: The authors declare that the research was conducted in the absence of any commercial or financial relationships that could be construed as a potential conflict of interest.

Publisher's Note: All claims expressed in this article are solely those of the authors and do not necessarily represent those of their affiliated organizations, or those of the publisher, the editors and the reviewers. Any product that may be evaluated in this article, or claim that may be made by its manufacturer, is not guaranteed or endorsed by the publisher.

frontiers in Immunology

HYPOTHESIS AND THEORY
published: 10 December 2020
doi: 10.3389/fimmu.2020.598444

OPEN ACCESS

Edited by:
Caroline Petitdemange, Institut Pasteur, France

Reviewed by:
Pio Conti, University of Studies G. d'Annunzio Chieti and Pescara, Italy
Chengping Wen, Zhejiang Chinese Medical University, China

***Correspondence:**
Ralf Kircheis
r.kircheis.rk@gmail.com
Oliver Planz
oliver.planz@uni-tuebingen.de

†Present address:
Ralf Kircheis, Syntacoll GmbH, Saal a.d. Donau, Germany
Emanuel Haasbach, State Agency for Nature, Environment and Consumer Protection of North Rhine-Westphalia, Recklinghausen, Germany
Daniel Lueftenegger, Biogen GmbH, Munich, Germany
Willm T. Heyken, TÜV SÜD Product Service, Munich, Germany
Matthias Ocker, Translational Medicine & Clinical Pharmacology, Boehringer Ingelheim Pharma GmbH, Ingelheim, Germany and Charité University Medicine Berlin, Berlin, Germany

Specialty section:
This article was submitted to Viral Immunology, a section of the journal Frontiers in Immunology

Received: *24 August 2020*
Accepted: *27 November 2020*
Published: *10 December 2020*

Citation:
Kircheis R, Haasbach E, Lueftenegger D, Heyken WT, Ocker M and Planz O (2020) NF-κB Pathway as a Potential Target for Treatment of Critical Stage COVID-19 Patients. Front. Immunol. 11:598444. doi: 10.3389/fimmu.2020.598444

NF-κB Pathway as a Potential Target for Treatment of Critical Stage COVID-19 Patients

Ralf Kircheis[1†], Emanuel Haasbach[2†], Daniel Lueftenegger[1†], Willm T. Heyken[1†], Matthias Ocker[3†] and Oliver Planz[2*]*

[1] Virologik GmbH, Erlangen, Germany, [2] Institute of Cell Biology and Immunology, Eberhard Karls University Tuebingen, Tuebingen, Germany, [3] Institute for Surgical Research, Philipps University of Marburg, Marburg, Germany

Patients infected with SARS-CoV-2 show a wide spectrum of clinical manifestations ranging from mild febrile illness and cough up to acute respiratory distress syndrome, multiple organ failure, and death. Data from patients with severe clinical manifestations compared to patients with mild symptoms indicate that highly dysregulated exuberant inflammatory responses correlate with severity of disease and lethality. Epithelial-immune cell interactions and elevated cytokine and chemokine levels, i.e. cytokine storm, seem to play a central role in severity and lethality in COVID-19. The present perspective places a central cellular pro-inflammatory signal pathway, NF-κB, in the context of recently published data for COVID-19 and provides a hypothesis for a therapeutic approach aiming at the simultaneous inhibition of whole cascades of pro-inflammatory cytokines and chemokines. The simultaneous inhibition of multiple cytokines/chemokines is expected to have much higher therapeutic potential as compared to single target approaches to prevent cascade (i.e. redundant, triggering, amplifying, and synergistic) effects of multiple induced cytokines and chemokines in critical stage COVID-19 patients.

Keywords: NF-KappaB, cytokines, chemokines, COVID-19, SARS-CoV-2 (2019-nCoV), proteasome inhibitor, NSAID, cytokine storm

INTRODUCTION

Coronaviruses—enveloped positive-sense, single-stranded RNA viruses—are broadly distributed in humans and animals. While most human coronavirus (hCoV) infections show mild symptoms, there are highly pathogenic hCoV, including the severe acute respiratory syndrome virus (SARS-CoV) and the Middle East respiratory syndrome coronavirus (MERS-CoV), with 10 and 37% mortality, respectively. The novel coronavirus SARS-CoV-2 with more than 42 mio infected persons and 1.2 mio deaths worldwide (https://coronavirus.jhu.edu/) End of October 2020 has become a global pandemic with enormous medical and socio-economic burden. Patients infected with SARS-CoV-2 show a wide spectrum of clinical manifestations ranging from mild febrile illness and cough up to acute respiratory distress syndrome (ARDS), multiple organ failure, and death, *i.e.* a clinical picture in severe cases that is very similar to that seen in SARS-CoV and MERS-CoV infected patients. While younger individuals show predominantly mild-to-moderate clinical symptoms, elderly individuals frequently exhibit severe clinical manifestations (1–4). Post-mortem analysis

showed Diffuse Alveolar Disease with capillary congestion, cell necrosis, interstitial oedema, platelet-fibrin thrombi, and infiltrates of macrophages and lymphocytes (5). Recently, the induction of endotheliitis in various organs (including lungs but also in heart and kidney and intestine) by SARS-CoV-2 infection as a direct consequence of viral involvement and of the host inflammatory response was shown (6, 7).

SARS-CoV-2 binds with its spike (S) protein to the angiotensin-converting enzyme-related carboxypeptidase-2 (ACE-2) receptor on the host cell using the cellular serine protease TMPRSS2 for S protein priming (8). The ACE-2 receptor is widely expressed in pulmonary and cardiovascular tissues, hematopoietic cells, including monocytes and macrophages which may explain the broad range of pulmonary and extra-pulmonary effects of SARS-CoV-2 infection including cardiac, gastrointestinal organs, and kidney affection (6, 8).

MATERIALS AND METHODS

Proteasome Inhibitor

The novel proteasome inhibitor VL-01 (Z-Trp-Trp-Phe-aminohydantoin, MW = 752.82 g/mol) has been described by Leban et al. (9) and was synthesized at Almac (Ireland).

Confocal Microscopy of Nuclear Translocation of NF-κB

Cells, seeded overnight on cover-slides, were incubated with increasing concentrations of inhibitors, and stimulated with TNFα (2 ng/ml) for 30 min. Cells were fixated with 2% paraformaldehyde, washed, and permeabilized with PBS/Tween®20. Cells were stained using primary antibodies for NF-κB (p65), (rabbit pAb, Santa Cruz, Cat. No.: sc-372, 1:1,000) and fluorescence-labeled secondary antibody [Alexa Fluor® 488 goat anti-rabbit IgG (H+L), Life Technologies Cat. No.: 11008, 1:2,000] for 30 min. Subsequently, the cell nuclei were stained using DAPI (1:40,000, Life Technologies, Cat. No.: D1306) for 30 min. The cover-slides were embedded with Flouramount G (Invitrogen), dried overnight at 4°C, and evaluated by confocal microscope (Leica, LSM3).

Inhibition of Cytokine Release *In Vivo* in H5N1 Infection Model

The highly pathogenic avian H5N1 influenza A virus strain A/Mallard/Bavaria/1/2006 (H5N1, MB1), obtained from the Bavarian Health and Food Safety Authority, Oberschleissheim, Germany was grown in embryonated chicken eggs.

Six to 8-week-old Balb/c mice from the animal breeding facilities at the Friedrich-Loeffler-Institute, Federal Research Institute for Animal Health, Tuebingen, Germany, were anaesthetized by intraperitoneal injection of 150 µl of a ketamine (1%, Sanofi)-rompun (0,2%, Bayer) solution before treatment. Balb/c mice were intranasal infected with avian H5N1 virus A/mallard/Bavaria/1/2006 (7 × 10exp2 or 100 pfu, i.e. 10-fold MLD50). Mice were i.v. treated with 25 mg/kg VL-01 or solvent (mock) 2 h prior to virus infection. Serum samples for cytokine analysis were collected before and 12, 30, or 72 h after infection. All animal studies were approved by the Institutional Animal Care and Use Committee of Tuebingen.

Inhibition of Cytokine Release *In Vivo* in LPS Challenge Model

To investigate the effect of VL-01 on LPS induced cytokine response, mice were i.v. treated with 25 mg/kg VL-01 2 h prior to LPS treatment (Lipopolysaccharides from *Escherichia coli* 055: B5, Sigma, Germany, 20 µg/mice). Serum samples for cytokine analysis were collected before (−4 h) and 1.5 and 3 h after LPS treatment.

Cytokine Analysis

Cytokine analysis was performed using Bio-Plex Protein Arrays from BioRad (Bio-Rad Laboratories, Munich). Bio-Plex-Pro-Mouse Cytokine 6-Plex or 23-Plex were used for cytokine analysis after H5N1 infection or LPS challenge, respectively.

RESULTS

Cytokine and Chemokine Storm Is a Hallmark of Acute Respiratory Viral Infections, Such as SARS-CoV-2, SARS-CoV, MERS-CoV, H5N1, and H1N1 (Spanish) Influenza A—Central Role of the NF-κB Pathway

The morbidity and mortality of highly pathogenic hCoV is still incompletely understood. Virus-induced cytopathic effects and viral evasion of the host immune response play a role in disease severity. However, clinical data from patients, in particular those with severe clinical manifestations indicate that highly dysregulated exuberant inflammatory and immune responses correlate with severity of disease and lethality (1, 5–7, 10–12). Significantly elevated cytokine and chemokine levels, *i.e.* cytokine storm, seem to play a central role in severity and lethality in SARS-CoV-2 infections, with elevated plasma levels of IL-1β, IL-7, IL-8, IL-9, IL-10, G-CSF, GM-CSF, IFNγ, IP-10, MCP-1, MIP-1α, MIP-1β, PDGF, TNFα, and VEGF in both ICU (Intensive care unit) patients and non-ICU patients. Significantly higher plasma levels of IL-2, IL-7, IL-10, G-CSF, IP-10, MCP-1, MIP-1α, and TNFα were found in patients with severe pneumonia developing ARDS and requiring ICU admission and oxygen therapy compared to non-ICU patients showing pneumonia without ADRS (1).

Immune profiling of COVID-19 patients revealed distinct immunotypes with therapeutic implications, *i.e.* immunotype 1 characterized by a robust CD4 T cell activation, proliferating effector CD8 T cells was connected to severe disease, immunotype 2 with more traditional effector CD8 T cell subsets, less CD4 T cell activation and memory B cells, showed intermediate clinical outcome, and immunotype 3 with only minimal lymphocyte activation response showed the least

clinical symptomatic picture (13). In the same line, asymptomatic SARS-CoV-2 infected individuals exhibited lower levels of a panel of 18 cytokines / chemokines (14).

Detailed insight into the underlying cellular interactions demonstrated by single-cell RNA sequencing analysis showed that COVID-19 severity correlates with the cellular airway epithelium-immune cell interaction. Critical COVID-19 cases —compared to moderate cases—exhibited stronger interaction between epithelial and immune cells, indicated by ligand-receptor expression profiles. Besides expression of pro-inflammatory cytokines, such as IL-1β and TNF-α, the expression of chemokines CCL2, CCL3, CCL20, CXCL1, CXCL3, CXCL10, IL-8 was shown likely to contribute to clinical observation of excessive inflammatory tissue damage, lung injury, and respiratory failure (15).

Regarding the cell types affected, single cell transcriptome and phenotyping studies show that SARS-CoV-2-induced hyper-activation seems to affect a broad spectrum of cells ranging from epithelial cells of the respiratory tract (16–18), lining endothelial cells (6, 7), cells of the innate immune system, including macrophages and mast cells located in the submucosa of the respiratory tract (15, 19), and PBMC (including monocytes, dendritic cells, CD4- and CD8 T-cells) (13, 15, 20).

Notably, also for SARS-CoV and MERS-CoV infected patients, increased levels of pro-inflammatory cytokines in serum, including IL-1β, IL-6, IL-12, IFNγ, TNFα, IL-15, IL-17 and chemokines including CCL2 (MCP-1), CXCL10 (IP-10), CXCL9 (MIG), CCL-5, IL-8 were associated with pulmonary inflammation and extensive lung damage (21–23). Furthermore, both the nucleocapsid protein and the spike protein of SARS-CoV were shown to induce pro-inflammatory cytokines *via* activation of the NF-κB pathway (24, 25). Using comprehensive genomic analyses Smits et al. showed that aged macaques have a stronger host response to virus infection compared to young macaques, with an increase in differential expression of genes associated with inflammation, with NF-κB as central player, whereas expression of type I interferon was reduced indicating a possible negative-feedback cross-talk between the pro-inflammatory NF-κB pathway and IFN-induced antiviral pathways (26).

Interestingly, beside the three highly pathogenic hCoV, also H5N1 and certain H1N1 influenza virus infections with high lethality in humans, showed excessive alveolar immune inflammatory infiltrates and high levels of pro-inflammatory cytokines and chemokines including IP10/CXCL10, IL-6, IL-8, and RANTES in human cell lines, mice, and macaques (27–32) and in humans infected with swine-origin Influenza A virus H1N1 (33).

A differential time-kinetic dependent expression of cytokines and chemokines with acute response cytokines TNFα and IL-1β and chemokines IL-8 and MCP-1 in the early minutes to hours after infection, followed by a more sustained increase in IL-6 was demonstrated by microarray-based transcriptional changes in H5N1 and 1918 H1N1 in comparison to seasonal H1N1 virus infection, with transcriptional changes in the NF-kB pathway central in the cytokine storm (34).

Importantly, recent transcriptome analysis from post-mortem lung tissue of COVID-19 patients and cell culture models infected with COVID-19, Respiratory Syncytial virus and influenza virus identified commonly regulated gene-expression modules of key inflammatory processes for all three acute respiratory viral infections. Key examples were TNF, NF-κB, IL-1, and ALOX5 signaling pathways (17). Several recent reports have demonstrated the NF-κB pathway as *the* central signaling pathway for the SARS-CoV-2 infection-induced pro-inflammatory cytokine/chemokine response (16–18, 35–37). Huang et al. showed in a human *in vitro* model that simulates the initial apical infection of alveolar epithelium with SARS-CoV-2 a rapid transcriptomic change in infected cells, characterized by a shift to an inflammatory phenotype with upregulation of NF-κB signaling and NF-κB target genes by day 1 post-infection, followed by a loss of the mature alveolar program (16). Moreover, SARS-CoV-2 spike protein subunit 1 (CoV2-S1) was shown to induce high levels of NF-κB activations, production of pro-inflammatory cytokines and chemokines (IL-1β, TNFα, IL-6, CCL2), and mild epithelial damage in human bronchial epithelial cells. CoV2-S1-induced NF-κB activation required S1 interaction with human ACE2 receptor and early activation of endoplasmic reticulum (ER) stress, associated unfolded protein response (UPR), and MAP kinase signaling pathways. Notably, a higher activity in NF-κB activation of CoV-2-S1 compared to CoV-S1 was found, probably correlating with the higher binding affinity of CoV-2-S1 to ACE2 receptor (37). Sohn et al. showed that C-C motif (CC) chemokines [CC chemokine ligand (CCL) 2, CCL7, CCL8, CCL24, CCL20, CCL13, and CCL3], C-X-C motif (CXC) chemokines [CXC chemokine ligand (CXCL) 2 and CXCL10], and chemokine receptor subfamilies, as well as IL-1β and its downstream inflammatory signaling molecules (IL1R1, MYD88, IRAK1, TRAF6, NFKBIA, NFKB1, RELA) were dramatically elevated in peripheral blood mononuclear cells (PBMC) from COVID-19 patients compared to healthy controls. Moreover, the expression of the toll-like receptor TLR4 and its related/downstream signaling molecules (CD14, MYD88, IRAK1, TRAF6, TIRAP, TICAM) and most NF-κB signaling pathway genes (NFKBIA, NFKB1, RELA, NFKB2) were significantly upregulated, indicating that TLR4-mediated NF-κB signaling pathway activation is involved in the upregulation of inflammatory responses in patients with COVID-19 infection (38).

Taken together, these multiple reports point to a potential common pathophysiological mechanism of highly dysregulated exuberant inflammatory reactions in response to various acute respiratory RNA virus infections.

Inhibition of NF-κB Can Inhibit Both Virus-Induced and LPS-Induced Cytokine Storm

We have previously shown that elevated cytokine release of IL-α/β, IL-6, MIP-1β, RANTES, and TNF-α induced by highly pathogenic avian H5N1 influenza A virus was significantly reduced by application of the proteasome inhibitor VL-01 *in vivo* (39). The underlying mechanism of this inhibitory effect of

proteasome inhibitors is supposed to be mediated largely by the inhibition of one of the most prominent cellular transcription pathways, NF-κB. The inhibition of the nuclear translocation of the transcription factor NF-κB by proteasome inhibitors has been described (40–42). This is mediated *via* the inhibition of the proteasomal degradation of the cytosolic inhibitor IκBα, this way keeping NF-κB sequestered by IκBα in the cytosol and thereby inhibiting the otherwise induced translocation of NF-κB to the nucleus where it would initiate the transcription of multiple pro-inflammatory proteins, such as cytokines, chemokines, adhesion molecules, and growth factors (**see Figure 1**). Activation of the NF-κB pathway has been described for very different signal-receptor bindings, including binding of LPS to Toll-like receptor TLR4, binding of cytokines like IL-1 and TNFα to their respective receptors, or recognition of RNA viruses by Toll-like receptors, TLR7/8 for single stranded RNA or TLR3 for double stranded RNA. TLR7/8 and TLR3 are inserted in membranes in such way that the RNA-recognition domains face towards the extracellular space or into the endosomal lumen (42, 43). For SARS-CoV-2 uptake into the endosomal compartment after binding to the ACE2 receptor (8) has been described and the activation of the endosomal TLR7/8 sensitive to single-stranded RNA is assumed (43). Furthermore, the activation of additional Toll-like receptors, such as TLR2, 3, and 4 has been postulated (44). The activation of TLR3 can be expected by double-stranded RNA intermediates generated during SARS-CoV-2 replication

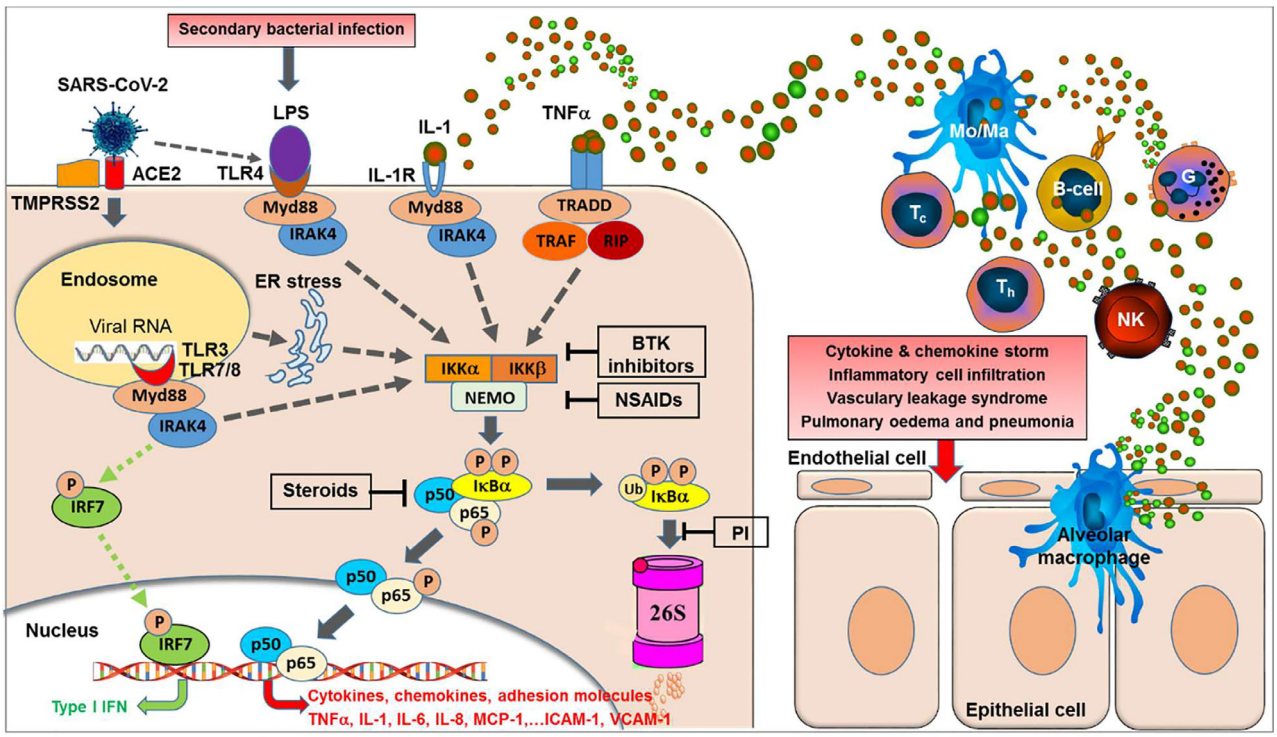

FIGURE 1 | NF-κB activation is central to the acute respiratory RNA virus-induced cytokine storm. Binding of SARS-CoV-2 to its receptor, *i.e.* the angiotensin-converting enzyme 2 (ACE2) and the help of the cellular serine protease TMPRSS2 trigger endocytosis into the host cell. Within the endosomes, RNA from single-stranded RNA virus is known to activate the Toll-like receptors TLR7 and TLR8. Double-stranded RNA intermediates generated during viral replication can be recognized by TLR3. TLR7/8 and/or TLR3 activation can lead to activation of transcription of the interferon-regulator factor (IRF) family and antiviral responses (green dotted lines). However, as a second major effect the activation of the TLRs can trigger—*via* various intermediates—the activation of IKK (IκB kinases) (gray dotted lines) resulting in phosphorylation of the cytoplasmic inhibitor factor IκBα triggering its ubiquitination followed by degradation by the 26S proteasome, thereby NF-κB (a heterodimer complex consisting of protein subunits p50 and p65) is released from IκBα and can now enter the nucleus and initiate transcription of various genes coding for pro-inflammatory proteins such as cytokines, chemokines, adhesion molecules, and growth factors. Importantly, this final sequence of NF-κB activation is shared with a multiple range of cytokine receptor- and Toll-like receptor mediated signal cascades, including binding of TNFα or IL-1 to their receptors or binding of LPS (e.g. from secondary bacterial infections) to TLR4. Furthermore, SARS-CoV-2 was reported to induce TLR4-mediated NF-κB activation as well as ER stress-induced NF-κB activation. Excessive NF-κB activation triggers the gene expression for a broad range of pro-inflammatory cytokines and chemokines, adhesion molecules, and acute phase proteins, resulting in inflammatory cell activation and infiltration, vascular leakage syndrome, finally leading to pulmonary edema and pneumonia. In contrast, interferon-response factor (IRF)-related antiviral responses are largely independent on NF-κB translocation. BTK inhibitors, Bruton Tyrosine Kinase inhibitors; PI, proteasome inhibitors; NSAIDs, nonsteroidal anti-inflammatory drugs; TNFα, tumor necrosis factor-alpha; IL-1, interleukin-1; MCP-1, macrophage chemotactic protein-1; ICAM-1, intercellular adhesion molecule-1; VCAM-1, vascular cell adhesion molecule-1; IRF7, interferon regulatory factor-7; Type I IFN, interferon type I; Myd88, myeloid differentiation primary response 88 protein (adaptor molecule); NEMO, NF-κB essential modulator; IKK, IκB kinase; TRAF, TNF receptor-associated factor; RIP, receptor-interacting protein; TRADD, tumor necrosis factor receptor type-1 associated DEATH domain protein; IRAK4, interleukin-1 receptor-associated kinase 4; ER, endoplasmatic reticulum; LPS, lipopolysaccharide.

(43). Furthermore, also the activation of TLR4 (at the outer membrane) by SARS-CoV-2 has been indicated by a recent study (38). TLR4 also can be activated by LPD derived from bacterial co-infection or secondary bacterial infections, which have been found in up to 14% of SARS-CoV-2 infected patients (45). Furthermore, a recent study has demonstrated that SARS-Cov-2 spike protein subunit 1 induces high levels of NF-κB activation, production of pro-inflammatory cytokines in human bronchial epithelial cells *via* early activation of endoplasmatic reticulum (ER) stress, and associated unfolded protein response (UPR), and MAP kinase signaling pathways (37).

Importantly, all these different signaling pathways join into a common downstream signaling sequence characterized by phosphorylation of the cytosolic inhibitor IκBα which triggers its ubiquitination and proteasomal degradation resulting in release and translocation of NF-κB into the nucleus (42). This sequence of events in the signal transduction pathways suggests that interfering at these late stages (*i.e.* phosphorylation, ubiquitination, and/or proteasomal degradation of IκBα) of the pathway will inhibit NF-κB activation, irrespectively of the initial triggering signal (see **Figure 1**).

We could demonstrate the inhibitory effect of proteasome inhibitors on nuclear translocation NF-κB in various cell types such as human macrophages after stimulation with TNFα *in vitro*. Without stimulation of the NF-κB pathway, p65/p50 (p65 FITC stained) is sequestered in the cytosol by its inhibitor IκB. Following stimulation by TNFα, NF-κB translocates to the nucleus (shown by coinciding p65 staining and nucleus staining by DAPI). NF-κB nuclear translocation after TNFα stimulation was inhibited by application of the proteasome inhibitor VL-01 showing p65 staining in the cytosol and only few cells with p65 positive nucleus (**Figure 2**).

The effect of VL-01 on the pro-inflammatory cytokine and chemokine response *in vivo* was demonstrated in a H5N1 influenza virus challenge mouse model. A strong cytokine and chemokine response was induced in Balb/c mice intranasally infected with avian H5N1 virus A/mallard/Bavaria/1/2006 (7×10^2 pfu, i.e. 10-fold MLD_{50}). Mice were treated i.v. either with 25 mg/kg VL-01 or solvent (mock) 2 h prior to virus infection. Serum samples for cytokine analysis were collected at different time points after infection. While some cytokines/chemokines such as TNFα and MIP-1β peaked very early after H5N1 infection (12 h), others, *i.e.* IL-1α and RANTES peaked somewhat later (at 30 h), followed by KC (neutrophil-activating protein-3) and IL-6, reaching their peak at 72 h after infection (**Figure 3**). Treatment with proteasome inhibitor significantly inhibited the release of IL-1, IL-6, TNFα, MIP-1β (*i.e.* CCL4), and KC (*i.e.* CXCL1) at their peak time-points in Balb/c mice after infection with the highly pathogenic avian H5N1 influenza A virus (**Figure 3**). Importantly, proteasome inhibition significantly decreased the release for *all*, *early and late* cytokines and chemokines, and resulted in significantly increased survival of mice after infection with the highly pathogenic avian H5N1 influenza A virus (39).

In order to investigate whether the inhibition of cytokine and chemokine release by inhibition of the nuclear translocation of

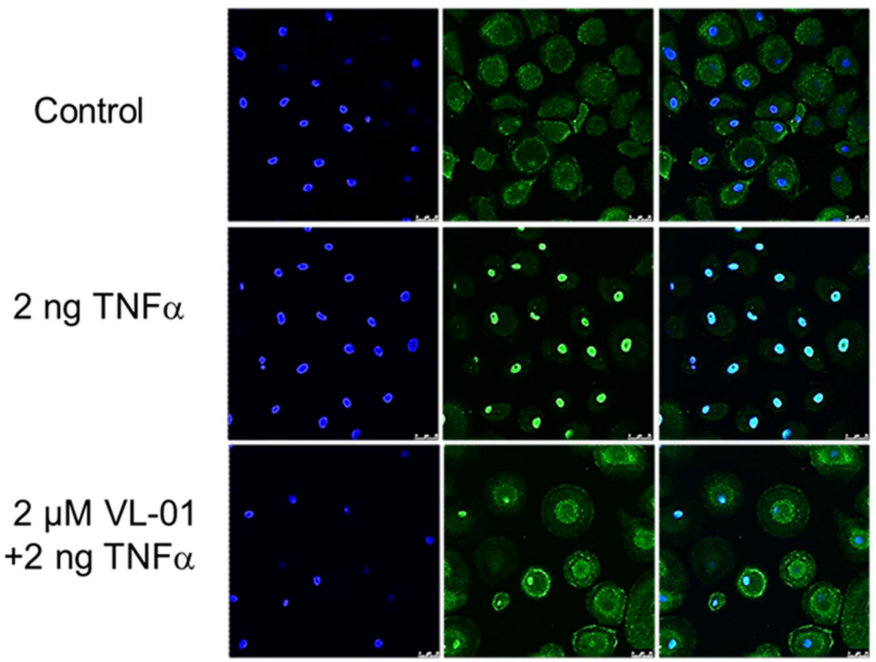

FIGURE 2 | Inhibition of TNFα induced nuclear translocation of NF-κB by the proteasome inhibitor VL-01. Human monocyte-derived macrophages were seeded on cover-slides, incubated overnight, and incubated in the presence or absence of the proteasome inhibitor VL-01 and stimulated with TNFα (2 ng/ml) for 30 min. Immunofluorescence staining of NF-κB was done using a FITC (green)-labeled p65 specific antibody (middle panel), and cell nuclei were counterstained with DAPI (blue, left panel) and evaluated by confocal microscope (Leica, LSM3). Staining of NF-κB (FITC) and nuclei (DAPI) superimposed are shown in the right panel.

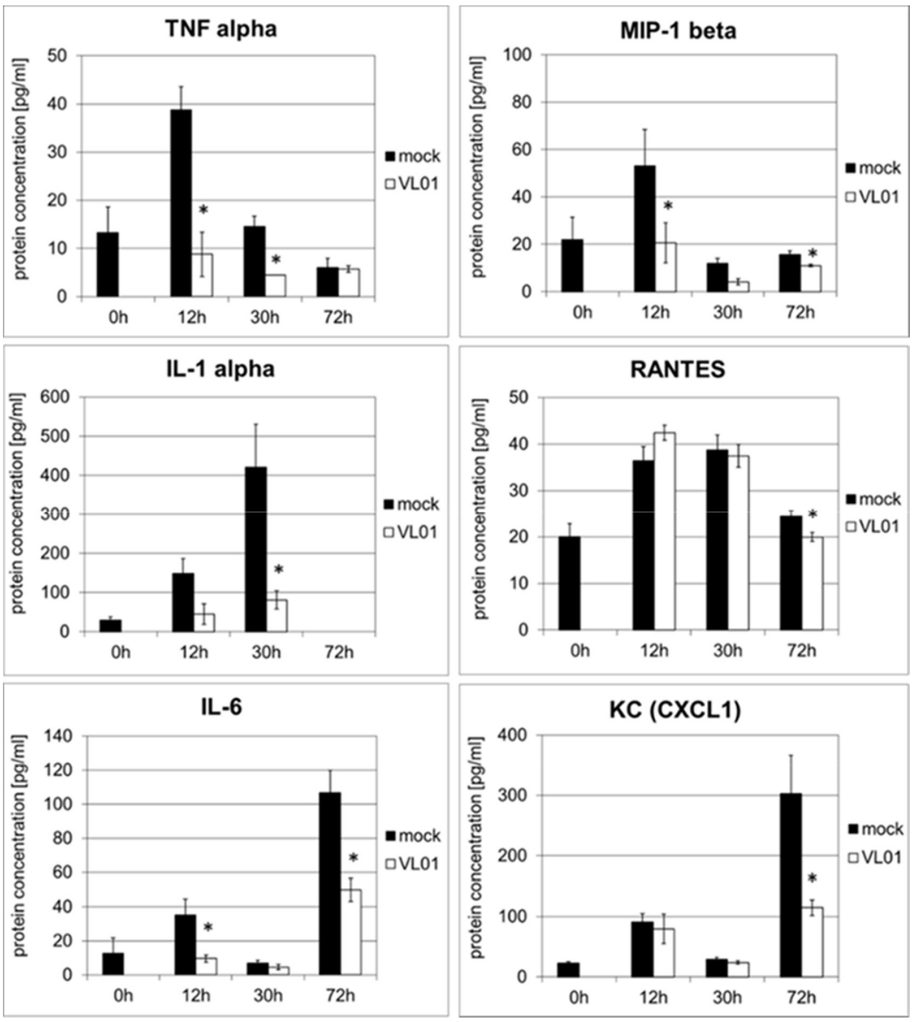

FIGURE 3 | Inhibition of cytokine release in BALB/c mice infected with H5N1 by treatment with the proteasome inhibitor VL-01. Balb/c mice (n = 4) were intranasal infected with avian H5N1 virus A/mallard/Bavaria/1/2006 (7×10^2 pfu, i.e. 10-fold MLD50). Mice were i.v. treated with 25 mg/kg VL-01 or solvent (mock) 2 h prior to virus infection. Cytokine levels in blood were determined before (0 h) and 12, 30, or 72 h after infection using the Bio-Plex Pro Mouse Cytokine 6-Plex Panel (Biorad). *$p < 0.05$.

NF-κB is a general mechanism, an acute lung injury (ALI) mouse model with LPS challenge was used. This model provides a rapid and strong systemic induction of pro-inflammatory cytokines and chemokines. Balb/c mice were treated i.v. with 25 mg/kg VL-01, followed by i.p. application of 20 µg LPS. Serum samples for cytokine analysis were collected before (−4 h) LPS treatment (control) and after LPS treatment (1.5 and 3 h). Again distinct release patterns were found for different cytokines/chemokines, with TNFα, IL-1β, MIP-1α (*i.e.* CCL3), and MIP-1β (*i.e.* CCL4) peaking already 1.5 h after LPS challenge, followed by MCP-1 (*i.e.* CCL2), Eotaxin, and G-CSF, further followed by cytokines with more delayed expression, such as IL-6, RANTES (*i.e.* CCL5), IL-12p40, and KC (*i.e.* CXCL1) peaking 3 h after LPS stimulus (**Figure 4**). In contrast, only a minimal or no increase was found for IL-4, IFNγ, and GM-CSF following LPS challenge. The panel of induced cytokines and chemokines in this acute lung injury model is rather similar to the panel of cytokines reported for COVID-19 patients, with cytokines/chemokines such as TNFα, IL-1, IL-6, IL-10, G-CSF, MIP-1α, MIP-1β , and MCP-1 correlating with critical stage in COVID-19 patients (1). Importantly, treatment of mice with proteasome inhibitor significantly reduced the release of the whole panel of the induced pro-inflammatory cytokines (Th1 profile) and chemokines. Taken together, these data generated in different models demonstrate the principal potency of proteasome inhibitors to interfere with the pro-inflammatory effects, by inhibiting the translocation of NF-κB to the nucleus.

As a second line of evidence for the potential role of the NF-κB pathway in acute respiratory viral infection DeDiego et al. have demonstrated, that the inhibition of NF-κB-mediated inflammation in SARS-CoV infected mice significantly decreased the expression of pro-inflammatory cytokines

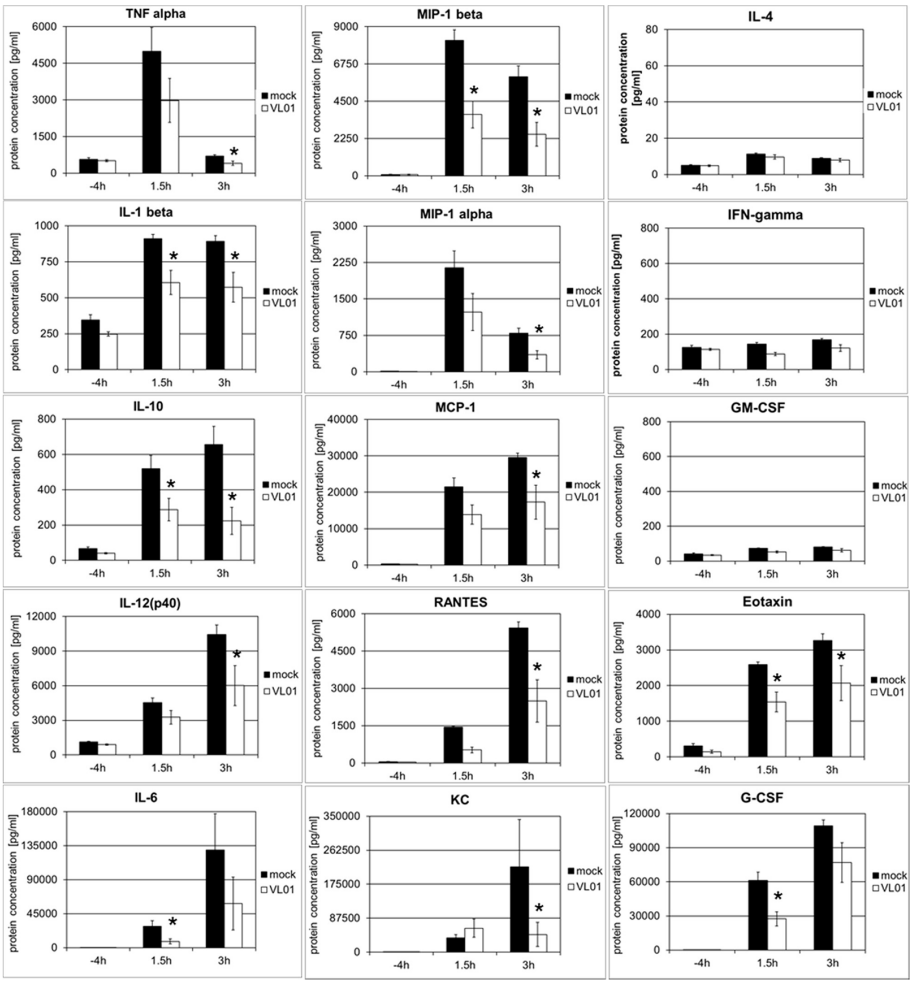

FIGURE 4 | Inhibition of LPS-induced cytokine release in BALB/c mice by the proteasome inhibitor VL-01. Balb/c mice (n = 7) were injected i.v. with VL-01 (25 mg/kg, in 200 µl i.v.) 2 h prior LPS stimulation (20 µg/mouse, 200 ml i.p.). Cytokine levels were determined for the time points before (–4 h), and 1.5 or 3 h after LPS injection, using the Bio-Plex Pro Mouse Cytokine 23-Plex Panel (Biorad). *$p < 0.05$.

including TNFα, IL-6, and chemokines including CCL2, CCL5, CXCL1, CXCL2, CXCL10, correlating with increased survival. In their study four different NF-κB inhibitors, with different mechanism of inhibition, i.e. CAPE, resveratrol, Bay11-7082, and parthenolide, were used. All four inhibitors were shown to inhibit NF-κB activity, and to decrease the expression levels of pro-inflammatory cytokines and chemokines, without affecting viral titers or cell viability (46).

Moreover, Acetylsalicylic acid (ASA) and other salicylates—in contrast to pure (COX) cyclooxygenase inhibitors, such as indomethacin—are well-known inhibitors of NF-κB activation by acting as specific inhibitors of IKK2 (*i.e.* IKKβ)—a kinase essential for phosphorylating IκB (47). Furthermore, D,L-lysine-acetylsalicylate glycine (LASAG) a water-soluble salt of ASA (licensed as Aspirin i.v.®) was shown to decrease activation of promoter constructs of NF-κB-dependent genes for IL-6 and IL-8 and to improve the time to alleviation of influenza symptoms in hospitalized patients in a phase II clinical trial (48). The well-known analgesic, antipyretic, anti-thrombotic, anti-inflammatory, and antiviral effects of ASA have led to initiation at least eight clinical studies investigating the effects of ASA in COVID-19 according to clinicaltrials.gov (49). A recently published study has demonstrated that indeed Aspirin use is associated with decreased mechanical ventilation, ICU admission, and In-hospital mortality in hospitalized COVID-19 patients (50).

Thirdly, the concept of a central role of NF-κB pathway in critical stage SARS-CoC-2 infected patients is supported by two recently published studies showing pronounced clinical effect in critical COVID-19 patients by Bruton tyrosine kinase (BTK) inhibitors, correlating with significantly decrease in inflammatory parameters (C-reactive protein and IL-6), normalized lymphopenia, and improved oxygenation (51, 52). Bruton tyrosine kinase is known to be involved in TLR7/8-induced TNFα transcription *via* NF-κB recruitment at the stage of phosphorylation of p65 (53).

Finally, support for the role of NF-κB pathway in critical stage COVID-19 patients is provided by recent results from the RECOVERY trial. Dexamethasone was found to significantly reduce death in patients with severe respiratory complications of COVID-19 requiring ventilation by up to one third (54). Dexamethasone—a broadly used glucocorticoid anti-inflammatory drug—is assumed to mediate its anti-inflammatory activity at least partially *via* downregulation of the NF-κB activity (55), probably by suppression of NF-κB expression (56) and/or increased expression of IκB in the cytoplasm (57).

All these data collectively strongly indicate that inhibition of the NF-κB signal pathway may be a promising target to control SARS-CoV-2 induced excessive immune activation associated with systemic cytokine and chemokine release, capillary leakage, and multi-organ tissue damage (**Figure 1**).

DISCUSSION

Various studies as referenced in the present review have shown that highly stimulated epithelial-immune cell interactions leading to highly dysregulated exuberant inflammatory responses with significantly (topically and systemically) elevated cytokine and chemokine release, play a central role in severity and lethality in various acute respiratory viral infections, including Influenza A H5N1, highly pathogenic H1N1, SARS-CoV, MERS-CoV, and SARS-CoV-2.

Even the higher COVID-19 mortality rate observed in male compared to female patients (58) may correlate with sex differences in the immune responses between male and female, with higher plasma levels cytokines and chemokines including IL-6, IL-8, IL-18, CCL5 found in male patients. In contrast, female patients showed higher IFNα2 levels and a higher T cell activation compared to male patients (59, 60). The reason for these differences may be speculated to be associated with the location of responsive genes on the X chromosomes and accordingly different expression in female and male (61).

Furthermore, while initial reports indicated that children typically have mild or no COVID-19 symptoms and lower rates of hospitalization and death than adults, there is a accumulating number of reports on the occurrence of Multisystem inflammatory syndrome in children (MIS-C) as a newly described condition associated with SARS-CoV-2 exposure that is reminiscent of both Kawasaki disease and toxic shock syndrome (62, 63). A recent study on peripheral immunophenotypes in children with multisystem inflammatory syndrome associated with SARS-CoV-2 infection showed high levels of IL-1β, IL-6, IL-8, IL-10, IL-17, IFN-γ together with high CD64 expression on neutrophils and monocytes, and high HLA-DR expression on γδ and CD4+CCR7+ T cells in the acute phase of MIS-C indicating high immune activation and cytokine release syndrome (64). For treatment of MIS-C blocking of pro-inflammatory cytokines and the use of anti-inflammatory cytokines IL-37 and IL-38 has been suggested as a potential therapeutic tool (65).

A variety of immunomodulatory approaches has been proposed and are being tested to inhibit various cytokines prominently elevated during COVID-19 infection, including monoclonal antibodies against the IL-6 receptor (66–69) or IL-1 receptor antagonist (70, 71). Whereas some clinical efficacy in COVID-19 patients has been recorded also several notable caveats and limitations to the efficacy of single-cytokine targeting approaches have been seen and have led to the question which cytokine to target in a raging storm (72, 73).

The question which particular cytokine / chemokine to target has been shown to be most difficult due to the cascade nature of the induced cytokine storm. There is a considerable degree of redundancy (or overlapping activities) (74) between the (patho) physiological activities of different cytokines, such as TNFα, IL-1, and IL-6, or also between various chemokines. The second characteristics of the cytokine cascade are the triggering effects, inducing downstream the expression of many additional cytokines / chemokines together with positive autocrine and paracrine feedback loops as illustrated for TNFα and IL-1 in **Figure 1**. Recently, the amplifying positive feedback loop between IL-6 / STATs and NF-κB signaling has been highlighted with regard to COVID-19 associated mortality (75). Finally, a recent study has shown that the cocktail of the cytokines found most highly upregulated in the circulation of patients with COVID-19 and in PBMCs infected with SARS-CoV-2, *i.e.* IL-6, IL-18, IFN-γ, IL-15, TNF-α, IL-1α, IL-1β, and IL-2 robustly induced cell death the marrow-derived macrophages whereas none of the cytokines individually induced high levels of cell death at the concentration used. Similarly a synergistic effect was found when a cocktail of two cytokines, *i.e.* TNFα and IFNγ, was applied indicating highly synergistic effects between various cytokines on the target cell level (76).

These redundant, triggering, positive feedback-loops (amplifying), and synergistic effects make it utmost difficult to select *the one* crucial cytokine / chemokine within this cascade calling for a systemic approach for simultaneous inhibition of multiple cytokines, including also early expressed cytokines and chemokines.

As summarized in the present review, there is accumulating evidence from recently published studies that indicate the NF-κB signal transduction pathway as a common pathway centrally involved in the generation of the observed cascades of pro-inflammatory cytokines and chemokines in acute respiratory virus infection, including SARS-CoV-2-triggered COVID-19. Reaching beyond the possibilities of currently evaluated drugs for single targets of the cytokine cascade, the inhibition of NF-κB pathway—preferably in parallel at several sensitive points (**Figure 1**)—could provide the unique potential to inhibit the release of multiple cytokines simultaneously, in particular strongly pro-inflammatory cytokines including IL-1, IL-6, TNFα, and chemokines including MIP-1α, MIP-1β, MCP-1, as well as adhesion molecules that are increased during highly inflammatory processes during acute COVID-19 stages.

Multiple approved medications with implicated NF-κB activity involving NSAIDs (*e.g.* acetylsalicylic acid, Aspirin), BTK

inhibitors (*e.g.* Ibrutinib, Acalabrutinib), steroids (*e.g.* Dexamethasone), are in wide-spread clinical use and have shown significant clinical efficacy, i.e. significant decrease in mortality was demonstrated (50–52, 54). Although impressive decrease in mortality has been observed, none of these treatments so far has resulted in complete prevention of mortality yet. This might be associated with a still not optimized dosage, start, and duration of treatment. On the other hand, from the sequence of transduction events during NF-kB pathway (see **Figure 1**) it seems plausible that highest effects might be achieved by targeting the latest common steps in NF-κB signal transduction pathway. In this respect inhibiting beside phosphorylation also the following steps of IκB inactivation, *i.e.* ubiquitination and/or proteasome degradation may provide additional treatment options. Several registered proteasome inhibitors (Bortezomib, Carfilzomib, or Ixazomib) are available for treatment of oncological indications (77). This class of substances is known to be powerful inhibitors of NF-κB pathway, with well-known side effect profile known from broad clinical application. In contrast to oncological indications where eight (or more) treatment cycles are routinely applied, it seems plausible that just few applications of proteasome inhibitors will be sufficient to downregulate the acute cytokine storm in COVID-19 patients, with a better side effect profile to be expected (77).

Importantly, in contrast to another recently suggested systemic approach for simultaneous inhibition of cytokines by JAK inhibitors (78), NF-κB inhibition will inhibit predominantly highly pro-inflammatory cytokines and chemokines, such as TNFα, IL-1, IL-6, MCP-1, MIP-1, which are expected to be primarily involved in exuberant systemic inflammatory responses (as proven at the cellular level for COVID-19 patients by the study of Chua et al. (15) rather than cytokines primarily involved in antiviral responsiveness, such as IFNγ (18, 20, 21, 26)—which is primarily dependent on other pathways, i.e. JAK/STAT.

Although there are still many open questions regarding e.g. which compound class—or which combination of—would be most effective, as well as the optimal timing to start treatment (72, 73), the potential to control the cytokine storm-induced severe lung failure and systemic organ failure by using already registered inhibitors of the centrally involved NF-κB pathway may be a real chance to get additional treatment options, hopefully decreasing the number of cases in need for artificial ventilation, multi-organ failure, and death.

DATA AVAILABILITY STATEMENT

The raw data supporting the conclusions of this article will be made available by the authors, without undue reservation.

ETHICS STATEMENT

The animal study was reviewed and approved by Institutional Animal Care and Use Committee of Tuebingen.

AUTHOR CONTRIBUTIONS

RK contributed project idea, discussion of data, writing of manuscript, literature search, and review of manuscript. EH contributed original data. DL contributed original data and discussion of data. WH contributed original data. MO contributed review of manuscript and literature research. OP contributed original data and review of manuscript. All authors contributed to the article and approved the submitted version.

ACKNOWLEDGMENTS

We acknowledge support by Open Access Publishing Fund of University of Tübingen.

REFERENCES

1. Huang C, Wang Y, Li X, Ren L, Zhao J, Hu Y, et al. Clinical features of patients infected with 2019 novel coronavirus in Wuhan, China. *Lancet* (2020) 395:497–506. doi: 10.1016/S0140-6736(20)30183-5
2. Xu Z, Shi L, Wang Y, Zhang J, Huang L, Zhang C, et al. Pathological findings of COVID-19 associated with acute respiratory distress syndrome. *Lancet Resp Lancet Respir Med* (2020) 8(4):420–2. doi: 10.1016/S2213-2600(20)30076-X
3. Zheng Z, Peng F, Xu B, Zhao J, Liu H, Peng J, et al. Risk factors of critical & mortal COVID-19 cases: A systematic literature review and meta-analysis. *J Infect* (2020) 81(2):e16–25. doi: 10.1016/j.jinf.2020.04.021
4. Wang D, Hu B, Hu C, Zhu F, Liu X, Zhang J, et al. Clinical characteristics of 138 hospitalized patients with 2019 novel Coronavirus-infected pneumonia in Wuhan, China. *JAMA* (2020) 323(11):1061–69. doi: 10.1001/jama.2020.1585
5. Carsana L, Sonzogni A, Nasr A, Rossi RS, Pellegrinelli A, Zerbi P, et al. Pulmonary post-mortem findings in a series of COVID-19 cases from northern Italy: a two-centre descriptive study. *Lancet Infect Dis* (2020) 20 (10):1135–40. doi: 10.1101/2020.04.19.20054262
6. Varga Z, Flammer AJ, Steiger P, Haberecker M, Andermatt R, Zinkernagel AS, et al. Endothelial cell infection and endotheliitis in COVID-19. *Lancet* (2020) 395(10234):1417–8. doi: 10.1016/S0140-6736(20)30937-5
7. Ackermann M, Verleden SE, Kuehnel M, Haverich A, Welte T, Laenger F, et al. Pulmonary vascular endothelialitis, thrombosis, and angiogenesis in COVOD-19. *New Engl J Med* (2020) 383(2):120–8. doi: 10.1056/NEJMoa2015432
8. Hoffmann M, Kleine-Weber H, Schroeder S, Krüger N, Herrler T, Erichsen S, et al. SARS-CoV-2 Cell Entry Depends on ACE2 and TMPRSS2 and Is Blocked by a Clinically Proven Protease Inhibitor. *Cell* (2020) 181(2):271–80.e8. doi: 10.1016/j.cell.2020.02.052
9. Leban J, Blisse M, Krauss B, Rath S, Baumgartner R, Seifert MH. Proteasome inhibition by peptide-semicarbazones. *Bioorg Med Chem* (2008) 16(8):4579–88. doi: 10.1016/j.bmc.2008.02.042
10. Tay MZ, Poh CM, Renia L, MacAry PA, Ng LFP. The trinity of COVID-19: immunity, inflammation and intervention. *Nat Rev Immunol* (2020) 20 (6):363–74. doi: 10.1038/s41577-020-0311-8
11. Schett G, Michael Sticherling M, Neurath MF. COVID-19: risk for cytokine targeting in chronic inflammatory diseases? *Nat Rev Immunol* (2020) 20 (5):271–2. doi: 10.1038/s41577-020-0312-7
12. Moore JB, June CH. Cytokine release syndrome in severe COVID-19. Lessons from arthritis and cell therapy in cancer patients point to therapy for sever disease. Viewpoint: COVID-19. *Science* (2020) 368(6490):473–74. doi: 10.1126/science.abb8925
13. Mathew D, Giles JR, Baxter AE, Oldridge DA, Greenplate AR, Wu JE, et al. Deep immune profiling of COVID-19 patients reveals distrinct immunotypes

with therapeutic implications. *Science* (2020) 369(6508):eabc8511. doi: 10.1126/science.abc8511
14. Long Q-X, Tang X-J, Shi Q-L, Li Q, Deng H-J, Yuan J, et al. Clinical and immunological assessment of asymptomatic SARS-CoV-2 infections. *Nat Med* (2020) 26(8):1200–4. doi: 10.1038/s41591-020-0965-6
15. Chua LR, Lukassen S, Trump S, Hennig BP, Wendisch D, Pott F, et al. COVID-19 severity correlates with airway epithelium-immune cell interactions identified by single-cell analysis. *Nat Biotechnol* (2020) 38 (8):970–9. doi: 10.1038/s41587-020-0602-4
16. Huang J, Hume AJ, Abo KM, Werder RB, Villacorta-Martin C, Alysandratos KD, et al. SARS-CoV-2 Infection of Pluripotent Stem Cell-Derived Human Lung Alveolar Type 2 Cells Elicits a Rapid Epithelial-Intrinsic Inflammatory Response. *Cell Stem Cell* (2020) 18:S1934–5909(20)30459-8. doi: 10.1016/j.stem.2020.09.013
17. Islam MR, Fischer AA. Transcriptome Analysis Identifies Potential Preventive and Therapeutic Approaches Towards COVID-19 Preprints. (2020) 2020040399. doi: 10.20944/preprints202004.0399.v1
18. Neufeldt CJ, Cerikan B, Cortese M, Frankish J, Lee J-Y, Plociennikowska A, et al. SARS-CoV-2 infection induces a pro-inflammatory cytokine response through cGAS-STING and NF-κB. *bioRxiv* (2020). doi: 10.1101/2020.07.21.212639. 2020.07.21.212639.
19. Kritas SK, Ronconi G, Caraffa A, Gallenga CE, Ross R, Conti P. Mast cells contribute to coronavirus-induced inflammation: new anti-inflammatory strategy. *J Biol Regul Homeost Agents* (2020) 34(1):9–14. doi: 10.23812/20-Editorial-Kritas
20. Lee JS, Park S, Jeong HW, Ahn JY, Choi SJ, Lee H, et al. Immunophenotyping of COVID-19 and influenza highlights the role of type I interferons in development of severe COVID-19. *Sci Immunol* (2020) 5(49):eabd1554. doi: 10.1126/sciimmunol.abd1554
21. Wong CK, Lam CW, Wu AKL, Ip WK, Lee NLS, Chan IHS, et al. Plasma inflammatory cytokines and chemokines in severe acute respiratory syndrome. *Clin Exp Immunol* (2004) 136(1):95–103. doi: 10.1111/j.1365-2249.2004.02415.x
22. Channappanavar R, Perlman S. Pathogenic human coronavirus infections: causes and consequences of cyokine storm and immunopathology. *Semin Immunopathol* (2017) 39(5):529–39. doi: 10.1007/s00281-017-0629-x
23. Mahallawi WH, Khabour OF, Zhang Q, Makhdoum HM, Suliman BA. MERS-CoV infection in humans is associated with a proinflammatory Th1 and Th17 cytokine profile. *Cytokine* (2018) 104:8–13. doi: 10.1016/j.cyto.2018.01.025
24. Wang W, Ye L, Ye L, Li B, Gao B, Zeng Y, et al. Up-regulation of IL-6 and TNF-α induced by SARS-coronavirus spike protein in murine macrophages via NF-κB pathway. *Virus Res* (2007) 128(1):1–8. doi: 10.1016/j.virusres.2007.02.007
25. Liao Q-J, Ye L-B, Timani KA, Zeng Y-C, She Y-L, Ye L, et al. Activation of NF-kappaB by the full-length nucleocapsid protein of the SARS coronavirus. *Acta Biochim Biophys Sin (Shanghai)* (2005) 37(9):607–12. doi: 10.1111/j.1745-7270.2005.00082.x
26. Smits SL, de Lang A, van den Brand JM, Leijten LM, van IJcken WF, Eijkemans MJ, et al. Exacerbated innate host response to SARS-CoV in aged non-human primates. *PloS Pathog* (2010) 6(2):e1000756. doi: 10.1371/journal.ppat.1000756
27. Cheung CY, Poon LL, Lau AS, Luk W, Lau YL, Shortridge KF, et al. Induction of proinflammatory cytokines in human macrophages by influenza A (H5N1) virues: a mechanism for the unusual severety of human disease. *Lancet* (2002) 360:1831–7. doi: 10.1016/s0140-6736(02)11772-7
28. de Jong MD, Simmons CP, Thanh CP, Hien VM, Smith GJD, Nguyen T, et al. Fatal outcome of human influenza A (H5N1) is associated with high viral load and hypercytokinemia. *Nat Med* (2006) 12:1203–07. doi: 10.1038/nm1477
29. Wong SS, Yuen KY. Avian influenza virus infections in humans. *Chest* (2006) 129:156–68. doi: 10.1378/chest.129.1.156
30. Droebner K, Reiling SJ, Planz O. Role of hypercytokinemia in NF-kB p50-deficient mice after H5N1 influenza A virus infection. *J Virol* (2008) 82:11461–66. doi: 10.1128/JVI.01071-08
31. Chan MC, Cheung CY, Chui WH, Tsao SW, Nicholls JM, Chan YO, et al. Proinflammatory cytokine responses induced by influenza A (H5N1) virues in primary human alveolar and bronchial epithelial cells. *Respir Res* (2005) 6:135. doi: 10.1186/1465-9921-6-135
32. Kobasa D, Jones SM, Shinya K, Kash JC, Copps J, Ebihara H, et al. Abberant innate immune response in lethal infection of macaques with the 1918 influenza virus. *Nature* (2007) 445:319–23. doi: 10.1038/nature05495
33. Perez-Padilla R, de la Rosa-Zamboni D, Ponce de Leon S, Hernandez M, Quiñones-Falconi F, Bautista E. Pneumonia and respiratory failure from swine-origin influenza A (H1N1) in Mexico. *N Engl J Med* (2009) 361(7):680–9. doi: 10.1056/NEJMoa0904252
34. Tisoncik JR, Korth MJ, Simmons CP, Farrar J, Martin TR, Katze MG. Into the eye of the cytokine storm. *Microbiol Mol Biol Rev* (2012) 76(1):16–32. doi: 10.1128/MMBR.05015-11
35. Rian K, Esteban-Medina M, Hidalgo MR, Çubuk C, Falco MM, Loucera C, et al. Mechanistic modeling of the SARS-CoV-2 disease map. *bioRxiv* (2020). doi: 10.1101/2020.04.12.025577
36. Ingraham NE, Lotfi-Emran S, Thielen BK, Techar K, Morris RS, Holtan SG, et al. Immunomodulation in COVID-19. *Lancet Respir Med* (2020) 8(6):544–6. doi: 10.1016/S2213-2600(20)30226-5
37. Hsu AC-Y, Wang G, Reid AT, Veerati PC, Pathinayake PS, Daly K, et al. SARS-CoV-2 Spike protein promotes hyper-inflammatory response that can be ameliorated by Spike-antagonistic peptide and FDA-approved ER stress and MAP kinase inhibitors in vitro. *bioRxiv* (2020). doi: 10.1101/2020.09.30.317818
38. Sohn KM, Lee S-G, Kim HJ, Cheon S, Jeong H, Lee J, et al. COVID-19 patients upregulate toll-like receptor 4-mediated inflammatory signaling that mimics bacterial sepsis. *J Korean Med Sci* (2020) 35(38):e343. doi: 10.3346/jkms.2020.35.e343. bioRxiv preprint.
39. Haasbach E, Pauli E-K, Spranger R, Mitzner D, Schubert U, Kircheis R, et al. Antiviral activity of the proteasome inhibitor VL-01 against influenza A viruses. *Antiviral Res* (2011) 91:304–13. doi: 10.1016/j.antiviral.2011.07.006
40. Chitra S, Nalini G, Rajasekhar. The ubiquitin proteasome system G. and efficacy of proteasome inhibitors in diseases. *Int J Rheum Dis* (2012) 15 (3):249–60. doi: 10.1111/j.1756-185X.2012.01737.x
41. van der Heijden JW, Oerlemans R, Lems WF, Scheper RJ, Dijkmans BA, Jansen G. The proteasome inhibitor bortezomib inhibits the release of NFkappaB-inducible cytokines and induces apoptosis of activated T cells from rheumatoid arthritis patients. *Clin Exp Rheumatol* (2009) 27(1):92–8.
42. Moynagh PN. TLR signalling and activation of IRFs: revisiting old friends from the NF-kappaB pathway. *Trends Immunol* (2005) 26(9):469–76. doi: 10.1016/j.it.2005.06.009CorpusID:31624452
43. Schmitz ML, Kracht M, Saul VV. The intricate interplay between RNA viruses and NF-κB. *Biochim Biophys Acta* (2014) 1843(11):2754–64. doi: 10.1016/j.bbamcr.2014.08.004
44. Conti P, Ronconi G, Caraffa A, Gallenga C, Ross R, Frydas I, et al. Induction of pro-inflammatory cytokines (IL-1 and IL-6) and lung inflammation by Coronavirus-19 (COVI-19 or SARS-CoV-2): anti-inflammatory strategies. *J Biol Regul Homeost Agents* (2020) 34(2):327–31. doi: 10.23812/CONTI-E
45. Langford BJ, So M, Raybardhan S, Leung V, Westwood D, MacFadden DR, et al. Bacterial co-infection and secondary infection in patients with COVID-19: a living rapid review and meta-analysis. *Clin Microbiol Infect* (2020) 26 (12):1622–9. doi: 10.1016/j.cmi.2020.07.016
46. DeDiego ML, Nieto-Torres JL, Regla-Nava JA, Jimenez-Guardeno, Fernandez-Delgado R, Fett C, et al. Inhibition of NF-kB-mediated inflammation in severe acute respiratory syndrome coronavirus-infected mice increases survival. *J Virol* (2013) 88(2):913–24. doi: 10.1128/JVL02576-13
47. Toner R, McAuley DF, Shyamsundar M. Aspirin as a potential treatment in sepsis or acute respiratory distress syndrome. *Crit Care* (2015) 19:374. doi: 10.1186/s13054-015-1091-6
48. Scheuch G, Canisius S, Nocker K, Hofmann T, Naumann R, Pleschka S, et al. Targeting intracellular signaling as an antiviral strategy: aerosolized LASAG for the treatment of influenza in hospitalized patients. *Emerg Microbes Infect* (2018) 7(1):21. doi: 10.1038/s41426-018-0023-3
49. Bianconi V, Violi F, Fallarino F, Pignatelli P, Sahebkar A, Pirro M. Is Acetylsalicylic Acid a Safe and Potentially Useful Choice for Adult Patients with COVID-19? *Drugs* (2020) 80(14):1383–96. doi: 10.1007/s40265-020-01365-1
50. Chow JH, Khanna AK, Kethireddy S, Yamane D, Levine A, Jackson AM, et al. Aspirin use is associated with decreased mechanical ventilation, ICU

admission, and In-hospital mortality in hospitalized patients with COVID-19. *Anesth Analg*. doi: 10.1213/ANE.0000000000005292
51. Treon SP, Castillo JJ, Skarbnik AP, Soumerai JD, Ghobrial IM, Guerrera ML, et al. The BTK inhibitor ibrutinib may protect against pulmonary injury in COVID-19-infected patients. *Blood May* (2010) 135(21):1913–5. doi: 10.1182/blood.2020006288
52. Roschewski M, Lionakis MS, Sharman JP, Roswarski J, Goy A, Monticelli MA, et al. Inhibition of Bruton tyrosine kinase in patients with sever COVID-19. *Sci Immunol* (2020) 5(48):eabd0110. doi: 10.1126/sciimmunol.abd0110
53. Page TH, Urbaniak AM, Espirito Santo AI, Danks L, Smallie T, Williams LM, et al. Bruton's tyrosine kinase regulates TLR7/8-induced TNF transcription via nuclear factor-κB recruitment. *Biochem Biophys Res Commun* (2018) 499 (2):260–6. doi: 10.1016/j.bbrc.2018.03.140
54. The RECOVERY Collaborative Group. Dexamethasone in hospitalized patients with COVID-19 – Preliminary Report. *N Engl J Med* (2020) NEJMoa2021436. doi: 10.1056/NEJMoa2021436
55. Meduri GU, Muthiah MP, Carratu P, Eltorky M, Chrousos GP. Nuclear factor-kappaB- and glucocorticoid receptor alpha- mediated mechanisms in the regulation of systemic and pulmonary inflammation during sepsis and acute respiratory distress syndrome. Evidence for inflammation-induced target tissue resistance to glucocorticoids. *Neuroimmunomodulation* (2005) 12(6):321–38. doi: 10.1159/000091126
56. Aghei ZH, Kumar S, Farbath S, Kumar MA, Saslow J, Nakhla T, et al. Dexamethasone suppresses expression of Nuclaer Factor-kappaB in the cells of tracheobronchial lavage fluid in premature neonates with respiratory distress. *Pediatr Res* (2006) 59(6):811–8015. doi: 10.1203/01.pdr.0000219120.92049.b3
57. Yamamoto Y, Richard BG. Therapeutic potential of inhibition of the NF-κB pathway in the treatment of inflammation and cancer. *J Cli Invest* (2001) 107 (2):135–42. doi: 10.1172/JCI11914
58. Bhopal SS, Bhopal R. Sex differences in COVID-19 mortality varies markedly by age. *Lancet* (2020) 396(10250):532–3. doi: 10.1016/S0140-6736(20)31748-7
59. Takahashi T, Ellingson MK, Wong P, Israelow B, Lucas C, Klein J, et al. Sex differences in immune responses that underlie COVID-19 disease outcomes. *Nature* (2020). doi: 10.1038/s41586-020-2700-3
60. Maleki DP, Sadoughi F, Hallajzadeh J, Asemi Z, Mansournia MA, Yousefi B, et al. An Insight into the Sex Differences in COVID-19 Patients: What are the Possible Causes? *Prehosp Disaster Med* (2020) 35(4):438–41. doi: 10.1017/S1049023X20000837
61. Conti P, Younes A. Coronavirus COV-19/SARS-CoV-2 affects women less than men: clinical response to viral infection. *J Biol Regul Homeost Agents* (2020) 34(2):339–43. doi: 10.23812/Editorial-Conti
62. Dufort EM, Koumans EH, Chow EJ, Rosenthal EM, Muse A, Rowlands J, et al. Multisystem Inflammatory Syndrome in Children in New York State. *N Engl J Med* (2020) 383:347–58. doi: 10.1056/NEJMoa2021756
63. Feldstein LR, Rose EB, Horwitz SM, Collins JP, Newhams MM, Son MBF, et al. Multisystem Inflammatory Syndrome in U.S. Children and Adolescents. *New Engl J Med* (2020) 383(4):334–46. doi: 10.1056/NEJMoa2021680
64. Carter MJ, Fish M, Jennings A, Doores KJ, Wellman P, Seow J, et al. Peripheral immunophenotypes in children with multisystem inflammatory syndrome associated with SARS-CoV-2 infection. *Nat Med* (2020) 26(11):1701–7. doi: 10.1038/s41591-020-1054-6
65. Ronconi G, Teté G, Kritas SK, Gallenga CE, Caraffa Al, Ross R, et al. SARS-CoV-2, which induces COVID-19, causes kawasaki-like disease in children: role of pro-inflammatory and anti-inflammatory cytokines. *J Biol Regul Homeost Agents* (2020) 34(3):767–73. doi: 10.23812/EDITORIAL-RONCONI-E-59
66. Radbel J, Narayanan N, Bhatt PJ. Use of tocilizumab for COVID-19 infection-induced cytokine release syndrome: A cautionary case report. *Chest* (2020) 158 (1):e15–e9. doi: 10.1016/j.chest.2020.04.024. S0012-3692(20)30764-9.
67. Aziz M, Fatima R, Assaly R. Elevated Interleukin-6 and Severe COVID-19: A Meta-Analysis [published online ahead of print, 2020 Apr 28]. *J Med Virol* (2020). doi: 10.1002/jmv.25948. 10.1002/jmv.25948
68. Zhang S, Li L, Shen A, Chen Y, Qi Z. Rational Use of Tocilizumab in the Treatment of Novel Coronavirus Pneumonia. *Clin Drug Investig* (2020) 40 (6):511–8. doi: 10.1007/s40261-020-00917-3
69. Xu X, Han M, Li T, Sun W, Wang D, Fu B, et al. Effective treatment of severe COVID-19 patients with tocilizumab. *Proc Natl Acad Sci U S A* (2020) 117 (20):10970–5. doi: 10.1073/pnas.2005615117
70. Cavalli G, De Luca G, Campochiaro C, Della-Torre E, Ripa M, Canetti D, et al. Interleukin-1 blockade with high-dose anakinra in patients with COVID-19, acute respiratory distress syndrome, and hyperinflammation: a retrospective cohort study. *Lancet Rheumatol* (2020) 2(6):e325–31. doi: 10.1016/S2665-9913(20)30127-2
71. Conti P, Gallenga CE, Tetè G, Caraffa Al, Ronconi G, Younes A, et al. How to reduce the likelihood of coronavirus-19 (CoV-19 or SARS-CoV-2) infection and lung inflammation mediated by IL-1. *J Biol Regul Homeost Agents* (2020) 34(2):333–8. doi: 10.23812/Editorial-Conti-2
72. Ye Q, Wang B, Mao J. The pathogenesis and treatment of the 'Cytokine Storm' in COVID-19. *J Infect* (2020) 80(6):607–13. doi: 10.1016/j.jinf.2020.03.037
73. Lu L, Zhang H, Zhan M, Jiang J, Yin H, Dauphars DJ, et al. Preventing Mortality in COVID-19 Patients: Which Cytokine to Target in a Raging Storm? *Front Cell Dev Biol* (2020) 8:677:677. doi: 10.3389/fcell.2020.00677. eCollection 2020.
74. Kany S, Vollrath JT, Relja B. Cytokines in Inflammatory Disease. *Int J Mol Sci* (2019) 20:6008. doi: 10.3390/ijms20236008
75. Hojyo S, Uchida M, Tanaka K, Hasebe R, Tanaka Y, Murakami M, et al. How COVID-19 induces cytokine storm with high mortality. *Inflammation Regen* (2020) 40:37. doi: 10.1186/s41232-020-00146-3. eCollection 2020.
76. Karki R, Sharma BR, Tuladhar S, Williams EP, Zalduondo L, Samir P, et al. COVID-19 cytokines and the hyperactive immune response: Synergism of TNF-α and IFN-γ in triggering inflammation, tissue damage, and death. *bioRxiv* (2020). doi: 10.1101/2020.10.29.361048
77. Richardson PG, Briemberg H, Jagannath S, Wen PY, Barlogie B, Berenson J, et al. Frequency, Characteristics, and reversibility of peripheral neuropathy during treatment of advanced multiple myeloma with Bortezomib. *J Clin Oncol* (2006) 24:3113–20. doi: 10.1200/JCO.2005.04.7779
78. Spinelli FR, Conti F, Gadina M. HiJAKing SARS-CoV-2? The potential role of JAK inhibitors in the management of COVID-19. *Sci Immunol* (2020) 5(47): eabc5367. doi: 10.1126/sciimmunol.abc5367

Conflict of Interest: RK, DL, and WH were employed by Virologik GmbH.

The remaining authors declare that the research was conducted in the absence of any commercial or financial relationships that could be construed as a potential conflict of interest.

frontiers in Immunology

ORIGINAL RESEARCH
published: 23 December 2020
doi: 10.3389/fimmu.2020.591269

Immunomodulation Induced During Interferon-α Therapy Impairs the Anti-HBV Immune Response Through CD24^{+}CD38^{hi} B Cells

Binqing Fu[1,2†], Dongyao Wang[1,2†], Xiaokun Shen[1,2], Chuang Guo[1,2], Yanyan Liu[3], Ying Ye[3], Rui Sun[1,2], Jiabin Li[3], Zhigang Tian[1,2*] and Haiming Wei[1,2*]*

[1] Division of Molecular Medicine, Hefei National Laboratory for Physical Sciences at Microscale, The CAS Key Laboratory of Innate Immunity and Chronic Disease, School of Life Sciences, University of Science and Technology of China, Hefei, China, [2] Institute of Immunology, University of Science and Technology of China, Hefei, China, [3] Department of Infectious Diseases, The First Affiliated Hospital of Anhui Medical University, Hefei, China

Type I interferon is widely used for antiviral therapy, yet has yielded disappointing results toward chronic HBV infection. Here we identify that PEG-IFNα-2b therapy toward persistent infection in humans is a double-edged sword of both immunostimulation and immunomodulation. Our studies of this randomised trial showed persistent PEG-IFNα-2b therapy induced large number of CD24^{+}CD38^{hi} B cells and launched a CD24^{+}CD38^{hi} B cells centered immunosuppressive response, including downregulating functions of T cells and NK cells. Patients with low induced CD24^{+}CD38^{hi} B cells have achieved an improved therapeutic effect. Specifically, using the anti-CD24 antibody to deplete CD24^{+}CD38^{hi} B cells without harming other B cell subsets suggest a promising strategy to improve the therapeutic effects. Our findings show that PEG-IFNα-2b therapy toward persistent infection constitutes an immunomodulation effect, and strategies to identifying the molecular basis for the antiviral versus immunomodulatory effects of PEG-IFNα-2b to selectively manipulate these opposing activities provide an opportunity to ameliorate anti-virus immunity and control viral infection.

Keywords: anti-virus function, immunomodulatory effects, CD24^{+}CD38^{hi} B, chronic hepatitis B virus infection, Peg-IFNα-2b

OPEN ACCESS

Edited by:
Caroline Petitdemange, Institut Pasteur, France

Reviewed by:
Kathrin Sutter, University of Duisburg-Essen, Germany
Cai Zhang, Shandong University, China
Yolande Richard, Institut National de la Santé et de la Recherche Médicale (INSERM), France
Qiuju Han, Shandong University, China

***Correspondence:**
Haiming Wei
ustcwhm@ustc.edu.cn
Zhigang Tian
tzg@ustc.edu.cn
Jiabin Li
lijiabin@ahmu.edu.cn

†These authors have contributed equally to this work

Specialty section:
This article was submitted to Viral Immunology, a section of the journal Frontiers in Immunology

Received: *04 August 2020*
Accepted: *18 November 2020*
Published: *23 December 2020*

Citation:
Fu B, Wang D, Shen X, Guo C, Liu Y, Ye Y, Sun R, Li J, Tian Z and Wei H (2020) Immunomodulation Induced During Interferon-α Therapy Impairs the Anti-HBV Immune Response Through CD24^{+}CD38^{hi} B Cells. Front. Immunol. 11:591269. doi: 10.3389/fimmu.2020.591269

INTRODUCTION

Human hepatitis B virus (HBV) establishes persistent infection and thus constitutes a major health burden worldwide (1–4). More than 240 million people are chronically infected with HBV globally, and 780,000 people die each year from HBV-associated liver diseases (5). Peg-IFNα-2b, which mediates both immunomodulatory and direct antiviral effects, is currently widely utilized for the treatment of HBV (6, 7). Interferon-α (IFNα) signaling occurs upstream of hundreds of inflammatory genes and leads to a hyper-activated immune response. These responses include activation of the adaptive and

Abbreviations: HBV, hepatitis B virus; IFNα, Interferon-α TH1, T helper 1 cells; TH17, T helper 17 cells; CHB, Chronic Hepatitis B; HBeAg, Hepatitis B e antigen; LCMV, lymphocytic choriomeningitis virus; IFN-I, Type I interferon; Breg, regulatory B.

innate immune systems, and increased production of antiviral proteins capable of suppressing viral replication and promoting viral clearance (3, 8–10). However, PEG-IFNα-2b yields disappointing therapeutic effects when used to treat chronic HBV infection. Actually, Hepatitis B e antigen (HBeAg)-positive CHB patients who received PEG-IFNα-2b, PEG-IFNα-2b plus lamivudine, or lamivudine alone demonstrated only a 32, 27, or 19% rate of HBeAg seroconversion, respectively (6). The explanation for these results remains unknown.

Recently, reports about persistent infections using lymphocytic choriomeningitis virus (LCMV) infection in mice revealed that Type I Interferon potentially initiates an immunosuppressive program that represses antiviral immunity and facilitates persistent infection. For example, in a model of persistent LCMV, the blockade of IFN-I signaling reduced immune system activation, decreased the levels of negative immune regulatory molecules, and promoted viral clearance and infection control (11, 12). Moreover, a rapid depletion of virus-specific B cells have been documented and this deletion can be completely reversed by blockade of Type I interferon (IFN-I) signaling, associated with suboptimal antibody responses (13–15). It would be very interesting to explore whether IFN-I induced the immunomodulatory effect also exist in virus infected human.

In HBeAg-negative chronic patients, the absolute number of HBV-specific $CD8^+$ T cells was strikingly reduced on PEG-IFNα-2b therapy whereas numbers of $CD56^{bright}$ NK cell increased, showing differential boosting of innate and adaptive antiviral responses (4, 16).Also in HBeAg-negative chronic patients, PEG-IFNα-2b therapy showed a major impact on peripheral B cell subsets and a complete remodeling of the B cell compartment (17). In HBeAg-positive chronic patients, PEG-IFNα-2b has shown to induce a distinct and rapid up-regulation of IFN signaling pathway that coincided with the up-regulation of the frequency of proliferating NK and activated total $CD8^+$ T cells in the first 14 days of IFN-α treatment (18). However, whether PEG-IFNα-2b therapy can induce an immunomodulatory program in chronic infected HBeAg-positive patients during the whole 48 weeks of PEG-IFNα-2b treatment has not yet been determined.

D24 is a small glycosyl phosphoinositol anchored protein that is able to provide costimulatory signals to T cells and the CD24-Siglec-G pathway has been identified to selectively suppresses the immune response to Danger-associated molecular patterns (DAMPs) (19). CD24 can be the dominant innate immune checkpoint and novel "Don't Eat Me" signal that promotes ovarian cancer and breast cancer immune escape (20). CD24 has also been identified as a marker of regulatory B (Breg) cells. $CD24^+CD38^{hi}$ Breg cells inhibit the differentiation of Th1 and Th17 cells, and suppress effector $CD4^+$ and $CD8^+$ T cells *via* the release of IL-10 (21–25). CD24 polymorphisms affect the risk and progression of chronic HBV infected patients. Targeted mutation of CD24 drastically reduced the size of spontaneous liver cancers in HBV transgenic mice (26). It has been reported the existence of IL-10-secreting $CD24^+CD38^{hi}$ B cells in HBV patients (27); however, the dynamic change and the function of these $CD24^+CD38^{hi}$ B cells during PEG-IFNα-2b therapy has not been uncovered.

To determine whether Peg-IFNα-2b therapy causes immunomodulatory effects, randomized clinical trial were conducted including 92 naive HBeAg-positive CHB patients. Patients were divided into two groups, one receiving Peg-IFNα-2b alone and one receiving Peg-IFNα-2b in combination with adefovir-dipivoxil, in order to simulate patients undergoing treatment with nucleoside analog (NUC). Samples were characterized at multiple time points through the whole 48 weeks of PEG-IFNα-2b therapy and also 24 weeks of follow-up. The data revealed a new mechanism in which Peg-IFNα-2b therapy during persistent infection in humans launches a $CD24^+CD38^{hi}$ B -centered immunomodulatory program. This mechanism counteracts the antiviral ability of the immune system in patients with chronic HBV infection.

MATERIALS AND METHODS

Ethics Statement

This multi-centered, randomized, open-label research study was conducted in accordance with the guidelines of China's regulatory requirements, the Declaration of Helsinki and the Principles of Good Clinical Practice. This trial was approved by the local Ethics Board of the First Affiliated Hospital of Anhui Medical University with the clinical trial registration number ChiCTR-TRC-12002226 (http://www.chictr.org.cn/index.aspx). The detail about this Clinical Trial protocol has been showed in the **Supplementary Materials**. All patients involved were HBV patients who had not undergone prior antiviral or immunomodulatory treatment, and each provided written informed consent. Peripheral blood samples from healthy donors were obtained from the Blood Center of Anhui Province. Ethical approval was obtained from the Ethics Committee of the University of Science and Technology of China.

Patients and Human Samples

The included patients had been positive for HBeAg and hepatitis B surface antigen (HBsAg) for longer than 6 months and had elevated serum alanine transaminase (ALT) (>2 × ULN and <10 × ULN) and detectable baseline serum HBV DNA (>2 × 10^4 IU/mL) on at least two occasions. Those who had liver cirrhosis, antibodies against HCV, hepatitis D virus, or HIV, or other acquired or inherited causes of liver disease were excluded. The patients were randomly assigned into one of two groups to receive Peg-IFNα-2b (1.5 μg/kg/week, PegIntron, Schering-Plough, Kenilworth, NJ, USA) alone or in combination with adefovir-dipivoxil (ADV) (10 mg/day, Hepsera, Gilead Sciences, Foster City, CA, USA) for 48 weeks with 24 weeks of follow-up (**Table S1**). An HBeAg seroconversion was defined as a patient with HBeAg loss (COI < 1.0) and seroconversion to anti-HBeAg at week 72 (**Table S2**). According to the European Association for the Study of the Liver guidelines (28), sustained response patients consisted of 17 responders in these 92 patients defined as persistently undetectable HBeAg and a result of HBV DNA <2,000 IU/ml, with the development of antibodies to HBeAg (anti-HBe) (29). Out of 100 HBeAg positive patients, 92 were

completed the final PEG-IFNα-2b treatment (**Figure 1**). NUC-alone patients are also patients had been positive for HBeAg and hepatitis B surface antigen (HBsAg) for longer than 6 months but voluntarily choose to use NUC medicines but not PEG-IFNα-2b therapy. The samples of NUC-alone patients were collected at 6 months or 9 months after the NUC therapy.

Other detailed materials and methods are available in the **Supplementary Material**.

RESULTS

$CD24^+CD38^{hi}$ B Cells Are Induced Significantly During Peg-IFNα-2b Therapy

Similar to previous studies (6), 30.4% of HBV patients in our study underwent HBeAg seroconversion. There was no significant difference (p = 0·501) between Group 1, the Peg-IFNα-2b group (26.7%), and Group 2, the Peg-IFNα-2b + adefovir-dipivoxil group (34.0%) (**Figure 1** and **Tables S1** and **S2**). No significant change of the total $CD3^-CD19^+$B cells during PEG-IFNα-2b therapy (**Figure 2B**). To investigate whether Peg-IFNα-2b therapy induced immunomodulatory effects, analysis of a variation among B cell subsets in HBV patients *in vivo* including $CD24^+CD38^{hi}$ B cells and $CD27^+CD38^{hi}$ B cells were done in the whole Peg-IFNα-2b therapy. These studies showed that the percentage and cell number of $CD24^+CD38^{hi}$ B cells increased rapidly after Peg-IFNα-2b was administered, remained stable at high levels during therapy, and decreased when Peg-IFNα-2b therapy was discontinued at week 48 (**Figures 2A, C, D**). Furthermore, $CD24^+CD38^{hi}$ B cells increased in patients from both Groups 1 and 2 (**Figures S1A, B**). To further exclude the changes of $CD24^+CD38^{hi}$ B cells is for the reason that CHB patients have hepatic flares time to time, negative control groups with no-treatment and NUC-alone therapy were also measured. Both negative control groups showed a low percentage of $CD24^+CD38^{hi}$ B cells (**Figures S1C, D**). On the other hand, previous researches showed that a rapid depletion of antibody-producing mature B cells correlated with IFNα signaling (13–15). In persistent HBV patients, there were no significant changes in the $CD27^+CD38^{hi}$ subset during Peg-IFNα-2b therapy, suggesting plasma B cells are always at low levels during Peg-IFNα-2b therapy (**Figures 2A, C, D**). Thus, persistent HBV patients have increased $CD24^+CD38^{hi}$ B cells during Peg-IFNα therapy.

Peg-IFNα-2b Induced $CD24^+CD38^{hi}$ B Cells Secret IL-10

Pro-inflammatory cytokines such as IFNα plays a pivotal role in B cell differentiation (25, 30–32). Thus, to determine whether Peg-IFNα-2b therapy increases the $CD24^+CD38^{hi}$ B cell population, Peripheral Blood Mononuclear Cells (PBMCs) from healthy donors and HBV patients were first cultured respectively through Peg-IFNα-2b stimulation (100 ng/ml) *in vitro*, which concentration was referred from previous researches (33). The percentage of $CD24^+CD38^{hi}$ B cells was significantly upregulated in both healthy donors and HBV patients when cells were cultured with Peg-IFNα-2b, indicating that IFNα stimulation induces the $CD24^+CD38^{hi}$ B cell population (**Figures 3A, B**). Interestingly, the frequency of $CD24^+CD38^{hi}$ B cells in PEG-IFNα-2b -treated HBV patient group were higher than those in PEG-IFNα-2b -treated healthy donor group, which is probably due to PBMC cells from HBV patient group were previously stimulated by Peg-IFNα-2b *in vivo*. To exclude the possibility that PEG-IFNα-2b treatment had a variable impact of the viability of diverse B cell subsets, and therefore may modulate the frequency of B cell subsets, the impact of PEG-IFNα-2b on survival of different B cell subsets was measured. The number of $CD24^+CD38^{hi}$ B cells from healthy controls was significantly increased. $CD24^+CD38^{hi}$ B subset from HBV patients were also the most variable subset compared with the other two subsets (**Figure S2**).

It has been reported the existence of IL-10-secreting B cells in HBV patients (27), however whether these IL-10-secreting B cells induced during PEG-IFNα-2b therapy has not been uncovered. PBMC were collected from HBV patients at 0 weeks or 12–36 weeks after the start of Peg-IFNα-2b therapy and cultured without Peg-IFNα-2b for 32 h. PBMCs collected from healthy donors were

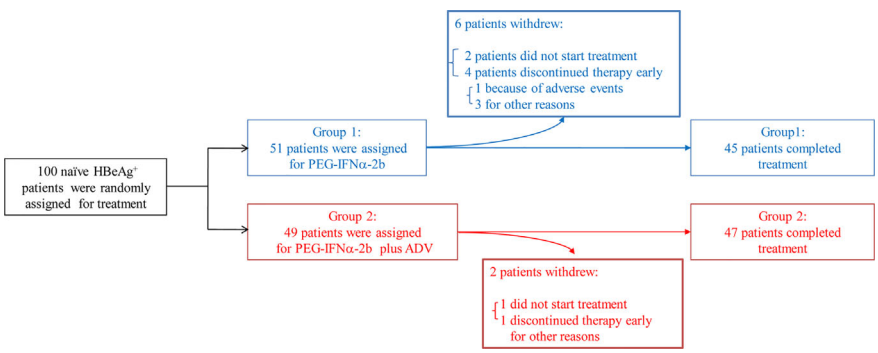

FIGURE 1 | Patients through the trial. One hundred patients that had been positive for HBeAg and hepatitis B surface antigen (HBsAg) for longer than 6 months and had elevated serum alanine transaminase (ALT) (>2 × ULN and <10 × ULN) and detectable baseline serum HBV DNA (>2 × 104 IU/ml) on at least two occasions have been involved into this clinical trial. Out of 100 HBeAg positive patients, 92 were completed the final Peg-IFNα-2b treatment. Randomized clinical trial were conducted including these 92 naive HBeAg-positive CHB patients. Patients were divided into two groups, one receiving Peg-IFNα-2b alone and one receiving Peg-IFNα-2b in combination with adefovir-dipivoxil in order to simulate patients undergoing treatment with nucleoside analog (NUC).

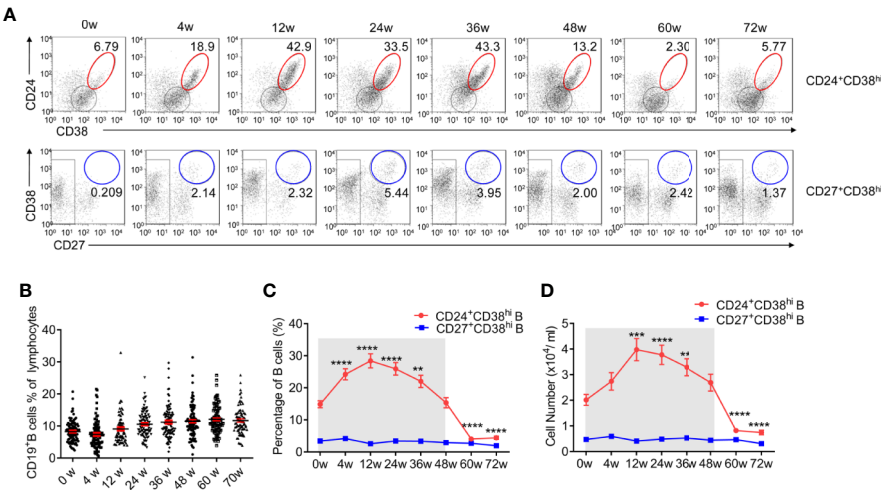

FIGURE 2 | $CD24^+CD38^{hi}$ B cells increase significantly in HBV patients during Peg-IFNα-2b therapy. Naive HBeAg-positive CHB patients were divided into two groups, one receiving Peg-IFNα-2b alone and one receiving Peg-IFNα-2b in combination with adefovir-dipivoxil, in order to simulate patients undergoing treatment with NUCs. Data were quantified from blood samples during routine visits to hepatitis clinics (weeks 0, 4, 12, 24, 36, and 48) and during follow-up (weeks 60 and 72). **(A)** Representative density plots showing CD24 and CD38 expression as well as CD27 and CD38 expression on gated $CD19^+$B cells at each time point during Peg-IFNα-2b therapy. **(B)** Percentage analysis of $CD19^+$B cells from HBV patients at 0-72w during Peg-IFNα-2b therapy. n = 75–90. Unpaired t test. **(C)** Percentage analysis of $CD24^+CD38^{hi}$ B cells and $CD27^+CD38^{hi}$ B cells from HBV patients at 0-72 week during PEG-IFNα-2b therapy. n = 47. Unpaired t test. **(D)** Cell numbers of $CD24^+CD38^{hi}$B cells and $CD27^+CD38^{hi}$ B cells from HBV patients at 0-72w during PEG-IFNα-2b therapy. n = 47. Unpaired t test. Significant differences are shown in **(C, D)** indicating differences compared with the data at 0w. Mean ± SEM, $^{**}P < 0{\cdot}01$, $^{***}P < 0{\cdot}005$, $^{****}P < 0{\cdot}0001$.

cultured with or without Peg-IFNα-2b (25 ng/ml) for 32 h. Much higher levels of IL-10 in PBMC cell supernatants from HBV patients during Peg-IFNα-2b therapy have been identified compared to the other groups (**Figure 3C**). To verify whether there are also other cells in the co-culture might produce IL-10, we have tested PBMC from HBV patients during Peg-IFNa therapy, Compared to non-B cells lymphocytes, including T cells, NK cells, B cells are the main source of IL-10 secreting (**Figure S3**). To uncover which subset is the main source of IL-10 in HBV patient during Peg-IFNα-2b therapy, B cells from freshly isolated PBMC of HBV patients and also healthy controls were analyzed. Data revealed that a higher percentage of $CD24^+CD38^{hi}$ B cells secreting IL-10 compared with other B cell subsets, suggesting the potential of these $CD24^+CD38^{hi}$ B cells to become IL-10-producing $CD24^+CD38^{hi}$ Breg cells (**Figures 3D, E**). To analyze whether PEG-IFNα-2b could induce expansion of these HBV-driven Bregs or prevent their death, we isolated PBMC from CHB patients with PEG-IFNα-2b treatment during 12–24 weeks, and CHB patients without PEG-IFNα-2b treatment. We tested the level of Ki67 expression and the percentage of apoptotic cells in Breg cells. The results showed that PEG-IFNα-2b might induce expansion of these HBV-driven Bregs (**Figures 3F–I**).

To identify whether these Breg cells however release other immunosuppressive cytokines such as IL-4, IL-4 expressions analysis have been done in HBV patient during PEG-IFNα-2b therapy. Our data showed that B cells from these HBV patients did not secret IL-4. In some patients, IL-4 has been identified to secrete from non-B cells but not B cells (**Figure S4**). Increase numbers of immature B cells might be a compensatory mechanism with accelerated emigration from BM or spleen. To demonstrate whether increase numbers of immature B cells is a compensatory mechanism with accelerated emigration from BM or spleen, we tested the circulating levels of BAFF, CXCL12, and CXCL13 of HBV patients at 12–36 weeks after the start of PEG-IFNα-2b therapy by ELISA. It seems CXCL12 has a positive correlation with Breg cells (**Figure S5**).

Patients With Fewer $CD24^+CD38^{hi}$ B Cells Exhibit Improved Therapeutic Effects

As $CD24^+CD38^{hi}$ B cells increased dramatically during Peg-IFNα-2b therapy, we further investigated whether these $CD24^+CD38^{hi}$ B cells are relevant for clinical outcomes. $CD24^+CD38^{hi}$ B cells are found at low frequencies (<5% of B cells) in normal healthy human controls (34). Depending on whether the percentage of $CD24^+CD38^{hi}$ B cells in HBV patients at 72 weeks after the start of PEG-IFNα-2b therapy are higher than that in the normal healthy controls or not, patients were classified into the more $CD24^+CD38^{hi}$ B cell group ($CD24^+CD38^{hi}$ B cells ≥ 5% of B cells) or the fewer $CD24^+CD38^{hi}$ B cell group ($CD24^+CD38^{hi}$ B cell <5% of B cells). These groups were then analyzed for the clinical outcomes of PEG-IFNα-2b therapy. Among all the 81 patients that have tested both $CD24^+CD38^{hi}$ B cells phenotype and HBV related serum analysis, 44.68% percent of patients in the fewer $CD24^+CD38^{hi}$ B cell group underwent HBV seroconversion (HBeAg < 1.0 COI) compared with only 17.6% HBV seroconversion in the more $CD24^+CD38^{hi}$ B cell group (**Figures 4A, B**). Furthermore, we compared HBsAg, HBV DNA and ALT between patients in fewer $CD24^+CD38^{hi}$ B cell group and more $CD24^+CD38^{hi}$ B cell group, and the results indicated that patients in fewer $CD24^+CD38^{hi}$ B cell group may have higher probability to obtain satisfactory therapy results

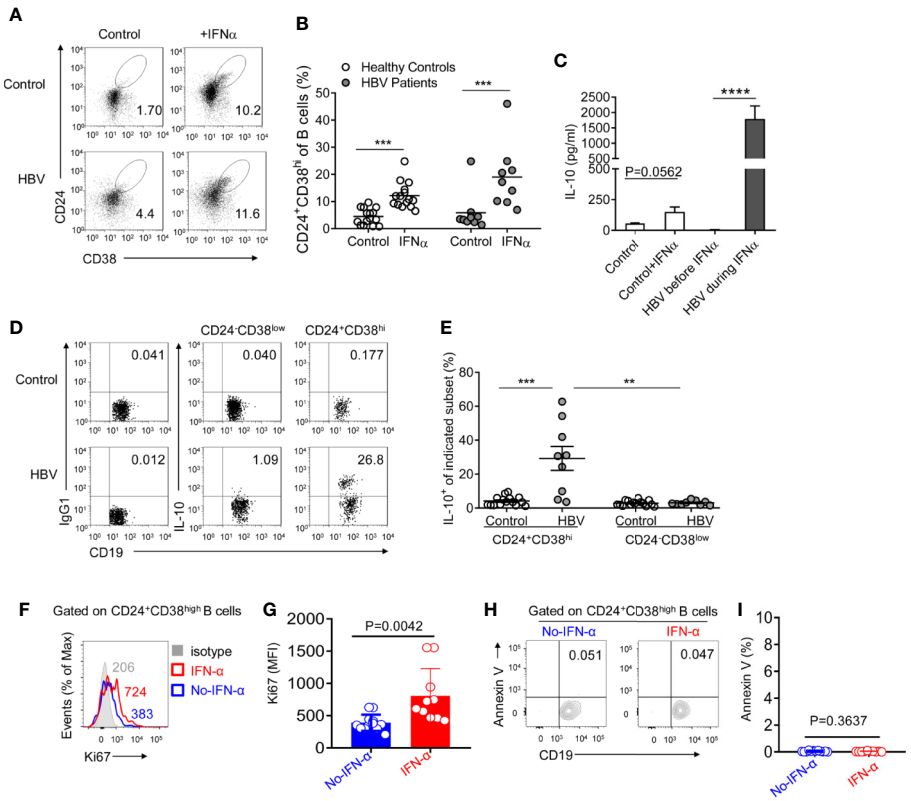

FIGURE 3 | CD24^{+}CD38^{hi} B cells are induced under Peg-IFNα-2b and produce plenty of IL-10. **(A, B)** PBMCs from HBV patients and healthy controls were cultured in complete RPMI medium 1640 with or without human Peg-IFNα-2b (100 ng/ml) for 36h. Representative density plots **(A)** and percentage analysis **(B)** showing CD24 and CD38 expression on gated B cells from HBV patients and healthy controls. n = 15 (healthy controls) and 9 (HBV patients). Paired t test. **(C)** ELISA analysis of IL-10 secretion in cell-free supernatants of cultured PBMCs from HBV patients before or during Peg-IFNα-2b therapy and healthy controls with or without re-stimulation by Peg-IFNα-2b (25 ng/ml) during a 32-h culture. PBMC from HBV patients were collected before PEG-IFNα-2b therapy or at 12-36 weeks after the start of Peg-IFNα-2b therapy. **(D)** Representative density plots and **(E)** percentage analysis of IL-10 expression on gated CD24^{+}*CD38^{hi}* B cells and CD24^{-}CD38^{low} mature B cells from HBV patients and healthy controls. These B cells were from freshly isolated PBMC in HBV patients and healthy controls. After 4 h of stimulation with PMA and ionomycin in the presence of monensin, intracellular flow cytometry staining was done and gated as CD19^{+}CD3^{-} cells. n = 15 (healthy controls) and 9 (HBV patients). Paired t-tests were used for the analysis in subsets from the same patient. Data are presented as Mean ± SEM, $^{**}P < 0{\cdot}01$, $^{***}P < 0{\cdot}005$, $^{****}P < 0{\cdot}0001$. **(F)** Flow cytometry analysis of Ki67 expression on the CD24^{+}CD38^{high} B cells from PBMC of HBV patients without (blue) or with (red) PEG-IFNα-2b therapy for 12-24 weeks. **(G)** Statistics calculated by the MFI of Ki67 from PBMC of HBV patients without (blue, n = 12) or with (red, n = 10) PEG-IFNα-2b therapy for 12-24 weeks. Unpaired t test. $^{**}P < 0.01$; $^{***}P < 0.001$; $^{****}P < 0.0001$. Data are presented as mean ± SD. **(H)** Flow cytometry analysis of Annexin V expression on the CD24^{+}CD38^{high} B cells from PBMC of HBV patients without (blue) or with (red) PEG-IFNα-2b therapy for 12–24 weeks. **(I)** Statistics calculated by the percentage of Annexin V^{+} Breg cells from PBMC of HBV patients without (blue, n = 12) or with (red, n = 10) PEG-IFNα-2b therapy for 12–24 weeks. Unpaired t test. $^{**}P < 0.01$; $^{***}P < 0.001$; $^{****}P < 0.0001$. Data are presented as mean ± SD.

(**Figures 4C–H**). No significant differences between patients from fewer CD24^{+}CD38^{hi} B cell group and more CD24^{+}CD38^{hi} B cell group in HBeAg, HBsAg, HBV DNA, and ALT before Peg-IFNα-2b therapy (**Figure S6**). Thus, our data revealed that CD24^{+}CD38^{hi} B cells have negative correlation with the therapeutic effects.

CD24^{+}CD38^{hi} B Cell-Centered Immunosuppressive Response by Inhibiting Anti-Virus Response

Our previous study has showed that increased NKp30 expression and degranulation on NK cells correlated with clinical outcomes during Peg-IFN-α-2b therapy (29). However, the number of NKp30^{+}NK cell increased for the first 6 month but decreased for the rest of the therapy. Given the close association between CD24^{+}CD38^{hi} B cells and clinical outcomes, the effects of CD24^{+}CD38^{hi} B cells on immune cells function was further examined. To indicate whether the CD24^{+}CD38^{hi} B cells have an inhibitory effect toward T cells and NK cells, high purity of PBMC with or without CD24^{+}CD38^{hi}B cells from HBV patients were sorted and re-stimulated with 50 μg/ml of HBsAg for 72 h. Cytokines were measured by intracellular staining. It has been shown that IFNγ, TNFα and CD107a positive T cells were significantly increased in CD24^{+}CD38^{hi}B cells depleted group (**Figures 5A, B, D**), suggesting CD24^{+}CD38^{hi} B cells impaired anti-virus effect in T cells. It is interesting that IFNγ^{+}NK cells, IFNγ^{+}CD107a^{+}NK cells were also significantly increased in CD24^{+}CD38^{hi}B cells depleted group compared with non-depleted group under the same culture condition (**Figures 5A, C, E**). These data showed that these CD24^{+}CD38^{hi} B cells inhibit the anti-virus immune functions of T cells and NK cells. To further investigate the effect of the CD24^{+}CD38^{hi} B cells on plasma cell function, antibody

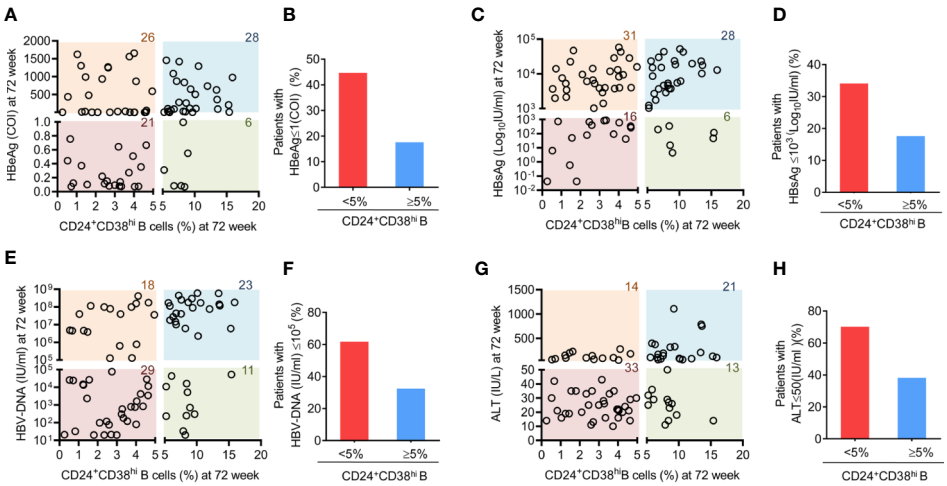

FIGURE 4 | Patients with fewer CD24+CD38hi B cells have an improved therapeutic effect. **(A)** Analysis between the percentage of CD24+CD38hi B cells in patients at 72 week and HBeAg expression at 72 weeks after the start of Peg-IFNα therapy. n = 81. **(B)** Percentage analysis of SRs among patients with fewer CD24+CD38hi B cells (<5%) group and more CD24+CD38hi B cells (≥5%) group. SR (seroconversion responder) was defined as the HBeAg seroconversion (COI < 1.0) at 72 weeks after the start of PEG-IFNα-2b therapy. **(C, E, G)** Analysis between the percentage of CD24+CD38hi B cells in patients at 72 week and HBsAg, HBVDNA and ALT expression at 72 weeks after the start of Peg-IFNα-2b therapy. n = 81. **(D, F, H)** Percentage analysis of patients with lower expression of HBsAg, HBVDNA and ALT expression at 72 weeks after the start of Peg-IFNα-2b therapy in fewer CD24+CD38hi B cells (<5%) group and more CD24+CD38hi B cells (≥5%) group. n = 81. Each circle in the Figure represents the data from a patient. The number marked on each color lump represent the sum number of patients.

secretion were investigated from HBV PBMC stimulated by HBV specific antigens with or without CD24+CD38hiB cells. These data showed that after depleted CD24+CD38hi B cells, HBV PBMC have higher IgG secretion (**Figure 5F**). To verify whether an increased IgG production has correlation with the percentage of CD24+CD38hiB cells, the correlation between CD24+CD38hiB cells and IgG increasing rate after CD24+CD38hiB cells have been analyzed. The IgG increase ratio (IgG in PBMC after CD24+CD38hiB cells depletion/IgG in PBMC before CD24+CD38hiB cells depletion) is positive correlated with the ratio between CD24+CD38hiB cells and whole PBMC from HBV patients (CD24+CD38hiB cells number/PBMC cell number) (**Figure 5G**). These data show that the CD24+CD38hi B cells have an inhibitory effect toward T cells, NK cells and also IgG secretion.

Defective monocyte-derived DC cells constitute a potential reason for the poor therapeutic efficacy of PEG-IFNα-2b (35). As CD64 has been identified to possess the capability to separate conventional DC cells from monocyte-derived DC cells (36), CD64+CD11c+ monocyte-derived DC cells on HBV patients were tested during PEG-IFNα-2b therapy. CD64+CD11c+DC cells were significantly decreased and remained at a very low level during PEG-IFNα-2b therapy, and increased after the PEG-IFNα-2b therapy stopped (**Figures 6A, B**). Combined with the dynamic changes of CD24+CD38hi B cells, the changes of CD64+ Mo-derived DC cells were negatively related to the changes of CD24+ CD38hiB cells during PEG-IFNα-2b therapy (**Figure 6C**). To confirm whether Breg cells have suppression capability of mo-DCs cells, Mo-DC cells were sorted from HBV patients as CD19- CD3-CD11c+HLA-DR+cells and co-cultured with or without sorted Breg cells at 1:1 cell ratio. After cultured 24 h, the important markers CD86 and CD80 were tested. These data showed that Breg can decrease the expression of CD80 and CD86 expression on mo-DC cells and this effected can be blocked by anti-IL-10 antibody (**Figures 6D, E**). To further identify whether the regulatory function of Breg cells toward mo-DC is cell-contact dependent or not, we did the transwell experiment to physically block cell-cell contact between mo-DC and Breg cell. The results showed that breg cells still can re-modulate mo-DC phenotype showing that this regulation is not cell-contact dependent but triggered by the immunosuppressive cytokines (**Figures 6F, G**). Thus, CD24+CD38hi B cells inhibit the functions of anti-virus immune system and result in immune suppression during Peg-IFNα therapy, which confirms that the immunomodulatory effects of PEG-IFNα-2b exist in human.

CD24 Is a Suitable Marker to Target CD24+CD38hi B Cells

Given that CD24+CD38hi B cells are significantly induced during PEG-IFNα-2b therapy, the strategies to selectively manipulate this opposing activity would be prospected to restore immune responses and improved persistent virus therapy. Anti-CD19 and anti-CD20 antibodies have previously been used to deplete B cells (37, 38). However, such treatments deplete all B cells, including CD27+CD38hi precursors of plasma B cells and CD24- mature B cells, which may be beneficial to the immune response. It is important to identify a target marker that is specifically expressed on CD24+CD38hi B cells but not on other B cell subsets and effector cells. We analyzed blood from HBV patients at 12 weeks after the

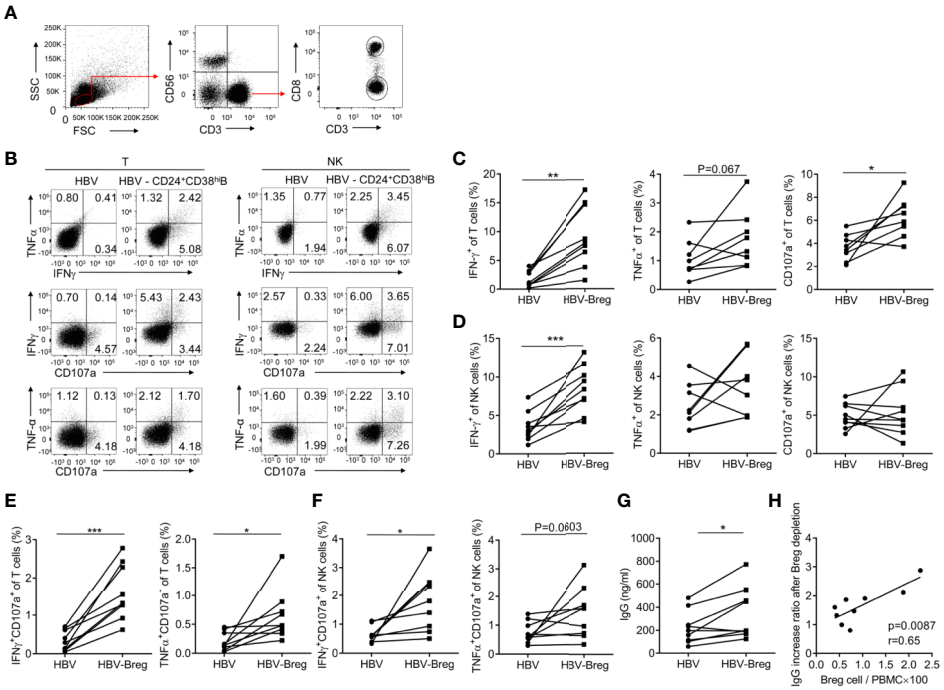

FIGURE 5 | CD24^{+} CD38^{hi} B cells inhibit the anti-virus functions of T cells and NK cells. PBMCs from HBV patients at 12-36 weeks after the start of PEG-IFNα-2b therapy were cultured in 24-well flat-bottom plates at a density of 1–2 × 106 cells per well in a complete RPMI medium 1640 with 10% fetal bovine serum plus streptomycin and penicillin as well as IL-2 (100 U/ml). PBMC from peripheral blood mononuclear cells of CHB patients with or without CD19+CD24+*CD38^{hi}* B cells were sorted and the purity of depleting CD19+CD24+*CD38^{hi}* B cells was determined to be >95% by post-purification FACS analysis. PBMC with or without CD19 +CD24+*CD38^{hi}* B cells were re-stimulated with 50 μg/ml of HBsAg (HyTest, 8HS7ay) for 72 h and cytokines were measured by intracellular staining. **(A)** The gating strategy for analyzing T- and NK cells. **(B)** Representative density plots of IFNγ, TNFα and CD107a expression on gated CD3^{+}T cells or CD56^{+} CD3^{-}NK cells from HBV patients with or without CD24^{+} CD38^{hi}B cells. **(C**, **D)** Percentage analysis of IFNγ, TNFα and CD107a expression on gated CD3^{+}T cells or CD56^{+}NK cells from HBV patients with or without CD24^{+} CD38^{hi}B cells (Breg). n = 8 in each group. Paired t-tests. **(E**, **F)** Percentage analysis of IFNγ^{+}CD107a^{+}, TNFα^{+}CD107a^{+} cells in gated CD3^{+}T cells or CD56^{+}CD3^{-}NK cells from HBV patients with or without CD24^{+} CD38^{hi}B cells (Breg). Paired t test. **(G)** Analysis of IgG secretion from HBV patients with or without CD24^{+}CD38^{hi}B cells. Paired t test. PBMC with or without CD19^{+}CD24^{+}CD38^{hi} B cells (Breg) were re-stimulated with 50 μg/ml of HBsAg for 72 h and cell-free supernatants of cultured PBMCs in each group were measured IgG by ELISA. **(H)** The IgG increase ratio (IgG level in PBMC after Breg depletion/ IgG level in PBMC before Breg depletion) is positive correlated with the ratio between Breg cells and whole PBMC from HBV patients (Breg cell number/PBMC cell number×100). n = 9. Mean ± SEM, *p < 0·05, **P < 0·01, ***P < 0·005.

start of Peg-IFNα-2b therapy when CD24^{+}CD38^{hi} B cells increased to very high levels. The CD24 surface marker was expressed primarily on CD19^{+} B cells but not on other effector immune cells, including T cells and NK cells, making CD24 a suitable target for CD24^{+}CD38^{hi} B cell depletion (**Figures 7A, B**). As approximately 95% of CD24^{+} lymphocytes were B cells (**Figures 7B**), the first thing we do is to sorting CD24^{+} B cells from the lymphocytes of HBV patients using the anti-CD24 antibody to identify whether we could deplete CD24^{+}CD38^{hi} B subsets using anti-CD24 antibody. After depleting CD24^{+}CD38^{hi} B subsets using anti-CD24 antibody, the percentage of CD24^{+}CD38^{hi} B cells decreased whereas other B cell subsets were maintained (**Figure 7C**). To determine whether the anti-CD24 antibody depleted CD24^{+} cells through complement dependent cytotoxicity and to simulate the situation *in vivo*, PBMCs from HBV patients were cultured with guinea pig serum with or without the anti-CD24 antibody. PBMCs co-cultured with the anti-CD24 antibody and the guinea pig serum showed significantly decreased percentages of CD24^{+}CD38^{hi} B cells compared with the guinea pig serum control group and the medium-only control group (**Figures 7D, E**). These results indicated the feasibility of using the anti-CD24 antibody to deplete CD24^{+}CD38^{hi} B cells without harming other B cell subsets, suggesting a promising strategy to improve the therapeutic effects of Peg-IFNα-2b during HBV persistence.

DISCUSSION

PEG-IFNα-2b has been widely applied in many diseases yet yields disappointing therapeutic effects in treating chronic HBV infection. In this report, we have identified that PEG-IFNα-2b therapy may also induce an immunomodulatory effect in chronic HBV patients through dramatically upregulating the CD24^{+}CD38^{hi} B cells, which drive an immunosuppressive program and reduce anti-virus therapeutic effects. The extent to which CD24^{+}CD38^{hi} B cells were retained in a given patient was negatively correlated with therapeutic effects. In this context, CD24 was found to be a suitable marker to target CD24^{+}CD38^{hi} B cells. Given that Type I IFNs exert

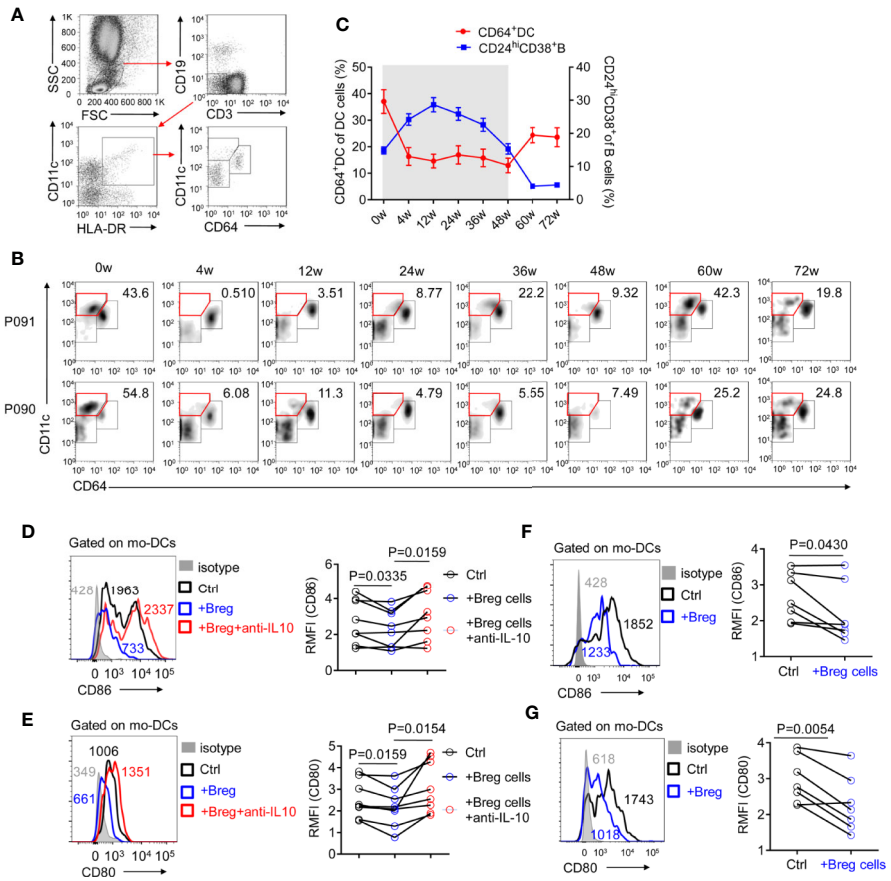

FIGURE 6 | CD24^{+} CD38^{hi} B cells are negatively correlated with monocyte-derived DC cells. **(A)** Representative density plots of the gating strategy used for CD64^{+}DC cells. **(B)** Representative density plots of CD11c and CD64 expressions on gated DC cells from HBV patients at each time point during PEG-IFNα-2b therapy. **(C)** Percentages analysis showing that CD24^{+}CD38^{hi} B cells are negatively correlated with CD64^{+}DC cells. n = 47. Mean ± SEM. **(D–G)** Mo-DCs were cultured in 48-well flat-bottom plates at a density of 0.5-1.0 × 10^{5} cells per well in a complete RPMI medium 1640 (Gibco, Grand Island, NY, U.S.A.) with 10% fetal bovine serum (HyClone, Logan, UT, U.S.A.) plus streptomycin and penicillin. Equal number of Breg cells were then added to the culture wells, with or without 3 μg/ml of anti-IL-10 (biolegend; #501427) for 24 h. **(D, E)** Left: mo-DCs were co-cultured with Breg cells (blue) or with Breg cells and 3 μg/ml of anti-IL-10 (red), stained with CD86 **(D)** or CD80 **(E)**, and analyzed by flow cytometry. Right: The relative mean fluorescence intensity (RMFI) of n = 8 patients are shown. **(F, G)** Left: mo-DCs were co-cultured with Breg cells (blue) in transwell system, stained with CD86 **(C)** or CD80 **(D)**, and analyzed by flow cytometry. Right: The relative mean fluorescence intensity (RMFI) of n = 7 patients are shown. Data were analyzed by two-way ANOVA **(D, E)**, or two-tailed paired Student's t-test **(F, G)**. Data are presented as mean ± SD.

diverse effects on innate and adaptive immune cells and have been widely employed to treat infection with viruses, bacteria, fungi, parasites and tumors (2, 8), the findings presented here are relevant not only for understanding HBV but also in ascertaining the role of immunomodulatory effect induced by the widely used PEG-IFNα-2b therapy.

Although early antiviral effects of IFN-α are critical, the potential immunomodulatory roles of IFNs later in chronic infection could explain paradoxical clinical observations using IFN-α based treatments. For example, IFN-α warrants the survival of the host in the acute phase of infection (39), while persistent IFN-α-induced inflammation may also paradoxically promote microbial evasion during chronic infection (11, 12). IFNα has been reported to lead to the production of immunosuppressive molecules in models of Simian Immunodeficiency Virus (SIV) (39) and LCMV infection (11, 12). In addition, IFNα reduces the responsiveness of macrophages to activation by IFNγ during *Listeria monocytogenes* and *Mycobacterium tuberculosis* infections (40–42). Data presented here confirms the effect of Peg-IFNα therapy to induce immunosuppressive CD24^{+}CD38^{hi} B cells in chronic infection. Interestingly, both the percentage and number of CD24^{+}CD38^{hi} B cells were at high level at 12–24 weeks after the beginning of Peg-IFNα therapy and then decline. This decline of CD24^{+}CD38^{hi} B cells may because long-term high concentrations of IFN-α overexposure. Type I IFN therapy in chronic HCV patients may result in lupus-like symptoms (43). In lupus patients, hyperactivated pDCs fail to induce Breg cells (30). It is possible that the chronic high concentrations of type I IFN is potential to induce autoimmune-like disease rather than generates CD24^{+}CD38^{hi} Breg cell at the late stage of the therapy. The specific mechanism of the Breg decline after long-term stimulation of IFNα is still unknown. It is also important to identify the molecular basis for the antiviral versus immunomodulatory effects of IFN-α to selectively manipulate these opposing activities.

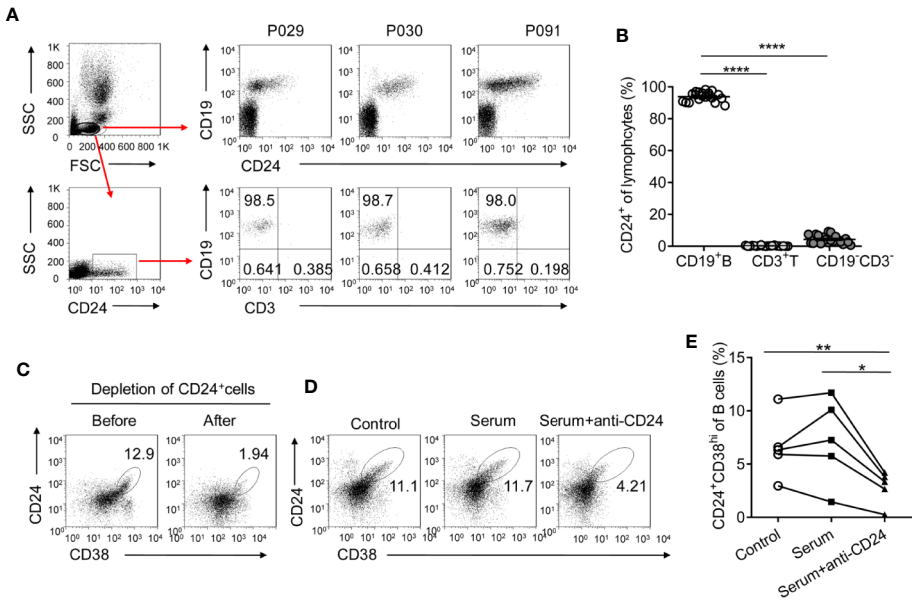

FIGURE 7 | CD24 is a suitable target for CD24^{+}CD38^{hi} B cell depletion. **(A)** Gating strategy and representative density plots of CD19 and CD24 expression on gated lymphocytes from HBV patients at 12 weeks (12w) after the initiation of PEG-IFNα-2b therapy. After gating on CD24^{+} lymphocytes, nearly 95% of cells were CD19^{+}CD3^{-} B cells. **(B)** Percentage analysis of gated CD24^{+} cells belonged to CD19^{+} B, CD3^{+} T cell, and CD19^{-}CD3^{-} other cell populations. n = 20. Paired two-tailed t-tests. **(C)** Representative density plots showing CD24 and CD38 expression on gated lymphocytes from HBV patients before and after CD24^{+} cells were sorted. CD24^{+} cells were sorted using an anti-CD24 antibody (BD Bioscience) and anti-FITC-MicroBeads (MiltenyiBiotec). **(D, E)** Representative density plots and percentage analysis of CD24 and CD38 expression in each group. PBMCs from HBV patients were cultured at a density of 1 × 10^{6} cells per 1 ml with 10 μg of anti-human CD24 antibody and 500 μl of guinea pig serum, with 500 μl of guinea pig serum only, or with 500 μl of complete RPMI medium 1640 (control) for 30min. n = 5. Paired two-tailed t-tests Mean ± SEM, *p < 0·05, **P < 0·01, ****P < 0·0001.

Previous reports have showed CD24 is a potential oncogene and overexpressed in a large variety of human malignancies (44). Many efforts have been done for early intervention about CD24 target in the prevention and treatment of cancer, such as colorectal cancer, pancreatic cancer (45), ovarian cancer (46) and bladder cancer (47). It seems promising that the therapeutic potential of CD24 blockade with monoclonal antibodies, which may promote the phagocytic clearance of CD24^{+} cancer cells both *in vitro* and *in vivo* (20). In this study, CD24^{+}CD38^{hi} B cells was observed along with subsequent negative correlation with monocyte-derived DC cells, NK cells, and T cells functions in HBV patients (**Figures 5** and **6**). It was potential that depleting CD24^{+}B cells using an anti-CD24 antibody would improve Peg-IFNα therapy against the virus *in vivo*. Nevertheless, more evidences about anti-CD24 antibody based on clinical studies are urgently needed.

In conclusion, Peg-IFNα-2b therapy is the most effective HBV therapy and yet is only capable of inducing an HBeAg seroconversion rate of approximately 30%. The study presented here uncovers the mechanism by which a CD24^{+}CD38^{hi} B-centered immunomodulatory response is induced by persistent Peg-IFNα-2b therapy. In addition, we demonstrate possible effective strategies to interrupt the immunosuppressive state using an anti-CD24 antibody. Other approaches which selectively manipulate these opposing activities between immune-activation and immunomodulation may also be possible to increase the anti-viruses immune response.

DATA AVAILABILITY STATEMENT

The original contributions presented in the study are included in the article/**Supplementary Material**. Further inquiries can be directed to the corresponding authors.

ETHICS STATEMENT

The studies involving human participants were reviewed and approved by the local Ethics Board of the First Affiliated Hospital of Anhui Medical University. The patients/participants provided their written informed consent to participate in this study.

AUTHOR CONTRIBUTIONS

BF designed and performed the experiments, analyzed and interpreted the data. DW performed the experiments and assessing outcomes. XS and CG helped to perform the experiments. RS established techniques of FACS and Immunohistochemistry, and interpreted the data. YL and YY generated the random allocation sequence, enrolled participants, collected tissue samples and information from patients. JL supervised the clinical trial and assigned participants to interventions. ZT provided strategic planning, conceived the project, and interpreted some data. HW

supervised the project, provided crucial ideas, and assisted with data interpretation. BF wrote the manuscript with HW. All authors contributed to the article and approved the submitted version.

FUNDING

This work was supported by the Ministry of Science and Technology of China (973 Basic Science Project 2012CB519004), the Natural Science Foundation of China (81330071, 81922028), Anhui Key Program of Medical Scientific Research of China (no.2010A010), and Youth Innovation Promotion Association of Chinese Academy of Sciences (grant 2019442).

SUPPLEMENTARY MATERIAL

The Supplementary Material for this article can be found online at: https://www.frontiersin.org/articles/10.3389/fimmu.2020.591269/full#supplementary-material

REFERENCES

1. Rehermann B. Pathogenesis of chronic viral hepatitis: differential roles of T cells and NK cells. *Nat Med* (2013) 19:859–68. doi: 10.1038/nm.3251
2. McNab F, Mayer-Barber K, Sher A, Wack A, O'Garra A. Type I interferons in infectious disease. *Nat Rev Immunol* (2015) 15:87–103. doi: 10.1038/nri3787
3. Belloni L, Allweiss L, Guerrieri F, Pediconi N, Volz T, Pollicino T, et al. IFN-alpha inhibits HBV transcription and replication in cell culture and in humanized mice by targeting the epigenetic regulation of the nuclear cccDNA minichromosome. *J Clin Invest* (2012) 122:529–37. doi: 10.1172/JCI58847
4. Micco L, Peppa D, Loggi E, Schurich A, Jefferson L, Cursaro C, et al. Differential boosting of innate and adaptive antiviral responses during pegylated-interferon-alpha therapy of chronic hepatitis B. *J Hepatol* (2013) 58:225–33. doi: 10.1016/j.jhep.2012.09.029
5. Schweitzer A, Horn J, Mikolajczyk RT, Krause G, Ott JJ. Estimations of worldwide prevalence of chronic hepatitis B virus infection: a systematic review of data published between 1965 and 2013. *Lancet* (2015) 386:1546–55. doi: 10.1016/S0140-6736(15)61412-X
6. Lau GKK, Piratvisuth T, Luo KX, Marcellin P, Thongsawat S, Cooksley G, et al. Peginterferon alfa-2a, lamivudine, and the combination for HBeAg-positive chronic hepatitis B. *New Engl J Med* (2005) 352:2682–95. doi: 10.1056/Nejmoa043470
7. Janssen HLA, van Zonneveld M, Senturk H, Zeuzem S, Akarca US, Cakaloglu Y, et al. Pegylated interferon alfa-2b alone or in combination with lamivudine for HBeAg-positive chronic hepatitis B: a randomised. *Lancet* (2005) 365:123–9. doi: 10.1016/S0140-6736(05)17701-0
8. Ivashkiv LB, Donlin LT. Regulation of type I interferon responses. *Nat Rev Immunol* (2014) 14:36–49. doi: 10.1038/nri3581
9. Wang BX, Fish EN. The yin and yang of viruses and interferons. *Trends Immunol* (2012) 33:190–7. doi: 10.1016/j.it.2012.01.004
10. Mayer-Barber KD, Yan B. Clash of the Cytokine Titans: counter-regulation of interleukin-1 and type I interferon-mediated inflammatory responses. *Cell Mol Immunol* (2017) 14:22–35. doi: 10.1038/cmi.2016.25
11. Wilson EB, Yamada DH, Elsaesser H, Herskovitz J, Deng JN, Cheng GH, et al. Blockade of Chronic Type I Interferon Signaling to Control Persistent LCMV Infection. *Sci (New York NY* (2013) 340:202–7. doi: 10.1126/science.1235208
12. Teijaro JR, Ng C, Lee AM, Sullivan BM, Sheehan KCF, Welch M, et al. Persistent LCMV Infection Is Controlled by Blockade of Type I Interferon Signaling. *Sci (New York NY* (2013) 340:207–11. doi: 10.1126/science.1235214
13. Moseman EA, Wu T, de la Torre JC, Schwartzberg PL, McGavern DB. Type I interferon suppresses virus-specific B cell responses by modulating CD8+ T cell differentiation. *Sci Immunol* (2016) (4):eaah3565. doi: 10.1126/sciimmunol.aah3565
14. Fallet B, Narr K, Ertuna YI, Remy M, Sommerstein R, Cornille K, et al. Interferon-driven deletion of antiviral B cells at the onset of chronic infection. *Sci Immunol* (2016) 1(4):eaah6817. doi: 10.1126/sciimmunol.aah6817
15. Sammicheli S, Kuka M, Di Lucia P, de Oya NJ, De Giovanni M, Fioravanti J, et al. Inflammatory monocytes hinder antiviral B cell responses. *Sci Immunol* (2016) 1(4):eaah6817. doi: 10.1126/sciimmunol.aah6789
16. Thimme R, Dandri M. Dissecting the divergent effects of interferon-alpha on immune cells: time to rethink combination therapy in chronic hepatitis B? *J Hepatol* (2013) 58:205–9. doi: 10.1016/j.jhep.2012.11.007
17. Aspord C, Bruder Costa J, Jacob MC, Dufeu-Duchesne T, Bertucci I, Pouget N, et al. Remodeling of B-Cell Subsets in Blood during Pegylated IFNalpha-2a Therapy in Patients with Chronic Hepatitis B Infection. *PloS One* (2016) 11:e0156200. doi: 10.1371/journal.pone.0156200
18. Tan AT, Hoang LT, Chin D, Rasmussen E, Lopatin U, Hart S, et al. Reduction of HBV replication prolongs the early immunological response to IFNalpha therapy. *J Hepatol* (2014) 60:54–61. doi: 10.1016/j.jhep.2013.08.020
19. Chen GY, Tang J, Zheng P, Liu Y. CD24 and Siglec-10 selectively repress tissue damage-induced immune responses. *Sci (New York NY* (2009) 323:1722–5. doi: 10.1126/science.1168988
20. Barkal AA, Brewer RE, Markovic M, Kowarsky M, Barkal SA, Zaro BW, et al. CD24 signalling through macrophage Siglec-10 is a target for cancer immunotherapy. *Nature* (2019) 572:392–+. doi: 10.1038/s41586-019-1456-0
21. Mauri C, Bosma A. Immune regulatory function of B cells. *Annu Rev Immunol* (2012) 30:221–41. doi: 10.1146/annurev-immunol-020711-074934
22. Mauri C, Nistala K. Interleukin-35 takes the 'B' line. *Nat Med* (2014) 20:580–1. doi: 10.1038/nm.3594
23. Blair PA, Norena LY, Flores-Borja F, Rawlings DJ, Isenberg DA, Ehrenstein MR, et al. CD19(+)CD24(hi)CD38(hi) B cells exhibit regulatory capacity in healthy individuals but are functionally impaired in systemic Lupus Erythematosus patients. *Immunity* (2010) 32:129–40. doi: 10.1016/j.immuni.2009.11.009
24. Flores-Borja F, Bosma A, Ng D, Reddy V, Ehrenstein MR, Isenberg DA, et al. CD19+CD24hiCD38hi B cells maintain regulatory T cells while limiting TH1 and TH17 differentiation. *Sci Trans Med* (2013) 5:173ra123. doi: 10.1126/scitranslmed.3005407
25. Yoshizaki A, Miyagaki T, DiLillo DJ, Matsushita T, Horikawa M, Kountikov EI, et al. Regulatory B cells control T-cell autoimmunity through IL-21-dependent cognate interactions. *Nature* (2012) 491:264–8. doi: 10.1038/nature11501
26. Li DL, Zheng LH, Jin L, Zhou YS, Li HY, Fu JL, et al. CD24 Polymorphisms Affect Risk and Progression of Chronic Hepatitis B Virus Infection. *Hepatology* (2009) 50:735–42. doi: 10.1002/hep.23047
27. Das A, Ellis G, Pallant C, Lopes AR, Khanna P, Peppa D, et al. IL-10-Producing Regulatory B Cells in the Pathogenesis of Chronic Hepatitis B Virus Infection. *J Immunol* (2012) 189:3925–35. doi: 10.4049/jimmunol.1103139
28. European Association For The Study Of The Liver. EASL clinical practice guidelines: Management of chronic hepatitis B virus infection. *J Hepatol* (2012) 57:167–85. doi: 10.1016/j.jhep.2012.02.010
29. Shen X, Fu B, Liu Y, Guo C, Ye Y, Sun R, et al. NKp30(+) NK cells are associated with HBV control during pegylated-interferon-alpha-2b therapy of chronic hepatitis B. *Sci Rep* (2016) 6:38778. doi: 10.1038/srep38778
30. Menon M, Blair PA, Isenberg DA, Mauri C. A Regulatory Feedback between Plasmacytoid Dendritic Cells and Regulatory B Cells Is Aberrant in Systemic Lupus Erythematosus. *Immunity* (2016) 44:683–97. doi: 10.1016/j.immuni.2016.02.012
31. Rosser EC, Blair PA, Mauri C. Cellular targets of regulatory B cell-mediated suppression. *Mol Immunol* (2014) 62:296–304. doi: 10.1016/j.molimm.2014.01.014
32. Sarvaria A, Madrigal JA, Saudemont A. B cell regulation in cancer and anti-tumor immunity. *Cell Mol Immunol* (2017) 14:662–74. doi: 10.1038/cmi.2017.35

33. Tang X, Zhang S, Peng Q, Ling L, Shi H, Liu Y, et al. Sustained IFN-I stimulation impairs MAIT cell responses to bacteria by inducing IL-10 during chronic HIV-1 infection. *Sci Adv* (2020) 6:eaaz0374. doi: 10.1126/sciadv.aaz0374
34. Saidova A, Bublin M, Schmidthaler K, Fajgelj V, Klinglmueller F, Spittler A, et al. Evidence for a Role of TGF-beta-Activated Kinase 1 and MAP3K7 Binding Protein 3 in Peanut-Specific T-Cell Responses. *Int Arch Allergy Immunol* (2019) 179(1):10–6. doi: 10.1159/000496438
35. Roy S, Goswami S, Bose A, Goswami KK, Sarkar K, Chakraborty K, et al. Defective dendritic cell generation from monocytes is a potential reason for poor therapeutic efficacy of interferon alpha 2b (IFN alpha 2b) in cervical cancer. *Transl Res* (2011) 158:200–13. doi: 10.1016/j.trsl.2011.03.003
36. Langlet C, Tamoutounour S, Henri S, Luche H, Ardouin L, Gregoire C, et al. CD64 Expression Distinguishes Monocyte-Derived and Conventional Dendritic Cells and Reveals Their Distinct Role during Intramuscular Immunization. *J Immunol* (2012) 188:1751–60. doi: 10.4049/jimmunol.1102744
37. Maloney DG. Anti-CD20 Antibody Therapy for B-Cell Lymphomas. *New Engl J Med* (2012) 366:2008–16. doi: 10.1056/NEJMct1114348
38. Maude SL, Frey N, Shaw PA, Aplenc R, Barrett DM, Bunin NJ, et al. Chimeric Antigen Receptor T Cells for Sustained Remissions in Leukemia. *New Engl J Med* (2014) 371:1507–17. doi: 10.1056/Nejmoa1407222
39. Sandler NG, Bosinger SE, Estes JD, Zhu RT, Tharp GK, Boritz E, et al. Type I interferon responses in rhesus macaques prevent SIV infection and slow disease progression. *Nature* (2014) 511:601–5. doi: 10.1038/nature13554
40. Auerbuch V, Brockstedt DG, Meyer-Morse N, O'Riordan M, Portnoy DA. Mice lacking the type I interferon receptor are resistant to Listeria monocytogenes. *J Exp Med* (2004) 200:527–33. doi: 10.1084/jem.20040976
41. Carrero JA, Calderon B, Unanue ER. Type I interferon sensitizes lymphocytes to apoptosis and reduces resistance to Listeria infection. *J Exp Med* (2004) 200:535–40. doi: 10.1084/jem.20040769
42. O'Connell RM, Saha SK, Vaidya SA, Bruhn KW, Miranda GA, Zarnegar B, et al. Type I interferon production enhances susceptibility to Listeria monocytogenes infection. *J Exp Med* (2004) 200:437–45. doi: 10.1084/jem.20040712
43. Wilson LE, Widman D, Dikman SH, Gorevic PD. Autoimmune disease complicating antiviral therapy for hepatitis C virus infection. *Semin Arthritis Rheumatism* (2002) 32:163–73. doi: 10.1053/sarh.2002.37277
44. Ni YH, Zhao X, Wang W. CD24, A Review of its Role in Tumor Diagnosis, Progression and Therapy. *Curr Gene Ther* (2020) 20:109–26. doi: 10.2174/1566523220666200623170738
45. Sagiv E, Starr A, Rozovski U, Khosravi R, Altevogt P, Wang T, et al. Targeting CD24 for treatment of colorectal and pancreatic cancer by monoclonal antibodies or small interfering RNA. *Cancer Res* (2008) 68:2803–12. doi: 10.1158/0008-5472.CAN-07-6463
46. Kleinmanns K, Fosse V, Davidson B, de Jalon EG, Tenstad O, Bjorge L, et al. CD24-targeted intraoperative fluorescence image-guided surgery leads to improved cytoreduction of ovarian cancer in a preclinical orthotopic surgical model. *EBioMedicine* (2020) 56:102783. doi: 10.1016/j.ebiom.2020.102783
47. Overdevest JB, Thomas S, Kristiansen G, Hansel DE, Smith SC, Theodorescu D, et al. CD24 offers a therapeutic target for control of bladder cancer metastasis based on a requirement for lung colonization. *Cancer Res* (2011) 71:3802–11. doi: 10.1158/0008-5472.CAN-11-0519

Conflict of Interest: The authors declare that the research was conducted in the absence of any commercial or financial relationships that could be construed as a potential conflict of interest.

frontiers in Immunology

MINI REVIEW
published: 12 February 2021
doi: 10.3389/fimmu.2021.637910

Dual Antiretroviral Therapy—All Quiet Beneath the Surface?

Berend J. van Welzen, Patrick G. A. Oomen and Andy I. M. Hoepelman*

Department of Internal Medicine and Infectious Diseases, University Medical Centre Utrecht, Utrecht, Netherlands

Infection with the human immunodeficiency virus (HIV) is characterized by progressive depletion of CD4+ lymphocytes cells as a result of chronic immune activation. Next to the decreases in the number of CD4+ cells which leads to opportunistic infections, HIV-related immune activation is associated with several prevalent comorbidities in the HIV-positive population such as cardiovascular and bone disease. Traditionally, combination antiretroviral therapy (cART) consists of three drugs with activity against HIV and is highly effective in diminishing the degree of immune activation. Over the years, questions were raised whether virological suppression could also be achieved with fewer antiretroviral drugs, i.e., dual- or even monotherapy. This is an intriguing question considering the fact that antiretroviral drugs should be used lifelong and their use could also induce cardiovascular and bone disease. Therefore, the equilibrium between drug-induced toxicity and immune activation related comorbidity is delicate. Recently, two large clinical trials evaluating two-drug cART showed non-inferiority with respect to virological outcomes when compared to triple-drug regimens. This led to adoption of dual antiretroviral therapy in current HIV treatment guidelines. However, it is largely unknown whether dual therapy is also able to suppress immune activation to the same degree as triple therapy. This poses a risk for an imbalance in the delicate equilibrium. This mini review gives an overview of the current available evidence concerning immune activation in the setting of cART with less than three antiretroviral drugs.

Keywords: HIV, antiretroviral therapy, immune activation, dual therapy, cART

OPEN ACCESS

Edited by:
Caroline Petitdemange, Institut Pasteur, France

Reviewed by:
Giulia Carla Marchetti, University of Milan, Italy
Claudia Cicala, National Institutes of Health (NIH), United States

****Correspondence:***
Berend J. van Welzen
b.j.vanwelzen@umcutrecht.nl

Specialty section:
This article was submitted to Viral Immunology, a section of the journal Frontiers in Immunology

Received: *04 December 2020*
Accepted: *22 January 2021*
Published: *12 February 2021*

Citation:
van Welzen BJ, Oomen PGA and Hoepelman AIM (2021) Dual Antiretroviral Therapy—All Quiet Beneath the Surface? Front. Immunol. 12:637910. doi: 10.3389/fimmu.2021.637910

INTRODUCTION

In 1983, a group of French virologists identified a T-lymphotropic retrovirus—now called the human immunodeficiency virus (HIV)—as causative agent of the acquired immunodeficiency syndrome (AIDS) (1). The clinical picture of AIDS is characterized by opportunistic infections such as pneumocystis jirovecii pneumonia and candida esophagitis (2). These opportunistic infections are the result of a severe depletion of CD4+ lymphocytes, which are central mediators of immune response, coordinating both cellular and humoral responses against infections (3).

Although HIV uses the CD4 receptor to gain access to target cells, the depletion of CD4+ lymphocytes is only partly due to a direct cytolytic effect of HIV (4). The current leading hypothesis states that chronic HIV infection is accompanied by a hyperactive inflammatory state in which there is an increased turnover of activated naïve T-cells, eventually leading to T-cell depletion by means of apoptosis (5, 6). Immune activation is driven by both the HIV viremia and bacterial translocation from the gut (7, 8) and is associated with numerous comorbidities in HIV-positive

patients (9–11). Therefore, immune activation is not only considered to be a predictor for the risk for progression to AIDS but also an important cause of HIV-related comorbidity (12, 13).

Till the end of 1995, the nucleoside reverse transcriptase inhibitors (NRTIs) were the only available antiretroviral agents – targeting reverse transcriptase, an enzyme essential for HIV replication (14). Unfortunately, NRTI mono- or dual therapy had only temporary effects due to rapid resistance development and virological failure (15). However, the perspective for people living with HIV changed dramatically as result of the introduction of a new class of drugs: the protease inhibitors (PIs) combined with a pharmacological booster (16). Combination antiretroviral therapy (cART)—drug regimens consisting of multiple antiretroviral classes—diminished the risk of resistance development and led to an spectacular increase in life expectancy (17). Over the years, the development of antiretroviral drugs took off and several other third drug ("anchors") classes—such as the non-nucleoside reverse transcriptase inhibitors (NNRTIs) and integrase strand transfer inhibitors (INSTIs) —were introduced (18, 19). Nowadays, triple antiretroviral therapy is highly successful with most patients reaching the main treatment goal of an "undetectable" viral load—defined as <50 copies/ml of HIV RNA when measured by polymerase chain reaction—and with the mortality risk declining (20, 21). Current immunoassays however, due to improvement of sensitivity, are able to detect viral loads that are below 50 copies/ml but can still be quantified: so-called "residual viremia." A small group of patients—"elite controllers"—are able to maintain an undetectable viral load in absence of antiretroviral drugs (22). However, these patients display significant immune activation when compared to HIV-negative controls (23, 24) and this is linked to an increased risk for cardiovascular disease in these patients (25). These findings emphasize the importance of immune activation in the pathophysiology of HIV-related comorbidity. In the modern antiretroviral era, there is no role for in depth monitoring of immune activation as these markers are generally considered to reduce simultaneously with the viral load, albeit they do not show complete normalization (26).

In the recent years, questions were raised whether there is a need to hold on to the mantra that cART should always consist of three antiretroviral drugs (27). Indeed, the current available agents have high genetic barriers for resistance and the life-long use of multiple drugs could lead to long-term toxicity. Numerous studies evaluated the efficacy of mono- or dual antiretroviral therapy (28–36) and some of these two-drug regimens gained ground in the current treatment guidelines (37, 38). However, there are concerns as to whether the two-drug regimens suppress the degree of HIV-related immune activation enough (39). A rebound in immune activation which occurs beneath the surface despite virological suppression could be harmful. In the end, the development of comorbidity in HIV is the net result of potential harmful effects of antiretroviral drugs vs. the degree in which these drugs suppress the virus and the related immune activation (**Figure 1**). Therefore, any change in the current standard of care might lead to disruption of this equilibrium. In this mini review, we will discuss the best current available data on immune activation in non-traditional cART regimens.

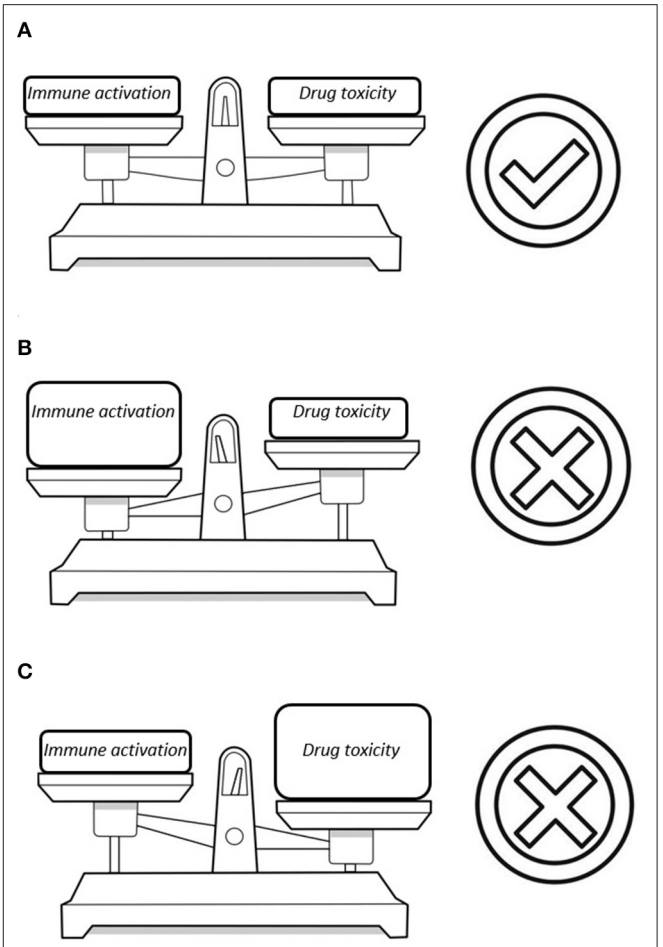

FIGURE 1 | Three possible scenarios in the equilibrium between drug toxicity and damage from HIV-related immune activation: **(A)** A perfect balance between these factors with the smallest possible risk for comorbidity. **(B)** The reduction in the number of antiretroviral drugs diminishes the risk for drug toxicity but a flare in immune activation could lead to HIV-associated comorbidity. **(C)** Multiple antiretroviral drugs are able to fully suppress the virus but this poses a significant risk for cART-associated toxicity.

IMMUNOLOGICAL MARKERS IN HIV-INFECTION

The test battery for HIV-related immune activation is extending ever since the recognition of the hyperactive inflammatory status. The available markers can be divided into soluble and cellular markers for inflammation and immune activation, with some being more readily available than others (40) (**Table 1**).

The soluble markers are easy to measure in a large number of test facilities and can subdivided into markers of inflammation, coagulation and microbial translocation. The most commonly used inflammation markers include high-sensitivity c-reactive protein (hs-CRP) and plasma interleukin-6 (IL-6), both considered to be extremely sensitive for systemic inflammation (41, 42) and associated with HIV-related mortality (43–46). Other soluble markers include tumor necrosis factor

TABLE 1 | An overview of the most important soluble and cellular markers for HIV-associated immune activation that are reported in current literature.

Markers	Biological and clinical characteristics	Ref.
Soluble markers		
Tumor necrosis factor α	- Produced by macrophages and T-cells - Used for cell signaling and cytokine stimulation - Associated with disease progression	47
Interferon-γ (IFN-γ)	- Produced by T-helper cells, CD8+ lymphocytes and NK cells - Induction of several pro-inflammatory cytokines and anti-viral characteristics - Especially active during acute HIV infection	52
Interleukin-6	- Released by monocytes and macrophages - Elevated during chronic stage of infection - Associated with disease progression, especially CVD	46
D-dimer	- Fibrin degradation product -Associated with disease progression, especially CVD	56
Soluble CD14	- Marker of monocyte activation and indirect marker of microbial translocation - Associated with disease progression	58
LPS	- Endotoxin, a marker for microbial translocation - Associated with disease progression	50
Bacterial 16s DNA	- Marker for microbial translocation - Prognostic value in HIV is unknown	50
Soluble CD27	- Marker of T-cel activation - Rapid increase in case of viral rebound	53
Soluble CD40 ligand	- Marker for platelet activation - Implicated to contribute to innate and adaptive immune dysfunction - Prognostic value in HIV is unknown	54
Cellular markers		
HLA-DR+	- MHC class II receptor on CD4+ and CD8+ lymphocytes - Upregulated in response to signaling and being a marker for T-cell activation	60
CD38+	- Glycoprotein expressed on lymphocytes and macrophages - Upregulation mediated by IFN- γ and LPS - Considered as a T cell activation marker	61
Ki67+	- Nuclear antigen being a marker for cell proliferation. Present in all cells during mitosis, including T lymphocytes	7
PD-1 co-stimulatory receptor	- Regulating T-cell response - High levels are considered to be result of T-cell exhaustion	63
Annexin-V+	- Marker for apoptosis	62

For parameters predictive of disease progression, it is not further specified whether this includes declining CD4+ cell counts or clinical AIDS-defining events. CVD, cardiovascular disease; LPS, lipopolysaccharide; Ref, reference; PD-1, programmed death-1.

alpha (TNF-α), interferon-γ, neopterin, mitochondrial DNA (mtDNA), β2-microglobulin, soluble CD27, and soluble CD40 ligand (47–54). The latter two are markers of T-cell activation. The main example for coagulation markers is D-dimer, which levels increase in several pro-inflammatory states and high levels being associated with cardiovascular disease (55, 56). The last group of soluble markers are surrogates of microbial translocation. These include bacterial lipopolysaccharide (LPS)—present in gram-negative bacteria—and bacterial DNA (16s ribosomal RNA subunit) (57). In addition, plasma soluble CD14 (sCD14) and soluble CD163 (sCD163)—products of monocyte activation—are also considered to be a markers for impaired mucosal integrity (58). None of these markers are exclusively found in the setting of HIV-infection (59).

Although the soluble markers can be assessed relatively easy, their reflection of inflammation and immune activation is considered to be less specific than the cellular activation markers in the setting of HIV (40). Assessing cellular markers is more labor-intensive, requiring the isolation of peripheral blood mononuclear cells and performing flow cytometry. For the cellular activity, some well-defined markers are available: CD38+/HLA-DR+ expression on lymphocytes for T-cell activation (60, 61), Ki-67 positivity for proliferation (7), annexin-V for apoptosis (62) and programmed-death-1 co-stimulatory receptor for T-cell exhaustion (63). The CD4+ lymphocyte counts and CD4/CD8 ratio are more readily available but these changes occur more slowly and are therefore kept out of this review (64).

RESIDUAL IMMUNE ACTIVATION DURING TRIPLE-DRUG THERAPY

The initiation of cART results in fast virological suppression and significant reduction in immune activation in most patients, subsequently leading to CD4+ cell recovery (65). However,

antiretroviral therapy does not normalize the HIV-induced inflammatory response with some residual immune activation persisting (66). Studies describing the effect of cART on the soluble markers report inconsistent outcomes (43, 67, 68), but especially the degree of T-cell activation rarely normalizes (69).

The clinical impact of this residual immune activation is largely unknown but, for example, the higher incidence of cardiovascular disease among HIV-positive individuals despite cART and the elite controllers implies clinical significance. The reason for residual immune activation in the setting of virological suppression has not been fully elucidated, but it is suggested that low-grade HIV replication in certain anatomical or cellular compartments is the main driver (70). These "sanctuary sites" are compartments, such as the central nervous system (CNS), gastrointestinal tract and lymph nodes, where cART reaches insufficient drug levels to completely suppress local viral replication and subsequent low-grade inflammation. The variable—and often suboptimal—drug penetration in lymph nodes (71), mucosal tissues (72) and the CNS (73) have been demonstrated in several papers. Besides these sites, persisting microbial translocation and the presence of viral coinfections are associated with persistent immune activation (74, 75). There is no consistent evidence that favors one anchor over another with respect to the degree of immune activation (76–78). Studies evaluating whether therapy intensification with additional anchors results in further suppression of immune activation, are conflicting (79–81).

IMMUNE ACTIVATION AND VIROLOGICAL EFFICACY IN MONOTHERAPY

After the introduction of cART in the mid-nineties, monotherapy for HIV-infection was abandoned because of virological inferiority. However, the idea of antiretroviral monotherapy made a comeback after the introduction of agents with a high antiviral potency and a high genetic barrier for resistance. Such a mono-drug regimen have significant advantages, including less side-effects and pill burden. The hypothesis that one powerful antiretroviral drug would be sufficient to maintain virological suppression, led to several trials comparing the virological efficacy of PI or INSTI monotherapy to traditional three-drug regimens (28, 30–33). Unfortunately, monotherapy with these drugs seem to result in higher rates of virological rebound when compared to cART. Therefore, current guidelines recommend against monotherapy as maintenance therapy in treatment-experienced patients with a undetectable viral load (37, 38). However, from a pathophysiological viewpoint it is interesting to have a closer look at the impact of monotherapy on immune activation markers.

One study that provides an insight in the mechanisms of immune activation rebound was published by BenMarzoek-Hidalgo et al. (82). In their paper, the authors describe the relationship between microbial translocation and viremia with immune activation in 71 patients receiving boosted darunavir monotherapy. In this cohort, only 26% of the patients maintained a viral load below 20 copies/ml, while 16 patients displayed virological failure (2 consecutive HIV-RNA levels exceeding 200 copies/mL). The remaining patients had (transitory) episodes of a detectable viral load during follow-up yet without meeting the criteria for virological failure. Although separate analysis per outcome group found that only patients with virological failure showed an increase in T-cell activation, it became clear that time with viral suppression was inversely correlated with T-cell activation (percentage HLA-DR+-CD38+ lymphocytes in both CD8+ and CD4+ lymphocyte subsets) at a follow-up of 24 months. In this study, there was a clear correlation between the viral load and the percentage of activated CD4+ and CD8+ lymphocytes. In addition, another study showed that intensification with INSTI (raltegravir) to PI monotherapy (either darunavir/ritonavir or lopinavir/ritonavir), resulted in a decline in the degree of residual viremia and a decrease in the percentage of activated CD8+ lymphocytes (83).

There are several studies that evaluated the non-specific soluble markers in highly selected populations (84–86), while other studies evaluated the cellular markers. The smallest study of Merlini et al. did not find a difference in T-cell activation between baseline and after 96 weeks for both patients receiving PI monotherapy with atazanavir ($n = 18$) and those receiving atazanavir-based cART [$n = 22$ (87)]. However, patients on monotherapy were more likely to display increased T-cell apoptosis than patients receiving three drugs. Torres et al. evaluated the markers for monocyte activation in 40 patients receiving PI monotherapy (either lopinavir/ritonavir or darunavir/ritonavir) and 20 patients on PI-based cART for at least 48 weeks and an undetectable viral load (88). This cross-sectional analysis showed that patients on monotherapy display higher levels of monocyte activation—CD14+CD16-CD163+ cells and sCD14 levels—when compared to those receiving standard therapy. The last, most well-designed, study of Petrara et al. described the dynamics of the HIV-1 viral reservoir and T- and B-cell activation markers at 48 and 96 weeks of therapy in patients switched to PI mono-therapy ($n = 32$) and patients continuing PI-based triple therapy ($n = 32$) (89). It should be noted that ten percent of the patients in the monotherapy group experienced virological failure compared to zero patients receiving cART. Furthermore, the authors observed a significant increase of T- and B-cell activation in patients receiving one drug, while these markers remained low in patients on cART.

So the best available evidence suggests that a switch to monotherapy is associated with an increase of T-cell activation and apoptosis markers, while soluble markers data are more inconsistent. These observations seem to be the result of (low-grade) viral rebound. The increased risk for virological failure and the suggestion of a rebound in immune activation, disqualify monotherapy as maintenance therapy.

IMMUNE ACTIVATION IN DUAL THERAPY

Antiretroviral monotherapy is not likely to play a role in the near future, so the current focus is on the effectiveness of dual therapy. In fact, two-drug regimens have already gained a

position in current HIV treatment guidelines; in 2018 a single-tablet regimen (STR) consisting of dolutegravir (INSTI) and rilpivirine (NNRTI) was introduced and in 2020 a STR with dolutegravir and lamivudine (NRTI) was registered as a first-line treatment option. Currently, there are several large trials that support the use of these two STRs in clinical practice: SWORD-1&2 (36), GEMINI-1&2 (35), and TANGO study (29).

The SWORD-1&2 studies evaluated the efficacy, safety and tolerability of dolutegravir/rilpivirine as maintenance therapy in patients with an undetectable viral load. Patients were randomized to either dual therapy ($n = 512$) vs. continuing triple-drug therapy ($n = 516$). After 148 weeks, the data showed that dolutegravir/rilpivirine was non-inferior with respect to virological outcomes to triple therapy (90). In the first paper evaluating this regimen, there was a brief mention on the dynamics of the inflammatory and cardiovascular markers in both groups. The authors state there was no consistent pattern of change from baseline to week 48 or differentiation between both groups in the following markers: IL-6, CRP, sCD14, sCD163, and D-dimer. Exact data were not shown and specific T-cell markers were not evaluated. The use of STR dolutegravir/lamivudine for treatment-experienced patients is supported by the TANGO study (29). In this study, 743 patients with an undetectable viral load were enrolled and were randomized to either dolutegravir/lamivudine or a triple drug regimen (two NRTIs as backbone and an anchor from one of major groups). In this study, dual therapy was also found to be non-inferior in maintaining virological suppression compared to triple therapy. In the study cohort, the authors describe a significantly smaller decrease in serum IL-6 levels in patients on dual therapy, but for sCD14 there was an exact opposite trend. The dynamics of D-dimer, hs-CRP and sCD163 were comparable for both groups. In the GEMINI-1&2 studies, it was shown that dolutegravir/lamivudine was virologically non-inferior to INSTI-based cART in treatment-naïve patients, but there were no data on immune activation (35).

As mentioned above, the registration trials briefly addressed the concerns regarding HIV-related immune activation in dual therapy. In general, the results were inconsistent and focused on soluble markers. Fortunately, a few other studies described this issue more extensively although not for the registered treatment regimens. In the study of Concepción Romero-Sánchez et al. 58 patients, having an undetectable viral load for at least 6 months, were switched to a two-drug regimen consisting of a boosted PI and Maraviroc, a HIV entry inhibitor; there was no control group in this study (91). The authors observed no change in β2-microglobuline, sCD40L, sCD14, hsCRP, D-dimer, and mtDNA at 24 (±12) weeks of follow-up when compared to baseline. However, for patients with high baseline levels of β2-microglobuline, sCD40L and hsCRP there was marked decrease at final follow-up. Two other papers evaluated the differences between patients on dual antiretroviral therapy vs. those on triple therapy. Belmonti et al. describe the dynamics of IL-6, CRP, sCD14 and D-dimer from baseline to 48 weeks (92). A switch to dual therapy ($n = 70$ boosted atazanavir plus lamivudine) did not result in a significant changes in the markers mentioned above and did not differ from the markers in patients continuing triple therapy ($n = 69$). In addition, Vallejo et al. published a cross-sectional pilot study evaluating a broad spectrum of inflammation and immune activation biomarkers (interferon-gamma-induced protein 10, hs-CRP, sCD14, D-dimer, interferon-γ, TNF-α and IL-4) in patients on dual therapy vs. those continuing triple therapy (93). The dual therapy group consisted of 13 patients that were evaluated at 24 weeks after switch and 36 patients at 48 weeks, the control group included 26 patients. The authors found the lowest IL-6 and sCD14 levels in the patients on dual therapy for 48 weeks; the other markers were not different from the triple-therapy groups. Other studies worth to mention were performed by Quiros-Roldan et al. and Mussini et al. but these papers reported less commonly used parameters such as CD4/CD8 ratio, platelet-to-lymphocyte and neutrophil-to-lymphocyte ratio (94, 95).

In the studies presented above, the switch from triple to dual therapy is not accompanied with a consistent increase in the soluble inflammatory markers. However, in contrast to the monotherapy studies none of the papers assessed T-cell activation, proliferation or apoptosis markers. At this moment, there is sufficient evidence to support certain two drug regimens as treatment options for HIV in terms of virological efficacy but robust data on effects on immune activation are lacking.

CONCLUSIONS

In this review we presented the current best available evidence on the dynamics in immune activation in non-traditional antiretroviral therapy. We found that the most well-designed studies show that monotherapy is associated with insufficient suppression of T-cell activation when compared to traditional triple therapy; there might be an association with a detectable viral load. Furthermore, we observed that the dynamics of T-cell activation, proliferation and apoptosis do not necessarily follow the trends observed in the soluble markers, confirming earlier observations.

Especially the last finding is of great importance when we have a look at the data presented for the two-drug regimens, which now have become a reasonable option in modern antiretroviral therapy. The fact that the large registration trials for treatment-experienced patients included inflammatory makers as secondary outcomes is laudable; it emphasizes the recognition of the importance of this outcome. In contrast, the founders of these studies missed an excellent opportunity for a thorough assessment of the immune activation markers in dual therapy. In SWORD-1&2 and TANGO, the soluble markers are only briefly mentioned or the authors stay away from firm statements. Furthermore, the studies only included soluble markers but there are no data on T-cell activation. As we learned from the monotherapy data, especially those markers might display abnormalities. The fact that T-cell activation is correlated with a detectable viremia and that the two-drug regimens show virological non-inferiority with the 50 copies/ml threshold, is reassuring. However, as we are not aware of the degree of residual viremia in the two-drug regimens, a

negative impact of dual drug therapy cannot be excluded at this moment.

Based on the presented studies, we believe there is insufficient evidence that mono- and dual therapy are non-inferior to triple therapy when it comes to the suppression of HIV-related immune activation. Although dual therapy is an attractive option as it diminishes the life-time exposure to antiretroviral drugs with potential toxicity, the impact of a rebound in immune activation are currently unknown. We need to keep the potential negative impact of cART in an equilibrium with the degree of immune activation, as a misbalance could lead to HIV or cART-related comorbidity. There is a need for well-designed, longitudinal studies with a proper, unbiased patients selection evaluating both the soluble and the cellular immune activation markers. Only such studies can tell us whether everything is quiet beneath the surface in dual therapy.

AUTHOR CONTRIBUTIONS

BW and PO: draft of the manuscript and editing. AH: critical review and editing. All authors contributed to the article and approved the submitted version.

REFERENCES

1. Barre-Sinoussi F, Chermann JC, Rey F, Nugeyre MT, Chamaret S, Gruest J, et al. Isolation of a T-lymphotropic retrovirus from a patient at risk for acquired immune deficiency syndrome (AIDS). *Science.* (1983) 220:868–71. doi: 10.1126/science.6189183
2. Deeks SG, Overbaugh J, Phillips A, Buchbinder S. HIV infection. *Nat Rev Dis Prim.* (2015) 1:15035. doi: 10.1038/nrdp.2015.35
3. Swain SL, McKinstry KK, Strutt TM. Expanding roles for CD4$^+$ T cells in immunity to viruses. *Nat Rev Immunol.* (2012) 12:136–48. doi: 10.1038/nri3152
4. Vidya Vijayan KK, Karthigeyan KP, Tripathi SP, Hanna LE. Pathophysiology of CD4+ T-cell depletion in HIV-1 and HIV-2 infections. *Front Immunol.* (2017) 8:580. doi: 10.3389/fimmu.2017.00580
5. Sodora DL, Silvestri G. Immune activation and AIDS pathogenesis. *AIDS.* (2008) 22:439–46. doi: 10.1097/QAD.0b013e3282f2dbe7
6. Yates A, Stark J, Klein N, Antia R, Callard R. Understanding the slow depletion of memory CD4+ T cells in HIV infection. *PLoS Med.* (2007) 4:e177. doi: 10.1371/journal.pmed.0040177
7. Orendi JM, Bloem AC, Borleffs JC, Wijnholds FJ, de Vos NM, Nottet HS, et al. Activation and cell cycle antigens in CD4+ and CD8+ T cells correlate with plasma human immunodeficiency virus (HIV-1) RNA level in HIV-1 infection. *J Infect Dis.* (1998) 178:1279–87. doi: 10.1086/314451
8. Brenchley JM, Price DA, Schacker TW, Asher TE, Silvestri G, Rao S, et al. Microbial translocation is a cause of systemic immune activation in chronic HIV infection. *Nat Med.* (2006) 12:1365–71. doi: 10.1038/nm1511
9. Teer E, Joseph DE, Driescher N, Nell TA, Dominick L, Midgley N, et al. HIV and cardiovascular diseases risk: exploring the interplay between T-cell activation, coagulation, monocyte subsets, and lipid subclass alterations. *Am J Physiol Heart Circ Physiol.* (2019) 316:H1146–57. doi: 10.1152/ajpheart.00797.2018
10. Goh SSL, Lai PSM, Tan ATB, Ponnampalavanar S. Reduced bone mineral density in human immunodeficiency virus-infected individuals: a meta-analysis of its prevalence and risk factors. *Osteoporos Int.* (2018) 29:595–613. doi: 10.1007/s00198-017-4305-8
11. van Welzen BJ, Mudrikova T, El Idrissi A, Hoepelman AIM, Arends JE. A review of non-alcoholic fatty liver disease in HIV-infected patients: the next big thing? *Infect Dis Ther.* (2019) 8:33–50. doi: 10.1007/s40121-018-0229-7
12. Giorgi J V, Liu Z, Hultin LE, Cumberland WG, Hennessey K, Detels R. Elevated levels of CD38+ CD8+ T cells in HIV infection add to the prognostic value of low CD4+ T cell levels: results of 6 years of follow-up. The Los Angeles Center, Multicenter AIDS Cohort Study. *J Acquir Immune Defic Syndr.* (1993) 6:904–12.
13. Hazenberg MD, Otto SA, van Benthem BHB, Roos MTL, Coutinho RA, Lange JMA, et al. Persistent immune activation in HIV-1 infection is associated with progression to AIDS. *AIDS.* (2003) 17:1881–8. doi: 10.1097/00002030-200309050-00006
14. Fischl MA, Richman DD, Grieco MH, Gottlieb MS, Volberding PA, Laskin OL, et al. The efficacy of azidothymidine (AZT) in the treatment of patients with AIDS and AIDS-related complex. A double-blind, placebo-controlled trial. *N Engl J Med.* (1987) 317:185–91. doi: 10.1056/NEJM198707233170401
15. Lorenzi P, Opravil M, Hirschel B, Chave JP, Furrer HJ, Sax H, et al. Impact of drug resistance mutations on virologic response to salvage therapy. Swiss HIV Cohort Study. *AIDS.* (1999) 13:F17–21. doi: 10.1097/00002030-199902040-00001
16. Kitchen VS, Skinner C, Ariyoshi K, Lane EA, Duncan IB, Burckhardt J, et al. Safety and activity of saquinavir in HIV infection. *Lancet.* (1995) 345:952–5. doi: 10.1016/S0140-6736(95)90699-1
17. Gulick RM, Mellors JW, Havlir D, Eron JJ, Gonzalez C, McMahon D, et al. Treatment with indinavir, zidovudine, and lamivudine in adults with human immunodeficiency virus infection and prior antiretroviral therapy. *N Engl J Med.* (1997) 337:734–9. doi: 10.1056/NEJM199709113371102
18. Vazquez E. Nevirapine approval expands combo possibilities–and HIV suppression. *Posit Aware.* (1996) 7:9.
19. Markowitz M, Nguyen B-Y, Gotuzzo E, Mendo F, Ratanasuwan W, Kovacs C, et al. Rapid and durable antiretroviral effect of the HIV-1 integrase inhibitor raltegravir as part of combination therapy in treatment-naive patients with HIV-1 infection: results of a 48-week controlled study. *J Acquir Immune Defic Syndr.* (2007) 46:125–33. doi: 10.1097/QAI.0b013e318157131c
20. van Sighem AI, Wit F, Boyd A, Smit C, Matser A, Reiss P. *Monitoring Report 2019. Human Immunodeficiency Virus (HIV) Infection in the Netherlands.* Amsterdam: Stichting HIV Monitoring (2019).
21. Smith CJ, Ryom L, Weber R, Morlat P, Pradier C, Reiss P, et al. Trends in underlying causes of death in people with HIV from 1999 to 2011 (D:A:D): a multicohort collaboration. *Lancet.* (2014) 384:241–8. doi: 10.1016/S0140-6736(14)60604-8
22. Gebara NY, El Kamari V, Rizk N. HIV-1 elite controllers: an immunovirological review and clinical perspectives. *J Virus Erad.* (2019) 5:163–6. doi: 10.1016/S2055-6640(20)30046-7
23. Hunt PW, Brenchley J, Sinclair E, McCune JM, Roland M, Page-Shafer K, et al. Relationship between T cell activation and CD4+ T cell count in HIV-seropositive individuals with undetectable plasma HIV RNA levels in the absence of therapy. *J Infect Dis.* (2008) 197:126–33. doi: 10.1086/524143
24. Prabhu VM, Singh AK, Padwal V, Nagar V, Patil P, Patel V. Monocyte based correlates of immune activation and viremia in HIV-Infected long-term non-progressors. *Front Immunol.* (2019) 10:2849. doi: 10.3389/fimmu.2019.02849
25. Crowell TA, Hatano H. Clinical outcomes and antiretroviral therapy in "elite" controllers: a review of the literature. *J Virus Erad.* (2015) 1:72–7. doi: 10.1016/S2055-6640(20)30488-X
26. Gandhi RT, McMahon DK, Bosch RJ, Lalama CM, Cyktor JC, Macatangay BJ, et al. Levels of HIV-1 persistence on antiretroviral therapy are not associated with markers of inflammation or activation. *PLoS Pathog.* (2017) 13:e1006285. doi: 10.1371/journal.ppat.1006285
27. Moreno S, Perno CF, Mallon PW, Behrens G, Corbeau P, Routy J-P, et al. Two-drug vs. three-drug combinations for HIV-1: do we have enough data to make the switch? *HIV Med.* (2019) 20 (Suppl. 4):2–12. doi: 10.1111/hiv.12716
28. Wijting I, Rokx C, Boucher C, van Kampen J, Pas S, de Vries-Sluijs T, et al. Dolutegravir as maintenance monotherapy for HIV (DOMONO): a phase 2, randomised non-inferiority trial. *Lancet HIV.* (2017) 4:e547–54. doi: 10.1016/S2352-3018(17)30152-2
29. van Wyk J. *Switching to DTG/3TC Fixed-Dose Combination (FDC) is Non-inferior to Continuing a TAF-Based Regimen in Maintaining Virological Suppression Through 48 Weeks (TANGO Study).* (2019). Mexico City: IAS.

30. Hocqueloux L, Raffi F, Prazuck T, Bernard L, Sunder S, Esnault J-L, et al. Dolutegravir monotherapy vs. dolutegravir/abacavir/lamivudine for virologically suppressed people living with chronic human immunodeficiency virus infection: the randomized noninferiority MONotherapy of TiviCAY trial. *Clin Infect Dis.* (2019) 69:1498–505. doi: 10.1093/cid/ciy1132
31. Braun DL, Turk T, Tschumi F, Grube C, Hampel B, Depmeier C, et al. Noninferiority of simplified dolutegravir monotherapy compared to continued combination antiretroviral therapy that was initiated during primary human immunodeficiency virus infection: a randomized, controlled, multisite, open-label, noninferiority trial. *Clin Infect Dis.* (2019) 69:1489–97. doi: 10.1093/cid/ciy1131
32. Seang S, Schneider L, Nguyen T, Lê MP, Soulie C, Calin R, et al. Darunavir/ritonavir monotherapy at a low dose (600/100 mg/day) in HIV-1-infected individuals with suppressed HIV viraemia. *J Antimicrob Chemother.* (2018) 73:490–3. doi: 10.1093/jac/dkx417
33. Galli L, Spagnuolo V, Bigoloni A, D'Arminio Monforte A, Montella F, Antinori A, et al. Atazanavir/ritonavir monotherapy: 96 week efficacy, safety and bone mineral density from the MODAt randomized trial. *J Antimicrob Chemother.* (2016) 71:1637–42. doi: 10.1093/jac/dkw031
34. Swindells S, Andrade-Villanueva J-F, Richmond GJ, Rizzardini G, Baumgarten A, Masiá M, et al. Long-acting cabotegravir and rilpivirine for maintenance of HIV-1 suppression. *N Engl J Med.* (2020) 382:1112–23. doi: 10.1056/NEJMoa1904398
35. Cahn P, Madero JS, Arribas JR, Antinori A, Ortiz R, Clarke AE, et al. Durable efficacy of dolutegravir plus lamivudine in antiretroviral treatment-naive adults with HIV-1 infection: 96-week results from the GEMINI-1 and GEMINI-2 randomized clinical trials. *J Acquir Immune Defic Syndr.* (2020) 83:310–8. doi: 10.1097/QAI.0000000000002275
36. Aboud M, Orkin C, Podzamczer D, Bogner JR, Baker D, Khuong-Josses M-A, et al. Efficacy and safety of dolutegravir-rilpivirine for maintenance of virological suppression in adults with HIV-1: 100-week data from the randomised, open-label, phase 3 SWORD-1 and SWORD-2 studies. *Lancet HIV.* (2019) 6:e576–87. doi: 10.1016/S2352-3018(19)30149-3
37. European AIDS Clinical Society (EACS). *Guidelines. Version 10.0 November 2019.* (2019). Available online at: https://www.eacsociety.org/files/2019_guidelines-10.0_final.pdf (accessed December 1, 2020).
38. *Panel on Antiretroviral Guidelines for Adults Adolescents. Guidelines for the Use of Antiretroviral Agents in Adults Adolescents With HIV*. Department of Health and Human Services. Available online at: http://aidsinfo.nih.gov/contentfiles/lvguidelines/ (accessed December 1, 2020).
39. Serrano-Villar S, Moreno S. Changes in inflammatory biomarkers in SWORD-1 and SWORD-2 studies. *Lancet HIV.* (2020) 7:e158. doi: 10.1016/S2352-3018(20)30028-X
40. Nixon DE, Landay AL. Biomarkers of immune dysfunction in HIV. *Curr Opin HIV AIDS.* (2010) 5:498–503. doi: 10.1097/COH.0b013e32833ed6f4
41. Kaur S, Bansal Y, Kumar R, Bansal G. A panoramic review of IL-6: structure, pathophysiological roles and inhibitors. *Bioorg Med Chem.* (2020) 28:115327. doi: 10.1016/j.bmc.2020.115327
42. Pepys MB, Baltz ML. Acute phase proteins with special reference to C-reactive protein and related proteins (pentaxins) and serum amyloid A protein. *Adv Immunol.* (1983) 34:141–212. doi: 10.1016/S0065-2776(08)60379-X
43. Baker J V, Neuhaus J, Duprez D, Kuller LH, Tracy R, Belloso WH, et al. Changes in inflammatory and coagulation biomarkers: a randomized comparison of immediate vs. deferred antiretroviral therapy in patients with HIV infection. *J Acquir Immune Defic Syndr.* (2011) 56:36–43. doi: 10.1097/QAI.0b013e3181f7f61a
44. Neuhaus J, Jacobs DRJ, Baker JV, Calmy A, Duprez D, La Rosa A, et al. Markers of inflammation, coagulation, and renal function are elevated in adults with HIV infection. *J Infect Dis.* (2010) 201:1788–95. doi: 10.1086/652749
45. Kalayjian RC, Machekano RN, Rizk N, Robbins GK, Gandhi RT, Rodriguez BA, et al. Pretreatment levels of soluble cellular receptors and interleukin-6 are associated with HIV disease progression in subjects treated with highly active antiretroviral therapy. *J Infect Dis.* (2010) 201:1796–805. doi: 10.1086/652750
46. Kedzierska K, Crowe SM. Cytokines and HIV-1: interactions and clinical implications. *Antivir Chem Chemother.* (2001) 12:133–50. doi: 10.1177/095632020101200301
47. Vaidya SA, Korner C, Sirignano MN, Amero M, Bazner S, Rychert J, et al. Tumor necrosis factor α is associated with viral control and early disease progression in patients with HIV type 1 infection. *J Infect Dis.* (2014) 210:1042–6. doi: 10.1093/infdis/jiu206
48. Hunt PW. HIV and inflammation: mechanisms and consequences. *Curr HIV AIDS Rep.* (2012) 9:139–47. doi: 10.1007/s11904-012-0118-8
49. Cobos Jiménez V, Wit F, Joerink M, Maurer I, Harskamp AM, Schouten J, et al. T-cell activation independently associates with immune senescence in HIV-infected recipients of long-term antiretroviral treatment. *J Infect Dis.* (2016) 214:216–25. doi: 10.1093/infdis/jiw146
50. Nasi M, Pecorini S, De Biasi S, Digaetano M, Chester J, Aramini B, et al. Short communication: circulating mitochondrial DNA and lipopolysaccharide-binding protein but not bacterial DNA are increased in acute human immunodeficiency virus infection. *AIDS Res Hum Retroviruses.* (2020) 36:817–20. doi: 10.1089/aid.2020.0098
51. Uysal HK, Sohrabi P, Habip Z, Saribas S, Kocazeybek E, Seyhan F, et al. Neopterin and soluble CD14 levels as indicators of immune activation in cases with indeterminate pattern and true positive HIV-1 infection. *PLoS ONE.* (2016) 11:e0152258. doi: 10.1371/journal.pone.0152258
52. Roff SR, Noon-Song EN, Yamamoto JK. The significance of interferon-γ in HIV-1 pathogenesis, therapy, and prophylaxis. *Front Immunol.* (2014) 4:498. doi: 10.3389/fimmu.2013.00498
53. De Milito A, Aleman S, Marenzi R, Sonnerborg A, Fuchs D, Zazzi M, et al. Plasma levels of soluble CD27: a simple marker to monitor immune activation during potent antiretroviral therapy in HIV-1-infected subjects. *Clin Exp Immunol.* (2002) 127:486–94. doi: 10.1046/j.1365-2249.2002.01786.x
54. Miller EA, Gopal R, Valdes V, Berger JS, Bhardwaj N, O'Brien MP. Soluble CD40 ligand contributes to dendritic cell-mediated T-cell dysfunction in HIV-1 infection. *AIDS.* (2015) 29:1287–96. doi: 10.1097/QAD.0000000000000698
55. Vos AG, Idris NS, Barth RE, Klipstein-Grobusch K, Grobbee DE. Pro-Inflammatory markers in relation to cardiovascular disease in HIV infection. A systematic review. *PLoS ONE.* (2016) 11:e0147484. doi: 10.1371/journal.pone.0147484
56. Borges AH, O'Connor JL, Phillips AN, Baker JV, Vjecha MJ, Losso MH, et al. Factors associated with D-dimer levels in HIV-infected individuals. *PLoS ONE.* (2014) 9:e90978. doi: 10.1371/journal.pone.0090978
57. Sandler NG, Douek DC. Microbial translocation in HIV infection: causes, consequences and treatment opportunities. *Nat Rev Microbiol.* (2012) 10:655–66. doi: 10.1038/nrmicro2848
58. Sandler NG, Wand H, Roque A, Law M, Nason MC, Nixon DE, et al. Plasma levels of soluble CD14 independently predict mortality in HIV infection. *J Infect Dis.* (2011) 203:780–90. doi: 10.1093/infdis/jiq118
59. Dayer E, Dayer JM, Roux-Lombard P. Primer: the practical use of biological markers of rheumatic and systemic inflammatory diseases. *Nat Clin Pract Rheumatol.* (2007) 3:512–20. doi: 10.1038/ncprheum0572
60. Kestens L, Vanham G, Gigase P, Young G, Hannet I, Vanlangendonck F, et al. Expression of activation antigens, HLA-DR and CD38, on CD8 lymphocytes during HIV-1 infection. *AIDS.* (1992) 6:793–7. doi: 10.1097/00002030-199208000-00004
61. Savarino A, Bottarel F, Malavasi F, Dianzani U. Role of CD38 in HIV-1 infection: an epiphenomenon of T-cell activation or an active player in virus/host interactions? *AIDS.* (2000) 14:1079–89. doi: 10.1097/00002030-200006160-00004
62. Niehues T, McCloskey TW, Ndagijimana J, Horneff G, Wahn V, Pahwa S. Apoptosis in T-lymphocyte subsets in human immunodeficiency virus-infected children measured immediately ex vivo and following in vitro activation. *Clin Diagn Lab Immunol.* (2001) 8:74–8. doi: 10.1128/CDLI.8.1.74-78.2001
63. Velu V, Shetty RD, Larsson M, Shankar EM. Role of PD-1 co-inhibitory pathway in HIV infection and potential therapeutic options. *Retrovirology.* (2015) 12:14. doi: 10.1186/s12977-015-0144-x
64. Mussini C, Lorenzini P, Cozzi-Lepri A, Lapadula G, Marchetti G, Nicastri E, et al. CD4/CD8 ratio normalisation and non-AIDS-related events in individuals with HIV who achieve viral load suppression with antiretroviral therapy: an observational cohort study. *Lancet HIV.* (2015) 2:e98–106. doi: 10.1016/S2352-3018(15)00006-5
65. Sereti I, Krebs SJ, Phanuphak N, Fletcher JL, Slike B, Pinyakorn S, et al. Persistent, albeit reduced, chronic inflammation in persons starting antiretroviral therapy in acute HIV infection. *Clin Infect Dis.* (2017) 64:124–31. doi: 10.1093/cid/ciw683

66. Bloch M, John M, Smith D, Rasmussen TA, Wright E. Managing HIV-associated inflammation and ageing in the era of modern ART. *HIV Med.* (2020) 21 (Suppl. 3):2–16. doi: 10.1111/hiv.12952
67. McComsey GA, Kitch D, Daar ES, Tierney C, Jahed NC, Melbourne K, et al. Inflammation markers after randomization to abacavir/lamivudine or tenofovir/emtricitabine with efavirenz or atazanavir/ritonavir. *AIDS.* (2012) 26:1371–85. doi: 10.1097/QAD.0b013e328354f4fb
68. Eastburn A, Scherzer R, Zolopa AR, Benson C, Tracy R, Do T, et al. Association of low level viremia with inflammation and mortality in HIV-infected adults. *PLoS ONE.* (2011) 6:e26320. doi: 10.1371/journal.pone.0026320
69. Robbins GK, Spritzler JG, Chan ES, Asmuth DM, Gandhi RT, Rodriguez BA, et al. Incomplete reconstitution of T cell subsets on combination antiretroviral therapy in the AIDS Clinical Trials Group protocol 384. *Clin Infect Dis.* (2009) 48:350–361. doi: 10.1086/595888
70. Massanella M, Fromentin R, Chomont N. Residual inflammation and viral reservoirs: alliance against an HIV cure. *Curr Opin HIV AIDS.* (2016) 11:234–41. doi: 10.1097/COH.0000000000000230
71. Dyavar SR, Gautam N, Podany AT, Winchester LC, Weinhold JA, Mykris TM, et al. Assessing the lymphoid tissue bioavailability of antiretrovirals in human primary lymphoid endothelial cells and in mice. *J Antimicrob Chemother.* (2019) 74:2974–8. doi: 10.1093/jac/dkz273
72. Thompson CG, Cohen MS, Kashuba ADM. Antiretroviral pharmacology in mucosal tissues. *J Acquir Immune Defic Syndr.* (2013) 63 (Suppl. 2):S240–7. doi: 10.1097/QAI.0b013e3182986ff8
73. Caniglia EC, Cain LE, Justice A, Tate J, Logan R, Sabin C, et al. Antiretroviral penetration into the CNS and incidence of AIDS-defining neurologic conditions. *Neurology.* (2014) 83:134–41. doi: 10.1212/WNL.0000000000000564
74. Cassol E, Malfeld S, Mahasha P, van der Merwe S, Cassol S, Seebregts C, et al. Persistent microbial translocation and immune activation in HIV-1-infected South Africans receiving combination antiretroviral therapy. *J Infect Dis.* (2010) 202:723–33. doi: 10.1086/655229
75. Boulougoura A, Sereti I. HIV infection and immune activation: the role of coinfections. *Curr Opin HIV AIDS.* (2016) 11:191–200. doi: 10.1097/COH.0000000000000241
76. Hileman CO, Kinley B, Scharen-Guivel V, Melbourne K, Szwarcberg J, Robinson J, et al. Differential reduction in monocyte activation and vascular inflammation with integrase inhibitor-based initial antiretroviral therapy among HIV-infected individuals. *J Infect Dis.* (2015) 212:345–54. doi: 10.1093/infdis/jiv004
77. Kelesidis T, Tran TTT, Stein JH, Brown TT, Moser C, Ribaudo HJ, et al. Changes in inflammation and immune activation with atazanavir-, raltegravir-, darunavir-based initial antiviral therapy: ACTG 5260s. *Clin Infect Dis.* (2015) 61:651–60. doi: 10.1093/cid/civ327
78. Martínez E, D'Albuquerque PM, Llibre JM, Gutierrez F, Podzamczer D, Antela A, et al. Changes in cardiovascular biomarkers in HIV-infected patients switching from ritonavir-boosted protease inhibitors to raltegravir. *AIDS.* (2012) 26:2315–26. doi: 10.1097/QAD.0b013e328359f29c
79. van Lelyveld SFL, Drylewicz J, Krikke M, Veel EM, Otto SA, Richter C, et al. Maraviroc intensification of cART in patients with suboptimal immunological recovery: a 48-week, placebo-controlled randomized trial. *PLoS ONE.* (2015) 10:e0132430. doi: 10.1371/journal.pone.0132430
80. Kim CJ, Rousseau R, Huibner S, Kovacs C, Benko E, Shahabi K, et al. Impact of intensified antiretroviral therapy during early HIV infection on gut immunology and inflammatory blood biomarkers. *AIDS.* (2017) 31:1529–34. doi: 10.1097/QAD.0000000000001515
81. Llibre JM, Buzón MJ, Massanella M, Esteve A, Dahl V, Puertas MC, et al. Treatment intensification with raltegravir in subjects with sustained HIV-1 viraemia suppression: a randomized 48-week study. *Antivir Ther.* (2012) 17:355–64. doi: 10.3851/IMP1917
82. BenMarzouk-Hidalgo OJ, Torres-Cornejo A, Gutiérrez-Valencia A, Ruiz-Valderas R, Viciana P, López-Cortés LF. Differential effects of viremia and microbial translocation on immune activation in HIV-infected patients throughout ritonavir-boosted darunavir monotherapy. *Medicine.* (2015) 94:e781. doi: 10.1097/MD.0000000000000781
83. Puertas MC, Gómez-Mora E, Santos JR, Moltó J, Urrea V, Morón-López S, et al. Impact of intensification with raltegravir on HIV-1-infected individuals receiving monotherapy with boosted PIs. *J Antimicrob Chemother.* (2018) 73:1940–8. doi: 10.1093/jac/dky106
84. Arenas-Pinto A, Milinkovic A, Peppa D, McKendry A, Maini M, Gilson R. Systemic inflammation and residual viraemia in HIV-positive adults on protease inhibitor monotherapy: a cross-sectional study. *BMC Infect Dis.* (2015) 15:138. doi: 10.1186/s12879-015-0889-9
85. Arribas J, Hill A, Xi N, van Delft Y, Moecklinghoff C. Interleukin-6 and C-reactive protein levels after 3 years of treatment with darunavir/ritonavir monotherapy or darunavir/ritonavir + two nucleoside reverse transcriptase inhibitors in the MONET trial. *J Antimicrob Chemother.* (2012) 67:1804–6. doi: 10.1093/jac/dks102
86. Estébanez M, Stella-Ascariz N, Mingorance J, Pérez-Valero I, Bernardino JI, Zamora FX, et al. Inflammatory, procoagulant markers and HIV residual viremia in patients receiving protease inhibitor monotherapy or triple drug therapy: a cross-sectional study. *BMC Infect Dis.* (2014) 14:379. doi: 10.1186/1471-2334-14-379
87. Merlini E, Galli L, Tincati C, Cannizzo ES, Galli A, Gianotti N, et al. Immune activation, inflammation and HIV DNA after 96 weeks of ATV/r monotherapy: a MODAt substudy. *Antivir Ther.* (2018) 23:633–7. doi: 10.3851/IMP3234
88. Torres B, Guardo AC, Leal L, Leon A, Lucero C, Alvarez-Martinez MJ, et al. Protease inhibitor monotherapy is associated with a higher level of monocyte activation, bacterial translocation and inflammation. *J Int AIDS Soc.* (2014) 17:19246. doi: 10.7448/IAS.17.1.19246
89. Petrara MR, Cattelan AM, Sasset L, Freguja R, Carmona F, Sanavia S, et al. Impact of monotherapy on HIV-1 reservoir, immune activation, and co-infection with Epstein-Barr virus. *PLoS ONE.* (2017) 12:e0185128. doi: 10.1371/journal.pone.0185128
90. van Wyk J, Orkin C, Rubio R, Bogner J, Baker D, Khuong-Josses M-A, et al. Brief report: durable suppression and low rate of virologic failure 3 years after switch to dolutegravir + rilpivirine 2-drug regimen: 148-week results from the SWORD-1 and SWORD-2 randomized clinical trials. *J Acquir Immune Defic Syndr.* (2020) 85:325–30. doi: 10.1097/QAI.0000000000002449
91. Romero-Sánchez MC, Alvarez-Ríos AI, Bernal-Morell E, Genebat M, Vera F, Benhnia MR-E-I, et al. Maintenance of virologic efficacy and decrease in levels of β2-microglobulin, soluble CD40L and soluble CD14 after switching previously treated HIV-infected patients to an NRTI-sparing dual therapy. *Antiviral Res.* (2014) 111:26–32. doi: 10.1016/j.antiviral.2014.08.011
92. Belmonti S, Lombardi F, Quiros-Roldan E, Latini A, Castagna A, Borghetti A, et al. Systemic inflammation markers after simplification to atazanavir/ritonavir plus lamivudine in virologically suppressed HIV-1-infected patients: ATLAS-M substudy. *J Antimicrob Chemother.* (2018) 73:1949–54. doi: 10.1093/jac/dky125
93. Vallejo A, Molano M, Monsalvo-Hernando M, Hernández-Walias F, Fontecha-Ortega M, Casado JL. Switching to dual antiretroviral regimens is associated with improvement or no changes in activation and inflammation markers in virologically suppressed HIV-1-infected patients: the TRILOBITHE pilot study. *HIV Med.* (2019) 20:555–60. doi: 10.1111/hiv.12749
94. Quiros-Roldan E, Magro P, Raffetti E, Izzo I, Borghetti A, Lombardi F, et al. Biochemical and inflammatory modifications after switching to dual antiretroviral therapy in HIV-infected patients in Italy: a multicenter retrospective cohort study from 2007 to 2015. *BMC Infect Dis.* (2018) 18:285. doi: 10.1186/s12879-018-3198-2
95. Mussini C, Lorenzini P, Cozzi-Lepri A, Marchetti G, Rusconi S, Gori A, et al. Switching to dual/monotherapy determines an increase in CD8+ in HIV-infected individuals: an observational cohort study. *BMC Med.* (2018) 16:79. doi: 10.1186/s12916-018-1046-2

Conflict of Interest: The authors declare that the research was conducted in the absence of any commercial or financial relationships that could be construed as a potential conflict of interest.

frontiers in Immunology

ORIGINAL RESEARCH
published: 26 February 2021
doi: 10.3389/fimmu.2021.639291

Long-Term Suppressive cART Is Not Sufficient to Restore Intestinal Permeability and Gut Microbiota Compositional Changes

*Giuseppe Ancona[1†‡], Esther Merlini[1†‡], Camilla Tincati[1], Alessandra Barassi[2], Andrea Calcagno[3], Matteo Augello[1], Valeria Bono[1], Francesca Bai[1], Elvira S. Cannizzo[1], Antonella d'Arminio Monforte[1] and Giulia Marchetti[1]**

[1] Clinic of Infectious Diseases, Department of Health Sciences, University of Milan, Azienda Socio Sanitaria Territoriale Santi Paolo e Carlo, Milan, Italy, [2] Biochemistry Laboratory, Department of Health Sciences, University of Milan, Azienda Socio Sanitaria Territoriale Santi Paolo e Carlo, Milan, Italy, [3] Unit of Infectious Diseases, Department of Medical Sciences, University of Turin, Turin, Italy

Background: We explored the long-term effects of cART on markers of gut damage, microbial translocation, and paired gut/blood microbiota composition, with a focus on the role exerted by different drug classes.

Methods: We enrolled 41 cART naïve HIV-infected subjects, undergoing blood and fecal sampling prior to cART (T0) and after 12 (T12) and 24 (T24) months of therapy. Fifteen HIV-uninfected individuals were enrolled as controls. We analyzed: (i) T-cell homeostasis (flow cytometry); (ii) microbial translocation (sCD14, EndoCab, 16S rDNA); (iii) intestinal permeability and damage markers (LAC/MAN, I-FABP, fecal calprotectin); (iv) plasma and fecal microbiota composition (alpha- and beta-diversity, relative abundance); (v) functional metagenome predictions (PICRUSt).

Results: Twelve and twenty four-month successful cART resulted in a rise in EndoCAb ($p = 0.0001$) and I-FABP ($p = 0.039$) vis-à-vis stable 16S rDNA, sCD14, calprotectin and LAC/MAN, along with reduced immune activation in the periphery. Furthermore, cART did not lead to substantial modifications of microbial composition in both plasma and feces and metabolic metagenome predictions. The stratification according to cART regimens revealed a feeble effect on microbiota composition in patients on NNRTI-based or INSTI-based regimens, but not PI-based regimens.

Conclusions: We hereby show that 24 months of viro-immunological effective cART, while containing peripheral hyperactivation, exerts only minor effects on the gastrointestinal tract. Persistent alteration of plasma markers indicative of gut structural and functional impairment seemingly parallels enduring fecal dysbiosis, irrespective of drug classes, with no effect on metabolic metagenome predictions.

Keywords: dysbiosis, cART initiation, intestinal damage, microbial translocation, gut health

OPEN ACCESS

Edited by:
Nicholas Funderburg, The Ohio State University, United States

Reviewed by:
Ivan Vujkovic-Cvijin, National Institutes of Health (NIH), United States
Sergio Serrano-Villar, Hospital Universitario Ramón y Cajal, Spain

***Correspondence:**
Giulia Marchetti
giulia.marchetti@unimi.it

† These authors have contributed equally to this work

‡ Present address:
Esther Merlini, Gilead Sciences Srl, Milan, Italy
Giuseppe Ancona, Infectious Diseases Unit, Fondazione IRCCS Ca' Granda Ospedale Maggiore Policlinico, Milan, Italy

Specialty section:
This article was submitted to Viral Immunology, a section of the journal Frontiers in Immunology

Received: *08 December 2020*
Accepted: *04 February 2021*
Published: *26 February 2021*

Citation:
Ancona G, Merlini E, Tincati C, Barassi A, Calcagno A, Augello M, Bono V, Bai F, Cannizzo ES, d'Arminio Monforte A and Marchetti G (2021) Long-Term Suppressive cART Is Not Sufficient to Restore Intestinal Permeability and Gut Microbiota Compositional Changes. Front. Immunol. 12:639291. doi: 10.3389/fimmu.2021.639291

BACKGROUND

HIV-infected individuals harbor a distinct gut microbiota (1–5) known to associate with immune activation (6–8), immune status (9–12), antiretroviral treatment (13, 14) and sexual orientation (15, 16). Despite the increasing recognition of the gut microbiome involvement in HIV pathogenesis (17–20), findings and interpretation of literature studies diverge quite significantly, due to differences in cohort size, sampling, lack of adjustment for confounding factors, such as sexual practice, age, and diet (13, 15).

One of the most consistent alterations described in untreated HIV infection is the dramatic subversion of the *Bacteroidetes* and *Proteobacteria* phyla, with, respectively, an unbalanced *Prevotella/Bacteroides* species ratio and enrichment in *Enterobacteriaceae* (19, 21–23). The increased abundance of gut-resident bacteria which are capable of directly driving inflammation in the host represents a reasonable mechanistic link between HIV-associated dysbiosis and high systemic immune activation in the natural history of disease (22).

Suppressive combination antiretroviral therapy (cART) appears to have a limited effect on the restoration of gut microbiota (1, 3, 12, 14, 23–27). Indeed, although gut microbial composition of cART-treated individuals is different from that of untreated subjects, the former also display a microbial community structure distinct from that reported in the HIV-uninfected population (3, 26, 28). These findings allow for the speculation that enduring gut dysbiosis may contribute to the pathogenesis of residual clinical disease in the course of cART. In addition, antiretroviral compounds *per se* could further promote dysbiosis (29) as well as impact on microbial translocation, inflammation/immune activation and the gut epithelial barrier damage (23, 24).

While focusing on a detailed definition of gut microbiota in HIV infection, literature studies have overlooked the possible role of blood microbiota, translocated from the gastrointestinal tract to the systemic circulation, in promoting inflammation and non-communicable diseases in HIV-infected subjects.

A previous report from our group demonstrated a polymicrobic flora in the blood of HIV-infected subjects with inadequate immune recovery on cART (30), raising the question of whether blood microbiota merely reflects the microbial composition in the gut or actively contributes to HIV pathogenesis. In keeping with this observation, recent studies have demonstrated a role of blood microbiota in the onset of diabetes and athero-thrombotic disease in the general population (31, 32), possibly confirming a role of blood dysbiosis in non-AIDS related co-morbidities (33).

In the attempt to shed light onto the mechanisms underlying gut dysbiosis, gastrointestinal damage, microbial translocation and systemic inflammation in the course of effective treatment, we conducted a longitudinal analysis of the microbial composition in paired blood and gut samples of HIV-infected subjects introducing cART and studied its association with microbial translocation, gastrointestinal damage and gut/systemic inflammation parameters.

MATERIALS AND METHODS

Study Population

HIV-positive, adult, antiretroviral-naïve subjects were consecutively enrolled at the Clinic of Infectious Diseases, Department of Health Sciences, University of Milan—ASST Santi Paolo e Carlo, Milan, after providing written, informed consent in accordance with the Declaration of Helsinki. The Institutional Review Board at the ASST Santi Paolo e Carlo specifically approved the study. Individuals with either signs/symptoms of gastrointestinal diseases were excluded from the study. Study subjects underwent paired blood and fecal sampling prior to cART (T0) and after 12 (T12) and 24 (T24) months of therapy. HIV-uninfected individuals were enrolled as controls.

T-Cell Immune Phenotypes

Lymphocyte surface phenotypes were evaluated by flow cytometry on fresh peripheral blood (FACSCanto II; BD Italy). We evaluated activation (CD45R0/CD38), naïve (CD45RA), and memory (CD45R0) subsets and IL-7 receptor (CD127) on CD4 and CD8 T-cells. Samples were stained with the following fluorochrome-labeled antibodies: L/D V500, CD4 PE-Cy7, CD8 PerCPCy5.5, CD38-FITC, CD45R0-PE, CD45RA-FITC, CD127-PE (BD Bioscience). The gating strategy used is presented in **Supplementary Figure 1**.

The following combinations were used: LD/CD8/CD38/CD45R0, LD/CD8/CD4/CD127, and LD/CD4/CD8/CD45RA/CD45R0. FACSDiva 6.1.3 software was used to analyze data.

Microbial Translocation Markers

Plasma sCD14 and Endotoxin Core Antibodies (EndoCab) were measured by ELISA (R&D systems), in accordance with the manufacturer's instructions. Samples were diluted 1000X and 200X, respectively. The total amount of 16S rDNA present in the samples was measured by qPCR in triplicate and normalized using a plasmid-based standard scale (Vaiomer SAS, Labége, France).

Urinary Lactulose-Mannitol Fractional Excretion Ratio (LAC/MAN) and Intestinal Fatty Acid Binding Protein (I-FABP)

Participants were asked to fast the night before and to collect morning urine before drinking a sugar probe solution containing 5 g lactulose and 2 g mannitol. Urine was collected for 5 h following administration of the double sugar solution and participants did not eat or drink (with the exception of water) until the end of the 5-h collection. The total volume of urine was recorded and a 30 mL aliquot of chlorhexidine-preserved (0.236 mg/mL of urine; Sigma Chemical, St Louis, MO, USA) was frozen and stored for High Performance Liquid Chromatography analysis of lactulose and mannitol (Dionex MA-1 ion exchange column with pulsed amperometric detection on a Dionex Ion Chromatograph 3000, Thermo Scientific, Sunnyvale, CA). The ratio of lactulose and mannitol excretion (LAC/MAN) was assessed. Normal values were considered <0.05 (34, 35).

Intestinal Fatty Acid Binding Protein (I-FABP) was assessed by ELISA (Hycult Biotech), according to manufacturer's instruction.

Fecal Calprotectin Levels

Calprotectin concentrations were measured by use of a commercial ELISA kit (Immundiagnostik, Bensheim, Germany), according to the manufacturer's instruction. Briefly, two 100-mg samples of feces from a single stool sample from each participant were assayed, and the mean of the two measurements was recorded.

Gut Persistence Score

A gut persistence score was calculated for all drug regimens. Briefly, given the known bioavailability for every single cART molecule, the percentage of non-absorbed drug was ranked in quartiles and given a score between 1 (low persistence score, <25%) and 4 (high persistence score, >75%). A regimen gut persistence score was calculated as the sum of each ARV score.

Metagenomic Sequencing of Blood and Fecal Samples

Fresh stool samples and plasma were collected from each subject, frozen immediately and stored until processing at −80°C. Total DNA was extracted as previously described (36). DNA from plasma was isolated and amplified in a strictly controlled environment at Vaiomer SAS (Labège, France) using a stringent contamination-aware approach as discussed previously (36–39), with no decontamination strategies.

However, plasma, which harbors only a small fraction of the blood bacterial DNA (39), could be impacted by technical contaminants, which suggests that plasma signatures should be taken with more caution than those obtained from feces. Potential contaminants usually impact all samples in a similar way and should not create artifactual differences in the statistical analyses.

Following DNA extraction, the V3–V4 hypervariable regions of the 16S rDNA were amplified and quantified by qPCR, sequenced with MiSeq technology, and clustered into operational taxonomic units (OTUs) before taxonomic assignment as described for fecal and plasma samples (36). PCR amplification was performed using 16S universal primers targeting the V3–V4 hypervariable region of the bacterial 16S ribosomal gene corresponding to 340F-781R sequence positions on the reference *E. coli* sequence.

The targeted metagenomic sequences from fecal and plasma microbiota were analyzed using the bioinformatics pipeline established by Vaiomer SAS from the FROGS guidelines. Briefly, after demultiplexing of the barcoded Illumina paired reads, single read sequences were cleaned and paired for each sample independently into longer fragments. Operational taxonomic units (OTU) were produced with via single-linkage clustering and taxonomic assignment was performed in order to determine community profiles. For parameters: the samples with < 5,000 sequences after FROGS processing were not included in the statistics.

Bioinformatics Analyses

Targeted metagenomic sequences from microbiota were analyzed using a bioinformatic pipeline based on FROGS (40), as described in (38). Briefly, the denoising was performed by removing amplicons missing the two PCR primer sequences (10% of mismatches were allowed), amplicons shorter than 350 bases or longer that 480 bases, amplicons with at least one ambiguous nucleotide ("N"), amplicons identified as chimera (with vsearch v1.9.5), and amplicons with a strong similarity (coverage and identity $\geq$ 80%) with the phiX genome (used as a control for Illumina sequencing runs). Clustering was produced in two passes of the swarm algorithm v2.1.6. The first pass was a clustering with an aggregation distance equal to 1. The second pass was a clustering with an aggregation distance equal to 3. As final denoising step, OTU with very low abundance ($\leq$0.005%) were regarded as sequencing errors and thus discarded. Taxonomic assignment of amplicons into operational taxonomic units (OTUs) was produced by Blast+ v2.2.30+ with the RDP V11.4 database.

Samples with fewer than 5,000 sequences classified in OTU (3 plasma samples, and none of the fecal samples) were excluded from diversity and LEFSE analyses as their taxonomic profile was not determined with enough precision. However, no other cut off was used, and all other samples were kept in the analysis.

Reads obtained from the MiSeq sequencing system have been processed using Vaiomer SAS bioinformatics pipeline. The relative proportion taxa for each taxonomic level (phylum, class, order, family, genus, and species) for both fecal and plasma samples were analyzed statistically.

Alpha-diversity (α-diversity) represents the mean of species diversity per sample in each group/class. Diversity analysis is presented at OTUs level for richness parameters for species taxa according to (1) observed, (2) Chao1 and (3) PD (Phylogenetic Diversity) indexes; and diversity/evenness parameters for species taxa according to (3) Shannon, (4) Simpson, and (5) inverse Simpson indexes.

Principal Coordinate Analysis (PCoA) was performed for comparison of sample groups/class based on four methodologies for β-diversity: (1) Bray-Curtis (a quantitative measure of community dissimilarity), (2) Jaccard (a qualitative measure of community dissimilarity), (3) Unweighted-Unifrac (a qualitative measure of community dissimilarity that incorporates phylogenetic relationships between the features), and (4) Weighted-Unifrac (a quantitative measure of community dissimilarity that incorporates phylogenetic relationships between the features).

Finally, the output matrix containing the relative abundance of OTUs per sample was processed with the linear discriminant analysis effect size (LEfSe) algorithm (41) using an alpha cut-off of 0.05 for both the factorial Kruskal-Wallis test among classes and the pairwise Wilcoxon test between subclasses, and an effect size cut-off of 2.0 for the logarithmic LDA score for discriminative features, and the strategy for multi-class analysis set to "all-against-all."

The functional metagenome has been predicted using PICRUSt v1.1.1 (42) as follow: the OTU representative sequences

were used to pick OTUs against the GreenGenes reference tree (May 18, 2012 database) at 97% identity in order to convert our initial OTU abundance table into PICRUSt-ready OTU abundance table. The metagenome was predicted for each sample and the related pathways were retrieved from the Kyoto encyclopedia of genes and genomes (KEGG) pathways database and formatted for STAMP analysis.

Statistical Analysis

Continuous variables were expressed as median and interquartile range (IQR), whereas categorical variables were expressed as absolute numbers and percentages. The different groups of patients and the different time points were compared using Chi-squared, Fisher's exact test for categorical variables. Mann-Whitney or Kruskal-Wallis for the comparison between HIV+ groups and HIV negative controls. Friedman paired test and Wilcoxon matched paired test for the comparison among HIV+ groups. Correlations among variables were tested by Spearman Rank correlation and presented through heatmaps created using the HEATPLOT module on Stata (v.14, StataCorp, USA). Data were analyzed with GraphPad 6.2 Prism (GraphPad Software Inc). Permanova analysis and Permdisp analysis for all Beta-diversity indexes were performed. $P < 0.05$ for both Pseudo F and *F*-values, respectively, for Permanova and Permdisp, were considered statistically significant. For Picrust analyses was used "STAMP analysis" using Welch's (uncorrected) 0.95 for *post-hoc* test, and Bonferroni correction.

RESULTS

Study Population

We consecutively enrolled 41 HIV-infected, cART-naïve individuals (**Table 1**). At baseline, 25/41 (61%) started a NNRTI-based regimen, 9/41 (22%) a PI-based regimen and 7/41 (17%) an INSTI-based regimen (**Table 1**). Compared to HIV-negative healthy controls, HIV-infected patients were older ($p = 0.0017$), with a higher proportion of MSM ($p = 0.039$; **Table 1**).

Following 12 and 24 months of suppressive cART, we observed viro-immunological improvements (**Supplementary Table 1**), coupled with decreased T-cell activation and a redistribution of memory and naïve T-cell subsets (**Supplementary Table 1**). With regards to microbial translocation and gut barrier markers, cART introduction resulted in stable 16S rDNA and sCD14 levels, along with a rise in EndoCAb ($p = 0.0001$) and I-FABP plasma levels ($p = 0.039$; **Supplementary Table 1**). Interestingly, while fecal calprotectin was stable over time in the whole population (**Supplementary Table 1**), it significantly decreased in HIV-infected subjects with baseline calprotectin values above the range of normality (i.e., $>50\,\mu g/g$) (168 mcg/g vs. 125 mcg/g vs. 60 mcg/g; $p = 0.018$). Likewise, despite a stable LAC/MAN ratio in the whole cohort (**Supplementary Table 1**), HIV-infected patients starting cART with a LAC/MAN ratio > 0.05 displayed a significant reduction at T12 (0.065 vs. 0.034; $p = 0.031$; **Supplementary Table 1**).

Fecal Bacterial Composition Is Affected by Both HIV Infection and Sexual Behavior

We first assessed fecal alpha- and beta-diversity, as well as bacterial relative abundance between in HIV-infected cART-naive individuals and HIV-uninfected controls. The alpha-diversity richness indexes, but not the evenness indexes, were higher in HIV-infected subjects compared to the control group (observed: $p = 0.029$; Chao1: $p = 0.011$; PD: $p = 0.08$; Shannon $p = 0.184$; Simpson $p = 0.303$; **Supplementary Figure 2A**).

Following the fecal relative abundance analyses of the diverse taxonomic levels (phylum, class, order, family, genus, and species) HIV-positive individuals displayed higher *Actinomycetaceae* ($p = 0.01$), *Prevotellaceae* ($p = 0.003$), *Lactobacillaceae* ($p = 0.003$), *Peptococcaceae* ($p < 0.0001$), *Succinivibrionaceae* ($p < 0.0001$), *Fusobacteriaceae* ($p = 0.01$) and lower *Bacteroidaceae* ($p < 0.0001$), *Ruminococcaceae* ($p = 0.066$), and *Rikenellaceae* ($p < 0.0001$) (**Supplementary Figure 2B**) compared to controls. In particular, while we did not find major differences at the phylum level, we observed significant modification within the lower taxonomic levels, such as families and genera. These differences were confirmed by the linear discriminant analysis (LDA) effect size (LEfSe) with LDA score>2 as the cut-off, which also displayed the involvement of other taxa (**Supplementary Figure 2C**).

Given data on the effect of sexual behavior, particularly men who have sex with men (MSM), as a driving factor of large microbiome differences [15, 16], we decided to perform a sensitivity analysis within the HIV-infected group according to sexual behavior (i.e., 28 HIV+ MSM vs. 13 HIV+ MSW). Although not detecting differences in alpha-diversity, we confirm Bacteroidetes unbalance (Prevotellaceae-rich/Bacteroidaceae-poor) in MSM (**Supplementary Figures 2E,F**).

Of note however, when restricting the analysis in MSW from both HIV-infected and HIV-uninfected populations we show a microbial signature unique to HIV infection with significantly less Rikenellaceae ($p = 0.012$) and Ruminococcaceae ($p = 0.012$) (**Supplementary Figures 2G,H**) as well as higher Actinomycetaceae ($p = 0.042$), Lactobacillaceae ($p = 0.012$), and Succinivibrionaceae ($p = 0.002$) (highlighted in bold italics in **Supplementary Figure 2D**).

These unique microbial changes in HIV-infected subjects lead us to hypothesize diverse metagenomic functions. To answer this question, we used the bioinformatics tool PICRUSt (http://picrust.github.io/picrust), that revealed similar predicted functional metagenomic pathways in the two groups (**Supplementary Figure 2H**).

Effect of 12 and 24 Months of Diverse cART Regimens on Fecal Bacteria Composition

We next asked whether diverse cART regimens might result in modifications of gut microbiota composition. To address this question, we first analyzed the impact of cART regimens overall,

TABLE 1 | Epidemiological, Clinical, and HIV-related features of HIV-infected cohort.

	HIV -infected (*N* = 41)	HIV negative (*N* = 15)	*p*-value
Age, years (IQR)*	42 (31.5–50.5)	29 (24–33)	**0.0017**
Sex, male (n) (%)°	37 (90)	15 (100)	0.56
Sexual behaviors MSM, n (%)°	28 (68.2)	5 (33.3)	**0.039**
BMI, n (IQR)*	22.66 (22.02–25.18)	22.71 (20.98–24.91)	0.86
Vegetarian/vegan diet, n subjects (%)°	3 (7.3)	0	0.55
Ongoing antibiotic prophylaxis, n (%)°	8 (19.5)	0	0.09
Hepatitis coinfection, n (%)°	2 (4.8)	0	1
First cART regimen, n (%)		n/a	n/a
NNRTI-based	25 (61)		
PI-based	9 (22)		
INSTI-based	7 (17)		

**Data are median (IQR), statistical analysis Mann-Whitney test. °data are n (%), statistical analysis Fisher's Exact Test. IQR, Interquartile; cART, combination of antiretroviral therapy; NNRTI, non-nucleoside reverse transcriptase inhibitor; PI, protease inhibitor; INI, integrase inhibitor.*

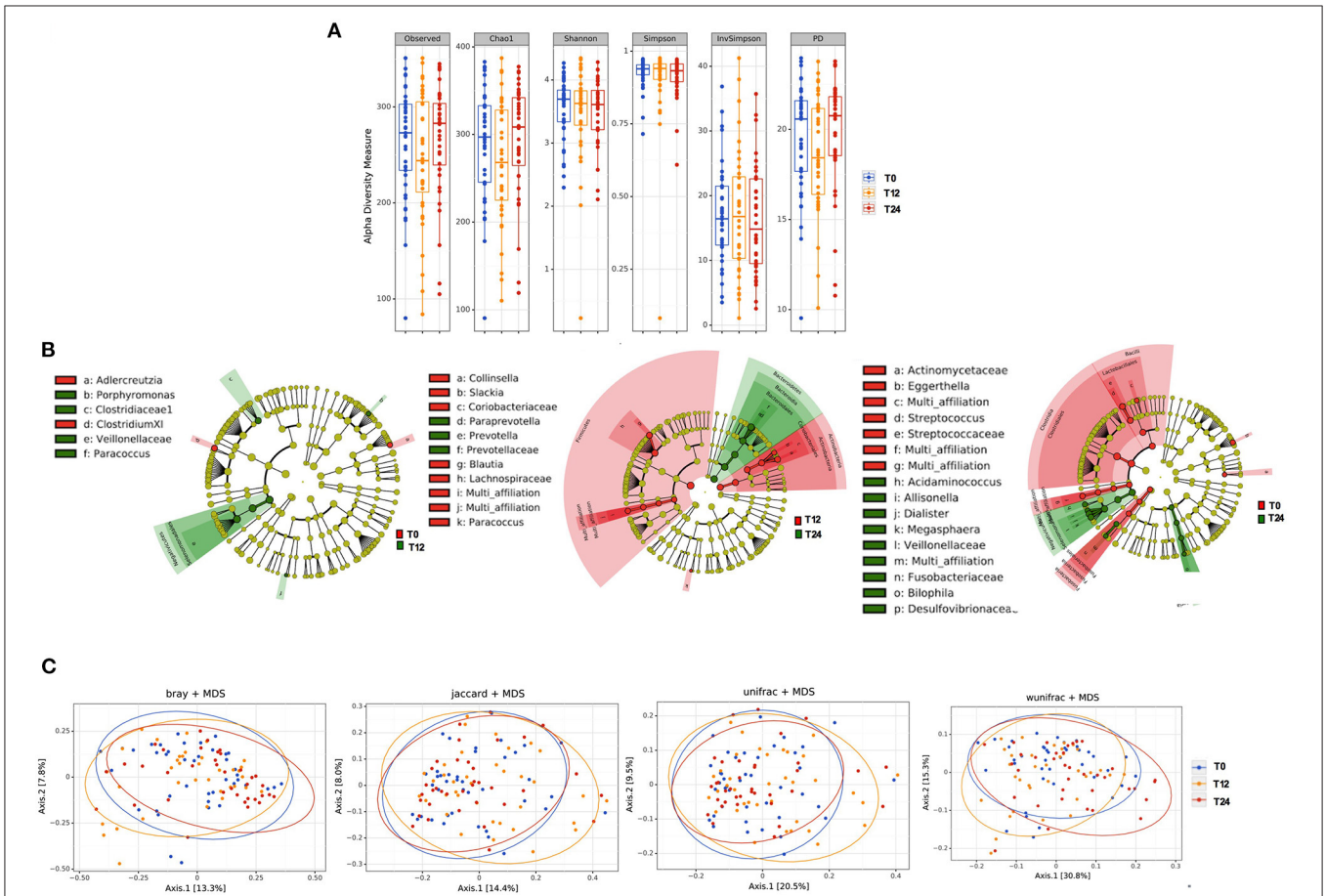

FIGURE 1 | Fecal alpha and beta diversity analyses following 12 and 24 months of cART. **(A)** Fecal alpha diversity (α-diversity) is represented as the mean of species diversity per sample in each group/class (total OTUs) according to Observed, Chao1, PD (richness parameters), Shannon and Simpson (diversity/evenness parameters) during cART. We failed to find any changes following 12 (T12) and 24 months of cART (T24), data analyzed by Friedman test. **(B)** Linear discriminant analysis (LDA) effect size (LEfSe) with LDA score>2 log as the cut-off for all taxa at the following time-points: T0 in red and T12 in green (left); T12 in red and 24 months in green (center); T0 in red and T24 in green (right); all OTUs showed are significant with $p < 0.05$. **(C)** The principal coordinate analyses (PCoA) based on fecal beta-diversity results revealed no significant differences in the course of the study according to Bray-Curtis, Jaccard, unweighted-Unifrac; of note weighted Unifrac showed a significant separation between T12 and T24 (Permanova analysis pseudo $F = 0.008$), but not confirmed by Permdisp $F = 0.92$. *P*-values are not adjusted for multiple comparisons.

then we stratified our cohort according to the 3rd drug, i.e., NNRTI, PI, or INSTI.

The initiation of antiretroviral therapy did not lead to substantial modifications of richness and evenness parameters, as shown in **Figure 1A**. Similarly, the beta-diversity LEfSe analyses showed a modest variation in gut bacterial composition following 12 and 24 months of cART (**Figure 1B**). In line with the above-mentioned results, the principal coordinate analyses based on beta-diversity results (Bray, Jaccard and Unifrac indexes) revealed minimal cluster changes of gut microbiota in the course of treated HIV infection, irrespective of cART duration (**Figure 1C**).

Following cART, the relative abundance analysis revealed a significant increase in *Veillonellaceae* ($p = 0.004$; **Figure 2A**) and a non-significant trend toward higher *Desulfovibrionaceae* ($p = 0.092$; **Figure 2B**), coupled with a parallel decrease in *Lactobacillaceae* ($p = 0.020$), *Coriobacteriaceae* ($p = 0.004$), and *Peptococcaceae* ($p = 0.027$); **Figures 2C–E**). Furthermore, at genus level we observed an increase in *Allisonella* ($p = 0.004$), and *Desulfovibrio* ($p = 0.037$); **Figures 2F,G**), with a significant decrease in *Lactobacillus* ($p = 0.020$), *Eggerthella* ($p = 0.049$), and *Peptococcus* ($p = 0.027$) (**Figures 2H–J**).

Because we initially demonstrated an influence of sexual behavior on fecal microbiome, in a sensitivity analysis we decided to investigate whether sexual orientation still accounts for fecal composition following 12 and 24- month cART. Most interestingly, MSM and MSW confirmed higher *Prevotellaceae* along with significant differences in the distribution of *Bifidobacteriaceae, Bacteroideaceae, Succinivibrionaceae* and *Desulfovibrionaceae* (**Supplementary Figures 3A–H**).

We next explored whether these cART-mediated microbiota shifts might be associated with markers of gut damage, microbial translocation, confirming possible associations between bacterial composition and their changes over time and gut damage/microbial translocation (**Figure 3**).

Changes in Gut Microbiota Composition According to the cART Class

Interestingly, when we stratified patients according to cART regimens, we found that only NNRTI-based therapy significantly reduced richness (observed: $p = 0.038$; Chao1: $p = 0.006$; **Figures 4A,B**), but not evenness indexes (**Figures 4C,D**) over time. Furthermore, the relative abundance analyses showed a different profile at both family and genus levels, with NNRTI-based regimens significantly reducing the families of *Coriobacteriaceae*, *Peptococcaceae* and increasing the *Veillonellaceae* family (**Figures 4E–G**). At the opposite, INSTI-based regimens resulted in decreased *Peptococcaceae* and increased *Veillonellaceae* families, as well as in higher *Allisonella* genus (**Figures 4H–J**). Interestingly, the changes in gut dysbiosis according to diverse cART regimens, was accompanied by stable metagenomics predictions (**Figures 4K,L**).

Having shown fecal microbiome changes specific to drug class, we next aimed to test whether this effect could be associated to differences in gut drug persistence across drug classes by calculating a "gut persistence score" (GPS), based on the drug bioavailability and the proportion of unchanged drug in feces. We found that the gut persistence score was similar between PI-, NNRTI- and INSTI-based regimens over time (**Figures 4M,N**), overall suggesting that, despite similar drug concentration in the gut, cART classes are associated with different microbiome signatures, not translating however in different predictive metagenomic functions.

Bacteria Alpha- and Beta-Diversity and Relative Abundance Analyses in Plasma

Given the presence of microbial bioproducts within the blood of HIV-infected individuals despite cART introduction (30, 43, 44), we also explored the composition of the translocating microbiota in plasma samples of our study cohort.

No differences were observed in richness parameters (observed, Chao1 and PD) and diversity/evenness parameters (Shannon and Simpson) in terms of bacteria composition over time (**Figure 5A**). In line with what observed in the feces, cART introduction modified the bacteria composition only partially, with slight variations of *Bacilli* genus ($p = 0.03$), *Sphingomonadales* order ($p = 0.01$) and *Sphingomonadaceae* family ($p = 0.04$) (**Figure 5B**). Similarly, beta- diversity analysis revealed no differences in plasma bacteria composition following the principal coordinate analysis during cART (**Figure 5C**).

Paired plasma and fecal subjects showed a completely different bacterial composition at phylum level, irrespective of HIV infection or cART introduction (**Supplementary Figure 4**).

DISCUSSION

It is now widely accepted that, aside from the direct effect on gastrointestinal mucosal immunity (45–48), HIV infection is characterized by gut microbiota compositional and functional changes, not fully reverted by cART (1, 3, 5, 12, 13, 18, 49–53). However, the causal relationship between altered intestinal microbiota composition, gut damage, and cART remains an open question that needs to be answered in order to improve microbiome-targeted therapies.

We hereby describe that 24 months of viro-immunological effective cART significantly reduced immune activation and corrected T-cell immune phenotype imbalances in the periphery, yet appeared to have a minor effect within the gut. Literature reports have demonstrated greater IFAB-P levels in HIV infection (54). Although IFAB-P measurements in HIV-uninfected subjects were not available in the present study, our results of a significant rise in plasma I-FABP during 24-month cART possibly suggest enduring enterocyte damage despite long-term cART. These findings complement previous data by Chevalier et al. (54) on the rise of I-FABP in acutely treated HIV-infected patients, implying the inefficiency of cART in preventing/correcting gut mucosal damage either in acute and in chronic infection. In keeping with this observation, the findings of a rise in both I-FABP and EndoCAb in the face of stable 16S rDNA might altogether suggest ongoing intestinal epithelium compromise, in turn conditioning the release in the systemic circulation of bacteria products that might however be cleared

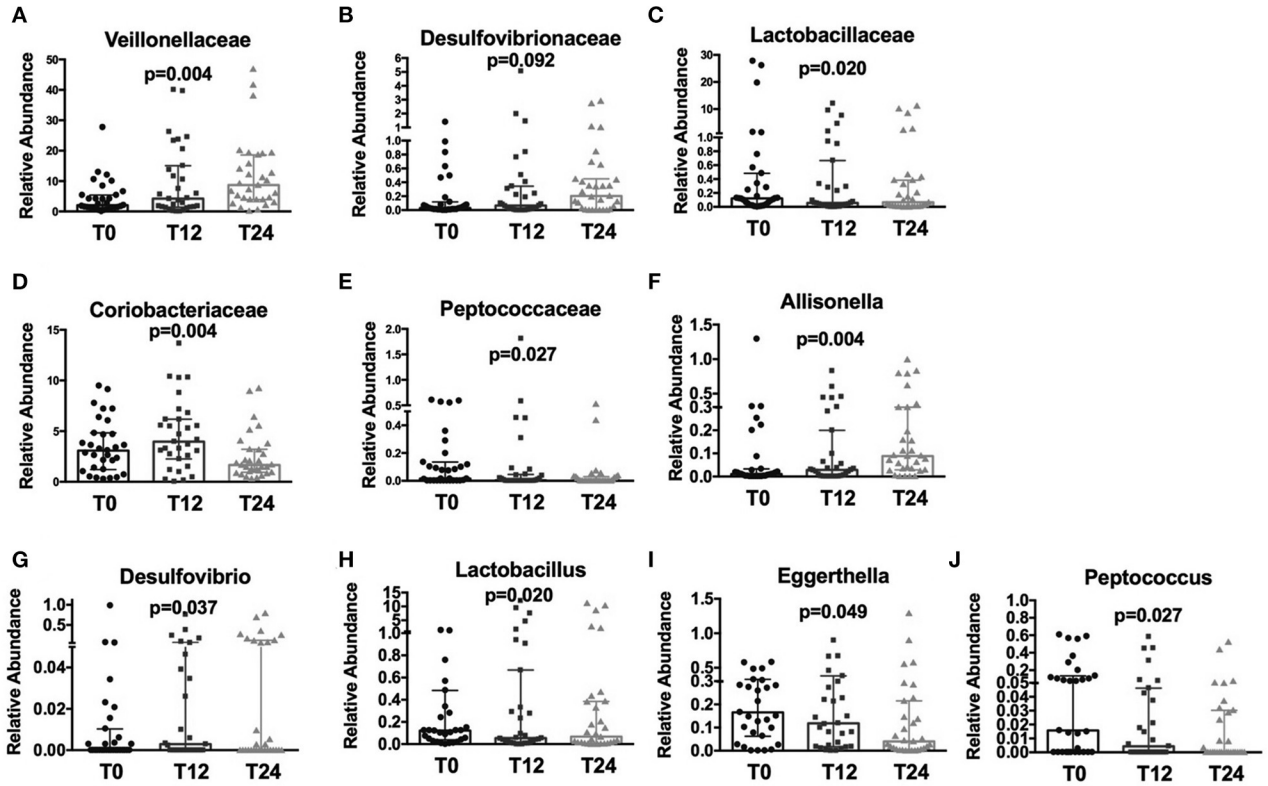

FIGURE 2 | Fecal relative abundance of bacteria Family and Genus taxa following cART introduction. The presented data refer to taxa at family and genus levels in HIV -infected patients before (T0) and after cART (T12, T24). **(A)** Significant increase in *Veillonellaceae* family ($p = 0.004$). **(B)** Increasing trend in *Desulfovibrionaceae* ($p = 0.92$); **(C–E)** significant decrease, respectively, in *Lactobacillaceae*, *Coriobacteriaceae,* and *Peptococcaceae* families ($p = 0.020$, $p = 0.004$, $p = 0.027$, respectively). **(F,G)** Significant increase in Allisonella and Desulfovibrio genera ($p = 0.004$, $p = 0.037$, respectively). **(H–J)** Significant decrease, respectively, in Lactobacillus, Eggerthella, and Peptococcus genera ($p = 0.020$, $p = 0.049$, $p = 0.027$, respectively). Data analyzed by Anova, *p*-values are not adjusted for multiple comparisons.

by naturally occurring EndoCAbs as previously suggested (55). Under this perspective, the finding of stable plasma sCD14 over 24 months is therefore not unexpected, given that sCD14 has been proven to interact with translocating bacteria products, in turn stimulating antigen-presenting cells via TLR signaling (56).

Although specific clinical indexes of gut permeability (i.e., LAC/MAN and fecal calprotectin) slightly and selectively improved in patients starting cART with advanced gut damage, our data overall point to the unproductive attempt of cART to repair the mucosal barrier.

The persistence of gut damage during long-term cART appears to mirror the limited effects of treatment on fecal microbiota composition, with modest increases in *Negativicutes, Selenomonadales, Veillonellaceae* and decreases in *Lactobacillaceae, Peptococcaceae*, *Coriobacteriaceae.* While some of these modifications might be helpful in restoring the balance between microbiota and immune system (57, 58), other changes, such as the emergence of *Allisonella* or *Desulfovibrio* genera, coupled with the possible positive association between the *Veillonellaceae* family and I-FABP levels, might indicate a perpetuation of gut damage. Further studies to finely investigate the associations between microbiome compositional signatures in both the stool and in gut tissue and markers of gut damage will be needed to better comprehend the possible interactions between gut microbiome and damage, in turn possibly affecting disease progression (59, 60).

Indeed, in line with previous literature reports (3, 12, 26, 28, 50), our cohort of chronically HIV-infected individuals maintained gut dysbiosis, featuring higher fecal α-diversity, a distinct cluster separation according to PCoA analysis and a *Prevotellaceae*-rich/*Bacteroidaceae* poor profile compared to uninfected individuals as well as a Ruminococcaceae/Rikenellaceae poor profile in MSW alone. Our finding is coherent with other authors, suggesting a complex scenario where the gut microbiota is altered by both HIV and other confounding factors (61).

Given that the enrichment or impoverishment of some key microbial species is linked to disease progression—i.e., the depletion of butyrate-producing bacteria has been associated with increased microbial translocation and immune activation (62, 63)–, our findings support the role of specific bacterial populations in the pathogenesis of non-communicable disorders in the context of treated HIV infection. Additionally, our finding of higher fecal α-diversity in HIV-infected patients seems to be

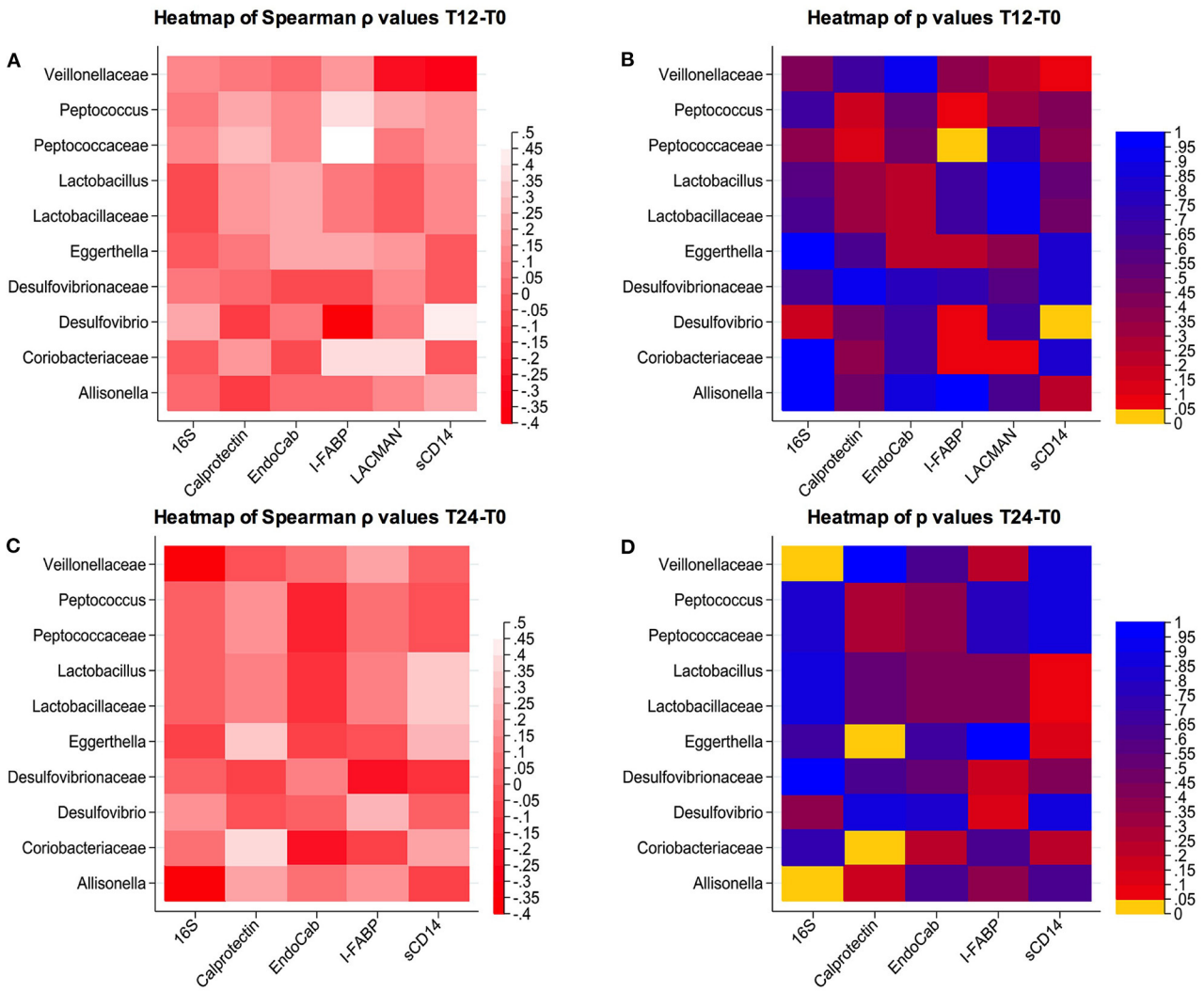

FIGURE 3 | Correlations between changes in microbial composition and soluble biomarkers. **(A,B)** Spearman correlation and *p*-values at T12-T0; **(C,D)** Spearman correlation and *p*-values at T24-T0.

in contrast with previous studies (12) and might be attributed in part to differences in sexual practices. Indeed, MSM were found to have greater fecal microbial differences than not-MSM, irrespective of HIV infection (15). In our cohort, however, the sensitive analysis on not-MSM confirmed the differences between HIV-infected and HIV- individuals, suggesting that factors other than sexual practice might have influenced the microbiota composition.

Antiretroviral drugs may contribute to the development of non-infectious comorbidities because of their widely described adverse effects on various organs and systems; further, cART may also determine compositional shifts in the gut microbiome and possibly fuel disease progression. In our study, aside from a small NNRTI-mediated decrease in α-diversity richness, we did not highlight marked changes according to PI- or INSTI-based combinations. Although in contrast with literature observations showing a possible role of cART-associated modifications in microbial composition (15, 23), the different cART regimens appear to have a similar impact on the composition of the microbiota.

We should also acknowledge that, given the low CD4 count at cART initiation, 19% of our cohort was on antibiotic prophylaxis, that was promptly interrupted when patients reached a good immune recovery level (generally within the first year). Thus, we could not exclude that part of the small modifications observed in gut microbiota composition might be mediated by antibiotic suspension. Besides, some cART regimens, particularly protease inhibitor-based combinations, could induce non-infectious diarrhea (64, 65), so it is also possible that the changes in microbiota might reflect these side-effects.

We next focused our research on the characterization of blood microbiota composition, given the role of translocated microbial bioproducts in disease progression (30, 44). Our analyses revealed a different composition of translocated microbial

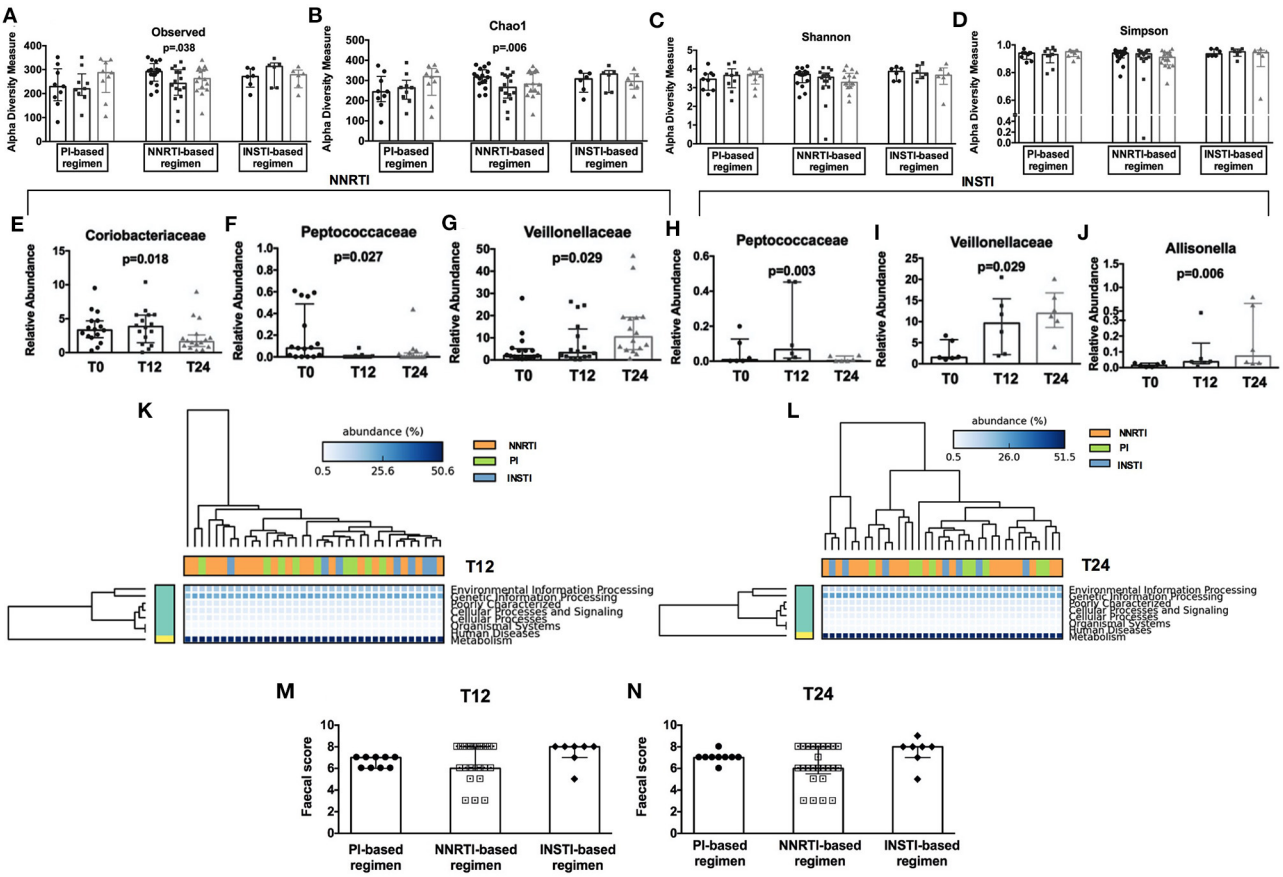

FIGURE 4 | Fecal alpha diversity indexes, relative abundance analyses, metagenomic prediction, and gut persistence score according to cART class. Comparison of alpha diversity measures in HIV-infected patients during cART (3 bars, from left to right: T0, T12, and T24) subdivided according to different cART regimens presented according to Observed **(A)**, Chao1 **(B)**, Shannon **(C)**, Simpson **(D)** at OTUs level. **(E–J)** Comparison of fecal relative abundance taxa according to cART regimens analyzed Friedman test, *p*-values not adjusted for multiple comparisons. **(K,L)** Predicted metagenomic functions according to class cART. Data analyzed by Welch's (uncorrected) 0.95 for *post-hoc* test, and Bonferroni correction. **(M,N)** No differences were found in terms of fecal Gut Persistence Score according to class cART in the course of the study analyzed by Friedman test, *p*-values are not adjusted for multiple comparisons.

products between plasma and fecal samples, in terms of both alpha and beta-diversity, suggesting, on the one hand, a selective passage of microbes through the gut barrier, and on the other, immune control over potentially pathogenic microorganisms. Interestingly, we describe predominance of the *Proteobacteria* phylum in plasma in contrast to its low intestinal abundance both before and after the introduction of cART. Our findings add to previous research describing the tempo and the signature of blood microbiota in both treated and untreated SIV and HIV-infected patients, and their possible influence on inflammation and immune homeostasis (21, 66, 67). Strikingly, a similar selective *Proteobacteria* overgrowth has been previously proven in the blood of experimentally SIV-infected asian macaques upon antiretroviral treatment, also associated with their increased metabolic activity within the gut and immune activation, altogether confirming the propensity to preferentially translocate in the systemic circulation, in turn conditioning the immune profile (21). Given that *Proteobacteria* in the blood have been associated with the onset of cardiovascular events (32), a detailed definition of the possible associations between the bacteria belonging to the *Proteobacteria* phylum and clinical outcomes in HIV-treated patients merits an in-depth investigation, to circumstantiate the role of dysbiosis in the development of residual disease during cART as recently suggested (68).

Several limitations in our study should be acknowledged: (i) our inability to study bacterial composition, gut damage and immunity at gut mucosal site, that might have shed light on the causal relationship between microbiota and immune system over the course of cART, (ii) the lack of an extensive analysis of microbial function, which would certainly widen the understanding of the possible interactions between gut microbial community and damage, as well as peripheral immune homeostasis, (iii) the lack of a standardized questionnaire on food habits, and (iv) the use of a non-validated drug penetration score into the feces, given the well-known distinctive ability of tissue penetrations exerts by the various drugs (69, 70). A further bias in our study might be represented by the younger age in control group. It is well-known that aging affects gut microbiota

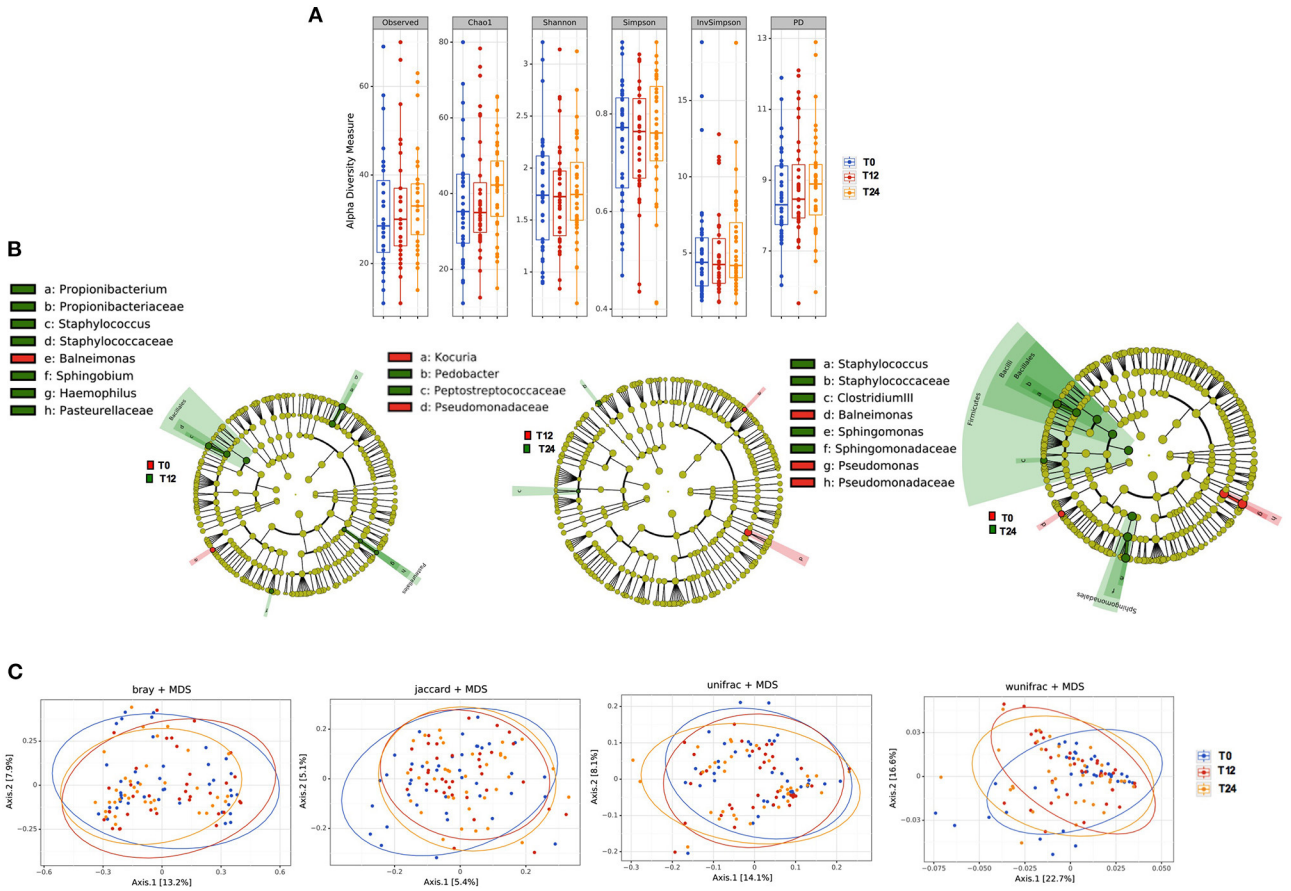

FIGURE 5 | Plasma microbiota composition: alpha and beta diversity analyses. **(A)** Plasma alpha diversity (α-diversity) represented as the mean of species diversity (total OTUs) per sample in each group/class according to Observed, Chao1, PD (richness parameters), Shannon, Simpson, and invSimpson (diversity/evenness parameters) before (T0) and after 12 (T12) and 24 (T24) months of cART. No significant differences following cART initiation were found (Friedman test). **(B)** Linear discriminant analysis (LDA) effect size (LEfSe) with LDA score>2 log as the cut-off for all taxa at the different time-points in study between baseline (T0) in red and 12 months (T12) in green of cART (left), T12 in red and 24 months (T24) in green of cART (center), T0 in red and T24 in green (right), all OTUs showed are significant with $p < 0.05$. **(C)** The principal coordinate analyses (PCoA) based on plasma beta-diversity results revealed no significant differences in the course of the study according to all parameters: BrayCurtis Permanova Pseudo $F = 0.49$, Perdsp. $F = 0.32$; Jaccard, pseudo $F = 0.94$, $F = 0.14$; unweighted Unifrac Pseudo $F = 0.99$, $F = 0.85$; weighted Unifrac 0.09, $F = 0.50$. *P*-values are not adjusted for multiple comparisons.

composition (71), however during adulthood (25–50 years) the composition tends to be stable (72, 73), thus we could assume that despite the statistical difference in age, the two study groups are homogeneous. Finally, we must acknowledge that specific plasma decontamination strategies were not applied in this data set. Given the possibility of plasma environmental contamination (39), although potential contaminants usually impact all samples in a similar way, they cannot be fully ruled out, and therefore microbial signatures in blood should be taken with more caution than those described in fecal samples.

In conclusion, despite the viro-immunological benefits, long-term effective cART, irrespective of drug classes, resulted in persistent gut damage that associates with gut dysbiosis. Besides, the finding of a compositional shift in fecal vs. plasma microbiota, with the enrichment of *Proteobacteria* in peripheral blood, opens new perspective on the clinical implication of circulating bacteria and HIV-associated non-communicable co-morbidities.

To our knowledge, this is the first study assessing the impact of 24 months of cART on both fecal and plasma microbiota composition. Whether the persistence of dysbiosis fuels intestinal damage and the consequent microbial translocation, or whether the HIV-mediated pro-inflammatory environment linked to gastrointestinal damage and microbial translocation promote dysbiosis remains to be elucidated.

DATA AVAILABILITY STATEMENT

The datasets presented in this study can be found in online repositories. The names of the repository/repositories and accession number(s) can be found at: ENA database under the project accession PRJEB41869.

ETHICS STATEMENT

The studies involving human participants were reviewed and approved by Ethics committee of ASST San Paolo e Carlo. The patients/participants provided their written informed consent to participate in this study.

AUTHOR CONTRIBUTIONS

GA and EM designed and performed experiments, analyzed and interpreted the data, and wrote the manuscript. AB was responsible for HPLC data. CT, FB, and AC helped in analyzing and interpreting the data. EC and VB participated to laboratory experiments. MA helped with patients recruitment and manuscript preparation. Ad'A contributed to data interpretation. GM conceived and designed the study and conducted the data analyses. All authors contributed to the editing of the manuscript. GM supervised the project.

FUNDING

This study was supported by the Italian Ministry of Health, Regione Lombardia, grant Giovani Ricercatori (number GR-2009-1592029) to GM, and grant Ricerca Finalizzata (number NET-2013-02355333-3) to GM.

ACKNOWLEDGMENTS

We are thankful to all the patients who participated in the study and the staff of the Clinic of Infectious Diseases and Tropical Medicine, University of Milan at ASST Santi Paolo e Carlo who cared for the patients. Presented in part at CROI 2017, February 13-16, 2017, Seattle (Washington), US—abstract #215.

SUPPLEMENTARY MATERIAL

The Supplementary Material for this article can be found online at: https://www.frontiersin.org/articles/10.3389/fimmu.2021.639291/full#supplementary-material

Supplementary Figure 1 | Gating strategy for the identification of $CD4^+$ and $CD8^+$ T-cell surface phenotypes. Lymphocytes were gated from forward (FSC) and side scatters (SSC), doublets were removed, live cells were selected and segregated for $CD4^+$ T-cells or CD8 T-cells. Within $CD4^+$ (or $CD8^+$) subsets, CD127, CD45RA, CD45R0, and/or CD38 gates were set up based on positive vs. negative peak. Depicted are representative plots from representative subject PBMCs.

Supplementary Figure 2 | (A) Fecal alpha diversity (α-diversity) represented as the mean of species diversity per sample in each group/class (total OTUs) according to Observed, Chao1 (richness parameters), Shannon and Simpson (diversity/evenness parameters) at baseline. We found a significant increase in HIV-infected patients compared to controls according to richness parameters (Observed $p = 0.029$; Chao1: $p = 0.011$, Mann-Whitney test); no differences according to diversity/evenness parameters (Shannon $p = 0.184$; Simpson $p = 0.3033$) were observed. **(B)** Fecal relative abundance at each taxonomic level (phylum, class, order, family, genus) between HIV-infected individuals at T0 and HIV-uninfected controls. ↑ indicates increase with significant $p < 0.05$, ↓ indicates decrease with significant values < 0.05 with exception for taxa Bifidobacteriales, Carnobacteriaceae, Acidaminococcus, Bifidobacterium, Collinsella, and Granulicatella that show trends with *p*-values between 0.05 and 0.07. Data analyzed by Mann-Whitney test. **(C)** Linear discriminant analysis (LDA) effect size (LEfSe) with LDA score>2 log as the cut-off at baseline. Significant results ($p < 0.05$) for all taxa are shown: higher abundance in HIV-infected subjects and HIV-uninfected controls represented in red and green, respectively. In Bold Italics are highlighted the families that remained altered in the sensitivity analysis according to sexual preferences (HIV-infected vs. HIV-uninfected men who have sex with women_MSW). **(D–G)** Sensitivity analysis of fecal microbial abundance according to sexual behavior and HIV-serostatus. HIV-infected men with different sexual behavior showed different microbial composition prior to cART (T0), with higher Prevotellaceae and lower Bacteriodaceae in MSM **(D,E)**. HIV-infected, cART-naive (T0) MSW displayed significantly lower Rikenellaceae and Ruminococcaceae compared to their sero-negative counterparts **(F,G)**. Data analyzed by Mann-Whitney test, $p < 0.05$. *P*-values are not adjusted for multiple comparisons. **(H)** Computed metagenomic functions between HIV-infected subjects prior to cART and HIV-uninfected subjects. Despite different microbial composition, similar functions were found in HIV-infected subjects prior to cART introduction and HIV-uninfected controls. Data anylzed by Welch's (uncorrected) 0.95 for *post-hoc* test, and Bonferroni correction.

Supplementary Figure 3 | Sensitivity analysis of fecal microbial abundance according to sexual behavior following 12 and 24 months of cART. HIV-infected men with different sexual behavior showed different microbial composition at a family taxa level during cART both at T12 and T24. MSM showed lower Bifidobacteriaceae compared to MSW at T12 **(A)** and T24 **(E)**, and higher Peptococcaceae, Prevotellaceae, and Succinivibrionaceae both at T12 **(B–D)** and at T24 **(F–H)**. Data analyzed Mann-Whitney test, $p < 0.05$. *P*-values are not adjusted for multiple comparisons.

Supplementary Figure 4 | Fecal and Plasma Phyla Distribution. The figure shows the relative abundance ratio between fecal (left bars) and plasma (right bars) samples among the most 4 representative phyla: Actinobacteria **(A)**, Proteobacteria **(B)**, Firmicutes **(C)**, and Bacteroidetes **(D)** for each group: HIV negative controls, HIV+ T0 (baseline), HIV+ T12 (after 12 months the introduction of cART) and HIV+ T24 (after 24 months the introduction of cART). **(A,B)** The relative abundance of Actinobacteria and Proteobacteria phyla was higher in plasma (right bars) than in feces (left bars) in all the study groups. **(C,D)** The relative abundance of Firmicutes and Bacteroidetes phyla was lower in plasma (right bars), as compared to feces (left bars), in both healthy controls and HIV-infected patients prior and after cART introduction. *P*-values are not adjusted for multiple comparisons.

Supplementary Table 1 | Viro-immunological parameters, T-cell phenotypes, microbial translocation, and gut barrier markers in 41 HIV-infected patients starting a first cART regimen.

Supplementary Table 2 | Viro-immunological parameters, T-cell phenotypes, microbial translocation/gut barrier markers in HIV-infected subjects treated with different classes of antiretrovirals.

REFERENCES

1. Zilberman-Schapira G, Zmora N, Itav S, Bashiardes S, Elinav HE. The gut microbiome in human immunodeficiency virus infection. *BMC Med.* (2016) 14:83. doi: 10.1186/s12916-016-0625-3
2. Rocafort M, Noguera-Julian M, Rivera J, Pastor L, Guillén Y, Langhorst J, et al. Evolution of the gut microbiome following acute HIV-1 infection. *Microbiome.* (2019) 7:73. doi: 10.1186/s40168-019-0687-5
3. Lozupone CA, Li M, Campbell TB, Flores SC, Linderman D, Gebert MJ, et al. Alterations in the gut microbiota associated with HIV-1 infection. *Cell Host Microbe.* (2013) 14:329–39. doi: 10.1016/j.chom.2013.08.006
4. Vujkovic-Cvijin I, Somsouk M. HIV and the gut microbiota: composition, consequences, and avenues for amelioration. *Curr HIV/AIDS Rep.* (2019) 16:204–13. doi: 10.1007/s11904-019-00441-w
5. Zhou Y, Ou Z, Tang X, Xu H, Wang X, Li K, et al. Alterations in the gut microbiota of patients with acquired immune deficiency

syndrome. *J Cell Mol Med.* (2018) 22:2263–71. doi: 10.1111/jcmm.13508
6. Mutlu EA, Keshavarzian A, Losurdo J, Swanson G, Siewe B, Forsyth C, et al. A compositional look at the human gastrointestinal microbiome and immune activation parameters in HIV infected subjects. *PLoS Pathog.* (2014) 10:e1003829. doi: 10.1371/journal.ppat.1003829
7. Neff CP, Krueger O, Xiong K, Arif S, Nusbacher N, Schneider JM, et al. Fecal microbiota composition drives immune activation in HIV-infected individuals. *EBioMedicine.* (2018) 30:192–202. doi: 10.1016/j.ebiom.2018.03.024
8. Zevin AS, McKinnon L, Burgener A, Klatt NR. Microbial translocation and microbiome dysbiosis in HIV-associated immune activation. *Curr Opin HIV AIDS.* (2016) 11:182–90. doi: 10.1097/COH.0000000000000234
9. Ji Y, Zhang F, Zhang R, Shen Y, Liu L, Wang J, et al. Changes in intestinal microbiota in HIV-1-infected subjects following cART initiation: influence of $CD4^+$ T cell count. *Emerg Microbes Infect.* (2018) 7:113. doi: 10.1038/s41426-018-0117-y
10. Lu W, Feng Y, Jing F, Han Y, Lyu N, Liu F, et al. Association between gut microbiota and CD4 recovery in HIV-1 infected patients. *Front Microbiol.* (2018) 9:1451. doi: 10.3389/fmicb.2018.01451
11. Guillén Y, Noguera-Julian M, Rivera J, Casadellà M, Zevin A S, Rocafort M, et al. Low nadir $CD4^+$ T-cell counts predict gut dysbiosis in HIV-1 infection. *Mucosal Immunol.* (2019) 12:232–46. doi: 10.1038/s41385-018-0083-7
12. Nowak P, Troseid M, Avershina E, Barqasho B, Neogi U, Holm K, et al. Gut microbiota diversity predicts immune status in HIV-1 infection. *AIDS.* (2015) 29:2409–18. doi: 10.1097/QAD.0000000000000869
13. Li SX, Armstrong A, Neff CP, Shaffer M, Lozupone CA, Palmer BE. Complexities of gut microbiome dysbiosis in the context of HIV infection and antiretroviral therapy. *Clin Pharmacol Ther.* (2016) 99:600–11. doi: 10.1002/cpt.363
14. Pinto-Cardoso S, Klatt NR, Reyes-Terán G. Impact of antiretroviral drugs on the microbiome: unknown answers to important questions. *Curr Opin HIV AIDS.* (2018) 13:53–60. doi: 10.1097/COH.0000000000000428
15. Noguera-Julian M, Rocafort M, Guillén Y, Rivera J, Casadellà M, Nowak P, et al. Gut microbiota linked to sexual preference and HIV infection. *EBioMed.* (2016) 5:135–46. doi: 10.1016/j.ebiom.2016.01.032
16. Li SX, Sen S, Schneider JM, Xiong KN, Nusbacher NM, Moreno-Huizar N, et al. Gut microbiota from high-risk men who have sex with men drive immune activation in gnotobiotic mice and in vitro HIV infection. *PLoS Pathog.* (2019) 15:e1007611. doi: 10.1371/journal.ppat.1007611
17. Tincati C, Douek DC, Marchetti G. Gut barrier structure, mucosal immunity and intestinal microbiota in the pathogenesis and treatment of HIV infection. *AIDS Res Ther.* (2016) 13:19. doi: 10.1186/s12981-016-0103-1
18. Dillon SM, Frank DN, Wilson CC. The gut microbiome and HIV-1 pathogenesis: a two-way street. *AIDS.* (2016) 30:2737–51. doi: 10.1097/QAD.0000000000001289
19. Mudd JC, Brenchley JM. Gut mucosal barrier dysfunction, microbial dysbiosis, and their role in HIV-1 disease progression. *J Infect Dis.* (2016) 214(Suppl. 2):S58–66. doi: 10.1093/infdis/jiw258
20. Luján JA, Rugeles MT, Taborda NA. Contribution of the microbiota to intestinal homeostasis and its role in the pathogenesis of HIV-1 infection. *Curr HIV Res.* (2019) 17:13–25. doi: 10.2174/1570162X17666190311114808
21. Klase Z, Ortiz A, Deleage C, Mudd JC, Quiñones M, Schwartzman E, et al. Dysbiotic bacteria translocate in progressive SIV infection. *Mucosal Immunol.* (2015) 8:1009–20. doi: 10.1038/mi.2014.128
22. Dillon SM, Lee EJ, Kotter CV, Austin GL, Dong Z, Hecht DK, et al. An altered intestinal mucosal microbiome in HIV-1 infection is associated with mucosal and systemic immune activation and endotoxemia. *Mucosal Immunol.* (2014) 7:983–94. doi: 10.1038/mi.2013.116
23. Pinto-Cardoso S, Lozupone C, Briceño O, Alva-Hernández S, Téllez N, Adriana A, et al. Reyes-terán: fecal bacterial communities in treated HIV infected individuals on two antiretroviral regimens. *Sci Rep.* (2017) 7:43741. doi: 10.1038/srep43741
24. Villanueva-Millán MJ, Pérez-Matute P, Recio-Fernández E, Lezana Rosales JM, Oteo JA. Differential effects of antiretrovirals on microbial translocation and gut microbiota composition of HIV-infected patients. *J Int AIDS Soc.* (2017) 20:21526. doi: 10.7448/IAS.20.1.21526
25. Vujkovic-Cvijin I, Dunham RM, Iwai S, Maher MC, Albright RG, Broadhurst MJ, et al. Dysbiosis of the gut microbiota is associated with HIV disease progression and tryptophan catabolism. *Sci Transl Med.* (2013) 5:193ra91. doi: 10.1126/scitranslmed.3006438
26. McHardy IH, Li X, Tong M, Ruegger P, Jacobs J, Borneman J, et al. HIV infection is associated with compositional and functional shifts in the rectal mucosal microbiota. *Microbiome.* (2013) 1:26. doi: 10.1186/2049-2618-1-26
27. Deusch S, Serrano-Villar S, Rojo D, Martínez-Martínez M, Bargiela R, Vázquez-Castellanos JF, et al. Effects of HIV, antiretroviral therapy and prebiotics on the active fraction of the gut microbiota. *AIDS.* (2018) 32:1229–37. doi: 10.1097/QAD.0000000000001831
28. Nowak RG, Bentzen SM, Ravel J, Crowell TA, Dauda W, Ma B, et al. Rectal microbiota among HIV-uninfected, untreated HIV, and treated HIV-infected in Nigeria. *AIDS.* (2017) 31:857–62. doi: 10.1097/QAD.0000000000001409
29. Shilaih M, Angst DC, Marzel A, Bonhoeffer S, Günthard HF, Kouyos RD. Antibacterial effects of antiretrovirals, potential implications for microbiome studies in HIV. *Antivir Ther.* (2018) 23:91–4. doi: 10.3851/IMP3173
30. Merlini E, Bai F, Bellistrì GM, Tincati C, d'Arminio A, Monforte G. Evidence for polymicrobic flora translocating in peripheral blood of HIV-infected patients with poor immune response to antiretroviral therapy. *PLoS ONE.* (2011) 6:e18580. doi: 10.1371/journal.pone.0018580
31. Amar J, Lange C, Payros G, Garret C, Chabo C, Lantieri O, et al. Blood microbiota dysbiosis is associated with the onset of cardiovascular events in a large general population: the D.E.S.I.R. study. *PLoS ONE.* (2013) 8:e54461. doi: 10.1371/journal.pone.0054461
32. Amar J, Serino M, Lange C, Chabo C, Iacovoni J, Mondot S, et al. Involvement of tissue bacteria in the onset of diabetes in humans: evidence for a concept. *Diabetologia.* (2011) 54:3055–61. doi: 10.1007/s00125-011-2329-8
33. Gelpi M, Vestad B, Hansen SH, Holm K, Drivsholm N, Goetz A, et al. Impact of human immunodeficiency virus-related gut microbiota alterations on metabolic comorbid conditions. *Clin Infect Dis.* (2020) 71:e359–67. doi: 10.1093/cid/ciz1235
34. Mishra A, Makharia GK. Techniques of functional and motility test: how to perform and interpret intestinal permeability. *J Neurogastroenterol Motil.* (2012) 18:443–7. doi: 10.5056/jnm.2012.18.4.443
35. Cobden I, Dickinson RJ, Rothwell J, Axon AT. Intestinal permeability assessed by excretion ratios of two molecules: results in coeliac disease. *Br Med J.* (1978) 2:1060. doi: 10.1136/bmj.2.6144.1060
36. Lluch J, Servant F, Païssé S, Valle C, Valière S, Kuchly C, et al. The characterization of novel tissue microbiota using an optimized 16S metagenomic sequencing pipeline. *PLoS ONE.* (2015) 10:e0142334. doi: 10.1371/journal.pone.0142334
37. Schierwagen R, Alvarez-Silva C, Servant F, Trebicka J, Lelouvier B, Arumugam M. Trust is good, control is better: technical considerations in blood microbiome analysis. *Gut.* (2020) 69:1362–3. doi: 10.1136/gutjnl-2019-319123
38. Anhê FF, Jensen BAH, Varin TV, Servant F, Van Blerk S, Richard D, et al. Type 2 diabetes influences bacterial tissue compartmentalisation in human obesity. *Nat Metab.* (2020) 2:233–42. doi: 10.1038/s42255-020-0178-9
39. Païssé S, Valle C, Servant F, Courtney M, Burcelin R, Amar J, et al. Comprehensive description of blood microbiome from healthy donors assessed by 16S targeted metagenomic sequencing. *Transfusion.* (2016) 56:1138–47. doi: 10.1111/trf.13477
40. Escudié F, Auer L, Bernard M, Mariadassou M, Cauquil L, Vidal K, et al. FROGS: find, rapidly, OTUs with galaxy solution. *Bioinformatics.* (2018) 34:1287–94. doi: 10.1093/bioinformatics/btx791
41. Segata N, Izard J, Waldron L, Gevers D, Miropolsky L, Garrett WS, et al. Metagenomic biomarker discovery and explanation. *Genome Biol.* (2011) 12:R60. doi: 10.1186/gb-2011-12-6-r60
42. Abubucker S, Segata N, Goll J, Schubert AM, Izard J, Cantarel BL, et al. Metabolic reconstruction for metagenomic data and its application to the human microbiome. *PLoS Comput Biol.* (2012) 8:e1002358. doi: 10.1371/journal.pcbi.1002358
43. Marchetti G, Tincati C, Silvestri G. Microbial translocation in the pathogenesis of HIV infection and AIDS. *Clin Microbiol Rev.* (2013) 26:2–18. doi: 10.1128/CMR.00050-12
44. Brenchley JM, Douek DC. Microbial translocation across the GI tract. *Annu Rev Immunol.* (2012) 30:149–73. doi: 10.1146/annurev-immunol-020711-075001

45. Somsouk M, Estes JD, Deleage C, Dunham RM, Albright R, Inadomi JM, et al. Gut epithelial barrier and systemic inflammation during chronic HIV infection. *AIDS.* (2015) 29:43–51. doi: 10.1097/QAD.0000000000000511
46. Paiardini M, Frank I, Pandrea I, Apetrei C, Silvestri G. Mucosal immune dysfunction in AIDS pathogenesis. *AIDS Rev.* (2008) 10:36–46.
47. Brenchley JM, Price DA, Douek DC. HIV disease: fallout from a mucosal catastrophe? *Nat Immunol.* (2006) 7:235–9. doi: 10.1038/ni1316
48. Tincati C, Merlini E, Braidotti P, Ancona G, Savi F, Tosi D, et al. Impaired gut junctional complexes feature late-treated individuals with suboptimal $CD4^+$ T-cell recovery upon virologically suppressive combination antiretroviral therapy. *AIDS.* (2016) 30:991–1003. doi: 10.1097/QAD.0000000000001015
49. Gori A, Tincati C, Rizzardini G, Torti C, Quirino T, Haarman M, et al. Early impairment of gut function and gut flora supporting a role for alteration of gastrointestinal mucosa in human immunodeficiency virus pathogenesis. *J Clin Microbiol.* (2008) 46:757–8. doi: 10.1128/JCM.01729-07
50. Ellis CL, Ma ZM, Mann SK, Li CS, Wu J, Knight TH, et al. Molecular characterization of stool microbiota in HIV-infected subjects by panbacterial and order-level 16S ribosomal DNA (rDNA) quantification and correlations with immune activation. *J Acquir Immune Defic Syndr.* (2011) 57:363–70. doi: 10.1097/QAI.0b013e31821a603c
51. Dinh DM, Volpe GE, Duffalo C, Bhalchandra S, Tai AK, Kane AV, et al. Intestinal microbiota, microbial translocation, and systemic inflammation in chronic HIV infection. *J Infect Dis.* (2015) 211:19–27. doi: 10.1093/infdis/jiu409
52. Ribeiro ABDT, Heimesaat MM, Bereswill S. Changes of the intestinal microbiome-host homeostasis in HIV-infected individuals - a focus on the bacterial gut microbiome. *Eur J Microbiol Immunol.* (2017) 7:158–67. doi: 10.1556/1886.2017.00016
53. Williams B. Gut microbiome in HIV infection: overcoming barriers? *Dig Dis Sci.* (2019) 64:1725–7. doi: 10.1007/s10620-019-05500-1
54. Chevalier MF, Petitjean G, Dunyach-Rémy C, Didier C, Girard PM, Manea ME, et al. The Th17/Treg ratio, IL-1RA and sCD14 levels in primary HIV infection predict the T-cell activation set point in the absence of systemic microbial translocation. *PLoS Pathog.* (2013) 9:e1003453. doi: 10.1371/journal.ppat.1003453
55. Brenchley JM, Price DA, Schacker TW, Asher TE, Silvestri G, Rao S, et al. Microbial translocation is a cause of systemic immune activation in chronic HIV infection. *Nat Med.* (2006) 12:1365–71. doi: 10.1038/nm1511
56. Kitchens RL, Thompson PA. Modulatory effects of sCD14 and LBP on LPS-host cell interactions. *J Endotoxin Res.* (2005) 11:225–9. doi: 10.1179/096805105X46565
57. Johansson MA, Björkander S, Mata Forsberg M, Qazi KR, Salvany Celades M, Bittmann J, et al. Sverremark-ekström: probiotic lactobacilli modulate staphylococcus aureus-induced activation of conventional and unconventional T cells and NK cells. *Front Immunol.* (2016) 7:273. doi: 10.3389/fimmu.2016.00273
58. Pérez-Santiago J, Gianella S, Massanella M, Spina CA, Karris MY, Var SR, et al. Gut Lactobacillales are associated with higher CD4 and less microbial translocation during HIV infection. *AIDS.* (2013) 27:1921–31. doi: 10.1097/QAD.0b013e3283611816
59. Figliuolo VR, Dos Santos LM, Abalo A, Nanini H, Santos A, Brittes NM, et al. Sulfate-reducing bacteria stimulate gut immune responses and contribute to inflammation in experimental colitis. *Life Sci.* (2017) 189:29–38. doi: 10.1016/j.lfs.2017.09.014
60. Coutinho CMLM, Coutinho-Silva R, Zinkevich V, Pearce CB, Ojcius DM, Beech I. Sulphate-reducing bacteria from ulcerative colitis patients induce apoptosis of gastrointestinal epithelial cells. *Microb Pathog.* (2017) 112:126–34. doi: 10.1016/j.micpath.2017.09.054
61. Gootenberg DB, Paer JM, Luevano JM, Kwon DS. HIV-associated changes in the enteric microbial community: potential role in loss of homeostasis and development of systemic inflammation. *Curr Opin Infect Dis.* (2017) 30:31–43. doi: 10.1097/QCO.0000000000000341
62. Dillon SM, Kibbie J, Lee EJ, Guo K, Santiago ML, Austin GL, et al. Low abundance of colonic butyrate-producing bacteria in HIV infection is associated with microbial translocation and immune activation. *AIDS.* (2017) 31:511–21. doi: 10.1097/QAD.0000000000001366
63. Louis P, Flint HJ. Formation of propionate and butyrate by the human colonic microbiota. *Environ Microbiol.* (2017) 19:29–41. doi: 10.1111/1462-2920.13589
64. Max B, Sherer R. Management of the adverse effects of antiretroviral therapy and medication adherence. *Clin Infect Dis.* (2000) 30(Suppl 2):S96–116. doi: 10.1086/313859
65. Kartalija M, Sande MA. Diarrhea and AIDS in the era of highly active antiretroviral therapy. *Clin Infect Dis.* (1999) 28:701–5; quiz 706–7. doi: 10.1086/515191
66. Ericsen AJ, Lauck M, Mohns MS, DiNapoli SR, Mutschler JP, Greene JM, et al. Microbial translocation and inflammation occur in hyperacute immunodeficiency virus infection and compromise host control of virus replication. *PLoS Pathog.* (2016) 12:e1006048. doi: 10.1371/journal.ppat.1006048
67. Serrano-Villar S, Sanchez-Carrillo S, Talavera-Rodríguez A, Lelouvier B, Gutiérrez C, Vallejo A, et al. Blood bacterial profiles associated with HIV infection and immune recovery. *J Infect Dis.* (2021) 223:471–81. doi: 10.1093/infdis/jiaa379
68. Vujkovic-Cvijin I, Sortino O, Verheij E, Sklar J, Wit FW, Kootstra NA, et al. HIV-associated gut dysbiosis is independent of sexual practice and correlates with noncommunicable diseases. *Nat Commun.* (2020) 11:2448. doi: 10.1038/s41467-020-16222-8
69. Fletcher CV, Staskus K, Wietgrefe SW, Rothenberger M, Reilly C, Chipman JG, et al. Persistent HIV-1 replication is associated with lower antiretroviral drug concentrations in lymphatic tissues. *Proc Natl Acad Sci USA.* (2014) 111:2307–12. doi: 10.1073/pnas.1318249111
70. Mitchell C, Roemer E, Nkwopara E, Robbins B, Cory T, Rue T, et al. Correlation between plasma, intracellular, and cervical tissue levels of raltegravir at steady-state dosing in healthy women. *Antimicrob Agents Chemother.* (2014) 58:3360–5. doi: 10.1128/AAC.02757-13
71. Mueller S, Saunier K, Hanisch C, Norin E, Alm L, Midtvedt T, et al. Differences in fecal microbiota in different European study populations in relation to age, gender, and country: a cross-sectional study. *Appl Environ Microbiol.* (2006) 72:1027–33. doi: 10.1128/AEM.72.2.1027-1033.2006
72. Power SE, O'Toole PW, Stanton C, Ross P, Fitzgerald GF. Intestinal microbiota, diet and health. *Br J Nutr.* (2014) 111:387–402. doi: 10.1017/S0007114513002560
73. Delgado S, Suárez A, Mayo B. Identification of dominant bacteria in feces and colonic mucosa from healthy Spanish adults by culturing and by 16S rDNA sequence analysis. *Dig Dis Sci.* (2006) 51:744–51. doi: 10.1007/s10620-006-3201-4

Conflict of Interest: The authors declare that the research was conducted in the absence of any commercial or financial relationships that could be construed as a potential conflict of interest.

frontiers in Immunology

ORIGINAL RESEARCH
published: 15 March 2021
doi: 10.3389/fimmu.2021.614436

Longitudinal Profiling of Antibody Response in Patients With COVID-19 in a Tertiary Care Hospital in Beijing, China

Xia Feng[1†], Jiming Yin[1,2†], Jiaying Zhang[1†], Yaling Hu[3], Yabo Ouyang[1,2], Shubin Qiao[4], Hong Zhao[5], Tong Zhang[1], Xuemei Li[1], Lili Zhang[1], Jie Zhang[6], Ronghua Jin[1], Yingmei Feng[1] and Bin Su[1*]*

[1] Beijing Youan Hospital, Capital Medical University, Beijing, China, [2] Beijing Institute of Hepatology, Beijing Youan Hospital, Capital Medical University, Beijing, China, [3] Sinovac Biotech Ltd., Beijing, China, [4] Beijing Fengtai Hospital of Integrated Traditional and Western Medicine, Beijing, China, [5] Department of Infectious Diseases, Peking University First Hospital, Beijing, China, [6] Beijing Key Laboratory of Monoclonal Antibody Research and Development, Sino Biological Inc., Beijing, China

The novel coronavirus named severe acute respiratory syndrome coronavirus 2 (SARS-CoV-2) caused a global pandemic of the coronavirus disease 2019 (COVID-19), which elicits a wide variety of symptoms, ranging from mild to severe, with the potential to lead to death. Although used as the standard method to screen patients for SARS-CoV-2 infection, real-time PCR has challenges in dealing with asymptomatic patients and those with an undetectable viral load. Serological tests are therefore considered potent diagnostic tools to complement real-time PCR-based diagnosis and are used for surveillance of seroprevalence in populations. However, the dynamics of the antibody response against SARS-CoV-2 currently remain to be investigated. Here, through analysis of plasma samples from 84 patients with COVID-19, we observed that the response of virus-specific antibodies against three important antigens, RBD, N and S, dynamically changed over time and reached a peak 5–8 weeks after the onset of symptoms. The antibody responses were irrespective of sex. Severe cases were found to have higher levels of antibody response, larger numbers of inflammatory cells and C-reactive protein levels. Within the mild/moderate cases, pairwise comparison indicated moderate association between anti-RBD vs. anti-N, anti-RBD vs. anti-S1S2, and anti-N vs. anti-S1S2. Furthermore, the majority of cases could achieve IgM and IgG seroconversion at 2 weeks since the disease onset. Analysis of neutralizing antibodies indicated that these responses were able to last for more than 112 days but decline significantly after the peak. In summary, our findings demonstrate the longitudinally dynamic changes in antibody responses against SARS-CoV-2, which can contribute to the knowledge of humoral immune response after SARS-CoV-2 infection and are informative for future development of vaccine and antibody-based therapies.

Keywords: COVID-19, SARS-CoV-2, spike, RBD, S antigen, neutralizing antibodies

OPEN ACCESS

Edited by:
Caroline Petitdemange, Institut Pasteur, France

Reviewed by:
Li Ye, Guangxi Medical University, China
Jianhui Nie, National Institutes for Food and Drug Control, China
Fei Xiao, The Fifth Affiliated Hospital of Sun Yat-sen University, China
Cong Jin, Chinese Center for Disease Control and Prevention, China

***Correspondence:**
Bin Su
binsu@ccmu.edu.cn
Yingmei Feng
yingmeif13@ccmu.edu.cn

[†] These authors have contributed equally to this work

Specialty section:
This article was submitted to Viral Immunology, a section of the journal Frontiers in Immunology

Received: *06 October 2020*
Accepted: *22 February 2021*
Published: *15 March 2021*

Citation:
Feng X, Yin J, Zhang J, Hu Y, Ouyang Y, Qiao S, Zhao H, Zhang T, Li X, Zhang L, Zhang J, Jin R, Feng Y and Su B (2021) Longitudinal Profiling of Antibody Response in Patients With COVID-19 in a Tertiary Care Hospital in Beijing, China. Front. Immunol. 12:614436. doi: 10.3389/fimmu.2021.614436

INTRODUCTION

Coronavirus disease 2019 (COVID-19), caused by a novel coronavirus named severe acute respiratory syndrome coronavirus 2 (SARS-CoV-2), has affected over 190 countries and was declared a global public health concern (1, 2). Although extensive efforts have been made to reduce person-to-person transmission of COVID-19 and control the outbreak, the number of cases is still increasing according to the situation report by the World Health Organization (WHO) (3). Globally, on February 13, 2021, more than 107 million cases have been reported, including about 2.3 million deaths caused by the novel coronavirus (3, 4). At this time, Chinese mainland has confirmed 89,763 cases, including 4,636 deaths (5).

The current COVID-19 pandemic rapidly spread globally, making the development of effective countermeasures to cure and prevent this disease a major global priority. It is known that four structural proteins of SARS-CoV-2, spike surface glycoprotein (S), membrane protein (M), envelope protein (E) and nucleocapsid protein (N), are essential for coronavirus assembly and infection (6, 7). S protein is the best studied coronavirus protein. The S protein consists of S1 and S2 subunits, which mediate viral attachment to host cells and fusion, respectively, in the process of infection. To engage the receptor of the host cell, the receptor-binding domain (RBD) at the N-terminal of the S1 subunit undergoes hinge-like conformational alterations (8–12). N protein oligomerizes to form a closed capsule that wraps the genomic coronavirus RNA, providing the first-line defense from the harsh conditions of the host (13–15). S and N proteins are also known as the major immunogens for the antibody response against coronaviruses (10, 14, 16). S protein has epitopes recognized by T and B cells, which can induce the production of neutralizing antibodies (nAbs); therefore, S protein represents a target for antibody-mediated neutralization and diagnostics (17–21). N protein can also potentially induce humoral and T-cell immune responses and be logically chosen as a target antigen for vaccination (22–24).

Serologic assays are urgently required for tracing patient contact, identifying the viral reservoir and conducting epidemiologic studies, although molecular diagnostic tests were rapidly developed to support case identification and track the outbreak of the SARS-CoV-2 pandemic. The ways in which the antibody responds to SARS-CoV-2 remain poorly understood, and specific data on the response of humoral immunity during infection are still unclear (25). In this study, with plasma specimens collected from patients with COVID-19 in a tertiary care hospital in Beijing, we performed longitudinal profiling of IgM and IgG against SARS-CoV-2-neutralizing and RBD-, S1S2- and N-specific antibodies, which revealed the duration of the antiviral immune response and the dynamics of these antibodies during the epidemic outbreak of SARS-CoV-2.

METHODS

Cohort Study

The COVID-19 case definition and clinical classification based on severity were defined according to the New Coronavirus Pneumonia Prevention and Control Protocol for COVID-19 (seventh edition) released by the National Health Commission of China (26). The clinical classification criteria were listed as follows. (1) Mild cases: clinical symptoms were mild without manifestation of pneumonia on imaging; (2) Moderate cases: fever, respiratory symptoms, and with radiological findings of pneumonia; (3) Severe cases: meeting any one of the following criteria: respiratory distress, hypoxia ($SpO2 \leq 93\%$), or abnormal blood gas analysis $PaO_2/FiO_2 \leq 300$ mmHg, or who required mechanical ventilation either invasively or noninvasively (26). Eighty-four patients diagnosed with SARS-CoV-2 from Beijing Youan Hospital, China, from February 03 to May 18, 2020, were enrolled in this study (**Table 1**). Weekly followed-up and SARS-CoV-2 RNA detection were performed timely. The whole follow-up lasted for over 112 days and were divided into 7 time points since symptom onset. The time points were defined as the days after symptom onset in which samples were collected, from the first to seventh time points were days 1–7, 8–14, 15–28, 29–56, 57–84, 85–112, and >112, respectively. The throat swabs from the upper respiratory tract and whole blood were collected from patients at various time-points after hospitalization and during followed-up. Sample collection, processing, and laboratory testing were performed as recommended by China CDC and complied with WHO guidance. All COVID-19 patients were confirmed as infected based on positive results from their respiratory swab samples by RT-PCR tests. None of the study participants was co-infected with HIV, hepatitis B virus/hepatitis C virus, or influenza viruses. All participants do not have a comorbid condition, tuberculosis, autoimmune diseases, or related drug usage. In this study, 3 healthy individuals were recruited as controls, and the code "0" represents the healthy condition.

Ethics Statement

This study and part of the relevant experiments were approved by the Beijing Youan Hospital Research Ethics Committee (No. 2020-037) and written informed consent was obtained from each participant in accordance with the Declaration of Helsinki. The clinical samples were collected for research use. The methods used conformed to approved guidelines and regulations.

Detection of the Antibodies Titer Against SARS-CoV-2

The titer of antibodies against structural protein RBD, N, and S1S2 were determined using indirect enzyme-linked immunosorbent assay (ELISA) kit supplied by Sino Biological Inc. (Cat: KIT004 for anti-S1S2 antibody; Cat: KIT005 for anti-N antibody; Cat: KIT006 for anti-RBD antibody, respectively). Briefly, corresponding recombinant proteins (RBD, N, and S1S2) have been pre-coated onto 96-well plates. The samples which were first diluted at 1:200 before measurement were added to the wells, followed by incubation with goat anti-human IgG conjugated with horseradish peroxidase for 1 h at 37°C after 5 washes with phosphate-buffered saline. The plates were developed using TMB, followed by 2 M sulfuric acid (H_2SO_4) addition to stop the reaction and colors developed in proportion

TABLE 1 | Demographic and clinical characteristics of COVID-19 patients.

Condition	Sex	Chronic respiratory disease	Coronary disease	Hypertension	Diabetes	Respiratory symptoms
Mild/moderate cases	62	1	3	6	7	48
Female	36	0	2	2	3	32
Male	26	1	1	4	4	16
Severe cases	22	1	7	9	2	21
Female	14	1	4	5	2	13
Male	8	0	3	4	0	8
Total	84	2	10	15	9	69

	Mild/moderate cases	Severe cases	*P*-value
Age (years)	44.84 ± 11.98	61.55 ± 14.76	<0.0001
Body temperature (°C)	38.01 ± 0.93	38.43 ± 0.83	0.0683
WBC ($\times 10^9$/L)	4.46 ± 1.55	5.37 ± 1.95	0.0304
NEU ($\times 10^9$/L)	2.69 ± 1.29	3.92 ± 2.08	0.0018
LYM ($\times 10^9$/L)	1.32 ± 0.54	1.03 ± 0.49	0.0177
MNC ($\times 10^9$/L)	0.32 ± 0.14	0.30 ± 0.14	0.0004
CRP (mg/L)	15.93 ± 21.56	54.27 ± 49.08	<0.0001

All the data are expressed as mean ± standard deviation (SD) or n (%). The statistic analysis was performed using t-test, with p-values < 0.05 were considered significant. WBC, White blood cells; NEU, Neutrophils; LYM, Lymphocytes; MNC, Monocytes; CRP, C-Reactive Protein.

to the amount of antibodies. To determine the final result, the ELISA plate was read at 450/630 nm by ELISA plate reader.

Detection of the IgG and IgM Antibodies Against SARS-CoV-2

The IgG and IgM antibodies against SARS-CoV-2 in plasma samples were tested using Immune Capture Colloidal Gold kit (Lot: 20200303) supplied by Bioscience (Yingnuote) Co., Ltd., China (CFDA approved), according to the manufacturer's instructions.

Neutralizing Antibody Titer Assay

The neutralizing antibody titers in plasma were measured by the Reed-Muench method on days 14 and 84 after discharge from the hospital. For calculation of geometric mean titer (GMT), antibody titers of <1:8, >1:512, and >1:1,024 were assigned values of 1:4, 1:(512 + 512/2), and 1:(1,024 + 1,024/2), respectively (27).

The titer of neutralizing antibody in plasma was determined with a modified cytopathogenic assay according to a previously published article (27). Briefly, plasma samples were inactivated at 56°C for 30 min and serially diluted with cell culture medium in 2-fold steps. The diluted plasma was mixed with a virus suspension of 100 CCID50 in 96-well plates at a ratio of 1:1, followed by 2 h incubation at 36.5°C in a 5% CO_2 incubator. Then, 1 – 2 × 10^4 Vero cells were added to the plasma-virus mixture, and the plates were incubated for 5 days at 36.5°C in a 5% CO_2 incubator. The cytopathic effect (CPE) of each well was recorded under microscopes, and the neutralizing titer was assayed by the dilution number of the 50% protective condition.

Statistical Analysis

Statistical difference was analyzed using Student's *t*-tests or Wilcoxon test with GraphPad Prism software version 5.03 (GraphPad Software, San Diego, California, USA). Differences were considered statistically significant at $p < 0.05$.

RESULTS

Demographic and Clinical Characteristics

A total of 84 patients with COVID-19 were enrolled in this study, including 34 males and 50 females. The average age of the patients was 48.85 ± 13.26 years for males and 49.48 ± 15.68 years for females (data is not shown in the **Table 1**). The clinical data for patients' disease history such as chronic respiratory disease, coronary disease, hypertension, and diabetes were summarized in **Table 1** (upper panel). Comparison analysis revealed that severe cases had higher levels of inflammatory cells and C-reactive protein (**Table 1**, down panel).

Enhanced Response of Antibodies Against SARS-CoV-2 Structural Proteins

To assess the response of antibodies against RBD, N, and S1S2, we performed in-house ELISAs to detect their presence in patients throughout the study. First, we compared the levels of these antibodies in patients with those in healthy individuals and observed that they were all markedly increased in patients ($p < 0.001$, **Figures 1A–C**). Furthermore, we classified the patients into two groups according to the severity of COVID-19 at admission and performed pairwise comparisons. For each type of antibody, we also observed that the levels were significantly higher in COVID-19 patients than in healthy controls, and this

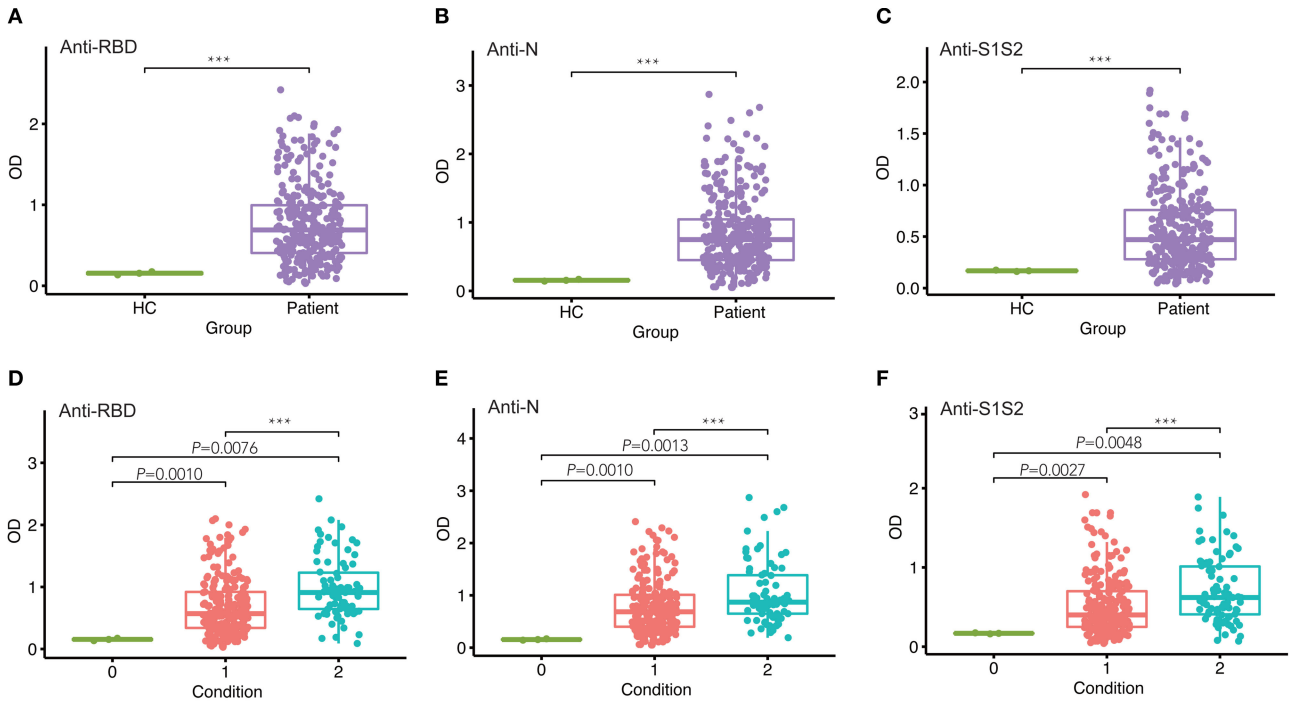

FIGURE 1 | Comparison of antibody responses between different groups. **(A–C)** Comparison of anti-RBD **(A)**, anti-N **(B)**, and anti-S1S2 **(C)** antibody responses between healthy controls (HC) and infected patients. **(D–F)** Pairwise comparison of anti-RBD **(D)**, anti-N **(E)**, and anti-S1S2 **(F)** antibody responses between healthy ("0"), mild/moderate ("1"), and severe ("2") conditions. *P*-values were calculated by Student's *t*-test for **(A–C)** and by one-way ANOVA for **(D–F)**. *P*-values < 0.05 were considered significant, and labeled with ***$P < 0.001$.

rising trend was maintained from mild/moderate conditions to severe conditions (**Figures 1D–F**).

Dynamics of Antibody Levels With Progression and Severity of Disease

Next, we investigated the dynamics of antibody levels throughout the study period. The observations in the period showed that the levels of anti-RBD, anti-N, and anti-S1S2 increased over time and peaked around at the fourth time point and then decreased slowly. These changing patterns were similar among patients in both mild/moderate and severe conditions (**Figure 2A**). Moreover, the levels of antibodies, including anti-RBD (**Figure 2B**), anti-N (**Figure 2C**), and anti-S1S2 (**Figure 2D**), in patients with a severe condition were relatively higher than those in patients with a mild/moderate condition. These differences were prominent in the late stage, especially for the anti-S1S2 antibody from the fourth to sixth time points.

In addition, we performed the same comparisons for the antibody levels between female and male patients. The dynamics of antibodies against N, RBD, and S1S2 proteins displayed similar wave patterns as those shown in previous analyses (**Figures 2A**, **3A**). Moreover, for the three types of antibodies at each time point, there were no differences between female and male patients (**Figures 3B–D**). These findings suggest that the levels of antibodies against the main SARS-CoV-2 immunogenic proteins are related to the progression and severity of COVID-19.

Furthermore, we screened 6 patients who had good follow-up compliance and observed their antibody responses individually. We collected plasma samples from these patients at 6 time points (first through the sixth). By the discharge time at the third time point, all patients except one exhibited the peak of the anti-RBD antibody (**Figure 4A**). In contrast, all patients achieved the peak response of anti-N antibody by that time (**Figure 4B**), and for the response of anti-S1S2 antibody, we observed that the peak response in three patients lagged until the fourth time point. Moreover, two patients had a rebounded response to anti-S1S2 antibody at the sixth time point (**Figure 4C**).

Dynamics of Antibody Seroconversion in Patients Since Symptom Onset

Among 84 patients, 66.7% (56/84) were positive for virus-specific IgM during the 4-month observation period. One patient was found to be positive for IgM on the day of symptom onset, and the last positive detection among the remaining patients who had IgM positive conversion was on the sixteenth day after symptom onset. Among IgM-positive patients, 57.1% (48/56) finally underwent IgM seronegative conversion, which occurred as early as day 32 after symptom onset. The median day of seronegative conversion for IgM was 57 (range: 19–82 days) after symptom onset. Eighty-four patients were all positive for virus-specific IgG, which became detectable as early as day 3 and as late as day 16 after symptom onset. However, 15.5% (13/84) underwent seronegative conversion, which occurred as early as day 51 after symptom onset. Among these patients with

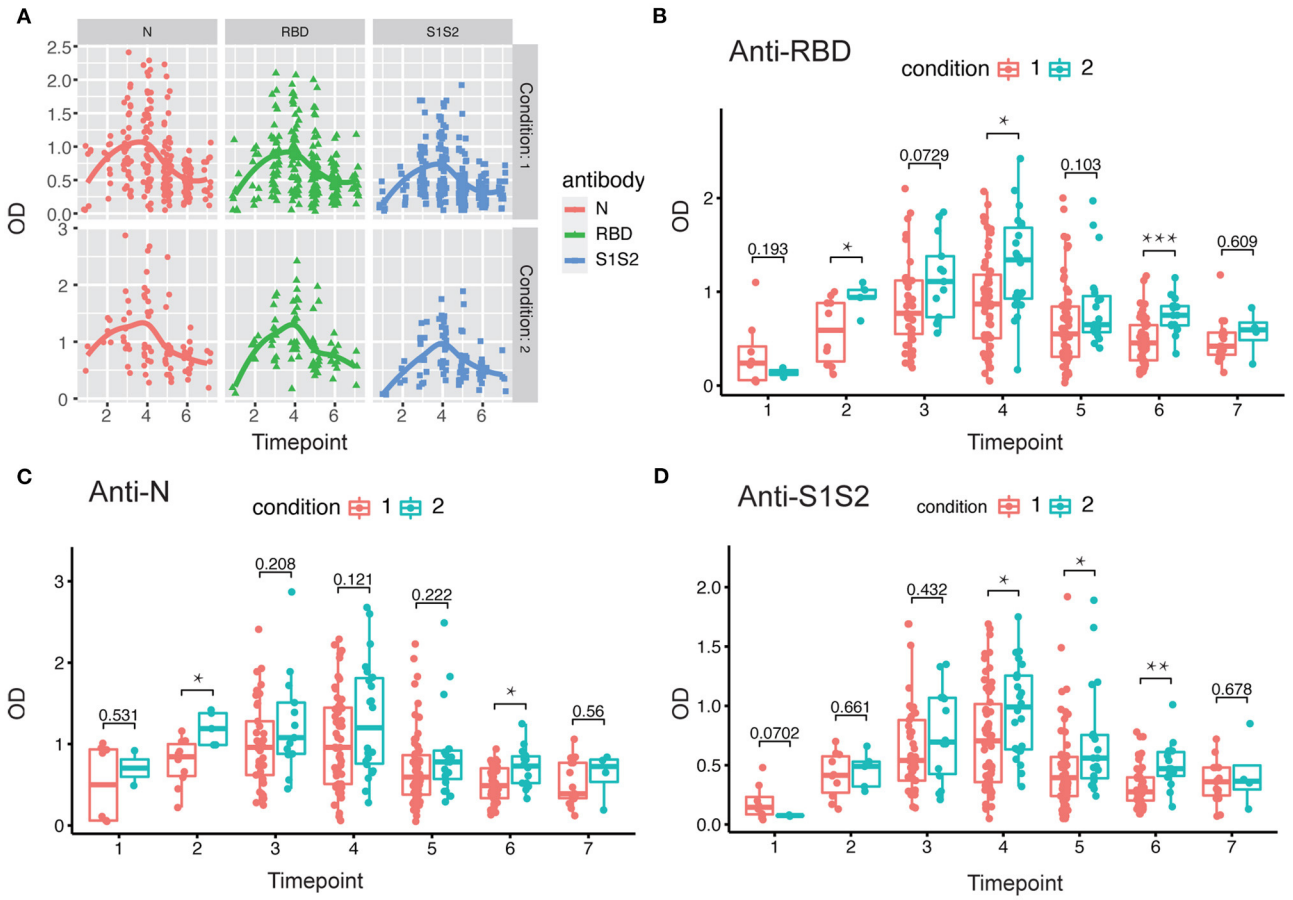

FIGURE 2 | Evaluation of antibody response between mild/moderate and severe patients. **(A)** Response of antibodies (anti-N, anti-RBD, and anti-S1S2) between mild/moderate and severe patients. **(B–D)** Comparison of anti-RBD **(B)**, anti-N **(C)**, and anti-S1S2 **(D)** antibody responses between mild/moderate ("1") and severe ("2") patients. Time points 1–7 represent days 1–7, 8–14, 15–28, 29–56, 57–84, 85–112, and >112, respectively, after symptom onset. *P*-values were calculated by Student's *t*-test. *P*-values < 0.05 were considered significant with *, **, and *** indicate $p < 0.05$, <0.01, and <0.001, respectively.

seronegative conversion, 92.3% (12/13) had a mild/moderate condition, and 7.7% (1/13) were had a critical condition. The negative seroconversion for IgG did not display a significant difference between mild/moderate and severe patients ($p > 0.05$, $\chi^2 = 2.722$). Overall, the longitudinal changes in virus-specific IgM and IgG antibodies in all patients are shown in **Figure 5**. The proportion of patients with detectable IgM reached 67% at the first time point (day 1–7 after onset), while the proportions of patients with detectable IgG were almost equal to 50% in the same monitoring period. The proportions of IgM- and IgG-positive patients reached 94 and 100%, respectively, at the peak in the second time point. Subsequently, the proportion of IgM-positive patients showed a rapid decrease over time, while the proportion of IgG-positive patients maintained relatively stable. Only from the fourth time point (day 29–56) did the proportion of IgG-positive patients decrease slightly.

Decline in Neutralizing Activities Over Time

Finally, we evaluated changes in the levels of nAbs against SARS-CoV-2 by measuring the titers of nAbs in 49 plasma samples collected at the first time point and the last time point during the monitoring period after discharge. The interval between two sampling times was approximately 2 months. The first sampling took place around the third or fourth time points (14 days after discharge), and the second sampling took place around the sixth time point (84 days after discharge). Initially, we compared the levels of nAbs between patients with a mild/moderate condition and severe condition. The results showed that there was no difference between these conditions either at the first follow-up monitoring at day 14 (**Figure 6A**) or the second follow-up monitoring at day 84 after discharge (**Figure 6B**). However, we performed a paired comparison for the levels of nAbs between the two follow-ups and found that there was an obvious decline in nAb levels over the period (**Figure 6C**). Furthermore, the remarkable change of nAb levels was found to maintain in mild/moderate patients (**Figure 6D**) instead of severe ones (**Figure 6E**), suggesting that the response of nAbs has to do with the disease conditions. Taken together, our study highlights the need for prospective serology studies assurance to better understand the humoral response to SARS-CoV-2 infection.

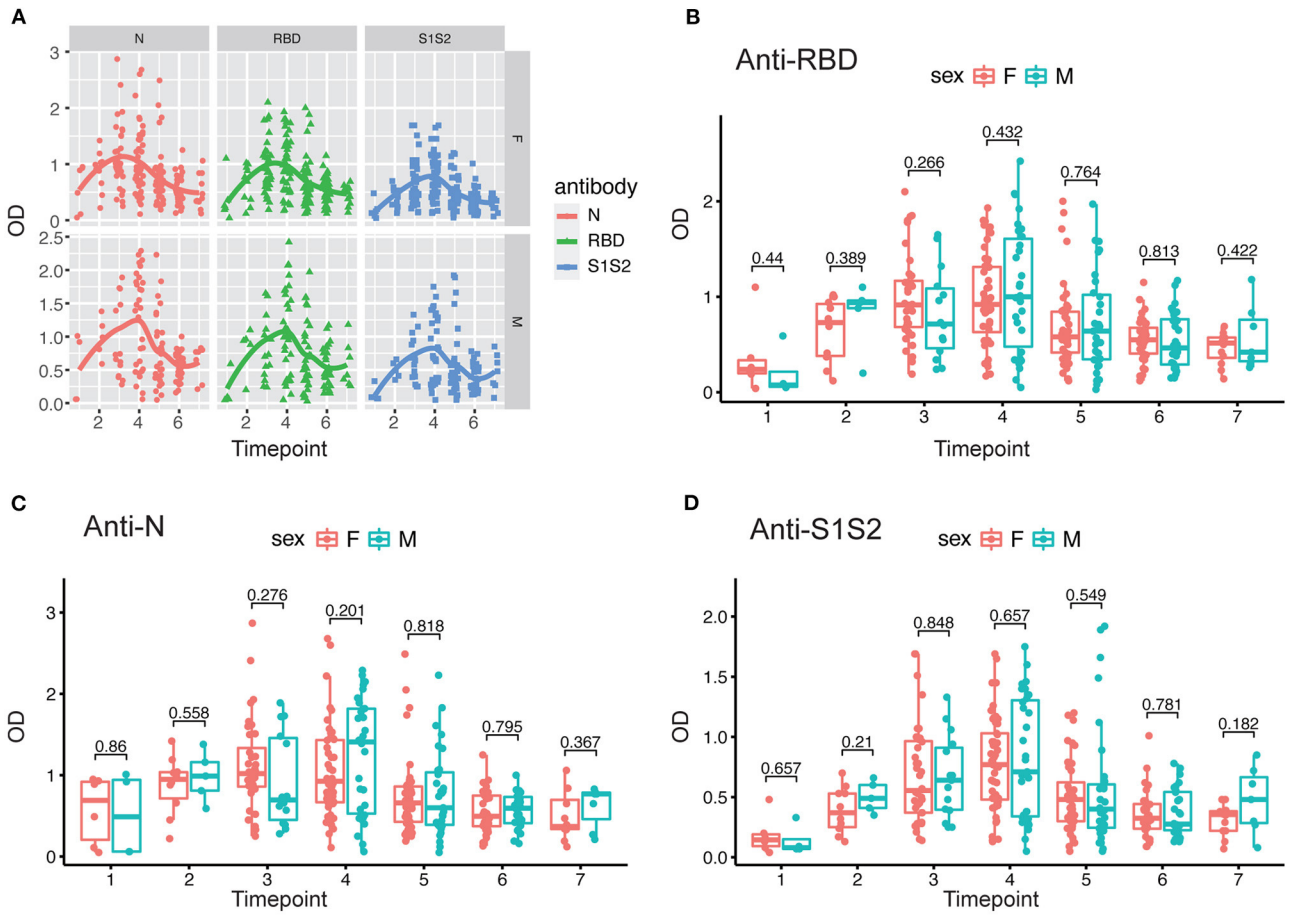

FIGURE 3 | Evaluation of antibody response between female and male patients. **(A)** Response of antibodies (anti-N, anti-RBD, and anti-S1S2) between female and male patients. **(B–D)** Comparison of anti-RBD **(B)**, anti-N **(C)**, and anti-S2S2 **(D)** antibody responses between female ("F") and male ("M") patients. Time points 1–7 represent days 1–7, 8–14, 15–28, 29–56, 57–84, 85–112, and >112, respectively, after symptom onset. *P*-values were calculated by Student's *t*-test, and *p*-values < 0.05 were considered significant.

DISCUSSION

In this study, we aimed to assess SARS-CoV-2 seroprevalence in patients hospitalized in a tertiary care hospital in Beijing as well as to evaluate longitudinal changes in antibody levels within the first 4 months after onset of disease and how the changes correlate with sex and COVID-19 symptoms. We tested plasma samples and monitored the dynamic changes in anti-RBD, anti-N, and anti-S1S2 antibodies in 84 COVID-19 patients (62 mild/moderate cases and 22 severe cases). Our results showed that antibodies were elicited against RBD, N, and S1S2 of SARS-CoV-2 over time, and in general, all the antibodies reached a peak 5–8 weeks after symptom onset. The three antibodies presented similar profiles regardless of patient condition and sex. The duration of antiviral antibodies could last for more than 112 days. However, the levels of antibodies (anti-RBD, anti-N, and anti-S1S2) were significantly higher in patients with a severe condition (**Figures 1**–**3**). Another difference was that anti-RBD and anti-N antibodies appeared to synchronously achieve seroconversion and reached a peak approximately 2–3 weeks after onset, while anti-S1S2 antibodies in some patients reached a peak more than 4 weeks after onset (**Figure 4**). In addition, we assessed the correlations among the anti-RBD, anti-N, and anti-S1S2 antibody levels at the discharge time point, and they exhibited moderate relationships with each other (anti-RBD vs. anti-N, $r = 0.76$; anti-RBD vs. anti-S1S2, $r = 0.83$; and anti-N vs. anti-S1S2, $r = 0.73$, respectively). We further performed multiple regression analyses with condition, sex and age as independent covariates and the antibody levels as the response; this analysis showed that none of these factors were significant (data not shown), probably due to small sample sizes.

In addition, the proportion of IgM seropositive conversion was higher than that of IgG the first week after symptom onset, which is consistent with the wide recognition that IgM provides the first line of defense during viral infection. Accordingly, IgM detection in the plasma also revealed the proportion of patients who had a recent exposure to SARS-CoV-2, while IgG detection suggested that the exposure happened several days before and

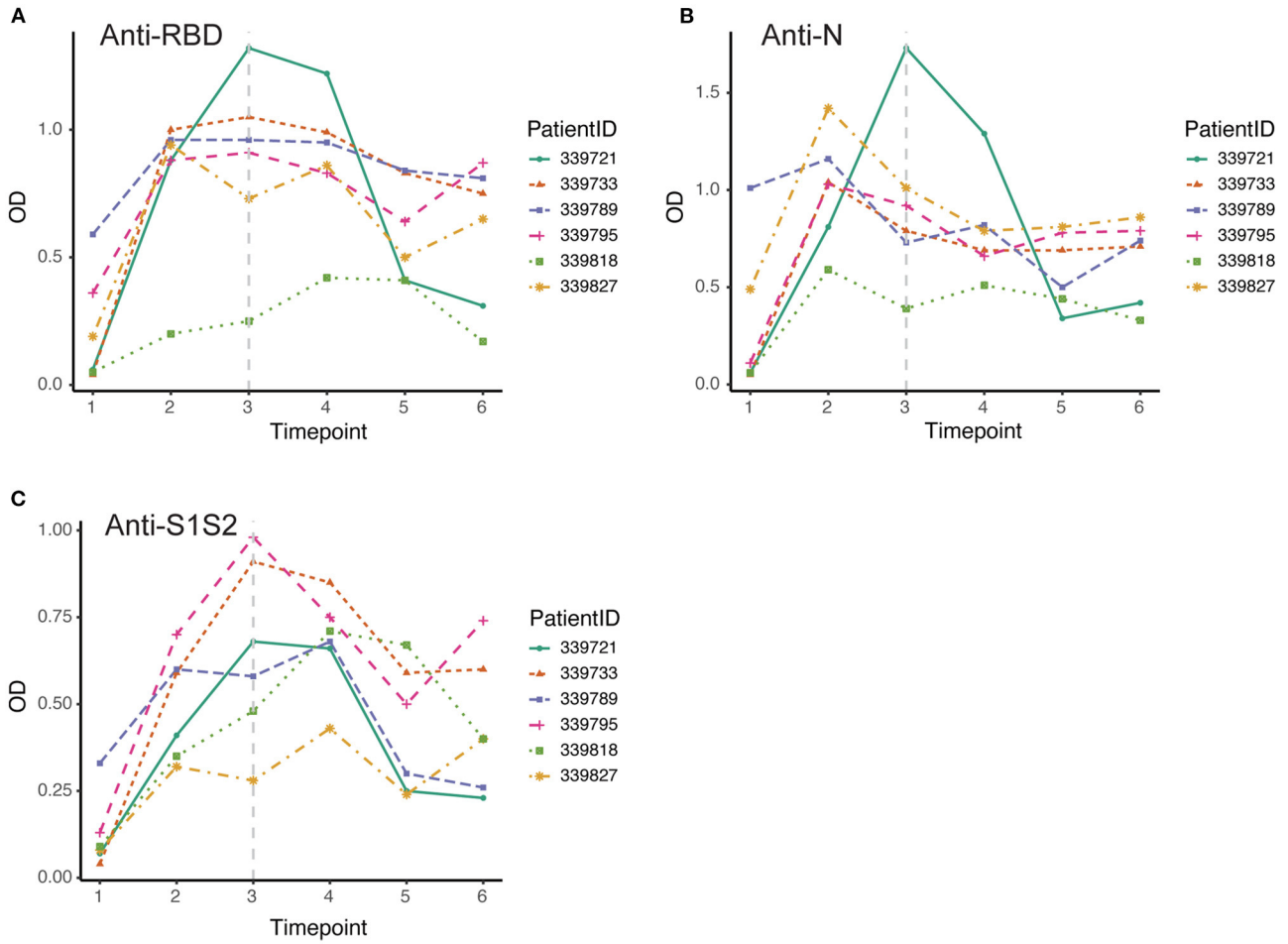

FIGURE 4 | Dynamic changes in antibodies against SARS-CoV-2 structural proteins. **(A–C)** Dynamic changes in anti-RBD antibody **(A)**, anti-N antibody **(B)** and anti-S1S2 **(C)** in representative patients over the monitoring period. Time points 1–6 represent days 1–7, 8–14, 15–28, 29–56, 57–84, and 85–112, respectively, after symptom onset. The gray vertical dashed line indicates the approximate time of discharge.

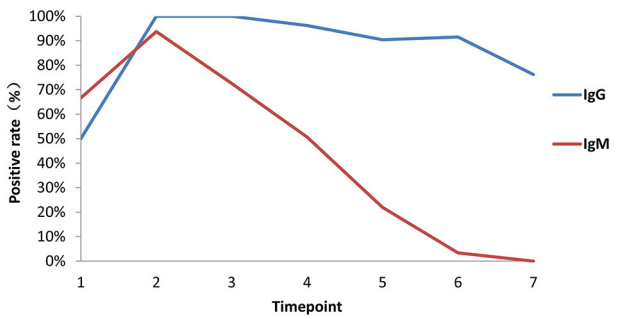

FIGURE 5 | Proportions of patients with seroconversion of IgM and IgG changes. Positive rates of virus-specific IgG (blue) and IgM (red) at different times in 84 plasma samples. Time points 1–7 represent days 1–7, 8–14, 15–28, 29–56, 57–84, 85–112, and >112, respectively, after symptom onset.

in the recovery phase. However, in most cases, it is difficult to accurately determine the exact time when a patient contracted the virus. The proportion of IgM conversion increased to the highest level (94%) 2 weeks after symptom onset, while that of IgG conversion reached 100% at the same time point. After the peak, both IgM and IgG declined, but IgM dropped more rapidly over time (**Figure 5**). Moreover, nAbs also showed a significant decline, reflecting the recovery of disease and clearance of viruses (**Figures 5**, **6**), consistent with other studies (28, 29). However, in our study, among the 49 samples of neutralizing activities, 37 cases decreased, 4 cases unchanged, and 8 cases increased, suggesting that the dynamic change of neutralizing responses varied greatly in individuals, but it tended to decline as a whole. Further studies are required to investigate this mechanism. Taken together, our findings raise concern that humoral immunity against SARS-CoV-2 may not be long lasting in persons with mild/moderate illness, who compose the majority of persons with COVID-19 (28).

Serologic assays are crucial for patient contact tracing and epidemiologic studies. Since the critical components of SARS-CoV-2, S and N proteins, are essential for the mediation of viral infection, they have already received much attention in studies on induced antibody responses (19, 20, 30–38). As described

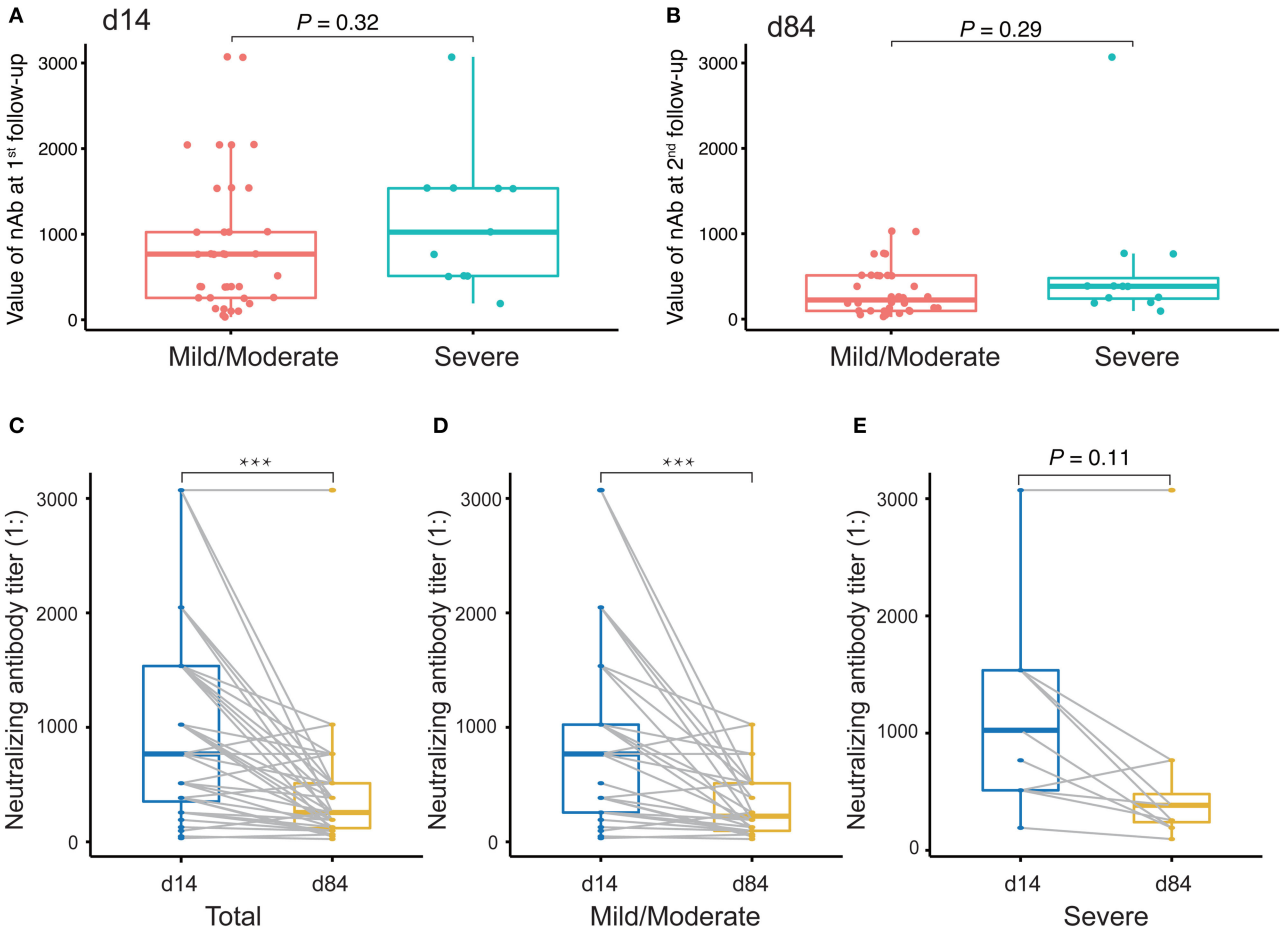

FIGURE 6 | Evaluation of neutralizing antibody (nAb) levels in COVID-19 patients discharged. **(A,B)** Unpaired *t*-test analysis to compare nAb levels in COVID-19 patients discharged between mild/moderate condition and severe condition at the first follow-up (at day 14 after discharge, **A**) and at the second follow-up (at day 84 after discharge, **B**). **(C–E)** Paired *t*-test analysis to compare nAb levels in patients between the first and the second follow-ups for both mild/moderate and severe conditions **(C)** as well as for each conditions, mild/moderate **(D)** and severe **(E)**, respectively. *P*-values < 0.05 were considered significant and labeled with $^{***}P < 0.001$.

in previous studies (39), our findings showed that the humoral immune response could be maintained for approximately 4 months (>112 days). However, almost all reports are based on a limited number of cases due to the urgent situation. These reports also have some discrepancies between each other with regard to the time of antibody response or seroconversion or the levels of antibodies or the proportions of seroconversion, probably because there is a lack of uniform standards for enrollment of study subjects or in-house assay development. Therefore, it is necessary to gather more information on the antibody response during the process of COVID-19 infection to provide more comprehensive and accurate knowledge. For example, in our study, only 66.7% of cases (56/84) showed positive IgM conversion, while Zhao et al. reported a ratio up to 82.7% (143/173) (32). Moreover, studying antibody responses can provide important clues for the development of vaccines and therapeutic antibodies for the prevention of the disease. S and N proteins, as critical immunogens, have been proposed to have the most clinically relevant value to provide protection against coronaviral infection. Recently, animal experiments demonstrated that the spike protein of SARS-CoV-2 can trigger strong protective antibody responses in rabbits (16). In addition, the combination of subunit vaccines with appropriate adjuvants may provide a good strategy for early clinical development (40).

Like others, our study has some limitations. First, due to the small sample size of patients with severe conditions, it is difficult to draw conclusions on the relationship between antibody response and clinical course. Second, because of the limited number of longitudinal plasma samples from the patients, it was also difficult to accurately assess the seroconversion time. Consequently, if the levels of antibodies are not high enough at the time of measurement, false negatives could be recorded. Therefore, a larger number of longitudinal samples is needed. Indeed, further investigation is needed to determine the reasons for negative IgM results in patients (28/84), and asymptomatic patients with an undetectable viral load. Previous studies showed possible reasons, including extreme low viral load and insufficient sensitivity of kit detection,

limitation of specimen types and irregular collection and intermittent virus shedding (41). Nevertheless, our findings contribute additional clinical information to the knowledge of antibody response during SARS-CoV-2 infection. As virological detection of SARS-CoV-2 through RT-PCR has limitations for surveillance, serological tests can detect if a person has been infected even months after viral clearance, which with very high sensitivity and specificity can be an important complementary approach (42, 43).

Taken together, our findings can benefit local researchers estimating the extent of the spread of the COVID-19 pandemic, provide comprehensive information on kinetics and neutralizing antibody responses in COVID-19 patients, and will improve our understanding for the development of vaccines as well as shed light on diagnosis, prognosis, and other treatments of SARS-CoV-2 infection (44).

DATA AVAILABILITY STATEMENT

The original contributions presented in the study are included in the article/supplementary material, further inquiries can be directed to the corresponding author/s.

ETHICS STATEMENT

The studies involving human participants were reviewed and approved by the Beijing Youan Hospital Research Ethics Committee (No. 2020-037) and written informed consent was obtained from each participant in accordance with the Declaration of Helsinki. The clinical samples were collected for research use. The methods used conformed to approved guidelines and regulations.

AUTHOR CONTRIBUTIONS

BS, YF, and RJ conceived the study, designed the experiments, and analyzed the data. XF, JY, JiaZ, YH, YO, SQ, HZ, XL, LZ, and JieZ performed the experiments, carried out the data collection and data analysis. TZ, RJ, and YF contributed to reagents and materials. XF, JY, and BS wrote the article and revised the manuscript. BS supervised the manuscript. All authors read and approved the final manuscript.

FUNDING

This work was supported by the National Natural Science Foundation of China (81772165 and 81974303), the Ministry of Science and Technology of the People's Republic of China (2020YFC0844900, 2020YFC0841700, and 2020YFC0848700), the Beijing Municipal of Science and Technology Major Project (Z201100005520062, Z201100005420018, and Z201100005420022), Beijing Municipal Administration of Hospitals Incubating Program (PX2021701), and the China Primary Health Care Foundation-Youan Medical Development Fund (BJYAYY-2020PY-01, BJYAYY-2020PY-05, and BJYAYY-2020ZQN-06). The funders had no role in study design, data collection and analysis, decision to publish, or preparation of the manuscript.

ACKNOWLEDGMENTS

The authors gratefully appreciated the participation of patients in this study. We thank Drs. Bing Xu and Wei Nie for their excellent assistance for sample preparation and data processing. We also thank Beijing MicroFuture Technology Co., Ltd. for its help in bioinformatics and statistical analysis.

REFERENCES

1. Rasmussen SA, Jamieson DJ. Public health decision making during Covid-19 - fulfilling the CDC pledge to the American people. *N Engl J Med.* (2020) 383:901–3. doi: 10.1056/NEJMp2026045
2. Ayenigbara IO. COVID-19: an international public health concern. *Cent Asian J Glob Health.* (2020) 9:e466. doi: 10.5195/cajgh.2020.466
3. *WHO Coronavirus Disease (COVID-19) Dashboard*. (2021). Available online at: https://covid19.who.int/ (accessed February 13, 2021).
4. World Health Organization. *Weekly Operational Update on COVID-19*. Available online at: https://www.who.int/publications/m/item/weekly-operational-update-on-covid-19---13-february-2021 (accessed February 13, 2021).
5. National Health Commission of the People's Republic of China. Available online at: http://www.nhc.gov.cn/cms-search/xxgk/getManuscriptXxgk.htm?id=6fc9a52ca4bd4a34b4c57330a2351cae (accessed February 13, 2021).
6. Wu F, Zhao S, Yu B, Chen YM, Wang W, Song ZG, et al. A new coronavirus associated with human respiratory disease in China. *Nature.* (2020) 579:265–9. doi: 10.1038/s41586-020-2008-3
7. Chen Y, Liu Q, Guo D. Emerging coronaviruses: genome structure, replication, and pathogenesis. *J Med Virol.* (2020) 92:2249. doi: 10.1002/jmv.26234
8. Wrapp D, Wang N, Corbett KS, Goldsmith JA, Hsieh CL, Abiona O, et al. Cryo-EM structure of the 2019-nCoV spike in the prefusion conformation. *Science.* (2020) 367:1260–3. doi: 10.1126/science.abb2507
9. Shang J, Wan Y, Liu C, Yount B, Gully K, Yang Y, et al. Structure of mouse coronavirus spike protein complexed with receptor reveals mechanism for viral entry. *PLoS Pathog.* (2020) 16:e1008392. doi: 10.1371/journal.ppat.1008392
10. Ou X, Liu Y, Lei X, Li P, Mi D, Ren L, et al. Characterization of spike glycoprotein of SARS-CoV-2 on virus entry and its immune cross-reactivity with SARS-CoV. *Nat Commun.* (2020) 11:1620. doi: 10.1038/s41467-020-15562-9
11. Lan J, Ge J, Yu J, Shan S, Zhou H, Fan S, et al. Structure of the SARS-CoV-2 spike receptor-binding domain bound to the ACE2 receptor. *Nature.* (2020) 581:215–20. doi: 10.1038/s41586-020-2180-5
12. Hoffmann M, Kleine-Weber H, Schroeder S, Kruger N, Herrler T, Erichsen S, et al. SARS-CoV-2 cell entry depends on ACE2 and TMPRSS2 and is blocked by a clinically proven protease inhibitor. *Cell.* (2020) 181:271–80.e278. doi: 10.1016/j.cell.2020.02.052
13. Zeng W, Liu G, Ma H, Zhao D, Yang Y, Liu M, et al. Biochemical characterization of SARS-CoV-2 nucleocapsid protein. *Biochem Biophys Res Commun.* (2020) 527:618–23. doi: 10.1016/j.bbrc.2020.04.136
14. Ye Q, West AMV, Silletti S, Corbett KD. Architecture and self-assembly of the SARS-CoV-2 nucleocapsid protein. *Protein Sci.* (2020) 29:1890–901. doi: 10.1002/pro.3909
15. Dutta NK, Mazumdar K, Gordy JT. The nucleocapsid protein of SARS-CoV-2: a target for vaccine development. *J Virol.* (2020) 94:e00647–20. doi: 10.1128/JVI.00647-20

16. Ravichandran S, Coyle EM, Klenow L, Tang J, Grubbs G, Liu S, et al. Antibody signature induced by SARS-CoV-2 spike protein immunogens in rabbits. *Sci Transl Med.* (2020) 12:eabc3539. doi: 10.1126/scitranslmed.abc3539
17. Walls AC, Park YJ, Tortorici MA, Wall A, McGuire AT, Veesler D. Structure, function, and antigenicity of the SARS-CoV-2 spike glycoprotein. *Cell.* (2020) 181:281–92.e286. doi: 10.1016/j.cell.2020.02.058
18. Tian X, Li C, Huang A, Xia S, Lu S, Shi Z, et al. Potent binding of 2019 novel coronavirus spike protein by a SARS coronavirus-specific human monoclonal antibody. *Emerg Microbes Infect.* (2020) 9:382–5. doi: 10.1080/22221751.2020.1729069
19. Ju B, Zhang Q, Ge J, Wang R, Sun J, Ge X, et al. Human neutralizing antibodies elicited by SARS-CoV-2 infection. *Nature.* (2020) 584:115–9. doi: 10.1038/s41586-020-2380-z
20. Cao Y, Su B, Guo X, Sun W, Deng Y, Bao L, et al. Potent neutralizing antibodies against SARS-CoV-2 identified by high-throughput single-cell sequencing of convalescent patients' B cells. *Cell.* (2020) 182:73–84.e16. doi: 10.1016/j.cell.2020.05.025
21. Rongqing Z, Li M, Song H, Chen J, Ren W, Feng Y, et al. Early detection of severe acute respiratory syndrome coronavirus 2 antibodies as a serologic marker of infection in patients with coronavirus disease 2019. *Clin Infect Dis.* (2020) 71:2066–72. doi: 10.1093/cid/ciaa523
22. Noorimotlagh Z, Karami C, Mirzaee SA, Kaffashian M, Mami S, Azizi M. Immune and bioinformatics identification of T cell and B cell epitopes in the protein structure of SARS-CoV-2: a systematic review. *Int Immunopharmacol.* (2020) 86:106738. doi: 10.1016/j.intimp.2020.106738
23. McAndrews KM, Dowlatshahi DP, Dai J, Becker LM, Hensel J, Snowden LM, et al. Heterogeneous antibodies against SARS-CoV-2 spike receptor binding domain and nucleocapsid with implications for COVID-19 immunity. *JCI Insight.* (2020) 5:e142386. doi: 10.1172/jci.insight.142386
24. Buchholz UJ, Bukreyev A, Yang L, Lamirande EW, Murphy BR, Subbarao K, et al. Contributions of the structural proteins of severe acute respiratory syndrome coronavirus to protective immunity. *Proc Natl Acad Sci USA.* (2004) 101:9804–9809. doi: 10.1073/pnas.0403492101
25. Siracusano G, Pastori C, Lopalco L. Humoral immune responses in COVID-19 patients: a window on the state of the art. *Front Immunol.* (2020) 11:1049. doi: 10.3389/fimmu.2020.01049
26. National Health Commission of the People's Republic of China (2020). Available online at: http://www.nhc.gov.cn/yzygj/s7653p/202003/46c9294a7dfe4cef80dc7f5912eb1989.shtml (accessed March 3, 2020).
27. Wang X, Guo X, Xin Q, Pan Y, Hu Y, Li J, et al. Neutralizing antibody responses to severe acute respiratory syndrome coronavirus 2 in coronavirus disease 2019 inpatients and convalescent patients. *Clin Infect Dis.* (2020) ciaa721:1–7. doi: 10.1093/cid/ciaa721
28. Ibarrondo FJ, Fulcher JA, Goodman-Meza D, Elliott J, Hofmann C, Hausner MA, et al. Rapid decay of anti-SARS-CoV-2 antibodies in persons with mild Covid-19. *N Engl J Med.* (2020) 383:1085–7. doi: 10.1056/NEJMc2025179
29. Korte W, Buljan M, Rosslein M, Wick P, Golubov V, Jentsch J, et al. SARS-CoV-2 IgG and IgA antibody response is gender dependent; and IgG antibodies rapidly decline early on. *J Infect.* (2020) 82:e11–4. doi: 10.1016/j.jinf.2020.08.032
30. Robbiani DF, Gaebler C, Muecksch F, Lorenzi JCC, Wang Z, Cho A, et al. Convergent antibody responses to SARS-CoV-2 in convalescent individuals. *Nature.* (2020) 584:437–42. doi: 10.1038/s41586-020-2456-9
31. Brochot E, Demey B, Handala L, Francois C, Duverlie G, Castelain S. Comparison of different serological assays for SARS-CoV-2 in real life. *J Clin Virol.* (2020) 130:104569. doi: 10.1016/j.jcv.2020.104569
32. Zhao J, Yuan Q, Wang H, Liu W, Liao X, Su Y, et al. Antibody responses to SARS-CoV-2 in patients with novel coronavirus disease 2019. *Clin Infect Dis.* (2020) 71:2027–34. doi: 10.1093/cid/ciaa344
33. Zhang L, Pang R, Xue X, Bao J, Ye S, Dai Y, et al. Anti-SARS-CoV-2 virus antibody levels in convalescent plasma of six donors who have recovered from COVID-19. *Aging.* (2020) 12:6536–42. doi: 10.18632/aging.103102
34. Wang K, Long QX, Deng HJ, Hu J, Gao QZ, Zhang GJ, et al. Longitudinal dynamics of the neutralizing antibody response to SARS-CoV-2 infection. *Clin Infect Dis.* (2020) ciaa1143. doi: 10.1093/cid/ciaa1143
35. Shu H, Wang S, Ruan S, Wang Y, Zhang J, Yuan Y, et al. Dynamic changes of antibodies to SARS-CoV-2 in COVID-19 patients at early stage of outbreak. *Virol Sin.* (2020) 35:744–51. doi: 10.1007/s12250-020-00268-5
36. Wang Y, Zhang L, Sang L, Ye F, Ruan S, Zhong B, et al. Kinetics of viral load and antibody response in relation to COVID-19 severity. *J Clin Invest.* (2020) 130:5235–44. doi: 10.1172/JCI138759
37. Wang P, Liu L, Nair MS, Yin MT, Luo Y, Wang Q, et al. SARS-CoV-2 neutralizing antibody responses are more robust in patients with severe disease. *Emerg Microbes Infect.* (2020) 9:2091–3. doi: 10.1080/22221751.2020.1823890
38. Long QX, Liu BZ, Deng HJ, Wu GC, Deng K, Chen YK, et al. Antibody responses to SARS-CoV-2 in patients with COVID-19. *Nat Med.* (2020) 26:845–8. doi: 10.1038/s41591-020-0897-1
39. Gudbjartsson DF, Norddahl GL, Melsted P, Gunnarsdottir K, Holm H, Eythorsson E, et al. Humoral immune response to SARS-CoV-2 in Iceland. *N Engl J Med.* (2020) 383:1724–34. doi: 10.1056/NEJMoa2026116
40. Shang W, Yang Y, Rao Y, Rao X. The outbreak of SARS-CoV-2 pneumonia calls for viral vaccines. *NPJ Vaccines.* (2020) 5:18. doi: 10.1038/s41541-020-0170-0
41. Guo X, Zeng L, Huang Z, He Y, Zhang Z, Zhong Z. Longer duration of SARS-CoV-2 infection in a case of mild COVID-19 with weak production of the specific IgM and IgG antibodies. *Front Immunol.* (2020) 11:1936. doi: 10.3389/fimmu.2020.01936
42. Zhang Z, Bi Q, Fang S, Wei L, Wang X, He J, et al. Insight into the practical performance of RT-PCR testing for SARS-CoV-2 using serological data: a cohort study. *Lancet Microbe.* (2021) 2:e79–87. doi: 10.1016/S2666-5247(20)30200-7
43. Lisboa Bastos M, Tavaziva G, Abidi SK, Campbell JR, Haraoui LP, Johnston JC, et al. Diagnostic accuracy of serological tests for covid-19: systematic review and meta-analysis. *BMJ.* (2020) 370:m2516. doi: 10.1136/bmj.m2516
44. Jeyanathan M, Afkhami S, Smaill F, Miller MS, Lichty BD, Xing Z. Immunological considerations for COVID-19 vaccine strategies. *Nat Rev Immunol.* (2020) 20:615–32. doi: 10.1038/s41577-020-00434-6

Conflict of Interest: YH was employed by Sinovac Biotech Ltd. JZ was employed by Sino Biological Inc.

The remaining authors declare that the research was conducted in the absence of any commercial or financial relationships that could be construed as a potential conflict of interest.

frontiers in Immunology

PERSPECTIVE
published: 24 March 2021
doi: 10.3389/fimmu.2021.649567

COVID-19 and HIV-Associated Immune Reconstitution Inflammatory Syndrome: Emergence of Pathogen-Specific Immune Responses Adding Fuel to the Fire

Nabila Seddiki[1,2†] *and Martyn French*[3,4*]

[1] Inserm, U955, Equipe 16, Créteil, 94000, France, Université Paris Est, Faculté de Médecine, Créteil, France, [2] Vaccine Research Institute (VRI), Créteil, France, [3] School of Biomedical Sciences, University of Western Australia, Perth, WA, Australia, [4] Division of Immunology, PathWest Laboratory Medicine, Perth, WA, Australia

OPEN ACCESS

Edited by:
Nicholas Funderburg,
The Ohio State University,
United States

Reviewed by:
Namal P. M. Liyanage,
The Ohio State University,
United States
Stephen Rawlings,
University of California, San Diego,
United States

***Correspondence:**
Martyn French
martyn.french@uwa.edu.au

†Present address
Nabila Seddiki,
IDMIT Department/IBFJ, Immunology of Viral Infections and Autoimmune Diseases (IMVA), INSERM U1184, CEA, Université Paris Sud, Fontenay-aux-Roses, France

Specialty section:
This article was submitted to Viral Immunology, a section of the journal Frontiers in Immunology

Received: 05 January 2021
Accepted: 08 March 2021
Published: 24 March 2021

Citation:
Seddiki N and French M (2021) COVID-19 and HIV-Associated Immune Reconstitution Inflammatory Syndrome: Emergence of Pathogen-Specific Immune Responses Adding Fuel to the Fire. Front. Immunol. 12:649567. doi: 10.3389/fimmu.2021.649567

Both coronavirus disease 2019 (COVID-19) and mycobacterial immune reconstitution inflammatory syndrome (IRIS) in patients with HIV-1 infection result from immunopathology that is characterized by increased production of multiple pro-inflammatory chemokines and cytokines associated with activation of myeloid cells (monocytes, macrophages and neutrophils). We propose that both conditions arise because innate immune responses generated in the absence of effective adaptive immune responses lead to monocyte/macrophage activation that is amplified by the emergence of a pathogen-specific adaptive immune response skewed towards monocyte/macrophage activating activity by the immunomodulatory effects of cytokines produced during the innate response, particularly interleukin-18. In mycobacterial IRIS, that disease-enhancing immune response is dominated by a Th1 $CD4^+$ T cell response against mycobacterial antigens. By analogy, it is proposed that in severe COVID-19, amplification of monocyte/macrophage activation results from the effects of a SARS-CoV-2 spike protein antibody response with pro-inflammatory characteristics, including high proportions of IgG3 and IgA2 antibodies and afucosylation of IgG1 antibodies, that arises from B cell differentiation in an extra-follicular pathway promoted by activation of mucosa-associated invariant T cells. We suggest that therapy for the hyperinflammation underlying both COVID-19 and mycobacterial IRIS might be improved by targeting the immunomodulatory as well as the pro-inflammatory effects of the 'cytokine storm'.

Keywords: COVID-19, immune reconstitution inflammatory syndrome, SARS-CoV-2, human immunodeficiency virus type 1, interleukin-18

INTRODUCTION

Infection with the novel coronavirus SARS-CoV-2 has very variable outcomes ranging from an asymptomatic infection through to coronavirus disease 2019 (COVID-19), which usually presents as respiratory tract disease ranging in severity from a flu-like illness to a severe viral pneumonia that may progress to acute respiratory distress syndrome (ARDS) and/or critical illness in about 20% of patients (1, 2). A coagulopathy is a prominent feature of critical illness in COVID-19 and contributes to morbidity and mortality (3). Deterioration of respiratory tract disease and progression to a critical state usually commences about 10 days after symptom onset (1). Risk factors for deterioration include older age, male sex and medical co-morbidities, such as obesity, diabetes mellitus and hypertension (1, 2). Children rarely develop respiratory tract disease caused by SARS-CoV-2 infection but may develop pediatric multisystem inflammatory syndrome (4).

It has become clear that most disease manifestations of SARS-CoV-2 infection are a consequence of hyperinflammation resulting from SARS-CoV-2-induced immunopathology, which is characterized by lymphopenia and neutrophilia (1, 2), increased production of multiple pro-inflammatory chemokines and cytokines detectable in plasma (5, 6) or broncho-alveolar lavage (BAL) fluid (7), and dysfunction and/or activation of myeloid cells (monocytes, macrophages and neutrophils), which has been demonstrated both in blood (8–10) and BAL fluid (11). Indeed, high plasma levels of D-dimers, ferritin, interleukin (IL)-6 and tumor necrosis factor-alpha (TNF-α) are strong predictors of mortality in COVID-19 (1, 6). Many of these abnormalities bear similarities to those observed in severely immunodeficient patients with human immunodeficiency virus type 1 (HIV-1) infection who develop an immune reconstitution inflammatory syndrome (IRIS) after commencing antiretroviral therapy (ART) consequent upon the restoration of an immune response against an opportunistic pathogen. Here, we compare the immunopathology underlying HIV-associated IRIS with that currently reported for COVID-19 and reason that new insights into the immunopathology underlying COVID-19 and treatment of it may arise from doing this.

MYCOBACTERIAL IRIS IS A MANIFESTATION OF MYELOID CELL ACTIVATION AMPLIFIED BY AN EMERGENT TH1 CD4$^+$ T CELL RESPONSE AGAINST MYCOBACTERIAL ANTIGENS

Approximately 20% of people with HIV-1 infection who commence ART with severe CD4$^+$ T cell depletion (CD4$^+$ T cell count <100/μL) experience an IRIS during the first 3 months of ART associated with a treated or unrecognized infection by various opportunistic pathogens (12). While clinical features of an IRIS may differ with different pathogens, an atypical and/or exaggerated inflammatory response is a characteristic finding. An IRIS may be associated with many types of mycobacteria, fungi, parasites and viruses that cause opportunistic infections but infections with mycobacteria are the most common cause, particularly *Mycobacterium tuberculosis* and *Mycobacterium avium* complex (MAC) (12). Research studies undertaken in patients with, or animal models of, mycobacterial IRIS have been most informative about the immunopathogenesis of IRIS and, therefore, mycobacterial IRIS will be focused on here. Notably, tuberculosis-associated IRIS (TB-IRIS) presents at a median time of 10-16 days after commencing ART (13–15).

Like COVID-19, increased production of multiple pro-inflammatory chemokines and cytokines is a prominent feature of mycobacterial IRIS (16–22), including increased production of TNF-α and IL-6. The latter has been shown to be a major mediator of immunopathology in animal models of MAC-IRIS (20). Furthermore, the IL-6-174*C variant of the IL-6 gene, as well as the TNFA-308*2 variant of the TNFA gene, were reported to be significantly less frequent in patients with mycobacterial IRIS compared with controls (23), suggesting a genetic susceptibility to the pro-inflammatory effects of IL-6 and TNF-α in mycobacterial IRIS. Corticosteroid therapy decreases the frequency and severity of TB-IRIS in patients at-risk of developing this condition (24) associated with suppressed production of pro-inflammatory cytokines, including IL-6 and TNF-α (18).

Patients with HIV infection who develop TB-IRIS also exhibit evidence of monocyte activation, not only after but also before commencing ART (19). In addition, higher blood neutrophil counts, increased neutrophil activation and elevation in plasma levels of neutrophil elastase and human neutrophil peptides have been observed in patients with TB-IRIS (25). Activation of circulating monocytes, and presumably tissue macrophages and neutrophils, is a likely explanation for increased plasma levels of pro-inflammatory cytokines and other biomarkers of inflammation being associated with an increased risk of developing TB-IRIS after ART is commenced. In a large prospective multinational study of patients with HIV-1 infection and CD4$^+$ T cell counts <100/μL (12), Vinhaes et al. defined an inflammatory profile that predicted the development of mycobacterial IRIS, which included several biomarkers of monocyte/macrophage activation, including IL-6, TNF-α, IL-27, sCD14 and D-dimers (26). Monocyte activation in patients with TB-IRIS is also associated with NLRP3-inflammasome activation both before and after ART (27), which probably explains why high plasma IL-18 levels are also predictive of the development of TB-IRIS (16, 21). Furthermore, monocyte/macrophage activation is a likely explanation for observations that high plasma levels of sCD14, IL-6 and D-dimers are predictors of death after ART is commenced in people with HIV-1 infection (28, 29).

Current evidence suggests that following commencement of ART in patients with HIV-1 and mycobacterial infections, activation of monocytes, and presumably other myeloid cells, is amplified directly or indirectly by the restoration of CD4$^+$ T cell responses against antigens of live or dead mycobacteria, resulting

in an aberrant inflammatory response. Exaggerated and/or atypical inflammatory responses against mycobacteria, subsequently defined as mycobacterial IRIS, were first identified in patients with HIV-1 infection who were unable to generate T cell responses against mycobacterial antigens, assessed by measuring tuberculin skin test (TST) responses, until shortly after the commencement of ART (30, 31). Analyses of T cell responses using various laboratory methods in patients who developed mycobacterial IRIS after commencing combination ART have demonstrated an association with expansion of mycobacterial-specific T cells (13, 22, 32–35) with skewing of $CD4^+$ T cells towards a Th1 phenotype during immune reconstitution (33–36), commensurate with the original observations of an association between mycobacterial IRIS and development of TST responses (30, 31). As IL-18 strongly promotes Th1 T cell responses (37), increased IL-18 production resulting from monocyte/macrophage activation (16, 18, 21, 27) may contribute to Th1 skewing of $CD4^+$ T cells during immune reconstitution in patients with TB-IRIS. Furthermore, proliferation of weakly suppressive regulatory $CD4^+$ T cells (38) may lead to inadequate regulation of T cell responses against mycobacteria in MAC-IRIS, though a relationship with decreased regulatory T cell numbers has not clearly been shown in TB-IRIS (33).

HYPERINFLAMMATION IN COVID-19 MAY BE A MANIFESTATION OF MYELOID CELL ACTIVATION AMPLIFIED BY A PRO-INFLAMMATORY ANTIBODY RESPONSE AGAINST SARS-COV-2

While there is robust evidence that the hyperinflammation complicating SARS-CoV-2 infection is a consequence of myeloid cell dysfunction and/or activation (8–11) resulting in the increased production of multiple pro-inflammatory cytokines and chemokines (5, 6), sometimes referred to as a cytokine storm (39), mechanisms remain unclear. A pro-inflammatory innate immune response associated with ineffective type I interferon anti-viral activity (40), which in some patients may be caused by neutralizing autoantibodies to type I interferons (41), may be a contributing factor. However, uncertainty remains as to why the onset of hyperinflammation is about 10 days after the onset of SARS-CoV-2 infection symptoms, and why older age, male sex and medical co-morbidities such as diabetes mellitus increase the risk of developing severe COVID-19.

Reports that critical illness in COVID-19 is associated with higher serum levels of IgG and IgA antibodies to SARS-CoV-2 spike protein (SP) (42–45), have raised the possibility that antibody responses against SARS-CoV-2 might be a determinant of the immunopathology in patients with COVID-19. Notably, patients with severe COVID-19 usually deteriorate about 10 days after symptom onset (1) just after IgG antibodies to SARS-CoV-2 SP are detectable (43). Furthermore, Cervia et al. reported that very high serum levels of IgA antibodies to SARS-CoV-2 SP are highly predictive of ARDS (44). Higher serum levels of SARS-CoV-2 SP antibodies in patients with severe COVID-19 might reflect higher SARS-CoV-2 viral loads (46) and/or an uncoordinated adaptive immune response that includes impaired T cell responses against SARS-CoV-2. Thus, several studies have demonstrated that patients with severe COVID-19, when compared to patients with mild COVID-19, exhibit less robust $CD4^+$ and $CD8^+$ T cell responses against SARS-CoV-2 membrane, nucleocapsid, and spike proteins (47–49). However, the findings of studies undertaken in non-human primates to elucidate the immunopathology of SARS-CoV-1 infection have provided evidence that binding of antibody-coated viruses to activatory Fc gamma receptors (FcγRs) on macrophages might have a disease-enhancing effect. Thus, induction of antibodies to SARS-CoV-1 SP by vaccination, or passive immunization with SARS-CoV-1 SP IgG antibodies, was associated with pulmonary inflammation after animals were infected by SARS-CoV-1 (50). This inflammation was characterized by "skewing" of pulmonary macrophages towards a pro-inflammatory M1 phenotype. Furthermore, incubation of M2 macrophages from healthy humans with plasma from SARS patients and SARS-CoV-1 pseudoviruses induced production of IL-8, CCL2 and IL-6 (50).

Evidence that IgG antibodies to the SP of SARS-CoV-2 might also exert a pro-inflammatory effect on monocytes/macrophages in patients with severe COVID-19 has been provided from several sources. In a very comprehensive analysis of antibody responses against SARS-CoV-2 undertaken by Zohar et al. (51), it was observed that patients with severe COVID-19 (requiring admission to an intensive care unit), when compared to patients with moderate COVID-19, possessed IgG antibodies at 2 weeks after presentation that exhibited functional characteristics likely to induce monocyte/macrophage activation. Those characteristics included higher serum levels of antibodies to the SARS-CoV-2 SP, including the receptor binding domain (RBD), belonging to the IgG3 subclass, the most pro-inflammatory IgG subclass (52), greater antibody binding to FcγRIIa, FcγRIIb, FcγRIIIa and FcγRIIIb, and greater antibody-dependent phagocytosis and NK cell activating activity. However, most of these differences were not observed in patients with severe COVID-19 who subsequently died suggesting that additional factors are determinants of mortality. Chakraborty et al. (53), also demonstrated that functional characteristics of IgG antibodies to the RBD domain of SARS-CoV-2 SP may be more important than serum antibody levels. Specifically, severe COVID-19 was associated with a SARS-CoV-2 RBD IgG antibody response that exhibited a higher proportion of IgG3 antibodies and decreased fucosylation of the Fc region glycans of IgG1 antibodies, both of which are antibody characteristics associated with increased binding of immune complexes to activatory FcγRs. These findings were confirmed in an independent study that demonstrated decreased fucosylation of SARS-CoV-2 SP IgG antibodies in COVID-19 patients with ARDS when compared to patients without ARDS (54). Chakraborty et al. (53) also demonstrated that decreased

antibody fucosylation was associated with higher binding of immune complexes to FcγRIIIa and increased production of the pro-inflammatory cytokines IL-6, TNF-α and IL-1β from monocytes incubated with immune complexes of antibodies and SARS-CoV-2 pseudoviruses. Notably, decreased antibody fucosylation did not appear to be directly related to the severity of SARS-CoV-2 infection but was more common in males with severe COVID-19. However, factors other than sex probably contributed to production of afucosylated antibodies because the association with male sex was not observed in patients with mild COVID-19.

Aberrant glycosylation of IgG1 Fc glycans is a consequence of B cell activation and/or metabolic activity driven by various extracellular stimuli, which include pro-inflammatory cytokines (55, 56). Such pro-inflammatory cytokines produced during an innate immune response against SARS-CoV-2 might include IL-6 because it promotes B cell differentiation (57). However, other cytokines are likely to contribute, including IL-18 because it plays a critical role in IgG antibody responses produced from B cells co-stimulated by subcapsular medullary macrophages in mice (58) and human B cells constitutively express IL-18R (59) but not IL-6R (60). Emerging evidence suggests that a pro-inflammatory antibody response in patients with severe COVID-19 may be derived from B cells that have differentiated into antibody secreting cells through an extrafollicular pathway (extrafollicular B cells). These cells are more abundant than normal in the blood of patients with severe COVID-19 (61, 62), as well as in lymphoid tissue, where they are increased in the context of marked germinal center depletion and impaired differentiation of germinal center T follicular helper cells (62). B cells that have differentiated through this pathway form a subpopulation of 'double negative' (DN; IgD^- $CD27^-$) B cells, which are characterized by the immunophenotype $CD11c^+$, $CXCR5^-$, $CXCR3^+$, T-bet^{hi} (type 2 DN [DN2] B cells) and programmed to differentiate through this pathway by IFN-γ in a TLR7-dependent manner (63). Immunoglobulin isotype switching of DN2 B cells in other infectious diseases is skewed towards pro-inflammatory isotypes of IgG, particularly IgG3 (64, 65). In the context of an early immune response against SARS-CoV-2, a major source of IFN-γ is likely to be mucosa-associated invariant T (MAIT) cells as these cells are activated and substantially depleted from blood in patients with severe COVID-19 (66, 67) and, furthermore, a fatal outcome of COVID-19 was associated with higher production of IFN-γ, compared with other cytokines, by MAIT cells (67). MAIT cells contribute to immune responses against viruses in an IL-18 dependent manner (68) and, importantly, MAIT cell activation was particularly associated with high plasma IL-18 levels in patients with severe COVID-19 (67). Th1 $CD4^+$ T cells, which are increased in frequency in lymphoid tissue of patients with severe COVID-19 (62), might also be a source of IFN-γ.

A notable finding from a study of sex differences in immune responses in patients with COVID-19 was that while all patients exhibited increased production of multiple pro-inflammatory cytokines, male patients exhibited higher production of IL-18, as well as IL-8, associated with greater activation of non-classical monocytes, when compared with female COVID-19 patients (69). Furthermore, in a study of a small number of children with pediatric multisystem inflammatory syndrome or COVID-19, plasma IL-18 levels were increased in addition to IL-6 levels (70). Moreover, Rodrigues et al. demonstrated that severe COVID-19 was associated with NLRP3-inflammasome activation in blood mononuclear cells and monocytes from post-mortem tissues, and that serum IL-18 levels correlated with disease severity (71). Increased IL-18 production and MAIT cell activation during an innate immune response against SARS-CoV-2 may therefore contribute to B cell activation through an extra-follicular pathway and production of a SARS-CoV-2 antibody response with pro-inflammatory characteristics, which include skewing towards IgG3 antibodies and decreased fucosylation of IgG1 antibodies to SARS-CoV-2 SP.

Higher serum levels of SARS-CoV-2 IgA antibodies, particularly those of the pro-inflammatory IgA2 subclass (72), and the greater binding of IgA antibodies to FcαR, reported in severe COVID-19 patients compared with moderate COVID-19 patients at 2 weeks after presentation (51), might also contribute to activation of alveolar macrophages *via* Fc alpha receptors (73). Finally, skewing of SARS-CoV-2 SP IgG antibody responses towards IgG3 antibody production in patients with severe COVID-19 (51, 53) might also adversely affect immune responses against SARS-CoV-2 by mechanisms other than myeloid cell activation. Combes et al. demonstrated that patients with severe COVID-19 produced SARS-CoV-2 antibodies that block the production of interferon-stimulated genes in several cell-types by activating conserved signaling circuits that dampen cellular responses to interferons (74). In other situations, this effect is associated with an anti-viral IgG antibody response that consists of IgG3 as well as IgG1 antibodies (75).

IMPLICATIONS FOR THERAPY OF COVID-19

Suppression of inflammatory responses by the use of corticosteroid therapy is at least partially effective in the prevention and treatment of TB-IRIS (18, 24) and treatment of severe COVID-19 (76). However, corticosteroid therapy may be complicated by opportunistic infections, such as Kaposi's sarcoma, in TB-IRIS (77) and potentially may further impair T cell responses against SARS-CoV-2. Anti-inflammatory therapies that target particular pro-inflammatory cytokines, such as TNF-α and IL-6, have been shown to be effective treatment for mycobacterial IRIS in studies of small numbers of patients (78) but observational studies and randomized controlled trials have not provided clear evidence of a benefit of IL-6 inhibitors, such as the IL-6R blocker tocilizumab, in the treatment of severe COVID-19 (79–81). An alternative or additional approach to controlling inflammation in severe COVID-19, as well as mycobacterial IRIS, is to modulate the effects of the cytokine milieu arising from the initial innate immune response that, as suggested here, might be a determinant of the functional characteristics of emerging adaptive immune responses. For example, investigating the effects of inhibiting IL-18 activity with

humanized monoclonal antibodies to IL-18 (82), or suppression of NLRP3-inflammasome activation, is supported by preliminary data from uncontrolled, but more than one, clinical studies in patients with COVID-19 reporting a beneficial effect of inhibiting NLRP3-inflammasome activity with colchicine (83, 84).

SUMMARY AND CONCLUSIONS

While COVID-19 is a complication of acute SARS-CoV-2 infection and HIV-associated IRIS occurs in the context of chronic HIV-1 infection, similarities between the two conditions are apparent (**Table 1**) and have been considered here in order to enlighten the immunopathology of severe COVID-19. Approximately 20% of HIV patients with severe $CD4^+$ T cell deficiency develop an IRIS after commencing ART, which presents at a median time of 10-16 days for TB-IRIS, while approximately 20% of people with symptomatic SARS-CoV-2 infection develop severe COVID-19 at about 10 days after symptom onset. We suggest that, in the absence of adaptive immune responses resulting from severe $CD4^+$ T cell depletion caused by HIV-1 infection, or infection with a novel pathogen in people with SARS-CoV-2 infection, innate immune responses against mycobacteria or SARS-CoV-2, respectively, are induced leading to activation of monocytes/macrophages, including NLRP3-inflammasome activation and IL-18 production. When adaptive immune responses emerge, through ART-induced immune reconstitution in people with HIV-1 infection or production of a primary antibody response in patients with SARS-CoV-2 infection, they directly or indirectly amplify the activation of monocytes/macrophages and neutrophils resulting in an exaggerated inflammatory response and immunopathology in infected tissues (**Figure 1**). In addition, we suggest that the initial innate immune response not only primes the immune system for hyperinflammation induced by emergent adaptive immune responses but also exerts an immunomodulatory effect on those adaptive immune responses resulting in a Th1-skewed $CD4^+$ T cell response against mycobacteria in mycobacterial IRIS and a SARS-CoV-2 IgG antibody response with pro-inflammatory characteristics, arising from extra-follicular B cell differentiation promoted by MAIT cell activation, in COVID-19. Based on our comparison of the immunopathology underlying mycobacterial IRIS and COVID-19, we suggest that IL-18 may play a central role in this process and should be investigated further as a possible therapeutic target.

TABLE 1 | Similarities between HIV-associated mycobacterial IRIS and severe COVID-19.

	HIV-associated mycobacterial IRIS	Severe COVID-19
Time of disease onset	Median time of 10-16 days after commencing ART (TB-IRIS)	Approximately 10 days after symptom onset
Markers of monocyte/macrophage activation associated with an increased risk of disease and death	sCD14, D-dimers	sCD14, D-dimers, ferritin
Increased plasma levels of pro-inflammatory cytokines and chemokines associated with disease	IL-6, IL-8, IL-12, IL-18, TNF-α, IFN-γ, CXCL10	IL-1β, IL-6, IL-8, IL-12, IL-17, IL-18, IFN-γ, TNF-α, CCL2, CCL3, CXCL10, GM-CSF
Emergent adaptive immune response that may amplify monocyte/macrophage activation associated with disease onset	Mycobacteria-specific Th1 $CD4^+$ T cell response	SARS-CoV-2 SP antibody response with pro-inflammatory characteristics

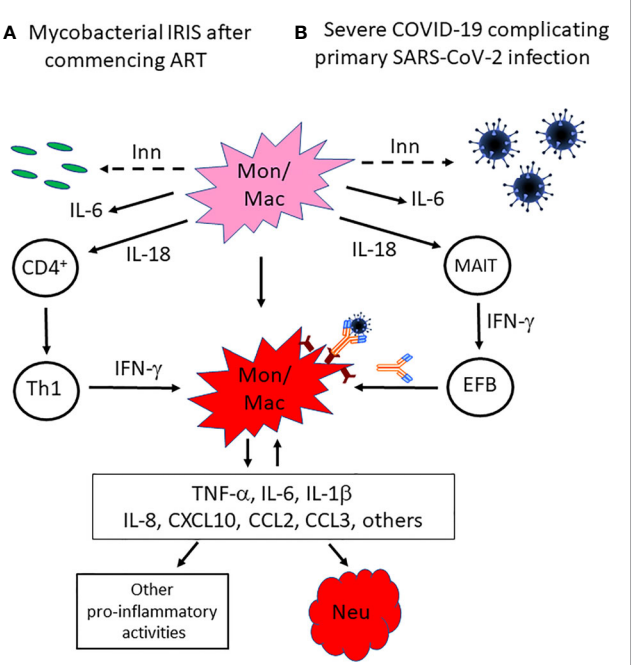

FIGURE 1 | Proposed mechanisms by which innate immune responses not only induce inflammation but also skew emerging adaptive immune responses towards a response that amplifies myeloid cell activation in mycobacterial IRIS or COVID-19. In the absence of effective adaptive immune responses against **(A)** mycobacteria in HIV patients with severe $CD4^+$ T cell deficiency and a mycobacterial co-infection, or **(B)** acute infection with the novel pathogen SARS-CoV-2, innate immune responses are generated that result in activation of monocytes/macrophages, including NLRP3-inflammasome activation. While this does not control the mycobacterial or SARS-CoV-2 infection, it generates a pro-inflammatory cytokine environment that includes IL-18, which skews $CD4^+$ T cell recovery towards a Th1 response after ART is commenced in HIV patients, or induces MAIT cell activation that promotes B cell differentiation through an extra-follicular pathway and the production of a SARS-CoV-2 SP antibody response with pro-inflammatory characteristics, including decreased fucosylation of IgG1 Fc glycans and higher proportions of IgG3 and IgA2 antibodies, which enhances binding of SARS-CoV-2/antibody complexes to activatory FcγRs on macrophages, in COVID-19 patients. In either situation, dysregulated production and activity of multiple pro-inflammatory cytokines and chemokines occurs and has multiple effects, including further recruitment and activation of neutrophils and monocytes, as well as macrophage activation in a positive feedback loop. Inn, innate immune response; Mon/mac, monocytes/macrophages; Neu, neutrophils; MAIT, mucosa-associated invariant T cells; EFB, extra-follicular B cells.

DATA AVAILABILITY STATEMENT

The original contributions presented in the study are included in the article/supplementary material. Further inquiries can be directed to the corresponding author.

AUTHOR CONTRIBUTIONS

MF conceived the hypothesis outlined in this paper, wrote the manuscript, and produced the figure. NS wrote the manuscript, produced the figure, and obtained funding for publication. All authors contributed to the article and approved the submitted version.

FUNDING

Publication of this work was supported by the Investissement d'Avenir program managed by the ANR under reference ANR-10-LABX-77, the Agence Nationale pour la Recherche sur le SIDA et les hépatites virales (ANRS), and the Vaccine Research Institute (VRI).

REFERENCES

1. Zhou F, Yu T, Du R, Fan G, Liu Y, Liu Z, et al. Clinical course and risk factors for mortality of adult inpatients with COVID-19 in Wuhan, China: a retrospective cohort study. *Lancet* (2020) 395:1054–62. doi: 10.1016/S0140-6736(20)30566-3
2. Wu C, Chen X, Cai Y, Xia J, Zhou X, Xu S, et al. Risk Factors Associated With Acute Respiratory Distress Syndrome and Death in Patients With Coronavirus Disease 2019 Pneumonia in Wuhan, China. *JAMA Intern Med* (2020) 180:934–43. doi: 10.1001/jamainternmed.2020.0994
3. Iba T, Levy JH, Levi M, Connors JM, Thachil J. Coagulopathy of Coronavirus Disease 2019. *Crit Care Med* (2020) 48:1358–64. doi: 10.1097/CCM.0000000000004458
4. Kabeerdoss J, Pilania RK, Karkhele R, Kumar TS, Danda D, Singh S. Severe COVID-19, multisystem inflammatory syndrome in children, and Kawasaki disease: immunological mechanisms, clinical manifestations and management. *Rheumatol Int* (2021) 41:19–32. doi: 10.1007/s00296-020-04749-4
5. Chi Y, Ge Y, Wu B, Zhang W, Wu T, Wen T, et al. Serum Cytokine and Chemokine Profile in Relation to the Severity of Coronavirus Disease 2019 in China. *J Infect Dis* (2020) 222:746–54. doi: 10.1093/infdis/jiaa363
6. Del Valle DM, Kim-Schulze S, Huang HH, Beckmann ND, Nirenberg S, Wang B. An inflammatory cytokine signature predicts COVID-19 severity and survival. *Nat Med* (2020) 26:1636–43. doi: 10.1038/s41591-020-1051-9
7. Chua RL, Lukassen S, Trump S, Hennig BP, Wendisch D, Pott F, et al. COVID-19 severity correlates with airway epithelium-immune cell interactions identified by single-cell analysis. *Nat Biotechnol* (2020) 38:970–9. doi: 10.1038/s41587-020-0602-4
8. Giamarellos-Bourboulis EJ, Netea MG, Rovina N, Akinosoglou K, Antoniadou A, Antonakos N, et al. Complex Immune Dysregulation in COVID-19 Patients with Severe Respiratory Failure. *Cell Host Microbe* (2020) 27:992–1000.e3. doi: 10.1016/j.chom.2020.04.009
9. Merad M, Martin JC. Pathological inflammation in patients with COVID-19: a key role for monocytes and macrophages. *Nat Rev Immunol* (2020) 20:355–62. doi: 10.1038/s41577-020-0331-4. Erratum in: Nat Rev Immunol 2020 Jun 2.
10. Schulte-Schrepping J, Reusch N, Paclik D, Baßler K, Schlickeiser S, Zhang B, et al. Severe COVID-19 Is Marked by a Dysregulated Myeloid Cell Compartment. *Cell* (2020) 82:1419–40.e23. doi: 10.1016/j.cell.2020.08.001
11. Liao M, Liu Y, Yuan J, Wen Y, Xu G, Zhao J, et al. Single-cell landscape of bronchoalveolar immune cells in patients with COVID-19. *Nat Med* (2020) 26:842–4. doi: 10.1038/s41591-020-0901-9
12. Sereti I, Sheikh V, Shaffer D, Phanuphak N, Gabriel E, Wang J, et al. Prospective international study of incidence and predictors of immune reconstitution inflammatory syndrome and death in people with HIV and severe lymphopenia. *Clin Infect Dis* (2020) 71:652–60. doi: 10.1093/cid/ciz877
13. Elliott JH, Vohith K, Saramony S, Savuth C, Dara C, Sarim C, et al. Immunopathogenesis and diagnosis of tuberculosis and tuberculosis-associated immune reconstitution inflammatory syndrome during early antiretroviral therapy. *J Infect Dis* (2009) 200:1736–45. doi: 10.1086/644784
14. Blanc FX, Sok T, Laureillard D, Borand L, Rekacewicz, Nerrienet E, et al. Earlier versus later start of antiretroviral therapy in HIV-infected adults with tuberculosis. *N Engl J Med* (2011) 365:1471–81. doi: 10.1056/NEJMoa1013911
15. Abdool Karim SS, Naidoo K, Grobler A, Padayatchi N, Baxter C, Gray AL, et al. Integration of antiretroviral therapy with tuberculosis treatment. *N Engl J Med* (2011) 365:1492–501. doi: 10.1056/NEJMoa1014181
16. Oliver BG, Elliott JH, Price P, Phillips M, Saphonn V, Vun MC, et al. Mediators of innate and adaptive immune responses differentially affect immune restoration disease associated with Mycobacterium tuberculosis in HIV patients beginning antiretroviral therapy. *J Infect Dis* (2010) 202:1728–37. doi: 10.1086/657082
17. Tadokera R, Meintjes G, Skolimowska KH, Wilkinson KA, Matthews K, Seldon R, et al. Hypercytokinaemia accompanies HIV-tuberculosis immune reconstitution inflammatory syndrome. *Eur Respir J* (2011) 37:1248–59. doi: 10.1183/09031936.00091010
18. Meintjes G, Skolimowska KH, Wilkinson KA, Matthews K, Tadokera R, Conesa-Botella A, et al. Corticosteroid-modulated immune activation in the tuberculosis immune reconstitution inflammatory syndrome. *Am J Respir Crit Care Med* (2012) 186:369–77. doi: 10.1164/rccm.201201-0094OC
19. Andrade BB, Singh A, Narendran G, Schechter ME, Nayak K, Subramanian S, et al. Mycobacterial antigen driven activation of CD14++CD16- monocytes is a predictor of tuberculosis-associated immune reconstitution inflammatory syndrome. *PloS Pathog* (2014) 10:e1004433. doi: 10.1371/journal.ppat.1004433
20. Barber DL, Andrade BB, McBerry C, Sereti I, Sher A. Role of IL-6 in Mycobacterium avium-associated immune reconstitution inflammatory syndrome. *J Immunol* (2014) 192:676–82. doi: 10.4049/jimmunol.1301004
21. Tan HY, Yong YK, Andrade BB, Shankar EM, Ponnampalavanar S, Omar SF, et al. Plasma interleukin-18 levels are a biomarker of innate immune responses that predict and characterize tuberculosis-associated immune reconstitution inflammatory syndrome. *AIDS* (2015) 29:421–31. doi: 10.1097/QAD.0000000000000557
22. Ravimohan S, Tamuhla N, Nfanyana K, Steenhoff AP, Letlhogile R, Frank I, et al. Robust Reconstitution of Tuberculosis-Specific Polyfunctional CD4+ T-Cell Responses and Rising Systemic Interleukin 6 in Paradoxical Tuberculosis-Associated Immune Reconstitution Inflammatory Syndrome. *Clin Infect Dis* (2016) 62:795–803. doi: 10.1093/cid/civ978
23. Price P, Morahan G, Huang D, Stone E, Cheong KY, Castley A, et al. Polymorphisms in cytokine genes define subpopulations of HIV-1 patients who experienced immune restoration diseases. *AIDS* (2002) 16:2043–7. doi: 10.1097/00002030-200210180-00009
24. Meintjes G, Stek C, Blumenthal L, Thienemann F, Schutz C, Buyze J, et al. Prednisone for the Prevention of Paradoxical Tuberculosis-Associated IRIS. *N Engl J Med* (2018) 379:1915–25. doi: 10.1056/NEJMoa1800762
25. Nakiwala JK, Walker NF, Diedrich CR, Worodria W, Meintjes G, Wilkinson RJ, et al. Neutrophil Activation and Enhanced Release of Granule Products in HIV-TB Immune Reconstitution Inflammatory Syndrome. *J Acquir Immune Defic Syndr* (2018) 77:221–9. doi: 10.1097/QAI.0000000000001582
26. Vinhaes CL, Sheikh V, de-Souza DO, Wang J, Rupert A, Roby G, et al. An inflammatory composite score predicts mycobacterial IRIS in people with HIV and severe lymphopenia: A prospective international cohort study. *J Infect Dis* (2020) 6:jiaa484. doi: 10.1093/infdis/jiaa484
27. Tan HY, Yong YK, Shankar EM, Paukovics G, Ellegard R, Larsson M, et al. Aberrant Inflammasome Activation Characterizes Tuberculosis-Associated Immune Reconstitution Inflammatory Syndrome. *J Immunol* (2016) 196:4052–63. doi: 10.4049/jimmunol.1502203

28. Boulware DR, Hullsiek KH, Puronen CE, Rupert A, Baker JV, French MA, et al. Higher levels of CRP, D-dimer, IL-6, and hyaluronic acid before initiation of antiretroviral therapy (ART) are associated with increased risk of AIDS or death. *J Infect Dis* (2011) 203:1637–46. doi: 10.1093/infdis/jir134
29. Siedner MJ, Bwana MB, Asiimwe S, Musinguzi N, Castillo-Mancilla J, Amanyire G, et al. Inflammatory biomarkers prior to antiretroviral therapy as prognostic markers of 12-month mortality in South Africa and Uganda. *AIDS* (2019) 33:2043–8. doi: 10.1097/QAD.0000000000002305
30. French MA, Mallal SA, Dawkins RL. Zidovudine-induced restoration of cell-mediated immunity to mycobacteria in immunodeficient HIV-infected patients. *AIDS* (1992) 6:1293–7. doi: 10.1097/00002030-199211000-00009
31. Narita M, Ashkin D, Hollender ES, Pitchenik AE. Paradoxical worsening of tuberculosis following antiretroviral therapy in patients with AIDS. *Am J Respir Crit Care Med* (1998) 158:157–61. doi: 10.1164/ajrccm.158.1.9712001
32. Bourgarit A, Carcelain G, Martinez V, Lascoux C, Delcey V, Gicquel B, et al. Explosion of tuberculin-specific Th1-responses induces immune restoration syndrome in tuberculosis and HIV co-infected patients. *AIDS* (2006) 20:F1–7. doi: 10.1097/01.aids.0000202648.18526.bf
33. Meintjes G, Wilkinson KA, Rangaka MX, Skolimowska K, Veen v, Abrahams M, et al. Type 1 helper T cells and FoxP3-positive T cells in HIV-tuberculosis-associated immune reconstitution inflammatory syndrome. *Am J Respir Crit Care Med* (2008) 178:1083–9. doi: 10.1164/rccm.200806-858OC
34. Bourgarit A, Carcelain G, Samri A, Parizot C, Lafaurie M, Abgrall S, et al. Tuberculosis-associated immune restoration syndrome in HIV-1-infected patients involves tuberculin-specific CD4 Th1 cells and KIR-negative gammadelta T cells. *J Immunol* (2009) 183:3915–23. doi: 10.4049/jimmunol.0804020
35. Vignesh R, Kumarasamy N, Lim A, Solomon S, Murugavel KG, Balakrishnan P, et al. TB-IRIS after initiation of antiretroviral therapy is associated with expansion of preexistent Th1 responses against Mycobacterium tuberculosis antigens. *J Acquir Immune Defic Syndr* (2013) 64:241–8. doi: 10.1097/QAI.0b013e31829f6df2. Erratum in: J Acquir Immune Defic Syndr (2014) 67:e44.
36. Silveira-Mattos PS, Narendran G, Akrami K, Fukutani KF, Anbalagan S, Nayak K, et al. Differential expression of CXCR3 and CCR6 on CD4(+) T-lymphocytes with distinct memory phenotypes characterizes tuberculosis-associated immune reconstitution inflammatory syndrome. *Sci Rep* (2019) 9:1502. doi: 10.1038/s41598-019-44429-3
37. Yasuda K, Nakanishi K, Tsutsui H. Interleukin-18 in Health and Disease. *Int J Mol Sci* (2019) 20:649. doi: 10.3390/ijms20030649
38. Seddiki N, Sasson SC, Santner-Nanan B, Munier M, van Bockel D, Ip S, et al. Proliferation of weakly suppressive regulatory CD4+ T cells is associated with over-active CD4+ T-cell responses in HIV-positive patients with mycobacterial immune restoration disease. *Eur J Immunol* (2009) 39:391–403. doi: 10.1002/eji.200838630
39. Fajgenbaum DC, June CH. Cytokine storm. *N Engl J Med* (2020) 383:2255–73. doi: 10.1056/NEJMra2026131
40. Hadjadj J, Yatim N, Barnabei L, Corneau A, Boussier J, Smith N, et al. Impaired type I interferon activity and inflammatory responses in severe COVID-19 patients. *Science* (2020) 369:718–24. doi: 10.1126/science.abc6027
41. Bastard P, Rosen LB, Zhang Q, Michailidis E, Hoffmann HH, Zhang Y, et al. Autoantibodies against type I IFNs in patients with life-threatening COVID-19. *Science* (2020) 370:eabd4585. doi: 10.1126/science.abd4585
42. Zhao J, Yuan Q, Wang H, Liu W, Liao X, Su Y, et al. Antibody Responses to SARS-CoV-2 in Patients With Novel Coronavirus Disease 2019. *Clin Infect Dis* (2020) 71:2027–34. doi: 10.1093/cid/ciaa344
43. Qu J, Wu C, Li X, Zhang G, Jiang Z, Li X, et al. Profile of IgG and IgM antibodies against severe acute respiratory syndrome coronavirus 2 (SARS-CoV-2). *Clin Infect Dis* (2020) 71:2255–8. doi: 10.1093/cid/ciaa489
44. Cervia C, Nilsson J, Zurbuchen Y, Valaperti A, Schreiner J, Wolfensberger A, et al. Systemic and mucosal antibody responses specific to SARS-CoV-2 during mild versus severe COVID-19. *J Allergy Clin Immunol* (2021) 147:545–57.e9. doi: 10.1016/j.jaci.2020.10.040
45. Garcia-Beltran WF, Lam EC, Astudillo MG, Yang D, Miller TE, Feldman J, et al. COVID-19 neutralizing antibodies predict disease severity and survival. *Cell* (2021) 184:476–88.e11. doi: 10.1016/j.cell.2020.12.015
46. Röltgen K, Powell AE, Wirz OF, Stevens BA, Hogan CA, Najeeb J, et al. Defining the features and duration of antibody responses to SARS-CoV-2 infection associated with disease severity and outcome. *Sci Immunol* (2020) 5: eabe0240. doi: 10.1126/sciimmunol.abe0240
47. Rydyznski Moderbacher C, Ramirez SI, Dan JM, Grifoni A, Hastie KM, Weiskopf D, et al. Antigen-Specific Adaptive Immunity to SARS-CoV-2 in Acute COVID-19 and Associations with Age and Disease Severity. *Cell* (2020) 183:996–1012.e19. doi: 10.1016/j.cell.2020.09.038
48. Sattler A, Angermair S, Stockmann H, Heim KM, Khadzhynov D, Treskatsch S, et al. SARS-CoV-2-specific T cell responses and correlations with COVID-19 patient predisposition. *J Clin Invest* (2020) 130:6477–89. doi: 10.1172/JCI140965
49. Oja AE, Saris A, Ghandour CA, Kragten NAM, Hogema BM, Nossent EJ, et al. Divergent SARS-CoV-2-specific T- and B-cell responses in severe but not mild COVID-19 patients. *Eur J Immunol* (2020) 50:1998–2012. doi: 10.1002/eji.202048908
50. Liu L, Wei Q, Lin Q, Fang J, Wang H, Kwok H, et al. Anti-spike IgG causes severe acute lung injury by skewing macrophage responses during acute SARS-CoV infection. *JCI Insight* (2019) 4:e123158. doi: 10.1172/jci.insight.123158
51. Zohar T, Loos C, Fischinger S, Atyeo C, Wang C, Slein MD, et al. Compromised Humoral Functional Evolution Tracks with SARS-CoV-2 Mortality. *Cell* (2020) 183:1508–1519.e12. doi: 10.1016/j.cell.2020.10.052
52. Vidarsson G, Dekkers G, Rispens T. IgG subclasses and allotypes: from structure to effector functions. *Front Immunol* (2014) 5:520. doi: 10.3389/fimmu.2014.00520
53. Chakraborty S, Gonzalez J, Edwards K, Mallajosyula V, Buzzanco AS, Sherwood R, et al. Proinflammatory IgG Fc structures in patients with severe COVID-19. *Nat Immunol* (2021) 22:67–73. doi: 10.1038/s41590-020-00828-7
54. Larsen MD, de Graaf EL, Sonneveld ME, Plomp HR, Linty F, Visser R, et al. Afucosylated immunoglobulin G responses are a hallmark of enveloped virus infections and show an exacerbated phenotype in COVID-19. *Science* (2021) 371(6532):eabc8378. doi: 10.1126/science.abc8378
55. Wang J, Balog CI, Stavenhagen K, Koeleman CA, Scherer HU, Selman MH, et al. Fc-glycosylation of IgG1 is modulated by B-cell stimuli. *Mol Cell Proteomics* (2011) 10:M110.004655. doi: 10.1074/mcp.M110.004655
56. Klarić L, Tsepilov YA, Stanton CM, Mangino M, Sikka TT, Esko T, et al. Glycosylation of immunoglobulin G is regulated by a large network of genes pleiotropic with inflammatory diseases. *Sci Adv* (2020) 6:eaax0301. doi: 10.1126/sciadv.aax0301
57. Muraguchi A, Hirano T, Tang B, Matsuda T, Horii Y, Nakajima K, et al. The essential role of B cell stimulatory factor 2 (BSF-2/IL-6) for the terminal differentiation of B cells. *J Exp Med* (1988) 167:332–44. doi: 10.1084/jem.167.2.332
58. Desbien AL, Dubois Cauwelaert N, Reed SJ, Bailor HR, Liang H, Carter D, et al. IL-18 and Subcapsular Lymph Node Macrophages are Essential for Enhanced B Cell Responses with TLR4 Agonist Adjuvants. *J Immunol* (2016) 197:4351–9. doi: 10.4049/jimmunol.1600993
59. Kunikata T, Torigoe K, Ushio S, Okura T, Ushio C, Yamauchi H, et al. Constitutive and induced IL-18 receptor expression by various peripheral blood cell subsets as determined by anti-hIL-18R monoclonal antibody. *Cell Immunol* (1998) 189:135–43. doi: 10.1006/cimm.1998.1376
60. Hirata Y, Taga T, Hibi M, Nakano N, Hirano T, Kishimoto T. Characterization of IL-6 receptor expression by monoclonal and polyclonal antibodies. *J Immunol* (1989) 143:2900–6.
61. Woodruff MC, Ramonell RP, Nguyen DC, Cashman KS, Saini AS, Haddad NS, et al. Extrafollicular B cell responses correlate with neutralizing antibodies and morbidity in COVID-19. *Nat Immunol* (2020) 21:1506–16. doi: 10.1038/s41590-020-00814-z
62. Kaneko N, Kuo HH, Boucau J, Farmer JR, Allard-Chamard H, Mahajan VS, et al. Loss of Bcl-6-Expressing T Follicular Helper Cells and Germinal Centers in COVID-19. *Cell* (2020) 183:143–57.e13. doi: 10.1016/j.cell.2020.08.025
63. Zumaquero E, Stone SL, Scharer CD, Jenks SA, Nellore A, Mousseau B, et al. IFNγ induces epigenetic programming of human T-bethi B cells and promotes TLR7/8 and IL-21 induced differentiation. *Elife* (2019) 8:e41641. doi: 10.7554/eLife.41641
64. Obeng-Adjei N, Portugal S, Holla P, Li S, Sohn H, Ambegaonkar A, et al. Malaria-induced interferon-γ drives the expansion of Tbethi atypical memory B cells. *PloS Pathog* (2017) 13:e1006576. doi: 10.1371/journal.ppat.1006576

65. Kardava L, Moir S. B-cell abnormalities in HIV-1 infection: roles for IgG3 and T-bet. *Curr Opin HIV AIDS* (2019) 14:240–5. doi: 10.1097/COH.0000000000000547
66. Parrot T, Gorin JB, Ponzetta A, Maleki KT, Kammann T, Emgård J, et al. MAIT cell activation and dynamics associated with COVID-19 disease severity. *Sci Immunol* (2020) 5:eabe1670. doi: 10.1126/sciimmunol.abe1670
67. Flament H, Rouland M, Beaudoin L, Toubal A, Bertrand L, Lebourgeois S, et al. Outcome of SARS-CoV-2 infection is linked to MAIT cell activation and cytotoxicity. *Nat Immunol* (2021) 22:322–35. doi: 10.1038/s41590-021-00870-z
68. Loh L, Wang Z, Sant S, Koutsakos M, Jegaskanda S, Corbett AJ, et al. Human mucosal-associated invariant T cells contribute to antiviral influenza immunity via IL-18-dependent activation. *Proc Natl Acad Sci USA* (2016) 113:10133–8. doi: 10.1073/pnas.1610750113
69. Takahashi T, Ellingson MK, Wong P, Israelow B, Lucas C, Klein J, et al. Sex differences in immune responses that underlie COVID-19 disease outcomes. *Nature* (2020) 588:315–20. doi: 10.1038/s41586-020-2700-3
70. Gruber CN, Patel RS, Trachtman R, Lepow L, Amanat F, Krammer F, et al. Mapping Systemic Inflammation and Antibody Responses in Multisystem Inflammatory Syndrome in Children (MIS-C). *Cell* (2020) 183:982–995.e14. doi: 10.1016/j.cell.2020.09.034
71. Rodrigues TS, de Sá K, Ishimoto AY, Becerra A, Oliveira S, Almeida L, et al. Inflammasomes are activated in response to SARS-CoV-2 infection and are associated with COVID-19 severity in patients. *J Exp Med* (2021) 218: e20201707. doi: 10.1084/jem.20201707
72. Steffen U, Koeleman CA, Sokolova MV, Bang H, Kleyer A, Rech J, et al. IgA subclasses have different effector functions associated with distinct glycosylation profiles. *Nat Commun* (2020) 11:120. doi: 10.1038/s41467-019-13992-8
73. Sibille Y, Depelchin S, Staquet P, Chatelain B, Coulie P, Shen L, et al. Fc alpha-receptor expression on the myelomonocytic cell line THP-1: comparison with human alveolar macrophages. *Eur Respir J* (1994) 7:1111–9.
74. Combes AJ, Courau T, Kuhn NF, Hu KH, Ray A, Chen WS, et al. Global absence and targeting of protective immune states in severe COVID-19. *Nature* (2021) 591:124-30. doi: 10.1038/s41586-021-03234-7
75. Hoepel W, Allahverdiyeva S, Harbiye H, de Taeye SW, van der Ham AJ, de Boer L, et al. IgG Subclasses Shape Cytokine Responses by Human Myeloid Immune Cells through Differential Metabolic Reprogramming. *J Immunol* (2020) 205:3400–7. doi: 10.4049/jimmunol.2000263
76. RECOVERY Collaborative Group, Horby P, Lim WS, Emberson JR, Mafham M, Bell JL, et al. Dexamethasone in Hospitalized Patients with Covid-19. *N Engl J Med* (2021) 384:693–704. doi: 10.1056/NEJMoa2021436
77. Manion M, Uldrick T, Polizzotto MN, Sheikh V, Roby G, Lurain K, et al. Emergence of Kaposi's Sarcoma Herpesvirus-Associated Complications Following Corticosteroid Use in TB-IRIS. *Open Forum Infect Dis* (2018) 5: ofy217. doi: 10.1093/ofid/ofy217
78. Cevaal PM, Bekker LG, Hermans S. TB-IRIS pathogenesis and new strategies for intervention: Insights from related inflammatory disorders. *Tuberculosis (Edinb)* (2019) 118:101863. doi: 10.1016/j.tube.2019
79. Malgie J, Schoones JW, Pijls BG. Decreased mortality in COVID-19 patients treated with Tocilizumab: a rapid systematic review and meta-analysis of observational studies. *Clin Infect Dis* (2020) 23:ciaa1445. doi: 10.1093/cid/ciaa1445
80. Stone JH, Frigault MJ, Serling-Boyd NJ, Fernandes AD, Harvey L, Foulkes AS, et al. Efficacy of Tocilizumab in Patients Hospitalized with Covid-19. *N Engl J Med* (2020) 383:2333–44. doi: 10.1056/NEJMoa2028836
81. Salama C, Han J, Yau L, Reiss WG, Kramer B, Neidhart JD, et al. Tocilizumab in Patients Hospitalized with Covid-19 Pneumonia. *N Engl J Med* (2021) 384:20–30. doi: 10.1056/NEJMoa2030340
82. Mistry P, Reid J, Pouliquen I, McHugh S, Abberley L, DeWall S, et al. Safety, tolerability, pharmacokinetics, and pharmacodynamics of single-dose antiinterleukin-18 mAb GSK1070806 in healthy and obese subjects. *Int J Clin Pharmacol Ther* (2014) 52:867–79. doi: 10.5414/CP202087
83. Scarsi M, Piantoni S, Colombo E, Airó P, Richini D, Miclini M, et al. Association between treatment with colchicine and improved survival in a single-centre cohort of adult hospitalised patients with COVID-19 pneumonia and acute respiratory distress syndrome. *Ann Rheum Dis* (2020) 79:1286–9. doi: 10.1136/annrheumdis-2020-217712
84. Sandhu T, Tieng A, Chilimuri S, Franchin G. A Case Control Study to Evaluate the Impact of Colchicine on Patients Admitted to the Hospital with Moderate to Severe COVID-19 Infection. *Can J Infect Dis Med Microbiol* (2020) 2020:8865954. doi: 10.1155/2020/8865954

Conflict of Interest: The authors declare that the research was conducted in the absence of any commercial or financial relationships that could be construed as a potential conflict of interest.

frontiers in Immunology

ORIGINAL RESEARCH
published: 25 March 2021
doi: 10.3389/fimmu.2021.638010

Markers of T Cell Exhaustion and Senescence and Their Relationship to Plasma TGF-β Levels in Treated HIV+ Immune Non-responders

Carey L. Shive[1,2], Michael L. Freeman[3], Souheil-Antoine Younes[3], Corinne M. Kowal[1], David H. Canaday[1,3], Benigno Rodriguez[3‡], Michael M. Lederman[3†] and Donald D. Anthony[1,3,4†]*

[1] Louis Stokes Cleveland VA Medical Center, Cleveland, OH, United States, [2] Center for AIDS Research, Department of Pathology, Case Western Reserve University, Cleveland, OH, United States, [3] Center for AIDS Research, Division of Infectious Diseases and HIV Medicine, Department of Medicine, Case Western Reserve University/University Hospitals Cleveland Medical Center, Cleveland, OH, United States, [4] MetroHealth Medical Center, Division of Rheumatic Disease, Case Western Reserve, Cleveland, OH, United States

OPEN ACCESS

Edited by:
John Zaunders,
St Vincent's Hospital Sydney, Australia

Reviewed by:
Christine Bourgeois,
Center for Immunology of Viral, Auto-immune, Hematological and Bacterial Diseases (IMVA-HB/IDMIT), UMR1184, France
Giulia Carla Marchetti,
University of Milan, Italy

***Correspondence:**
Carey L. Shive
carey.shive@case.edu

[†] These authors have contributed equally to this work

[‡] Deceased

Specialty section:
This article was submitted to Viral Immunology, a section of the journal Frontiers in Immunology

Received: 04 December 2020
Accepted: 16 February 2021
Published: 25 March 2021

Citation:
Shive CL, Freeman ML, Younes S-A, Kowal CM, Canaday DH, Rodriguez B, Lederman MM and Anthony DD (2021) Markers of T Cell Exhaustion and Senescence and Their Relationship to Plasma TGF-β Levels in Treated HIV+ Immune Non-responders. Front. Immunol. 12:638010. doi: 10.3389/fimmu.2021.638010

Background: Immune non-responders (INR) are HIV+, ART-controlled (>2 yrs) people who fail to reconstitute their CD4 T cell numbers. Systemic inflammation and markers of T cell senescence and exhaustion are observed in INR. This study aims to investigate T cell senescence and exhaustion and their possible association with soluble immune mediators and to understand the immune profile of HIV-infected INR. Selected participants were <50 years old to control for the confounder of older age.

Methods: Plasma levels of IL-6, IP10, sCD14, sCD163, and TGF-β and markers of T cell exhaustion (PD-1, TIGIT) and senescence (CD57, KLRG-1) were measured in ART-treated, HIV+ participants grouped by CD4 T cell counts (n = 63). Immune parameters were also measured in HIV-uninfected, age distribution-matched controls (HC; n = 30). Associations between T cell markers of exhaustion and senescence and plasma levels of immune mediators were examined by Spearman rank order statistics.

Results: Proportions of CD4 T cell subsets expressing markers of exhaustion (PD-1, TIGIT) and senescence (CD57, KLRG-1) were elevated in HIV+ participants. When comparing proportions between INR and IR, INR had higher proportions of CD4 memory PD-1+, EM CD57+, TEM TIGIT+ and CD8 EM and TEM TIGIT+ cells. Plasma levels of IL-6, IP10, and sCD14 were elevated during HIV infection. IP10 was higher in INR. Plasma TGF-β levels and CD4 cycling proportions of T regulatory cells were lower in INR. Proportions of CD4 T cells expressing TIGIT, PD-1, and CD57 positively correlated with plasma levels of IL-6. Plasma levels of TGF-β negatively correlated with proportions of TIGIT+ and PD-1+ T cell subsets.

Conclusions: INR have lower levels of TGF-β and decreased proportions of cycling CD4 T regulatory cells and may have difficulty controlling inflammation. IP10 is elevated in INR and is linked to higher proportions of T cell exhaustion and senescence seen in INR.

Keywords: HIV+ immune non-responders, inflammation, senescence, exhaustion, T regulatory cells, TGF-β, IL-6, age

INTRODUCTION

HIV infection, even when successfully controlled with antiretroviral therapy (ART), upsets the homeostasis of the immune system and is associated with increased morbidities such as cardiovascular disease (CVD) and cancer (1). While the life expectancy of a person infected with HIV has increased dramatically with the use of ART, it still remains shorter than in an HIV-uninfected person (2).

ART-treated HIV+ people exhibit continued elevation of systemic inflammation as indicated by plasma levels of soluble immune mediators that are associated with non-AIDS morbidities (3–5). Systemic inflammation is also prevalent in HIV-uninfected elderly, often referred to as "inflammaging" in those over 65 years old (6). Chronic elevated plasma levels of soluble immune mediators are also associated with morbidities and mortality in HIV-uninfected elderly (7, 8). Interleukin 6 (IL-6), tumor necrosis factor (TNF), and interleukin 1 beta (IL-1b) are among the earliest cytokines produced during an immune response, but when elevated levels of these cytokines persist they are linked to pathologies associated with chronic inflammation (9).

Immune senescence is also characteristic of both aging and chronic viral infection. T cell expression of inhibitory markers can identify exhausted (PD-1, TIGIT) or senescent (CD57, KLRG-1) T cells. Exhausted T cells undergo cell cycle arrest and lose polyfunctionality, including cytokine production (10). Programed cell death protein 1 (PD-1) is an inhibitory receptor associated with T cell exhaustion and is elevated in HIV disease (11, 12) and uninfected elderly (13, 14). T cell Immunoglobulin and ITIM Domain (TIGIT) is an inhibitory receptor on T cells that out-competes the activating receptor CD226 for its ligand-CD155. Increased frequencies of TIGIT+ effector CD8 T cells correlated with parameters of HIV disease progression (15) and TIGIT was upregulated on CD8 T cells in uninfected elderly adults (14). These two studies also found higher proportions of CD8 T cells co-expressing TIGIT and PD1. Like exhausted T cells, senescent T cells undergo cell cycle arrest; however, they continue to generate cytokines (10). Senescent cells produce large volumes of inflammatory cytokines such as IL-6 and IL-8 and are described as having a senescence-associated secretory phenotype (SASP) (16). T cell expression of CD57 is generally used to identify senescent T cells and HIV-specific CD8 T cells expressing CD57 lacked the ability to proliferate in response to antigen (17). Lastly, Killer cell lectin-like receptor subfamily G (KLRG-1) expresses an ITIM motif and after blocking its ligand, E-cadherin, KLRG-1 expressing CD8 T cells regained proliferative function (18). CD8 T cell expression of KLRG-1 is increased with age (19).

Cellular exhaustion or senescence often results after multiple rounds of proliferation which can lead to dysfunctional telomeres and the DNA damage response and cellular stress resulting in cell cycle arrest (20). Therefore, memory cells that have clonally expanded repeatedly are often the T cell maturation subsets that express markers of exhaustion and senescence.

Immune failure is a condition in HIV infection in which circulating CD4 T cell numbers fail to recover, or are very slow to recover, even when viremia is controlled by ART for >2 years. HIV+ people with immune failure are referred to as immune non-responders (INR), in contrast to immune responders (IR) who do recover CD4 T cell numbers. Immune failure is associated with increased non-AIDS morbidities (1), and INRs have both elevated systemic inflammation (21) and T cell exhaustion (22). We showed previously that INR express elevated levels of CD57 and PD-1 on their CD4 and CD8 T cells (22). In addition, we demonstrated that plasma levels of IL-6 and sCD14 were elevated in INR compared to plasma levels in IR (21). However, the INR in those studies were significantly older than the IR (21, 22). In the previous study INRs were more likely to be male and white, and they had lower CD4 nadir and were older at initiation of ART.

The objective of the current study was to examine the expression of T cell exhaustion and senescence markers and their possible associations with soluble immune mediators that have been associated with morbidity and mortality in HIV infection and aging; accounting for CD4 T cell counts and age. To determine if age may have influenced the results in the previous study of INR, we chose samples from participants that were <50 years old and would not be considered elderly (>65 years old).

HIV+ participants were on ART with controlled viremia for at least 2 years and were primarily male. The HIV+ participants were placed into three groups according to CD4 T cell status: INR (<350 cells/uL), intermediate (IT; 350–500 cells/uL), and IR (>500 cells/uL). HIV-uninfected, age distribution-matched controls (HC) were included for comparison. There was no significant difference in CD4 nadir or age at initiation of ART among the three groups of HIV+ participants.

This study was designed to examine systemic inflammation and markers of T cell exhaustion and senescence in ART-treated HIV+ INR and in age-matched uninfected controls. We found that T cell exhaustion and senescence negatively correlated with levels of TGF-β and positively correlated with plasma levels of IP10 and IL-6. Thus, we hypothesize that systemic inflammation contributes to the continuous activation of T cells resulting in T cell exhaustion and senescence.

METHODS

Ethics Statement and Participant Samples

All subjects provided written informed consent in accordance with the Declaration of Helsinki. Participant studies were approved by the University Hospitals Cleveland Medical Center Institutional Review Board or the Cleveland VA Medical Center Institutional Review Board. Frozen peripheral blood mononuclear cell (PBMC) and plasma samples from ART-treated, HIV-infected patients were selected from the Case Western Reserve University Center for AIDS Research (CFAR) repository. Annually, patients in the HIV clinic at University Hospitals of Cleveland are asked if they would like to donate a blood sample to the CFAR repository. Patients who are interested are consented and PBMC and plasma samples are stored for future HIV research. For the current study, samples were requested from the repository from patients who had both PBMCs and plasma stored from the same date, were 50 years old or younger, were on HIV ART therapy for at least 2 years with controlled viremia and had similar CD4 nadir levels

(no significant difference among INR, IT, IR groups). PBMC and plasma from healthy, HIV and HCV negative, consented participants 50 years old or younger were processed and stored as above.

Flow Cytometry

T cell phenotype was assessed using the following fluorochrome conjugated monoclonal antibodies: anti-CD3 PerCP (clone SK7), anti-CD57 FITC (clone NK-1) (BD Biosciences, San Jose, CA), anti- KLRG-1 APC (clone 13F12F2) (eBiosciences, San Diego, CA), anti-CD4 Pacific Blue (clone RPA-T4), anti-CD8 APC-Cy7 (clone SK1), anti-CD45RA PE-Cy7 (clone HI100), anti-CD27 AlexaFluor 700 (clone M-T271), anti-PD-1/CD274 BV711 (clone EH12.2H7), anti-TIGIT PE (clone A15153G) (Biolegend, San Diego, CA). PBMCs were incubated with viability dye (LIVE/DEAD-Aqua, Invitrogen, Grand Island, NY) at room temperature for 20 min then washed. Monoclonal antibodies were added for 20 min in the dark at room temperature, washed, fixed in PBS containing 2% formaldehyde, and events were acquired on a BD LSRFortessa flow cytometer (Becton Dickinson, San Jose, CA). For detection of the intracellular proteins, Ki67 (anti-Ki67-PE, BD Biosciences, San Jose, CA) and FoxP3 (anti-FoxP3-Vio667/APC, Miltenyi Biotec, Auburn, CA) cells were surface stained as described above, fixed, and permeabilized using the reagents and instructions in the Treg Detection kit (Miltenyi Biotec, Auburn, CA). Data were analyzed using FACSDIVA, (version 6.2 BD Bioscience, San Diego CA) or FlowJo (version 10.5.0) software. Maturation subsets were determined based on expression of CD45RA and CD27; naïve = CD45RA+CD27+; central memory (CM) CD45RA-CD27+; effector memory (EM) CD45RA-CD27-; terminal effector memory (TEM) CD45RA+CD27-. If there were fewer than 100 events in any T cell memory subset, those data were excluded from analysis. The CD4 TEM T cell subset sometimes had fewer than 100 events and may have a lower "*n*" value.

ELISA

Plasma IL-6 was measured by high sensitivity ELISA (Quantikine HS, R&D Systems, Minneapolis, MN), and soluble CD14 (sCD14), soluble CD163 (sCD163), Interferon gamma-induced protein 10 (IP10) or C-X-C motif chemokine 10 (CXCL10), and transforming growth factor-b1 (TGF-β1) were measured by ELISA (Quantikine, R&D Systems, Minneapolis, MN). Before measurement of TGF-β1, plasma was activated by 1N HCL as instructed in the manufacturer's protocol.

Statistics

Dichotomous variables (gender and CMV sero-status) were examined using the Chi-squared test. Comparisons among three or more groups were performed with non-parametric Kruskal-Wallis tests. Comparisons between two unrelated groups were performed using non-parametric two-tailed Mann Whitney *U*-tests. Associations between continuous variables were explored by Spearman's rank order correlation coefficient. All statistics were performed using GraphPad version 6 and significance thresholds were set at p-values ≤ 0.05.

RESULTS

Participant Characteristics

All HIV+ patients were ≤50 years old and had successful control of virus with ART for at least 2 years. Immune responder (IR) patients were more likely to have a protease inhibitor (PI) in their ART regimen (**Table 1**). No participants had a recognized viral illness at time of blood draw, no anti-neoplastic or immune modulatory treatment for cancer for at least 24 weeks, and no known immunological/inflammatory diseases (excepting HIV infection). There were no significant differences in age among the HC group and the INR, IT, and IR groups (Kruskal-Wallis $p = 0.511$; **Table 1**). There were no significant differences in CD4 nadir among the three HIV+ participant groups (Kruskal-Wallis $p = 0.910$; **Table 1**). Participants in all groups were primarily male. The HC participant group was primarily white (88%) and the HIV+ participant groups were about half white (INR 55%, IT 50%, and IR 42%). Nearly all HIV+ participants were serum antibody positive for cytomegalovirus (CMV) [INR 100% (23/23), IT 100% (14/14), IR 85% (22/26)] while 30% (9/30) of the HC participants were seropositive for CMV (**Table 1**).

Proportions of T Cell Subsets and T Cell Subset Expression of Exhaustion and Senescence Markers in Treated, HIV-Infected Participants

Supplementary Figure 1A shows the gating strategy used to identify live CD3+ lymphocytes, CD4+ or CD8+ T cells, and naïve (CD45RA+CD27+), central memory [(CM) CD45RA-CD27+], effector memory [(EM) CD45RA-CD27-], and terminal effector memory [(TEM) CD45RA+CD27-] T cell maturation subsets. The proportions of naïve CD4 and CD8 T cells were lower in INR and IT compared to proportions in HC and IR, while proportions of effector memory T cells were higher in INR and IT than in HC. Effector memory CD8 T cell proportions were also elevated in IR compared to proportions in HC and effector memory CD4 T cell proportions were higher in in INR than in IR (**Figure 1**). Proportions of CD8 TEM T cells were elevated in both INR and IR compared to proportions in HC (**Figure 1**).

Examples of PD-1, KLRG-1, TIGIT (**Supplementary Figure 1B**), and CD57 (**Supplementary Figure 1C**) staining on CD4 and CD8 T cells, maturation subsets and isotype controls are shown in **Supplementary Figures 1B,C**. In general, the proportions of memory CD4 T cell subsets expressing CD57, PD-1, TIGIT, and KLRG-1 were elevated in HIV+ participants compared to proportions in uninfected participants (**Figure 2**). CD4 CM T cell proportions expressing TIGIT were higher in INR, IT and IR than proportions in HC. PD-1+ proportions of CD4 CM T cells were higher in INR and IT compared to proportions in HC. Proportions of KLRG-1+ CD4 CM T cells were higher in HC compared to those in the HIV-infected groups. Proportions of CD57+, PD-1+, and TIGIT+ CD4 EM T cells were higher in INR, IT, and IR compared to proportions in HC. CD4 TEM proportions of CD57+ and KLRG-1+ T cells were higher in INR, IT, and IR than in HC. Proportions of PD-1+ TEM T cells were higher in INR and IT compared to

TABLE 1 | Participant characteristics.

	HIV^{neg} HC	HIV^{pos} INR	HIV^{pos} IT	HIV^{pos} IR	
***n*=**	**30**	**23**	**14**	**26**	***P*-value**
Median age (range)	41 (24–50)	43 (25–50)	44 (38–48)	41 (33–49)	*0.511
Median CD4 count (range)	NA	251 (80–347)	388 (352–491)	611 (503–1505)	*<0.0001
Median CD4+ Nadir (range)	NA	62 (0–255)	79 (0–203)	89 (3–249)	*0.91
Gender	76% male	77% male	100% male	75% male	**0.207
CMV % sero pos	30.0%	100%	100%	85%	**all grps = <0.0001 HIV+ grps = 0.048
Race	8% black	41% black	50% black	54% black	
	88%white	55% white	50% white	42% white	
	4% Other	4% Other		4% Other	
ART regimen	NA				
	NRTI + NNRTI	61%	57%	35%	
	NRTI + PI	30%[$]	36%	62%	
	NRTI + INSTI	4%	7%^	4%	

NA, not available; CMV, cytomegalovirus; NRTI, nucleoside reverse transcriptase inhibitors; NNRTI, non-nucleoside reverse transcriptase inhibitors; PI, protease inhibitor; INSTI, integrase strand transfer inhibitor.

***HC**= uninfected age distribution-matched control (≤50 years old).*

***INR**= immune non-responders; ART treated; <350 CD4 T cells/uL; < 50 years old.*

***IT**= intermediate CD4 counts; ART treated; 350–500 CD4 T cells/uL; < 50 years old.*

***IR**= immune responders; ART treated; >500 CD4 T cells/uL; <50 years old.*

There was no significant difference in age among INR, IT, IR, or HC populations.

[*]Kruskal-Wallis; [**]Chi Squared; one patient received PI only; one patient received PI also.

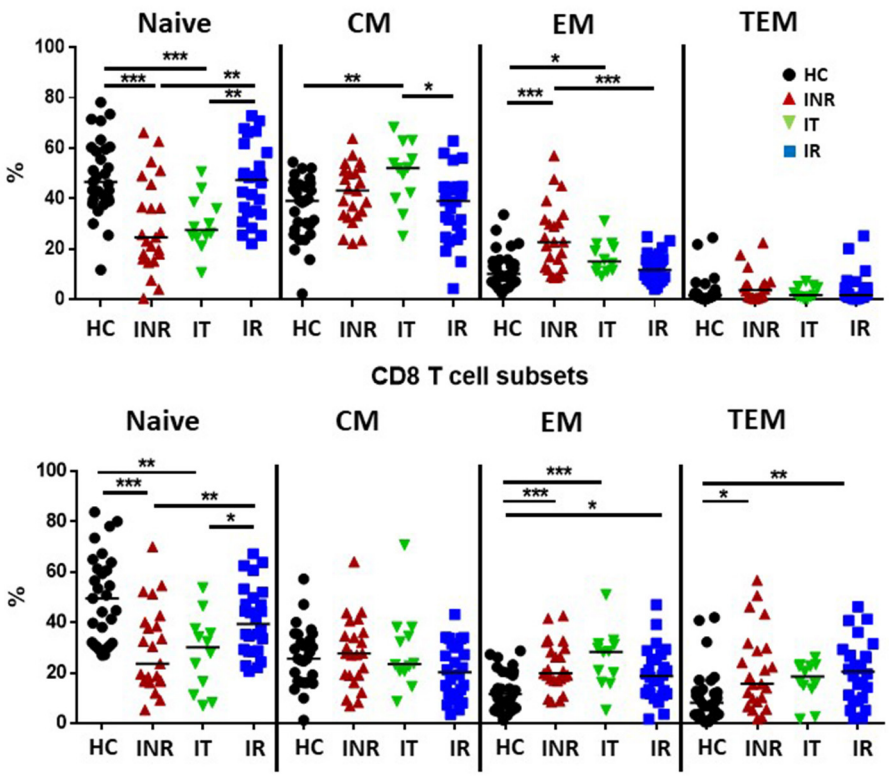

FIGURE 1 | Proportions of T cell maturation subsets in healthy controls, immune non-responders, intermediate, and immune responders. Thawed PBMCs were stained with live/dead stain, for CD4 and CD8 T cell subsets, and for CD45RA and CD27 to determine maturation subsets (naïve= CD45RA+CD27+; central memory CM= CD45RA-CD27+; effector memory EM= CD45RA-CD27-; terminal effector memory TEM= CD45RA+CD27-). Comparisons between 2 groups were made using the non-parametric, unpaired Mann-Whitney test. *$p = <0.05$; **$p = <0.01$; ***$p = <0.001$.

proportions in HC. Proportions of TIGIT+ TEM T cells were higher in INR when compared to proportions in HC.

In INR, the proportions of CD4 EM T cells expressing CD57 (**Figure 2A**) and PD-1 (**Figure 2B**) were elevated compared to the proportions in IR (**Figures 2A,B**). The proportions of TEM CD4 T cells expressing PD-1 and TIGIT were also elevated in INR compared to IR (**Figures 2B,C**).

In general, the proportions of CD8 T cells expressing markers of exhaustion and senescence were higher than that on CD4 T cells, especially in CM and TEM subsets, but the number of significant differences among the groups were not as great (**Figures 2**, **3**). CD8 CM T cell proportions expressing TIGIT were higher in INR and IT compared to proportions in HC and EM proportions of TIGIT+ and KLRG-1+ T cells were higher in INR and IT compared to CD8 EM T cell proportions in uninfected participants (**Figure 3**). CD8 EM proportions of CD57+ T cells were higher in INR, IT, and IR compared to HC (**Figure 3**). CD8 T cells from INR expressed higher proportions of TIGIT+ (EM and TEM) and KLRG-1+ (CM) T cells than did memory CD8 T cells from IR. Surprisingly, the proportions of KLRG-1+ CM CD8 T cells and TIGIT+ TEM T cells were lower in IR than proportions in HC (**Figures 3C,D**).

Plasma Levels of IL-6, IP10 (CXCL10), sCD14, and sCD163 in Treated, HIV+ Participants

Plasma IL-6 levels have been strongly associated with morbidities in HIV+ patients (3, 4) and were previously found to be elevated in the plasma of INR (21). However, in this cohort of relatively young (<50 years old) HIV+ patients, levels of IL-6 were not elevated in the plasma from INR when compared to plasma levels in the IR patients (**Figure 4**). Plasma levels of IL-6 were elevated in all HIV+ participant groups when compared to IL-6 levels in the HC group (**Figure 4**). Plasma IP10 levels were significantly elevated in the INR as compared to levels in IR and IT, and in all HIV+ groups compared to plasma levels in HC (**Figure 4**). There was a trend to higher plasma levels of sCD14 in HIV+ participants with lower CD4 counts, but this was only significant in the IT group compared to the IR group (**Figure 4**). Plasma levels of sCD14 were higher in HIV+ participant regardless of CD4 counts when compared to plasma levels in HC (**Figure 4**). Lastly, in this study, the only statistically significant difference in plasma sCD163 levels was an increase in plasma sCD163 in the IR compared to the plasma levels in the HC (**Figure 4**).

Plasma Levels of TGF-β and Proportions of Cycling CD4 Cells That Are T Regulatory Cells in Treated HIV+ Participants

We recently examined cycling CD4 T cells in INR and found that although cycling CD4 T cells were enriched for T regulatory cells (Tregs), frequencies of Tregs among cycling cells were lower in INR than in IR (23). Here, we examined the proportion of cycling (Ki67+) CD4 T cells that were Tregs in our three groups of HIV+ participants. Consistent with our previous report, we found that the proportion of $CD45RA^{neg}$ CD4+ Ki67+ T cells that were Tregs (CD4+ CD45RA- CD25+ CD127-FoxP3+) were significantly lower in INR (**Figure 5A**) than in the IR group. TGF-β promotes the development of Tregs (24). Therefore, we examined TGF-β in the HIV+ participants and found that plasma TGF-β levels were significantly lower in the INR and IT groups when compared to plasma levels in the IR group (**Figure 5B**). Due to differences in collection protocols, plasma levels of TGF-β in HC were not directly comparable to HIV+ participant groups, and so have been excluded from these analyses. In addition, there was a positive correlation between CD4 T cell counts and plasma levels of TGF-β in INR ($r = 0.437$, $p = 0.050$) and IT ($r = 0.551$, $p = 0.044$) but not IR participants ($r = 0.331$, $p = 0.114$) (**Figure 5C**).

The Association of Plasma Levels of IL-6, IP10, TGF-β, and sCD14 With T Cell Markers of Exhaustion and Senescence in Treated, HIV+ Participants

Next, we examined the correlation of plasma levels of IL-6, IP10, TGF-β, sCD14, and sCD163 with the proportions of markers of T cell exhaustion (PD-1, TIGIT) and senescence (CD57, KLRG-1) expressed on T cell maturation subsets in HIV+ participants. Only those associations that were significant are shown in **Supplementary Table 1**. **Figure 6** shows representative graphs of the association between plasma levels of TGF-β and TIGIT+ T cell subset proportions in INR and plasma TGF-β levels and T cell subset proportions of TIGIT+ and PD-1+ cells in IR. Plasma levels of TGF-β negatively correlated with proportions TIGIT+ (CD4 EM, CD8 CM, EM) T cells in INR and proportions of TIGIT+ (CD8 EM, naïve) and PD-1+ (CD4 EM, TEM) T cells in IR (**Supplementary Table 1**). Proportions of naïve KLRG-1+ T cells also negatively correlated with plasma levels of TGF-β in INR and IR (**Supplementary Table 1**). There was a positive correlation between plasma levels of TGF-β and proportions of CD4 EM CD57 in INR (**Supplementary Table 1**).

The associations of plasma levels of TGF-β with markers of T cell exhaustion were mostly negative associations, however the associations between plasma levels of IP10 and IL-6 and T cell markers of exhaustion and senescence were primarily positive (**Supplementary Table 1**). **Figure 7** shows representative graphs of the positive association between plasma levels of IL-6 and proportions of CD4 EM TIGIT+ T cells and plasma levels of IP10 and proportions of CD8 EM TIGIT and CM CD57 in INR (upper panel). Plasma levels of IP10 also positively associated with proportions of CD4 EM PD-1 and CD8 CM PD-1+ cells in INR (**Supplementary Table 1**). The lower panels show the positive association between plasma levels of IL-6 with CD4 CM proportions of TIGIT+, PD-1+ and CD57+ cells in IR. There were no significant associations between plasma levels of IP10 and T cell markers of exhaustion or senescence in IR (**Supplementary Table 1**). There were few significant associations between sCD163 and markers of exhaustion and senescence (data not shown). Interestingly, in INR there was a negative association between plasma levels of sCD14 and proportions of CD8 T cell subsets expressing markers of exhaustion and senescence (**Supplementary Table 1**).

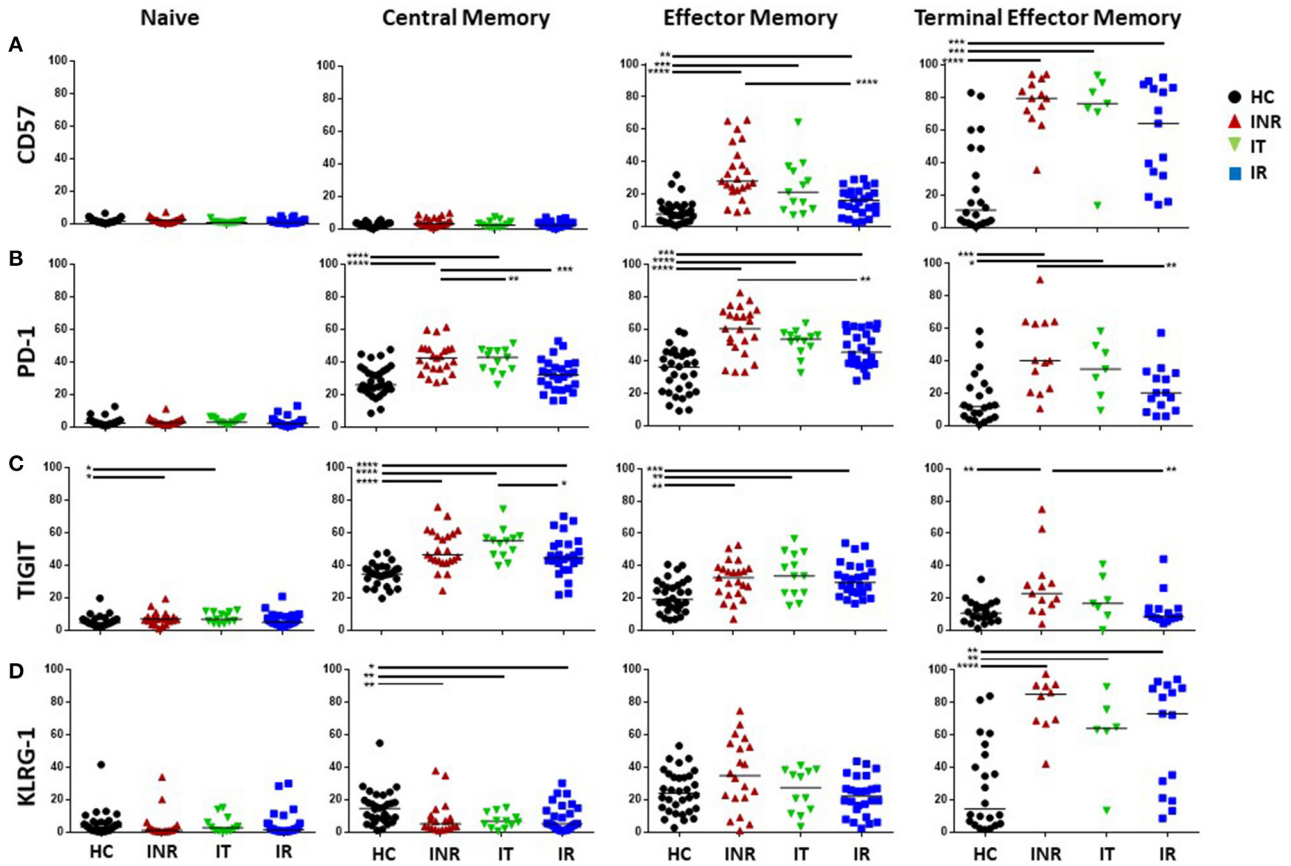

FIGURE 2 | Proportions of T cell exhaustion and senescence markers on CD4 naïve, CM, EM, and TEM T cell subsets. Thawed PBMCs were stained with live/dead stain, for CD4 and CD8 T cell subsets, and for CD45RA and CD27 to determine maturation subsets (naïve = CD45RA+CD27+; central memory CM = CD45RA-CD27+; effector memory EM = CD45RA-CD27-; terminal effector memory TEM = CD45RA+CD27-). Live gated CD3+CD4+ T cells were assessed for the proportion of CD57 **(A)**, PD-1 **(B)**, TIGIT **(C)**, and KLRG-1 **(D)** within each maturation subset. Each symbol represents one participant, *black circles* = uninfected <50 years old; *red triangles* = ART treated HIV-infected INR CD4 <350/uL, <50 years old; *green inverted triangles* = ART treated HIV-infected IT CD4 350–500/uL, <50 years old; *blue squares* = ART treated HIV-infected IR CD4 >500/uL, <50 years old. Short black bars indicate median. Comparisons between 2 groups were made using the non-parametric, unpaired Mann-Whitney test. *p = <0.05; **p = <0.01; ***p = <0.001; ****p = <0.0001.

DISCUSSION

Our previous studies found elevated plasma levels of IL-6 and sCD14 (21) and increased T cell expression of CD57 and PD-1 (22) in INR. However, in those studies the INR were significantly older than the IR, and both INR and IR were significantly older than the uninfected controls (21, 22). IL-6 and sCD14 are elevated in HIV-uninfected elderly and are associated with morbidity and mortality (7, 8). In addition, T cell expression of PD-1 (13), TIGIT (14), and KLRG-1 (19) were elevated in HIV-uninfected elderly. Therefore, in the current study we chose treated, HIV-infected participants that were <50 years old and a group of uninfected, age distribution-matched healthy controls. All HIV+ participants had controlled viremia for at least 2 years. They were divided into groups based on CD4 T cell counts as described above. The other objective of the current study was to examine the expression of T cell exhaustion and senescence markers and their possible associations with soluble immune mediators in treated HIV infection.

As mentioned, markers of exhaustion and senescence are most often found on memory T cells that have undergone multiple rounds of replication and activation. Proportions of memory T cells are elevated during aging and in chronic viral infections and our data confirm these findings. In this study we did not calculate absolute naïve T cell counts.

Proportions of PD-1 expressing exhausted T cells are elevated in HIV disease (11, 12) and may be related to the ability to recover CD4 T cells after control of virus with ART (25). Examination of HIV-specific CD8 T cells found that many expressed CD57 and lacked the ability to proliferate in response to antigen (17) and T cell expression of CD57 may be associated with the inability to reconstitute CD4 T cells despite ART control of virus (26). In the current study we saw increased proportions of CD4 EM T cells expressing PD-1, TIGIT and CD57 and increased CD8 EM proportions of CD57, TIGIT and KLRG-1 in treated, HIV+ participants when compared to proportions expressed in uninfected controls. We also found that proportions of CD4 EM T cells expressing PD-1 and CD57 were elevated in

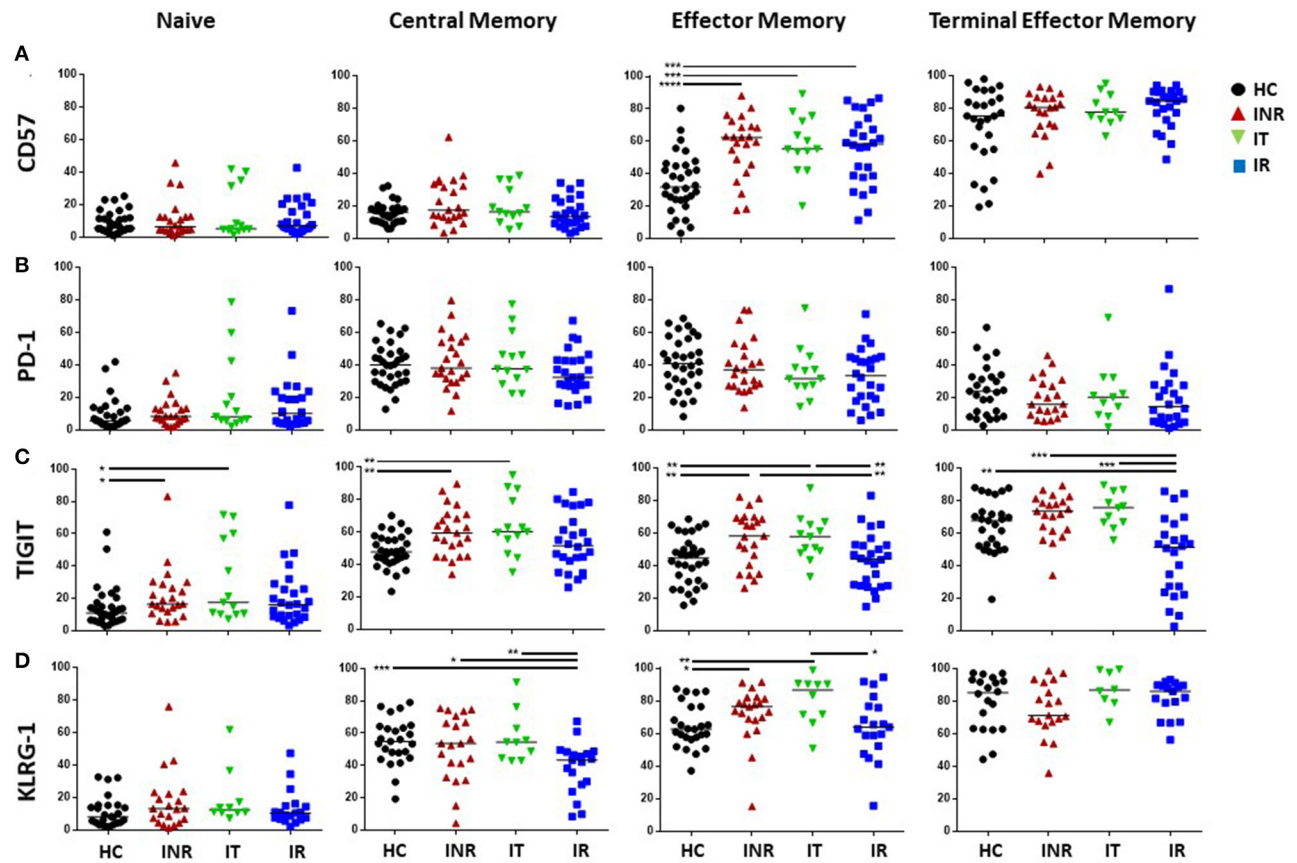

FIGURE 3 | Proportions of T cell exhaustion and senescence markers on CD8 naïve, CM, EM, and TEM T cell subsets**.** Thawed PBMCs were stained with live/dead stain, for CD4 and CD8 T cell subsets, and for CD45RA and CD27 to determine maturation subsets (naïve = CD45RA+CD27+; central memory CM = CD45RA-CD27+; effector memory EM = CD45RA-CD27-; terminal effector memory TEM = CD45RA+CD27-). Live gated CD3+CD8+ T cells were assessed for the proportion of CD57 **(A)**, PD-1 **(B)**, TIGIT **(C)**, and KLRG-1 **(D)** within each maturation subset. Each symbol represents one participant, *black circles* = uninfected <50 years old; *red triangles* = ART treated HIV-infected INR CD4 <350/uL, <50 years old; *green inverted triangles* = ART treated HIV-infected IT CD4 350–500/uL, <50 years old; *blue squares* = ART treated HIV-infected IR CD4 >500/uL, <50 years old. Short black bars indicate median. Comparisons between 2 groups were made using the non-parametric, unpaired Mann-Whitney test. *p = <0.05; **p = <0.01; ***p = <0.001; ****p = <0.0001.

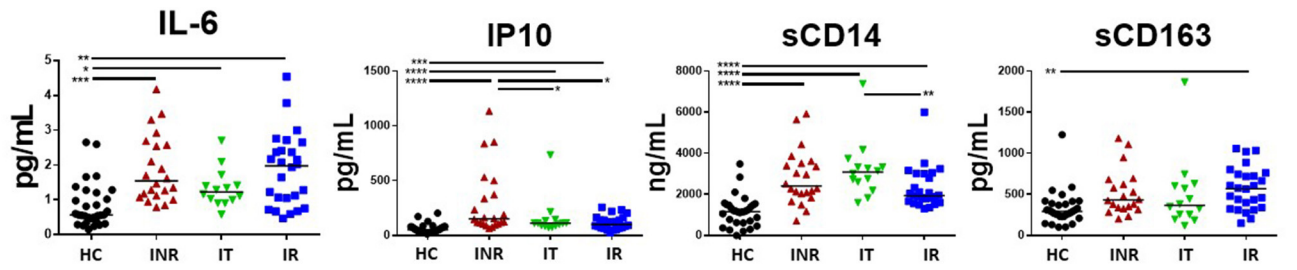

FIGURE 4 | Plasma levels of IL-6, IP10 (CXCL10), sCD14, and sCD163 in treated, HIV+ participants**.** Plasma was measured by ELISA for IP10 (CXCL10), sCD14, sCD163, and IL-6 (high sensitivity) following the manufacture's protocol. Each symbol represents one participant, *black circles* = uninfected age-matched controls (HC) <50 years old; *red triangles* = ART treated HIV-infected INR CD4 <350/uL, <50 years old; *green inverted triangles* = ART treated HIV-infected IT CD4 350–500/uL, <50 years old; *blue squares* = ART treated HIV-infected IR CD4 >500/uL, <50 years old. Black bars indicate median. Comparisons between 2 groups were made using a Mann-Whitney *U*-test. *p = <0.05; **p = <0.01; ***p = <0.001; ****p = <0.0001.

INR when compared to proportions expressed in IR. Although the proportions of memory T cells were elevated in INR, we calculated the proportion of CD57, PD-1, TIGIT, and KLRG-1 expressing cells within each T cell maturation subset, therefore expression level should be independent of the proportion of the maturation subset.

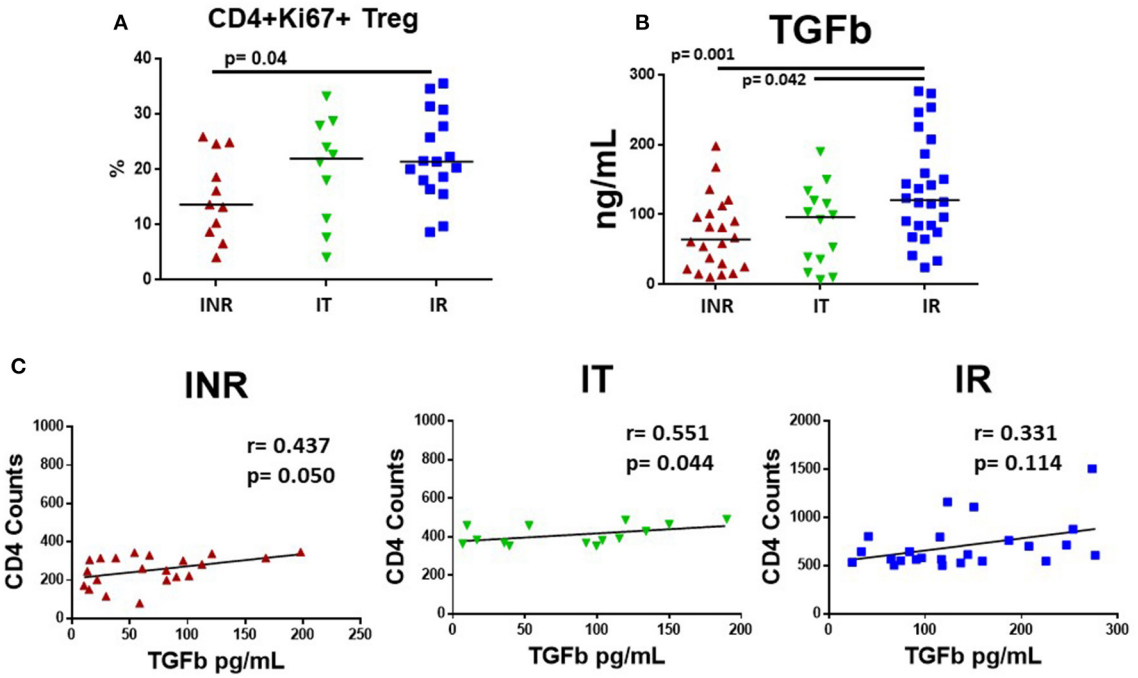

FIGURE 5 | Plasma levels of TGF-β and proportions of cycling memory CD4+ cells that are T regulatory cells in HIV+, treated participants**.** PBMCs were stained for Tregs using Miltenyi Biotec's Treg Detection kit and plasma was measured for TGF-β using R&D System ELISA kit. Each symbol represents one subject, *red triangles* = INR, CD4 <350/uL, <50 years old; *green inverted triangles* = IT CD4 350–500/uL, <50 years old; *blue squares* = IR CD4 >500/uL, <50 years old. **(A)** Proportions of CD3+CD4+CD45RA-Ki67+ cells that were CD127-CD25+ and FoxP3+, identified as Tregs are shown. **(B)** TGF-β was activated with 1N HCL and measured following manufacture's protocol; plasma levels are shown. Comparisons between 2 groups were made using a Mann-Whitney *U*-test. **(C)** Plasma levels of TGF-β were compared to CD4 T cell counts in treated, HIV-infected INR, IT, and IR participants using a rank order Spearman's analysis. Significance thresholds were set at *p*-values equal to or <0.05.

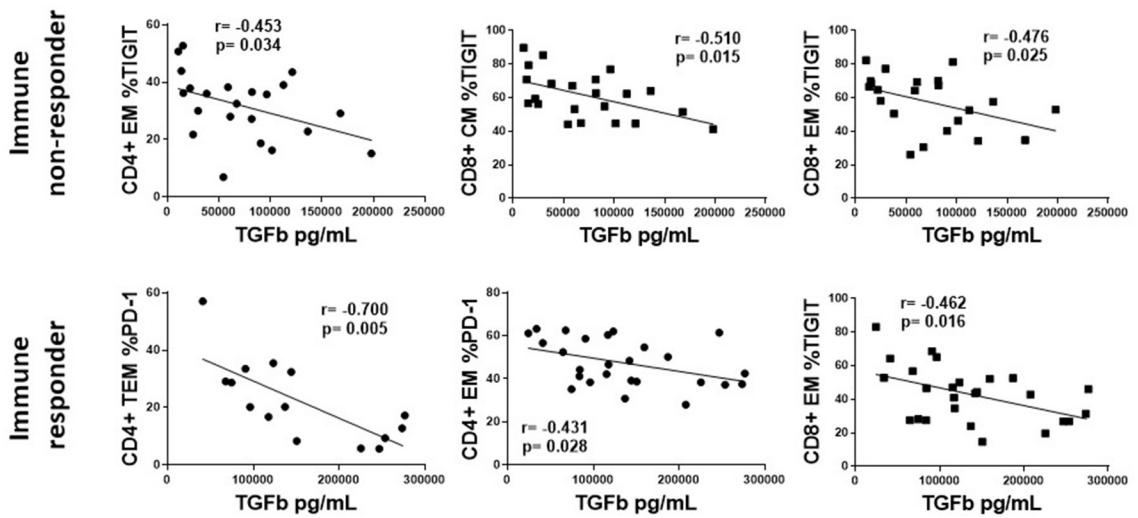

FIGURE 6 | The association of plasma levels of TGF-β with T cell markers of exhaustion and senescence in treated, HIV-infected immune non-responders and responders**.** Representative correlations from **Supplemental Table 1** are show. Top row, immune non-responders (INR); Plasma levels of TGF-β (x-axis) vs. CD4+ EM proportion of TIGIT, or CD8+ CM and EM proportions of TIGIT (y-axis). Bottom row, immune responders (IR); Plasma levels of TGF-β (x-axis) vs. CD4+ EM and TEM proportion of PD-1, or CD8+ EM proportions of TIGIT. Correlations were calculated using a Spearman's rank order analysis; $p = <0.05$ considered statistically significant.

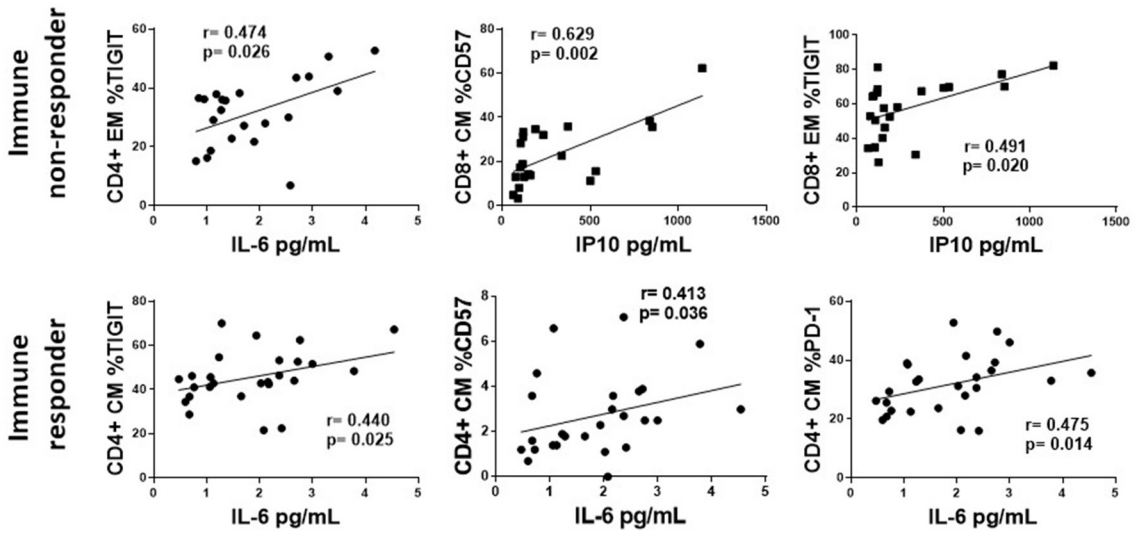

FIGURE 7 | The association of plasma levels of IP10 and IL-6 with T cell exhaustion and senescence**.** Representative correlations from **Supplemental Table 1** are show. Top row, immune non-responders (INR); Plasma levels of IL-6 or IP10 (x-axis) vs. CD4+ EM proportion of TIGIT, or CD8+ CM CD57 and EM proportions of TIGIT (y-axis, respectively). Bottom row, immune responders (IR); Plasma levels of IL-6 (x-axis) vs. CD4+ CM proportion of TIGIT, CD57, and PD-1. Correlations were calculated using a Spearman's rank order analysis; $p = <0.05$ considered statistically significant.

We also examined T cell expression of the inhibitory markers, KLRG-1 and TIGIT. Increased frequencies of TIGIT expressing CD8 T cells correlated with parameters of HIV disease progression (15) and TIGIT was also upregulated on CD8 T cells in uninfected elderly adults (14). We found elevated proportions of TIGIT expressing CD4 (CM, EM, TEM) and CD8 (CM, EM) T cells in treated HIV+ participants compared to proportions in HC and proportions of TIGIT+ CD4 and CD8 TEM T cells tended to be higher in INR.

We found it interesting that proportions of TIGIT+ naive CD4 and CD8 T cells were elevated in INR and IT compared to proportions in HC. In a study of elderly patients, TIGIT was also elevated in naïve (CD45RA+CCR7+) CD8 T cells (14). The expression of exhaustion and senescence markers on naïve T cells from elderly participants may reflect a population of CD8 T cells that are phenotypically naïve (CD45RA+, CCR7+, CD27+ CD95-) but are actually antigen-experienced (13, 27). This population of memory T cells with a naïve phenotype (T_{MNP}) may be present in INR as well. Our future studies in INR will examine this possibility in more detail.

Circulating inflammatory cytokines like IL-6 and IP10 are indicators of immune cell activation. Circulating soluble receptors are also an indication of innate immune cell activation. Activation of monocytes and macrophages causes the release of soluble forms of the surface receptors CD14 and CD163 (28, 29). In the current study, in which all HIV+ participant groups were similarly aged, plasma levels of IL-6 were higher in the HIV+ participants compared to plasma levels in HC, but among HIV+ donors, we observed no significant difference between INR and IR. IP10 is induced by Type I and Type II IFNs and in acute HIV infection, IP10 plasma levels were predictive of rapid disease progression and were negatively associated with CD4 T cell number set point (30). In the current study, plasma levels of IP10 were significantly higher in INR than in all other groups.

One factor that may contribute to systemic inflammation and T cell exhaustion and senescence observed in the current study is chronic infection with CMV. Indeed, CMV seropositivity is associated with immunosenescence (31) and our studies in HIV infection demonstrated that CMV coinfection is associated with elevated CD57 expression on both CD4 and CD8 memory T cells in treated HIV infection (32, 33). Another study found higher proportions of CD8+ CD28- T cells expressing CD57 in uninfected CMV seropositive participants compared to proportions in CMV seronegative participants (34). Proportions of CD8+CD28-T cells expressing CD57 were also associated with age (34). During primary CMV infection, IL-6 and IP10 are induced, and IP10 persists even during CMV latency (35). Previously, we found that plasma IP10 levels were significantly elevated in treated HIV+ CMV-seropositive donors compared to levels in treated HIV+ CMV-seronegative donors (36). It is possible that immune mechanisms that induce IP10, such as Type I or Type II IFNs, may arise early in HIV infection or as a result of CMV infection and persist after virus suppression by ART. Sorting out the immune manifestations of CMV infection is difficult because in immune competent hosts, infection is largely asymptomatic, and most HIV+ persons are CMV seropositive (93.7% in this cohort) (37). One limitation of the current study was that it was not powered to examine the effects of CMV infection on inflammation or T cell exhaustion/senescence, as nearly all of our HIV+ participants were CMV-seropositive, but only 30% of HC were CMV-seropositive. When we compared results from the CMV+ ($n = 9$) and CMV- ($n = 21$) uninfected healthy controls in the current study, we observed higher proportions of CD57+, PD-1+ and KLRG-1+ CD4 (EM and

TEM) T cells in CMV seropositive HIV-uninfected controls compared to proportions in CMV seronegative HIV-uninfected controls. We did not see any significant difference in CD8 subset expression of markers of T cell exhaustion or senescence, nor did we see any significant difference in plasma levels of IL-6, IP10, sCD14, or sCD163 when results among CMV seropositive and seronegative controls were compared.

We hypothesize that systemic inflammation contributes to the continuous activation and turnover of T cells resulting in T cell exhaustion and senescence in INR. We saw a significant positive correlation between plasma levels of IL-6 and T cell expression of exhaustion and senescence markers in both INR and IR and between plasm levels of IP10 and T cell expression of exhaustion and senescence markers in INR. Although associations do not confirm causality or directionality, these data are consistent with the interpretation that systemic immune mediators are related to T cell exhaustion and senescence. Importantly, we have evidence suggesting causality in our earlier study in which we showed that *in vitro* stimulation of healthy PBMCs for 7 days with IL-6 or IL-1b can induce the expression of PD-1 and CD57 on T cells (22).

Perhaps even more striking in the current study was the negative association of plasma levels of TGF-β and expression of T cell markers of exhaustion and senescence in the INR and IR. TGF-β is an important anti-inflammatory cytokine and promotes the development of T regulatory cells (24). In our previous study examining INR, we paradoxically found higher levels of cycling (Ki67+) CD4 T cells in INR, even though they sustain low CD4 T cell numbers (21). In our more recent study that examined this finding in more detail, we found that many of the cycling CD4 T cells were Tregs regardless of the extent of CD4 T cell recovery. Previously, when we examined the cycling CD4 T cells, we found that cycling cells from INR had lower frequencies of CD4 Tregs overall, and the Tregs that remained had evidence of mitochondrial dysfunction (23). We also found that the cycling CD4 T cells in INR had transcriptomic profiles consistent with decreased TGF-β signaling and increased apoptosis signaling (23). Here, we found significantly lower plasma levels of TGF-β and cycling CD4+ T cells that were Tregs, as well as higher levels of T cell exhaustion and senescence in INR than among IR. We propose that there are mechanistic links among low TGF-β levels, reduced CD4 T cell recovery, impaired Treg functionality, and dysregulated T cell phenotypes.

In summary, treated, HIV+ participants ≤50 years old showed greater expression of T cell exhaustion (CD4 EM PD-1 and TIGIT; CD8 EM TIGIT) and senescence (CD4 and CD8 EM CD57) markers and higher plasma levels of IL-6, IP10 and sCD14 than did age matched HC. INR in particular, generally had greater T cell exhaustion (CD4 PD-1; CD8 TIGIT) and senescence (CD4 EM CD57) and elevated plasma levels of IP10. There was a positive correlation between plasma levels of IL-6 and CD4 T cell exhaustion [in INR and IT (EM TIGIT); in IR (CM TIGIT and PD-1)] and senescence [in IR (CM CD57)]. There was also a positive correlation between plasma IP10 and T cell exhaustion in INR (CD4 EM PD-1, CD8 CM PD-1, CD8 EM TIGIT) and T cell senescence in INR (CD8 CM CD57). Plasma levels of TGF-β and proportions of cycling CD4+ T cells that were Tregs were significantly lower in INR compared to levels in IR. Lastly, plasma levels of TGF-β negatively correlated with markers of T cell exhaustion in INR (CD4 EM TIGIT, CD8 CM EM TIGIT) and IR (CD4 EM TEM PD-1, CD8 EM TIGIT).

In conclusion, we hypothesize that a "tug-of-war" exists between inflammation and the associated T cell exhaustion and senescence on one side, and anti-inflammatory TGF-β levels and Tregs on the other. Our data support a model whereby INR have dysfunctional CD4 T cell cycling (23), lower levels of TGF-β, and decreased generation of Tregs, and therefore, may have difficulty controlling inflammation. Elevated plasma levels of IP10 and IL-6 were positively associated with T cell expression of exhaustion and senescence markers in INR in this study. Our previous *in vitro* studies showed that IL-6 and IL-1b can induce the upregulation of PD-1 and CD57 on T cells (22). Whether these effects contribute to or are a result of immune failure is an open question, and is the focus of current research in our laboratories. Future studies will examine this model in other settings of lymphopenia and in the HIV-uninfected elderly.

DATA AVAILABILITY STATEMENT

The raw data supporting the conclusions of this article will be made available by the authors, without undue reservation.

ETHICS STATEMENT

The studies involving human participants were reviewed and approved by the University Hospitals Cleveland Medical Center Institutional Review Board or the Cleveland VA Medical Center Institutional Review Board. The patients/participants provided their written informed consent to participate in this study.

AUTHOR CONTRIBUTIONS

CS conceived study design, performed and analyzed experiments, and wrote manuscript. MF and S-AY contributed to experiment analysis and manuscript preparation. CK performed and analyzed experiments and CK, DC, and BR provided patient samples. DC, BR, ML, and DA contributed to study design and manuscript preparation. All authors reviewed and approved manuscript.

FUNDING

This work was supported by VA CDA2 51K2CX001471 (Shive), NIH AG044325-subaward WFUHS 115068 (Shive), VA Merit 1IO1CX001104 (Anthony), BX001894 (Anthony), R21AG062386 (Younes). The content is solely the responsibility of the authors and does not necessarily represent the official views of the VA.

ACKNOWLEDGMENTS

We would like to thank Dominic Dorazio, Michelle Gallagher, Robert Asaad, Jeffrey Jacobson, and other members of the AIDS Clinical Trial Unit (ACTU) for their support.

SUPPLEMENTARY MATERIAL

The Supplementary Material for this article can be found online at: https://www.frontiersin.org/articles/10.3389/fimmu.2021.638010/full#supplementary-material

Supplementary Figure 1 | Gating strategy. **(A)** Shows the gating strategy for CD4 and CD8 T cell maturation subsets in two participants (INR and IR). After singlet gating, lymphocytes were gated on a FSC/SSC plot. Live cells were gated based on the negative staining of InVitrogen live/dead aqua stain, then live cells expressing CD3 were gated. CD3+ T cells were then gated for CD4 or CD8 expression. For each subset (CD4 or CD8) CD45RA vs. CD27 was examine and a quadrant gate was used to determine naïve (CD45RA+CD27+), central memory (CD45RA-CD27+), effector memory (CD45RA-CD27-), and terminal effector memory (CD45RA+CD27-) subsets. **(B)** Shows PD-1, CD57, KLRG-1, and TIGIT staining from one participant. The top row shows isotype staining in CD4 (blue) or CD8 (purple) T cells. The center row show PD-1, CD57, KLRG-1, and TIGIT staining in CD4 (blue) or CD8 (purple) T cells. The bottom row shows the PD-1, CD57, KLRG-1, and TIGIT staining in overlapping histographs of maturation subset in CD4 or CD8 T cells. The participant in **(B)** did not show positive CD57 staining, therefore we included a different participant who did show positive CD57 staining in **(C)**.

Supplementary Table 1 | The association of plasma levels of IL-6, IP10, TGF-β, and sCD14 with markers of T cell exhaustion and senescence. The correlation of plasma levels of IL-6, IP10, TGFb, sCD14, and sCD163 were compared to the proportions of CD4 and CD8 T cell maturation subsets expressing CD57, PD-1, TIGIT, and KLRG-1 in treated, HIV+ INR, IT, and IR using Spearman's rank order analysis. Only correlations that were significant are shown in table. *P* and *r* values are shown for each significant correlation; $p = <0.05$ considered statistically significant. Gray boxes are significant negative correlations; white boxes are significant positive correlations.

REFERENCES

1. Smith C, Sabin CA, Lundgren JD, Thiebaut R, Weber R, Law M, et al., Factors associated with specific causes of death amongst HIV-positive individuals in the D:A:D Study. *AIDS*. (2010) 24:1537–48. doi: 10.1097/QAD.0b013e32833a0918
2. Wandeler G, Johnson LF, Egger M. Trends in life expectancy of HIV-positive adults on antiretroviral therapy across the globe: comparisons with general population. *Curr Opin HIV AIDS*. (2016) 11:492–500. doi: 10.1097/COH.0000000000000298
3. Hunt PW, Sinclair E, Rodriguez B, Shive C, Clagett B, Funderburg N, et al. Gut epithelial barrier dysfunction and innate immune activation predict mortality in treated HIV infection. *J Infect Dis*. (2014) 210:1228–38. doi: 10.1093/infdis/jiu238
4. Tenorio AR, Zheng Y, Bosch RJ, Krishnan S, Rodriguez B, Hunt PW, et al. Soluble markers of inflammation and coagulation but not T-cell activation predict non-AIDS-defining morbid events during suppressive antiretroviral treatment. *J Infect Dis*. (2014) 210:1248–59. doi: 10.1093/infdis/jiu254
5. Armah KA, McGinnis K, Baker J, Gibert C, Butt AA, Bryant KJ, et al. Status HIV, burden of comorbid disease, and biomarkers of inflammation, altered coagulation, and monocyte activation. *Clin Infect Dis*. (2012) 55:126–36. doi: 10.1093/cid/cis406
6. Franceschi C, Bonafe M, Valensin S, Olivieri F, M. De Luca, Ottaviani E, et al. Inflamm-aging. An evolutionary perspective on immunosenescence. *Ann N Y Acad Sci*. (2000) 908:244–54. doi: 10.1111/j.1749-6632.2000.tb06651.x
7. Wikby A, Nilsson BO, Forsey R, Thompson J, Strindhall J, Lofgren S, et al. The immune risk phenotype is associated with IL-6 in the terminal decline stage: findings from the Swedish NONA immune longitudinal study of very late life functioning. *Mech Ageing Dev*. (2006) 127:695–704. doi: 10.1016/j.mad.2006.04.003
8. Reiner AP, Lange EM, Jenny NS, Chaves PH, Ellis J, Li J, et al. Soluble CD14: genomewide association analysis and relationship to cardiovascular risk and mortality in older adults. *Arterioscler Thromb Vasc Biol*. (2013) 33:158–64. doi: 10.1161/ATVBAHA.112.300421
9. Bruunsgaard H, Pedersen M, Pedersen BK. Aging and proinflammatory cytokines. *Curr Opin Hematol*. (2001) 8:131–6. doi: 10.1097/00062752-200105000-00001
10. Pawelec G. Is there a positive side to T cell exhaustion? *Front Immunol*. (2019) 10:111. doi: 10.3389/fimmu.2019.00111
11. Breton G, Chomont N, Takata H, Fromentin R, Ahlers J, Filali-Mouhim A, et al. Programmed death-1 is a marker for abnormal distribution of naive/memory T cell subsets in HIV-1 infection. *J Immunol*. (2013) 191:2194–204. doi: 10.4049/jimmunol.1200646
12. Day CL, Kaufmann DE, Kiepiela P, Brown JA, Moodley ES, Reddy S, et al. PD-1 expression on HIV-specific T cells is associated with T-cell exhaustion and disease progression. *Nature*. (2006) 443:350–4. doi: 10.1038/nature05115
13. Dolfi DV, Mansfield KD, Polley AM, Doyle SA, Freeman GJ, Pircher H, et al. Increased T-bet is associated with senescence of influenza virus-specific CD8 T cells in aged humans. *J Leukoc Biol*. (2013) 93:825–36. doi: 10.1189/jlb.0912438
14. Song. T-cell immunoglobulin and ITIM domain contributes to CD8+ T-cell immunosenescence. *Aging Cell*. (2017). 17:e12716. doi: 10.1111/acel.12716
15. Chew GM, Fujita T, Webb GM, Burwitz BJ, Wu HL, Reed JS, et al. TIGIT marks exhausted cells T, correlates with disease progression, and serves as a target for immune restoration in HIV and SIV infection. *PLoS Pathog*. (2016) 12:e1005349. doi: 10.1371/journal.ppat.1005349
16. Coppe JP, Patil CK, Rodier F, Sun Y, Munoz DP, Goldstein J, et al. Senescence-associated secretory phenotypes reveal cell-nonautonomous functions of oncogenic RAS and the p53 tumor suppressor. *PLoS Biol*. (2008) 6:2853–68. doi: 10.1371/journal.pbio.0060301
17. Brenchley JM, Karandikar NJ, Betts MR, Ambrozak DR, Hill BJ, Crotty LE, et al. Expression of CD57 defines replicative senescence and antigen-induced apoptotic death of CD8+ T cells. *Blood*. (2003) 101:2711–20. doi: 10.1182/blood-2002-07-2103
18. Henson SM, Franzese O, Macaulay R, Libri V, Azevedo RI, S. Kiani-Alikhan, et al. KLRG1 signaling induces defective Akt (ser473) phosphorylation and proliferative dysfunction of highly differentiated CD8+ T cells. *Blood*. (2009) 113:6619–28. doi: 10.1182/blood-2009-01-199588
19. Henson SM, Akbar AN. KLRG1–more than a marker for T cell senescence. *Age (Dordr)*. (2009) 31:285–91. doi: 10.1007/s11357-009-9100-9
20. Campisi J, d'Adda di Fagagna F. Cellular senescence: when bad things happen to good cells. *Nat Rev Mol Cell Biol*. (2007) 8:729–40. doi: 10.1038/nrm2233
21. Lederman MM, Calabrese L, Funderburg NT, Clagett B, Medvik K, Bonilla H, et al. Immunologic failure despite suppressive antiretroviral therapy is related to activation and turnover of memory CD4 cells. *J Infect Dis*. (2011) 204:1217–26. doi: 10.1093/infdis/jir507
22. Shive CL, Clagett B, McCausland MR, Mudd JC, Funderburg NT, Freeman ML, et al. Inflammation perturbs the IL-7 axis, promoting senescence and exhaustion that broadly characterize immune failure in treated HIV infection. *J Acquir Immune Defic Syndr*. (2015) 71:483–92. doi: 10.1097/QAI.0000000000000913
23. Younes SA, Talla A, Pereira Ribeiro S, Saidakova EV, Korolevskaya LB, Shmagel KV, et al. Cycling CD4+ T cells in HIV-infected immune nonresponders have mitochondrial dysfunction. *J Clin Invest*. (2018) 128:5083–94. doi: 10.1172/JCI120245
24. Yoshimura A, Muto G. TGF-β function in immune suppression. In: Ahmed R, Honjo T, editors. *Negative Co-Receptors and Ligands*. Berlin, Heidelberg: Springer Berlin Heidelberg (2011). p. 127–47. doi: 10.1007/82_2010_87

25. Grabmeier-Pfistershammer K, Steinberger P, Rieger A, Leitner J, Kohrgruber N. Identification of PD-1 as a unique marker for failing immune reconstitution in HIV-1-infected patients on treatment. *J Acquir Immune Defic Syndr*. (2011) 56:118–24. doi: 10.1097/QAI.0b013e3181fbab9f
26. Fernandez S, Price P, McKinnon EJ, Nolan RC, French MA. Low CD4+ T-cell counts in HIV patients receiving effective antiretroviral therapy are associated with CD4+ T-cell activation and senescence but not with lower effector memory T-cell function. *Clin Immunol*. (2006) 120:163–70. doi: 10.1016/j.clim.2006.04.570
27. Pulko V, Davies JS, Martinez C, Lanteri MC, Busch MP, Diamond MS, et al. Human memory T cells with a naive phenotype accumulate with aging and respond to persistent viruses. *Nat Immunol*. (2016) 17:966–75. doi: 10.1038/ni.3483
28. Shive CL, Jiang W, Anthony DD, Lederman MM. Soluble CD14 is a nonspecific marker of monocyte activation. *AIDS*. (2015) 29:1263–5. doi: 10.1097/QAD.0000000000000735
29. Burdo TH, Lo J, Abbara S, Wei J, DeLelys ME, Preffer F, et al. Soluble CD163, a novel marker of activated macrophages, is elevated and associated with noncalcified coronary plaque in HIV-infected patients. *J Infect Dis*. (2011) 204:1227–36. doi: 10.1093/infdis/jir520
30. Liovat AS, Rey-Cuille MA, Lecuroux C, Jacquelin B, Girault I, Petitjean G, et al. Acute plasma biomarkers of T cell activation set-point levels and of disease progression in HIV-1 infection. *PLoS ONE*. (2012) 7:e46143. doi: 10.1371/journal.pone.0046143
31. Pawelec G, Derhovanessian E, Larbi A, Strindhall J, Wikby A. Cytomegalovirus and human immunosenescence. *Rev Med Virol*. (2009) 19:47–56. doi: 10.1002/rmv.598
32. Chen B, Morris SR, Panigrahi S, Michaelson GM, Wyrick JM, Komissarov AA, et al. Cytomegalovirus coinfection is associated with increased vascular-homing CD57(+) CD4 T cells in HIV infection. *J Immunol*. (2020) 204:2722–33. doi: 10.4049/jimmunol.1900734
33. Morris SR, Chen B, Mudd JC, Panigrahi S, Shive CL, Sieg SF, et al. Inflammescent CX3CR1+CD57+CD8+ T cells are generated and expanded by IL-15. *JCI Insight*. (2020) 5:132963. doi: 10.1172/jci.insight.132963
34. Lee SA, Sinclair E, Hatano H, Hsue PY, Epling L, Hecht FM, et al. Impact of HIV on CD8+ T cell CD57 expression is distinct from that of CMV and aging. *PLoS ONE*. (2014) 9:e89444. doi: 10.1371/journal.pone.0089444
35. van de Berg PJ, Griffiths SJ, Yong SL, Macaulay R, Bemelman FJ, Jackson S, et al. Cytomegalovirus infection reduces telomere length of the circulating T cell pool. *J Immunol*. (2010) 184:3417–23. doi: 10.4049/jimmunol.0903442
36. Freeman ML, Mudd JC, Shive CL, Younes SA, Panigrahi S, Sieg SF, et al. CD8 T-cell expansion and inflammation linked to CMV coinfection in ART-treated HIV infection. *Clin Infect Dis*. (2016) 62:392–6. doi: 10.1093/cid/civ840
37. Freeman ML, Lederman MM, Gianella S. Partners in crime: the role of CMV in immune dysregulation and clinical outcome during HIV infection. *Curr HIV/AIDS Rep*. (2016) 13:10–90. doi: 10.1007/s11904-016-0297-9

Conflict of Interest: The authors declare that the research was conducted in the absence of any commercial or financial relationships that could be construed as a potential conflict of interest.

frontiers in Immunology

ORIGINAL RESEARCH
published: 30 March 2021
doi: 10.3389/fimmu.2021.663843

Residual Viremia Is Linked to a Specific Immune Activation Profile in HIV-1-Infected Adults Under Efficient Antiretroviral Therapy

Mehwish Younas[1†], Christina Psomas[1,2†], Christelle Reynes[3], Renaud Cezar[4], Lucy Kundura[1], Pierre Portalès[5], Corinne Merle[2], Nadine Atoui[2], Céline Fernandez[2], Vincent Le Moing[2,6,7], Claudine Barbuat[8], Albert Sotto[7,8], Robert Sabatier[3], Audrey Winter[1], Pascale Fabbro[9], Thierry Vincent[5,7], Jacques Reynes[2,6,7] and Pierre Corbeau[1,4,7]*

[1] Institute for Human Genetics, CNRS, Montpellier, France, [2] Infectious Diseases Department, Montpellier University Hospital, Montpellier, France, [3] Institute for Functional Genomics, Montpellier University, Montpellier, France, [4] Immunology Department, University Hospital, Nîmes, France, [5] Immunology Department, University Hospital, Montpellier, France, [6] IRD UMI 233, INSERM U1175, Montpellier University, Montpellier, France, [7] Faculty of Medicine, Montpellier University, Montpellier, France, [8] Infectious Diseases Department, University Hospital, Nîmes, France, [9] Medical Informatics Department, University Hospital, Nîmes, France

Chronic immune activation persists in persons living with HIV-1 even though they are aviremic under antiretroviral therapy, and fuels comorbidities. In previous studies, we have revealed that virologic responders present distinct profiles of immune activation, and that one of these profiles is related to microbial translocation. In the present work, we tested in 140 HIV-1-infected adults under efficient treatment for a mean duration of eight years whether low-level viremia might be another cause of immune activation. We observed that the frequency of viremia between 1 and 20 HIV-1 RNA copies/mL (39.5 ± 24.7% versus 21.1 ± 22.5%, p = 0.033) and transient viremia above 20 HIV-1 RNA copies/mL (15.1 ± 16.9% versus 3.3 ± 7.2%, p = 0.005) over the 2 last years was higher in patients with one profile of immune activation, Profile E, than in the other patients. Profile E, which is different from the profile related to microbial translocation with frequent CD38+ CD8+ T cells, is characterized by a high level of CD4+ T cell (cell surface expression of CD38), monocyte (plasma concentration of soluble CD14), and endothelium (plasma concentration of soluble Endothelial Protein C Receptor) activation, whereas the other profiles presented low CD4:CD8 ratio, elevated proportions of central memory CD8+ T cells or HLA-DR+ CD4+ T cells, respectively. Our data reinforce the hypothesis that various etiological factors shape the form of the immune activation in virologic responders, resulting in specific profiles. Given the type of immune activation of Profile E, a potential causal link between low-level viremia and atherosclerosis should be investigated.

Keywords: low-level viremia, blip, inflammation, virologic responder, endothelium activation, coagulation

OPEN ACCESS

Edited by:
Remi Cheynier, INSERM U1016 Institut Cochin, France

Reviewed by:
Jean-Pierre Routy, McGill University, Canada
Petronela Ancuta, Université de Montréal, Canada

***Correspondence:**
Pierre Corbeau
pcorbeau@igh.cnrs.fr

†These authors have contributed equally to this work and share first authorship

Specialty section:
This article was submitted to Viral Immunology, a section of the journal Frontiers in Immunology

Received: *03 February 2021*
Accepted: *15 March 2021*
Published: *30 March 2021*

Citation:
Younas M, Psomas C, Reynes C, Cezar R, Kundura L, Portalès P, Merle C, Atoui N, Fernandez C, Le Moing V, Barbuat C, Sotto A, Sabatier R, Winter A, Fabbro P, Vincent T, Reynes J and Corbeau P (2021) Residual Viremia Is Linked to a Specific Immune Activation Profile in HIV-1-Infected Adults Under Efficient Antiretroviral Therapy. Front. Immunol. 12:663843. doi: 10.3389/fimmu.2021.663843

INTRODUCTION

Immune activation (IA)-related comorbidities are becoming a major concern in aviremic HIV-infected persons under antiretroviral therapy (ART) (1). For instance, atherosclerosis has been linked to inflammation and coagulation, interleukin-6 (IL-6) and D-dimer correlating positively with a greater risk of fatal cardiovascular disease (2), as well as to CD8+ T cell activation (HLA-DR and CD38 coexpression) (3) and monocyte (soluble CD163 level and cell surface coexpression of CD14 and CD16) activation (3, 4). It is therefore important to better identify the causes of this IA. HIV itself may be one of these drivers. Although HIV RNA levels are below the detection level of routine tests in these patients, most of them still produce low levels of virus, and HIV (glyco)proteins may be detected in their lymph nodes (5). Many HIV components may directly activate the innate immune system. For example, gp120 (6) Nef and Vpr (7) have been reported to directly activate monocytes and macrophages, and gp41 T cells (8). It has also been reported that HIV RNA induces interferon-α production by plasmacytoid dendritic cells *via* TLR-7 and TLR-9. Moreover, HIV antigens detected by specific B lymphocytes and T cells trigger an adaptive immune response. Finally, even a truncated CD4+ T cell infection may induce caspase-1 activation and IL-1β production in CD4+ T cells (9). In addition, HIV might also favor other causes of IA (10). Thus, Nef protein is also known to interact with the adenosine-triphosphate-binding cassette A1 transporter. This interaction interferes with cholesterol metabolism, and may promote pro-inflammatory metabolic disorders (11). Likewise, HIV-mediated IA might promote immune senescence, which is an additional cause of IA.

Yet authors looking for correlations between residual viremia and IA markers obtained contradictory results. Some authors found a link between residual viremia and inflammation (12), CD4+ T cell activation (13), and monocyte activation (12). By contrast, other authors did not observe such correlations (14–17).

Recent data however argue for a role of persistent viral production in IA. First, in virologic responders, higher levels of the inflammatory markers C-reactive protein (CRP), Tumor Necrosis Factor α (TNFα), IL-6, interferon γ (IFNγ) and/or the monocyte activation marker soluble CD14 (sCD14) have been reported in non-fully adherent patients than in fully adherent patients (18, 19). Second, in elite controllers, who are aviremic in the absence of treatment, intermittent bouts of viremia, so-called blips, are associated with a low CD4/CD8 ratio which is a global marker of IA (20). Moreover, the initiation of ART in these patients reduces CD4+ T cell and CD8+ T cell activation in the blood as well as in the gastrointestinal associated lymphoid tissues (21). Third, switching from a 3-drug regimen to some 2-drug ART regimens may result in an increase in CD8+ T cell counts (22, 23).

Knowing whether low-level viremia is a cause of IA is particularly important at a time when 2-drug regimens rather than 3-drug ART regimens (24), day-on, day-off schedules (25), and intermittent four-days-a-week treatments (26) are being proposed.

In a previous study, we analyzed 64 soluble and cell surface markers of inflammation and CD4+ and CD8+ T cell, B cell, monocyte, NK cell, and endothelial activation in 140 adults under effective ART. A double hierarchical clustering of patients and markers unveiled that these virologic responders had 5 different IA profiles (27). The first profile was characterized by a high percentage of central memory CD8+ T cells, the second by a low CD4:CD8 ratio, the third by frequent HLA-DR+ CD4+ T cells, and the two last profiles by an elevated proportion of CD38-expressing CD8+ and CD4+ T cells, respectively. In this present study, we looked for a link between one of those profiles and residual viremia.

MATERIALS AND METHODS

Study Design

This cross-sectional observational study has already been previously described (27). We recruited 140 HIV-1-infected adults with CD4 count above 200 cells/μL. Viremia of all participants, under stable ART, was below 50 copies per mL for at least 6 months before inclusion. We also recruited 150 persons with a mean ± SD age of 62 ± 4 years in the general population. Pregnant or breastfeeding women, persons under treatment or presenting a disease likely to modify the immune system were not included. Blood samples for immune profiling were collected once between April 2014 and June 2016. This study was approved by the Ethics Committee of Montpellier University Hospital. All patients provided written informed consent. The trial was registered on ClinicalTrials.gov (NCT02334943).

Immune Activation Markers

Using flow cytometry as previously described (28), we determined cell surface markers for the differentiation, activation, senescence, and/or exhaustion of CD4+ T lymphocytes, CD8+ T lymphocytes, and NK cells. We used ELISA to quantify soluble TNF receptor I (sTNFRI), sCD14 and soluble CD163 (sCD163), tissue Plasminogen Activator (tPA), soluble Thrombomodulin (sTM), and soluble Endothelial Protein C Receptor (sEPCR) and, by turbidimetry, CRP, immunoglobulins (Ig) and D-dimers also as previously reported (28).

Residual Viremia

HIV-1 RNA plasma level was quantified using the Amplicor HIV-1 Monitor test (Roche Diagnostic Systems). The test has a positive threshold of 20 copies/mL, and discriminates samples containing no detectable copies in 1mL from samples containing 1 to 20 copies/mL. We also recorded the percentage of blips, defined as isolated episodes of viremia > 20 copies/mL, within the 2 years preceding the analysis of the immune profile. The frequency of detectable viremia and blips over the 2 last years was determined on 4 to 8 measurements.

Statistical Analysis

Fisher's exact test or $\chi 2$ test was used to compare qualitative covariates. For quantitative covariates, on one hand, when comparing two groups (e.g. undetectable vs detectable viremia), we compared the distributions of covariates using the Student T-test or the Wilcoxon-Mann-Whitney test as appropriate. On the other hand, when comparing profiles together for example (i.e. more than two groups), the comparison was made using Anova or the Kruskal-Wallis H test as appropriate. Correlations were evaluated by Pearson, Spearman or Kendall test as appropriate. Normality was assessed using the Shapiro-Wilk test.

All analyses were performed using R software, version 3.6.1 (R Development Core Team, A Language and Environment for Statistical Computing, Vienna, Austria, 2016. https://www.R-project.org/).

Funding Source

Nîmes and Montpellier University Hospitals, MSD and MSDAVENIR.

RESULTS

Study Subjects

HIV-1-infected adults (n = 140), under efficient ART for a mean (SD) duration of 7.9 (4.1) years, were recruited at the University Hospitals of Nîmes and Montpellier, France. Eighty-one percent of patients were male, with a mean age of 56 (9) years. Their pretherapeutic CD4 count and viremia were 199 (119) cells/μL and 1,4372,216 (9,602,969) HIV RHA copies/mL, respectively. Their current mean CD4 count was 733 ± 375 cells/μL, and their CD4/CD8 ratio 1.24 (0.88). ART regimens and co-infections are given in **Table 1**.

Residual Viremia

In this study population, the frequency of residual viremia (1-20 copies/mL) at the time of study was 26%. There was no difference, neither in age (56.1 ± 8.5 versus 55.9 ± 10.1 years, p = 0.771), duration of infection (14.5 ± 8.0 versus 16.8 ± 7.7 years, p = 0.168) nor aviremia (7.0 ± 3.5 versus 8.3 ± 4.2 years, p = 0.155), nor in pretherapeutic CD4 count (164 ± 110 versus 159 ± 103 cells/mL, p = 0.980) nor pretherapeutic viremia (4,782,630 ± 20,381,332 versus 530,006 ± 1,733,809 copies/mL, p = 0.831) between patients with detectable and undetectable viremia, respectively. Likewise, no link could be established between residual viremia and the use of nucleoside reverse transcriptase inhibitors (p = 0.999), non-nucleoside reverse transcriptase inhibitors (p = 0.999), protease inhibitors (p = 0.969), or integrase inhibitors (p = 0.900).

The percentage of samples with detectable viremia (1-20 HIV-1 RNA copies/mL) or blips (isolated viremia > 20 HIV-1 RNA copies/mL) during the two years preceding the study was available for 135 out of 140 participants. These percentages of samples with detectable viremia (47.1 ± 21.0% versus 19.0 ± 21.0%, $p < 10^{-4}$, **Figure 1A**) and blips (9.8 ± 11.5% versus 2.1 ± 5.9%, $p < 10^{-4}$, **Figure 1B**) were higher in patients with detectable viremia than in patients with undetectable viremia at the time of the study.

TABLE 1 | Bioclinical characteristics of the study population.

Characteristics		HIV+ Treated
Number of individuals		140
Nucleoside reverse transcriptase inhibitor	N (%)	128 (91)
Non-nucleoside reverse transcriptase inhibitor	N (%)	50 (36)
Protease inhibitor	N (%)	67 (48)
Integrase inhibitor	N (%)	44 (31)
HBs Ag+	N (%)	3 (2)
Anti-HBs Ab+	N (%)	61 (44)
Anti-HBc Ab+	N (%)	54 (39)
HCV coinfection	N (%)	6 (4)
CMV coinfection	N (%)	124 (89)
EBV coinfection	N (%)	138 (99)
HAV coinfection	N (%)	97 (69)

HBs Ag, Hepatitis B surface antigen; HBc, Hepatitis B core; HCV, Hepatitis C Virus; CMV, Cytomegalovirus; EBV, Epstein-Barr Virus; HAV, Hepatitis A Virus.

Relationships Between Residual Viremia and Biomarkers

We determined the numbers and percentages of the following subpopulations: (i) activated (HLA-DR+ and/or CD38+), exhausted (PD-1+), senescent (CD57+, eventually CD27- and CD28-), naïve (CD45RA+CD27+), central and effector (CD45RA-CD27+ and CD45RA-CD27-, respectively) memory CD4+ and CD8+ T cells, (ii) activated (HLA-DR+), dysfunctional (CD56-), and senescent (CD57+) NK cells. Monocyte activation was evaluated by measuring sCD14 and sCD163, and B cell activation by measuring IgM, IgG, and IgA levels. Inflammation was monitored by quantifying sTNFRI and CRP. tPA, sTM, and sEPCR were used as markers of endothelium activation, and D-dimers were used as an indicator of fibrinolysis.

We compared residual viremia and blip frequency, i.e. for each participant, the frequency where the participant displayed low-level viremia or blips during the two last years with each one of these markers. The only link we revealed was with D-dimers. Patients with 1-20 HIV-1 RNA copies at the time of the study presented higher D-dimer levels than patients with undetectable viremia (n = 119, 708 ± 841 versus 411 ± 535 ng/mL, p = 0.015, **Figure 1C**). Moreover, there was a correlation between blip frequency over the two last years and D-dimer levels (n = 119, Kendall coefficient = 0.190, p = 0.009, **Figure 1D**). Looking for correlations between D-dimers and patient characteristics as well as other markers, we observed links between the coagulation marker, participant age (r = 0.295, p = 0.001, **Figure 2A**), pretherapeutic CD4 count (r = -0.182, p = 0.046, **Figure 2B**), the inflammation markers CRP (r = 0.364, $p < 10^{-4}$, **Figure 2C**) and sTNFRI (r = 0.293, p = 0.001, **Figure 2D**), the monocyte activation marker sCD163 (r = 0.253, p = 0.005, **Figure 2E**), and the endothelial activation marker sEPCR (r = 0.265, p = 0.003, **Figure 2F**).

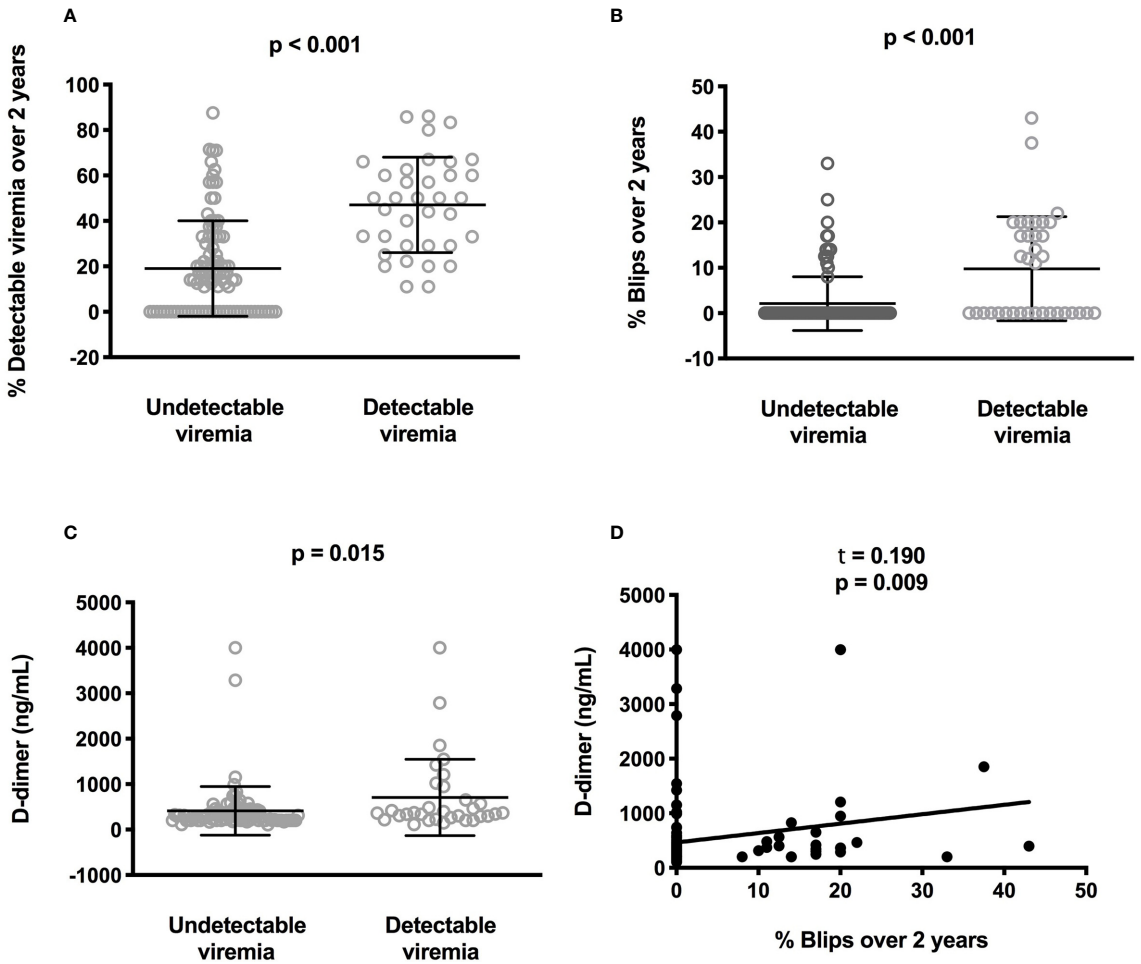

FIGURE 1 | Correlations between low-level viremia, blips, and D-dimer plasma levels. Difference for each participant in the frequency where the participant displayed low-level viremia **(A)** or blips **(B)** over the two last years between participants with or without current detectable viremia. Difference in circulating D-dimer concentrations between participants with or without current detectable viremia. Statistical analyses were performed using a Mann-Whitney test **(C)**. Correlation between the frequency of blips over the two last years and D-dimer plasma levels. Statistical analysis was performed using Kendall correlation **(D)**.

Residual Viremia Over Time Is Related to a Specific Immune Activation Profile

We previously reported that two independent hierarchical clustering analyses of the activation markers for the 140 patients had identified 5 groups of individuals presenting different IA profiles (Profiles A to E). Duration of infection and aviremia, nadir CD4, pretherapeutic viral load and CD4:CD8 ratio, as well as age were not different between Profile E and the other Profiles (27). There was differences neither in nucleoside reverse transcriptase inhibitor (p = 0.565), non-nucleoside reverse transcriptase inhibitor (p = 0.999), protease inhibitor (p = 0.165), nor in integrase inhibitor (0.999) usage between Profile E and the other profiles. The only difference was a tendency to a higher proportion of females in Profile E (p = 0. 061) (27). Yet, the frequency of detectable viremia (p = 0.999) or blips (p = 0.278) during the two years were not different between males and females (data not shown).

Interestingly, one of these profiles, Profile D, was linked to microbial translocation (27). We reasoned that another IA profile could be linked to another cause of IA, residual viral production. To test this hypothesis, we compared the frequency of residual viremia and the occurrence of blips over time between the IA profiles. Detectable viremia at the time of the study was more frequent in patients with Profile E than in the other patients (66.7% versus 23.8%, p = 0.011, **Figure 3A**). The frequency of detectable viremia over the 2 last years was also higher in Profile E patients than in patients with other profiles (39.5 ± 24.7% versus 21.1 ± 22.5%, p = 0.033, **Figure 3B**). Likewise, previous blip frequency was higher in Profile E patients than in the patients with other profiles (15.1 ± 16.9% versus 3.3 ± 7.2%, p = 0.005, **Figure 3C**).

Characterization of the Immune Activation Profile Related to Residual Viremia

No difference in duration of infection (p = 0.191) and of viral suppression (p = 0.285), in pretherapeutic viremia (p = 0.881) or

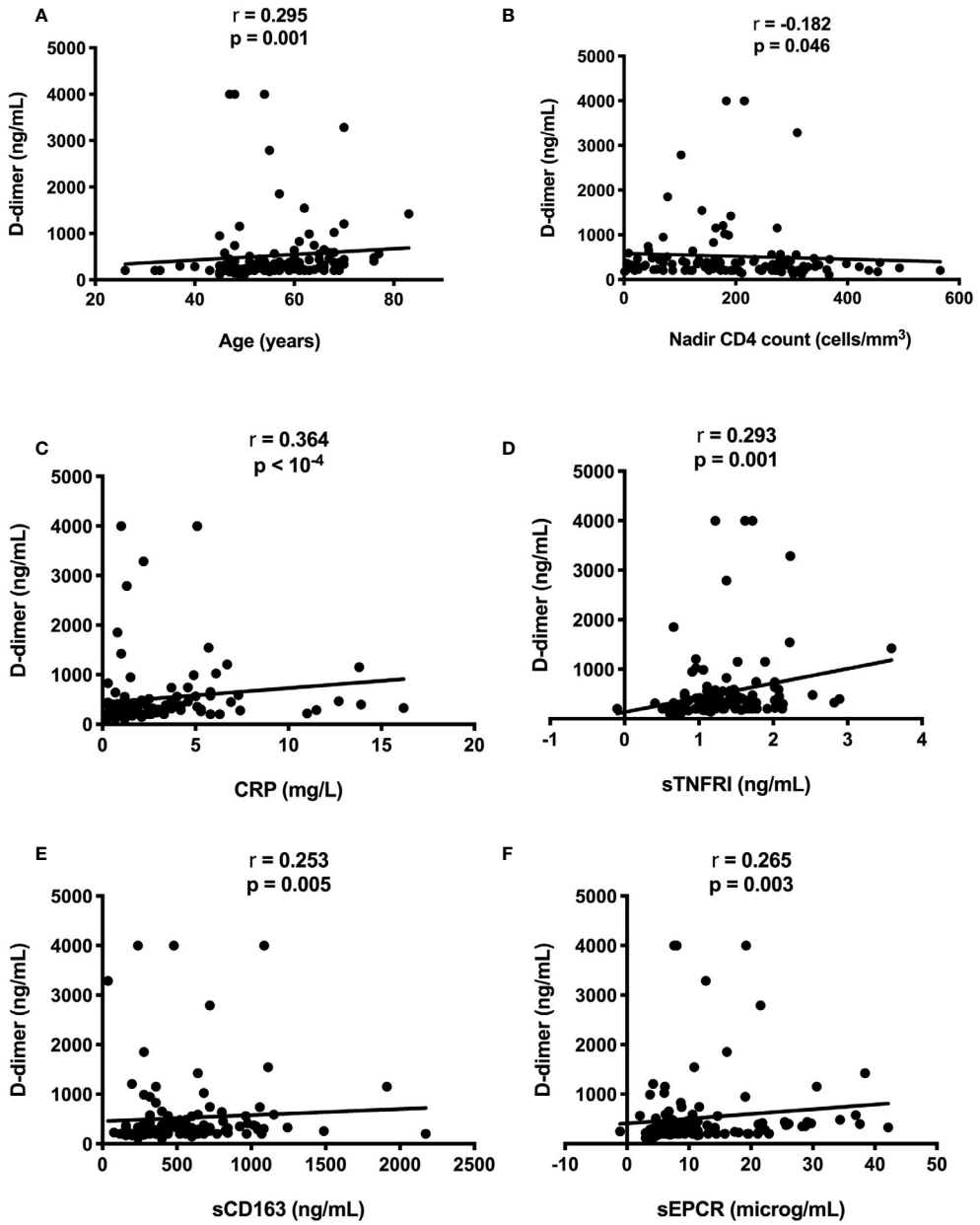

FIGURE 2 | Correlations between D-dimer level, participant age **(A)** and pretherapeutic CD4 count **(B)**, CRP **(C)**, sTNFRI **(D)**, sCD163 **(E)**, and sEPCR **(F)**.

CD4 count (0.285), and in age (p = 0.138) was observed between Profile E patients and patients with other profiles (data not shown). Compared with the other patients, Profile E patients had higher CD4 counts (1567 ± 451 versus 669 ± 288 cells/mL, $p < 10^{-4}$, **Figure 4A**) and CD4:CD8 ratios (2.79 ± 2.48 versus 1.14 ± 0.57, p < 0.001, **Figure 4B**). They also presented higher levels of sCD14 (3.76 ± 0.50 versus 3.37 ± 1.08 mg/mL, p = 0.030, **Figure 4C**) and higher percentages of CD38-positive CD4+ T-cells (73.1 ± 11.4% versus 55.9 ± 12.4%, $p < 10^{-4}$, **Figure 4D**) compared with the other patients. Profile E was also characterized by a high level of the endothelium activation marker sEPCR (18 ± 12% versus 10 ± 8%, p = 0.035, **Figure 4E**). Moreover, in Profile E patients there was a strong link between frequency of detectable viremia over the 2 last years and another endothelium activation marker, tPA (r = 0.687, p = 0.006, **Figure 4F**).

DISCUSSION

It is logical to assume that residual viremia should fuel immune activation in virological responders. Yet, although some authors have indeed found a link between low-level

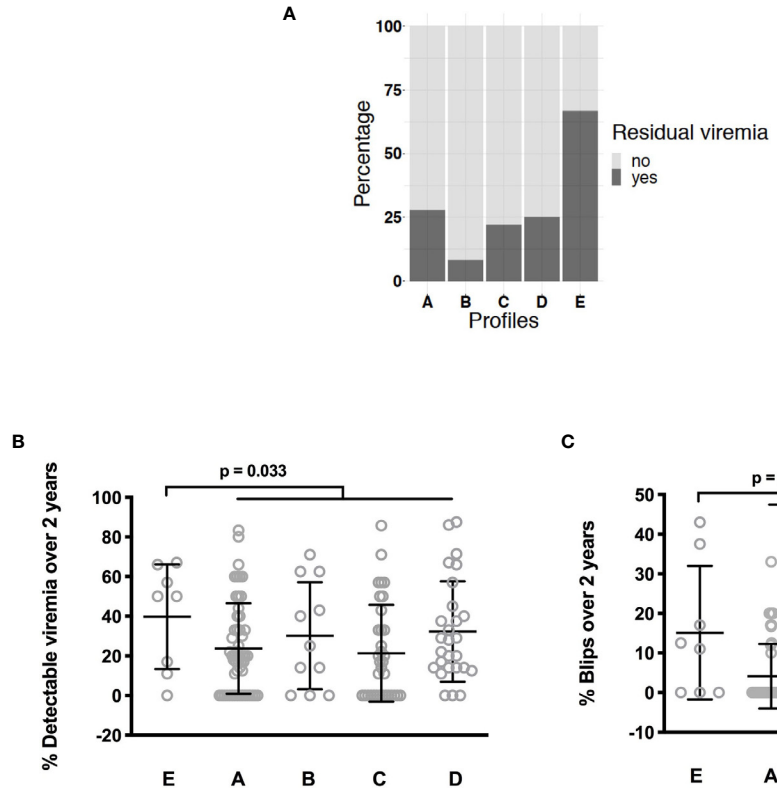

FIGURE 3 | Differences in the frequency of current low-level viremia between the various IA profiles. Statistical analyses were performed using a Kruskal-Wallis H test **(A)**. Differences in the frequency of low-level viremia **(B)** and blips **(C)** over the two last years between the various IA profiles. Statistical analyses were performed using a Mann-Whitney test.

viremia and IA (12, 13), others have not (14–17). This discrepancy might be due to differences in the size and/or bioclinical characteristics of the populations under study, as well as the actual definition of residual viremia. Here, we show that the frequency of detectable HIV-1 RNA and blips over a period of 2 years is associated with a specific profile of IA, Profile E. There may be two explanations for why we observed such a correlation whereas other authors had failed to identify it. First, a 24-month follow-up of viral load is more sensitive than a single measurement. Second, our two-step approach, consisting of clustering IA profiles in the patient population and thereafter looking for correlations between each of these profiles and residual viremia, may have unveiled links which would have been hidden in searches for such links in the global population. For instance, in our study, whereas high sCD14 levels and percentages of CD4+ T cells expressing CD38 characterize Profile E, these markers are not associated with residual viremia when taking into account the 140 participants.

The high circulating concentrations of sCD14 that we observed in Profile E patients is in line with the link between this IA marker and residual viremia reported by other authors (12). This link might be explained by the fact that the presence of viral components within the gut-associated lymphoid tissues might be responsible for local inflammation and thereby an increase in gut permeability facilitating microbial translocation (29). This could thus be a first argument in favor of a causal link between residual viremia and Profile E.

Previously, CD4+ T cell activation has also been found to be associated with residual viremia (13). Here again, it may be the presence of viral components that trigger this form of IA. Indeed, gp41 has been reported to interact with the T cell receptor and to facilitate thereby T lymphocyte activation (8). Moreover, Doitsh et al. observed that the presence of HIV DNA in CD4+ T cell provokes inflammasome activation, even though the viral life cycle is truncated (9). Consequently, CD4+ T cell activation in Profile E patients may be induced by the presence of the virus.

Compared with the other IA profiles, Profile E is also characterized by a high level of sEPCR. sEPCR results from the cleavage of the external portion of the protein C receptor on the surface of endothelial cells activated by thrombin, TNFα, IL-1 or endotoxins (30). An increase in sEPCR has already been reported in HIV infection (31, 32). A decrease in sEPCR under 48-week ART has even been correlated with HIV RNA changes (32). This is in line with the hypothesis that the presence of HIV may provoke EPCR cleavage, and further argues for a model in which Profile E is the consequence of residual viral production.

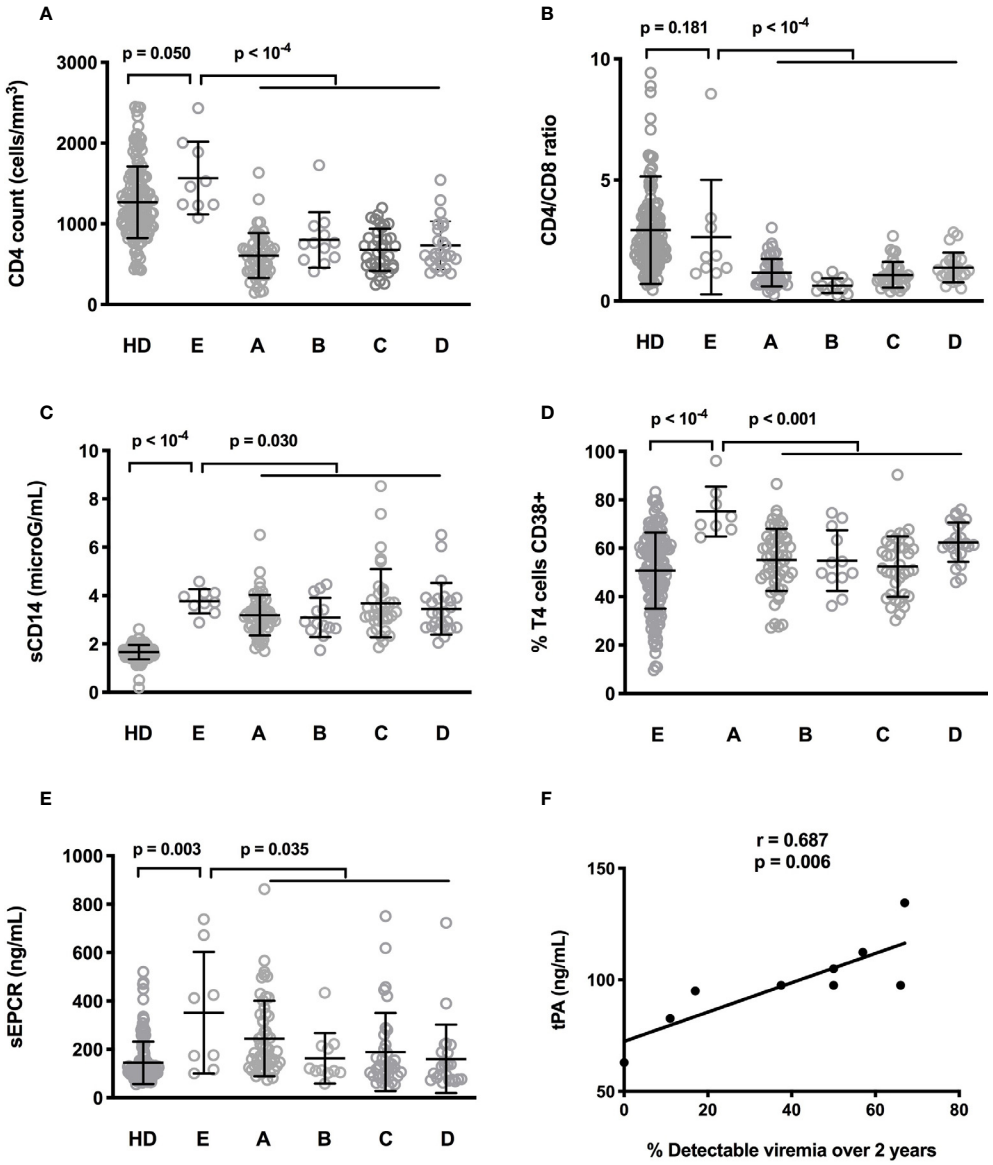

FIGURE 4 | Differences in CD4 count **(A)**, CD4:CD8 ratio **(B)**, sCD14 **(C)**, frequency of CD4+ T cells expressing CD38 **(D)**, and sEPCR **(E)** between healthy donors (HD) and people living with HIV-1 with the five IA profiles. Statistical analyses were performed using a Mann-Whitney test. Correlation between low-level viremia over the two last years and tPA in Profile E participants. Statistical analysis was performed using Spearman correlation **(F)**.

One consequence of our results is that we now know that residual viremia should be sought in patients with increased proportions of CD38+CD4+ T cell, sCD14 and/or sEPCR. Moreover, in these patients, potential causes of this residual viremia, e.g., non-optimal adherence to treatment or partial resistance to the current antiretroviral regimen, should also be investigated.

Globally, the present data support the idea that, depending on the etiological factor at work, microbial translocation for Profile D patients (27) and residual viremia for Profile E patients (present study), virologic responders develop a particular IA profile. As we have also established that a specific IA profile may be related to a specific comorbidity, insulin resistance (28), we propose a model in which a cause of IA may fuel an IA profile that may favor an IA-related morbidity. To further test this hypothesis, tissue evaluation of the IA, particularly in secondary lymphoid organs, and functional assays would be necessary. According to this model, the fact that we have shown that residual viremia is associated with a marker of monocyte activation (sCD14), two markers of endothelial activation (sEPCR and tPA), and a marker of coagulation (D-dimer), three forms of activation known to favor atherothrombosis (33–35), should encourage us to search for a link between residual viremia and atherosclerosis.

DATA AVAILABILITY STATEMENT

The raw data supporting the conclusions of this article will be made available by the authors, without undue reservation.

ETHICS STATEMENT

The studies involving human participants were reviewed and approved by Ethics Committee of Montpellier University Hospital, France. The patients/participants provided their written informed consent to participate in this study.

AUTHOR CONTRIBUTIONS

MY and LK contributed to the design of the flow cytometry study, and acquired, analyzed, and interpreted cell surface and soluble marker data. CP contributed to the design of the study, the enrolment of patients, and acquired, analyzed and interpreted the data. RC, PP, and TV contributed to the design of the flow cytometry study and acquired, analyzed and interpreted cell surface markers. CR, RS, AW, and PF contributed to the design of the statistical study and acquired, analyzed, and interpreted the statistical data. CM, NA, CF, VL, CB, and AS acquired, analyzed, and interpreted clinical data. JR contributed to the design of the study and analyzed and interpreted the data. PC contributed to the design of the study, analyzed, and interpreted data, and wrote the first draft of the manuscript. All authors contributed to the article and approved the submitted version.

FUNDING

The study was funded by MSD, MSDAvenir, and the university hospitals of Montpellier and Nîmes. These sponsors had no role in the study design, the collection, analysis, or interpretation of data, the writing of the report, nor in the decision to submit the paper for publication.

ACKNOWLEDGMENTS

We are grateful to the persons who volunteered for this study and to Teresa Sawyers for the critical reading of the manuscript.

REFERENCES

1. Miller CJ, Baker JV, Bormann AM, Erlandson KM, Hullsiek KH, Justice AC, et al. Adjudicated morbidity and mortality outcomes by age among individuals with HIV infection on suppressive antiretroviral therapy. *PLoS One* (2014) 9:e95061. doi: 10.1371/journal.pone.0095061
2. Nordell AD, McKenna M, Borges AH, Duprez D, Neuhaus J, Neaton JD, et al. Severity of cardiovascular disease outcomes among patients with HIV is related to markers of inflammation and coagulation. *J Am Heart Assoc* (2014) 3:e000844. doi: 10.1161/JAHA.114.000844
3. Longenecker CT, Funderburg NT, Jiang Y, Debanne S, Storer N, Labbato DE, et al. Markers of inflammation and CD8 T-cell activation, but not monocyte activation, are associated with subclinical carotid artery disease in HIV-infected individuals. *HIV Med* (2013) 14:385–90. doi: 10.1111/hiv.12013
4. Fitch KV, Srinivasa S, Abbara S, Burdo TH, Williams KC, Eneh P, et al. Noncalcified coronary atherosclerotic plaque and immune activation in HIV-infected women. *J Infect Dis* (2013) 208:1737–46. doi: 10.1093/infdis/jit508
5. Popovic M, Tenner-Racz K, Pelser C, Stellbrink H-J, van Lunzen J, Lewis G, et al. Persistence of HIV-1 structural proteins and glycoproteins in lymph nodes of patients under highly active antiretroviral therapy. *Proc Natl Acad Sci U S A* (2004) 102:14807–12. doi: 10.1073/pnas.0506857102
6. Planès R, Serrero M, Leghmari K, BenMohamed L, Bahraoui B. HIV-1 Envelope Glycoproteins Induce the Production of TNF-α and IL-10 in Human Monocytes by Activating Calcium Pathway. *Sci Rep Sci Rep* (2018) 8(1):17215. doi: 10.1038/s41598-018-35478-1
7. Lawn SD, Butera ST, Folks TM. Contribution of immune activation to the pathogenesis and transmission of human immunodeficiency virus type 1 infection. *Clin Microbiol* (2001) 14:753–77. doi: 10.1128/CMR.14.4.753-777.2001
8. Yakovian O, Schwarzer R, Sajman J, Neve-Oz Y, Razvag Y, Herrmann A, et al. Gp41 dynamically interacts with the TCR in the immune synapse and promotes early T cell activation. *Sci Rep* (2018) 8:9747. doi: 10.1038/s41598-018-28114-5
9. Doitsh G, Cavrois M, Lassen KG, Zepeda O, Yang Z, Santiago ML, et al. Abortive HIV infection mediates CD4 T cell depletion and inflammation in human lymphoid tissue. *Cell* (2010) 143:789–801. doi: 10.1016/j.cell.2010.11.001
10. Younas M, Psomas C, Reynes J, Corbeau P. Immune activation in the course of HIV-1 infection: Causes, phenotypes and persistence under therapy. *HIV Med* (2016) 17:89–105. doi: 10.1111/hiv.12310
11. Mujawar Z, Rose H, Morrow MP, Pushkarsky T, Dubrovsky L, Mukhamedova N, et al. Human immunodeficiency virus impairs reverse cholesterol transport from macrophages. *PLoS Biol* (2006) 4:e365. doi: 10.1371/journal.pbio.0040365
12. Falasca F, Di Carlo D, De Vito C, Bon I, d'Ettorre G, Fantauzzi A, et al. Evaluation of HIV-DNA and inflammatory markers in HIV-infected individuals with different viral load patterns. *BMC Infect Dis* (2017) 17:581. doi: 10.1186/s12879-017-2676-2
13. Hatano H, Jain V, Hunt PW, Lee TH, Sinclair E, Do TD, et al. Cell-based measures of viral persistence are associated with immune activation and programmed cell death protein 1 (PD-1)-expressing CD4+ T cells. *J Infect Dis* (2013) 213:370–8. doi: 10.1093/infdis/jis630
14. Guihot A, Dentone C, Assoumou L, Parizot C, Calin R, Seang S, et al. Residual immune activation in combined antiretroviral therapy-treated patients with maximally suppressed viremia. *AIDS* (2016) 30:327–30. doi: 10.1097/QAD.0000000000000815
15. Gandhi RT, McMahon DK, Bosch RJ, Lalama CM, Cyktor JC, Macatangay BJ, et al. Levels of HIV-1 persistence on antiretroviral therapy are not associated with markers of inflammation or activation. *PLoS Pathog* (2011) 13:e1006285. doi: 10.1371/journal.ppat.1006285
16. Chun T-W, Murray D, Justement JS, Hallahan CW, Moir S, Kovacs C, et al. Relationship between residual plasma viremia and the size of HIV proviral DNA reservoirs in infected individuals receiving effective antiretroviral therapy. *J Infect Dis* (2011) 204:135–8. doi: 10.1093/infdis/jir208
17. Allavena C, Rodallec A, Sécher S, Reliquet V, Baffoin S, André-Garnier E, et al. Evaluation of residual viremia and quantitation of soluble CD14 in a large cohort of HIV-infected adults on a long-term non-nucleoside reverse transcriptase inhibitor-based regimen. *J Med Virol* (2013) 85:1878–82. doi: 10.1002/jmv.23679
18. Castillo-Mancilla JR, Brown TT, Erlandson KM, Palella FJJ, Gardner EM, Macatangay BJC, et al. Suboptimal Adherence to Combination Antiretroviral Therapy Is Associated With Higher Levels of Inflammation Despite HIV Suppression. *Clin Infect Dis* (2016) 63:1661–7. doi: 10.1093/cid/ciw650
19. Castillo-Mancilla JR, Morrow M, Boum Y, Byakwaga H, Haberer JE, Martin JN, et al. Brief Report: Higher ART Adherence Is Associated With Lower

Systemic Inflammation in Treatment-Naive Ugandans Who Achieve Virologic Suppression. *J Acquir Immune Defic Syndr* (2018) 77:507–13. doi: 10.1097/QAI.0000000000001629
20. Chereau F, Madec Y, Sabin C, Obel N, Ruiz-Mateos E, Chrysos G, et al. Impact of CD4 and CD8 dynamics and viral rebounds on loss of virological control in HIV controllers. *PLoS One* (2017) 12:e0173893. doi: 10.1371/journal.pone.0173893
21. Hatano H, Yukl SA, Ferre AL, Graf EH, Somsouk M, Sinclair E, et al. Prospective antiretroviral treatment of asymptomatic, HIV-1 infected controllers. *PLoS Pathog* (2013) 9:e1003691. doi: 10.1371/journal.ppat.1003691
22. Mussini C, Lorenzini P, Cozzi-Lepri A, Marchetti G, Rusconi S, Gori A, et al. Switching to dual/monotherapy determines an increase in CD8+ in HIV-infected individuals: an observational cohort study. *BMC Med* (2018) 16:79. doi: 10.1186/s12916-018-1046-2
23. Quiros-Roldan E, Magro P, Raffetti E, Izzo I, Borghetti A, Lombardi F, et al. Biochemical and inflammatory modifications after switching to dual antiretroviral therapy in HIV-infected patients in Italy: a multicenter retrospective cohort study from 2007 to 2015. *BMC Infect Dis* (2018) 18285. doi: 10.1186/s12879-018-3198-2
24. Moreno S, Perno CF, Mallon PW, Behrens G, Corbeau P, Routy JP, et al. Two-drug vs. three-drug combinations for HIV-1: Do we have enough data to make the switch? *HIV Med* (2019) 20(Suppl 4):2–12. doi: 10.1111/hiv.12716
25. Costantini A, Tontini C, Rocchi M, Martini M, Butini L. Day-On, Day-Off emtricitabine, tenofovir disoproxil fumarate and efavirenz single tablet regimen (DODO) as maintenance therapy in HIV-infected patients. *Infez Med* (2018) 26:126–32.
26. de Truchis P, Assoumou L, Landman R, Mathez D, Le Dû D, Bellet J, et al. Four-days-a-week antiretroviral maintenance therapy in virologically controlled HIV-1-infected adults: the ANRS 162-4D trial. *J Antimicrob Chemother* (2018) 73:738–47. doi: 10.1093/jac/dkx434
27. Younas M, Psomas C, Reynes C, Cezar R, Kundura L, Portales P, et al. Microbial Translocation Is Linked to a Specific Immune Activation Profile in HIV-1-Infected Adults With Suppressed Viremia. *Front Immunol* (2019) 10:2185. doi: 10.3389/fimmu.2019.02185
28. Psomas C, Younas M, Reynes C, Cezar R, Portales P, Tuaillon E, et al. One of the immune activation profiles observed in HIV-1-infected adults with suppressed viremia is linked to metabolic syndrome: The ACTIVIH study. *EBioMedicine* (2016) 8:265–76. doi: 10.1016/j.ebiom.2016.05.008
29. Reus S, Portilla J, Sánchez-Payá J, Giner L, Francés R, Such J, et al. Low-level HIV viremia is associated with microbial translocation and inflammation. *J Acquir Immune Defic Syndr* (2013) 62:129–34. doi: 10.1097/QAI.0b013e3182745ab0
30. Van de Wouwer M, Collen D, Conway EM. Thrombomodulin-protein C-EPCR system: integrated to regulate coagulation and inflammation. *Arterioscler Thromb Vasc Biol* (2004) 24:1374–83. doi: 10.1161/01.ATV.0000134298.25489.92
31. Nozza S, Pogliaghi M, Chiappetta S, Spagnuolo V, Fontana G, Razzari C, et al. Levels of soluble endothelial protein C receptor are associated with CD4+ changes in Maraviroc-treated HIV-infected patients. *PLoS One* (2012) 7:e37032. doi: 10.1371/journal.pone.0037032
32. Chiappetta S, Ripa M, Galli L, Razzari C, Longo V, Galli A, et al. Soluble endothelial protein C receptor (sEPCR) as an inflammatory biomarker in naive HIV-infected patients during ART. *J Antimicrob Chemother* (2016) 71:1627–31. doi: 10.1093/jac/dkw010
33. Reynolds HR, Buyon J, Kim M, Rivera TL, Izmirly P, Tunick P, et al. Association of plasma soluble E-selectin and adiponectin with carotid plaque in patients with systemic lupus erythematosus. *Atherosclerosis* (2010) 210:569–74. doi: 10.1016/j.atherosclerosis.2009.12.007
34. Masiá M, Padilla S, García JA, García-Abellán J, Fernández M, Bernardino I, et al. Evolving understanding of cardiovascular, cerebrovascular and peripheral arterial disease in people living with HIV and role of novel biomarkers. A study of the Spanish CoRIS cohort, 2004-2015. *PLoS One* (2019) 14:e0215507. doi: 10.1371/journal.pone.0215507
35. Engelberger RP, Limacher A, Kucher N, Baumann F, Silbernagel G, Benghozi R, et al. Biological variation of established and novel biomarkers for atherosclerosis: Results from a prospective, parallel-group cohort study. *Clin Chim Acta* (2015) 447:16–22. doi: 10.1016/j.cca.2015.05.003

Conflict of Interest: The authors declare that the research was conducted in the absence of any commercial or financial relationships that could be construed as a potential conflict of interest.

frontiers in Immunology

ORIGINAL RESEARCH
published: 12 April 2021
doi: 10.3389/fimmu.2021.641230

Naïve CD4+ T Cell Lymphopenia and Apoptosis in Chronic Hepatitis C Virus Infection Is Driven by the CD31+ Subset and Is Partially Normalized in Direct-Acting Antiviral Treated Persons

Ann W.N. Auma[1†], Carey L. Shive[1,2], Alyssa Lange[2], Sofi Damjanovska[2], Corinne Kowal[2], Elizabeth Zebrowski[2], Pushpa Pandiyan[1], Brigid Wilson[2], Robert C. Kalayjian[3], David H. Canaday[2] and Donald D. Anthony[1,2,3]*

[1] Department of Pathology, Case Western Reserve University, Cleveland, OH, United States, [2] GRECC, VA Northeast Ohio Healthcare System, Cleveland, OH, United States, [3] Department of Medicine, MetroHealth Medical Center, Case Western Reserve University, Cleveland, OH, United States

OPEN ACCESS

Edited by:
John Zaunders,
St Vincent's Hospital Sydney,
Australia

Reviewed by:
Kehmia Titanji,
Emory University,
United States
Tao Shen,
Peking University,
China
Angela M. Crawley,
Ottawa Hospital Research Institute
(OHRI), Canada

***Correspondence:**
Donald D. Anthony
dda3@case.edu

[†]These data in part fulfill the department of Pathology PhD degree requirement for Ann Auma

Specialty section:
This article was submitted to Viral Immunology, a section of the journal Frontiers in Immunology

Received: 13 December 2020
Accepted: 24 March 2021
Published: 12 April 2021

Citation:
Auma AWN, Shive CL, Lange A, Damjanovska S, Kowal C, Zebrowski E, Pandiyan P, Wilson B, Kalayjian RC, Canaday DH and Anthony DD (2021) Naïve CD4+ T Cell Lymphopenia and Apoptosis in Chronic Hepatitis C Virus Infection Is Driven by the CD31+ Subset and Is Partially Normalized in Direct-Acting Antiviral Treated Persons. Front. Immunol. 12:641230. doi: 10.3389/fimmu.2021.641230

Background: The mechanisms underlying naïve CD4+ lymphopenia during chronic Hepatitis C Virus (HCV) infection are unclear. Whether direct-acting antiviral (DAA) therapy restores peripheral naïve CD4+ T cell numbers and function is unknown.

Methods: We enumerated frequencies and counts of peripheral naïve CD4+, CD4+CD31+ and CD4+CD31- T cells by flow cytometry in a cross sectional analysis comparing chronic HCV infected (n=34), DAA-treated(n=29), and age-range matched controls (n=25), as well as in a longitudinal cohort of HCV DAA treated persons (n=16). The cross-sectional cohort was stratified by cirrhosis state. Cell apoptosis/survival (AnnexinV+7AAD+/BCL-2 labeling) and cell cycle entry (Ki67 expression) of CD31+ and CD31- naïve CD4+ T cells was analyzed directly *ex vivo* and following 3 and 5 days of *in vitro* culture with media, interleukin (IL) -7 or CD3/CD28 activator.

Results: In the cross-sectional cohort, naïve CD4+ proportions were lower in chronic HCV infected persons compared to controls and DAA-treated persons, an effect in part attributed to cirrhosis. Age was associated with naïve cell counts and proportions in HCV infected and treated persons as well. Naïve CD4+ cell proportions negatively correlated with plasma levels of soluble CD14 following therapy in DAA-treated persons. Naïve CD4+ cells from HCV infected persons exhibited greater direct *ex vivo* apoptosis and cell-cycling compared to cells from DAA-treated persons and controls, and this was localized to the CD4+CD31+ subset. On the other hand, no remarkable differences in expression of BCL-2 or IL-7 Receptor (CD127) at baseline or following *in vitro* media or IL7 containing culture were observed. In the longitudinal cohort, naïve CD4+CD31+/CD31- ratio tended to increase 24 weeks after DAA therapy initiation.

Conclusions: Activation and apoptosis of peripheral naïve CD4+CD31+ T cells appear to contribute to naïve CD4+ lymphopenia in chronic HCV infection, and this defect is partially reversible with HCV DAA therapy. Age and cirrhosis -associated naïve CD4+ lymphopenia is present both before and after HCV DAA therapy. These findings have implications for restoration of host immune function after DAA therapy.

Keywords: hepatitis c virus infection, naïve cd4+ T cells, apoptosis, lymphopenia, direct-acting antiviral

INTRODUCTION

Chronic Hepatitis C virus (HCV) infection is associated with impaired immunity against neoantigens contained in vaccines and new infections (1). Immunity to neoantigens is dependent upon naïve CD4+ T cell recognition of a broad antigen repertoire (2–4), a function primarily executed by CD31 expressing naïve CD4+ T cells that have been demonstrated to contain a polyclonal and diverse T cell receptor (TCR) repertoire (5). Indeed, naïve CD4+CD31+ lymphopenia attributed to age-related thymic involution and subsequently diminished thymic output in the elderly was associated with impaired immunity to vaccines and new infections (6, 7). Along these lines, the poor vaccine responses in chronic HCV infected persons (1) may be partly attributable to the naïve CD4+CD31+ lymphopenia observed in this group (8). Furthermore, the naïve CD4+CD31+ T cells are considered to be enriched for recent thymic emigrants (RTEs) and have greater numbers of TRECs (T cell receptor excision circles); deoxyribonucleic acid (DNA) by-products of TCR gene rearrangement (9). Naïve CD4+CD31+ T cell lymphopenia is associated with low TREC numbers in the elderly and both are biomarkers of thymic function (9, 10). Previous studies have used these parameters to demonstrate low thymic function during ageing and chronic HCV infection (5, 11, 12). Whether chronic HCV infection treatment can improve naïve CD4+ cell numbers, particularly during older age, is not clear. Interferon therapy has been observed to lower naïve CD4+CD31+ T cell counts (13), but the impact of direct-acting antiviral (DAA) interferon-free therapy is unknown and thus addressed here.

CD4+CD31- T cells undergo peripheral homeostatic proliferation, resulting in reduction of TRECs (TRECs are non-replicating and therefore diluted with each cellular division) (14), a distinguishing feature of this naïve CD4+ subset (9, 10). Further, CD4+CD31- T cells possess a significantly restricted and oligoclonal TCR repertoire when compared to the CD4+CD31+ T cells due to deletion of the CD4+CD31- T cells that receive insufficient homeostatic signals (including IL-7), with a resultant net loss of those specific TCRs from the naïve T cell pool (5). Similar to the CD4+CD31+ subset, naïve CD4+CD31- lymphopenia is also observed in chronic HCV and HIV infections (12, 15). However, in contrast to CD4+CD31+ T cell numbers that decline with age, the CD4+CD31- T cell numbers are either stable or increase with age (15, 16), suggesting that distinct mechanisms underlie naïve CD4+CD31+ and CD4+CD31- T cell homeostasis. CD31 is also expressed on CD8+ naïve T cells but at significantly higher levels compared to CD4+ naïve T cells (17) and it is not clear whether CD31 is a reliable marker for CD8+ RTEs since the published literature is not robust (12, 18–20). In the present study, we aimed to understand the impact of chronic HCV infection on absolute counts and proportions of naïve CD4+ T cells and corresponding CD31+ and CD31- subsets before and after DAA therapy and in uninfected controls. We also investigated the relationship between age and numbers of each naïve CD4+ T cell subtype and determined whether this relationship differed before or after DAA therapy. Finally, we evaluated direct *ex vivo* cell death and cycling, and *in vitro* response to TCR and interleukin (IL) -7 stimulation to gain insight into mechanisms underlying naïve CD4 lymphopenia.

METHODS

Study Population

Study participants provided written informed consent under protocols approved by the institutional review boards for human studies at the Cleveland Veterans Affairs Medical Center and University Hospitals of Cleveland. The cross-sectional study cohort included age-range matched uninfected controls (n=34), chronic HCV infected (n=29) and HCV DAA-treated (n=25, 1-5 years post-therapy start with successful therapy outcome/sustained virologic response (SVR)) participant groups. The longitudinal study cohort included chronic HCV infected persons scheduled for initiation of HCV DAA therapy and were followed up at weeks 0 (Start), 4, 8, and 24 following therapy initiation. Chronic HCV infected persons were positive for HCV antibody (for >6 months) and HCV RNA and were seronegative for HIV (by enzyme-linked immunosorbent assay [ELISA]) and HBV (HBSag negative, HBVcore ab negative). HCV treated persons underwent DAA regimens (primarily Sofosbuvir/Ledipasvir, though also Sofosbuvir/Velpatasvir, Ombitasvir/Paritaprevir/Ritonavir, Dasabuvir/Ombitasvir/Paritaprevir/Ritonavir or Elbasvir/Grazoprevir) depending on the HCV genotype, drug/drug interactions, renal function, and prior treatment experience for a period of 8 or 12 weeks as per standard of care.

Clinical Laboratory and Radiology Investigations

Certified clinical laboratories performed investigations to determine the extent of liver function; aspartate transaminase (AST), alanine transaminase (ALT) and albumin levels and liver damage index; Fibrosis 4 index (Fib-4) score (Age x AST level/

Platelet count x √ALT level) and AST to platelet ratio index (APRI). Liver stiffness was determined by transient elastography (TE) in kilopaskals (kPa). Ten consecutive and successful measurements were performed per patient and only those obtained with a success rate of at least 60% and an interquartile range/median value (IQR/M) less than 30% were considered reliable. Cirrhosis status was determined here by participants having a TE score >12.5 kPa, anAPRI >1.5, or a liver biopsy consistent with cirrhosis.

CD4+ T Cell Frequency and Absolute Count

PBMCs were labeled with anti- CD3-PERCP/CD4-Pacific Blue/CD8-APC-CY7/CD27-AF700/CD45RA-PE-CY7/CD31-BUV-395 (BD Biosciences, San Jose, CA). Absolute cell counts were obtained in fresh blood using Trucount™ absolute counting tubes (BD Biosciences, San Jose, CA). Flow cytometric analysis was performed on a BD LSRFortessa (BD Biosciences, San Jose, CA). Compensation was performed using single antibody labeled compensation beads; Live/Dead™ Fixable Aqua Dead cell stain-labeled Amine Reactive compensation beads (Life Technologies Corporation, Eugene, Oregon) and BD™ CompBeads (BD Biosciences, San Jose, CA) for cell-surface marker antibodies and analyzed with FACS DIVA software on the BD LSRFortessa.7 Population-based gating strategy was used to determine lymphocytes that were singlets and live cells, CD3+ T cells were divided into CD4+ and CD8+ subsets and thereafter CD4+ T cell subsets were defined by CD27 and CD45RA expression: naïve (CD27+CD45RA+), central memory (CM, CD27+CD45RA-) and effector memory (EM, CD27+CD45RA-) (**Supplemental Figure 1**). Naïve CD4+ T cell subsets were further defined as either CD31+ or CD31- based on isotype gating (21).

Naïve CD4+ T Cell Isolation

Memory CD4+ T cells and non-CD4+ T cells were depleted from PBMCs by incubation with CD45RO, CD8, CD14, CD15, CD16, CD19, CD25, CD34, CD36, CD56, CD123, anti-TCRγ/δ, anti-HLA-DR, and CD235a (glycophorin A) antibodies (Miltenyi Biotech, Sunnyvale, CA). Naive CD4+ T cells were isolated using negative selection magnetic bead methods (Miltenyi Biotech, Sunnyvale, CA).

Naive CD4+ T Cell Proliferation, Survival and Cell Death

Purified naïve CD4 T cells were cultured (10^5 cells/200μL) in the presence and absence of 10 ng/ml of recombinant human IL-7 (Cytheris, Issy-les-Moulineaux, France) or 1 μl of ImmunoCult™ human CD3/CD28 T Cell Activator (Stemcell Technologies, Cambridge, MA) and incubated under conditions of 37°C and 5% CO_2 for 5 days per condition. Cells were evaluated at days 0 (baseline), 3 and 5 of culture. Cells were washed and surface labeled in the dark at room temperature for 30 minutes with LIVE/DEAD™ Fixable Aqua Dead Cell Stain Kit (Thermo Fisher Scientific, Waltham, MA) and anti- CD3-PercP/CD4-Pacific Blue/CD8-APC-Cy7/CD27-AF700/CD45RA-PE-Cy7/CD31-BUV395/CD127-BV711 (BD Biosciences, San Jose, CA). Naive CD4+ T cells were identified based on expression of CD3, CD4, CD27 and CD45RA and lack of expression of CD8 markers and subsets were identified based on expression or absence of CD31. For detection of intracellular Ki67 (CD3/CD28 stimulation) and BCL-2 (IL-7 stimulation), cells were surface labeled, fixed, and permeabilized with a saponin-based buffer (BD Biosciences, San Jose, CA), followed by incubation with anti-Ki67-PE or anti-BCL-2- PE (BD Biosciences, San Jose, CA) for 40 minutes on ice. After labeling completion, cells were washed and fixed in phosphate-buffered saline containing 2% formaldehyde, and acquired on the BD LSRFortessa. For detection of apoptotic cells (after IL-7 stimulation), cells were labeled for 15 minutes with anti-AnnexinV-PE and anti-7AAD-FITC in Annexin V Binding Buffer (BD Biosciences, San Jose, CA) and evaluated on the BD LSRFortessa within 30 min of labeling completion.

ELISA

Plasma from HCV infected and DAA-treated persons was assessed for inflammatory markers including soluble cluster of differentiation 14 (sCD14), interferon-inducible protein-10 (IP10), Autotaxin (ATX), sCD163, soluble Tumor Necrosis Factor Receptor II (sTNFRII) and IL-6; homeostatic cytokine IL-7; cytomegalovirus (CMV) IgG, by ELISA

(CMV ELISA kit from Diagnostic Automation/Cortez Diagnostics, Woodland Hills, CA and all other ELISA kits from R&D Systems, Minneapolis, MN).

Statistical Analysis

Differences between two study groups were determined by Mann Whitney test and between two time-points within group by Related-Samples Wilcoxon Signed Rank tests. Associations between continuous variables per group were evaluated using Spearman's rank correlation coefficient and Linear regression. Inter-group comparisons of linear regression lines were evaluated by covariance analysis. All tests were performed in GraphPad Prism, version 8 or SPSS for Windows v. 24.0 (IBM Corp, Armonk, New York). P value <0.05 considered statistically significant for all tests.

RESULTS

Study Participant Characteristics

In the cross-sectional study, chronic HCV infected (n=34) and DAA-treated (n=29) persons and uninfected controls (n=25) were predominantly male and black (**Table 1**), consistent with our VA Northeast Ohio Healthcare system. HCV infected persons were age-distribution matched with controls (median 61 vs 59 years, p=0.6) and younger compared to DAA-treated persons (median 61 vs 65 years, p=0.01). The TE score (obtained prior to therapy) was higher in DAA-treated persons compared to active HCV infected persons (median 10.1 vs 5.0, p=0.0003). The HCV genotype 1A was predominant in both cross-sectional and longitudinal cohorts (**Table 1**). Additionally, features of the

longitudinal cohort include an age similar to DAA-treated individuals in the cross-sectional cohort, and TE score similar to the untreated HCV cross-sectional group, and a modestly greater proportion of non-black males.

Naïve CD4+ Lymphopenia Is Associated With Cirrhosis and DAA HCV Therapy Is Associated With Partial Normalization

We previously reported naïve CD4+ and CD4+CD31+ lymphopenia in chronic HCV infection (8). Here, we extended our initial observation, evaluating CD4+ T cell distribution in a cross-sectional cohort of chronic HCV infected (n=34) and DAA-treated (n=29) persons and age-range matched uninfected controls (n=25). In the cross-sectional analysis, naïve CD4+ proportions were lower in HCV infected persons compared to controls (p=0.008) and DAA-treated persons (p=0.01) (**Figure 1A**) while the CD4+CD31+ and CD4+CD31- proportions were comparable in all 3 groups (not shown). Naïve CD4+ (p=0.03), CD4+CD31+ (p=0.06) and CD4+CD31- (p=0.008) counts were lower in HCV infected persons compared to controls, though similar to DAA-treated persons (not shown). When stratified by cirrhosis status. The cirrhotics displayed lower naïve CD4+ (p=0.02) and CD4+CD31+ (p=0.008) proportions compared to non-cirrhotics in the HCV infected group (**Figure 1B**). In the DAA-treated group, cirrhotics tended to display lower naïve CD4+CD31+ (p=0.11) proportions compared to non-cirrhotics (**Figure 1C**).

In the longitudinal cohort analysis of chronic HCV infected persons before and after DAA therapy initiation (0, 4, 8 and 24 weeks), before therapy naïve CD4+ (p=0.04), CD4+CD31+ (p=0.02) and CD4+CD31+:CD4+CD31- ratio (p=0.03) proportions were lower in HCV infected persons compared to controls **Supplemental Figure 2A-C**), while CD4+CD31- proportions were higher (p=0.02) compared to controls (not shown). Within 24 weeks of DAA therapy initiation, there was a trend towards increased CD4+CD31+:CD4+CD31- ratios (p=0.18) (**Supplemental Figure 2C**) and trend for decreased CD4+CD31- frequency (p=0.18) (not shown). Further, before

TABLE 1 | Clinical characteristics of cross-sectional cohorts.

Sample size	HCV Infected n = 34	HCV Treated n = 29	Uninfected Control n = 25	P value Infected vs Treated	P value Infected vs Control	P value Treated vs Control
Age, years	61 (58; 65)	65 (62; 68)	59 (44; 71)	0.01*	0.7	0.2
Gender; No. (%)						
Male	32 (89%)	28 (97%)	22 (88%)			
Female	4 (11%)	1 (3%)	3 (12%)			
Race; No. (%)						
Black	21 (58%)	17 (60%)	18 (72%)			
White	13 (36%)	12 (40%)	6 (24%)			
Other	2 (6%)	0 (0%)	1 (4%)			
Albumin level (g/dL)	3.7 (3.5; 3.9)	3.8 (3.5; 4.0)	3.9 (3.7; 4.1)	0.5	0.04*	0.2
ALT level (U/L)	54 (35; 72)	25 (19; 31)	29 (25; 33)	<0.0001*	<0.0001*	NS
AST level (U/L)	43 (30; 63)	26 (18; 36)	21 (18; 24)	0.0004*	<0.0001*	NS
Platelets (x10^9/L)	211 (162; 258)	190 (153; 232)	225 (201; 271)	0.3	0.2	0.02*
APRI; No. (%)						
<0.4	11 (37%)	10 (40%)	17 (89%)			
0.4-1.5	15 (50%)	14 (56%)	2 (11%)			
>1.5	4 (13%)	1 (4%)	0 (0%)			
Fibrosis 4 index	1.8 (1.3; 2.4)	1.9 (0.9; 3.2)	1.0 (0.8; 1.4)	0.9	0.002*	0.01*
Transient Elastography score	5.0 (4.4; 5.9)	10.1 (6.3; 21.9)	…	0.0003*	…	…
Transient Elastography score (%)						
<9.5	22 (92%)	7 (50%)	…			
9.5-12.5	1 (4%)	1 (7%)	…			
>12.5	1 (4%)	6 (43%)	…	,.		
HCV Genotype; No. (%)						
1a	24 (67%)	14 (47%)	…		…	…
1b	6 (17%)	8 (27%)	…		…	…
2	3 (8.5%)	4 (14%)	…		…	…
3	3 (8.5%)	1 (3%)	…		…	…
4	0 (0%)	1 (3%)	…		…	…
Unknown	0 (0%)	2 (6%)	…	…	…	…
Plasma HCV RNA level (IU/L)	4,816,448 (701,431; 4,355,261)	…	…	…	…	…

Median (25th, 75th percentiles) shown unless otherwise indicated [No. (%)].

**Statistically significant (P value <0.05) using Mann Whitney test for unpaired comparison.*

ALT, alanine aminotransferase; APRI, aspartate aminotransferase to platelet ratio index; AST, aspartate amino transferase; HCV, hepatitis C virus.

APRI calculated as AST/PLT.

Fibrosis 4 index calculated as [age × AST level]/[platelet count ×√ALT level].

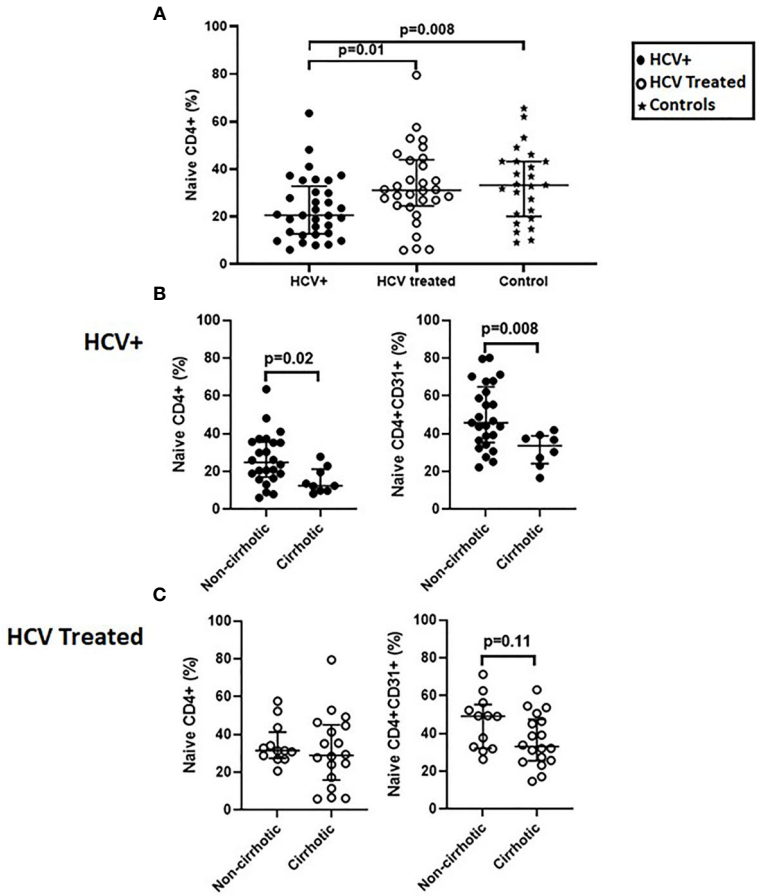

FIGURE 1 | Naïve CD4+ proportions are lower in HCV infected persons compared to direct-acting antiviral (DAA) -treated persons and age-range matched uninfected controls and the HCV infected persons with cirrhosis have lower naïve CD4+ and CD4+CD31+ proportions compared to those without cirrhosis before and after DAA therapy. In a cross-sectional cohort study; chronic HCV infected persons (n=34), HCV DAA-treated persons at 1-5 years post-DAA therapy initiation (n=29) and age-range matched uninfected controls (n=25) we compared proportions (%) of lymphocyte gated T cells that were naïve CD4 T cells (CD3+CD4+ CD27+CD45RA+) **(A)**. The HCV infected and DAA-treated groups were stratified by cirrhosis status defined by Transient Elastography scores with cirrhotics: >12.5 kilopaskals (kPa) and non-cirrhotics: <12.5 kPa. Proportions of naïve CD4+ and naïve CD4+CD31+ T cells were assessed **(B, C)**. Mann Whitney p values shown when $p<0.05$.

therapy absolute counts of naïve CD4+ (p=0.01), CD4+CD31+ (p=0.007) and CD4+CD31+:CD4+CD31- ratios (p=0.02) (**Supplemental Figures 2D–F**) and CD4+CD31- (p=0.03, not shown) were lower in HCV infected persons compared to controls. Within 24 weeks of DAA therapy initiation, there was a trend for increased CD4+CD31+:CD4+CD31- ratio (p=0.18) (**Supplemental Figure 2F**). Proportions of memory CD4+ T cell subsets remained unchanged after DAA initiation (not shown).

Collectively, these data indicate naïve CD4 lymphopenia is present during chronic active HCV infection, is localized to the CD31+ subset, and is more pronounced in those persons with cirrhosis. After therapy, naïve CD4+ and CD4+CD31+ lymphopenia appears partially normalized, though CD31+ subset frequency tends to remain lower in those with cirrhosis. The smaller longitudinal cohort data add further support for these findings.

Age Is Associated With Naïve CD4+ T Cell Proportions in Untreated and Treated HCV Infection

Prior studies indicate that age is negatively associated with naïve CD4+CD31+ proportions in healthy individuals (11, 22, 23). We therefore evaluated the relation between age and naïve CD4 cells here, and determined if HCV treatment state impacted the relationship between age and naïve CD4+, CD4+CD31+ and CD4+CD31- counts and proportions in our cross-sectional cohort. In active HCV infection, age negatively correlated with naïve CD4+ (r=-0.43, p=0.008) and CD4+CD31+ (r=-0.51, p=0.002); proportions and positively correlated with CD4+CD31- proportions (r=0.50, p=0.002) (**Figure 2**). In the DAA-treated group this correlation between age and CD4+CD31+ (r=-0.44, p=0.02) and CD4+CD31- (r=0.5, p=0.006) subsets was preserved (**Figure 2**). Similarly, naïve CD4+ (r=-0.41, p=0.01) and CD4+CD31+ (r=-0.49, p=0.004)

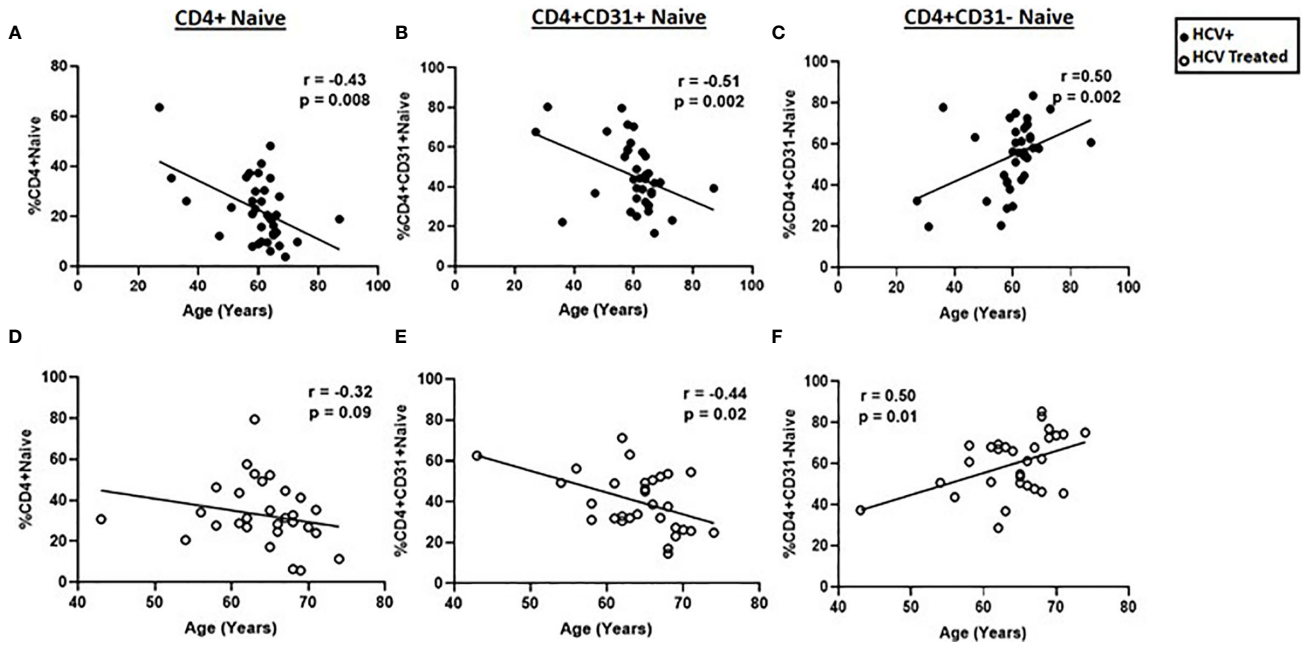

FIGURE 2 | Age negatively correlates with naïve CD4+ and CD4+CD31+ proportions and positively correlates with naïve CD4+CD31- proportions. The correlations between age and the naïve CD4+, **(A, D)** CD4+CD31+ **(B, E)** and CD4+CD31- **(C, F)** T cell proportions were determined in chronic HCV infected (filled circles, n=34) and HCV DAA-treated (open circles, n=29) individuals. Spearman's rank sum test was used; p= <0.05 considered significant.

counts negatively correlated with age in active HCV infection. In DAA-treated persons, the correlation between naïve CD4+CD31+ counts and age (r=-0.40, p=0.03) was preserved. Naïve CD4+ CD31- counts were not correlated with age in HCV infected or DAA-treated groups (not shown). Using linear regression, evaluating the interaction between age and naïve CD4+ cell subsets across groups, age associations with naïve CD4+ (p=0.96, -0.55 pooled slope), CD4+CD31+ (p=0.40, -0.74 pooled slope) and CD4+CD31- (p=0.40, 0.74 pooled slope) proportions did not differ between HCV infected and DAA-treated groups (**Supplemental Figure 3**), consistent with both age and HCV infection status driving naïve CD4+ cell lymphopenia. Naïve CD4+ T cell frequency/count and subset distribution did not differ by HCV genotype, sex or race.

Low Albumin Level, Liver Inflammation, Fibrosis, HCV Level and Soluble CD14 Level Are Associated With Naïve CD4+ and CD4+CD31+ Lymphopenia

Liver disease, regardless of etiology, may result in naïve T cell loss (8, 22, 24). Although splenic sequestration is one possible underlying mechanism (25), other factors may contribute. Chronic HCV infection contributes to liver inflammation and fibrosis, and impaired liver function, which in turn are associated with elevated systemic soluble immune activation markers (26). To better understand mechanisms underlying naïve CD4+ lymphopenia, we evaluated relationships between naïve CD4+ T cell numbers and plasma HCV level, markers of ongoing liver damage (ALT, AST), liver stiffness/fibrosis (TE, APRI, and FIB-4), liver synthetic function (albumin) and markers of systemic immune activation (sCD14, sCD163, ATX, TNFRII, IL-6 and IP-10 plasma levels). IP-10 levels (p=0.002) were elevated in HCV infected persons compared to DAA-treated persons while the levels of sCD14, sCD163, ATX, TNFRII and IL-6 were comparable between the two groups (**Supplemental Table 2**). FIB-4 score tended to negatively correlate with naïve CD4+ proportions (r=-0.35, p=0.06) and negatively correlated with CD4+CD31+ counts (r=-0.38, p=0.04), while HCV level tended to negatively correlate with naïve CD4+ counts (r=-0.30, p=0.06) in HCV infected persons. TE score negatively correlated with CD4+CD31+ proportions (r=-0.63, p=0.02) in DAA-treated persons. Albumin level positively correlated with CD4+CD31+ counts (r=0.60, p=0.01) in controls and CD4+ CD31+ proportions (r=-0.63, p=0.02) in DAA-treated persons. No other correlations were observed in controls. For immune activation markers, sCD14 negatively correlated with naïve CD4+ proportions (r=-0.45, p=0.02) in DAA-treated persons. No correlations were observed for the CD4+CD31- subset. Collectively, naïve CD4+ and CD4+CD31+ lymphopenia was associated with liver inflammation and fibrosis (FIB-4 and TE scores), immune activation (sCD14 level) and low liver albumin synthesis in chronic HCV infection even after DAA therapy.

Ex vivo Apoptosis in Naïve CD4+CD31+ T Cells During Chronic HCV Infection Is Greater Compared to DAA-Treated HCV

To address HCV infection mediated mechanisms of naïve CD4+ T cell homeostasis, we examined two important functions; naïve

CD4+ T cell direct *ex vivo* cell death and their death and capacity to respond to media vs. interleukin-7 (IL-7) *in vitro*. IL-7 is a homeostatic cytokine that can enhance the peripheral expansion and survival of naïve CD4+ T cells (27, 28), or TCR stimulus. We determined whether DAA therapy for chronic HCV infection was associated with naïve CD4+ T cell survival by direct *ex vivo* AnnexinV and 7AAD labeling, expression of pro-survival factor BCL-2 and IL-7R (CD127), or response to *in vitro* IL-7 stimulation. Furthermore, TCR induced activation of naïve CD4 + T cells is the first of three T cell activation signals (in addition to co-stimulation and cytokine-mediated differentiation) and impaired T cell activation following antigenic-stimulation during chronic HCV infection may dampen vaccine responses. We therefore evaluated the capacity of each naïve CD4+ T cell subset to undergo cell cycling (Ki67 labeling) following TCR stimulus before and after treatment of chronic HCV infection.

The early and late stages of cell death can be detected using AnnexinV (binds phosphatidylserine on outer leaflet of plasma membrane of apoptotic cells) and 7AAD (penetrates dead and apoptotic cells to bind double-stranded nucleic acids) respectively. Using AnnexinV and 7AAD, we evaluated the susceptibility of naïve CD4+ subsets to undergo cell death *in vivo* by examining purified naïve CD4+ cells and PBMCs for direct *ex vivo* apoptosis in naïve (CD31+ and CD31-) and memory (CM and EM) CD4+ T cell subsets respectively in HCV-infected (n=8) and DAA-treated (n=6) persons and controls (n=8). Cells from HCV infected persons exhibited greater AnnexinV+7AAD- labeling (early-stage apoptosis) in naïve (CD31+ p=0.03, CD31- p=0.04; **Figure 3A**) and memory (CM p=0.03, EM p=0.005; not shown) T cell subsets compared to DAA-treated persons and controls respectively. Compared to CD4+CD31-, CD4+CD31+ T cells displayed greater AnnexinV+7AAD- and AnnexinV+7AAD+ (late-stage apoptosis) labeling in HCV infected persons (p=0.004, p=0.01) and controls (p=0.02, p=0.04) (**Figures 3A, B**). These data are consistent with greater AnnexinV+7AAD+ CD4+CD31+:CD4+CD31- T cell ratios in HCV infected persons compared to DAA-treated persons (p=0.04, not shown). We also investigated the spontaneous apoptosis of naïve CD4+ subsets by examining purified CD4+ naïve T cells with or without IL-7 stimulation after 3 days. The IL-7 stimulated CD4+CD31- T cells displayed lower AnnexinV+7AAD+ labeling compared to media treated CD4+CD31- T cells from the HCV infected (p=0.02), DAA-treated (p=0.03) and control (p=0.02) persons while no differences were observed for the CD4+CD31+ T cells (**Supplemental Figure 4**). Further, media treated CD4+CD31- T cells displayed greater levels of AnnexinV+7AAD- labeling compared to media treated CD4+CD31+ T cells from the HCV infected (p=0.03) and DAA-treated persons (p=0.03) and controls (p=0.008) (not shown).

To further delineate mechanisms of apoptosis, we examined intracellular levels of pro-survival factor; BCL-2, and Ki67 (cell

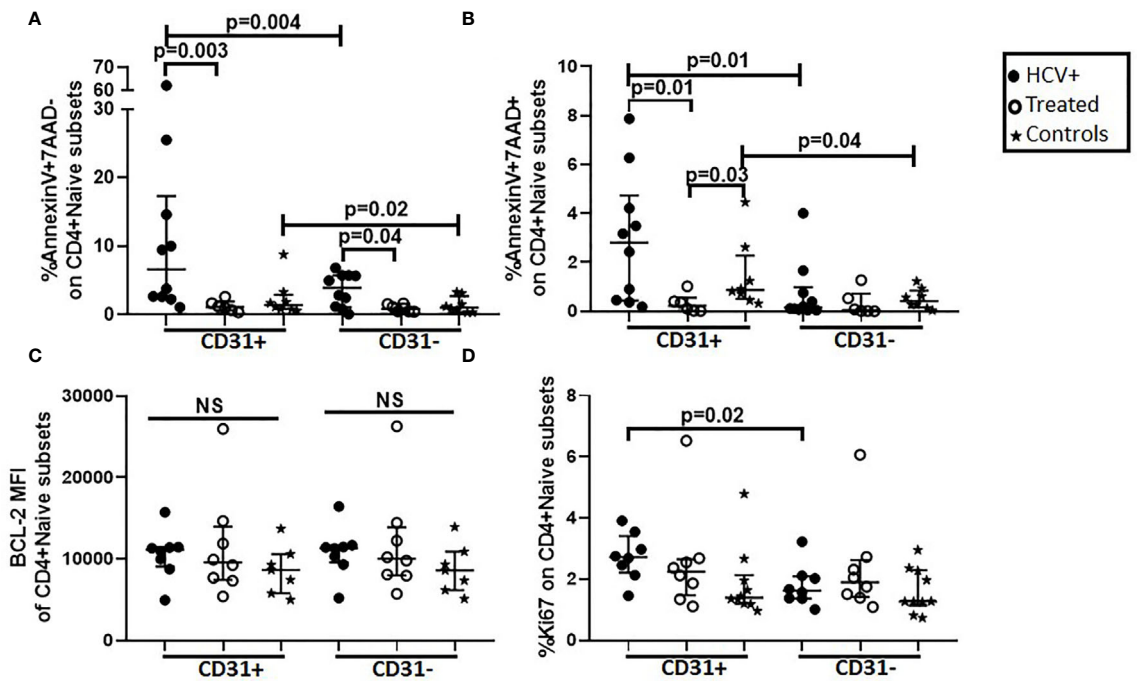

FIGURE 3 | Direct *ex vivo* apoptosis in CD31+ and CD31- naïve CD4+ T cell subsets is greater in HCV infected individuals compared to HCV DAA-treated individuals and uninfected controls and the CD4+CD31+ subset exhibits greater *ex vivo* apoptosis and cell cycling (Ki67 expression) compared to the CD4+CD31- subset. Magnetic bead purified (negative selection) naïve CD4 T cells from chronic HCV infected (filled circles, n=8), HCV DAA-treated (open circles, n=8) and age-range matched uninfected control (stars, n=7) groups were analyzed by flow cytometry for apoptosis (AnnexinV and 7AAD) **(A, B)**, BCL-2 **(C)** and cell cycling (Ki67) **(D)** on naïve (CD27+CD45RA+) CD4+CD31+ and CD4+CD31- T cells. Mann Whitney test was used for comparisons between two groups and between the CD4+CD31+ and CD4+CD31- subsets; p= <0.05 considered significant. NS represents non-significant p values.

cycling) in purified naïve CD4+ cells *ex vivo*. Naïve CD4+ subsets were all BCL-2 positive and the median fluorescence intensity (MFI) enabled the differentiation of the magnitude of BCL-2 expression MFI was comparable in gated naïve CD4+ T cell subsets across the 3 study groups (**Figure 3C**). Ki67 labeling was greater in CD4+CD31+ compared to CD4+CD31- naïve T cells (p=0.02) in HCV infected persons (**Figure 3D**). Inter-group comparisons revealed HCV infected persons exhibited greater in CD4+CD31+:CD4+CD31- Ki67+ T cell ratios when compared to DAA-treated persons (p=0.03, not shown). Together, the data demonstrated more enhanced *ex vivo* early-stage apoptosis in naïve and memory CD4+ T cells in HCV infection compared to treated HCV and controls respectively, and greater *ex vivo* late-stage apoptosis and cell cycling in CD4+CD31+ compared to CD4+CD31- subsets in HCV infection and controls.

IL-7 Induced BCL-2 Expression in Naïve CD4+ T Cell Subsets Is Greater in Chronic HCV Infected Persons Compared to DAA-Treated Persons

We next investigated if *in vitro* 5-day stimulation with recombinant IL-7 or CD3/CD28 activator would impact survival (apoptosis and BCL-2 expression), and cell cycling (Ki67 labeling) in our cross-sectional cohort. At Day 5 of IL-7 stimulation, BCL-2 upregulation in CD4+CD31+ cells of HCV infected persons was greater compared to cells of HCV treated persons (p=0.02) and controls (p=0.02, **Figure 4A**). BCL-2 upregulation in CD4+CD31- cells of HCV infected persons was also greater compared to cells of HCV treated persons (p=0.02), but similar to controls (**Figure 4B**). To determine if IL-7R (CD127) expression levels contributed to differential IL-7-induced BCL-2 upregulation between the groups, we examined IL-7R (CD127) levels on naïve CD4+ subsets. At baseline (Day 0), IL-7R MFI or positive% of naïve CD4+ subsets were comparable between the 3 study groups. In addition, the CD4+CD31+ subsets displayed greater IL-7R MFI compared to CD4+CD31- subsets in HCV infection (p=0.008) and treated HCV (p=0.03) (not shown). Following 5-day IL-7 stimulus, no inter-group or naïve subset differences in IL-7R down-regulation were observed (not shown). Plasma IL-7 levels were also comparable across groups (not shown).

At baseline (Day 0), no inter-group differences in bulk naïve CD4+ subset Ki67 labeling were observed (**Figure 4B**), however, Ki67+ CD4+CD31+:CD4+CD31- T cell ratios were greater in HCV infection compared to treated HCV (p=0.03, not shown). Following 5-day TCR stimulus (CD3/CD28), no inter-group

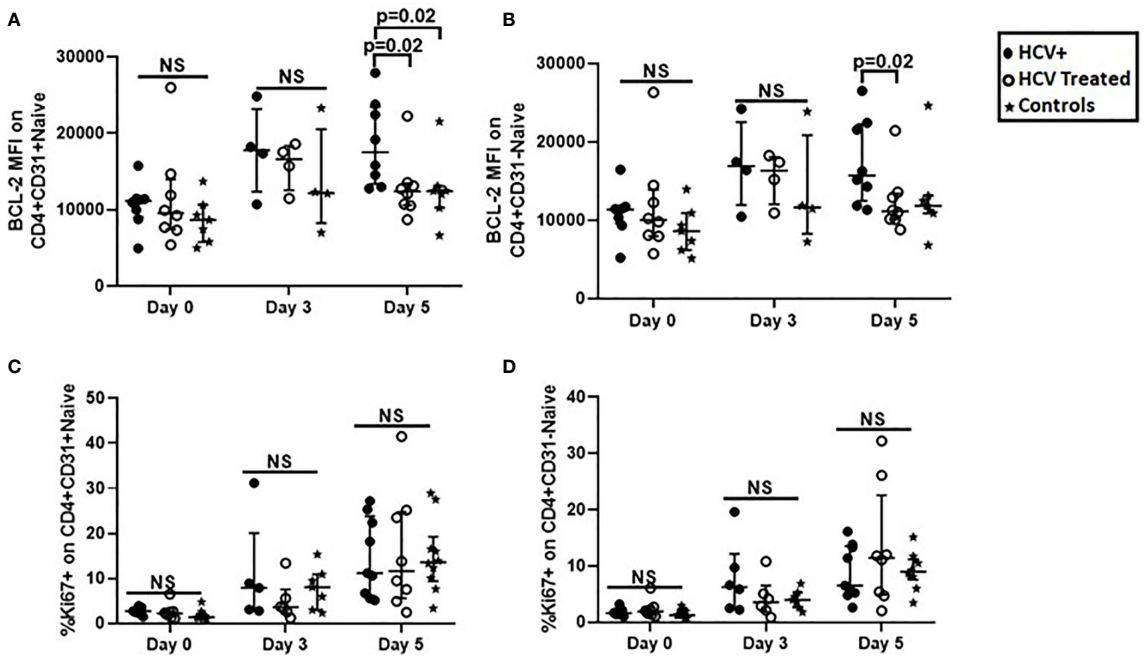

FIGURE 4 | BCL-2 expression after IL-7-stimulation was greater in CD31+ and CD31- naïve CD4+ T cell subsets from HCV infected persons compared to naïve CD4+ T cells from HCV DAA-treated persons and uninfected controls, while T cell Receptor-dependent cell cycle entry was similar in naïve CD4+ T cell subsets in all three groups. Magnetic bead purified (negative selection) naïve CD4 T cells from chronic HCV infected (filled circles, n=8), HCV DAA-treated (open circles, n=8) and age-range matched uninfected control (stars, n=7) groups were stimulated with 10ng/ml of recombinant human IL-7 or 1ul anti-CD3/anti-CD28 Activator for 5 days. On 0, 3, and 5 days, flow cytometric analysis of BCL-2 following IL-7 stimulation **(A, B)** and Ki67 following anti-CD3/anti-CD28 stimulation **(C, D)** on naïve (CD27+CD45RA+) CD4+CD31+ and CD4+CD31- T cells was performed. Mann Whitney test was used for comparisons between two groups; p= <0.05 considered significant. NS represents non-significant p values.

differences in naïve CD4+ subset Ki67 labeling were observed (**Figures 4C, D**). Notably, CD31 expression on naïve CD4+ T cells was similar after stimulation with IL-7 or CD3/CD28 activator, with exception of a modest increase in CD31 after 5 days of CD3/CD28 stimulation for control subject samples (**Supplementary Figure** for reviewer only.

Overall, IL-7-induced BCL-2 up-regulation in naïve CD4+ subsets was greater in HCV infected persons compared to HCV-treated and control persons, while IL-7R down-regulation was similar across groups. At baseline, cell cycling in CD31+ relative to CD31- subsets was greater in active HCV infection, and no differences in cell cycling were observed between groups before or after TCR stimulus.

DISCUSSION

In the present study, we observed lower naïve CD4+ T cell proportions in chronic HCV infected persons compared to DAA-treated persons and age-range matched uninfected controls. Further, HCV infected persons with cirrhosis displayed lower naïve CD4+ and CD4+CD31+ T cell proportions compared to those without cirrhosis before DAA therapy and this partially normalized when evaluating persons treated with DAA therapy. Results were consistent in the much smaller longitudinal cohort. Age negatively correlated with naïve CD4+ and CD4+CD31+ proportions, and positively correlated with CD4+CD31- proportions before and after HCV DAA therapy. Direct *ex vivo* apoptosis in naïve and memory CD4+ T cells was elevated in chronic HCV infection, and the CD4+ CD31+ subset exhibited greater apoptosis and cell cycling compared to the CD4+CD31- naïve subset. *In vitro* IL-7-induced BCL-2 upregulation was greater in naïve CD4+ cells from HCV infected persons compared to cells from HCV-treated persons and controls. Taken together, chronic HCV infection state, cirrhosis state, and age impact naïve CD4+ T cell proportions, likely by differing mechanisms. DAA therapy is associated with numerical and fractional normalization of naïve CD4+ lymphopenia. Plausible mechanisms underlying naïve CD4+ lymphopenia attributable to HCV infection include enhanced cellular apoptosis and activation (cycling), more so in the recent thymic emigrant CD4+CD31+ subset.

Naïve CD4+ and CD4+CD31+ T cell lymphopenia in chronic HCV infection was previously reported by our group and others (8, 12, 29). Here, we confirm this prior literature and extend previous reports to the impact of DAA treatment on naïve CD4+ T cell lymphopenia. Before therapy the proportions and counts of naïve CD4+, CD4+CD31+ and CD4+CD31- T cells in chronic HCV infected persons were lower compared to controls. DAA therapy was associated with partial normalization of naïve CD4+ proportions to levels observed in age-range matched controls, with a residual trend toward lower naïve CD4+CD31+ frequencies in cirrhotics compared to non-cirrhotics (**Figure 1**).

Age is also associated with naïve CD4+ T cell lymphopenia, largely thought to be due to thymic involution and decreased thymopoiesis in older individuals with subsequent reduction of naïve CD4+CD31+ T cell export into the periphery (7, 11). Here, associations between age and both proportions and counts of naïve CD4+ T cells and corresponding subsets were present both before and after DAA therapy, indicating that the age-related mechanisms regulating naïve CD4+ T cell homeostasis are observed regardless of, and perhaps independent of, HCV treatment status, suggesting different mechanisms. Indeed, data provided here indicate HCV mediated cell death of the naïve CD4+ T cell pool, contrasting with reduced thymic output in aged persons. Notably, age was negatively correlated with CD4+CD31+ counts but not correlated with CD4+CD31- counts regardless of HCV infection state, consistent with an age effect selective for the CD31+ subset. Overall, mechanisms of both age- and HCV- driven (reversed with DAA) lymphopenia were operative in our cohorts of chronic HCV infected persons of older age.

Mechanisms underlying HCV-associated naïve CD4+ lymphopenia have not been clearly defined. One potential mechanism is naïve CD4+ T cell anatomic redistribution due to portal hypertension and splenic sequestration (25), however, this does explain the selective association of HCV infection with lymphopenia in the CD4+CD31+ but not CD4+CD31- subset. Alternatively, insufficient DNA (deoxyribonucleic acid) repair enzyme can result in naïve CD4+ T cell accumulation of damaged DNA triggering intrinsic apoptosis and T cell loss during HCV infection (30). Here, since 7AAD binds to intra-cytoplasmic double-stranded nucleic acid fragments in apoptotic cells, the observed enhanced Annexin+7AAD+ labeling of naïve CD4+ T cells (direct *ex vivo*) from HCV infected persons could be consistent with this mechanism. At the same time direct *ex vivo* analysis of BCL-2 expression within naïve CD4+ T cells was similar between untreated and treated HCV and control persons, consistent with prior studies in chronic HCV (31–33) and suggesting that alteration of this intrinsic anti-apoptotic mechanism is not likely operative here. In fact *in vitro* media cultured cell apoptosis (measure of intrinsic resistance to apoptosis) does not appear to remarkably differ between groups but as expected resistance is enhanced by IL-7 culture (34, 35). Notably after IL-7 culture, HCV infected person cells exhibited greater BCL-2 expression compared to HCV-treated person cells, while IL-7-induced IL-7R downregulation was similar in cells from the two groups.

Another potential mechanism of HCV infection associated naïve CD4+ lymphopenia is activation-induced cell death, particularly in the CD4+CD31+ subset, following antigen specific or non-specific activation. In support of this, we observed greater late-stage (AnnexinV+7AAD+) apoptosis and cycling (Ki67 expression) in CD4+CD31+ compared to CD4+CD31- T cells in HCV infected persons and controls. Non-antigen specific naïve CD4+ T cell activation in HCV infection may be mediated by HCV envelope protein E2 interaction with cell surface receptor CD81 on naïve T cells (36) or by soluble immune activation factors secreted by inflamed livers. In support, we observed a negative correlation between sCD14 level (released from activated monocytes and Kupffer cells) and naïve CD4+ proportions in DAA-treated persons. Notably, sCD14 plasma levels were similar between

HCV untreated and treated persons, consistent with previous reports (26, 37), raising the possibility that residual liver inflammation after DAA therapy is one possible driver of naïve CD4 lymphopenia, while other factors are likely also involved before DAA therapy. Notably, lower liver biosynthetic function (albumin) and elevated liver inflammation and fibrosis (Fib-4 and TE scores) levels were associated with lower naïve CD4+ and CD4+CD31+ numbers before and after DAA therapy, demonstrating that the long-term effects of HCV infection and advanced liver damage may persist despite HCV cure possibly contributing to mechanisms that interfere with naïve CD4+ T cell homeostasis. Here, cirrhotics exhibited more naïve CD4+ and CD4+CD31+ lymphopenia during HCV infection, a finding that persisted despite effective DAA treatment, consistent with previous reports of CD4+CD31+ lymphopenia during liver cirrhosis regardless of cause (22, 38).

Lastly, the extrinsic apoptotic pathway *via* surface death receptors (including Fas receptor) may also contribute to naïve CD4+ T cell lymphopenia. HCV infection has been described to associate with greater Fas expression on peripheral bulk T cells, greater serum FasL levels, and apoptosis of bulk peripheral T cells (32, 39, 40). The liver may be one source of peripheral FasL since it is highly expressed within the liver immune cells in HCV infection (41). While these studies did not specifically evaluate naïve CD4+ T cells, it is likely this mechanism contributes here. Indeed, literature from the mouse system suggests naïve T cells may be more susceptible to Fas-mediated apoptosis following antigenic stimulation (33), and this is consistent with our observation of late-stage (Annexin+ 7AAD+) apoptosis in only naïve but not memory CD4+ T cells.

The current study has a number of limitations. The study participants are reflective of the North East Ohio VA population with African-American and male predominance. Female and non-black populations were under-represented and further study is needed to understand how these results extend to the general U.S. population. Investigations of longitudinal changes after DAA therapy initiation were severely limited by small sample size and inconsistent follow-up. Relationships between age and naïve CD4+ T cell numbers in the uninfected controls did not reach significance here, contrasting with published data, also perhaps due to small sample size or additional confounding factors in our sample set. Our measurements were peripheral blood based, and perhaps limited in ability to reflect events within the liver and thymus. However, these results build upon prior literature, focusing here on naïve CD4+ subsets, effects of DAA therapy on naïve CD4+ homeostasis, and mechanisms of cellular activation and cell death associated with DAA treatment status.

In summary, we have described naïve CD4+ T cell lymphopenia and apoptosis, associated with cell cycling in the CD31+ naïve CD4 T cell compartment, that is partially normalized after initiation of DAA therapy in chronic HCV infection. Age related naïve CD4 lymphopenia appears to be the result of alternative mechanism, such as reduced thymic output, and this is superimposed upon the state of chronic HCV infection and apoptosis. The downstream effect of restoration of this compartment after HCV DAA therapy is yet to be determined.

DATA AVAILABILITY STATEMENT

The original contributions presented in the study are included in the article/**Supplementary Material**. Further inquiries can be directed to the corresponding author.

ETHICS STATEMENT

The studies involving human participants were reviewed and approved by VA Northeast Ohio Healthcare System Institutional Review Board (IRB). The patients/participants provided their written informed consent to participate in this study.

AUTHOR CONTRIBUTIONS

Study concept and design: DA, AA CS, DC, and PP. Technical support and Manuscript review: AL, SD, CK, and EZ. Data acquisition: AA and AL. Data analysis and interpretation: AA and DA. Statistical analysis: AA, BW, and DA. Manuscript drafting: AA and DA. Critical revision of manuscript: AA, DA, CS, DC, and PP. Study supervision: AA, DA and CS. All authors contributed to the article and approved the submitted version.

FUNDING

This study was Supported by D43TW010319 (AA), IK2CX001471 (CS), BX001894 (DA), CX001791 (DA).

ACKNOWLEDGMENTS

We thank the study participants for the contribution of their samples.

SUPPLEMENTARY MATERIAL

The Supplementary Material for this article can be found online at: https://www.frontiersin.org/articles/10.3389/fimmu.2021.641230/full#supplementary-material

Supplementary Table 1 | Clinical characteristics of HCV DAA-treated longitudinal cohort. Median (25^{th};75^{th} percentiles) shown unless otherwise indicated.

Supplementary Table 2 | Soluble markers of systemic immune activation markers of cross-sectional cohorts. Median (25^{th}; 75^{th} percentiles). *Statistically significant (P value <0.05) using Mann Whitney test for unpaired comparison. **Samples not available for full cohort

Supplementary Figure 1 | Flow cytometry gating strategy for naïve CD4+ T cells and corresponding subsets.

Supplementary Figure 2 | Naïve CD4+, CD4+CD31+ and CD4+CD31- proportions and counts are lower in HCV infected individuals compared to age-range matched uninfected controls and initiation of direct-acting antiviral (DAA) therapy tended to increase naïve CD4+ and CD4+CD31+ but not CD4+CD31- counts. In a longitudinal cohort study, chronic HCV infected individuals were treated with 8 or 12 weeks of DAA therapy and followed from baseline (start; n=16) to time-points after DAA therapy initiation; Weeks 4 (n=13), 8 (n=6) and 24 (n=6). Proportions **(A–C)** and counts **(D–F)** of naïve CD4+ T cells (A and D), CD4+CD31+ T cells **(B, E)** and CD431+:CD31- T cell ratios **(C, F)** were assessed. Age-range matched uninfected controls (n=25) we compared for each T cell parameter. Wilcoxon signed rank test was used for paired comparisons between two time points; p= <0.05 considered significant.

Supplementary Figure 3 | The degree of association between age and the naïve CD4+, CD4+CD31+ and CD4+CD31- proportions does not significantly differ before and after HCV DAA therapy. The associations between age and the naïve CD4+, CD4+CD31+ and CD4+CD31- T cell proportions in the chronic HCV infected (filled circles, n=34) and HCV DAA-treated (open circles, n=29) groups and the differences between the two study groups were determined. R and p values for correlations within each group (HCV infected and HCV treated) are shown, and p values to determine differences in correlations between groups are shown. We can discuss whether we want p value for y axis intercept as well. The Linear regression test was used.

Supplementary Figure 4 | The naïve CD4+CD31- T cells undergo spontaneous apoptosis at higher levels compared to the naïve CD4+CD31+ T cells before and after HCV DAA therapy and in absence of HCV infection. Magnetic bead purified (negative selection) naïve CD4 T cells from chronic HCV infected (filled circles, n=4), HCV DAA-treated (open circles, n=4) and age-range matched uninfected control (stars, n=5) groups were stimulated with or without 10ng/ml of recombinant human IL-7 for 3 days. On third day, flow cytometric analysis for apoptosis (AnnexinV and 7AAD) on naïve (CD27+CD45RA+) CD4+CD31+ **(A)** and CD4+CD31- **(B)** T cells was performed. Mann Whitney test was used for comparisons between two groups; p= <0.05 considered significant.

Supplementary Figure 5 | CD31 expression on naïve CD4+ T cells is mostly stable during *in vitro* stimulation with recombinant IL-7 or CD3/CD28 activator in cells from HCV infected and DAA-treated persons. Magnetic bead purified (negative selection) naïve CD4 T cells from chronic HCV infected (filled circles, n=8; **A, D**), HCV DAA-treated (open circles, n=8; **B, E**) and age-range matched uninfected control (stars, n=7; **C, F**) groups were stimulated with 10ng/ml of recombinant human IL-7 **(A–C)** or 1ul anti-CD3/anti-CD28 Activator **(D–F)** for 5 days. On 0 (direct *ex vivo*), 3, and 5 days, flow cytometric analysis of CD31 expression on naïve (CD27+CD45RA+) CD4+ T cells was performed. Mann Whitney test was used for comparisons between two groups; p= <0.05 considered significant.

REFERENCES

1. Shive CL, Judge CJ, Clagett B, Kalayjian RC, Osborn M, Sherman KE, et al. Pre-vaccine plasma levels of soluble inflammatory indices negatively predict responses to HAV, HBV, and tetanus vaccines in HCV and HIV infection. *Vaccine* (2018) 36(4):453–60. doi: 10.1016/j.vaccine.2017.12.018
2. Nanda NK, Apple R, Sercarz E. Limitations in plasticity of the T-cell receptor repertoire. *Proc Natl Acad Sci* (1991) 88(21):9503–7. doi: 10.1073/pnas.88.21.9503
3. Woodland D, Kotzin B, Palmer E. Functional consequences of a T cell receptor D beta 2 and J beta 2 gene segment deletion. *J Immunol* (1990) 144(1):379–85.
4. Bousso P, Wahn V, Douagi I, Horneff G, Pannetier C, Le Deist F, et al. Diversity, functionality, and stability of the T cell repertoire derived in vivo from a single human T cell precursor. *Proc Natl Acad Sci* (2000) 97(1):274–8. doi: 10.1073/pnas.97.1.274
5. Kohler S, Wagner U, Pierer M, Kimmig S, Oppmann B, Mowes B, et al. Post-thymic in vivo proliferation of naive CD4+ T cells constrains the TCR repertoire in healthy human adults. *Eur J Immunol* (2005) 35(6):1987–94. doi: 10.1002/eji.200526181
6. Čičin-Šain L, Smyk-Paerson S, Currier N, Byrd L, Koudelka C, Robinson T, et al. Loss of naive T cells and repertoire constriction predict poor response to vaccination in old primates. *J Immunol* (2010) 184(12):6739–45. doi: 10.4049/jimmunol.0904193
7. Schulz AR, Mälzer JN, Domingo C, Jurchott K, Grutzkau A, Babel N, et al. Low Thymic Activity and Dendritic Cell Numbers Are Associated with the Immune Response to Primary Viral Infection in Elderly Humans. *J Immunol* (2015) 1500598.
8. Yonkers NL, Sieg S, Rodriguez B, Anthony DD. Reduced naive CD4 T cell numbers and impaired induction of CD27 in response to T cell receptor stimulation reflect a state of immune activation in chronic hepatitis C virus infection. *J Infect Dis* (2011) 203(5):635–45. doi: 10.1093/infdis/jiq101
9. Kimmig S, Przybylski GK, Schmidt CA, Laurisch K, Mowes B, Radbruch A, et al. Two subsets of naive T helper cells with distinct T cell receptor excision circle content in human adult peripheral blood. *J Exp Med* (2002) 195(6):789–94. doi: 10.1084/jem.20011756
10. Junge S, Kloeckener-Gruissem B, Zufferey R, Keisker A, Salgo B, Fauchere JC, et al. Correlation between recent thymic emigrants and CD31+ (PECAM-1) CD4+ T cells in normal individuals during aging and in lymphopenic children. *Eur J Immunol* (2007) 37(11):3270–80. doi: 10.1002/eji.200636976
11. Kilpatrick R, Rickabaugh T, Hultin L, Hultin P, Hausner M, Detels R, et al. Homeostasis of the Naive CD4+ T Cell Compartment during Aging. *J Immunol (Baltimore Md 1950)* (2008) 180:1499–507. doi: 10.4049/jimmunol.180.3.1499
12. Hartling HJ, Gaardbo JC, Ronit A, Salem M, Laye M, Clausen MR, et al. Impaired thymic output in patients with chronic hepatitis C virus infection. *Scand J Immunol* (2013) 78(4):378–86. doi: 10.1111/sji.12096
13. Beq S, Rozlan S, Pelletier S, Willems B, Bruneau J, Lelievre J-D, et al. Altered thymic function during interferon therapy in HCV-infected patients. *PloS One* (2012) 7(4):e34326. doi: 10.1371/journal.pone.0034326
14. Takeshita S, Toda M, Yamagishi H. Excision products of the T cell receptor gene support a progressive rearrangement model of the alpha/delta locus. *EMBO J* (1989) 8(11):3261–70. doi: 10.1002/j.1460-2075.1989.tb08486.x
15. Rickabaugh TM, Kilpatrick RD, Hultin LE, Hultin PM, Hausner MA, Sugar CA, et al. The dual impact of HIV-1 infection and aging on naïve CD4+ T-cells: additive and distinct patterns of impairment. *PloS One* (2011) 6(1):e16459. doi: 10.1371/journal.pone.0016459
16. Gomez I, Hainz U, Jenewein B, Schwaiger S, Wolf A, Grubeck-Loebenstein B. Changes in the expression of CD31 and CXCR3 in CD4+ naıve T cells in elderly persons. *Mech Ageing Dev* (2003) 124(4):395–402. doi: 10.1016/S0047-6374(03)00014-9
17. Tanaka Y, Albelda SM, Horgan KJ, Van Seventer GA, Shimizu Y, Newman W, et al. CD31 expressed on distinctive T cell subsets is a preferential amplifier of beta 1 integrin-mediated adhesion. *J Exp Med* (1992) 176(1):245–53. doi: 10.1084/jem.176.1.245
18. Tanaskovic S, Fernandez S, Price P, Lee S, French MA. CD31 (PECAM-1) is a marker of recent thymic emigrants among CD4+ T-cells, but not CD8+ T-cells or γδ T-cells, in HIV patients responding to ART. *Immunol Cell Biol* (2010) 88(3):321–7. doi: 10.1038/icb.2009.108
19. Cunningham CA, Helm EY, Fink PJ. Reinterpreting recent thymic emigrant function: defective or adaptive? *Curr Opin Immunol* (2018) 51:1–6. doi: 10.1016/j.coi.2017.12.006
20. Fink PJ. The biology of recent thymic emigrants. *Annu Rev Immunol* (2013) 31:31–50. doi: 10.1146/annurev-immunol-032712-100010
21. Morimoto C, Schlossman SP. Rambotti Lecture. Human naive and memory T cells revisited: new markers (CD31 and CD27) that help define CD4+ T cell subsets. *Clin Exp Rheumatol* (1993) 11(3):241–7.
22. Lario M, Muñoz L, Ubeda M, Borrero M-J, Martinez J, Monserrat J, et al. Defective thymopoiesis and poor peripheral homeostatic replenishment of T-helper cells cause T-cell lymphopenia in cirrhosis. *J Hepatol* (2013) 59(4):723–30. doi: 10.1016/j.jhep.2013.05.042
23. Tong Q-Y, Zhang J-C, Guo J-L, et al. Human Thymic Involution and Aging in Humanized Mice. *Front Immunol* (2020) 11(1399). doi: 10.3389/fimmu.2020.01399

24. Albillos A, Hera A, Reyes E, Monserra J, Munoz L, Nieto M, et al. Tumour necrosis factor-alpha expression by activated monocytes and altered T-cell homeostasis in ascitic alcoholic cirrhosis: amelioration with norfloxacin. *J Hepatol* (2004) 40(4):624–31. doi: 10.1016/j.jhep.2003.12.010
25. McGovern BH, Golan Y, Lopez M, Pratt D, Lawton A, Moore G, et al. The impact of cirrhosis on CD4+ T cell counts in HIV-seronegative patients. *Clin Infect Dis* (2007) 44(3):431–7. doi: 10.1086/509580
26. Kostadinova L, Shive CL, Zebrowski E, Fuller B, Rife K, Hirsch A, et al. Soluble markers of immune activation differentially normalize and selectively associate with improvement in AST, ALT, albumin, and transient elastography during IFN-free HCV therapy. *Pathog Immun* (2018) 3(1):149. doi: 10.20411/pai.v3i1.242
27. Tan JT, Dudl E, LeRoy E, Murray R, Sprent J, Weinberg KI, et al. IL-7 is critical for homeostatic proliferation and survival of naive T cells. *Proc Natl Acad Sci* (2001) 98(15):8732–7. doi: 10.1073/pnas.161126098
28. Moniuszko M, Fry T, Tsai W-P, Morre M, Assouline B, Cortez P, et al. Recombinant interleukin-7 induces proliferation of naive macaque CD4+ and CD8+ T cells in vivo. *J Virol* (2004) 78(18):9740–9. doi: 10.1128/JVI.78.18.9740-9749.2004
29. Shmagel KV, Saidakova EV, Korolevskaya LB, Shmagel NG, Chereshnev VA, Anthony DD, et al. Influence of hepatitis C virus coinfection on CD4+ T cells of HIV-infected patients receiving HAART. *Aids* (2014) 28(16):2381–8. doi: 10.1097/QAD.0000000000000418
30. Zhao J, Dang X, Zhang P, Nguyen LN, Cao D, Wang L, et al. Insufficiency of DNA repair enzyme ATM promotes naive CD4 T-cell loss in chronic hepatitis C virus infection. *Cell Discov* (2018) 4(1):1–13. doi: 10.1038/s41421-018-0015-4
31. Toubi E, Kessel A, Goldstein L, Slobodin G, Sabo E, Shmuel Z, et al. Enhanced peripheral T-cell apoptosis in chronic hepatitis C virus infection: association with liver disease severity. *J Hepatol* (2001) 35(6):774–80. doi: 10.1016/S0168-8278(01)00207-0
32. El-Bendary M, Hawas S, Elhammady D, Al-Hadidy A-HM, Rizk H. Expression of Fas (CD95) and Bcl-2 in peripheral blood mononuclear cells in patients with chronic HCV and schistosomiasis. *Egypt J Basic Appl Sci* (2014) 1(3-4):136–43. doi: 10.1016/j.ejbas.2014.10.002
33. Inaba M, Kurasawa K, Mamura M, Kumano K, Saito Y, Iwamoto I. Primed T cells are more resistant to Fas-mediated activation-induced cell death than naive T cells. *J Immunol* (1999) 163(3):1315–20.
34. Khaled AR, Durum SK. Lymphocide: cytokines and the control of lymphoid homeostasis. *Nat Rev Immunol* (2002) 2(11):817–30. doi: 10.1038/nri931
35. Rathmell JC, Farkash EA, Gao W, Thompson CB. IL-7 enhances the survival and maintains the size of naive T cells. *J Immunol* (2001) 167(12):6869–76. doi: 10.4049/jimmunol.167.12.6869
36. Wack A, Soldaini E, Tseng CTK, Nuti S, Klimpel GR, Abrignani S. Binding of the hepatitis C virus envelope protein E2 to CD81 provides a co-stimulatory signal for human T cells. *Eur J Immunol* (2001) 31(1):166–75. doi: 10.1002/1521-4141(200101)31:1<166::AID-IMMU166>3.0.CO;2-L
37. Kostadinova L, Shive CL, Judge C, Zebrowski E, Compan A, Rife K, et al. During Hepatitis C Virus (HCV) Infection and HCV-HIV Coinfection, an Elevated Plasma Level of Autotaxin Is Associated With Lysophosphatidic Acid and Markers of Immune Activation That Normalize During Interferon-Free HCV Therapy. *J Infect Dis* (2016) 214(9):1438–48. doi: 10.1093/infdis/jiw372
38. Vranjkovic A, Deonarine F, Kaka S, Angel JB, Cooper CL, Crawley AM. Direct-acting antiviral treatment of HCV infection does not resolve the dysfunction of circulating CD8+ T-cells in advanced liver disease. *Front Immunol* (2019) 10:1926. doi: 10.3389/fimmu.2019.01926
39. Taya N, Torimoto Y, Shindo M, Hirai K, Hasebe C, Kohgo Y. Fas-mediated apoptosis of peripheral blood mononuclear cells in patients with hepatitis C. *Br J Haematol* (2000) 110(1):89–97. doi: 10.1046/j.1365-2141.2000.01945.x
40. Zhu L-X, Liu J, Xie Y-H, Kong Y-Y, Ye Y, Wang C-L, et al. Expression of hepatitis C virus envelope protein 2 induces apoptosis in cultured mammalian cells. *World J Gastroenterol: WJG* (2004) 10(20):2972. doi: 10.3748/wjg.v10.i20.2972
41. Mita E, Hayashi N, Iio S, Takehara T, Hijioka T, Kasahara A, et al. Role of Fas Ligand in Apoptosis Induced by Hepatitis C Virus Infection. *Biochem Biophys Res Commun* (1994) 204(2):468–74. doi: 10.1006/bbrc.1994.2483

Conflict of Interest: The authors declare that the research was conducted in the absence of any commercial or financial relationships that could be construed as a potential conflict of interest.

frontiers in Immunology

REVIEW
published: 12 April 2021
doi: 10.3389/fimmu.2021.656414

Gut Leakage of Fungal-Related Products: Turning Up the Heat for HIV Infection

Stéphane Isnard[1,2,3], *John Lin*[1,2], *Simeng Bu*[1,2], *Brandon Fombuena*[1,2], *Léna Royston*[1,2] *and Jean-Pierre Routy*[1,2,4*]

[1] Infectious Diseases and Immunity in Global Health Program, Research Institute, McGill University Health Centre, Montreal, QC, Canada, [2] Chronic Viral Illness Service, McGill University Health Centre, Montreal, QC, Canada, [3] CIHR Canadian HIV Trials Network, Vancouver, BC, Canada, [4] Division of Hematology, McGill University Health Centre, Montreal, QC, Canada

The intestinal epithelial layer serves as a physical and functional barrier between the microbiota in the lumen and immunologically active submucosa. Th17 T-cell function protects the gut epithelium from aggression from microbes and their by-products. Loss of barrier function has been associated with enhanced translocation of microbial products which act as endotoxins, leading to local and systemic immune activation. Whereas the inflammatory role of LPS produced by Gram-negative bacteria has been extensively studied, the role of fungal products such as β-D-glucan remains only partially understood. As HIV infection is characterized by impaired gut Th17 function and increased gut permeability, we critically review mechanisms of immune activation related to fungal translocation in this viral infection. Additionally, we discuss markers of fungal translocation for diagnosis and monitoring of experimental treatment responses. Targeting gut barrier dysfunction and reducing fungal translocation are emerging strategies for the prevention and treatment of HIV-associated inflammation and may prove useful in other inflammatory chronic diseases.

Keywords: fungi, inflammation, HIV, beta-D-glucan [BDG], immune activation

OPEN ACCESS

Edited by:
Caroline Petitdemange, Institut Pasteur, France

Reviewed by:
Giulia Carla Marchetti, University of Milan, Italy
Kehmia Titanji, Emory University, United States

***Correspondence:**
Jean-Pierre Routy
jean-pierre.routy@mcgill.ca

Specialty section:
This article was submitted to Viral Immunology, a section of the journal Frontiers in Immunology

Received: *20 January 2021*
Accepted: *22 March 2021*
Published: *12 April 2021*

Citation:
Isnard S, Lin J, Bu S, Fombuena B, Royston L and Routy J-P (2021) Gut Leakage of Fungal-Related Products: Turning Up the Heat for HIV Infection. Front. Immunol. 12:656414. doi: 10.3389/fimmu.2021.656414

INTRODUCTION

Gut damage and increased gut permeability constitute hallmarks of both acute and chronic phases of HIV infection (1, 2). CD4+ T cells loss in the gut mucosa, including interleukin (IL)-17-producing T-helper cells (Th17), disturbs mucosal homeostasis and contributes to epithelial gut damage (3). HIV-associated loss of epithelial integrity induces the non-physiological passage of microbial by-products from the gut lumen into the systemic circulation, referred to as microbial translocation. Brenchley et al. first reported in 2006 that increased plasma levels of the Gram-negative bacterial cell wall antigen lipopolysaccharide (LPS) triggers systemic immune activation in both people living with HIV (PLWH) and SIV-infected rhesus macaques (2), and eventually contributes to disease progression in PLWH (4–8). Moreover, in macaque models, gut epithelium

damage precedes immune activation (9). Although antiretroviral therapy (ART) successfully controls HIV replication and prevents AIDS, the gut epithelium is not fully repaired in long-term ART-treated PLWH (4, 10, 11). As such, microbial translocation persists along with systemic immune activation in ART-treated PLWH (4, 12–15). This chronic inflammation in ART-treated PLWH likewise increases the risks of non-AIDS comorbidities such as cardiovascular and metabolic diseases, neurocognitive dysfunction and cancer (16). Therefore, understanding the link between epithelial gut damage and systemic immune activation in PLWH is crucial in both ART-naïve and ART-treated PLWH.

On the luminal side of the gut epithelium lives a complex microbiota. Different in almost every individual, the gut microbiota composition is well-controlled by both the microbiota itself and the host. Composed of bacteria, fungi, archaea, protozoa and viruses, the microbiota plays key physiological and immune roles through the metabolism of different nutrients, regulation of the immune system and control of pathogen invasion. Yet, microbiota composition studies predominantly focus on bacteria. As such, microbial translocation of bacterial products such as LPS is primarily studied alongside the subsequent immune response, quantified by host factor soluble CD14 (sCD14) produced by macrophages/monocytes in response to LPS stimulation, and LPS-binding protein (LBP) mostly produced by the liver in the presence of LPS.

Fungal mass constitutes the second player after bacterial mass in the composition of gut microbiota. Fungi are thus found in the gut of all healthy individuals and PLWH (17, 18), with *Saccharomyces cerevisiae*, *Malassezia restricta* and *Candida albicans* being the most often found in stools. As such, one can hypothesize that fungal product would also translocate into the circulation in the presence of a leaky gut. (1→3)-β- D-Glucan BDG is a major cell wall component of most fungi and is used as a clinical biomarker for diagnosing and managing invasive fungal infection (IFI). Although other cell wall molecules such as mannans and galactomannans are also common across fungi species colonizing humans, BDG is the only marker associated with fungal translocation in PLWH. Morris et al. first showed elevated plasma levels of BDG in PLWH in 2012 (19). Since then, several other groups including ours reported an association between BDG and epithelial gut damage, immune activation, inflammation, and risk of developing non-AIDS comorbidities (4, 15, 20–24). These findings suggest a significant role for BDG in chronic immune activation and the development of non-AIDS comorbidities in PLWH, although the mechanisms involved remain poorly understood.

The development of non-AIDS comorbidities despite long-term ART represents the main concern in care for PLWH (16, 25–27). As fungal translocation appears to play a key role in immune activation, understanding mechanisms behind this phenomenon could help in designing novel therapies aiming at improving the quality of life of ART-treated individuals. Herein, we delve into the literature regarding the contribution and mechanism by which fungal translocation induces systemic immune activation and non-AIDS comorbidities in PLWH.

EVIDENCE OF GUT LEAKAGE OF FUNGAL PRODUCTS IN ANIMAL MODELS

Fungi are peaceful colonizers of the skin but also lungs and genital tract of most mammals including humans. They're also naturally present in the gut microbiota in absence of invasive fungal infection (IFI) (28). However, fungal products that are found in the blood usually result either from IFI or from translocation of fungal products predominantly from the gut (17, 18, 29–31).

The gastrointestinal tract (GI) encompasses multifaceted physical and immunological barriers preventing translocation of microbes and their by-products, while allowing for the absorption of nutrients. The gut mucosa is protected by both physical and immune components: the mucus and epithelial tight junctions on the apical pole of intestinal cells form a physical barrier; patrolling leukocytes in the lamina propria constitute an immune barrier ensuring that any translocated pathogens are phagocytosed, cleared, and/or transferred to mesenteric lymph nodes.

Fungi in the gut microbiota are abundant in mammals and play key roles in the balance between bacteria and other communities, as well as immune development in mice (32, 33). Animal models of gut damage that are frequently used include oral treatment with Dextran sulfate sodium (DSS), which impairs the gut epithelium and creates an experimental colitis (34). Upon DSS treatment, fungal products were found in the systemic circulation in different mice models (35, 36). Moreover, translocated fungal products, including BDG, were shown to participate in inflammation (37).

These mouse models suggest that upon gut damage, microbial translocation of fungal products occurs and participates in inflammation induction. As fungi are also present in the gut microbiota of non-human primates, studies could be performed to confirm the origin of translocated fungal products in different pathologies (31, 38).

EVIDENCE OF GUT LEAKAGE OF BDG IN PEOPLE LIVING WITH HIV

Increased gut permeability is a hallmark of HIV infection and has been shown to increase microbial translocation and inflammation (2). Markers of gut damage, Zonulin and intestinal fatty acid binding protein (I-FABP), as well as the marker of gut permeability regenerating islet-derived protein 3-α (REG3α) were found at higher levels in PLWH (10, 39). Beside translocation of bacterial products, higher circulating levels of fungal products were also found in PLWH, suggesting microbial translocation of fungal products (reviewed in **Table 1**).

Morris et al. were the first to report elevated levels of fungal product BDG in the blood of PLWH, grouping together ART-treated and viremic untreated individuals (19). Clinically, higher circulating BDG levels were associated with absence of ART, higher viral load and lower CD4 T-cell count (19).

TABLE 1 | Main studies assessing the influence of fungal translocation in people living with HIV.

	Country	Sample size	Population	Study design	Main findings	Reference
2012	USA	132	CHI, mostly ART+	Cross sectional	Higher BDG values associated with inflammation, CD8 T-cell activation, and pulmonary abnormalities.	(19)
2015	USA	41	CHI ART+	Cross sectional	Blood BDG levels correlated with neopterin levels and tended to correlate with TNF-α levels.	(15)
2016	USA	11	Early infection, before and after ART	Cross sectional	Blood BDG and sCD14 levels were associated with lower colonization of *Lactobacilli* in stools.	(23)
2016	USA	21	CHI ART+	Cross sectional	Higher blood BDG levels were associated with neurocognitive dysfunction.	(22)
2018	USA	451	Before and after ART	Cross sectional	suPAR and BDG plasma levels after ART initiation were associated with increased risk of non-AIDS comorbidities.	(40)
2019	Canada	146	Early and chronic, ART naïve or ART+	Longitudinal Cross sectional	Plasma BDG levels were higher in chronically infected people than early infection, and were associated with inflammation and immune activation.	(4)
2019	USA	231	ART naïve before and after ART, comparison of TDF/FTC, ATV + DRV, or RAL	Longitudinal	BDG increased after ART initiation, in association with increase in body fat.	(20)
2019	USA	61	CHI ART+	Cross sectional	BDG levels in plasma were associated with neurocognitive function.	(21)
2019	USA	176	CHI ART+ and uninfected controls	Cross sectional	Lower levels of BDG in HIV+ participants compared to uninfected controls. BDG levels correlated with levels of inflammation markers in HIV+ participants. No difference in levels of anti-fungal antibodies were found.	(24)
2020	USA	14	CHI ART+, compared to people with liver cirrhosis and healthy controls	Longitudinal and cross sectional	Oral challenge with BDG rich food did not increase blood levels of BDG.	(41)
2020	Uganda	171	Children (2-10 years old) HIV+ ART+, and uninfected, HIV exposed or not	Cross sectional	Blood BDG levels were higher in HIV infected children. In children with a history of breastfeeding, BDG levels correlated with soluble TNF receptor levels.	(42)
2020	Uganda	101	Children (10-18 years old) HIV+ ART+, and uninfected, HIV exposed or not	Cross sectional	Blood BDG levels were higher in HIV infected children. BDG levels were associated with immune activation in monocytes and T-cells.	(43)
2020	Canada	11	CHI ART+	Longitudinal	24 hours follow-up of participant showed no significant variations of BDG levels in blood.	(44)
2021	The Netherlands	40	CHI ART^{+} and uninfected controls	Cross-sectional	A higher proportion of ART-treated PLWH had detectable BDG levels in blood, and those levels were associated with inflammatory markers.	(14)
2021	Canada	145	CHI ART+ and uninfected control	Cross-sectional	BDG levels were associated with subclinical coronary atherosclerosis plaque in PLWH but not uninfected controls.	(45)

CHI, chronic HIV infection; ART, antiretroviral therapy; TDF, tenofovir disoproxil fumarate; FTC, emtricitabine; ATV, atazanavir; DRV, darunavir; RAL, raltegravir.

Weiner et al. found lower levels of BDG in PLWH compared to uninfected controls, although high levels of BDG were also found in the control group (24). Interestingly, this study also showed no difference in levels of anti-*Saccharomyces* antibodies (ASCA) between both groups (IgG and IgA).

We previously compared plasma levels of distinct gut damage and microbial translocation markers in different groups of PLWH without IFI and showed that plasma levels of BDG were higher in PLWH compared to uninfected controls, while galactomannan levels were low and similar between both groups. We also found higher levels of BDG in chronically infected PLWH compared to those in the early phase of the infection (4). Surprisingly, BDG levels were not statistically lower in ART-treated PLWH compared to their ART-naïve counterpart. Moreover, those levels correlated with markers of gut damage I-FABP and gut permeability REG3α in PLWH and uninfected controls, in accordance with the hypothesis that fungal translocation originates from gut microbiota (4, 10). Also, BDG and LPS levels correlated, and both were hypothesized to originate from the gut. Moreover, after a 2-year follow-up, PLWH not taking ART had increased levels of blood BDG levels, while those treated during the early phase of the infection had stable BDG levels (4). Early ART initiation was also associated with lower BDG levels, suggesting that early ART decreases the magnitude of gut damage and prevents further BDG translocation. All in all, these results demonstrated that fungal BDG translocation occurs in PLWH and suggest that these molecules originate from the gut.

VALIDATING BDG AS A MARKER OF MICROBIAL TRANSLOCATION IN PLWH

Recent findings tend to validate BDG as a marker of microbial translocation. Indeed, BDG can be found in several types of food including oatmeal, mushrooms, and seaweed. One would expect that increased intake of food rich in BDG might lead to its

increased absorption. Therefore, Hoenigl et al. designed a clinical trial where people were fed with high-BDG food in a controlled environment (41). This study included participants with advanced HCV-associated liver cirrhosis as positive controls, as those patients have elevated microbial translocation levels (46–49). Other included participants constituted of PLWH with detectable viral loads, ART-suppressed PLWH, and HCV negative/HIV negative controls. Although BDG testing of the BDG-rich food confirmed an elevated concentration, no significant variation of plasma BDG levels were detected in any participants up to 8 hours after food intake. This study strengthened the hypothesis that translocated BDG is originating from fungal communities in the GI tract rather than from food intake.

In addition, we also demonstrated that BDG levels were stable throughout 24 hours in ART-treated PLWH, as opposed to LPS levels (44). Interestingly, LPS levels increased after lunch and dinner, and decreased during the night, while BDG levels were stable over 24 hours. Although we were not able to exclude a circadian regulation mechanism, we hypothesized that detoxification of LPS might explain its variation. Indeed, BDG levels were stable upon ART initiation in PLWH, when gut damage marker levels decreased, suggesting that translocated BDG is not detoxified as efficiently as LPS (11, 50).

CONSEQUENCES OF BDG TRANSLOCATION IN PLWH

Inflammation

Translocated products are recognized by the immune system as pathogen-associated molecular patterns (PAMPs) and induce inflammation. As such, several studies found associations between BDG and inflammation or immune-activation markers in PLWH.

Morris et al. found that participants with higher BDG levels had increased circulating levels of inflammatory cytokines IL-8 and tumor necrosis factor α (TNF-α), as well as higher levels of activated CD8 T-cells in ART-naïve and ART-treated PLWH (19).

Interestingly, in PLWH in the primary phase of the infection starting ART, circulating BDG, but not LPS, levels were inversely associated with gut colonization of *Lactobacilli*, which are associated with reduced colon inflammation (23). This association was demonstrated 12 weeks after ART initiation and tended to persist 12 weeks later.

In ART-treated PLWH, Hoenigl et al. found that BDG levels, although in the normal range (below 60 pg/mL), were associated with plasma levels of Neopterin, a marker of inflammation, and tended to correlate with plasma levels of pro-inflammatory cytokines IL-6 and IL-8 (15). However, no association between BDG levels and the marker of bacterial-related inflammation sCD14 could be observed.

Higher BDG levels have been associated with markers of disease progression: in ART-naïve PLWH, we found an association between viral load and BDG, but not LPS levels (4). Furthermore, in both ART-naïve and ART-treated PLWH, BDG levels were associated with lower CD4 count and lower CD4/CD8 ratio, indicating a link between BDG translocation and markers of disease progression.

BDG levels were also associated with pro-inflammatory cytokines IL-6, IL-8 and CXCL13 in blood, as well as the frequency of activated blood CD4 and CD8 cells (4, 51) (**Table 1**). Moreover, Weiner et al. showed that levels of BDG, but not ASCA, in PLWH correlated with inflammation markers such as IP-10, IL-6, markers of monocyte/macrophage activation sCD14 and sCD163 and percentage of activated CD4 and CD8 T-cells (24).

In Ugandan ART-treated children, BDG levels were also elevated compared to HIV-exposed or unexposed children (42, 43). Also, BDG levels were associated with levels of the soluble TNF-receptor, another marker of inflammation (42).

Van der Heijden reported that PLWH with higher levels of BDG exhibited higher plasma levels of the inflammatory marker IL-1β, as well as higher response of monocytes to imiquimod or *Mycobacterium tuberculosis* stimulations (14).

Altogether, these findings indicate that fungal translocation of BDG is associated with inflammation, in both ART-naïve and ART-treated individuals, possibly participating in disease progression.

Non-AIDS Comorbidities

Persisting inflammation, even in ART-treated PLWH, is associated with increased risk of developing non-AIDS comorbidities including cardiovascular and metabolic diseases, and neurocognitive dysfunction. As translocation of fungal products has been associated with inflammation, the link between BDG and those comorbidities was investigated in several studies.

In 2018, Hoenigl et al. performed a cross sectional analysis of 451 PLWH, followed up to 11 years after ART initiation, and looked at the frequency of non-AIDS comorbidities, including myocardial infarction or stroke, non-AIDS malignancy or serious bacterial infection, or death from a non-AIDS related event. Among other markers of inflammations, only blood levels of soluble urokinase plasminogen activator receptor (suPAR), a marker of T-cell and monocyte activation, as well as BDG, were associated with non-AIDS comorbidity occurrence (40). Interestingly, only post-ART and pre-comorbidity BDG levels were associated with development of those comorbidities, independently of CD4 count but not smoking status pre-event.

Morris et al. found that PLWH with higher BDG levels had higher frequency of cardiopulmonary abnormalities including reduced diffusing capacity for carbon monoxide, higher pulmonary artery systolic pressure and increased tricuspid regurgitant jet velocity (19).

We also showed an association between plasma BDG levels and subclinical coronary atherosclerosis plaque in ART-treated PLWH but not uninfected controls, independently of age sex and other typical factors. Interestingly, we found that BDG levels were more strongly associated with plaque prevalence than age, smoking habits, hypertension, statin use or obesity (45).

Moreover, a study assessing metabolic and weight changes showed that after ART-initiation, blood BDG levels increased

two years after ART initiation, and were associated with larger trunk and total body fat accumulation (20).

Several studies have shown a link between BDG levels and cognitive functions in PLWH. Plasma BDG levels were associated with Global Deficit Score in ART-treated PLWH (22). Interestingly, this study showed that the 2 participants (out of 21) who had the worst deficit were also the only ones with elevated BDG levels in cerebrospinal fluid. Also, although IL-8 levels in plasma were associated with the deficit score, no correlation between BDG levels and IL-8 levels was observed in this study (22). The same team expanded such findings in 61 ART-treated PLWH and found that suPAR and BDG plasmatic levels were associated with the Global Deficit Score, independently of CD4 T-cell count (21) **(Table 1).**

Although BDG appears as a new marker of non-AIDS comorbidities, current observations rely on associations only. More studies are thus needed to puzzle out the mechanism linking fungal translocation and comorbidities.

DETECTION OF FUNGAL PRODUCTS IN PLWH—INSIGHTS ON MECHANISMS

Fungal PAMPs induce inflammation following their detection by pattern recognition receptor (PRRs) expressed on different cell types. Fungal PRRs include C-type lectin receptors such as Dectin-1, Toll-like receptor 2, integrins, scavenger receptors, and hyaluronic acid receptors (52). The receptor ephrin type-A receptor 2 (EphA2) has also been shown to mediate detection of fungal BDG in the mouth and upper GI, inducing protective innate immunity (53). EphA2 is also expressed at lower levels throughout the gut. Whether this receptor is implicated in fungal product induction of inflammation in PLWH has not been elucidated yet.

Effect on Antigen Presenting Cells and Neutrophils

Antigen presenting cells (APCs) are specialized in the detection of pathogens through conserved PAMPs, allowing the development of appropriate immune responses. APC include dendritic cells, macrophages/monocytes, and B cells, and are highly abundant in tissue, notably in the gut.

APCs can sense fungi through different receptors including Dectin-1, Toll-like receptor 2 (TLR2) and Complement receptor 3 (CR3) (**Figure 1**).

Dectin-1 is the main receptor interacting with BDG on macrophages, monocytes, dendritic cells, B-cells, and neutrophils (54–57). Expressed at the cell surface, Dectin-1 recognizes circulating or membrane-bound BDG, activating the NF-κB pathway through activation of the CARD9/BCL10/MALT1 complex.

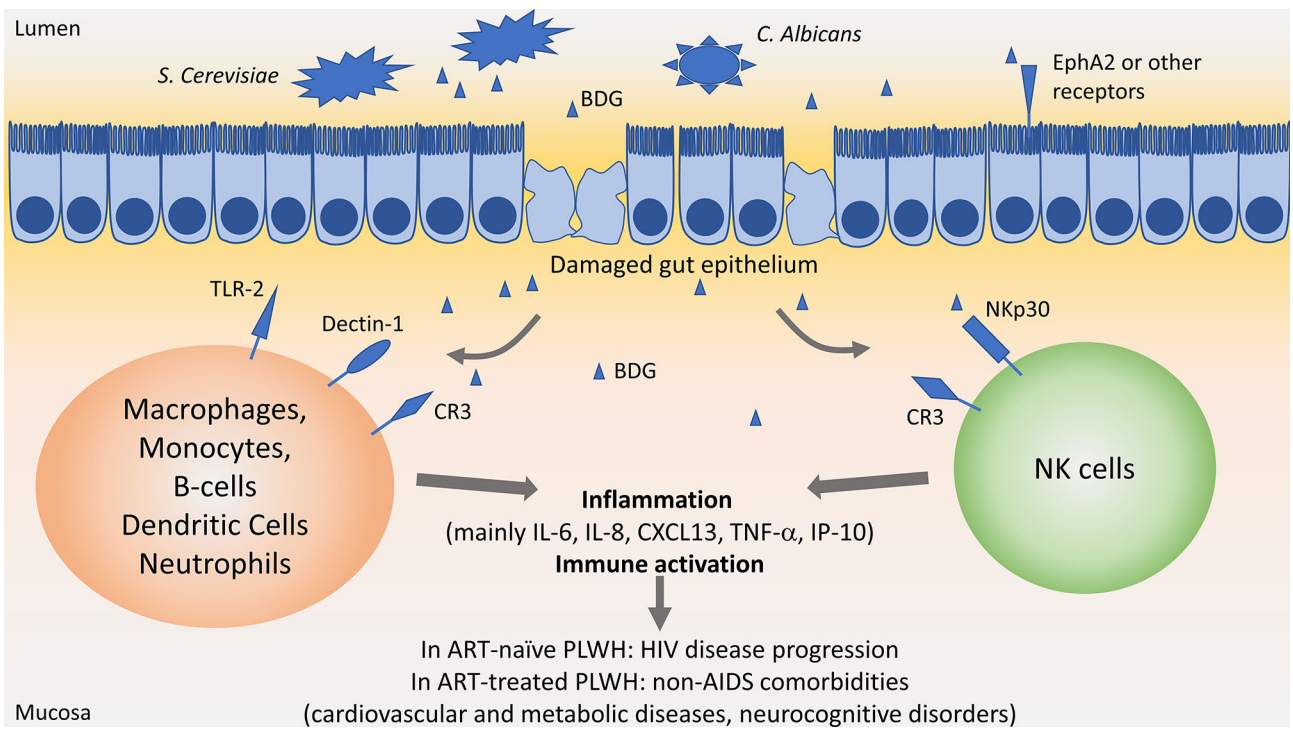

FIGURE 1 | Influence of β-D-Glucan in people living with HIV. In the gut lumen, *Saccharomyces Cerevisiae* and *Candida albicans* are largely present in the microbiota. Upon HIV-associated epithelial gut damage, fungal products such as β-D-Glucan (BDG) translocate in the mucosa. BDG is recognized by immune cells through Toll-like receptor 2 (TLR-2), Dectin-1, complement receptor 3 (CR3) or NKp30, activating immune cells and inducing inflammation. Persisting inflammation has been associated with disease progression in people living with HIV (PLWH) not taking antiretroviral therapy (ART), and with increased risk of non-AIDS comorbidities in ART-treated PLWH.

TLR2 is expressed on Dendritic cells, macrophages, and monocytes, and also activates the NF-κB pathway through activation of MyD88 upon recognition of soluble or particulate BDG.

Both stimulation of Dectin-1 and TLR2 on macrophages and monocyte induce the secretion of pro-inflammatory cytokines such as IL-6, IL-8, TNF-α, as well as anti-inflammatory mediator IL-10 (55) (**Figure 1**). It is worth noting that stimulation of monocytes with BDG induced internalization of Dectin-1 and decreased its surface expression as soon as 30 min after stimulation (54, 55). Size of BDG molecules play a key role in the induction of inflammatory responses, with larger-sized BDG inducing higher IL-1β, IL-6 and IL-23 secretion compared to smaller-sized BDG. However, secretion of chemokines involved in recruitment and maturation of T-cells was not affected by BDG size (58).

CR3 can also trigger BDG recognition on macrophages, monocytes, and neutrophils. However, neutrophils recognize BDG through CR3 only after opsonization with complement (59).

In vitro or animal models indicated that APC and neutrophils secrete inflammatory cytokines when stimulated by BDG, however the indication of such direct effect in PLWH is still lacking. As an initial foray, we found that circulating levels of BDG, but not LPS, inversely correlated with Dectin-1 expression on monocytes in PLWH (4), suggesting a direct interaction between BDG and its receptor Dectin-1 on monocytes. To validate this mechanism, we stimulated PBMC *in vitro* with *Saccharomyces Cerevisiae*-extracted BDG and found decreased Dectin-1 expression on monocytes at 24 and 48 hours. LPS did not induce such variation [personal communication (60)]. Moreover, stimulation of monocytes and macrophages with BDG was shown to primarily induce IL-1β and IL-8, which correlated with BDG levels in plasma samples in PLWH.

Detection by NK Cells

NK cells are a key player of innate immunity responsible for eliminating infected cells, cancer cells, as well as fungi. The main fungal receptor on NK cells is NKp30, also called Natural cytotoxicity triggering receptor 3 (NCR3). Recent work has shown that NKp30 recognizes membrane bound BDG, allowing elimination of fungal cells. NKp30 is required for elimination of *Cryptococcus* in a mouse model (61, 62). As such, NKp30 is the PRR responsible for direct recognition of fungus and BDG by NK cells. Unexpectedly, soluble BDG also binds to NKp30, activating NK cells and allowing the secretion of cytotoxic molecules Perforins and Granzymes (61, 62). Addition of BDG to NK increased *Candida*-killing activity. Earlier, this group showed that NKp30 surface expression is reduced on NK cells from ART-treated PLWH (62). We later confirmed those results in both ART-naïve and ART-treated chronically infected PLWH and also found that surface NKp30 expression was negatively correlated with circulating BDG but not LPS levels (4). *In vitro*, stimulation with *S. Cerevisiae*-extracted BDG but not with LPS decreased NKp30 expression at 24 and 48h (60), confirming the direct role of BDG in reducing NKp30 expression. Reduced NKp30 expression was associated with lower cytotoxic function against fungi and cancer cells (61–63).

Altogether, these findings indicate that BDG has a direct stimulating role of NK cells, including in PLWH on ART. This could lead to inflammation and decreased efficiency in infection or cancer suppression, leading to increased non-AIDS comorbidities.

BDG and Trained Immunity in HIV

Recent findings have put fungal products under the spotlight as they robustly induce trained immunity. This type of innate immune memory has been shown to be induced by β-glucans (including BDG) and BCG vaccines (64, 65). Trained immunity is defined as the process by which a stimulation programs a cell to respond with greater efficiency to a second stimulation after returning to steady state following the first stimulation. Trained immunity is functionally different from priming and differentiation and opposed to tolerance (64). In animal and human models, BDG has been shown to activate immune cells, especially monocytes, and induce epigenetic changes allowing those cells to respond with greater intensity to a second stimulation. Trained immunity is not antigen restricted as it potentiates the response to subsequent stimuli differently from the first antigen encounter and has been shown to act throughout the body *via* modulation of hematopoiesis and cell trafficking.

Whether translocated BDG plays a role in inducing trained immunity in PLWH is still unknown. In 2020, Van Der Heijden identified a link between circulating BDG levels and a trained immunity phenotype in ART-treated PLWH (14). Whether this phenotype is induced by trained immunity or priming of monocytes will have to be elucidated in further studies.

However, several indications lead to the hypothesis that this trained immunity is unlikely in PLWH. The first clue concerns the dynamics: most models of trained immunity require the removal of the initial stimulus to potentiate a second response, while BDG persists chronically even at low levels in PLWH. The second clue relies on the complexity of microbial translocation in PLWH: BDG translocation is accompanied by other microbial products such as LPS, inducing various inflammatory signals, while trained immunity has been shown to mostly rely on single instances of antigenic stimulation with β-glucans or BCG. The last hint is clinically relevant: glucan-induced trained immunity has been shown to increase protective responses to diverse infections and cancer, while PLWH have increased risks of both infection and cancer. However, trained immunity could also participate in sustained chronic inflammation such as in atherosclerosis, notably through the recognition of oxidized low-density lipoprotein particles (66). Indeed, BDG levels have been linked with cardiovascular disease in PLWH (19, 40, 45).

Hence, and due to the difficulty in deciphering priming from trained immunity, the influence of microbial translocation of BDG on trained immunity in PLWH should be assessed in future studies.

TARGETING FUNGAL TRANSLOCATION IN PLWH

We and others have shown that starting ART as early as possible appears to stabilize BDG levels, in accordance with current

guidelines recommending ART initiation as soon as the diagnostic is confirmed (4, 20). Therefore, as fungal translocation has been associated with inflammation and non-AIDS comorbidities in ART-treated PLWH, strategies targeting fungal translocation are needed.

Treatment with the antifungal agent fluconazole in ART-treated PLWH with neurocognitive disorders barely changed levels of markers of inflammation IL-1α, IL-6, IL-8 and IP-10 (67). However, levels of fungal products translocation have not been assessed in this study, rendering it difficult to draw conclusions on the effect of anti-fungal treatment on fungal microbial translocation.

Specific strategies have not been developed to prevent microbial translocation of fungal products in ART-treated PLWH. Fecal microbiota transplantation (FMT) could influence the mass of the mycobiome and allow improvement of gut epithelium integrity, reducing fungal translocation (68). Although several pilot trials of FMT have been initiated in PLWH, few have studied fungal translocation before and after treatment. In 2020, a study by Utay et al. consisting in six weekly FMT rounds in six ART-treated PLWH reported neither significant variations of circulating BDG levels, nor changes in inflammation and gut permeability markers I-FABP (69).

However, BDG levels have been used as markers of translocation in several other clinical trials:

In one study, metformin was expected to decrease inflammation in ART-treated PLWH (70, 71). Pilot results showed that 3 months of metformin treatment in addition to ART slightly decreased the marker of inflammation sCD14, but did not decrease LPS nor BDG translocation (72).

In a randomized placebo-controlled double-blind study, dipyridamole treatment was shown to increase extracellular adenosine levels and decrease CD8 T-cell activation in ART-treated PLWH (73). However, this treatment did not modify BDG levels in either group (74).

CONCLUSION

Translocation of fungal products, mainly inferred from BDG levels in the blood, has been shown to be associated with inflammation and comorbidities in PLWH. Whether BDG contributes directly to inflammation remains unknown, although assessment of BDG-receptors in PLWH pledges in this favor. Further studies are required to examine the role of fungal translocation in PLWH, especially those receiving ART. Overall, BDG appears as a robust biomarker of microbial translocation linked with inflammation and non-AIDS comorbidities in PLWH. Targeted strategies are critically needed to reduce the contribution of fungal translation to inflammation in PLWH, and eventually improve the quality of life of this population.

AUTHOR CONTRIBUTIONS

SI wrote the first draft, constructed the figure and table, and made revisions to the final draft of the manuscript. JL, SB, BF, and LR participated in the discussion and critically read and edited the manuscript. J-PR designed the review and critically revised the manuscript. All authors contributed to the article and approved the submitted version.

FUNDING

This work was funded by the Canadian Institutes of Health Research (CIHR; grants MOP 103230 and PTJ 166049), the Vaccines & Immunotherapy Core of the CIHR Canadian HIV Trials Network (CTN, grant CTN 257, CTN PT032, and CTNPT038), the CIHR-funded Canadian HIV Cure Enterprise (CanCURE) Team Grant HB2-164064 and réseau Fonds de la recherche-Santé (FRQ-S) SIDA Maladies infectieuses and thérapies cellulaires. SI is a post-doctoral fellow supported by the FRQ-S and CIHR-CTN. BF is supported by a William Turner award from the McGill University Health Centre. LR is a post-doctoral fellow supported by the "Fonds de perfectionnement" of the Geneva University Hospitals, Switzerland. J-PR is the holder of the Louis Lowenstein Chair in Hematology and Oncology, McGill University.

ACKNOWLEDGMENTS

We are highly grateful to Angie Massicotte, Josée Girouard, and Cezar Iovi for coordination and assistance. The authors would like to thank study participants for their time and contribution.

REFERENCES

1. Brenchley JM, Douek DC. Microbial translocation across the GI tract. *Annu Rev Immunol* (2012) 30:149–73. doi: 10.1146/annurev-immunol-020711-075001
2. Brenchley JM, Price DA, Schacker TW, Asher TE, Silvestri G, Rao S, et al. Microbial translocation is a cause of systemic immune activation in chronic HIV infection. *Nat Med* (2006) 12:1365–71. doi: 10.1038/nm1511
3. Ghosn J, Taiwo B, Seedat S, Autran B, Katlama C. Hiv. *Lancet* (2018) 392:685–97. doi: 10.1016/s0140-6736(18)31311-4
4. Mehraj V, Ramendra R, Isnard S, Dupuy FP, Ponte R, Chen J, et al. Circulating (1–>3)-beta-D-Glucan is associated with immune activation during HIV infection. *Clin Infect Dis* (2019) 70:232–41. doi: 10.1093/cid/ciz212
5. Tudesq JJ, Dunyach-Remy C, Combescure C, Doncesco R, Laureillard D, Lavigne JP, et al. Microbial translocation is correlated with HIV evolution in HIV-HCV co-infected patients. *PloS One* (2017) 12:e0183372. doi: 10.1371/journal.pone.0183372
6. Epeldegui M, Magpantay L, Guo Y, Halec G, Cumberland WG, Yen PK, et al. A prospective study of serum microbial translocation biomarkers and risk of AIDS-related non-Hodgkin lymphoma. *AIDS* (2018) 32:945–54. doi: 10.1097/QAD.0000000000001771
7. Marchetti G, Cozzi-Lepri A, Merlini E, Bellistri GM, Castagna A, Galli M, et al. Microbial translocation predicts disease progression of HIV-infected antiretroviral-naive patients with high CD4+ cell count. *AIDS* (2011) 25:1385–94. doi: 10.1097/QAD.0b013e3283471d10
8. Marchetti G, Tincati C, Silvestri G. Microbial translocation in the pathogenesis of HIV infection and AIDS. *Clin Microbiol Rev* (2013) 26:2–18. doi: 10.1128/CMR.00050-12
9. Hensley-McBain T, Berard AR, Manuzak JA, Miller CJ, Zevin AS, Polacino P, et al. Intestinal damage precedes mucosal immune dysfunction in SIV

infection. *Mucosal Immunol* (2018) 11:1429–40. doi: 10.1038/s41385–018-0032-5.
10. Isnard S, Ramendra R, Dupuy FP, Lin J, Fombuena B, Kokinov N, et al. Plasma levels of C-type lectin REG3alpha and gut damage in people with HIV. *J Infect Dis* (2019) 221:110–21. doi: 10.1093/infdis/jiz423
11. Ramendra R, Isnard S, Mehraj V, Chen J, Zhang Y, Finkelman M, et al. Circulating LPS and (1–>3)-beta-D-Glucan: A Folie a Deux Contributing to HIV-Associated Immune Activation. *Front Immunol* (2019) 10:465. doi: 10.3389/fimmu.2019.00465
12. Ramendra R, Isnard S, Lin J, Fombuena B, Ouyang J, Merhaj V, et al. CMV seropositivity is associated with increased microbial translocation in people living with HIV and uninfected controls. *Clin Infect Dis* (2019) 71:1438–46. doi: 10.1093/cid/ciz1001
13. Cassol E, Misra V, Holman A, Kamat A, Morgello S, Gabuzda D. Plasma metabolomics identifies lipid abnormalities linked to markers of inflammation, microbial translocation, and hepatic function in HIV patients receiving protease inhibitors. *BMC Infect Dis* (2013) 13:203. doi: 10.1186/1471-2334-13-203
14. van der Heijden WA, van de Wijer L, Keramati F, Trypsteen W, Rutsaert S, Ter Horst R, et al. Chronic HIV infection induces transcriptional and functional reprogramming of innate immune cells. *JCI Insight* (2021). doi: 10.1172/jci.insight.145928
15. Hoenigl M, de Oliveira MF, Perez-Santiago J, Zhang Y, Woods SP, Finkelman M, et al. Correlation of (1–>3)-beta-D-glucan with other inflammation markers in chronically HIV infected persons on suppressive antiretroviral therapy. *GMS Infect Dis* (2015) 3. doi: 10.3205/id000018
16. Hsu DC, Sereti I. Serious Non-AIDS Events: Therapeutic Targets of Immune Activation and Chronic Inflammation in HIV Infection. *Drugs* (2016) 76:533–49. doi: 10.1007/s40265-016-0546-7
17. Hager CL, Ghannoum MA. The mycobiome in HIV. *Curr Opin HIV AIDS* (2018) 13:69–72. doi: 10.1097/COH.0000000000000432
18. Nash AK, Auchtung TA, Wong MC, Smith DP, Gesell JR, Ross MC, et al. The gut mycobiome of the Human Microbiome Project healthy cohort. *Microbiome* (2017) 5:153. doi: 10.1186/s40168-017-0373-4
19. Morris A, Hillenbrand M, Finkelman M, George MP, Singh V, Kessinger C, et al. Serum (1–>3)-beta-D-glucan levels in HIV-infected individuals are associated with immunosuppression, inflammation, and cardiopulmonary function. *J Acquir Immune Defic Syndr* (2012) 61:462–8. doi: 10.1097/QAI.0b013e318271799b
20. Dirajlal-Fargo S, Moser C, Rodriguez K, El-Kamari V, Funderburg NT, Bowman E, et al. Changes in the Fungal Marker β-D-Glucan After Antiretroviral Therapy and Association With Adiposity. *Open Forum Infect Dis* (2019) 6. doi: 10.1093/ofid/ofz434
21. Gianella S, Letendre SL, Iudicello J, Franklin D, Gaufin T, Zhang Y, et al. Plasma (1 –> 3)-beta-D-glucan and suPAR levels correlate with neurocognitive performance in people living with HIV on antiretroviral therapy: a CHARTER analysis. *J Neurovirol* (2019) 25:837–43. doi: 10.1007/s13365-019-00775-6
22. Hoenigl M, de Oliveira MF, Perez-Santiago J, Zhang Y, Morris S, McCutchan AJ, et al. (1–>3)-beta-D-Glucan Levels Correlate With Neurocognitive Functioning in HIV-Infected Persons on Suppressive Antiretroviral Therapy: A Cohort Study. *Med (Baltimore)* (2016) 95:e3162. doi: 10.1097/MD.0000000000003162
23. Hoenigl M, Perez-Santiago J, Nakazawa M, de Oliveira MF, Zhang Y, Finkelman MA, et al. (1–>3)-beta-d-Glucan: A Biomarker for Microbial Translocation in Individuals with Acute or Early HIV Infection? *Front Immunol* (2016) 7:404. doi: 10.3389/fimmu.2016.00404
24. Weiner L, Retuerto M, Hager C, El Kamari V, Shan L, Sattar A, et al. Fungal Translocation is Associated with Immune Activation and Systemic Inflammation in Treated HIV. *AIDS Res Hum Retroviruses* (2019) 25:461–72. doi: 10.1089/AID.2018.0252
25. Alzahrani J, Hussain T, Simar D, Palchaudhuri R, Abdel-Mohsen M, Crowe SM, et al. Inflammatory and immunometabolic consequences of gut dysfunction in HIV: Parallels with IBD and implications for reservoir persistence and non-AIDS comorbidities. *EBioMedicine* (2019) 46:522–31. doi: 10.1016/j.ebiom.2019.07.027
26. Bonnet F, Le Marec F, Leleux O, Gerard Y, Neau D, Lazaro E, et al. Evolution of comorbidities in people living with HIV between 2004 and 2014: cross-sectional analyses from ANRS CO3 Aquitaine cohort. *BMC Infect Dis* (2020) 20:850. doi: 10.1186/s12879-020-05593-4
27. Nanditha NGA, Paiero A, Tafessu HM, St-Jean M, McLinden T, Justice AC, et al. Excess burden of age-associated comorbidities among people living with HIV in British Columbia, Canada: a population-based cohort study. *BMJ Open* (2021) 11:e041734. doi: 10.1136/bmjopen-2020-041734
28. Hallen-Adams HE, Suhr MJ. Fungi in the healthy human gastrointestinal tract. *Virulence* (2017) 8:352–8. doi: 10.1080/21505594.2016.1247140
29. Findley K, Oh J, Yang J, Conlan S, Deming C, Meyer JA, et al. Topographic diversity of fungal and bacterial communities in human skin. *Nature* (2013) 498:367–70. doi: 10.1038/nature12171
30. Hamm PS, Taylor JW, Cook JA, Natvig DO. Decades-old studies of fungi associated with mammalian lungs and modern DNA sequencing approaches help define the nature of the lung mycobiome. *PloS Pathog* (2020) 16: e1008684. doi: 10.1371/journal.ppat.1008684
31. Lai GC, Tan TG, Pavelka N. The mammalian mycobiome: A complex system in a dynamic relationship with the host. *Wiley Interdiscip Rev Syst Biol Med* (2019) 11:e1438. doi: 10.1002/wsbm.1438
32. van Tilburg Bernardes E, Pettersen VK, Gutierrez MW, Laforest-Lapointe I, Jendzjowsky NG, Cavin JB, et al. Intestinal fungi are causally implicated in microbiome assembly and immune development in mice. *Nat Commun* (2020) 11:2577. doi: 10.1038/s41467-020-16431-1
33. Scupham AJ, Presley LL, Wei B, Bent E, Griffith N, McPherson M, et al. Abundant and Diverse Fungal Microbiota in the Murine Intestine. *Appl Environ Microbiol* (2006) 72:793–801. doi: 10.1128/aem.72.1.793-801.2006
34. Wang T, Fan C, Yao A, Xu X, Zheng G, You Y, et al. The Adaptor Protein CARD9 Protects against Colon Cancer by Restricting Mycobiota-Mediated Expansion of Myeloid-Derived Suppressor Cells. *Immunity* (2018) 49:504–514 e4. doi: 10.1016/j.immuni.2018.08.018
35. Issara-Amphorn J, Surawut S, Worasilchai N, Thim-Uam A, Finkelman M, Chindamporn A, et al. The Synergy of Endotoxin and (1–>3)-beta-D-Glucan, from Gut Translocation, Worsens Sepsis Severity in a Lupus Model of Fc Gamma Receptor IIb-Deficient Mice. *J Innate Immun* (2018) 10:189–201. doi: 10.1159/000486321
36. Leelahavanichkul A, Worasilchai N, Wannalerdsakun S, Jutivorakool K, Somparn P, Issara-Amphorn J, et al. Gastrointestinal Leakage Detected by Serum (1–>3)-beta-D-Glucan in Mouse Models and a Pilot Study in Patients with Sepsis. *Shock* (2016) 46:506–18. doi: 10.1097/SHK.0000000000000645
37. Panpetch W, Somboonna N, Bulan DE, Issara-Amphorn J, Finkelman M, Worasilchai N, et al. Oral administration of live- or heat-killed Candida albicans worsened cecal ligation and puncture sepsis in a murine model possibly due to an increased serum (1–>3)-beta-D-glucan. *PloS One* (2017) 12: e0181439. doi: 10.1371/journal.pone.0181439
38. Mann AE, Mazel F, Lemay MA, Morien E, Billy V, Kowalewski M, et al. Biodiversity of protists and nematodes in the wild nonhuman primate gut. *ISME J* (2020) 14:609–22. doi: 10.1038/s41396-019-0551-4
39. Cheru LT, Park EA, Saylor CF, Burdo TH, Fitch KV, Looby S, et al. I-FABP Is Higher in People With Chronic HIV Than Elite Controllers, Related to Sugar and Fatty Acid Intake and Inversely Related to Body Fat in People With HIV. *Open Forum Infect Dis* (2018) 5:ofy288. doi: 10.1093/ofid/ofy288
40. Hoenigl M, Moser C, Funderburg N, Bosch R, Kantor A, Zhang Y, et al. Soluble Urokinase Plasminogen Activator Receptor (suPAR) is predictive of Non-AIDS Events during Antiretroviral Therapy-mediated Viral Suppression. *Clin Infect Dis* (2018) 69:676–86. doi: 10.1093/cid/ciy966
41. Hoenigl M, Lin J, Finkelman M, Zhang Y, Karris MY, Letendre S, et al. Glucan rich nutrition does not increase gut translocation of Beta glucan. *Mycoses* (2020) 64:24–9. doi: 10.1111/myc.13161
42. Dirajlal-Fargo S, El-Kamari V, Weiner L, Shan L, Sattar A, Kulkarni M, et al. Altered Intestinal Permeability and Fungal Translocation in Ugandan Children With Human Immunodeficiency Virus. *Clin Infect Dis* (2020) 70:2413–22. doi: 10.1093/cid/ciz561
43. Dirajlal-Fargo S, Albar Z, Bowman E, Labbato D, Sattar A, Karungi C, et al. Increased monocyte and T-cell activation in treated HIV+ Ugandan children: associations with gut alteration and HIV factors. *AIDS* (2020) 34:1009–18. doi: 10.1097/QAD.0000000000002505
44. Ouyang J, Isnard S, Lin J, Fombuena B, Chatterjee D, Wiche Salinas TR, et al. Daily variations of gut microbial translocation markers in ART-treated HIV-infected people. *AIDS Res Ther* (2020) 17:15. doi: 10.1186/s12981-020-00273-4

45. Isnard S, Fombuena B, Sadouni M, Lin J, Richard C, Routy B, et al. Circulating β-D-Glucan as a marker of subclinical coronary plaque in ART-treated people living with HIV. *Open Forum Infect Dis* (2021). doi: 10.1093/ofid/ofab109
46. Moon MS, Quinn G, Townsend EC, Ali RO, Zhang GY, Bradshaw A, et al. Bacterial Translocation and Host Immune Activation in Chronic Hepatitis C Infection. *Open Forum Infect Dis* (2019) 6. doi: 10.1093/ofid/ofz255
47. Balagopal A, Philp FH, Astemborski J, Block TM, Mehta A, Long R, et al. Human immunodeficiency virus-related microbial translocation and progression of hepatitis C. *Gastroenterology* (2008) 135:226–33. doi: 10.1053/j.gastro.2008.03.022
48. Marchetti G, Nasta P, Bai F, Gatti F, Bellistri GM, Tincati C, et al. Circulating sCD14 is associated with virological response to pegylated-interferon-alpha/ribavirin treatment in HIV/HCV co-infected patients. *PloS One* (2012) 7: e32028. doi: 10.1371/journal.pone.0032028
49. Peters L, Neuhaus J, Duprez D, Neaton JD, Tracy R, Klein MB, et al. Biomarkers of inflammation, coagulation and microbial translocation in HIV/HCV co-infected patients in the SMART study. *J Clin Virol* (2014) 60:295–300. doi: 10.1016/j.jcv.2014.03.017
50. Finkelman MA. Specificity Influences in (1–>3)-beta-d-Glucan-Supported Diagnosis of Invasive Fungal Disease. *J Fungi (Basel)* (2020) 7. doi: 10.3390/jof7010014
51. Mehraj V, Ramendra R, Isnard S, Dupuy FP, Lebouche B, Costiniuk C, et al. CXCL13 as a Biomarker of Immune Activation During Early and Chronic HIV Infection. *Front Immunol* (2019) 10:289. doi: 10.3389/fimmu.2019.00289
52. Patin EC, Thompson A, Orr SJ. Pattern recognition receptors in fungal immunity. *Semin Cell Dev Biol* (2019) 89:24–33. doi: 10.1016/j.semcdb.2018.03.003
53. Swidergall M, Solis NV, Lionakis MS, Filler SG. EphA2 is an epithelial cell pattern recognition receptor for fungal beta-glucans. *Nat Microbiol* (2018) 3:53–61. doi: 10.1038/s41564-017-0059-5
54. Brown GD, Taylor PR, Reid DM, Willment JA, Williams DL, Martinez-Pomares L, et al. Dectin-1 Is A Major β-Glucan Receptor On Macrophages. *J Exp Med* (2002) 196:407–12. doi: 10.1084/jem.20020470
55. Bonfim CV, Mamoni RL, Blotta MH. TLR-2, TLR-4 and dectin-1 expression in human monocytes and neutrophils stimulated by Paracoccidioides brasiliensis. *Med Mycol* (2009) 47:722–33. doi: 10.3109/13693780802641425
56. Taylor PR, Brown GD, Reid DM, Willment JA, Martinez-Pomares L, Gordon S, et al. The -Glucan Receptor, Dectin-1, Is Predominantly Expressed on the Surface of Cells of the Monocyte/Macrophage and Neutrophil Lineages. *J Immunol* (2002) 169:3876–82. doi: 10.4049/jimmunol.169.7.3876
57. Ali MF, Driscoll CB, Walters PR, Limper AH, Carmona EM. beta-Glucan-Activated Human B Lymphocytes Participate in Innate Immune Responses by Releasing Proinflammatory Cytokines and Stimulating Neutrophil Chemotaxis. *J Immunol* (2015) 195:5318–26. doi: 10.4049/jimmunol.1500559
58. Elder MJ, Webster SJ, Chee R, Williams DL, Hill Gaston JS, Goodall JC. beta-Glucan Size Controls Dectin-1-Mediated Immune Responses in Human Dendritic Cells by Regulating IL-1beta Production. *Front Immunol* (2017) 8:791. doi: 10.3389/fimmu.2017.00791
59. McDonald JU, Rosas M, Brown GD, Jones SA, Taylor PR. Differential dependencies of monocytes and neutrophils on dectin-1, dectin-2 and complement for the recognition of fungal particles in inflammation. *PloS One* (2012) 7:e45781. doi: 10.1371/journal.pone.0045781
60. Isnard S, Ramendra R, Dupuy FP, Mehraj V, Ponte R, Chen J, et al. Circulating beta-D-Glucan and Induction of Immune activation. In: *CROI 2019 Poster 2109*. Conference on Retroviruses and Opportunistic infections 2019 (2019).
61. Li SS, Ogbomo H, Mansour MK, Xiang RF, Szabo L, Munro F, et al. Identification of the fungal ligand triggering cytotoxic PRR-mediated NK cell killing of Cryptococcus and Candida. *Nat Commun* (2018) 9:751. doi: 10.1038/s41467-018-03014-4
62. Li SS, Kyei SK, Timm-McCann M, Ogbomo H, Jones GJ, Shi M, et al. The NK receptor NKp30 mediates direct fungal recognition and killing and is diminished in NK cells from HIV-infected patients. *Cell Host Microbe* (2013) 14:387–97. doi: 10.1016/j.chom.2013.09.007
63. Han B, Mao FY, Zhao YL, Lv YP, Teng YS, Duan M, et al. Altered NKp30, NKp46, NKG2D, and DNAM-1 Expression on Circulating NK Cells Is Associated with Tumor Progression in Human Gastric Cancer. *J Immunol Res* (2018) 2018:6248590. doi: 10.1155/2018/6248590
64. Divangahi M, Aaby P, Khader SA, Barreiro LB, Bekkering S, Chavakis T, et al. Trained immunity, tolerance, priming and differentiation: distinct immunological processes. *Nat Immunol* (2020) 22:2–6. doi: 10.1038/s41590-020-00845-6
65. Netea MG, Dominguez-Andres J, Barreiro LB, Chavakis T, Divangahi M, Fuchs E, et al. Defining trained immunity and its role in health and disease. *Nat Rev Immunol* (2020) 20:375–88. doi: 10.1038/s41577-020-0285-6
66. Bekkering S, Quintin J, Joosten LA, van der Meer JW, Netea MG, Riksen NP. Oxidized low-density lipoprotein induces long-term proinflammatory cytokine production and foam cell formation via epigenetic reprogramming of monocytes. *Arterioscler Thromb Vasc Biol* (2014) 34:1731–8. doi: 10.1161/ATVBAHA.114.303887
67. Sacktor N, Skolasky RL, Moxley R, Wang S, Mielke MM, Munro C, et al. Paroxetine and fluconazole therapy for HIV-associated neurocognitive impairment: results from a double-blind, placebo-controlled trial. *J Neurovirol* (2018) 24:16–27. doi: 10.1007/s13365-017-0587-z
68. Ouyang J, Isnard S, Lin J, Fombuena B, Peng X, Nair Parvathy S, et al. Treating from the inside out: relevance of fecal microbiota transplantation to counteract gut damage in GVHD and HIV infection. *Front Med* (2020) 7:421. doi: 10.3389/fmed.2020.00421
69. Utay NS, Monczor AN, Somasunderam A, Lupo S, Jiang ZD, Alexander AS, et al. Evaluation of Six Weekly Oral Fecal Microbiota Transplants in People with HIV. *Pathog Immun* (2020) 5:364–81. doi: 10.20411/pai.v5i1.388
70. Routy JP, Isnard S, Mehraj V, Ostrowski M, Chomont N, Ancuta P, et al. Effect of metformin on the size of the HIV reservoir in non-diabetic ART-treated individuals: single-arm non-randomised Lilac pilot study protocol. *BMJ Open* (2019) 9:e028444. doi: 10.1136/bmjopen-2018-028444
71. Planas D, Pagliuzza A, Ponte R, Fert A, Marchand LR, Massanella M, et al. LILAC pilot study: Effects of metformin on mTOR activation and HIV reservoir persistence during antiretroviral therapy. *EBioMedicine* (2021) 65:103270. doi: 10.1016/j.ebiom.2021.103270
72. Isnard S, Lin J, Fombuena B, Ouyang J, Varin TV, Richard C, et al. Repurposing metformin in non-diabetic people living with HIV: Influence on weight and gut microbiota. *Open Forum Infect Dis* (2020). doi: 10.1093/ofid/ofaa338
73. Macatangay BJC, Jackson EK, Abebe KZ, Comer D, Cyktor J, Klamar-Blain C, et al. Placebo-Controlled, Pilot Clinical Trial of Dipyridamole to Decrease Human Immunodeficiency Virus-Associated Chronic Inflammation. *J Infect Dis* 221 (2020) 221:1598–606. doi: 10.1093/infdis/jiz344
74. Mallarino-Haeger C, Abebe KZ, Jackson EK, Zyhowski A, Klamar-Blain C, Cyktor JC, et al. Brief Report: Dipyridamole Decreases Gut Mucosal Regulatory T-Cell Frequencies Among People With HIV on Antiretroviral Therapy. *J Acquir Immune Defic Syndr* (2020) 85:665–9. doi: 10.1097/QAI.0000000000002488

Conflict of Interest: The authors declare that the research was conducted in the absence of any commercial or financial relationships that could be construed as a potential conflict of interest.

frontiers in Immunology

ORIGINAL RESEARCH
published: 31 May 2021
doi: 10.3389/fimmu.2021.688886

Preservation of Gastrointestinal Mucosal Barrier Function and Microbiome in Patients With Controlled HIV Infection

Gerald Mak[1†], John J. Zaunders[2†], Michelle Bailey[3], Nabila Seddiki[4], Geraint Rogers[5,6], Lex Leong[7], Tri Giang Phan[1,8], Anthony D. Kelleher[3], Kersten K. Koelsch[3], Mark A. Boyd[3,5,9] and Mark Danta[1,10]*

[1] St. Vincent's Clinical School, UNSW, Darlinghurst, NSW, Australia, [2] Centre for Applied Medical Research, St Vincent's Hospital, Sydney, NSW, Australia, [3] Kirby Institute, UNSW Sydney, Sydney, NSW, Australia, [4] IDMIT Department/IBFJ, Immunology of Viral Infections and Autoimmune Diseases (IMVA), INSERM U1184, CEA, Université Paris Sud, Paris, France, [5] South Australian Health and Medical Research Institute (SAHMRI), Adelaide, SA, Australia, [6] Faculty of Science, Flinders University, Adelaide, SA, Australia, [7] Microbiology and Infectious Diseases, South Australia (SA) Pathology, Adelaide, SA, Australia, [8] Immunology Division Garvan Institute of Medical Research, Sydney, NSW, Australia, [9] Faculty of Health and Medical Sciences, University of Adelaide, Adelaide, SA, Australia, [10] Department of Gastroenterology, St. Vincent's Hospital, Sydney, NSW, Australia

OPEN ACCESS

Edited by:
Remi Cheynier, U1016 Institut Cochin (INSERM), France

Reviewed by:
Jean-Pierre Routy, McGill University, Canada
Stephen Kent, The University of Melbourne, Australia

***Correspondence:**
Mark Danta
m.danta@unsw.edu.au

[†]These authors have contributed equally to this work

Specialty section:
This article was submitted to Viral Immunology, a section of the journal Frontiers in Immunology

Received: *31 March 2021*
Accepted: *04 May 2021*
Published: *31 May 2021*

Citation:
Mak G, Zaunders JJ, Bailey M, Seddiki N, Rogers G, Leong L, Phan TG, Kelleher AD, Koelsch KK, Boyd MA and Danta M (2021) Preservation of Gastrointestinal Mucosal Barrier Function and Microbiome in Patients With Controlled HIV Infection. Front. Immunol. 12:688886. doi: 10.3389/fimmu.2021.688886

Background: Despite successful ART in people living with HIV infection (PLHIV) they experience increased morbidity and mortality compared with HIV-negative controls. A dominant paradigm is that gut-associated lymphatic tissue (GALT) destruction at the time of primary HIV infection leads to loss of gut integrity, pathological microbial translocation across the compromised gastrointestinal barrier and, consequently, systemic inflammation. We aimed to identify and measure specific changes in the gastrointestinal barrier that might allow bacterial translocation, and their persistence despite initiation of antiretroviral therapy (ART).

Method: We conducted a cross-sectional study of the gastrointestinal (GIT) barrier in PLHIV and HIV-uninfected controls (HUC). The GIT barrier was assessed as follows: *in vivo* mucosal imaging using confocal endomicroscopy (CEM); the immunophenotype of GIT and circulating lymphocytes; the gut microbiome; and plasma inflammation markers Tumour Necrosis Factor-α (TNF-α) and Interleukin-6 (IL-6); and the microbial translocation marker sCD14.

Results: A cohort of PLHIV who initiated ART early, during primary HIV infection (PHI), n=5), and late (chronic HIV infection (CHI), n=7) infection were evaluated for the differential effects of the stage of ART initiation on the GIT barrier compared with HUC (n=6). We observed a significant decrease in the CD4 T-cell count of CHI patients in the left colon (p=0.03) and a trend to a decrease in the terminal ileum (p=0.13). We did not find evidence of increased epithelial permeability by CEM. No significant differences were found in microbial translocation or inflammatory markers in plasma. In gut biopsies, CD8 T-cells, including resident intraepithelial CD103+ cells, did not show any significant elevation of activation in PLHIV, compared to HUC. The majority of residual circulating activated

CD38+HLA-DR+ CD8 T-cells did not exhibit gut-homing integrins α4ß7, suggesting that they did not originate in GALT. A significant reduction in the evenness of species distribution in the microbiome of CHI subjects (p=0.016) was observed, with significantly higher relative abundance of the genus *Spirochaeta* in PHI subjects (p=0.042).

Conclusion: These data suggest that substantial, non-specific increases in epithelial permeability may not be the most important mechanism of HIV-associated immune activation in well-controlled HIV-positive patients on antiretroviral therapy. Changes in gut microbiota warrant further study.

Keywords: HIV, CD4, antiretroviral therapy (ART), gut-associated lymphoid tissues (GALT), microbiome

INTRODUCTION

Chronic HIV-1 infection is associated with persistent elevated systemic immune activation, including increases in levels of pro-inflammatory cytokines (1), lymph node germinal centre activity, immunoglobulin secretion by B-cells (2, 3) and activation and increased turnover of T-cells (4), particularly including target CCR5+ CD4 T-cells (5). A proposed cause for this is gut microbial translocation, which is the pathological translocation of luminal micro-organisms from the gastrointestinal tract (GIT) to the portal and systemic circulation as a consequence of depletion and impaired reconstitution of gut-associated lymphoid tissue (GALT) CD4 T-cells (6, 7).

Effects of HIV in the GIT include epithelial apoptosis (8, 9) and loss of epithelial barrier integrity (10, 11) with evidence of increased epithelial tight junction permeability (12, 13). Focal loss of CD4 T-cells in the mucosa (14–16) and dysregulation of T-cell subtypes (17–20) have also been implicated. Microbial translocation is believed to lead to systemic immune activation, seen as a correlation between plasma LPS levels and circulating activated CD38+HLA-DR+ CD8 T-cells (7). Furthermore, gut microbiome composition correlates with increased immune activation in HIV-infected individuals (21–23). The effect of antiretroviral therapy (ART) on the gut microbiome and mucosal and systemic lymphocytes suggests partial but not complete normalization of the dysbiosis resulting from HIV-1 infection (24). Therefore, there is a need to further study the relationship between enduring changes in the microbiome, the mucosal barrier and systemic immune responses during ART.

Studies to date directly assessing the functional integrity of the intestinal barrier in HIV-infected individuals have generally investigated impairment using immunohistochemical or transcriptional analysis of biopsies (8, 11–13). Conventional techniques such as mannitol and lactulose permeability measuring intestinal barrier function (25) have also been used to study HIV-1 infected subjects (8, 9).

Confocal endomicroscopy (CEM) shows promise for accurate, focal analysis of the intestinal barrier *in vivo*. CEM is a novel technique utilising a laser confocal endomicroscope integrated into a colonoscope, gathering images at 1000x magnification (26, 27). CEM has been successful in identifying gastrointestinal barrier changes in inflammatory bowel disease (28, 29), in which microbial translocation is thought to play a role (30). To the best of our knowledge, this technique has only been used once to study the gastrointestinal barrier of PLHIV. This was done in a set of mainly elite controllers, with evidence of permeability, but no quantitative comparison to HIV-uninfected controls (31).

Our study aimed to confirm and quantify the increased permeability of the gut mucosal barrier, as directly observed *in vivo* using CEM, compared to HIV-uninfected controls, and explore potential relationships between gut microbiome, mucosal immune function, intestinal barrier integrity and markers of immune activation in PLHIV who commenced ART during either primary or established chronic HIV infection. All parameters were compared to HIV-uninfected controls.

METHODS

Subjects

This cross-sectional pilot cohort study enrolled PLHIV who initiated ART during primary (PHI) and chronic (CHI) infection and had maintained virological control for >2 years, and a control group of HIV-uninfected controls (HUC). The HUC were matched for age and sex. PLHIV were considered treated in primary HIV infection (PHI) if ART was initiated within six months of HIV infection (HIV), and in chronic HIV infection (CHI) if treatment was initiated at least 12-months after HIV infection, as defined in the PINT study (32). Volunteers were excluded if they were unfit for colonoscopy, had a fluorescein allergy, or had specific inflammatory gastrointestinal conditions associated with colitis. This study was approved by the St Vincent's Human Research Ethics Committee (HREC 14/214). All participants provided written informed consent.

Confocal Endomicroscopy (CEM)

Colonoscopy with confocal endomicroscopy was conducted by a single colonoscopist using an Optiscan CIS-2 prototype confocal laser endomicroscope (Notting Hill, VIC, Australia). This device replaces one of two air/water channels of a conventional Olympus CF-H180AL endoscope (Tokyo, Japan) with a 488nm laser microscope. The endoscopic probe was applied perpendicular to the mucosal surface, and serial microscopic images of the terminal

ileum were captured at scanning depths of 15-70μm during and after intravenous administration of 5mL 10% fluorescein sodium contrast (Alcon, Australia) in 1mL increments.

Two blinded observers reviewed the images with patient grouping identifiers removed. Images where villi and lumen were indistinguishable were discarded. The two observers then independently analysed the remaining images for evidence of cell junction enhancement and fluorescein leak (see **Figure 1**). Cell junction enhancement was defined as an area of increased, equal fluorescence between two epithelial cells, extending from the basal to the apical surface of the cell layer. Fluorescein leak was characterised by a distinct plume of contrast leakage into the lumen stemming from the epithelial luminal border. Both features have previously been used in studies to gauge mucosal barrier function and permeability in gastrointestinal pathologies (28, 29, 33, 34).

Flow Cytometry

Ten pinch biopsies each were taken from the terminal ileum and left colon using endoscopic biopsy forceps during colonoscopy and separately stored in containers of media solution containing 10mL Roswell Park Memorial Institute (RPMI) culture media (Invitrogen, USA) with 10% foetal bovine serum (Bovogen, Australia) and 100U PenStrep (Invitrogen). Blood was concurrently collected in Vacutainer tubes with sodium heparin anti-coagulant (Becton Dickinson, NJ, USA).

Biopsy samples were weighed, then minced with sterile scissors, before enzymatic digestion using collagenase type III (Sigma-Aldrich) and DNase (Sigma-Aldrich), in order to prepare single cell suspensions for flow cytometry, as previously described (35). All samples were stained for surface markers according to manufacturer instructions, as previously described (35). Additionally, samples from the terminal ileum and left colon were stained for epithelial cells using the monoclonal antibody EpCam-FITC (BD Biosciences, CA, USA). Samples were washed with PBS (Dulbecco's Phosphate Buffered Saline (DPBS) with 0.5% BSA and 0.1% sodium azide) and fixed in a solution of 0.5% paraformaldehyde in DPBS. Peripheral blood samples were stained, lysed and fixed as previously described (35).

Cells were analysed using a four-laser LSR-II flow cytometer (BD Biosciences) and BD FACSDiva version 8.0 (BD Biosciences), then further analysed using FlowJo version 10.7.1 (Ashland, OR). The gating strategy for lymphocytes isolated from gastrointestinal biopsies has been previously described (35), and is shown in **Supplementary Figure 1A**. Gating of peripheral blood lymphocytes utilised a similar strategy as shown in **Supplementary Figure 1B**.

Microbiome Analysis

Stool samples were collected and preserved using OMNIgene GUT microbial stabilisation kit (DNA Genotek, Ontario, Canada). Genomic DNA was extracted using DNeasy PowerLyzer PowerSoil DNA isolation kits (Qiagen, Hilden, Germany) as per manufacturer's instructions. 16S rRNA sequencing was performed by first preparing the amplicon library using a previously described protocol (36), and sequenced on the Illumina Miseq sequencing platform using Illumina Miseq v3 kit with 2 x 300 bp cycle (Illumina Inc., CA, USA). Downstream processing of the amplicon sequencing reads was carried out as described (36). Briefly, reads were quality filtered and merged, followed by assigning operational taxonomic units (OTUs) using the Quantitative Insights into Microbial Ecology (37) software. No samples were eliminated following subsampling to the depth of 8,079 reads.

Plasma Marker Analysis

The plasma level of soluble CD14 (sCD14) was used as a marker of monocyte activation by lipopolysaccharide and microbial translocation. Other cytokines included TNF and IL6. EDTA anti-coagulated blood was centrifuged at 1600rpm for 15 minutes to obtain plasma for testing in ELISAs using commercially available kits for sCD14, IL-6 and TNF-α (all R&D systems, MN, USA) according to manufacturer's instructions.

Data Analysis

CD4 and CD8 T-cells in gastrointestinal biopsies at each sample site were counted as absolute cell numbers as previously described (35), but were also normalised by weight of biopsies and by the number of epithelial cells in the biopsies (35). Data was analysed using Prism software version 9.0 (GraphPad, La Jolla, CA). Quantitative analysis was performed using Kruskal-Wallis one-way ANOVA, with two-tailed Mann-Whitney U post-hoc analysis. Spearman's correlation was used to compare two continuous variables. Cohen's kappa score was used to measure inter-observer agreement in confocal endomicroscopy image

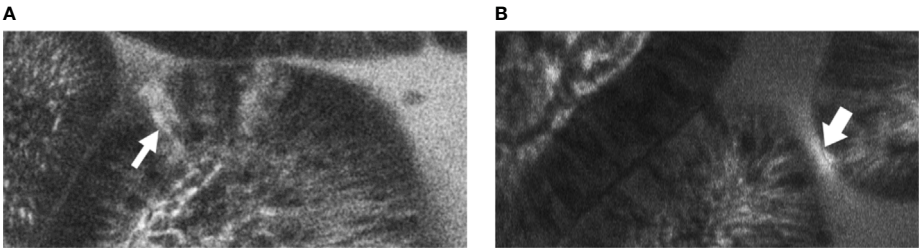

FIGURE 1 | Example images of terminal ileal villi exhibiting **(A)** fluorescein leak and **(B)** cell junction enhancement **(A)** Cell junction enhancement, characterised by an area of increased fluorescence from the basal to the apical surface between two epithelial cells. **(B)** Fluorescein leak, characterised by increased fluorescence in the epithelial cell layer, and a distinct plume of contrast leakage into the lumen.

interpretation. Faecal microbiota variation was analysed using Shannon and Simpson diversity indices, while group diversity as calculated using Bray-Curtis dissimilarity distance was illustrated using non-metric multidimensional scaling (NMDS) ordination, and tested using permutational multivariate analysis of variance (PERMANOVA). Kruskal-Wallis with Benjamini-Hochberg false-discovery rate adjustment was employed to assess significant difference in specific bacterial taxa between groups.

RESULTS

Participants

Of the 16 HIV-positive participants from the PINT study, which prospectively studied the effect of commencing a raltegravir-containing regimen during either primary HIV-1 infection (PHI) or chronic infection (CHI) (32), five primary and two chronic HIV participants re-enrolled into this study. A further six HIV-positive participants and six HIV-uninfected controls (HUC) were recruited from outpatient clinics at St Vincent's Hospital, Sydney. One patient in the PHI group did not attend for study procedures. Hence, a total of six HUC, five PHI and seven CHI subjects attended their allocated study session (**Figure 2**). All participants were male, with baseline characteristics outlined in **Table 1**. The CHI subjects had ART for a median 7 years (range 4-23) and the PHI subjects for 7 years (range 7-7).

One patient from the CHI group and one patient from the HUC group were excluded from confocal endomicroscopy and lymphocyte analysis due to inadequate visualisation of the terminal ileum, confocal imaging calibration issues, or non-attendance. One patient in the HUC group and two patients in the CHI group were excluded from microbiome analysis due to inadequate faecal sample.

Preservation of Gastrointestinal Mucosal Barrier Integrity Using Confocal Endomicroscopy (CEM)

The median time taken to examine and capture the CEM images in the terminal ileum per patient was 9 minutes (range 6-20). A median of 889 (382-2046) images taken per patient were analysed after removal of 282 (22-993) unfocused images per patient. Fluorescein leak (**Figure 1A**) and cell junction enhancement (**Figure 1B**) were able to be identified by the two observers. Of images identified by one or the other observer to contain fluorescein leak or cell junction enhancement, 29.8% were identified by the other observer. Inter-observer agreement for the presence of features identified per patient was moderate (κ=0.43) for cell junction enhancement and substantial (κ=0.75) for fluorescein leak. There was also a strong correlation between the total number of features identified by each observer separately and features identified by both observers (Spearman r 0.81; 95%CI 0.51-0.93; p<0.01).

The number of images with fluorescein leak and cell junction enhancement was small as a proportion of the total number of images (median 0.15%, range 0-0.54%). There was no statistically significant difference in the median percentage of CEM features seen in participants across the three groups (HUC=0.26% *vs* PHI 0% *vs* CHI 0.11%; p=0.51) (**Figure 3**). No significant differences were found when fluorescein leak and cell junction enhancement were analysed separately (data not shown).

Characterisation of CD4 and CD8 T-Cells in Gastrointestinal Tissue

In addition to absolute counts of CD4 and CD8 T-cells in gastrointestinal biopsies at each sample site, as previously described (35), numbers of these cells were also normalised by weight of biopsies and also by the number of epithelial cells in the biopsies (35). This revealed similar weights and epithelial cell

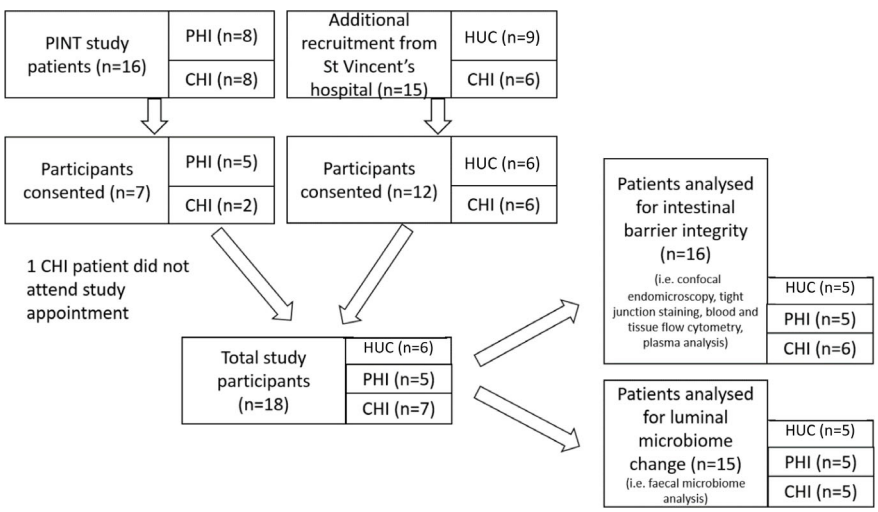

FIGURE 2 | Patient recruitment flowchart outlining selection of patients for confocal endomicroscopy imaging, tight junction, blood and tissue lymphocyte, plasma marker and faecal microbiome analyses. HUC, HIV-uninfected control; PHI, HIV-positive participant who initiated antiretroviral therapy during primary HIV infection; CHI, HIV-positive participant who initiated antiretroviral therapy during chronic HIV infection.

TABLE 1 | Baseline characteristics and clinical parameters of study participants.

	HIV-Uninfected controls (n=6)	HIV-positive participants treated with antiretroviral therapy in primary infection (n=5)	HIV-positive participants treated with antiretroviral therapy in chronic infection (n=7)	p-value
Age years median (range)	49 (33-58)	52 (48-55)	49 (35-53)	0.42
Gender Male n (%)	6 (100%)	5 (100%)	7 (100%)	1.00
Years since diagnosis of HIV median (range)	–	7 (7-7)	17.5 (8-33)	<0.01
Years since commencement of ART median (range)	–	7 (7-7)	6.5 (4-23)	0.48
Time between diagnosis and commencement of ART years median (range)	–	0 (0-0)	7 (2-20)	<0.01
Current antiretroviral therapy regimen	–	RAL/TDF/FTC RAL/TDF/FTC RAL/TDF/FTC EVG/c/TDF/FTC DTG/TDF/FTC	TDF/FTC/NVP EVG/c/TDF/FTC EVG/c/TDF/FTC RPV/TDF/FTC RAL/TDF/FTC ABC/3TC ABC/3TC/NVP/RAL	–
CD4 T-cell count on visit cells/mm^3 median (range)*	881.9 (748.3-1278)	792.2 (421.5-888.3)	708.9 (602.1-809.8)	0.11
CD8 T-cell count on visit cells/mm^3 median (range)*	734.8 (658.8-1045)	519.8 (264.5-1305)	733.6 (523.7-2417)	0.65
Last measured plasma viral load	–	Undetectable	Undetectable	–
Acute infections or vaccinations in past month n (%)	3 (50%)	0 (0%)	3 (43%)	0.06
Antibiotic use in past month Yes n (%)	1 (17%)	0 (0%)	2 (29%)	0.42
Overseas travel in past year Yes n (%)	3 (50%)	1 (20%)	4 (57%)	0.42
Current Smoker Yes n (%)	0 (0%)	1 (20%)	2 (29%)	0.38
Current Alcohol Use Yes n (%)	5 (83%)	4 (80%)	6 (86%)	0.97

**Systemic lymphocyte counts were only analysed in patients where confocal imaging, blood and tissue samples were collected. Chi-square test was used to analyse categorical data for significance. Mann Whitney U and Kruskal Wallis tests were used to analyse continuous data for 2 and >2 groups, respectively. RAL, raltegravir; TDF, tenofovir disoproxil fumarate; FTC, emtricitabine; EVG, elvitegravir; DTG, dolutegravir; NVP, nevirapine; RPV, rilpivirine; ABC, abacavir; 3TC, lamivudine.*

counts between groups, but no correlation between the weight and epithelial cell count.

By absolute count from biopsies, there was no significant difference between CD4 T-cell counts in terminal ileum (TI) biopsies across the three study groups by Kruskal-Wallis test, but there was a significant difference between HUC and CHI groups in left colon (LC) biopsies (**Figure 4A**). By weight, there was an absolute decrease in CD4 T-cell numbers per mg in PLHIV in the LC compared with HUC participants, (HUC 1434.5 vs PHI 392.56 *vs* CHI 515.6 cells/mg; p=0.03) (**Figure 4B**). A similar decreasing trend was found in the TI samples (HUC 2987.8 *vs* PHI 751.8 *vs* CHI 577.9 cells/mg; p=0.20) (**Figure 4B**). There was no significant change in the CD4 T-cell count:epithelial cell number ratio in the TI (HUC 0.027 *vs* PHI 0.014 *vs* CHI 0.016; p=0.56) or LC (HUC 0.026 *vs* PHI 0.013 vs CHI 0.008; p=0.17) (**Figure 4C**).

There were no significant changes in the CD8 T-cell count by biopsy, weight or epithelial cell ratio, in either the TI or LC across the three groups (**Figures 4D–F**).

Association Between Circulating and Gastrointestinal Lymphocyte Numbers

When analysing the samples of all volunteers in our study, a significant positive correlation was found between the CD4 T-cell count in peripheral blood and the number of CD4 T-cell count in gastrointestinal tissue in both the TI (p<0.01 r=0.76) and LC (p=0.02 r=0.57) (**Table 2**); the degree of correlation was higher in the TI than in the LC. A significant positive correlation was also found between peripheral blood CD8 T-cell count and CD8 T-cell number in the TI (p<0.01 r=0.69) (**Table 3**).

CD8 T Cell Activation in Peripheral Blood and Biopsies

Circulating activated CD38+HLA-DR+ CD8 T-cells, as a proportion of total CD8 T-cells in the peripheral blood, was measured as a marker of systemic immune activation. No statistically significant differences were found across the percentages in the three subject groups of the current study

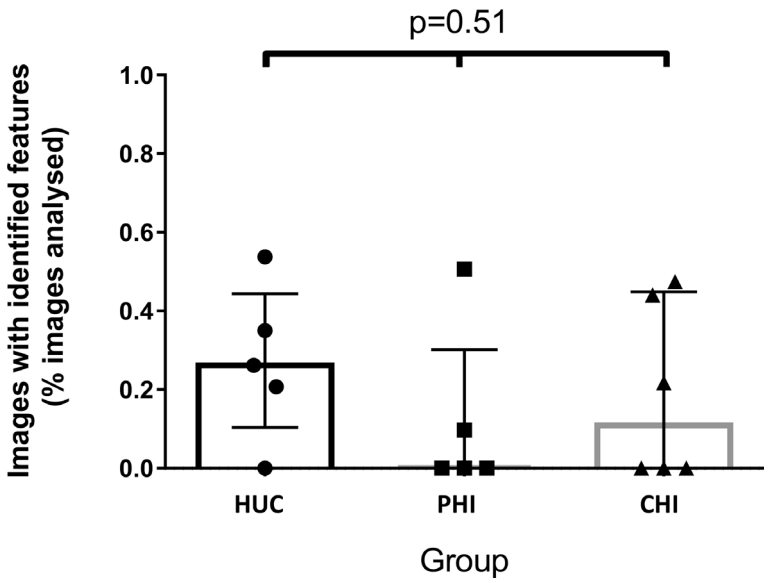

FIGURE 3 | Images with identified confocal endomicroscopy features (fluorescein leak and cell junction enhancement) as a percentage of total images analysed for the participant, across three groups. Median percentage of images was 0.26% for HIV-uninfected controls (HUC), 0.00% for HIV-positive participants treated in primary infection (PHI), and 0.11% for HIV-positive participants treated in chronic infection (CHI). Statistical analysis was conducted using Kruskal Wallis one-way analysis of variation.

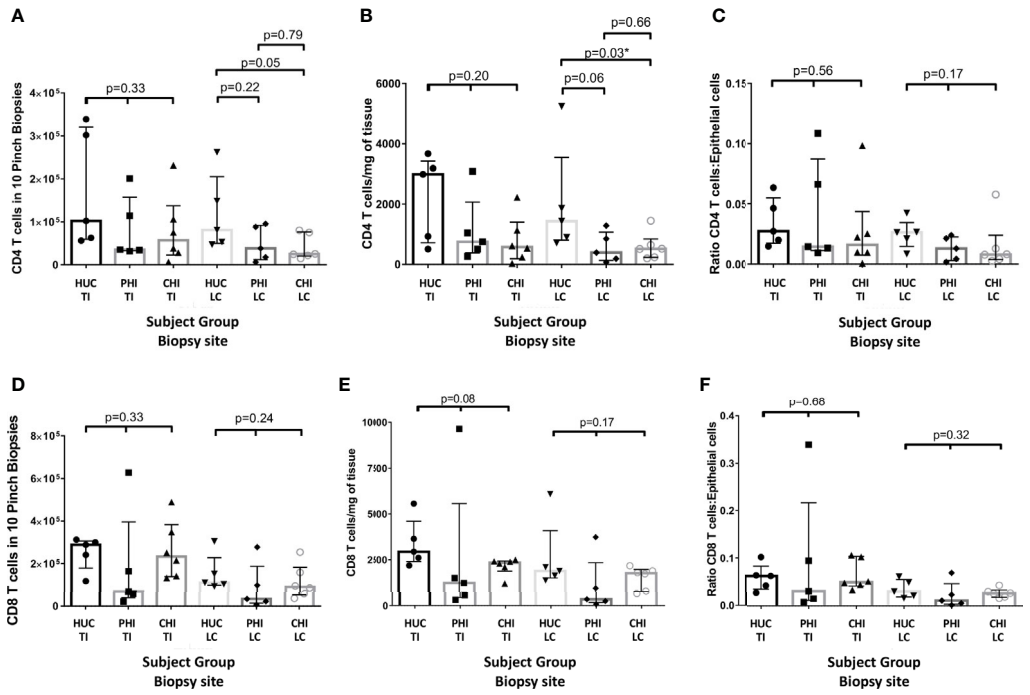

FIGURE 4 | Changes in CD4 panels **(A–C)** and CD8 **(D–F)** cell numbers in the terminal ileum and left colon between patient groups as: **(A, D)** an absolute count from ten biopsies; **(B, E)** standardised per milligram of tissue; and **(C, F)** standardized by epithelial cell number HUC, HIV-uninfected controls; PHI, HIV-positive patients treated during primary infection; CHI, HIV-positive patients treated during chronic infection; TI, terminal ileum; LC, left colon, *statistically significant ($p \leq 0.05$). Statistical analysis was conducted using Kruskal Wallis one-way analysis of variance with pairwise post-hoc testing using Mann Whitney U.

TABLE 2 | Relationship between systemic CD4 T-cell concentration measured using peripheral blood and measured gastrointestinal lymphocyte numbers, for all study groups combined, and for HIV-positive study participants only.

	All Patients			HIV-positive Patients		
	n	p-value	r	n	p-value	r
CD4 T-cell count for all biopsies						
TI	16	<0.01**	0.76	11	0.03*	0.65
LC	16	0.02*	0.57	11	0.27	0.36
CD4 T-cell count per milligram of tissue						
TI	16	<0.01**	0.81	11	<0.01**	0.76
LC	16	0.02*	0.59	11	0.20	0.42
Ratio of CD4 T-cells:Epithelial cells						
TI	16	0.01*	0.61	11	0.19	0.43
LC	16	0.09	0.44	11	0.17	0.45

*Spearman Correlation was used for analysis of significance. *p ≤ 0.05. **p ≤ 0.01.*

(medians: HUC 2.75% PHI 3.53% CHI 3.45% Kruskal-Wallis test p=0.69) (**Figure 5A** left). As comparator data, a previous larger sample of HUC and all longitudinal data from the PINT study (38) showed that there was a small but significant elevation of activated CD38+HLA-DR+ CD8 T-cells in PLHIV on long-term suppressive ART (medians: HUC 1.5%, HIV+ PINT subjects 4.0%; Mann-Whitney test p<0.0001) (38) (**Figure 5A**, right). For the PLHIV in PINT, 25/67 observations were above 4.6%, which was the 95th percentile of the normal range.

We also measured the activated CD38+HLA-DR+ % of CD8 T-cells in the gut biopsies and compared them to the corresponding peripheral blood levels (**Figure 5B**). In general, the level of activation was in the same range as for circulating CD8 T-cells, and no significant elevations were seen in gut biopsies from PLHIV, compared to the HUC gut biopsies (**Figure 5B**).

When we further subdivided the activated CD38+HLA-DR+ CD8 T-cells in the gut biopsies into CD103+ resident intraepithelial cells (39) versus CD103- presumptively migratory cells (**Supplementary Figure 1A**), we found that, in most biopsies, the majority of CD38+HLA-DR+ CD8 T-cells were CD103+ tissue resident cells that are unlikely to recirculate (**Figure 5C**).

Conversely, we examined the expression of integrins α4ß7, that determine whether the cells traffic through GALT, on CD38+HLA-DR+ CD8 T-cells in peripheral blood (**Supplementary Figure 1B**). The results show that the majority of circulating activated CD38+HLA-DR+ CD8 T-cells do not express integrins α4ß7 (**Figure 5D**). We also did not see any correlation between the levels of circulating activated CD38+HLA-DR+ CD8 T-cells with the corresponding cells in either TI biopsies (**Figure 5E**) or LC biopsies (**Figure 5F**). Finally, when there were larger percentages of activated CD38+HLA-DR+ CD8 T-cells in gut biopsies, they were mostly CD103- in TI (**Figure 5G**) and in LC (**Figure 5H**), suggesting that they were migratory.

Overall, the results indicate that while it appears that there are slightly more circulating activated CD38+HLA-DR+ CD8 T-cells in PLHIV on fully suppressive ART, they appear to be more systemic in origin and not directly associated with activation within GALT.

We also used an alternative CD38+CD127- phenotype of activated CD8 T cells since it has been reported that levels of this phenotype differed between HIV+ subjects and uninfected controls, in both rectal mucosa and blood (40). When we studied these cells (**Supplementary Figure 1B**) we did not find any significant differences in CD38+CD127- CD8 T-cells between PLHIV and HIV-uninfected subjects in either blood or gut biopsies (**Supplementary Figure 2**).

Plasma Markers of Immune Activation

There were no significant differences between the levels of sCD14 (pg/mL) found in the three study groups (HUC $1.78x10^6$ *vs* PHI $1.32x10^6$ *vs* CHI $1.68x10^6$ pg/ml; p=0.55) (**Figure 6A**). The majority of study participants (68.75%) had undetectable concentrations of TNF-α in plasma (**Figure 6B**). A higher number of patients in the CHI group had detectable plasma TNF-α levels compared with those in both the HIV-uninfected and PHI groups (n=3, n=1, n=1 respectively), but this was not

TABLE 3 | Relationship between systemic CD8 T-cell concentration measured in peripheral blood and measured gastrointestinal lymphocyte numbers, for all study groups combined, and for HIV-positive study participants only.

	All Patients			HIV-positive Patients		
	n	p-value	r	n	p-value	r
CD8 T-cell count for all biopsies						
TI	16	<0.01**	0.69	11	<0.01**	0.76
LC	16	0.07	0.46	11	0.03*	0.65
CD8 T-cell count per milligram of tissue						
TI	16	<0.01**	0.65	11	<0.01**	0.79
LC	16	0.17	0.36	11	0.08	0.56
Ratio of CD8 T-cells:Epithelial cells						
TI	16	<0.01**	0.67	11	<0.01**	0.80
LC	16	0.08	0.45	11	0.03*	0.68

*Spearman Correlation was used for analysis of significance. *p ≤ 0.05. **p ≤ 0.01.*

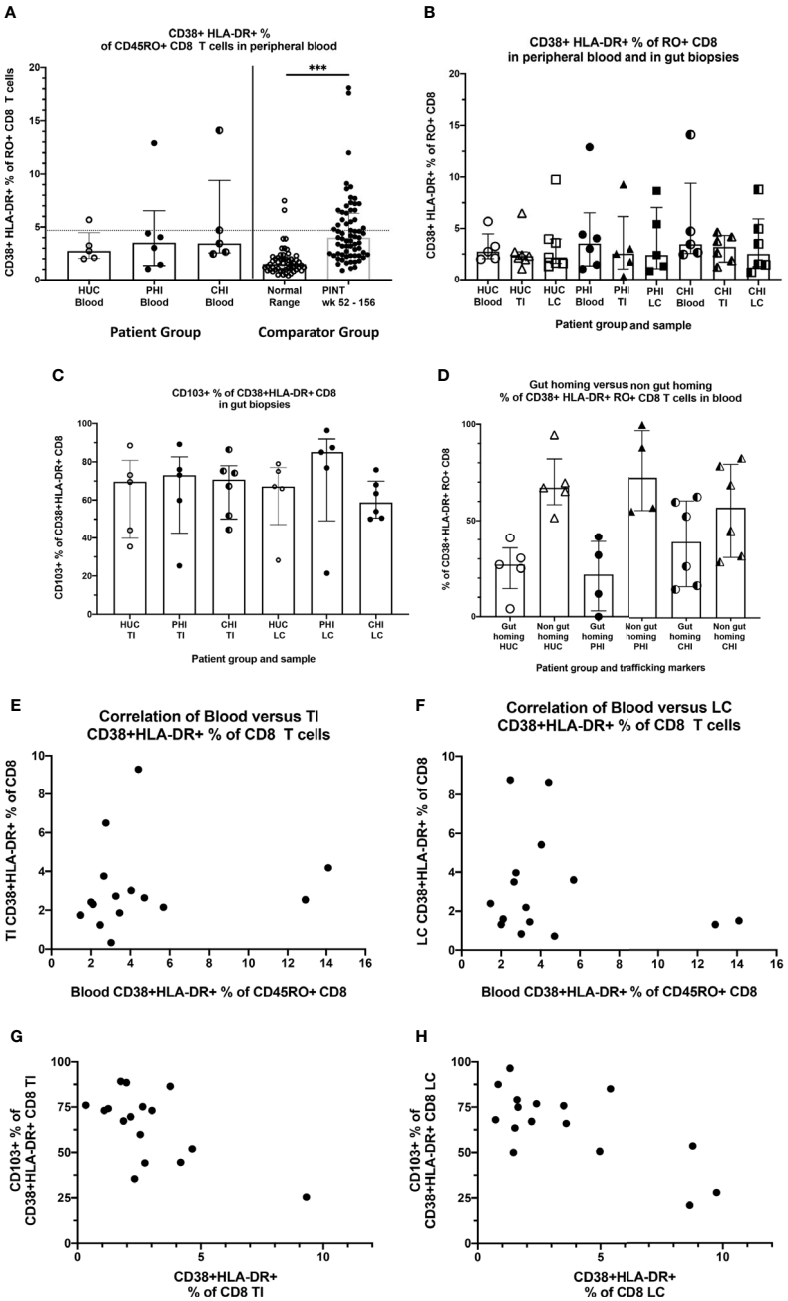

FIGURE 5 | Activated CD38+HLA-DR+ CD8 T-cells in blood and tissues. **(A)** Activated CD38+HLA-DR+ as % of CD45RA- CD8 T cells in peripheral blood, by study group. HUC, HIV-uninfected controls; PHI, HIV-positive patients treated during primary infection; CHI, HIV-positive patients treated during chronic infection. The Comparator Groups are (left) normal range for HUC subjects from reference (38) and the 95th percentile (4.6%) is shown as the dotted horizontal line, and (right) PINT subjects longitudinal observations from reference (38). Statistical analysis between HUC, PHI and CHI groups was conducted using Kruskal Wallis one-way analysis of variance. Statistical analysis between comparator normal range and PINT groups was done using Mann-Whitney test. **(B)** Comparison of activated CD38+HLA-DR+ as % of CD45RA- CD8 T-cells in peripheral blood, TI biopsies and LC biopsies, respectively by study group. **(C)** Percentage of activated CD38+HLA-DR+ CD8 T-cells in TI and LC biopsies that are also CD103+. **(D)** Percentage of activated CD38+HLA-DR+ CD8 T-cells in peripheral blood that are either CD49d+integrin ß7+ gut-homing or CD49d+integrin ß7+-negative non-gut-homing, by study group. **(E)** Correlation of activated CD38+HLA-DR+ as % of CD8 T-cells in peripheral blood with activated CD38+HLA-DR+ as % of CD8 T cells in TI biopsies. **(F)** Correlation of activated CD38+HLA-DR+ as % of CD8 T-cells in peripheral blood with activated CD38+HLA-DR+ as % of CD8 T cells in LC biopsies. **(G)** Correlation of CD103+ as % of activated CD38+HLA-DR+ CD8 T-cells in TI biopsies with activated CD38+HLA-DR+ as % of CD8 T cells in TI biopsies. **(H)** Correlation of CD103+ as % of activated CD38+HLA-DR+ CD8 T-cells in LC biopsies with activated CD38+HLA-DR+ as % of CD8 T cells in LC biopsies. ***$p < 0.0001$.

statistically significant. Of the five participants with detectable TNF-α concentrations, 4 (80%) had detectable cell junction enhancement or fluorescein leak seen on confocal endomicroscopy (HUC n=1, PHI n=1, CHI n=2). There were no significant differences in IL-6 concentrations across the three groups (HUC 1.49pg/mL *vs* PHI 1.79pg/mL *vs* CHI 1.69pg/mL; p=0.22) (**Figure 6C**). Finally, the relationship between epithelial integrity and both local immune parameters in the TI as well as systemic parameters was explored. No significant differences were found between the presence of confocal endomicroscopy features and the immune parameters measured (**Table 4**).

Characterisation of Gut Microbiota

Microbiota composition across all patients was dominated by fermentative bacterial taxa, including members of the *Faecalibacterium* (median 0.10; interquartile range [IQR] 0.05-0.12), *Prevotella* (median 0.21; IQR 0.09-0.38) and Bacteroides (median 0.01, IQR 0.003-0.12) genera (**Figure 7A**). There was no significant difference between groups in overall microbiota composition based on Bray Curtis dissimilarity, as assessed by PERMANOVA (P(perm)=0.202, pseudo-F=1.272, 9551 permutations). A non-significant decreasing trend in taxa diversity was also found using the Shannon diversity index H' (**Figure 7B**). However, a significant difference (p=0.03) was found between PLHIV and HIV-uninfected participants in the distribution evenness of taxa, as measured by the Simpson diversity index (**Figure 7C**). The relative abundance of the *Spirochaeta* genus was significantly higher in the PHI group (p=0.042; **Figure 7D**), while the *Acidaminococcus* genus showed a non-significant trend towards increased relative abundance in the CHI group (**Figure 7E**). Patients in the CHI group exhibited a trend of increasing *Prevotella* relative abundance, and a trend of decreasing *Faecalibacterium* relative abundance. There was no correlation between the microbiota and the CEM or the cytokines (data not shown).

DISCUSSION

In this study, we aimed to confirm and characterise the *in vivo* intestinal permeability of study participants with treated HIV infection, compared to HIV-uninfected controls, using CEM, as well as define associations with parameters of mucosal barrier integrity and systemic immune activation and inflammation. Contrary to expectations, however, we could not confirm significant differences for *in vivo* intestinal permeability between study groups.

In our study methodology, the amount of fluorescein used was matched with other studies which successfully identified changes in gastrointestinal villi, determining the timeframe in which contrast-enhanced images could be taken with the confocal microscope (28, 29). Fluorescein leak and cell junction enhancement were features chosen as indicative of increased epithelial permeability in intestinal villi as interpretation could be easily standardised and due to their previous association with damage to epithelial barrier integrity in other contexts (41). These features were identifiable in our images, but, importantly, there were no significant quantitative differences between the subject groups.

A recent study had also utilized *in vivo* microscopic imaging of rectal mucosa and reported that there was increased fluorescein leakage and intramucosal bacteria in most of the 10 HIV+ subjects studied (31). However, unlike our study, there was no quantitative comparison to HIV-uninfected controls, and 7/10 HIV+ subjects were Elite Controllers (31), who are not representative of PLHIV on long-term ART.

Although *in vitro* studies have reported increased tight junction permeability, epithelial inflammation and apoptosis (10) on direct exposure to the HIV-1, this effect could be reduced *in vivo* due to the fast turnover rate of epithelial cells (42) and sustained suppression of HIV replication with long term ART. Certainly, this would be consistent with both this small study's results and results from an *in vitro* study of intestinal permeability by Epple et al. in 2009 (12). Although inter-observer agreement on cell junction enhancement was low compared to other studies (28, 41, 43), the comparable agreement on presence of fluorescein leak with other studies, and the high percentage of study participants with CEM features suggest the methodology is sufficiently sensitive. Larger studies utilising this method in treated and untreated PLHIV with comparison to other inflammatory gastrointestinal diseases, such as ulcerative colitis or Crohn's disease, would help place these findings in a clearer context.

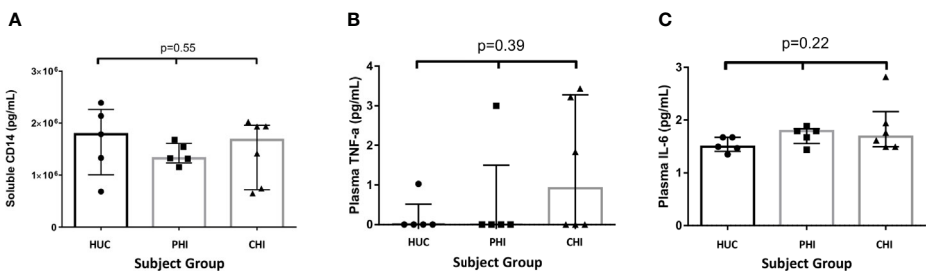

FIGURE 6 | Levels of soluble proteins measured in plasma between the study groups. **(A)** Levels of soluble CD14 measured in plasma between the study groups. **(B)** Levels of TNF-α measured in plasma between the study groups. **(C)** Levels of IL-6 measured in plasma between the study groups. Statistical significance was calculated using the Kruskal Wallis test.

TABLE 4 | Relationship of confocal endomicroscopy features identified in patients and measured parameters.

	All patient groups (n=16)			HIV-positive patients only (n=11)		
Parameter	CEM no abnormalities (n=7)	CEM abnormalities (n=9)	P	CEM no abnormalities (n=6)	CEM abnormalities (n=5)	P
Systemic CD4 (cells/mm^3)	697.3	769.7	0.30	694.5	752.0	0.33
Systemic CD8 (cells/mm^3)	769.0	674.3	0.84	733.6	661.6	0.79
Systemic activated CD8%	3.17	1.63	0.28	3.21	1.55	0.25
Terminal Ileum CD4 T-cells/mg	614.7	1133	0.41	577.9	1133	0.33
Terminal Ileum CD8 T-cells/mg	2105	2412	0.41	1803	2290	0.93
sCD14 (pgx10^6/mL)	1.538	1.417	0.68	1.430	1.417	0.93
TNF-α (pg/mL)	0.000	0.000	1.00	0.000	3.003	0.11
IL-6 (pg/mL)	1.762	1.613	0.26	1.777	1.613	0.42

Median values are shown for each group. TI, terminal ileum; IgA, immunoglobulin A; sCD14, soluble CD14; TNF-α, tumour necrosis factor alpha; IL-6, interleukin 6. Analysis was performed using Mann Whitney U rank sum tests.

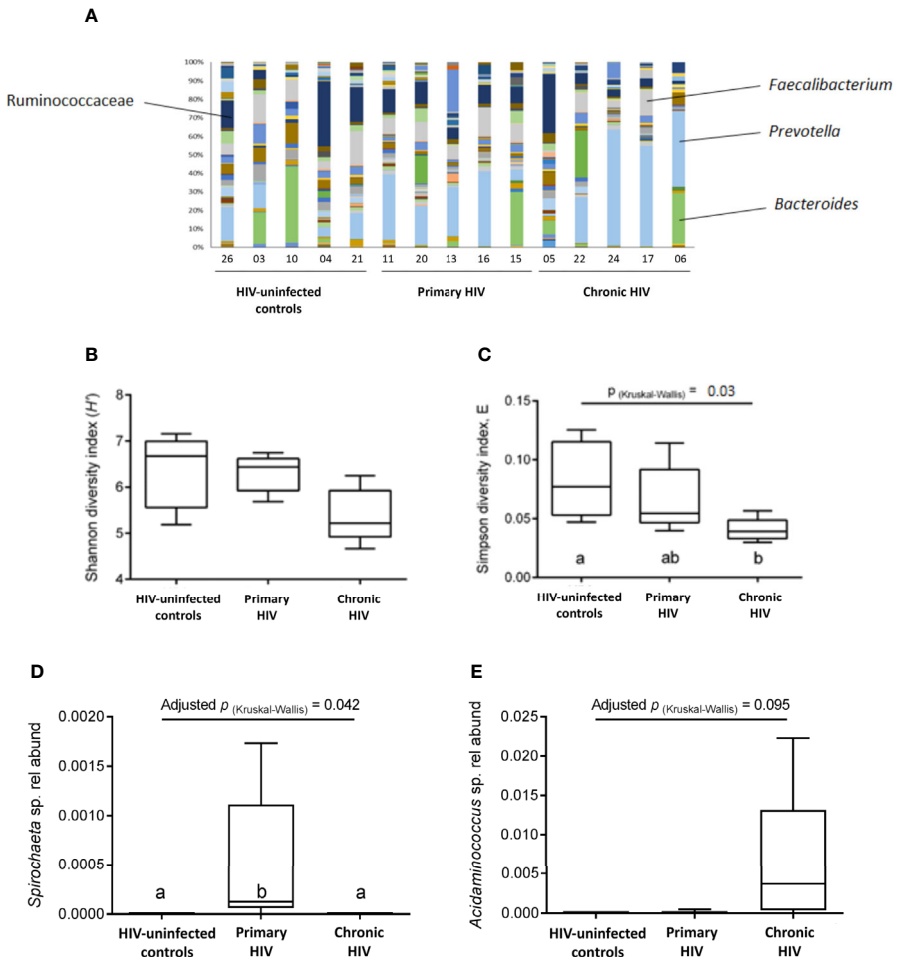

FIGURE 7 | Faecal microbiota composition. **(A)** Bacterial composition from analysis of faecal samples from study participants prior to bowel preparation. A total of 145 types of taxa are represented, with increased representation of fermentative taxa (i.e., Ruminococcaceae, Faecalibacterium, Prevotella, Bacteroides) compared to other taxa. **(B)** Species diversity and taxa distribution in study participants as measured by Shannon diversity index (H') **(C)** Species diversity and taxa distribution in study participants as measured by Simpson diversity index E **(D)** Relative abundance of the *Spirochaeta* genus between groups. **(E)** Relative abundance of the *Acidaminococcus* genus between groups.

Ours is the first study to directly explore the effect of early and late initiation of effective ART on intestinal permeability. A secondary hypothesis was that gastrointestinal lymphocyte depletion would be more profound in PLHIV who commenced ART during CHI. Consistent with this hypothesis, our study found a significant decrease in LC CD4 T-cell counts and a decreasing trend in TI CD4 T-cell counts of CHI participants compared to HIV-uninfected controls, and is consistent with our

previous studies (35). This result is supported in previous studies on T-lymphocyte cell counts in gastrointestinal tissue (14, 16, 44) in untreated and treated (6, 44–46) PLHIV, but the effect of early ART initiation in the literature is unclear. While studies have reported limited reconstitution of the proportion of CD4 T-cells in intestinal tissue even when treated during primary infection (6, 47), a study by Allers et al. on absolute CD4 T-cell numbers reported treatment during early HIV infection led to complete preservation of CD4 T-cells in duodenal tissue (45).

Our study found a decreasing trend in LC CD4 T-cell numbers of PLHIV treated in primary infection. The association was less clear in the TI. Data from a study by Yukl et al. (48) previously showed a larger quantifiable decrease in the proportion of CD4 T-cells in ileal samples of HIV-positive volunteers than in rectal samples. It has been suggested that the effect of HIV infection on T-cell numbers is variable depending on the gastrointestinal sample site due to different frequencies of gut-homing and regulatory T cells (48). A possible identified contributor to the variability of lymphocyte counts was the nature of lymphoid follicles being concentrated in Peyer's patches in the TI (49), making representative sampling of this site difficult. Our group's larger analysis of gastrointestinal lymphocyte counts have revealed significant decreases in CD4 T-cells in both the LC and TI, using both absolute cell counts and epithelial cell ratio, although in that study samples were not analysed by weight (35).

Earlier studies quantified the CD4 T-cells as a percentage of total CD3+ T-cells. However, absolute CD8+ CD3+ T-cell levels may be increased in HIV-positive patients with untreated infection, with high variability in the levels in patients on ART (14, 45), resulting in either a decrease in, or increased variability, in mucosal CD4 T-cell percentages. This study is one of few to use absolute lymphocyte counts to preclude the effects of CD8 T-cell proliferation. As a standard method of normalisation is not documented, both epithelial cell counts and biopsy weight were used as normalisation methods due to possible variations in size of biopsy samples. However, we found stronger correlations between peripheral blood and tissue lymphocytes when normalising by weight. This suggests that lymphocyte loss may be more concentrated in areas of lymphoid aggregation, which are deeper in the tissue, compared to tissue-resident lymphocytes near the epithelial border. Weight may be more representative of biopsy volume, and epithelial cells representative of total biopsy tissue area. This might be a useful area of investigation, which could involve comparison of immuno-histochemistry and flow cytometry methods.

Despite systemic CD4 activation being central to HIV pathogenesis (50), we have concentrated on the study of activated CD38+HLA-DR+ CD8 T-cells, rather than activation of CD4 T-cells for several reasons. Firstly, levels of activated CD38+HLA-DR+ CD8 T-cells in blood samples from untreated patients have been clearly correlated with disease progression (51). Secondly, in patients receiving ART, we and others have documented residual elevation of activated CD8 T-cells (38, 52, 53) despite suppression of HIV replication; these levels have been correlated with plasma LPS levels, consistent with the microbial translocation hypothesis (7). Finally, the frontline CD8 T-cells in GALT can be identified as CD103+ intraepithelial resident memory cells, and these cells should be most activated by barrier dysfunction. In contrast, levels of CD4 activation in gut biopsy samples are complicated by the presence of germinal centres containing activated CD4 T follicular helper cells (35), and these cells do not leave GALT.

Instead, we have found that there was no difference in CD8 T-cell activation in gut biopsy samples between PLHIV on ART compared to HIV-uninfected controls, and in particular, we documented for the first time that CD103+ CD8 T-cells were generally more activated than CD103- migratory CD8+ T-cells. Furthermore, there was only a minority of activated CD8 T-cells in peripheral blood that expressed the gut-homing integrins α4ß7, and there was no obvious correlation of levels of activation of CD8 T-cells between the GALT and blood compartments. Altogether, our detailed results suggest that it is unlikely that the main source of activated CD8 T-cells in blood is due to gastrointestinal barrier dysfunction.

We have previously found that crucial CD4 T follicular helper cells in GALT are not significantly depleted in HIV+ subjects on ART, nor are their important downstream effector cells, IgA+ B-cells (35), which will help maintain microbial homeostasis of this tissue. Instead, in these GALT germinal centres as well as in other lymphoid tissues, it is possible that CD4 T follicular helper cells act as a residual underlying HIV reservoir (3, 54) and may contribute to lingering CD8 T-cell activation. Undoubtedly, GALT CD4 T-cells continue to contribute to the HIV reservoir under ART (55, 56). However, we have previously found that in the circulation, gut-homing CD4 T cells only contain a small proportion of the HIV-1 DNA in PBMC (57). Other tissues, despite fully suppressed plasma viremia, are likely to contain HIV-1 reservoirs that activate CD8 T-cells, such as CD4 T follicular helper cells in peripheral lymph nodes (3, 54), infected alveolar macrophages (58) and infected cells in the CNS (59, 60).

An increased relative abundance of *Spirochaeta*, *Prevotella*, *Acidaminococcus* species in those with HIV, and a reduced abundance of *Faecalibacterium* species, as suggested by our data, are consistent with gut microbiome changes described in PLHIV in other studies (22, 23, 61). *Faecalibacterium prausnitzii*, a member of clostridial cluster IV, is one of a number of obligate anaerobic gut commensal bacteria that are responsible for the production of the short chain fatty acid butyrate through the fermentation of carbohydrates in the colon by inducing (62). Butyrate, in turn, contributes to gut barrier function by inducing tight junction assembly through an AMPK-dependent pathway (63). In contrast, increased prevalence of *Prevotella* species is associated with increased susceptibility to gut inflammation through indirect suppression of IL-18 production (64). However, while it has been suggested that an increased presence of potentially pathogenic bacteria in the gastrointestinal lumen may induce expression of pro-inflammatory cytokines, thereby increasing epithelial layer permeability (65, 66), these changes in microbiota composition were not reflected in the confocal imaging results.

There are a number of reasons why interpretation of the microbiome data is difficult. First, the cohort was small, and the study was cross-sectional, not permitting longitudinal microbiome follow-up. Three participants were treated for a sexually transmitted infection with antibiotics before enrolment. Finally, it has been recognised that ART has a variable impact on the composition of the microbiome, and this could not be assessed in this study (67, 68).

Plasma sCD14 concentration is a measure of monocyte activation in response to lipopolysaccharide from the cell walls of gram-negative bacteria (45, 69). We did not find, however, an increasing trend in levels of sCD14 in CHI patients. Recent studies have revealed differing findings on the effect of ART on levels of sCD14 (45, 70, 71). This variability may be due to a number of confounding factors, such as the duration of ART, although variability persists when individual patients are followed longitudinally (71); behavioural factors such as smoking may also be implicated (72, 73). The measured levels of sCD14 varied highly between previously published studies, varying from $0.7x10^6$pg/mL (74) to $4x10^6$pg/mL (45) in HIV-uninfected controls. Our study's median of $1.8x10^6$ pg/mL for HIV-uninfected controls and $1.4x10^6$ pg/mL for PLHIV is consistent with results from other studies (45, 74). No increasing trend in levels of TNF-α, IL-6 or systemic activated HLA-DR+CD38+ CD8+ T-cells was found in the CHI patients.

Presentation of intraluminal antigens from the intestinal lumen is part of normal physiology in the regulation of immune responses and establishment of immunotolerance (75, 76), and it is possible for increased bacterial products to enter the portal and systemic circulation due to dysregulation of immune lymphocytes despite maintenance of epithelial barrier integrity. HIV-1 can infect hepatic Kupffer cells, which express CD14 and other receptors responding to LPS, altering measured levels of these markers (77). However, partial restoration of Kupffer cells has been found following initiation of ART (78).

The strength of this study was the detailed comparison with HIV-uninfected controls, including not only the confocal imaging, but also the detailed study of immune activation locally and systemically, as well as of the microbiome. This study was however limited by its cross-sectional design. Hence, we were unable to demonstrate whether the lack of changes in intestinal permeability was due to recovery following ART initiation. A more significant limitation of this study was the small sample size, which increases the possibility of type II errors. Finally, the small sample including only men makes generalisability difficult. As a pilot study, the main aim was to identify trends in measures of the gastrointestinal barrier that could contribute to microbial translocation and contribute exploratory data to support further larger studies of barrier dysfunction and microbial dysbiosis.

In conclusion, our results indicate that despite slightly impaired CD4+ T-cell recovery in the gastrointestinal tissue of CHI patients, no changes to physical epithelial integrity were found, nor significantly increased activation of CD8 T-cells within GALT. Furthermore, microbial translocation and inflammatory markers trended towards return to baseline. Our study raises doubts about the significance of microbial translocation and systemic inflammation in HIV-positive participants on effective ART. Analyses have suggested that there is little difference in life expectancy in PLHIV compared to HIV-uninfected individuals when controlling for other risk factors (79), although a more recent study suggests that PLHIV who commenced ART in the US between 2011-2016 with high CD4 counts still had about 7 years less life expectancy, plus more years of comorbidities. Several issues remain, such as whether dysregulation of intestinal CD4+ lymphocytes alone facilitates increased passage of bacterial by-products into the portal circulation. In summary, our study suggests that the importance of microbial translocation and its contribution to systemic immune activation in well-controlled HIV-positive patients may not be as significant as widely reported and believed.

DATA AVAILABILITY STATEMENT

The raw data supporting the conclusions of this article will be made available by the authors, without undue reservation.

ETHICS STATEMENT

This study was approved by the St Vincent's Human Research Ethics Committee (HREC 14/214). All participants provided written informed consent. The patients/participants provided their written informed consent to participate in this study.

AUTHOR CONTRIBUTIONS

Experimental work and data analysis: GM, JZ, MB, NS, GR, LL, and MD. Project conception: MD, MAB, KK, AK, and TP. Patient recruitment and procedures: MD, GM, KK, and AK. Manuscript written by GM, JZ, and MD. All authors contributed to the article and approved the submitted version.

FUNDING

The study was funded by a St Vincent's Clinic Foundation Project Grant. Cancer Institute NSW Equipment Grant 10REG114, Australia Research Council (ARC) Linkage Project LP10020080. TP is supported by National Health and Medical Research Council (NHMRC) Senior Research Fellowship (APP1155678) and the Ernest Heine Family Foundation. JZ was supported by NHMRC Fellowship 1063422 and ADK by NHMRC Program Grant 1052979.

ACKNOWLEDGMENTS

The authors would like to thank Dr Yin Xu for expert technical assistance.

SUPPLEMENTARY MATERIAL

The Supplementary Material for this article can be found online at: https://www.frontiersin.org/articles/10.3389/fimmu.2021.688886/full#supplementary-material

Supplementary Figure 1 | – Representative flow plots and gating of CD8 T-cell subsets. **(A)**– Top row: Gating of CD45+ SSC^{low} lymphocytes, then CD3+ and EpCAM-negative, then CD45RA-negative, then CD8 T-cells (CD3+ CD4 negative). -Bottom row: CD8 T-cells then analysed for CD38 *vs* HLA-DR and CD38 *vs* CD127. -Then CD38+HLA-DR+ and CD38+CD127^{low} cells, respectively, were analysed for CD103 expression. **(B)**– Top row: Gating of CD45+ SSC^{low} lymphocytes, then CD3+ and CD20-negative, then CD45RA-negative, then CD8 T-cells (CD3+ CD4 negative). -Bottom row: CD8 T cells then analysed for CD38 *vs* HLA-DR, and CD49d *vs* integrin ß7, and CD38+CD127^{low} cells. -Then CD38+HLA-DR+ cells were analysed for CD49d *vs* integrin ß7 expression

Supplementary Figure 2 | Activated CD38+CD127^{low} CD8 T-cells in blood and tissues. Activated CD38+CD127^{low} as % of CD45RA- CD8 T cells in peripheral blood, and in TI and LC biopsies, by study group. HUC: HIV-uninfected controls, PHI: HIV-positive patients treated during primary infection, CHI: HIV-positive patients treated during chronic infection.

REFERENCES

1. Esser R, Von Briesen H, Brugger W, Ceska M, Glienke W, Müller S, et al. Secretory Repertoire of HIV-Infected Human Monocytes/Macrophages. *Pathobiology* (1991) 59(4):219–22. doi: 10.1159/000163649
2. Lane HC, Masur H, Edgar LC, Whalen G, Rook AH, Fauci AS. Abnormalities of B-cell Activation and Immunoregulation in Patients With the Acquired Immunodeficiency Syndrome. *New Engl J Med* (1983) 309(8):453–8. doi: 10.1056/NEJM198308253090803
3. Hey-Nguyen WJ, Xu Y, Pearson CF, Bailey M, Suzuki K, Tantau R, et al. Quantification of Residual Germinal Center Activity and HIV-1 DNA and RNA Levels Using Fine Needle Biopsies of Lymph Nodes During Antiretroviral Therapy. *AIDS Res Hum Retroviruses* (2017) 33(7):648–57. doi: 10.1089/aid.2016.0171
4. Hazenberg MD, Stuart JWC, Otto SA, Borleffs JC, Boucher CA, de Boer RJ, et al. T-Cell Division in Human Immunodeficiency Virus (HIV)-1 Infection is Mainly Due to Immune Activation: A Longitudinal Analysis in Patients Before and During Highly Active Antiretroviral Therapy (HAART). *Blood* (2000) 95(1):249–55. doi: 10.1182/blood.V95.1.249.001k40_249_255
5. Zaunders JJ, Kaufmann GR, Cunningham PH, Smith D, Grey P, Suzuki K, et al. Increased Turnover of CCR5+ and Redistribution of CCR5- Cd4 T Lymphocytes During Primary Human Immunodeficiency Virus Type 1 Infection. *J Infect Dis* (2001) 183(5):736–43. doi: 10.1086/318827
6. Guadalupe M, Sankaran S, George MD, Reay E, Verhoeven D, Shacklett BL, et al. Viral Suppression and Immune Restoration in the Gastrointestinal Mucosa of Human Immunodeficiency Virus Type 1-Infected Patients Initiating Therapy During Primary or Chronic Infection. *J Virol* (2006) 80 (16):8236–47. doi: 10.1128/JVI.00120-06
7. Brenchley JM, Price DA, Schacker TW, Asher TE, Silvestri G, Rao S, et al. Microbial Translocation is a Cause of Systemic Immune Activation in Chronic HIV Infection. *Nat Med* (2006) 12(12):1365–71. doi: 10.1038/nm1511
8. Epple HJ, Allers K, Tröger H, Kühl A, Erben U, Fromm M, et al. Acute HIV Infection Induces Mucosal Infiltration With CD4+ and CD8+ T Cells, Epithelial Apoptosis, and a Mucosal Barrier Defect. *Gastroenterology* (2010) 139(4):1289–300. e2. doi: 10.1053/j.gastro.2010.06.065
9. Somsouk M, Estes JD, Deleage C, Dunham RM, Albright R, Inadomi JM, et al. Gut Epithelial Barrier and Systemic Inflammation During Chronic HIV Infection. *AIDS* (2015) 29(1):43–51. doi: 10.1097/QAD.0000000000000511
10. Nazli A, Chan O, Dobson-Belaire WN, Ouellet M, Tremblay MJ, Gray-Owen SD, et al. Exposure to HIV-1 Directly Impairs Mucosal Epithelial Barrier Integrity Allowing Microbial Translocation. *PloS Pathog* (2010) 6(4): e1000852. doi: 10.1371/journal.ppat.1000852
11. Tincati C, Merlini E, Braidotti P, Ancona G, Savi F, Tosi D, et al. Impaired Gut Junctional Complexes Feature Late-Treated Individuals With Suboptimal CD4+ T-Cell Recovery Upon Virologically Suppressive Combination Antiretroviral Therapy. *AIDS* (2016) 30(7):991–1003. doi: 10.1097/QAD.0000000000001015
12. Epple HJ, Schneider T, Troeger H, Kunkel D, Allers K, Moos V, et al. Impairment of the Intestinal Barrier is Evident in Untreated But Absent in Suppressively Treated HIV-Infected Patients. *Gut* (2009) 58(2):220–7. doi: 10.1136/gut.2008.150425
13. Chung CY, Alden SL, Funderburg NT, Fu P, Levine AD. Progressive Proximal-to-Distal Reduction in Expression of the Tight Junction Complex in Colonic Epithelium of Virally-Suppressed HIV+ Individuals. *PloS Pathog* (2014) 10(6):e1004198. doi: 10.1371/journal.ppat.1004198
14. Brenchley JM, Schacker TW, Ruff LE, Price DA, Taylor JH, Beilman GJ, et al. Cd4+ T Cell Depletion During All Stages of HIV Disease Occurs Predominantly in the Gastrointestinal Tract. *J Exp Med* (2004) 200(6):749–59. doi: 10.1084/jem.20040874
15. Guadalupe M, Reay E, Sankaran S, Prindiville T, Flamm J, McNeil A, et al. Severe CD4+ T-Cell Depletion in Gut Lymphoid Tissue During Primary Human Immunodeficiency Virus Type 1 Infection and Substantial Delay in Restoration Following Highly Active Antiretroviral Therapy. *J Virol* (2003) 77 (21):11708–17. doi: 10.1128/JVI.77.21.11708-11717.2003
16. Mehandru S, Poles MA, Tenner-Racz K, Horowitz A, Hurley A, Hogan C, et al. Primary HIV-1 Infection is Associated With Preferential Depletion of CD4+ T Lymphocytes From Effector Sites in the Gastrointestinal Tract. *J Exp Med* (2004) 200(6):761–70. doi: 10.1084/jem.20041196
17. DaFonseca S, Niessl J, Pouvreau S, Wacleche SV, Gosselin A, Cleret-Buhot A, et al. Impaired Th17 Polarization of Phenotypically Naive CD4+ T-Cells During Chronic HIV-1 Infection and Potential Restoration With Early ART. *Retrovirology* (2015) 12(1). doi: 10.1186/s12977-015-0164-6
18. D'Ettorre G, Baroncelli S, Micci L, Ceccarelli G, Andreotti M, Sharma P, et al. Reconstitution of Intestinal CD4 and Th17 T Cells in Antiretroviral Therapy Suppressed HIV-Infected Subjects: Implication for Residual Immune Activation From the Results of a Clinical Trial. *PloS One* (2014) 9(10): e109791. doi: 10.1371/journal.pone.0109791
19. Estes JD, Harris LD, Klatt NR, Tabb B, Pittaluga S, Paiardini M, et al. Damaged Intestinal Epithelial Integrity Linked to Microbial Translocation in Pathogenic Simian Immunodeficiency Virus Infections. *PloS Pathog* (2010) 6(8):e1001052. doi: 10.1371/journal.ppat.1001052
20. Kim CJ, McKinnon LR, Kovacs C, Kandel G, Huibner S, Chege D, et al. Mucosal Th17 Cell Function is Altered During HIV Infection and is an Independent Predictor of Systemic Immune Activation. *J Immunol* (2013) 191 (5):2164–73. doi: 10.4049/jimmunol.1300829
21. Gori A, Tincati C, Rizzardini G, Torti C, Quirino T, Haarman M, et al. Early Impairment of Gut Function and Gut Flora Supporting a Role for Alteration of Gastrointestinal Mucosa in Human Immunodeficiency Virus Pathogenesis. *J Clin Microbiol* (2008) 46(2):757–8. doi: 10.1128/JCM.01729-07
22. Dillon SM, Lee EJ, Kotter CV, Austin GL, Dong Z, Hecht DK, et al. An Altered Intestinal Mucosal Microbiome in HIV-1 Infection is Associated With Mucosal and Systemic Immune Activation and Endotoxemia. *Mucosal Immunol* (2014) 7(4):983–94. doi: 10.1038/mi.2013.116
23. Vujkovic-Cvijin I, Dunham RM, Iwai S, Maher MC, Albright RG, Broadhurst MJ, et al. Dysbiosis of the Gut Microbiota is Associated With HIV Disease Progression and Tryptophan Catabolism. *Sci Trans Med* (2013) 5 (193):193ra91. doi: 10.1126/scitranslmed.3006438
24. Liu J, Williams B, Frank D, Dillon SM, Wilson CC, Landay AL. Inside Out: HIV, the Gut Microbiome, and the Mucosal Immune System. *J Immunol* (2017) 198(2):605–14. doi: 10.4049/jimmunol.1601355
25. Smecuol E, Bai JC, Sugai E, Vazquez H, Niveloni S, Pedreira S, et al. Acute Gastrointestinal Permeability Responses to Different non-Steroidal Anti-Inflammatory Drugs. *Gut* (2001) 49(5):650–5. doi: 10.1136/gut.49.5.650
26. Buchner AM, Wallace MB. In-Vivo Microscopy in the Diagnosis of Intestinal Neoplasia and Inflammatory Conditions. *Histopathology* (2015) 66(1):137–46. doi: 10.1111/his.12597

27. Goetz M, Malek NP, Kiesslich R. Microscopic Imaging in Endoscopy: Endomicroscopy and Endocytoscopy. *Nat Rev Gastroenterol Hepatol* (2014) 11(1):11–8. doi: 10.1038/nrgastro.2013.134
28. Kiesslich R, Duckworth CA, Moussata D, Gloeckner A, Lim LG, Goetz M, et al. Local Barrier Dysfunction Identified by Confocal Laser Endomicroscopy Predicts Relapse in Inflammatory Bowel Disease. *Gut* (2012) 61(8):1146–53. doi: 10.1136/gutjnl-2011-300695
29. Lim LG, Neumann J, Hansen T, Goetz M, Hoffman A, Neurath MF, et al. Confocal Endomicroscopy Identifies Loss of Local Barrier Function in the Duodenum of Patients With Crohn's Disease and Ulcerative Colitis. *Inflammatory Bowel Dis* (2014) 20(5):892–900. doi: 10.1097/MIB.0000000000000027
30. Caradonna L, Amati L, Magrone T, Pellegrino N, Jirillo E, Caccavo D. Invited Review: Enteric Bacteria, Lipopolysaccharides and Related Cytokines in Inflammatory Bowel Disease: Biological and Clinical Significance. *J Endotoxin Res* (2000) 6(3):205–14. doi: 10.1177/09680519000060030101
31. Etcheverry-Rufino F, Lucero C, Lopez-Ceron M, Alenar-Gelabert Y, Fernandez I, Ugarte A, et al. Local Barrier Dysfunction Identified by Confocal Laser Endomicroscopy Predicts Bacterial Translocation in HIV Infection. *AIDS* (2020) 34(2):328–31. doi: 10.1097/QAD.0000000000002415
32. Koelsch KK, Boesecke C, McBride K, Gelgor L, Fahey P, Natarajan V, et al. Impact of Treatment With Raltegravir During Primary or Chronic HIV Infection on RNA Decay Characteristics and the HIV Viral Reservoir. *Aids* (2011) 25(17):2069–78. doi: 10.1097/QAD.0b013e32834b9658
33. Turcotte JF, Kao D, Mah SJ, Claggett B, Saltzman JR, Fedorak RN, et al. Breaks in the Wall: Increased Gaps in the Intestinal Epithelium of Irritable Bowel Syndrome Patients Identified by Confocal Laser Endomicroscopy (With Videos). *Gastrointestinal Endoscopy* (2013) 77(4):624–30. doi: 10.1016/j.gie.2012.11.006
34. Li C-Q, Xie X-J, Yu T, Gu X-M, Zuo X-L, Zhou C-J, et al. Classification of Inflammation Activity in Ulcerative Colitis by Confocal Laser Endomicroscopy. *Am J Gastroenterol* (2010) 105(6):1391–6. doi: 10.1038/ajg.2009.664
35. Zaunders J, Danta M, Bailey M, Mak G, Marks K, Seddiki N, et al. Cd4+ T Follicular Helper and Iga+ B Cell Numbers in Gut Biopsies From HIV-infected Subjects on Antiretroviral Therapy are Comparable to HIV-uninfected Individuals. *Front Immunol* (2016) 7(438):438. doi: 10.3389/fimmu.2016.00438
36. Jervis-Bardy J, Leong L, Marri S, Smith RJ, Choo JM, Smith-Vaughan HC, et al. Deriving Accurate Microbiota Profiles From Human Samples With Low Bacterial Content Through Post-Sequencing Processing of Illumina MiSeq Data. *Microbiome* (2015) 3(1):1–11. doi: 10.1186/s40168-015-0083-8
37. Caporaso JG, Kuczynski J, Stombaugh J, Bittinger K, Bushman FD, Costello EK, et al. QIIME Allows Analysis of High-Throughput Community Sequencing Data. *Nat Methods* (2010) 7(5):335–6. doi: 10.1038/nmeth.f.303
38. Hey-Cunningham WJ, Murray JM, Natarajan V, Amin J, Moore CL, Emery S, et al. Early Antiretroviral Therapy With Raltegravir Generates Sustained Reductions in HIV Reservoirs But Not Lower T-cell Activation Levels. *AIDS* (2015) 29(8):911–9. doi: 10.1097/QAD.0000000000000625
39. Schenkel JM, Masopust D. Tissue-Resident Memory T Cells. *Immunity* (2014) 41(6):886–97. doi: 10.1016/j.immuni.2014.12.007
40. Shaw JM, Hunt PW, Critchfield JW, McConnell DH, Garcia JC, Pollard RB, et al. Short Communication: HIV+ Viremic Slow Progressors Maintain Low Regulatory T Cell Numbers in Rectal Mucosa But Exhibit High T Cell Activation. *AIDS Res Hum Retroviruses* (2013) 29(1):172–7. doi: 10.1089/aid.2012.0268
41. Chang J, Ip M, Yang M, Wong B, Power T, Lin L, et al. The Learning Curve: Inter-Observer and Intra-Observer Agreement of Endoscopic Confocal Laser Endomicroscopy in the Assessment of Mucosal Barrier Defects. *Gastrointestinal Endoscopy* (2015) 83(4):785–91. doi: 10.1016/j.gie.2015.08.045
42. Lipkin M. Growth and Development of Gastrointestinal Cells. *Annu Rev Physiol* (1985) 47(1):175–97. doi: 10.1146/annurev.ph.47.030185.001135
43. Neumann H, Vieth M, Atreya R, Grauer M, Siebler J, Bernatik T, et al. Assessment of Crohn's Disease Activity by Confocal Laser Endomicroscopy. *Inflammatory Bowel Dis* (2012) 18(12):2261–9. doi: 10.1002/ibd.22907
44. Gordon SN, Cervasi B, Odorizzi P, Silverman R, Aberra F, Ginsberg G, et al. Disruption of Intestinal CD4+ T Cell Homeostasis is a Key Marker of Systemic CD4+ T Cell Activation in HIV-infected Individuals. *J Immunol* (2010) 185(9):5169–79. doi: 10.4049/jimmunol.1001801
45. Allers K, Puyskens A, Epple HJ, Schurmann D, Hofmann J, Moos V, et al. The Effect of Timing of Antiretroviral Therapy on CD4 T-Cell Reconstitution in the Intestine of HIV-infected Patients. *Mucosal Immunol* (2016) 9(1):265–74. doi: 10.1038/mi.2015.58
46. Hayes TL, Asmuth DM, Critchfield JW, Knight TH, McLaughlin BE, Yotter T, et al. Impact of Highly Active Antiretroviral Therapy Initiation on CD4+ T-Cell Repopulation in Duodenal and Rectal Mucosa. *AIDS (London England)* (2013) 27(6):867. doi: 10.1097/QAD.0b013e32835d85b4
47. Mehandru S, Poles MA, Tenner-Racz K, Jean-Pierre P, Manuelli V, Lopez P, et al. Lack of Mucosal Immune Reconstitution During Prolonged Treatment of Acute and Early HIV-1 Infection. *PloS Med* (2006) 3(12):2335–48. doi: 10.1371/journal.pmed.0030546
48. Yukl SA, Shergill AK, Girling V, Li Q, Killian M, Epling L, et al. Site-Specific Differences in T Cell Frequencies and Phenotypes in the Blood and Gut of HIV-uninfected and ART-treated HIV+ Adults. *PloS One* (2015) 10(3):e0121290. doi: 10.1371/journal.pone.0121290
49. Van Kruiningen HJ, West AB, Freda BJ, Holmes KA. Distribution of Peyer's Patches in the Distal Ileum. *Inflammatory Bowel Dis* (2002) 8(3):180–5. doi: 10.1097/00054725-200205000-00004
50. Zaunders J, Xu Y, Kent SJ, Koelsch KK, Kelleher AD. Divergent Expression of CXCR5 and CCR5 on CD4+ T Cells and the Paradoxical Accumulation of T Follicular Helper Cells During HIV Infection. *Front Immunol* (2017) 8:495. doi: 10.3389/fimmu.2017.00495
51. Giorgi JV, Liu Z, Hultin LE, Cumberland WG, Hennessey K, Detels R. Elevated Levels of CD38+ Cd8+ T Cells in HIV Infection Add to the Prognostic Value of Low CD4+ T Cell Levels: Results of 6 Years of Follow-Up. The Los Angeles Center, Multicenter Aids Cohort Study. *J Acquir Immune Defic Syndr* (1993) 6(8):904–12.
52. Younas M, Psomas C, Reynes J, Corbeau P. Immune Activation in the Course of HIV-1 Infection: Causes, Phenotypes and Persistence Under Therapy. *HIV Med* (2016) 17(2):89–105. doi: 10.1111/hiv.12310
53. Zaunders JJ, Cunningham PH, Kelleher AD, Kaufmann GR, Jaramillo AB, Wright R, et al. Potent Antiretroviral Therapy of Primary Human Immunodeficiency Virus Type 1 (HIV-1) Infection: Partial Normalization of T Lymphocyte Subsets and Limited Reduction of HIV-1 DNA Despite Clearance of Plasma Viremia. *J Infect Dis* (1999) 180(2):320–9. doi: 10.1086/314880
54. Banga R, Procopio FA, Noto A, Pollakis G, Cavassini M, Ohmiti K, et al. Pd-1(+) and Follicular Helper T Cells are Responsible for Persistent HIV-1 Transcription in Treated Aviremic Individuals. *Nat Med* (2016) 22(7):754–61. doi: 10.1038/nm.4113
55. Yukl SA, Shergill AK, McQuaid K, Gianella S, Lampiris H, Hare CB, et al. Effect of Raltegravir-Containing Intensification on HIV Burden and T-cell Activation in Multiple Gut Sites of HIV-positive Adults on Suppressive Antiretroviral Therapy. *Aids* (2010) 24(16):2451–60. doi: 10.1097/QAD.0b013e32833ef7bb
56. Anderson JL, Khoury G, Fromentin R, Solomon A, Chomont N, Sinclair E, et al. Human Immunodeficiency Virus (Hiv)-Infected CCR6+ Rectal Cd4+ T Cells and HIV Persistence On Antiretroviral Therapy. *J Infect Dis* (2020) 221(5):744–55. doi: 10.1093/infdis/jiz509
57. McBride K, Xu Y, Bailey M, Seddiki N, Suzuki K, Gao Y, et al. The Majority of HIV-1 DNA in Circulating CD4+ T Lymphocytes is Present in non-Gut Homing Resting Memory CD4+ T Cells. *AIDS Res Hum Retroviruses* (2013) 29(10):1330–9. doi: 10.1089/aid.2012.0351
58. Cribbs SK, Lennox J, Caliendo AM, Brown LA, Guidot DM. Healthy HIV-1-infected Individuals on Highly Active Antiretroviral Therapy Harbor HIV-1 in Their Alveolar Macrophages. *AIDS Res Hum Retroviruses* (2015) 31(1):64–70. doi: 10.1089/aid.2014.0133
59. Spudich S, Robertson KR, Bosch RJ, Gandhi RT, Cyktor JC, Mar H, et al. Persistent HIV-infected Cells in Cerebrospinal Fluid are Associated With Poorer Neurocognitive Performance. *J Clin Invest* (2019) 129(8):3339–46. doi: 10.1172/JCI127413
60. Suzuki K, Zaunders J, Levert A, Butterly S, Liu Z, Ishida T, et al. Neuron Damage and Reservoir are Secondary to HIV Transcripts Despite Suppressive ART. *Topics in Antiviral Medicien*. (2021) 29(1):49
61. Mutlu EA, Keshavarzian A, Losurdo J, Swanson G, Siewe B, Forsyth C, et al. A Compositional Look At the Human Gastrointestinal Microbiome and

Immune Activation Parameters in HIV Infected Subjects. *PloS Pathog* (2014) 10(2):e1003829. doi: 10.1371/journal.ppat.1003829
62. Riviere A, Selak M, Lantin D, Leroy F, De Vuyst L. Bifidobacteria and Butyrate-Producing Colon Bacteria: Importance and Strategies for Their Stimulation in the Human Gut. *Front Microbiol* (2016) 7:979. doi: 10.3389/fmicb.2016.00979
63. Peng L, Li ZR, Green RS, Holzman IR, Lin J. Butyrate Enhances the Intestinal Barrier by Facilitating Tight Junction Assembly Via Activation of AMP-activated Protein Kinase in Caco-2 Cell Monolayers. *J Nutr* (2009) 139 (9):1619–25. doi: 10.3945/jn.109.104638
64. Iljazovic A, Roy U, Galvez EJC, Lesker TR, Zhao B, Gronow A, et al. Perturbation of the Gut Microbiome by Prevotella Spp. *enhances Host susceptibility to Mucosal inflammation Mucosal Immunol* (2021) 14(1):113–24. doi: 10.1038/s41385-020-0296-4
65. Ma TY, Iwamoto GK, Hoa NT, Akotia V, Pedram A, Boivin MA, et al. Tnf-α-Induced Increase in Intestinal Epithelial Tight Junction Permeability Requires NF-κb Activation. *Am J Physiol Gastrointest Liver Physiol* (2004) 286(3): G367–G76. doi: 10.1152/ajpgi.00173.2003
66. Al-Sadi RM, Ma TY. Il-1β Causes an Increase in Intestinal Epithelial Tight Junction Permeability. *J Immunol* (2007) 178(7):4641–9. doi: 10.4049/jimmunol.178.7.4641
67. BenMarzouk-Hidalgo OJ, Torres-Cornejo A, Gutierrez-Valencia A, Ruiz-Valderas R, Viciana P, Lopez-Cortes LF. Differential Effects of Viremia and Microbial Translocation on Immune Activation in HIV-Infected Patients Throughout Ritonavir-Boosted Darunavir Monotherapy. *Medicine* (2015) 94 (17):e781. doi: 10.1097/MD.0000000000000781
68. Li Z, Li W, Li N, Jiao Y, Chen D, Cui L, et al. γδ T Cells are Involved in Acute HIV Infection and Associated With AIDS Progression. *PloS One* (2014) 9(9): e106064. doi: 10.1371/journal.pone.0106064
69. Rajasuriar R, Booth D, Solomon A, Chua K, Spelman T, Gouillou M, et al. Biological Determinants of Immune Reconstitution in HIV-infected Patients Receiving Antiretroviral Therapy: The Role of Interleukin 7 and Interleukin 7 Receptor α and Microbial Translocation. *J Infect Dis* (2010) 202(8):1254–64. doi: 10.1086/656369
70. Cioe PA, Baker J, Kojic EM, Onen N, Hammer J, Patel P, et al. Elevated Soluble CD14 and Lower D-Dimer Are Associated With Cigarette Smoking and Heavy Episodic Alcohol Use in Persons Living With Hiv. *JAIDS J Acquired Immune Deficiency Syndromes* (2015) 70(4):400–5. doi: 10.1097/QAI.0000000000000759
71. Valiathan R, Miguez MJ, Patel B, Arheart KL, Asthana D. Tobacco Smoking Increases Immune Activation and Impairs T-cell Function in HIV Infected Patients on Antiretrovirals: A Cross-Sectional Pilot Study. *PloS One* (2014) 9 (5):e97698. doi: 10.1371/journal.pone.0097698
72. Chege D, Sheth PM, Kain T, Kim CJ, Kovacs C, Loutfy M, et al. Sigmoid Th17 Populations, the HIV Latent Reservoir, and Microbial Translocation in Men on Long-Term Antiretroviral Therapy. *Aids* (2011) 25(6):741–9. doi: 10.1097/QAD.0b013e328344cefb
73. Miron N, Cristea V. Enterocytes: Active Cells in Tolerance to Food and Microbial Antigens in the Gut. *Clin Exp Immunol* (2012) 167(3):405–12. doi: 10.1111/j.1365-2249.2011.04523.x
74. Mowat AM. Anatomical Basis of Tolerance and Immunity to Intestinal Antigens. *Nat Rev Immunol* (2003) 3(4):331–41. doi: 10.1038/nri1057
75. Hufert FT, Schmitz J, Schreiber M, Schmitz H, Rácz P, von Laer DD. Human Kupffer Cells Infected With HIV-1 In Vivo. *JAIDS J Acquired Immune Deficiency Syndromes* (1993) 6(7):772–7.
76. Balagopal A, Ray SC, De Oca RM, Sutcliffe CG, Vivekanandan P, Higgins Y, et al. Kupffer Cells are Depleted With HIV Immunodeficiency and Partially Recovered With Antiretroviral Immunereconstitution: HIV, Kupffer Cells and Antiretroviral Therapy. *AIDS (London England)* (2009) 23(18):2397. doi: 10.1097/QAD.0b013e3283324344
77. Sabin CA. Do People With HIV Infection Have a Normal Life Expectancy in the Era of Combination Antiretroviral Therapy? *BMC Med* (2013) 11(1):251. doi: 10.1186/1741-7015-11-251
78. Justice A, Falutz J. Aging and HIV: An Evolving Understanding. *Curr Opin HIV AIDS* (2014) 9(4):291–3. doi: 10.1097/COH.0000000000000081
79. Marcus JL, Leyden WA, Alexeeff SE, Anderson AN, Hechter RC, Hu H, et al. Comparison of Overall and Comorbidity-Free Life Expectancy Between Insured Adults With and Without Hiv Infection, 2000-2016. *JAMA Netw Open* (2020) 3(6):e207954. doi: 10.1001/jamanetworkopen.2020.7954

Conflict of Interest: The authors declare that the research was conducted in the absence of any commercial or financial relationships that could be construed as a potential conflict of interest.

The handling editor has declared a shared affiliation, though no other collaboration with one of the authors NS at the time of review.

frontiers in Immunology

REVIEW
published: 18 June 2021
doi: 10.3389/fimmu.2021.670566

Contribution of Adipose Tissue to the Chronic Immune Activation and Inflammation Associated With HIV Infection and Its Treatment

Christine Bourgeois[1], Jennifer Gorwood[2], Anaelle Olivo[1], Laura Le Pelletier[2], Jacqueline Capeau[2], Olivier Lambotte[1,3], Véronique Béréziat[2*†] and Claire Lagathu[2*†]*

[1] CEA - Université Paris Saclay - INSERM U1184, Center for Immunology of Viral Infections and Autoimmune Diseases, IDMIT Department, IBFJ, Fontenay-aux-Roses, France, [2] Sorbonne Université, INSERM UMR_S 938, Centre de Recherche Saint-Antoine, Institut Hospitalo-Universitaire de Cardio-métabolisme et Nutrition (ICAN), FRM EQU201903007868, Paris, France, [3] AP-HP, Groupe Hospitalier Universitaire Paris Saclay, Hôpital Bicêtre, Service de Médecine Interne et Immunologie Clinique, Le Kremlin-Bicêtre, France

OPEN ACCESS

Edited by:
Nicholas Funderburg, The Ohio State University, United States

Reviewed by:
Cristian Apetrei, University of Pittsburgh, United States
Karen Ingrid Tasca, São Paulo State University, Brazil

***Correspondence:**
Christine Bourgeois
christine.bourgeois@u-psud.fr
Véronique Béréziat
veronique.bereziat@inserm.fr
Claire Lagathu
claire.lagathu@inserm.fr

[†]These authors have contributed equally to this work

Specialty section:
This article was submitted to Viral Immunology, a section of the journal Frontiers in Immunology

Received: *21 February 2021*
Accepted: *24 May 2021*
Published: *18 June 2021*

Citation:
Bourgeois C, Gorwood J, Olivo A, Le Pelletier L, Capeau J, Lambotte O, Béréziat V and Lagathu C (2021) Contribution of Adipose Tissue to the Chronic Immune Activation and Inflammation Associated With HIV Infection and Its Treatment. Front. Immunol. 12:670566. doi: 10.3389/fimmu.2021.670566

White adipose tissue (AT) contributes significantly to inflammation – especially in the context of obesity. Several of AT's intrinsic features favor its key role in local and systemic inflammation: (i) large distribution throughout the body, (ii) major endocrine activity, and (iii) presence of metabolic and immune cells in close proximity. In obesity, the concomitant pro-inflammatory signals produced by immune cells, adipocytes and adipose stem cells help to drive local inflammation in a vicious circle. Although the secretion of adipokines by AT is a prime contributor to systemic inflammation, the lipotoxicity associated with AT dysfunction might also be involved and could affect distant organs. In HIV-infected patients, the AT is targeted by both HIV infection and antiretroviral therapy (ART). During the primary phase of infection, the virus targets AT directly (by infecting AT CD4 T cells) and indirectly (via viral protein release, inflammatory signals, and gut disruption). The initiation of ART drastically changes the picture: ART reduces viral load, restores (at least partially) the CD4 T cell count, and dampens inflammatory processes on the whole-body level but also within the AT. However, ART induces AT dysfunction and metabolic side effects, which are highly dependent on the individual molecules and the combination used. First generation thymidine reverse transcriptase inhibitors predominantly target mitochondrial DNA and induce oxidative stress and adipocyte death. Protease inhibitors predominantly affect metabolic pathways (affecting adipogenesis and adipocyte homeostasis) resulting in insulin resistance. Recently marketed integrase strand transfer inhibitors induce both adipocyte adipogenesis, hypertrophy and fibrosis. It is challenging to distinguish between the respective effects of viral persistence, persistent immune defects and ART toxicity on the inflammatory profile present in ART-controlled HIV-infected patients. The host metabolic status, the size of the pre-established viral reservoir, the quality of the immune restoration, and the natural ageing with associated comorbidities may mitigate and/or reinforce the contribution of antiretrovirals (ARVs)

toxicity to the development of low-grade inflammation in HIV-infected patients. Protecting AT functions appears highly relevant in ART-controlled HIV-infected patients. It requires lifestyle habits improvement in the absence of effective anti-inflammatory treatment. Besides, reducing ART toxicities remains a crucial therapeutic goal.

Keywords: adipose tissue, HIV infection, fat, antiretroviral treatment, chronic inflammation, chronic immune activation

THE BIOLOGY OF ADIPOSE TISSUE

Several "Colors" of Adipose Tissue: White, Brown, Beige, and Pink

Adipose tissue (AT) is a loose connective tissue composed of differentiated adipocytes and stroma/vascular cells (a heterogeneous cell population including endothelial cells, immune cells, fibroblasts, and adipocyte precursors). White adipocytes are characterized by a single, large droplet of cytoplasmic fat and a flattened nucleus. Brown adipocytes contain several small lipid droplets and large numbers of mitochondria and lysosomes; the latter are responsible for the tissue's brown color. Beige adipocytes (white adipocytes that have differentiated into brown adipocytes) are characterized by multilocular lipid droplets. Lastly, pink adipocytes are white adipocytes that have differentiated into milk-producing gland cells during pregnancy, lactation, and post-lactation (1).

The various ATs differ with regard to their metabolic activity, sites, plasticity, vascularization and innervation. White adipose tissue (WAT) is the main site for lipid storage and mobilization and has a high secretion capacity. The activity of WAT is strongly linked to inflammation in healthy individuals (where low-grade inflammation is required for correct metabolic activity) (2), and even more so in ageing and in people with fat gain/obesity (where the more intense inflammation contributes to the loss of metabolic activity) (3). Brown adipose tissue (BAT, mainly characterized in rodents) ensures non-shivering thermogenesis; it can maintain thermal homeostasis by dissipating large amounts of energy in the form of heat. It used to be thought that BAT was only present in meaningful amounts in infants and that it regressed and become metabolically inactive in adults. However, recent positron emission tomography (PET) imaging studies of glucose uptake have revealed the presence of substantial deposits of thermogenic fat in adult humans (4, 5). Besides being highly metabolically active, BAT is densely innervated by the sympathetic nervous system (6) and is relatively insensitive to inflammatory signals. Recent studies have demonstrated the presence of brown-like adipocytes in WAT. These "Beige" adipocytes (also referred to as "browned" or "brite" ["brown in white"] adipocytes) are highly thermogenic adipocytes (6). They are functionally flexible and can either store or dissipate energy, depending on the environmental or physiological circumstances. Like brown adipocytes, beige adipocytes oxidize fatty acids and glucose and have large numbers of mitochondria. In response to various stimuli, the energy is dissipated as heat through uncoupled respiration (7). This mechanism is mediated by the uncoupling protein-1 (UCP-1) present in the inner mitochondrial membrane. Beige adipocytes can enhance energy expenditure by inducing a futile cycle that involves free fatty acid (FFA) β-oxidation and re-esterification (8, 9). This process might constitute a crucial adaptive response to excess energy supplies. In humans, the correlation between leanness and high levels of brown and beige fat activity suggests that these ATs have an important metabolic role (4, 5, 10).

Adipocytes are highly plastic, as exemplified by the beiging process, which corresponds to recruitment of the adaptive thermogenic adipocytes. Beiging may be a novel therapeutic target for mitigating lipid storage, alleviating metabolic disorders and thus dampening the associated inflammatory profile.

A Focus on WAT and Its Unique Properties

WAT Is Influential Because of Its Large Mass and Broad Distribution

WAT is the body's main energy reservoir; it stores energy as triglycerides and releases energy (in response to hormonal stimuli) as FFAs. This AT accounts for 15 to 25% of body weight in lean, healthy individuals and much greater percentage in overweight and obese people. In contrast to BAT, WAT is distributed throughout the body. There are two main types of WAT: subcutaneous adipose tissue (SCAT, accounting for about 80% of AT in lean individuals) and visceral adipose tissue (VAT, located in the intra-abdominal cavity, e.g. at omental, mesenteric, and retroperitoneal sites). Although lean individuals have a small amount of VAT, this tissue expands considerably in people with metabolic disorders. Intra-abdominal VAT is able to communicate with nearby internal organs, such as the intestinal tract and the liver. Several mechanisms are involved in this communication, with the release of metabolites, hormones, cytokines and miRNAs (11, 12). Perivascular AT, epicardial AT, lymph-node (LN)-associated AT, bone-marrow (BM)-infiltrating AT, and (in the context of metabolic disorders) ectopic AT in liver or muscles have been described (see section 4). Lastly, the anatomical distribution of WAT in contact with the external environment (such as the intestinal tract and the skin) and with immune structures (LNs, BM, and thymus) might be crucial in the modulation of local immune responses.

WAT Is Also a Major Endocrine Organ

WAT is less metabolically active than BAT but has a unique endocrine profile. The main endocrine activity in WAT is adipokine secretion [for a review, see (13)]. In fact, WAT secretes over 400 different adipokines, which are usually

categorized as being anti-inflammatory or pro-inflammatory but also contribute to metabolic regulation. Some of these adipokines are produced by the adipocytes themselves (such as the prototypical adipokines leptin and adiponectin), whereas others are mainly produced by immune cells located in the AT (interleukin (IL)-6, tumor necrosis factor (TNF)-α, IL-8, monocyte chemoattractant protein 1 (MCP-1), regulated upon activation, normal T cell expressed and presumably secreted chemokine (RANTES), *etc.*) (**Table 1**). The well-known satiety factor leptin is secreted specifically by adipocytes in SCAT and (to a lesser extent) VAT and has a role in energy regulation. Blood leptin levels are correlated with the AT mass. Adiponectin is the other main adipocyte-specific adipokine. It is mainly secreted by VAT and is known to enhance fatty acid oxidation by muscle tissue and to increase the action of insulin in the liver. Thus, blood adiponectin levels are inversely correlated with insulin resistance. Importantly, both leptin and adiponectin also have immunomodulatory functions (20, 21).

The influence of adipose-secreted factors on systemic and distal inflammation, angiogenesis, vascular homeostasis, fibrolysis, and the immune system is not fully understood (22) and is being evaluated in various diseases [including inflammatory arthritis, autoimmunity (23), inflammatory bowel disease (24), and cancer (25)]. The AT's adipokine secretion profile is strongly modulated by the metabolic and inflammatory context. The various bioactive adipokines exert autocrine, paracrine and endocrine effects on local and systemic targets. The AT's endocrine activity appears to depend on the adipokine in question and the tissue site: SCAT produces IL-6 and TNF-α but the latter does not have an endocrine effect (26, 27). In contrast, the TNF-α produced by mesenteric AT contributes to inflammation in the mesentery (28). Most recently, AT has also been identified as a site of miRNA production; miRNAs with endocrine activity are packaged into exosomes and then released into the circulation (11).

Metabolic and Immune Cells Coexist in AT

The influence of AT on acute or chronic immune responses depends on the resident immune cells. As mentioned above, AT contains differentiated adipocytes and stromal/vascular cells. Virtually all the known types of immune cell have been detected in WAT: eosinophils, neutrophils, mast cells, macrophages, T lymphocytes (including regulatory T cells, CD4 and CD8 αβ T cells, γδ T cells, and natural killer (NK) T cells), type I and II innate lymphoid cells, and invariant NK cells (29). Remarkably, the presence of immune cells is required for the full metabolic activity of AT under normal conditions. Macrophages (including M2 anti-inflammatory and M1 pro-inflammatory subsets) and T lymphocytes are the most numerous immune cells in AT. The macrophages clear dead adipocytes, buffer lipids and contribute to angiogenesis (30). The regulatory CD4 T cell (Tregs) fraction is highly represented in lean AT in some mouse models (31). Other Th2-like cells (e.g. eosinophils) also help to limit excessive inflammation and modulate lipogenesis (32). Importantly, a degree of inflammation in AT is essential for homeostasis (2). Whereas adipose stem cells (ASCs) are crucial for metabolic homeostasis, they also send immunomodulatory signals to immune cells. In an *in vitro* study of the immunomodulatory effect of ASCs on macrophages isolated from osteoarthritic synovial tissue, the secretion of prostaglandin E2 favored the M1-to-M2 transition (33). *In vitro* culture of human ASCs with T lymphocytes also induces immunosuppression through the PD1/PDL1 Gal-9/TIM-3 pathways (34). The interplay between immune and metabolic cells is subtle, and metabolic stress induce changes in the immune cells' composition and functions.

TABLE 1 | Cytokine production by AT.

	Differences between VAT and SCAT			Cell source	
				Adipocytes	Stromal/vascular cells
Pro-inflammatory factors					
IL-6	VAT	>	SCAT	++	++
TNF-α	VAT	=	SCAT	+	+++
IL-1β	VAT	>	SCAT	+	++
Resistin	VAT	>	SCAT	+	++
Leptin	SCAT	>	VAT	+++	–
Chemokines					
IL-8	VAT	>	SCAT	+	++
RANTES	VAT	>	SCAT	+	++
MCP-1	VAT	>	SCAT	+	++
Anti-inflammatory factors					
IL-10	VAT	=	SCAT	+	++
IL-1Rα	VAT	=	SCAT	+	+
IL-4	VAT	>	SCAT	+	++
Adiponectin	VAT	>	SCAT	+++	–

The table gives a non-exhaustive list of adipokines/cytokines with prominent pro- or anti-inflammatory activities from among the 400 produced by AT. Three groups are defined here: pro-inflammatory cytokines (IL-6, Tumor necrosis factor (TNF-α), IL-1β, resistin, and leptin); chemokines (IL-8, monocyte chemoattractant protein 1 (MCP-1), regulated upon activation, normal T cell expressed and presumably secreted chemokine (RANTES)), and anti-inflammatory factors (IL-10, IL-1Rα, IL-4, and adiponectin). The secretion profile depends on the site (i.e. SCAT vs. VAT) and the cell type (14–19).

SCAT, Subcutaneous adipose tissue; VAT, Visceral adipose tissue; IL, Interleukin.

In addition to having key roles in metabolic regulation, these immune cells notably exhibit immune and cytokine-secreting activities that might contribute directly to systemic inflammation and/or sustain/exacerbate local inflammation in AT. Recent research has suggested that tissue-resident T lymphocytes contribute to secondary immune responses by migrating towards lymphoid sites, although the underlying mechanisms have not been fully evaluated (35, 36). If this process occurs in AT (e.g. with the release of memory T cells into draining LNs), it might constitute a novel way in which AT contributes to chronic immune activation.

Functional Differences Between SCAT and VAT

Although SCAT and VAT are morphologically similar; the latter is more densely vascularized and innervated and contains larger numbers of adipocytes, and immune cells (37).

Metabolic Differences

A growing body of evidence suggests that SCAT and VAT differ in their metabolic characteristics (38, 39) and thus their functions. VAT has a lower proportion of preadipocytes and a higher proportion of large adipocytes (39). Furthermore, VAT adipocytes are more insulin-resistant than SCAT adipocytes but also have a higher metabolic rate. In fact, VAT is more sensitive to adrenergic stimulation and thus more prone to lipolysis and FFA release. In contrast, SCAT buffers levels of FFAs and triglycerides. The progenitor cells' adipogenic capacity is closely linked to metabolic changes. In obesity, hypertrophic adipocytes (which contribute to contribute to insulin resistance) are frequently observed in VAT (40), and VAT expansion is correlated with the onset of metabolic disorders (41, 42). Adipocyte precursors isolated from SCAT displayed a higher adipogenic potential than those from VAT (40). In rodent models of obesity, it has been shown that SCAT is metabolically beneficial. Indeed, the intra-abdominal transplantation of SCAT ameliorates several metabolic parameters, including insulin resistance (43). Likewise, removal of VAT can prevent the onset of insulin resistance (44).

Endocrine and Immune Differences

VAT *vs.* SCAT differences in endocrine activity have been documented in both healthy lean individuals and obese individuals (**Table 1**). The differences are more pronounced in the context of obesity. In healthy individuals, differences in C-C chemokine receptor type 2 (CCR2) and macrophage migration inhibitory factor (MIF) (45, 46) have been reported, and adiponectin is secreted more by VAT than by SCAT. However, VAT is prone to being pro-inflammatory in response to obesity. IL-6 is secreted more by VAT than by abdominal SCAT, whereas leptin is secreted more by SCAT. On the cellular level, no difference in the number of macrophages has been detected, although VAT has a more pro-inflammatory profile than SCAT (47). In mice fed a high-fat diet, macrophage infiltration is increased rapidly in VAT but not in SCAT (48, 49). It is noteworthy that macrophages and inflammation also contribute to the remodeling of the extracellular matrix (ECM). In VAT in obese individuals, increased fibrosis (characterized by the excessive production of ECM components) interrupts normal metabolic functions and accentuates inflammatory responses (48, 49) (see the following section).

Differences Between Subcutaneous Upper Versus Lower Fat

The SCAT is the greater fat mass in healthy individuals, and differential capacity for certain subcutaneous regions are described, notably lower-body (gluteal fat, subcutaneous leg fat, and intramuscular fat), and upper-body subcutaneous fat (including abdominal SCAT) (50). Although the accumulation of upper fat (abdominal obesity, including visceral and abdominal subcutaneous) is associated with the development of cardiovascular disease and type 2 diabetes mellitus, lower-body fat has protective properties that are associated with an improved cardiometabolic risk profile in men and women (51). However, the underlying mechanisms for the functional differences between upper and lower-body AT remain elusive (52). The observation that regional characteristics are retained *in vitro* strongly indicates that the differences in adipocyte functions are inherent to the depot rather than a consequence of the local microenvironment. Abdominal and gluteofemoral SCAT present differentially-expressed developmental genes (53, 54) including members of the homeobox (HOX) family, HOX-domain encoding genes and T-box genes. In addition, lower-body AT is characterized by low lipid mobilization (55, 56) through α-adrenergic (antilipolytic) receptors. The release rates of non-esterified fatty acid (NEFA) are lower, in accordance with the reduced overall turnover of the triglyceride pool of this tissue (52). On the other side, abdominal SCAT is characterized by smaller adipocytes, higher expression of adipogenic, lipolytic, and mitochondrial genes associated with lower oxygen consumption (57) and the capacity to recruit new adipocytes seems limited in this tissue. Thus, different metabolic pathways regulate lipid metabolism in upper- *versus* lower-body fat and these tissues respond differently to weight gain in favor of a causality between lower-body fat accumulation and reduced risk of cardiometabolic diseases.

The Plasticity of AT and Fibrosis in the Context of Obesity/Metabolic Disorders

AT is highly plastic, so that it can regulate energy influx and efflux. Adipocytes react to energy overload by initiating hypertrophy (an increase in cell size, due to lipogenesis and triglyceride accumulation) and hyperplasia (an increase in cell number, due to adipogenesis); both of these processes are associated with metabolic and endocrine changes, as extensively reviewed elsewhere (13, 58, 59). During AT expansion, the ECM requires remodeling to accommodate adipocyte growth. In AT, the ECM is characterized by collagens; these are produced mainly by adipocytes but also by stromal/vascular cells. Adipocytes are maintained within an ECM network whose deposition is impaired during obesity. Fibrosis can mechanically limit tissue plasticity and contribute to metabolic impairments (60). In obese individuals, the presence

of pericellular fibrosis and fibrosis bundles was negatively correlated with hypertrophy (61). In this context, fibrosis is associated with inflammation and insulin resistance (60, 62, 63). Moreover, ECM deposition was found to be higher in SCAT than in VAT in both lean and obese subjects (63),, although adipocyte hypertrophy in VAT coincides with increased adipocyte death, formation of crown-like structure, inflammation, and insulin resistance (60, 64, 65). Simultaneous changes in the immune cell compartment are also observed and drastically modify the AT's secretory profile (66). Although adipocytes secrete some pro-inflammatory cytokines (IL-6, TNFα, and IL-8) at low levels, immune cells account for most of the cytokine secretion.

Immune System Activation and Inflammatory Activity of AT in Obese Contexts

AT inflammation is a standard feature of obesity, and mainly involves AT macrophages. Macrophage accumulation and a progressive shift from an M2 phenotype to an M1 phenotype are observed in AT during obesity (49). This translates into a shift from the secretion of immunosuppressive cytokines [such as IL-10 and transforming growth factor β (TGF-β)] to the secretion of pro-inflammatory cytokines (such as IL-6, TNF-α, MCP-1, IL-12, IL-23, and IL-1β). However, several mechanisms are involved in the shift in the AT's inflammatory profile; they include the direct impact of adipocyte dysfunction and M1 differentiation (both through the adipocyte's cytokine production (67) and lipid buffering) and the local influence of other immune events, such as neutrophil accumulation, Th1 bias (leading to greater IFN-γ production), and a reduction in the proportion of Tregs. The recruitment of neutrophils (rather than eosinophils) also contributes to the AT's pro-inflammatory secretion profile; the production of superoxide, elastase and myeloperoxidase by neutrophils and IL-1β production contribute to the inflammatory response (68). The Th2-Th1 shift and the recruitment of CD8 T cells increase the level of IFN-γ production, favors M1 macrophage polarization, and activates adipocytes (69). Additionally, Th17 cells are also recruited in AT in obese contexts, under the combined influences of AT macrophages, ASC and adipocytes (70). Recruitment of NK cells is also described in visceral (epididymal) but not subcutaneous AT in the HFD mouse model. The upregulation of NK activating ligands by adipocytes contributes to the increase in NK cells in SCAT, that will subsequently contribute to M1 macrophage differentiation (48, 71). The exact sequence of events is still not fully known, although neutrophils and CD8 T cells appear to have crucial roles in the initiation of local inflammatory responses (68, 72) because they are detected before the accumulation of macrophages. Moreover, inflammatory macrophages disrupt ECM homeostasis, which leads to fibrosis (2). Lastly, advanced glycation end-products (AGE) that are increased in obese diabetic patients, impact both adipocyte and immune cells functions, as both cell types express the receptor for AGE (RAGE) (73, 74). On the whole, inflammation in AT is triggered by several integrated mechanisms and involves the various cell subsets in the AT, i.e. immune cells, adipocytes, and (presumably) ASCs - a shift towards a more inflammatory profile has not been described for the latter. In a vicious circle, the concomitant pro-inflammatory signals produced by these various cell types help to drive local inflammation.

Contribution of AT to Low-Grade Inflammation During Obesity

Obesity is associated with low-grade inflammation (75–77) and insulin resistance (78). It is generally acknowledged that the secretion of adipokines by AT contributes to overall inflammation, although the exact contribution of a given pro-inflammatory cytokine to local and/or systemic inflammation is difficult to evaluate. The complexity of the inflammatory network that develops in AT (involving intricate, redundant, time-framed interactions between pro-inflammatory signals) is an initial hurdle. The integrated metabolic and inflammatory processes that drive each other in the AT (79) and thus amplify local inflammation constitute a second hurdle. Lastly, a third level of complexity relates to the opposing influences of cytokines produced by metabolic vs. immune cells, since the results appear to depend on the type of producing cell for IL-6 (80) and type I interferon [as reviewed in (81)] (82, 83). Although the secretion of adipokines by AT contributes to overall inflammation, the low-grade inflammation observed in the blood is due to many inflammatory factors, including lipotoxicity, disruption of gut microbiota, and systemic immune activation. The severity of obesity and the development of metabolic comorbidities (84) must also be taken into account.

CAUSES OF ADIPOSE TISSUE ALTERATIONS DURING HIV INFECTION

HIV infection in ART-naive patients is characterized by wasting, affecting both muscle and fat mass. ART-naive patients have lower SCAT volume and decreased whole tissue expression of pro-adipogenic genes compared to HIV-negative controls together with decreased mitochondrial DNA (mtDNA) content and reduced expression of mitochondria-encoded proteins that are required for adequate adipocyte metabolic function (85). Different AT alterations were observed in HIV-infected patients receiving ART. Although HIV impacts AT biology per se and metabolic profile (86), these changes were mainly attributed to the ART. The first-generation drugs taken by patients had lipotoxic effects; the resulting lipoatrophy gave rise to a syndrome called "ART-related lipodystrophy". Once lipotoxic molecules had been replaced by less toxic drugs, patients progressively gained fat (mainly on the trunk). The broad use of the newer class of integrase strand transfer inhibitors (INSTIs) now means that some patients can increase their overall fat mass. Understanding why AT mass, distribution, and function are often altered in HIV-infected patients (regardless of the type of ART) is a real challenge. Viral persistence certainly has an

important role, together with HIV-related changes in the immune context inside and outside AT. The fact that the patients' fat alterations became severe only after the introduction of ART molecules (i) emphasizes the drugs' essential contribution to harmful changes and (ii) suggests that HIV and some antiretrovirals (ARVs) act in synergy on adipocytes and other adipose cells to induce metabolic and inflammatory dysfunctions in AT and thus trigger adverse events in other tissues.

HIV-Related Fat Alterations: The Impact of HIV Infection on AT Biology

Although ART is clearly associated with adverse events, the presence of metabolic alterations in treatment-naive, HIV-infected people (86) suggests that the virus itself also has an impact on AT biology. All the studies performed in the 2000s found that adipocytes were not infected by HIV (87, 88) and that no HIV components were present in these cells. However, other HIV-related mechanisms have been identified (**Figure 1**).

Viral Proteins

Since viral proteins are present in patients with no detectable viral load (87, 89, 90), it has been suggested that Vpr, Nef, Tat and Gag have an impact on AT.

The mechanisms whereby viral proteins might affect adipocyte functions have been investigated *in vitro*. Nef, the accessory protein Vpr, and the regulatory protein Tat have been shown to alter adipogenesis (85, 91, 92) and might also contribute to the onset of insulin resistance in adipocytes (92). Interestingly, some studies have shown that Tat induces mitochondrial dysfunction [probably through mitochondrial membrane permeabilization and the generation of mitochondrial reactive oxygen species (ROS) (93)], which might account for the observed AT dysfunction and insulin resistance. It was established that HIV infection upregulated the expression of collagen 6, fibronectin and the profibrotic factor TGF-β in SCAT and (to a lesser extent) VAT. These observations were confirmed *in vitro*, where Tat and Nef promoted the acquisition of a profibrotic phenotype and increased the production of ECM components by adipocytes and their precursors (91).

The impact of the viral proteins on immune cells is well documented in general but has not been specifically investigated for AT-resident immune cells. It is known that the intracellular diffusion of viral proteins influences the function of T cells (94–96) and macrophages (97, 98). Nef binds to CXCR4 and modulates T cell activation (99). Lastly, T cells are activated (as expected) after exposure to viral proteins but the impact on the immune response in AT has not been extensively investigated.

Direct Infection of AT-Resident CD4 T Cells

The observation of high numbers of immune cells (and notably CD4 T cells and macrophages) in AT in obese individuals prompted reexamination of whether AT was directly infected by HIV. Couturier et al. detected HIV in the stromal vascular fraction prepared from AT (100). Subsequently, HIV (and SIV,

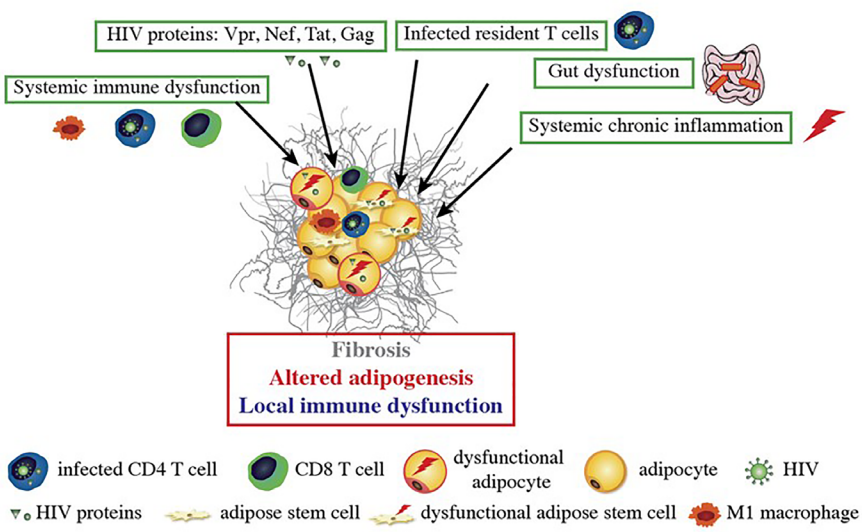

FIGURE 1 | HIV-related alterations in AT. HIV itself and the viral proteins produced by infected cells induce fibrosis and alter adipogenesis and local immune functions. HIV proteins are secreted by infected cells within AT and can impact the nearby adipose stem cells (ASCs) and adipocytes. Dysfunctional ASCs present mitochondrial dysfunction, elevated levels of oxidative stress and a profibrotic phenotype. The proteins impede the ASCs' ability to differentiate into adipocytes; this leads to dysfunctional adipocytes with low expression of adipogenic markers, lipid accumulation, and leptin and adiponectin secretion. HIV-protein-treated adipocytes also acquired a pro-inflammatory phenotype that is involved in local inflammation and immune dysfunction. Systemic factors (gut dysfunction, systemic chronic inflammation, and immune dysfunction) also contribute to AT dysfunction, with the induction of CD8 T cells, macrophages infiltration, and a shift towards a pro-inflammatory M1 macrophage profile.

in macaque models) were detected in the CD4 T cell fraction (101, 102) in both viremic and controlled ART-experienced patients. Lastly, several research groups have confirmed that the virus found in AT is replication-competent (102, 103). It is noteworthy that unambiguous data on the macrophage fraction are not available: the virus was found in the viremic macaque model but not in samples from ART-experienced, HIV-infected patients (102).

Systemic effects of HIV infection on AT functions

Although HIV is undetectable in the blood of ART responders, some dysfunctions persist. An ART-controlled HIV infection is known to be associated with low-grade chronic inflammation and persistent immune dysfunction (104–107), although the extent of these defects is subject to debate. Schematically, three main HIV-related factors may indirectly impact AT functions: gut dysfunction, immune dysfunction, and inflammation.

Gut Dysfunction

A crucial event during the first stage of an HIV infection is the severe, rapid depletion of the CD4 T cell compartment in the gut. ART enables only partial restoration of the gut mucosa (108) and does lasting damage to the gut's functional properties. In some ART-controlled patients, gut dysfunction impacts both the immune responses and the AT functions. The intactness of the epithelial barrier is weakened, leading to greater microbial load and viral persistence that are factors in chronic immune activation and inflammation. The disruption of the gut microbiota (109) modulates AT functions and subsequently impacts AT immune cells. Indeed, gut microbiota has a causal role in the development of obesity and associated metabolic disorders (12, 110, 111): microbiota transplanted from obese mice induces obesity. Given the central role of gut microbiota on metabolic and immune responses, multiples pathways are presumably involved (increase in LPS that may directly favor AT expansion, changes in metabolites and miRNA production by the gut, resulting in changes in AT immune cells inflammatory potential and in metabolites, adipokines and miRNA production by AT…). We currently lack data on changes in metabolite and miRNA production in the gut during chronic ART-controlled HIV infection.

Immune Dysfunction

The immune responses that develop during HIV infection lead to a progressive loss of cell function. For example, HIV-specific CD8 T cells exhibit an exhausted profile (112). The loss of immune function has several known causes, and others probably remain to be found. The following causes are commonly cited: (i) persistent antigenic stimulation; (ii) dysregulated immunoregulation (the important immunosuppressive population of Tregs are targeted by HIV, albeit to a lesser extent than conventional CD4 T cells, and thus control the immune responses less tightly; (iii) immune activation caused by exposure to a pro-inflammatory environment, (iv) the differentiation of T cells into less functional cells (such as senescent and/or exhausted cells), which in turn favors antigen persistence. Given that the AT is also a site of immune cell accumulation (predominantly CD4 T cells and immunoregulatory T cells in lean individuals), immune dysfunction during chronic HIV infection can particularly disturb the AT-resident immune cells' immune and metabolic functions.

Chronic Inflammation

The low-grade inflammation observed in chronic HIV-controlled patients has several causes. It combines immune dysfunctions (CD4 depletion, which is partially restored; defects in immunomodulatory mechanisms, and gut disruption), metabolic inflammation ("meta-inflammation"), inflammation associated with pathogen persistence/overload (leading to constant immune activation, i.e. "infectious inflammation") and "inflammageing" (HIV infection has been linked to accentuated ageing) (3). The residual inflammatory signature also depends on several factors, including the CD4 T cell count (both at the nadir and after treatment), the timing of ART, the patient's age and gender of the patients, and non-HIV-related factors (overweight, viral co-infections, smoking, alcohol consumption, recreational drug abuse, drug toxicity, etc.) (106, 113). Regardless of the exact nature of the inflammation that develops during a chronic ART-controlled HIV infection, the AT is highly sensitive to the inflammatory environment. As described above, systemic inflammation may contribute to or initiate local inflammation in AT. Reciprocally, AT inflammation may contribute to the systemic low-grade inflammation observed in HIV-infected patients (**Figure 2**). Importantly, the amplitude and nature of this chronic inflammation is also highly dependent on effective ART. This therapy restores the CD4 T cell count fully or partially (as defined by the patient's status as an "immune responder" or an "immune nonresponder") and reduces microbial translocation, viral persistence in reservoirs, and inflammation. Although ART is highly beneficial, it is also associated with metabolic side effects – notably within AT. ART can thus drastically change the nature of the inflammation that persists during chronic HIV infection.

ART-Related Lipodystrophy

Description

Prior to the development of ART, HIV-infected patients were seen to experience severe changes in body composition (including loss of muscle and AT) during the first few years of HIV infection. This resulted in cachexia, especially when patients had progressed to AIDS (85).

The introduction of the first thymidine nucleoside reverse transcriptase inhibitors (NRTIs), such as zidovudine and stavudine, enabled partial control of the HIV infection and delayed the onset of AIDS. Next, the introduction of protease inhibitors (PIs) enabled the "resurrection" of patients with AIDS who were already in a state of profound, life-threatening immunodeficiency. Triple therapy (a combination of two NRTIs and a PI) enabled real control of the virus, with an increase in the CD4 cell count and a marked decreased in the HIV load. However, patients with controlled infections

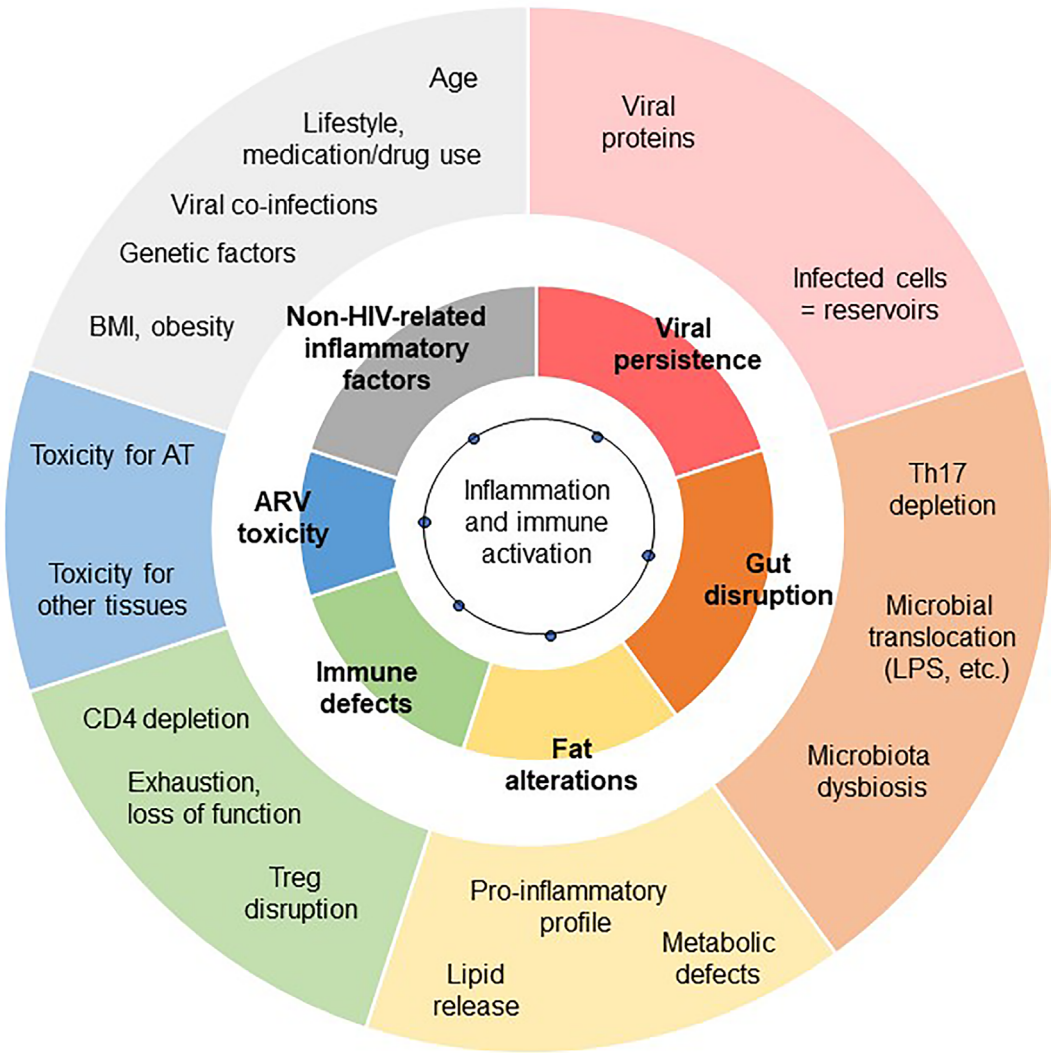

FIGURE 2 | Contribution of AT dysfunction to HIV-related low-grade inflammation. The exact degree of low-grade inflammation associated with chronic, controlled HIV infections remains subject to debate. The inflammation profile depends on the biomarkers studied and the clinical context of chronic HIV infection (including the time of ART initiation, and the severity of the primary phase of the infection). However, various triggers of inflammation are commonly reported to contribute to low-grade chronic inflammation: viral persistence, gut disruption, immunoregulatory defects, and non-HIV related comorbidities. Each of these main factors (shown in the inner circle) has several subfactors (shown in the outer circle). Fat alterations and the toxicity of ARVs also contribute.

commonly lost fat, even though the muscle mass was unaffected. This lipoatrophy was observed at all SCAT locations (the limbs, trunk, face, and buttocks). In particular, facial lipoatrophy gave the patient a striking, stigmatizing, cadaveric appearance – a hallmark of HIV infection. Furthermore, the levels of visceral fat variously decreased or increased, giving a mixed lipodystrophy phenotype (peripheral lipoatrophy plus central lipohypertrophy). Lastly, some patients developed a "buffalo neck", with the accumulation of fat at the back of the neck.

It was soon determined that thymidine NRTIs (mainly stavudine but also zidovudine) were responsible for the lipodystrophy, and these drugs were replaced by NRTIs with little or no AT toxicity. However, the features of lipoatrophy can persist for years (with long-term cardiometabolic consequences) after a patient has switched from thymidine NRTIs.

The Impact of First-Generation ARVs on Adipocytes and Their Progenitors

The mechanisms underlying the effects of individual drugs on AT have been investigated *ex vivo* and *in vitro*. The *ex vivo* studies of fat samples from patients were limited by the fact that none of the latter were being treated with a single ART and that the triple therapy at that time constituted of a PI and two NRTIs. In general, only subcutaneous fat samples were available. The

in vitro studies of each ART on adipose cells in cultured models were limited by the absence of a true, three-dimensional AT milieu comprising the different cell types (**Figure 3**).

The First-Generation Thymidine NRTIs Stavudine and Zidovudine

Ex vivo analyses of samples taken from lipoatrophic areas indicated that AT was deeply affected, with small adipocytes, fibrosis, and crown-like structures indicating the infiltration of macrophages around dead adipocytes (114, 115). This situation was unusual because crown-like structures are observed during obesity, when adipocytes are enlarged. In cases of lipoatrophy, these histological features pointed to a toxic effect of ART on adipocytes. Furthermore, expression levels of the main adipogenic factors (peroxisome proliferator activated receptor γ (PPAR-γ), CCAAT/enhancer-binding protein alpha (C/EBP-α), and sterol regulatory element-binding transcription factor 1 (SREBP-1)), adipose markers, adiponectin, and leptin were abnormally low. Greater levels of inflammation were characterized by increased gene and protein expression of proinflammatory cytokines (like IL-6 and TNF-α) by stressed adipocytes and immune cells infiltrating the AT. Furthermore, the AT from lipoatrophic subjects has a low mitochondrial DNA (mtDNA) content and low expression levels of the mitochondria-encoded proteins required for adequate metabolic function in adipocytes (116, 117). In end-stage lipoatrophy, all the subcutaneous ASCs and adipocytes were destroyed. In contrast to SCAT, few studies have evaluated alterations in VAT in ART-treated patients. However, NRTIs appear to be less toxic for VAT adipocytes than for SCAT adipocytes (85).

The role of thymidine NRTIs was further investigated in patients who switched from these drugs. Progressive AT recovery was observed, although recovery from severe lipoatrophy was often only partial - probably due to irreversible exhaustion of the ASCs in subcutaneous fat (118).

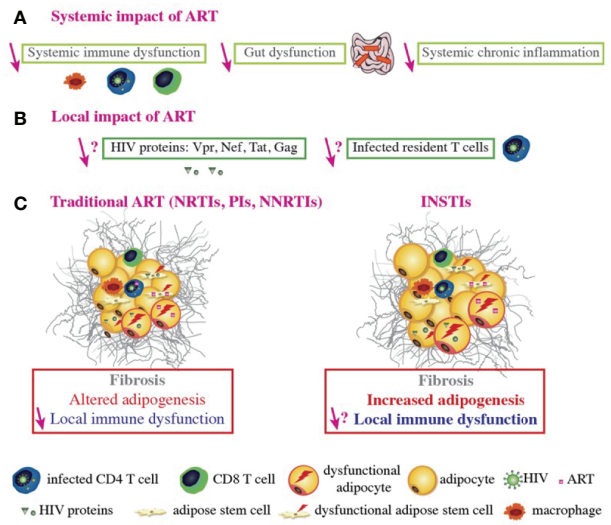

FIGURE 3 | ART-related fat alterations. ART controls HIV replication, improves systemic immune function, decreases chronic inflammation, promotes immune reconstitution and function, improves gut function and integrity, and decreases the viral load and viral protein concentration in the blood **(A)**. However, it is not known whether ART decreases the number of infected T cells or the viral protein concentration within AT **(B)**. Regarding conventional ART, the NRTIs stavudine and zidovudine, some PIs boosted by ritonavir, and the NNRTI efavirenz (EFV) induce alterations in AT such as fibrosis, altered adipogenesis, and local immune dysfunction. ART does improve immune function and expression levels of some adipogenic markers (e.g. PPARγ) in the AT, relative to treatment-naive HIV-infected patients. However, adipogenic marker expression is still lower than in non-infected people. ART induces mitochondria dysfunction and alters adipogenesis in both ASCs and adipocytes. ART-treated adipocytes present with oxidative stress and insulin resistance. Furthermore, some ARVs induce pro-inflammatory adipokine/cytokine secretion by adipocytes, ASCs and macrophages and CD8 T cells accumulation; this contributes to AT immune dysfunction and inflammation. It was recently reported that some INSTIs can be associated with fat and weight gain, adipogenesis, fibrosis, and adipocyte hypertrophy/dysfunction, with increased insulin resistance *in vitro*. INSTIs also induce collagen production, mitochondrial dysfunction, and oxidative stress in both ASCs and adipocytes, which might promote fibrosis. Nonetheless, the local impact of INSTIs on immune cells within the AT remains to be determined **(C)**.

The First-Generation PIs Indinavir and Nelfinavir

Studying PIs in clinical AT samples was difficult since the patients were receiving two NRTIs (including one thymidine NRTI) at the same time as a PI. Therefore, most of the information on the effects of indinavir and nelfinavir has been obtained *in vitro* (see below). It has been suggested that some PIs have a role in the shift from a brown/beige phenotype to a white phenotype because the expression of the micro-RNA processing enzyme Dicer was found to be low in lipoatrophic areas, and this decrease was proportional to the duration of PI use.

ART-Related Changes in Fat With Combinations of Today's ARVs

Description

More recently, HIV-infected patients with long-term control of the infection were generally receiving triple therapy with two NRTIs and a PI or a nonnucleoside reverse transcriptase inhibitor (NNRTI, such as efavirenz). As the treated patients aged, however, the prevalence of comorbidities increased. The patients often gained weight and fat, with the classical truncal distribution seen during ageing (85, 119). These changes were associated with adverse cardiometabolic outcomes, as atherosclerotic cardiovascular disease (CVD), diabetes, and non-alcoholic fatty liver disease (NAFLD).

This increase in trunk fat is seen in both women and men and in all ethnic groups. It can result in obesity, particularly when the initial bodyweight is already high (as observed frequently in North America and less so in Europe). As the person ages, the fat gain is often accompanied by the loss of muscle mass. This situation is called sarcopenic obesity and is associated with harmful cardiometabolic outcomes.

Nowadays, the recently developed class of INSTIs is widely used to control HIV infections. Although the INSTIs are effective and safe, combination therapy (with the addition of an NRTI) is typically required to control the virus. However, some patients

gain weight and fat mass (mainly on the limbs, trunk, and abdomen) and become obese (85).

Weight gain can affect treatment-naive patients initiating ART. A large proportion of this gain is due to a return to good health; patients with a low CD4 and a high viral load gain the most weight during the first two years of ART. Nevertheless, this weight/fat mass gain is excessive in some individuals taking an INSTI [mainly dolutegravir (DTG) and bictegravir], especially in women (vs. men) and African ethnic groups (vs. Caucasians) (120, 121). Weight gain is also observed in some ART-controlled patients who switch to an INSTI; female sex and older age are risk factors for this increase. Nevertheless, it is unclear why some patients (but not others) gain weight disproportionally. Recent studies have indicated that along with INSTIs, commonly used "older" drugs can also modulate weight gain. For example, the NNRTI efavirenz and the NRTI tenofovir diproxil fumarate (TDF) have been linked to lower weight gains, while tenofovir alafenamide (TAF, a derivative of TDF that concentrates within cells) is associated with a greater weight gain (121).

The Impact of INSTIs and TAF/TDF on Fat

In AT, adipocytes can sequester ARTs inside the adipocyte lipid droplet, which contributes to viral persistence (87). Adipocytes have consistently been shown to reduce the antiviral efficacy of TDF and TAF *in vitro*, and some INSTIs have been found in AT (122).

Effect of INSTIs. Recent *ex vivo* studies have found that fibrosis, adipocyte size, and adipogenic marker expression are greater in SCAT and VAT samples from INSTI-treated macaques than in samples from untreated animals. Similarly, SCAT and VAT from obese INSTI-treated HIV-infected patients show higher levels of fibrosis than samples from INSTI-naïve obese patients (85, 123).

DTG has been detected within adipocytes and in the stromal vascular fraction prepared from VAT (122), suggesting that it has access to ASCs and adipocytes *in vivo*. Raltegravir (RAL) has a high level of tissue penetration and is therefore likely to accumulate in AT (124). These features might explain the fat mass gain in treated patients (**Figure 3**).

Recent results suggest that INSTIs can decrease SCAT inflammation. In the OBEVIH cohort of obese subjects undergoing bariatric surgery, the level of inflammation was lower in HIV-infected patients treated with an INSTI than in patients not receiving an INSTI and in HIV-negative controls (Pourchez V, unpublished data). Accordingly, our study of SCAT samples from HIV-infected patients switched from a PI-containing regimen to combination therapy with RAL and the CCR5 inhibitor maraviroc revealed very low expression levels of genes involved in T lymphocyte signaling (125).

Effects of TAF vs. TDF. Differences in pharmaceutical formulation mean that TAF has lower circulating concentrations but higher intracellular concentrations than TDF. It remains to be determined why TDF prevents weight gain and TAF enhances it. However, it is possible that these effects are related to differences in the level of drug-induced oxidative stress.

A Third Factor: The Host Status Prior Infection

Inflammation Is an Integrative Process

It is challenging to distinguish between the respective effects of HIV infection, ART toxicity and personal factors on the inflammatory profile developing in ART-controlled HIV-infected patients. The interplay between HIV and the ARVs are multiple. Firstly, ART reduces viral persistence and virus-related immune defects, suggesting that the persisting low-grade inflammation observed in ART-controlled patients may partly relate to ARV-toxicities when immune restoration is achieved. Among host-related factors, the severity of the primary phase, the size of the pre-established viral reservoir may affect the quality of the immune restoration and also participate to the development of low-grade inflammation. Immune and tissue-specific natural senescence together with the presence of age-related comorbidities may also contribute to the development of an exacerbated immune responses. In aged patients, ART toxicity is increased probably due to reduced capacities to detoxify and eliminate drugs (kidney and liver failures) and to the prescription of other drugs (polypharmacy).

Importantly, patients with efficient immune restoration present inflammatory profile close to healthy individuals (106, 113), suggesting a limited impact of currently used ARVs per se on inflammation. However, the question of the relative impact of HIV infection and ARV remains open when considering patients with partial immune restoration. One may hypothesize sequential impacts of HIV infection and ARV on AT. It could be hypothesized that ARV may impact differently AT that was previously disrupted by HIV infection compared to uninfected AT, possibly acting in synergy to amplify adipose dysfunction. The same notion may apply to other infections that target AT (tuberculosis, CMV, …) and may alter the metabolic and immune parameters of AT. Lastly, because HIV persist in AT even after ART induction, one may consider the combined impacts of HIV infection and ARVs on the alteration of AT. These questions are difficult to address *ex vivo* since ARV are prescribed only to HIV-infected patients and very limited data are available in animal models regarding the study of ARV toxicity with/out HIV/SIV infection, and the associated inflammation.

An Important Factor: The Host Metabolic Status Prior Infection

Importantly, the impact of HIV infection and ARV on AT may also directly rely on the host metabolic status prior infection. In that respect, preexisting obesity may exacerbate the pathophysiology of HIV infection and the toxicity of ARVs. Studies in NHP demonstrate the higher severity of SIV pathogenesis in animals fed with high fat diet with resulting cardiovascular (CV) and liver alterations (126, 127), but ARV were not administered in this setting. Data in humans are obviously less consensual. Before ART's availability, HIV infected patients with higher BMI showed slower HIV progression compared to underweight patients (128, 129),

presumably due to delayed wasting/cachexia effects. In ART-treated patients, obese or underweight patients exhibited higher cumulative mortality rates, delineating an optimal BMI range between 24 and 28 (130) and obesity has been identified as a risk factor for multimorbidity (131). Regarding the impact of obesity on CD4 T cell reconstitution, patients with higher BMI before ART initiation exhibit higher (132, 133) or comparable (134) immune reconstitution. This apparent discrepancy between mortality rate and CD4 T cell restoration exemplified the diverse impacts of obesity which is associated simultaneously with positive and negative effects. However, the impact of obesity on the toxicity of ARV remains ill-documented. It has been hypothesized that the sequestration and metabolism of ARV may differ in obese versus lean patients. ART plasma concentrations were lower in obese patients, although not impacting the viral control (135).

As a whole, the close interplay between HIV infection, ARV toxicity and metabolic status prior infection and/or following ART introduction may be considered as a combination rather than as independent factors of inflammation.

PHENOTYPIC AND MECHANISTIC CHANGES IN AT

Metabolic Changes

Local Effects

A number of *in vitro* studies have sought to describe the mechanisms involved in the detrimental effects of individual PIs, NRTIs and NNRTIs on adipogenesis, insulin signaling, adipokine secretion, and apoptosis (85).

In vitro studies of adipocytes cultured with individual thymidine NRTIs showed that stavudine and (to a lesser extent) zidovudine were toxic for AT. The drugs inhibited the mitochondrial DNA polymerase (required for mtDNA replication) and also induced severe oxidative stress. Thus, toxic effects on mitochondria might result in an energy deficiency and high levels of oxidative stress (136). Inter-individual differences in sensitivity to the lipoatrophic effect of stavudine or zidovudine might be related (at least in part) to mtDNA haplogroups, some of which are variously associated with a greater risk of lipoatrophy (the H, I and K haplogroups) or a lower risk (the T and W haplogroups) (137, 138).

The effects of first-generation PIs on adipose cells have also been evaluated *in vitro*. These effects might result (at least in part) from the inhibition of the enzyme ZMPSTE24, which is responsible for the maturation of the precursor prelamin A into the nuclear protein lamin A. First-generation PIs were able to inhibit the enzyme, which led to the accumulation of prelamin A around the nucleus and to mislocalization of SREBP-1 (139, 140). The accumulation of prelamin A favored cell senescence, adipocyte dysfunction, and insulin resistance. First-generation PIs could also induce endoplasmic reticulum (ER) stress. Furthermore, a recent study showed that both short- and long-term treatment with the first-generation PI lopinavir promoted whitening of brown adipocytes differentiated *in vitro*. This shift impeded fatty acid oxidation and favored insulin resistance (141–143).

Efavirenz has been used for a long time and is still given to HIV-infected people today. However, it can reduce adipogenesis and adiponectin expression whilst increasing the expression of proinflammatory markers (144).

More recently, several research groups have started to identify and characterize the mechanisms involved in the INSTIs' effect on weight/fat gain. The etiology of INSTI-related weight/fat gain is unclear but may include indirect effects on thermogenesis, appetite or energy regulation, or a direct effect on AT. We have observed that some INSTIs do indeed have a direct impact on adipocytes: DTG and (to a lesser extent) RAL increased ECM accumulation and adipocyte hypertrophy. Despite the increase in adipogenesis, INSTIs also promote oxidative stress and insulin resistance (123). The mechanisms involved are being studied but one can reasonably hypothesize that adipocyte hypertrophy in the abdominal SCAT of patients on INSTIs compensates for the decreases in beige AT and energy expenditure. Interestingly, a recent study showed that the brown AT transcription factor PRDM16 might protect against the development of fibrosis in WAT (145). Furthermore, TGF-β inhibits the beiging of adipocyte precursors (146). A decline in beiging might therefore also be involved in the fibrosis observed in the AT of INSTI-treated patients. These associations highlight the need to determine whether people living with HIV (PLWH) are at risk of cardiometabolic disease as a result of reduced beiging capacity in WAT; this might constitute a novel mechanism for metabolic dysregulation in this population.

Another hypothesis relates to the effect of INSTIs on food intake. It has been shown that DTG inhibits the binding of α-melanocyte-stimulating hormone (αMSH) and melanocortin 4 receptor (MC4R) in the hypothalamus; this might promote hyperphagia (147, 148). However, the serum DTG levels in patients are much lower than those required for hyperphagia (149).

In the context of obesity, elevated fibrosis is mainly due to periadipocyte fibrosis; the latter has been linked to metabolic disorders (60) and was observed in the AT of INSTI-treated macaques and patients. These alterations might result from increased oxidative stress. Indeed, lipohypertrophy in PLWH has previously been linked to mitochondrial toxicity in AT (150). Accordingly, we found that DTG and RAL promoted ROS production and mitochondrial dysfunction. We hypothesized that in the context of HIV infection and stressed adipocytes in a profibrotic environment (due to the impact of HIV, obesity, or antiretrovirals other than INSTIs), INSTIs might alleviate adipocyte stress (thereby favoring hypertrophy/expansion) but might also increase oxidative stress, reduce metabolic flexibility, and accentuate insulin resistance.

Systemic Effects

After secretion by AT, the hormones adiponectin and leptin regulate key pathways in lipid and glucose metabolism (151). Adiponectin has a potent anti-inflammatory and anti-atherogenic action, and a decrease in adiponectin levels is correlated with the development of insulin resistance (152).

Adiponectin also has an important role in lipid metabolism by increasing fatty acid oxidation in skeletal muscle and in the liver and thus lowering circulating FFA levels (153). In contrast, leptin regulates the energy balance by inhibiting hunger but also has major effects on insulin sensitivity and inflammation (154). In accordance with the observed alterations in AT function, circulating levels of adiponectin and leptin are low in both ART-treated and treatment-naive patients (155). Furthermore, some studies have shown that DTG and RAL lower circulating adiponectin levels (156–160). Recently, it has been suggested that the adiponectin/leptin ratio is a marker of AT dysfunction; threshold values for cardiometabolic risk have been determined (161, 162) and could therefore be explored in ART-experienced HIV-infected patients.

Metabolite profiles are altered not only in plasma/serum but also in a variety of other biological fluids. In cerebrospinal fluid, alterations in energy metabolites were found to be correlated with neurocognitive impairments and increased inflammation in ART-experienced HIV-infected individuals. These alterations overlap with the metabolic alterations seen in older HIV-negative individuals and suggest that aging is accelerated by exposure to ART (163).

Immune Changes

AT-Resident Immune Cells

Studies of samples collected from HIV-infected people (mostly ART patients) and HIV-negative controls are difficult to interpret because of large intergroup differences in infectious, metabolic and treatment-related parameters. In this respect, nonhuman primates are interesting models for determining the effect of HIV in the presence or absence of ART, and provide a more controlled experimental setting with regard to the individuals' infectious and metabolic histories. Regardless of the model and the stage of infection considered, mRNA/protein quantification (on supernatants or microscopy) and flow cytometry studies (102, 103, 164) have shown that chronic HIV/SIV infection is associated with a shift towards a pro-inflammatory immune profile in AT. In humans, levels of adipose-macrophage-derived cytokine (IL-12, IL-6, IL-8, and MCP-1) are higher in HIV-infected individuals than in noninfected individuals. In cynomolgus macaques, the overall macrophage count in AT was similar in HIV-infected and noninfected individuals but the former group had a higher proportion of non-M2 macrophages (based on the expression of CD206 and CD163 as M2 markers) (102). Changes in the T cell compartment have been reviewed in detail (165). The most important change is a decrease in the CD4/CD8 ratio, with an accumulation of CD8 T cells during chronic untreated SIV infections (101, 102). Research on the CD4 T cell fraction (166, 167) in both humans and nonhuman primates revealed an AT-specific phenotype, whereas differences between HIV/SIV+ and HIV/SIV noninfected animals were limited. AT-resident CD4 T cells are characterized by higher expression levels of PD-1 and CD57 and higher proportions of effector memory (Tem) and CD45RA+ Tem (Temra) - suggesting a more activated/exhausted profile. High expression of CD69 on AT-resident T cells has also been reported (166, 167), although this marker is associated with resident memory cell differentiation and/or activation. The Treg fraction (a seminal immunoregulatory subset) was reportedly prominent in the AT in some mouse models (31, 168). In contrast, baseline Foxp3 expression was low in both HIV-infected and noninfected people, even though the proportion of Tregs was slightly higher in SIV-positive animals (166).

Overall, chronic HIV infection appears to have the same effects on AT as obesity (a shift towards M1 macrophages and CD8 T cell accumulation), albeit to a lesser extent. Data on the modulation of other immune cell fractions present in AT during HIV infection (in the presence or absence of ART) are lacking. Likewise, HIV-related changes in the status of neutrophils, CD4 Th1 T cells, and type 1 innate lymphoid cells as effectors or partners in pro-inflammatory immune responses have not yet been studied. However, this knowledge may be needed to fully understand the complex crosstalk between immune and metabolic cells in AT and to further evaluate local inflammation in AT during HIV infection.

Inflammation

The pro-inflammatory cytokine profile of AT in HIV/SIV-infected individuals vs. noninfected individuals has been characterized by detecting proteins or mRNA in AT lysates or supernatants of AT fractions. Although the studies differed with regard to the experimental methods and the cytokines assayed (91, 101, 167), all found a greater pro-inflammatory potential (with IL-2, IL-7, IL-15, CCL19, and TGF-β) in AT collected from HIV/SIV-infected individuals vs. noninfected individuals. Koethe et al. also contributed important insights into the transcriptional upregulation of genes coding for chemokines, chemokine receptors, and Toll-like receptors (167). Taken as a whole, these data suggest that chronic infection induces a pro-inflammatory profile in AT. Importantly, all the studies performed on human samples were limited by high inter-individual heterogeneity, which presumably reflects differences in metabolic and infectious histories. Important, Couturier et al. compared the AT cytokine secretion profiles in ART-experienced patients and treatment-naive patients; ART appeared to be associated with a less inflammatory profile in the AT (101).

The net impact of ART is thus obviously highly beneficial because it controls the HIV infection. ART reduces the viral load, restores (at least partially) the CD4 T cell count, and dampens inflammatory processes. This benefit is also observed within the AT, with regard to inflammatory cytokines. However, ART induces metabolic side effects (which are highly dependent on the combination used) that change the nature of the chronic inflammation associated with a controlled HIV infection. As described in this section, the ARVs' side effects affect ASCs and/or adipocytes and can induce oxidative stress, ECM remodeling (with a consequential reduction in the metabolic responsiveness of AT), and insulin resistance. Importantly, recent studies have also evidenced a direct impact of ARVs on immune cell functions (169). DTG and elvitegravir reduce the oxidative and proliferative activities of peripheral blood CD4 T cells and thus induce a "stress" immune response with strong production of TNF but no polyfunctional cytokine

responses.Based on these data, the ARV's impact on immune activity (and not just metabolic activity) in AT should also be investigated.

Oxidative Stress, Endothelial Dysfunction, and the Renin-Angiotensin-Aldosterone System

In the context of AT disease such as obesity, vascular damage, including endothelial dysfunction, has been observed, along with oxidative stress. Increased oxidative stress develops in obese AT as a result of multiple factors: dysfunctional adipocytes in response to nutrient overload (hypertrophy, increased mitochondrial oxidation, increased levels of reactive oxygen species (ROS)), AT hypoxia, increased pro-oxidant cytokines production (such as TNF-α) by AT and increased release of FFAs. These parameters contribute to systemic oxidative stress and inflammation (170). Obesity is also associated with vascular remodeling and fibrosis in both VAT and SCAT (171). This vascular remodeling is associated with inflammation characterized by macrophage infiltration especially in SCAT and has been associated with systemic endothelial dysfunction and insulin resistance in obese patients (172).

The renin-angiotensin system (RAS) plays an important pathophysiological role. The production of RAS components by adipocytes is exacerbated during obesity, contributing to the systemic RAS which then affects the cardiovascular system (171). The up-regulation of adipose RAS, and especially the increase of angiotensin II production, promotes inflammation through increased chemokine production, oxidative stress and fibrosis (171). Conversely, blocking or preventing RAS activation in AT can reduce oxidative stress, improve insulin resistance and reduce inflammation (173, 174). Interactions between the RAS and HIV infection have been described, and could contribute to AT inflammation, but also to the onset of metabolic syndrome and hypertension in PLWH (175, 176).

Insulin Resistance and Lipotoxicity

AT dysfunction, as seen in obesity and diabetes, is generally associated with insulin resistance, a metabolic disorder affecting multiple tissues. The proposed mechanisms involved in insulin resistance include both whole body aspects, such as inflammation and metabolic inflexibility; as well as cellular phenomena, such as lipotoxicity, ER stress, and mitochondrial dysfunction. Lipotoxicity, as a result of increased lipolysis in AT and release of FFAs, is a type of cellular stress induced by the accumulation of lipid intermediates such as diacylglycerols (DAGs), ceramides, and triglycerides that facilitate the development of insulin resistance and ectopic fat deposition in muscle, liver, and adipose tissue together with a pro-inflammatory response (177). Lipotoxicity participates to the enhanced cardiometabolic risk observed in PLWH (178, 179).

COMORBIDITIES ASSOCIATED WITH LOW-GRADE INFLAMMATION

In the general population, a number of age-related comorbidities (including cardiometabolic diseases, neurocognitive impairments, cancer, and frailty) are associated with a state of low-grade chronic inflammation. Circulating levels of several cytokines and inflammatory markers [such as IL-6 and C-reactive protein (CRP)] rise with age and might trigger these comorbidities. AT is the main source of circulating IL-6, and the cytokine triggers the synthesis of CRP in the liver. Accordingly, obesity is associated with low-grade, chronic inflammation. Hence, an increase in the mass of AT might contribute to these comorbidities by enhancing low-grade inflammation.

Several studies have evidenced a state of low-grade inflammation in ageing HIV-infected patients who are well controlled by ART. This level of inflammation is greater than in non-infected subjects (180, 181) and is thought to be involved in the elevated prevalence of certain comorbidities. The inflammation might result from HIV-related factors, such as the presence of the virus inside reservoirs, greater gut permeability, dysbiosis, an effect on gut-associated lymphoid tissue, and coinfections (which are nevertheless observed in ART-controlled patients). AT might be a key factor - first as an HIV reservoir and then as a source of inflammatory markers in the context of ART-related fat mass gain.

Some patients treated with thymidine NRTIs present persistent fat alterations several years after treatment discontinuation. In the AGEhIV cohort, long-term-infected, ART-controlled patients had a greater waist circumference, a lower hip circumference, and a greater incidence of hypertension than HIV-negative people (180). In the COCOMO study, cumulative exposure to stavudine, zidovudine or didanosine was associated with elevated amounts of VAT, lower amounts of SCAT, and a higher risk of hypertension and dyslipidemia (182).

Trunk fat accumulation is one facet of the broader condition of ectopic lipid deposition in HIV-infected patients; accumulation is also observed in the liver, epicardial tissue, and skeletal muscle. In this situation (also referred to as "metabolically unhealthy obesity", due to its association with cardiometabolic outcomes), the storage capacity of SCAT (the largest WAT depot) is limited, and further calory overload leads to fat accumulation in ectopic tissues (e.g., liver, skeletal muscle, and heart) and in VAT depots - an event commonly referred to as "lipotoxicity". Excessive ectopic lipid accumulation leads to local inflammation and insulin resistance (42). The clinical consequences of ectopic fat deposition are summarized in **Figure 4**.

Atherosclerotic Cardiovascular Disease

Epicardial fat is physiologically similar to visceral fat and is located close to the coronary arteries. It might therefore have a major role in the development of coronary atherosclerosis (183, 184). Groups of adipocytes are close to the right ventricular myocardium and might release fatty acids to fuel the cardiomyocytes. Epicardial fat also releases adipokines, cytokines, and vasoactive products that regulate coronary artery tone. In obese patients with several CV risk factors, epicardial fat around the coronary arteries releases pro-inflammatory cytokines and presents a high macrophage count and high levels of TNF-α, IL-6, and IL-8 (185). It has been suggested that the greater volume of epicardial fat in obese subjects contributes to the elevated CV risk (186).

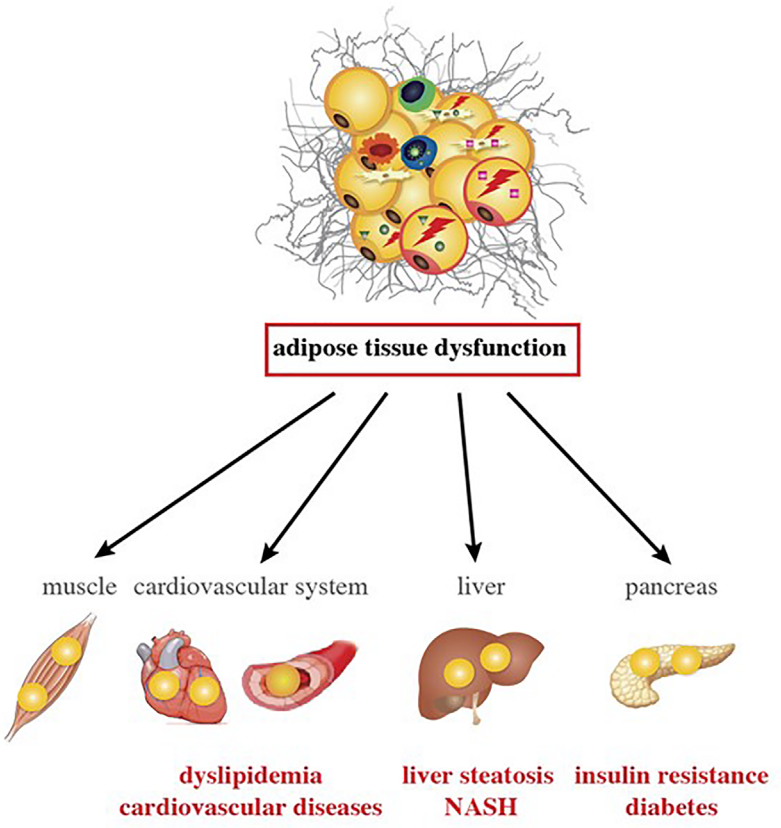

FIGURE 4 | Inflammation changes in AT and are associated with comorbidities in ART-experienced, HIV-infected patients. AT alterations with VAT expansion, local and systemic inflammation, and gut dysfunction promote lipotoxicity in ART-experienced, HIV-infected people. Lipids accumulate in metabolic organs other than the AT, such as muscle, heart, blood vessels, liver, and pancreas. Lipotoxicity and inflammation might contribute to the development of atherogenic dyslipidemia, cardiovascular diseases, insulin resistance, diabetes, liver steatosis and NASH in the context of HIV infection and ART.

Several studies of ART-controlled patients have evidenced greater volumes of epicardial fat; along with traditional risk factors for atherosclerosis and the duration of ART, the amount of epicardial fat is associated with the amount of VAT and with insulin resistance. In HIV-infected patients, the epicardial fat volume is related to endothelial dysfunction and the progression of carotid atherosclerosis (187–189).

More recently, the overall fat gain observed in some patients raises the question of whether treatment with INSTIs influences cardiometabolic outcomes. At present, there is no indication of an elevated CV risk for this class of ART molecules, although long-term follow-up data (i.e. for at least 5 years) are missing.

Metabolic Liver Diseases

Liver steatosis corresponds to another type of ectopic fat deposition. An elevated liver fat content has been reported in patients with lipoatrophy and in those with central obesity - two situations associated with systemic low-grade inflammation. In HIV-mono-infected patients, the prevalence of steatosis is relatively high, relative to the body mass index (BMI) (30-35%) (190). In some people, simple steatosis can progress to a more worrying situation: non-alcoholic steatohepatitis (NASH), with liver inflammation and often progressive fibrosis. Severe fibrosis (cirrhosis) and progression to hepatocarcinoma are life-threatening.

Several studies have highlighted the strong relationship between trunk fat accumulation and steatosis or fibrosis in HIV-infected subjects. In a matched cohort of 468 HIV-mono-infected patients the prevalence of significant liver fibrosis (≥Fibroscan grade 2) was 25.1% in patients with metabolic syndrome and 7.9% in those without. In a multivariate analysis, obesity and insulin resistance were independently associated with advanced fibrosis (≥Fibroscan grade 3). Leptin and soluble (s) CD163 were strongly associated with fibrosis/cirrhosis, whereas HIV parameters and ART were not. Thus, AT and macrophage activation might be key players in the development of liver fibrosis in HIV-infected patients (191). In a study of 62 HIV-infected adults with elevated aminotransferase levels, insulin resistance, obesity, and the presence of either of two minor alleles in the *PNPLA3* gene were significantly associated with an elevated risk of NASH and fibrosis. NASH and/or fibrosis were not associated with the duration of HIV infection or ART (192).

Insulin Resistance and Diabetes

In the APROCO cohort of HIV-infected patients followed up for 10 years after the initiation of first-generation PIs, the incidence diabetes peaked in 1999-2000, and was linked to treatment with indinavir, stavudine and didanosine. As expected, diabetes was associated with age and adiposity. The main risk factor was the waist-to-hip ratio (hazard ratio: 3.9), which highlighted the key role of truncal obesity (193). In a longer-term study of 352 patients from the cohort, the prevalence of diabetes was 11%, and the prevalence of atherogenic dyslipidemia (a high triglyceride/high-density lipoprotein ratio, observed mainly in diabetic subjects) was 9%. Diabetes and atherogenic dyslipidemia were associated with elevated levels of systemic markers of oxidative stress and inflammation (194).

The more recent use of INSTIs has resulted in overall fat gain in some patients. While blood lipid levels are generally lower, the outcome for insulin resistance is less clear. We have observed elevated insulin resistance in well-controlled, aging patients switched from a PI-containing regimen to RAL/etravirine; this is probably linked to INSTI-related weight gain (195). Regarding diabetes, 722 of the 22,884 eligible individuals (3%) in the USA/Canadian NA-ACCORD study of ART-initiators developed this condition. Persons initiating INSTIs + NNRTIs had the same incident risk of diabetes as those initiating PIs+ NNRTIs. This effect was most pronounced for RAL. The association between INSTI and diabetes was attenuated by accounting for 12-month weight gain. Initiating combination ART regimens with INSTIs or PIs + NNRTIs may confer a greater risk of diabetes; this is probably mediated by weight gain (196). In the French DAT'AIDS study, 265 of the 19,462 HIV-infected patients initiating ART developed diabetes. Multivariate and survival analyses did not highlight an increase in new-onset diabetes in patients undergoing combination ART with an INSTI as a third agent (relative to an NNRTI or a PI). BMI, age, African or Hispanic ethnicity, arterial hypertension, and AIDS were associated with a higher incidence of diabetes (197).

Hence, it is currently not clear whether INSTIs have an additional effect on the incidence of diabetes, other than that related to weight gain. However, clinicians should be aware of this possible metabolic comorbidity - particularly in older patients and in patients with a high BMI.

Relative to non-infected subjects, HIV-infected patients present a higher prevalence of age-related comorbidities associated with a higher level of systemic inflammation. This might result from a number of factors related to HIV infection and coinfections (with hepatitis C virus or CMV) but also modifiable risk factors such as smoking, alcohol abuse and substance abuse (181, 198). Furthermore, adiposity and particularly truncal fat accumulation are associated with low-grade inflammation and comorbidities resulting from greater ectopic fat deposition.

THERAPEUTIC STRATEGIES

Here, the goal of treatment (in addition to ART) is to decrease inflammation, immune activation, and thus the related comorbidities. Even though these strategies do not specifically address AT, they might act on this tissue in addition to other organs. As observed for obesity-related cardiometabolic complications in the general population, weight reduction has been consistently associated with lower AT inflammation and results in better cardiovascular, hepatic and metabolic outcomes (i.e. a lower incidence of NAFLD, insulin resistance, and diabetes) (199). This approach is relevant in overweight or obese HIV-infected patients with central fat accumulation. Furthermore, regular exercise is an excellent strategy for reducing inflammation and cardiometabolic complications (199).

Other strategies aiming at reducing systemic inflammation to reduce comorbidities have been tested in HIV-infected patients and are reviewed elsewhere (198). The lasting association between inflammation and atherosclerosis has prompted significant interest in strategies for inhibiting inflammatory proteins upstream of CRP - particularly IL-6 and IL-1β. The strongest evidence to date in favor of preventing CVD by reducing inflammation comes from the CANTOS study using canakinumab, inhibiting IL-1β, albeit in HIV-negative participants (200). In HIV-infected patients, Hsue et al. recently demonstrated that IL-1β inhibition with canakinumab reduced atherosclerotic inflammation (201) but was not associated with other improvements. In a phase II trial, HIV-infected patients at an increased risk of atherosclerotic events were treated with low-dose methotrexate or placebo for 24 weeks (202). Low-dose methotrexate had no effect on the primary endpoint (brachial artery flow-mediated dilation) or levels of various inflammatory biomarkers, and the trial was stopped prematurely. The potential effect of the Janus kinase inhibitor ruxolitinib was evaluated in an open-label trial in HIV-positive patients (Marcolin VC, unpublished data). At week 5, the sCD14 level was significantly lower in the ruxolitinib arm than in the ART-alone arm but the IL-6 level was not. Since D-dimer elevation is linked to the pro-inflammatory profile reported in PLWH, it has been suggested that anticoagulant drugs may be of value in treating the pro-coagulant state. Orally administered edoxaban (a direct factor Xa inhibitor) was tested against placebo in the TACTICAL-HIV trial (Baker JV, unpublished data). However, four months of edoxaban treatment did not lead to lower levels of biomarkers associated with inflammation or monocyte activation.

The anti-inflammatory activity of 3-hydroxymethyl-3-methylglutaryl coenzyme A reductase inhibitors (i.e. statins) is well documented (203), and several clinical trials have assessed the benefits of these drugs on surrogate markers of CVD (along with LDL-lowering activity) in ART-suppressed HIV-infected patients. In the SATURN-HIV trial, rosuvastatin (10 mg/day) was significantly associated with low levels of sCD14, with a fall of approximately 10% at 48 weeks (204). Lower levels of several markers of vascular inflammation were also observed. In the INTREPID trial, similar results were observed for pitavastatin but not for pravastatin (205). It is now necessary to determine whether the statin-induced reduction of inflammatory/immune activation and cardiovascular biomarkers translates into a reduction in morbidity and mortality in HIV-infected patients. The ongoing REPRIEVE study is addressing this question (206).

Taken as a whole, strategies designed to decrease systemic inflammation/immune activation in HIV-infected patients have not produced a clear reduction in comorbidities. Again, combinations of simple lifestyle modifications (e.g. exercise and weight loss) with decreased AT inflammation have been validated for reducing the incidence of cardiovascular events, diabetes, and NAFLD.

CONCLUSION

AT is targeted by both HIV infection and ART. HIV targets AT both directly (direct infection of AT CD4 T cells) and indirectly (viral protein release, inflammatory signals, and gut disruption). Schematically, ART impacts adipogenesis, adipocyte homeostasis, and ECM remodeling (including fibrosis), whereas viral persistence directly impacts the metabolic and immune functions of AT immune cells. In a chronic ART-controlled HIV infection, the direct impact of HIV *per se* is less severe than that of ART. Indeed, ART efficiently reduces the viral load and the various immune defects associated with the early stage of infection. However, restoration of the immune system is only partial, and the persisting damage inflicted on the immune system during the early stages of infection might contribute to AT inflammation. Given the close links between the gut and AT, the latter's functions may also be indirectly impacted by the massive CD4 T cell depletion observed in the gut in the early stages of infection. Subsequently, AT's endocrine activity and its release of metabolites will increase systemic immune activation and inflammation. Furthermore, ART reduces the viral load to undetectable levels in the circulation blood but does not eradicate the virus in reservoir sites such as AT.

In the longer term, the various direct toxic effects of ARVs might drive low-grade inflammation in HIV-infected patients. These effects are highly dependent on the classes/combinations of ARV used, that variously target ASCs and/or adipocytes, and can induce oxidative stress, ECM remodeling (with a consequential reduction in the metabolic responsiveness of AT), and insulin resistance (125). Ongoing research is also evaluating the direct impact of ARVs on immune cells. Given the crucial, pleiotropic, metabolic role of AT and the complex, intricate dialogue between AT and HIV-related or ART-related parameters, it is still very difficult to evaluate the contribution to systemic inflammation of AT in general and HIV-related changes in AT in particular. These contributions might also depend strongly on metabolic alterations and comorbidities present at the start of the infection.

AUTHOR CONTRIBUTIONS

All authors contributed to the article and approved the submitted version.

FUNDING

The research was funded by the French National Research Agency for HIV and Viral Hepatitis (ANRS), the French National Research Agency (reference: RHU CARMMA ANR-15-RHUS-0003), Sidaction, DIM OneHealth, Fondation Dormeur, and Gilead.

ACKNOWLEDGMENTS

The authors thank the staff at the IDMIT facility working on the SIVART program: the project manager (Dr. D. Desjardins), the animal welfare group (Dr Ho Tsong Fang), and the biomonitoring groups (Dr. N. Dereuddre-Bosquet, and AS. Gallouet), and the director (Dr. R. Le Grand). We thank the surgery departments at Bicêtre Hospital and Institut Mutualiste Montsouris Hospital (Dr G Pourcher) and Pr V Pourcher (Pitié-Salpétrière Hospital, APHP) for access to human AT samples. Lastly, we thank the patients for agreeing to participate in the research on AT.

REFERENCES

1. Giordano A, Smorlesi A, Frontini A, Barbatelli G, Cint S. White, Brown and Pink Adipocytes: The Extraordinary Plasticity of the Adipose Organ. *Eur J Endocrinol* (2014) 170:159–71. doi: 10.1530/EJE-13-0945
2. Wernstedt Asterholm I, Tao C, Morley TS, Wang QA, Delgado-Lopez F, Wang ZV, et al. Adipocyte Inflammation Is Essential for Healthy Adipose Tissue Expansion and Remodeling. *Cell Metab* (2014) 20:103–18. doi: 10.1016/j.cmet.2014.05.005
3. Zamboni M, Nori N, Brunelli A, Zoico E. How Does Adipose Tissue Contribute to Inflammageing? *Exp Gerontol* (2021) 143:111162. doi: 10.1016/j.exger.2020.111162
4. Cypess AM, Lehman S, Williams G, Tal I, Rodman D, Goldfine AB, et al. Identification and Importance of Brown Adipose Tissue in Adult Humans. *N Engl J Med* (2009) 360:1509–17. doi: 10.1056/NEJMoa0810780
5. Saito M, Okamatsu-Ogura Y, Matsushita M, Watanabe K, Yoneshiro T, Nio-Kobayashi J, et al. High Incidence of Metabolically Active Brown Adipose Tissue in Healthy Adult Humans: Effects of Cold Exposure and Adiposity. *Diabetes* (2009) 58:1526–31. doi: 10.2337/db09-0530
6. Wang W, Seale P. Control of Brown and Beige Fat Development. *Nat Rev Mol Cell Biol* (2016) 17:691–702. doi: 10.1038/nrm.2016.96
7. Fedorenko A, Lishko PV, Kirichok Y. Mechanism of Fatty-Acid-Dependent UCP1 Uncoupling in Brown Fat Mitochondria. *Cell* (2012) 151:400–13. doi: 10.1016/j.cell.2012.09.010
8. Cypess AM, White AP, Vernochet C, Schulz TJ, Xue R, Sass CA, et al. Anatomical Localization, Gene Expression Profiling and Functional Characterization of Adult Human Neck Brown Fat. *Nat Med* (2013) 19:635–9. doi: 10.1038/nm.3112
9. Jespersen NZ, Larsen TJ, Peijs L, Daugaard S, Homoe P, Loft A, et al. A Classical Brown Adipose Tissue mRNA Signature Partly Overlaps With Brite in the Supraclavicular Region of Adult Humans. *Cell Metab* (2013) 17:798–805. doi: 10.1016/j.cmet.2013.04.011
10. van Marken Lichtenbelt WD, Vanhommerig JW, Smulders NM, Drossaerts JM, Kemerink GJ, Bouvy ND, et al. Cold-Activated Brown Adipose Tissue in Healthy Men. *N Engl J Med* (2009) 360:1500–8. doi: 10.1056/NEJMoa0808718
11. Thomou T, Mori MA, Dreyfuss JM, Konishi M, Sakaguchi M, Wolfrum C, et al. Adipose-Derived Circulating miRNAs Regulate Gene Expression in Other Tissues. *Nature* (2017) 542:450–5. doi: 10.1038/nature21365

12. Virtue AT, McCright SJ, Wright JM, Jimenez MT, Mowel WK, Kotzin JJ, et al. The Gut Microbiota Regulates White Adipose Tissue Inflammation and Obesity Via a Family of Microrrnas. *Sci Transl Med* (2019) 11:eaav1892. doi: 10.1126/scitranslmed.aav1892
13. Hotamisligil GS. Inflammation and Metabolic Disorders. *Nature* (2006) 444:860–7. doi: 10.1038/nature05485
14. Lafontan M, Berlan M. Do Regional Differences in Adipocyte Biology Provide New Pathophysiological Insights? *Trends Pharmacol Sci* (2003) 24:276–83. doi: 10.1016/S0165-6147(03)00132-9
15. Bruun JM, Lihn AS, Pedersen SB, Richelsen B. Monocyte Chemoattractant Protein-1 Release Is Higher in Visceral than Subcutaneous Human Adipose Tissue (AT): Implication of Macrophages Resident in the AT. *J Clin Endocrinol Metab* (2005) 90:2282–9. doi: 10.1210/jc.2004-1696
16. Madani R, Karastergiou K, Ogston NC, Miheisi N, Bhome R, Haloob N, et al. RANTES Release by Human Adipose Tissue In Vivo and Evidence for Depot-Specific Differences. *Am J Physiol Endocrinol Metab* (2009) 296: E1262–8. doi: 10.1152/ajpendo.90511.2008
17. Rakotoarivelo V, Lacraz G, Mayhue M, Brown C, Rottembourg D, Fradette J, et al. Inflammatory Cytokine Profiles in Visceral and Subcutaneous Adipose Tissues of Obese Patients Undergoing Bariatric Surgery Reveal Lack of Correlation With Obesity or Diabetes. *EBioMedicine* (2018) 30:237–47. doi: 10.1016/j.ebiom.2018.03.004
18. Bouloumié A, Curat CA, Sengenès C, Lolmède K, Miranville A, Busse R. Role of Macrophage Tissue Infiltration in Metabolic Diseases. *Curr Opin Clin Nutr Metab Care* (2005) 8:347–54. doi: 10.1097/01.mco.0000172571.41149.52
19. Bruun JM, Lihn AS, Verdich C, Pedersen SB, Toubro S, Astrup A, et al. Regulation of Adiponectin by Adipose Tissue-Derived Cytokines: In Vivo and In Vitro Investigations in Humans. *Am J Physiol Endocrinol Metab* (2003) 285:E527–33. doi: 10.1152/ajpendo.00110.2003
20. Matarese G, La Cava A. The Intricate Interface Between Immune System and Metabolism. *Trends Immunol* (2004) 25:193–200. doi: 10.1016/j.it.2004.02.009
21. Luo Y, Liu M. Adiponectin: A Versatile Player of Innate Immunity. *J Mol Cell Biol* (2016) 8:120–8. doi: 10.1093/jmcb/mjw012
22. Maximus PS, Al Achkar Z, Hamid PF, Hasnain SS, Peralta CA. Adipocytokines: Are They the Theory of Everything? *Cytokine* (2020) 133:155144. doi: 10.1016/j.cyto.2020.155144
23. Neumann E, Hasseli R, Ohl S, Lange U, Frommer KW, Müller-Ladner U. Adipokines and Autoimmunity in Inflammatory Arthritis. *Cells* (2021) 10:216. doi: 10.3390/cells10020216
24. Tsai Y-W, Fu S-H, Dong J-L, Chien M-W, Liu Y-W, Hsu C-Y, et al. Adipokine-Modulated Immunological Homeostasis Shapes the Pathophysiology of Inflammatory Bowel Disease. *Int J Mol Sci* (2020) 21:9564. doi: 10.3390/ijms21249564
25. Angelucci A, Clementi L, Alesse E. Leptin in Tumor Microenvironment. *Adv Exp Med Biol* (2020) 1259:89–112. doi: 10.1007/978-3-030-43093-1_6
26. Mohamed-Ali V, Goodrick S, Rawesh A, Katz DR, Miles JM, Yudkin JS, et al. Subcutaneous Adipose Tissue Releases Interleukin-6, But Not Tumor Necrosis Factor-Alpha, In Vivo. *J Clin Endocrinol Metab* (1997) 82:4196–200. doi: 10.1210/jcem.82.12.4450
27. Carey AL, Bruce CR, Sacchetti M, Anderson MJ, Olsen DB, Saltin B, et al. Interleukin-6 and Tumor Necrosis Factor-Alpha Are Not Increased in Patients With Type 2 Diabetes: Evidence That Plasma Interleukin-6 Is Related to Fat Mass and Not Insulin Responsiveness. *Diabetologia* (2004) 47:1029–37. doi: 10.1007/s00125-004-1403-x
28. Desreumaux P, Ernst O, Geboes K, Gambiez L, Berrebi D, Müller-Alouf H, et al. Inflammatory Alterations in Mesenteric Adipose Tissue in Crohn's Disease. *Gastroenterology* (1999) 117:73–81. doi: 10.1016/s0016-5085(99)70552-4
29. Bourgeois C, Gorwood J, Barrail-Tran A, Lagathu C, Capeau J, Desjardins D, et al. Specific Biological Features of Adipose Tissue, and Their Impact on HIV Persistence. *Front Microbiol* (2019) 10:2837. doi: 10.3389/fmicb.2019.02837
30. Ivanov S, Merlin J, Lee MKS, Murphy AJ, Guinamard RR. Biology and Function of Adipose Tissue Macrophages, Dendritic Cells and B Cells. *Atherosclerosis* (2018) 271:102–10. doi: 10.1016/j.atherosclerosis.2018.01.018
31. Feuerer M, Herrero L, Cipolletta D, Naaz A, Wong J, Nayer A, et al. Lean, But Not Obese, Fat Is Enriched for a Unique Population of Regulatory T Cells That Affect Metabolic Parameters. *Nat Med* (2009) 15:1–11. doi: 10.1038/nm.2002
32. Duffaut C, Zakaroff-Girard A, Bourlier V, Decaunes P, Maumus M, Chiotasso P, et al. Interplay Between Human Adipocytes and T Lymphocytes in Obesity: CCL20 as an Adipochemokine and T Lymphocytes as Lipogenic Modulators. *Arterioscler Thromb Vasc Biol* (2009) 29:1608–14. doi: 10.1161/ATVBAHA.109.192583
33. Manferdini C, Paolella F, Gabusi E, Gambari L, Piacentini A, Filardo G, et al. Adipose Stromal Cells Mediated Switching of the Pro-Inflammatory Profile of M1-like Macrophages Is Facilitated by PGE2: In Vitro Evaluation. *Osteoarthr Cartil* (2017) 25:1161–71. doi: 10.1016/j.joca.2017.01.011
34. Zhou K, Guo S, Tong S, Sun Q, Li F, Zhang X, et al. Immunosuppression of Human Adipose-Derived Stem Cells on T Cell Subsets Via the Reduction of NF-kappaB Activation Mediated by PD-L1/PD-1 and Gal-9/TIM-3 Pathways. *Stem Cells Dev* (2018) 27:1191–202. doi: 10.1089/scd.2018.0033
35. Beura LK, Wijeyesinghe S, Thompson EA, Macchietto MG, Rosato PC, Pierson MJ, et al. T Cells in Nonlymphoid Tissues Give Rise to Lymph-Node-Resident Memory T Cells. *Immunity* (2018) 48:327–338.e5. doi: 10.1016/j.immuni.2018.01.015
36. Behr FM, Parga-Vidal L, Kragten NAM, van Dam TJP, Wesselink TH, Sheridan BS, et al. Tissue-Resident Memory CD8+ T Cells Shape Local and Systemic Secondary T Cell Responses. *Nat Immunol* (2020) 21:1070–81. doi: 10.1038/s41590-020-0723-4
37. Ibrahim MM. Subcutaneous and Visceral Adipose Tissue: Structural and Functional Differences. *Obes Rev* (2009) 11:11–8. doi: 10.1111/j.1467-789X.2009.00623.x
38. Gealekman O, Guseva N, Hartigan C, Apotheker S, Gorgoglione M, Gurav K, et al. Depot-Specific Differences and Insufficient Subcutaneous Adipose Tissue Angiogenesis in Human Obesity. *Circulation* (2011) 123:186–94. doi: 10.1161/CIRCULATIONAHA.110.970145
39. Hwang I, Kim JB. Two Faces of White Adipose Tissue With Heterogeneous Adipogenic Progenitors. *Diabetes Metab J* (2019) 43:752–62. doi: 10.4093/dmj.2019.0174
40. Kim JI, Huh JY, Sohn JH, Choe SS, Lee YS, Lim CY, et al. Lipid-Overloaded Enlarged Adipocytes Provoke Insulin Resistance Independent of Inflammation. *Mol Cell Biol* (2015) 35:1686–99. doi: 10.1128/MCB.01321-14
41. Bray GA, Jablonski KA, Fujimoto WY, Barrett-Connor E, Haffner S, Hanson RL, et al. Relation of Central Adiposity and Body Mass Index to the Development of Diabetes in the Diabetes Prevention Program. *Am J Clin Nutr* (2008) 87:1212–8. doi: 10.1093/ajcn/87.5.1212
42. Longo M, Zatterale F, Naderi J, Parrillo L, Formisano P, Raciti GA, et al. Adipose Tissue Dysfunction as Determinant of Obesity-Associated Metabolic Complications. *Int J Mol Sci* (2019) 20:2358. doi: 10.3390/ijms20092358
43. Hocking SL, Stewart RL, Brandon AE, Suryana E, Stuart E, Baldwin EM, et al. Subcutaneous Fat Transplantation Alleviates Diet-Induced Glucose Intolerance and Inflammation in Mice. *Diabetologia* (2015) 58:1587–600. doi: 10.1007/s00125-015-3583-y
44. Gabriely I, Ma XH, Yang XM, Atzmon G, Rajala MW, Berg AH, et al. Removal of Visceral Fat Prevents Insulin Resistance and Glucose Intolerance of Aging: An Adipokine-Mediated Process? *Diabetes* (2002) 51:2951–8. doi: 10.2337/diabetes.51.10.2951
45. Alvehus M, Burén J, Sjöström M, Goedecke J, Olsson T. The Human Visceral Fat Depot has a Unique Inflammatory Profile. *Obesity (Silver Spring)* (2010) 18:879–83. doi: 10.1038/oby.2010.22
46. Ayari A, Wolowczuk I. Physiology and Pathophysiology of Adipose Tissue-Derived Cytokine Networks. In: *Cytokine Effector Functions in Tissues*. Elsevier Inc. Academic Press (2017) p. 33–50. doi: 10.1016/B978-0-12-804214-4.00001-4
47. Kralova Lesna I, Kralova A, Cejkova S, Fronek J, Petras M, Sekerkova A, et al. Characterisation and Comparison of Adipose Tissue Macrophages From Human Subcutaneous, Visceral and Perivascular Adipose Tissue. *J Transl Med* (2016) 14:208. doi: 10.1186/s12967-016-0962-1
48. Lee B-C, Kim M-S, Pae M, Yamamoto Y, Eberlé D, Shimada T, et al. Adipose Natural Killer Cells Regulate Adipose Tissue Macrophages to Promote Insulin Resistance in Obesity. *Cell Metab* (2016) 23:685–98. doi: 10.1016/j.cmet.2016.03.002

49. Weisberg SP, McCann D, Desai M, Rosenbaum M, Leibel RL, Ferrante AW. Obesity Is Associated With Macrophage Accumulation in Adipose Tissue. *J Clin Invest* (2003) 112:1796–808. doi: 10.1172/JCI200319246.Introduction
50. Tchkonia T, Thomou T, Zhu Y, Karagiannides I, Pothoulakis C, Jensen MD, et al. Mechanisms and Metabolic Implications of Regional Differences Among Fat Depots. *Cell Metab* (2013) 17:644–56. doi: 10.1016/j.cmet.2013.03.008
51. White UA, Tchoukalova YD. Sex Dimorphism and Depot Differences in Adipose Tissue Function. *Biochim Biophys Acta - Mol Basis Dis* (2014) 1842:377–92. doi: 10.1016/j.bbadis.2013.05.006
52. Karpe F, Pinnick KE. Biology of Upper-Body and Lower-Body Adipose Tissue - Link to Whole-Body Phenotypes. *Nat Rev Endocrinol* (2015) 11:90–100. doi: 10.1038/nrendo.2014.185
53. Pinnick KE, Nicholson G, Manolopoulos KN, McQuaid SE, Valet P, Frayn KN, et al. Distinct Developmental Profile of Lower-Body Adipose Tissue Defines Resistance Against Obesity-Associated Metabolic Complications. *Diabetes* (2014) 63:3785–97. doi: 10.2337/db14-0385
54. Karastergiou K, Fried SK, Xie H, Lee MJ, Divoux A, Rosencrantz MA, et al. Distinct Developmental Signatures of Human Abdominal and Gluteal Subcutaneous Adipose Tissue Depots. *J Clin Endocrinol Metab* (2013) 98:362–71. doi: 10.1210/jc.2012-2953
55. Tan GD, Goossens GH, Humphreys SM, Vidal H, Karpe F. Upper and Lower Body Adipose Tissue Function: A Direct Comparison of Fat Mobilization in Humans. *Obes Res* (2004) 12:114–8. doi: 10.1038/oby.2004.15
56. McQuaid SE, Humphreys SM, Hodson L, Fielding BA, Karpe F, Frayn KN. Femoral Adipose Tissue may Accumulate the Fat That has Been Recycled as VLDL and Nonesterified Fatty Acids. *Diabetes* (2010) 59:2465–73. doi: 10.2337/db10-0678
57. Vogel MAA, Jocken JWE, Sell H, Hoebers N, Essers Y, Rouschop KMA, et al. Differences in Upper and Lower Body Adipose Tissue Oxygen Tension Contribute to the Adipose Tissue Phenotype in Humans. *J Clin Endocrinol Metab* (2018) 103:3688–97. doi: 10.1210/jc.2018-00547
58. Choe SS, Huh JY, Hwang IJ, Kim JI, Kim JB. Adipose Tissue Remodeling: Its Role in Energy Metabolism and Metabolic Disorders. *Front Endocrinol (Lausanne)* (2016) 7:30. doi: 10.3389/fendo.2016.00030
59. Gregor MF, Hotamisligil GS. Inflammatory Mechanisms in Obesity. *Annu Rev Immunol* (2011) 29:415–45. doi: 10.1146/annurev-immunol-031210-101322
60. Sun K, Tordjman J, Clément K, Scherer PE. Fibrosis and Adipose Tissue Dysfunction. *Cell Metab* (2013) 18:470–7. doi: 10.1016/j.cmet.2013.06.016
61. Divoux A, Tordjman J, Lacasa D, Veyrie N, Hugol D, Aissat A, et al. Fibrosis in Human Adipose Tissue: Composition, Distribution, and Link With Lipid Metabolism and Fat Mass Loss. *Diabetes* (2010) 59:2817–25. doi: 10.2337/db10-0585
62. Abdennour M, Reggio S, Le Naour G, Liu Y, Poitou C, Aron-Wisnewsky J, et al. Association of Adipose Tissue and Liver Fibrosis With Tissue Stiffness in Morbid Obesity: Links With Diabetes and BMI Loss After Gastric Bypass. *J Clin Endocrinol Metab* (2014) 99:898–907. doi: 10.1210/jc.2013-3253
63. Muir LA, Neeley CK, Meyer KA, Baker NA, Brosius AM, Washabaugh AR, et al. Adipose Tissue Fibrosis, Hypertrophy, and Hyperplasia: Correlations With Diabetes in Human Obesity. *Obesity* (2016) 24:597–605. doi: 10.1002/oby.21377
64. Weyer C, Foley JE, Bogardus C, Tataranni PA, Pratley RE. Enlarged Subcutaneous Abdominal Adipocyte Size, But Not Obesity Itself, Predicts Type II Diabetes Independent of Insulin Resistance. *Diabetologia* (2000) 43:1498–506. doi: 10.1007/s001250051560
65. Skurk T, Alberti-Huber C, Herder C, Hauner H. Relationship Between Adipocyte Size and Adipokine Expression and Secretion. *J Clin Endocrinol Metab* (2007) 92:1023–33. doi: 10.1210/jc.2006-1055
66. Apostolopoulos V, de Courten MPJ, Stojanovska L, Blatch GL, Tangalakis K, de Courten B. The Complex Immunological and Inflammatory Network of Adipose Tissue in Obesity. *Mol Nutr Food Res* (2016) 60:43–57. doi: 10.1002/mnfr.201500272
67. Klein-Wieringa IR, Andersen SN, Kwekkeboom JC, Giera M, de Lange-Brokaar BJE, van Osch GJVM, et al. Adipocytes Modulate the Phenotype of Human Macrophages Through Secreted Lipids. *J Immunol* (2013) 191:1356–63. doi: 10.4049/jimmunol.1203074
68. Watanabe Y, Nagai Y, Honda H, Okamoto N, Yanagibashi T, Ogasawara M, et al. Bidirectional Crosstalk Between Neutrophils and Adipocytes Promotes Adipose Tissue Inflammation. *FASEB J* (2019) 33:11821–35. doi: 10.1096/fj.201900477RR
69. Wang Q, Wu H. T Cells in Adipose Tissue: Critical Players in Immunometabolism. *Front Immunol* (2018) 9:2509. doi: 10.3389/fimmu.2018.02509
70. Chehimi M, Vidal H, Eljaafari A. Pathogenic Role of IL-17-Producing Immune Cells in Obesity, and Related Inflammatory Diseases. *J Clin Med* (2017) 6:68. doi: 10.3390/jcm6070068
71. Wensveen FM, Jelenčić V, Valentić S, Šestan M, Wensveen TT, Theurich S, et al. NK Cells Link Obesity-Induced Adipose Stress to Inflammation and Insulin Resistance. *Nat Immunol* (2015) 16:376–85. doi: 10.1038/ni.3120
72. Nishimura S, Manabe I, Nagasaki M, Eto K, Yamashita H, Ohsugi M, et al. CD8+ Effector T Cells Contribute to Macrophage Recruitment and Adipose Tissue Inflammation in Obesity. *Nat Med* (2009) 15:914–20. doi: 10.1038/nm.1964
73. Strieder-Barboza C, Baker NA, Flesher CG, Karmakar M, Neeley CK, Polsinelli D, et al. Advanced Glycation End-Products Regulate Extracellular Matrix-Adipocyte Metabolic Crosstalk in Diabetes. *Sci Rep* (2019) 9:1–10. doi: 10.1038/s41598-019-56242-z
74. Feng Z, Zhu L, Wu J. RAGE Signalling in Obesity and Diabetes: Focus on the Adipose Tissue Macrophage. *Adipocyte* (2020) 9:563–6. doi: 10.1080/21623945.2020.1817278
75. Pradhan AD, Manson JE, Rifai N, Buring JE, Ridker PM. C-Reactive Protein, Interleukin 6, and Risk of Developing Type 2 Diabetes Mellitus. *J Am Med Assoc* (2001) 286:327–34. doi: 10.1001/jama.286.3.327
76. Ouchi N, Parker JL, Lugus JJ, Walsh K. Adipokines in Inflammation and Metabolic Disease. *Nat Publ Gr* (2011) 11:85–97. doi: 10.1038/nri2921
77. Fontana L, Eagon JC, Trujillo ME, Scherer PE, Klein S. Visceral Fat Adipokine Secretion Is Associated With Systemic Inflammation in Obese Humans. *Diabetes* (2007) 56:1010–3. doi: 10.2337/db06-1656
78. McLaughlin T, Liu L-F, Lamendola C, Shen L, Morton J, Rivas H, et al. T-Cell Profile in Adipose Tissue Is Associated With Insulin Resistance and Systemic Inflammation in Humans. *Arterioscler Thromb Vasc Biol* (2014) 34:2637–43. doi: 10.1161/ATVBAHA.114.304636
79. Liu R, Nikolajczyk BS. Tissue Immune Cells Fuel Obesity-Associated Inflammation in Adipose Tissue and Beyond. *Front Immunol* (2019) 10:1587. doi: 10.3389/fimmu.2019.01587
80. Han MS, White A, Perry RJ, Camporez JP, Hidalgo J, Shulman GI, et al. Regulation of Adipose Tissue Inflammation by Interleukin 6. *Proc Natl Acad Sci U S A* (2020) 117:2751–60. doi: 10.1073/pnas.1920004117
81. Gessani S, Belardelli F. Type I Interferons as Joint Regulators of Tumor Growth and Obesity. *Cancers (Basel)* (2021) 13:1–18. doi: 10.3390/cancers13020196
82. Wieser V, Adolph TE, Grander C, Grabherr F, Enrich B, Moser P, et al. Adipose Type I Interferon Signalling Protects Against Metabolic Dysfunction. *Gut* (2018) 67:157–65. doi: 10.1136/gutjnl-2016-313155
83. Chan CC, Damen MSMA, Moreno-Fernandez ME, Stankiewicz TE, Cappelletti M, Alarcon PC, et al. Type I Interferon Sensing Unlocks Dormant Adipocyte Inflammatory Potential. *Nat Commun* (2020) 11:2745. doi: 10.1038/s41467-020-16571-4
84. Iacobini C, Pugliese G, Blasetti Fantauzzi C, Federici M, Menini S. Metabolically Healthy Versus Metabolically Unhealthy Obesity. *Metabolism* (2019) 92:51–60. doi: 10.1016/j.metabol.2018.11.009
85. Koethe JR, Lagathu C, Lake JE, Domingo P, Calmy A, Falutz J, et al. HIV and Antiretroviral Therapy-Related Fat Alterations. *Nat Rev Dis Prim* (2020) 6:48. doi: 10.1038/s41572-020-0181-1
86. Giralt M, Domingo P, Villarroya F. Adipose Tissue Biology and HIV-Infection. *Best Pract Res Clin Endocrinol Metab* (2011) 25:487–99. doi: 10.1016/j.beem.2010.12.001
87. Dupin N, Buffet M, Marcelin A-G, Lamotte C, Gorin I, Ait-Arkoub Z, et al. HIV and Antiretroviral Drug Distribution in Plasma and Fat Tissue of HIV-Infected Patients With Lipodystrophy. *AIDS* (2002) 16:2419–24. doi: 10.1097/00002030-200212060-00006
88. Munier S, Borjabad A, Lemaire M, Mariot V, Hazan U. In Vitro Infection of Human Primary Adipose Cells With HIV-1: A Reassessment. *AIDS* (2003) 17:2537–9. doi: 10.1097/01.aids.0000096866.36052.84

89. Raymond AD, Campbell-Sims TC, Khan M, Lang M, Huang MB, Bond VC, et al. HIV Type 1 Nef Is Released From Infected Cells in CD45(+) Microvesicles and Is Present in the Plasma of HIV-infected Individuals. *AIDS Res Hum Retroviruses* (2011) 27:167–78. doi: 10.1089/aid.2009.0170
90. Agarwal N, Iyer D, Patel SG, Sekhar RV, Phillips TM, Schubert U, et al. HIV-1 Vpr Induces Adipose Dysfunction In Vivo Through Reciprocal Effects on PPAR/GR Co-Regulation. *Sci Transl Med* (2013) 5:213ra164. doi: 10.1126/scitranslmed.3007148
91. Gorwood J, Bourgeois C, Mantecon M, Atlan M, Pourcher V, Pourcher G, et al. Impact of HIV/simian Immunodeficiency Virus Infection and Viral Proteins on Adipose Tissue Fibrosis and Adipogenesis. *AIDS* (2019) 33:953–64. doi: 10.1097/QAD.0000000000002168
92. Gorwood J, Ejlalmanesh T, Bourgeois C, Mantecon M, Rose C, Atlan M, et al. SIV Infection and the HIV Proteins Tat and Nef Induce Senescence in Adipose Tissue and Human Adipose Stem Cells, Resulting in Adipocyte Dysfunction. *Cells* (2020) 9:854. doi: 10.3390/cells9040854
93. Pérez-Matute P, Pérez-Martínez L, Blanco JR, Oteo JA, Perez-Matute P, Perez-Martinez L, et al. Role of Mitochondria in HIV Infection and Associated Metabolic Disorders: Focus on Nonalcoholic Fatty Liver Disease and Lipodystrophy Syndrome. *Oxid Med Cell Longev* (2013) 2013:493413. doi: 10.1155/2013/493413
94. Vendeville A, Rayne F, Bonhoure A, Bettache N, Montcourrier P, Beaumelle B. HIV-1 Tat Enters T Cells Using Coated Pits Before Translocating From Acidified Endosomes and Eliciting Biological Responses. *Mol Biol Cell* (2004) 15:2347–60. doi: 10.1091/mbc.E03-12-0921
95. Debaisieux S, Rayne F, Yezid H, Beaumelle B. The Ins and Outs of HIV-1 Tat. *Traffic* (2012) 13:355–63. doi: 10.1111/j.1600-0854.2011.01286.x
96. Clark E, Nava B, Caputi M. Tat Is a Multifunctional Viral Protein That Modulates Cellular Gene Expression and Functions. *Oncotarget* (2017) 8:27569–81. doi: 10.18632/oncotarget.15174
97. Herbein G, Gras G, Khan KA, Abbas W. Macrophage Signaling in HIV-1 Infection. *Retrovirology* (2010) 7:34. doi: 10.1186/1742-4690-7-34
98. Datta PK, Deshmane S, Khalili K, Merali S, Gordon JC, Fecchio C, et al. Glutamate Metabolism in HIV-1 Infected Macrophages: Role of HIV-1 Vpr. *Cell Cycle* (2016) 15:2288–98. doi: 10.1080/15384101.2016.1190054
99. Jacob RA, Johnson AL, Pawlak EN, Dirk BS, Van Nynatten LR, Haeryfar SMM, et al. The Interaction Between HIV-1 Nef and Adaptor Protein-2 Reduces Nef-mediated CD4+ T Cell Apoptosis. *Virology* (2017) 509:1–10. doi: 10.1016/j.virol.2017.05.018
100. Couturier J, Suliburk JW, Brown JM, Luke DJ, Agarwal N, Yu X, et al. Human Adipose Tissue as a Reservoir for Memory CD4+ T Cells and HIV. *AIDS* (2015) 29:667–74. doi: 10.1097/QAD.0000000000000599
101. Couturier J, Agarwal N, Nehete PN, Baze WB, Barry MA, Jagannadha Sastry K, et al. Infectious SIV Resides in Adipose Tissue and Induces Metabolic Defects in Chronically Infected Rhesus Macaques. *Retrovirology* (2016) 13:30. doi: 10.1186/s12977-016-0260-2
102. Damouche A, Lazure T, Avettand-Fènoël V, Huot N, Dejucq-Rainsford N, Satie A-PA-P, et al. Adipose Tissue Is a Neglected Viral Reservoir and an Inflammatory Site During Chronic HIV and SIV Infection. *PloS Pathog* (2015) 11:e1005153. doi: 10.1371/journal.ppat.1005153
103. Couturier J, Lewis DE. HIV Persistence in Adipose Tissue Reservoirs. *Curr HIV/AIDS Rep* (2018) 15:60–71. doi: 10.1007/s11904-018-0378-z
104. Sabin CA. Do People With HIV Infection Have a Normal Life Expectancy in the Era of Combination Antiretroviral Therapy? *BMC Med* (2013) 11:251. doi: 10.1186/1741-7015-11-251
105. Hunt PW. HIV and Inflammation: Mechanisms and Consequences. *Curr HIV/AIDS Rep* (2012) 9:139–47. doi: 10.1007/s11904-012-0118-8
106. Novelli S, Lécuroux C, Goujard C, Reynes J, Villemant A, Blum L, et al. Persistence of Monocyte Activation Under Treatment in People Followed Since Acute HIV-1 Infection Relative to Participants at High or Low Risk of HIV Infection. *EBioMedicine* (2020) 62:103129. doi: 10.1016/j.ebiom.2020.103129
107. Sereti I, Krebs SJ, Phanuphak N, Fletcher JL, Slike B, Pinyakorn S, et al. Persistent, Albeit Reduced, Chronic Inflammation in Persons Starting Antiretroviral Therapy in Acute HIV Infection. *Clin Infect Dis* (2017) 64:124–31. doi: 10.1093/cid/ciw683
108. Brenchley JM, Price DA, Schacker TW, Asher TE, Silvestri G, Rao S, et al. Microbial Translocation Is a Cause of Systemic Immune Activation in Chronic HIV Infection. *Nat Med* (2006) 12:1365–71. doi: 10.1038/nm1511
109. Bandera A, De Benedetto I, Bozzi G, Gori A. Altered Gut Microbiome Composition in HIV Infection: Causes, Effects and Potential Intervention. *Curr Opin HIV AIDS* (2018) 13:73–80. doi: 10.1097/COH.0000000000000429
110. Bäckhed F, Ding H, Wang T, Hooper LV, Koh GY, Nagy A, et al. The Gut Microbiota as an Environmental Factor That Regulates Fat Storage. *Proc Natl Acad Sci U S A* (2004) 101:15718–23. doi: 10.1073/pnas.0407076101
111. Spencer SP, Sonnenburg JL. When Gut Microbiota Creep Into Fat, the Fat Creeps Back. *Cell* (2020) 183:589–91. doi: 10.1016/j.cell.2020.10.008
112. Day CL, Kaufmann DE, Kiepiela P, Brown JA, Moodley ES, Reddy S, et al. PD-1 Expression on HIV-Specific T Cells Is Associated With T-Cell Exhaustion and Disease Progression. *Nature* (2006) 443:350–4. doi: 10.1038/nature05115
113. Ghislain M, Bastard J-P, Meyer L, Capeau J, Fellahi S, Gérard L, et al. Late Antiretroviral Therapy (ART) Initiation Is Associated With Long-Term Persistence of Systemic Inflammation and Metabolic Abnormalities. *PloS One* (2015) 10:e0144317. doi: 10.1371/journal.pone.0144317
114. Bastard J-P, Caron M, Vidal H, Jan V, Auclair M, Vigouroux C, et al. Association Between Altered Expression of Adipogenic Factor SREBP1 in Lipoatrophic Adipose Tissue From HIV-1-Infected Patients and Abnormal Adipocyte Differentiation and Insulin Resistance. *Lancet* (2002) 359:1026–31. doi: 10.1016/S0140-6736(02)08094-7
115. Jan V, Cervera P, Maachi M, Baudrimont M, Kim M, Vidal H, et al. Altered Fat Differentiation and Adipocytokine Expression Are Inter-Related and Linked to Morphological Changes and Insulin Resistance in HIV-1-Infected Lipodystrophic Patients. *Antivir Ther* (2004) 9:555–64. doi: 10.1038/nm1511
116. Mallal SA, John M, Moore CB, James IR, McKinnon EJ. Contribution of Nucleoside Analogue Reverse Transcriptase Inhibitors to Subcutaneous Fat Wasting in Patients With HIV Infection. *AIDS* (2000) 14:1309–16. doi: 10.1097/00002030-200007070-00002
117. Nolan D, Hammond E, Martin A, Taylor L, Herrmann S, McKinnon E, et al. Mitochondrial DNA Depletion and Morphologic Changes in Adipocytes Associated With Nucleoside Reverse Transcriptase Inhibitor Therapy. *AIDS* (2003) 17:1329–38. doi: 10.1097/01.aids.0000060385.18106.35
118. Martin A, Mallon PW. Therapeutic Approaches to Combating Lipoatrophy: Do They Work? *J Antimicrob Chemother* (2005) 55:612–5. doi: 10.1093/jac/dki062
119. Lake JE, Stanley TL, Apovian CM, Bhasin S, Brown TT, Capeau J, et al. Practical Review of Recognition and Management of Obesity and Lipohypertrophy in Human Immunodeficiency Virus Infection. *Clin Infect Dis* (2017) 64:1422–9. doi: 10.1093/cid/cix178
120. Calmy A, Tovar Sanchez T, Kouanfack C, Mpoudi-Etame M, Leroy S, Perrineau S, et al. Dolutegravir-Based and Low-Dose Efavirenz-Based Regimen for the Initial Treatment of HIV-1 Infection (NAMSAL): Week 96 Results From a Two-Group, Multicentre, Randomised, Open Label, Phase 3 Non-Inferiority Trial in Cameroon. *Lancet HIV* (2020) 7:e677–87. doi: 10.1016/S2352-3018(20)30238-1
121. Venter WDF, Moorhouse M, Sokhela S, Fairlie L, Mashabane N, Masenya M, et al. Dolutegravir Plus Two Different Prodrugs of Tenofovir to Treat HIV. *N Engl J Med* (2019) 381:803–15. doi: 10.1056/NEJMoa1902824
122. Couturier J, Winchester LC, Suliburk JW, Wilkerson GK, Podany AT, Agarwal N, et al. Adipocytes Impair Efficacy of Antiretroviral Therapy. *Antiviral Res* (2018) 154:140–8. doi: 10.1016/j.antiviral.2018.04.002
123. Gorwood J, Bourgeois C, Pourcher V, Pourcher G, Charlotte F, Mantecon M, et al. The Integrase Inhibitors Dolutegravir and Raltegravir Exert Pro-Adipogenic and Profibrotic Effects and Induce Insulin Resistance in Human/Simian Adipose Tissue and Human Adipocytes. *Clin Infect Dis* (2020) 71:e549–60. doi: 10.1093/cid/ciaa259
124. Patterson KB, Prince HA, Stevens T, Shaheen NJ, Dellon ES, Madanick RD, et al. Differential Penetration of Raltegravir Throughout Gastrointestinal Tissue: Implications for Eradication and Cure. *AIDS* (2013) 27:1413–9. doi: 10.1097/QAD.0b013e32835f2b49
125. Bastard JP, Pelloux V, Alili R, Fellahi S, Aron-Wisnewsky J, Emilie C, et al. Altered Subcutaneous Adipose Tissue Parameters After Switching ART-Controlled HIV+ Patients to Raltegravir/Maraviroc. *AIDS* (2021). doi: 10.1097/QAD.0000000000002900
126. Mansfield KG, Carville A, Wachtman L, Goldin BR, Yearley J, Li W, et al. A Diet High in Saturated Fat and Cholesterol Accelerates Simian Immunodeficiency Virus Disease Progression. *J Infect Dis* (2007) 196:1202–10. doi: 10.1086/521680

127. Milner JJ, Sheridan PA, Karlsson EA, Schultz-Cherry S, Shi Q, Beck MA. Diet-Induced Obese Mice Exhibit Altered Heterologous Immunity During a Secondary 2009 Pandemic H1N1 Infection. *J Immunol* (2013) 191:2474–85. doi: 10.4049/jimmunol.1202429
128. Crum-Cianflone NF, Roediger M, Eberly LE, Vyas K, Landrum ML, Ganesan A, et al. Obesity Among HIV-infected Persons: Impact of Weight on CD4 Cell Count. *AIDS* (2010) 24:1069–72. doi: 10.1097/QAD.0b013e328337fe01
129. Shor-Posner G, Campa A, Zhang G, Persaud N, Miguez-Burbano M-J, Quesada J, et al. When Obesity Is Desirable: A Longitudinal Study of the Miami HIV-1–Infected Drug Abusers (MIDAS) Cohort. *J Acquir Immune Defic Syndr* (2000) 23:81–8. doi: 10.1097/00126334-200001010-00011
130. Jiang J, Qin X, Liu H, Meng S, Abdullah AS, Huang J, et al. An Optimal BMI Range Associated With a Lower Risk of Mortality Among HIV-Infected Adults Initiating Antiretroviral Therapy in Guangxi, China. *Sci Rep* (2019) 9:7816. doi: 10.1038/s41598-019-44279-z
131. Kim DJ, Westfall AO, Chamot E, Willig AL, Mugavero MJ, Ritchie C, et al. Multimorbidity Patterns in HIV-Infected Patients: The Role of Obesity in Chronic Disease Clustering. *J Acquir Immune Defic Syndr* (2012) 61:600–5. doi: 10.1097/QAI.0b013e31827303d5
132. Koethe JR, Jenkins CA, Shepherd BE, Stinnette SE, Sterling TR. An Optimal Body Mass Index Range Associated With Improved Immune Reconstitution Among HIV-infected Adults Initiating Antiretroviral Therapy. *Clin Infect Dis* (2011) 53:952–60. doi: 10.1093/cid/cir606
133. Koethe JR, Jenkins CA, Lau B, Shepherd BE, Wester W, Rebeiro PF, et al. Higher Time-Updated Body Mass Index: Association With Improved CD4+ Cell Recovery on HIV Treatment. *J Acquir Immune Defic Syndr* (2016) 73:197–204. doi: 10.1097/QAI.0000000000001035
134. Tedaldi EM, Brooks JT, Weidle PJ, Richardson JT, Baker RK, Buchacz K, et al. Increased Body Mass Index Does Not Alter Response to Initial Highly Active Antiretroviral Therapy in HIV-1-Infected Patients. *J Acquir Immune Defic Syndr* (2006) 43:35–41. doi: 10.1097/01.qai.0000234084.11291.d4
135. Madelain V, Le MP, Champenois K, Charpentier C, Landman R, Joly V, et al. Impact of Obesity on Antiretroviral Pharmacokinetics and Immunovirological Response in HIV-Infected Patients: A Case-Control Study. *J Antimicrob Chemother* (2017) 72:1137–46. doi: 10.1093/jac/dkw527
136. Caron M, Auclair M, Lagathu C, Lombes A, Walker UA, Kornprobst M, et al. The HIV-1 Nucleoside Reverse Transcriptase Inhibitors Stavudine and Zidovudine Alter Adipocyte Functions In Vitro. *AIDS* (2004) 18:2127–36. doi: 10.1097/00002030-200411050-00004
137. De Luca A, Nasi M, Di Giambenedetto S, Cozzi-Lepri A, Pinti M, Marzocchetti A, et al. Mitochondrial DNA Haplogroups and Incidence of Lipodystrophy in HIV-Infected Patients on Long-Term Antiretroviral Therapy. *J Acquir Immune Defic Syndr* (2012) 59:113–20. doi: 10.1097/QAI.0b013e31823daff3
138. Hulgan T, Haubrich R, Riddler SA, Tebas P, Ritchie MD, McComsey GA, et al. European Mitochondrial DNA Haplogroups and Metabolic Changes During Antiretroviral Therapy in AIDS Clinical Trials Group Study A5142. *AIDS* (2011) 25:37–47. doi: 10.1097/QAD.0b013e32833f9d02
139. Caron M, Auclair M, Donadille B, Béréziat V, Guerci B, Laville M, et al. Human Lipodystrophies Linked to Mutations in A-type Lamins and to HIV Protease Inhibitor Therapy Are Both Associated With Prelamin A Accumulation, Oxidative Stress and Premature Cellular Senescence. *Cell Death Differ* (2007) 14:1759–67. doi: 10.1038/sj.cdd.4402197
140. Caron M, Auclair M, Sterlingot H, Kornprobst M, Capeau J. Some HIV Protease Inhibitors Alter Lamin A/C Maturation and Stability, SREBP-1 Nuclear Localization and Adipocyte Differentiation. *AIDS* (2003) 17:2437–44. doi: 10.1097/00002030-200311210-00005
141. Torriani M, Srinivasa S, Fitch KV, Thomou T, Wong K, Petrow E, et al. Dysfunctional Subcutaneous Fat With Reduced Dicer and Brown Adipose Tissue Gene Expression in HIV-Infected Patients. *J Clin Endocrinol Metab* (2016) 101:1225–34. doi: 10.1210/jc.2015-3993
142. Ravaud C, Pare M, Yao X, Azoulay S, Mazure NM, Dani C, et al. Resveratrol and HIV-Protease Inhibitors Control UCP1 Expression Through Opposite Effects on P38 MAPK Phosphorylation in Human Adipocytes. *J Cell Physiol* (2020) 235:1184–96. doi: 10.1002/jcp.29032
143. Srinivasa S, Torriani M, Fitch KV, Maehler P, Iyengar S, Feldpausch M, et al. Brief Report: Adipogenic Expression of Brown Fat Genes in HIV and HIV-Related Parameters. *J Acquir Immune Defic Syndr* (2019) 82:491–5. doi: 10.1097/QAI.0000000000002180
144. El Hadri K, Glorian M, Monsempes C, Dieudonne MN, Pecquery R, Giudicelli Y, et al. In Vitro Suppression of the Lipogenic Pathway by the Nonnucleoside Reverse Transcriptase Inhibitor Efavirenz in 3T3 and Human Preadipocytes or Adipocytes. *J Biol Chem* (2004) 279:15130–41. doi: 10.1074/jbc.M312875200
145. Hasegawa Y, Ikeda K, Chen Y, Alba DL, Stifler D, Shinoda K, et al. Repression of Adipose Tissue Fibrosis Through a PRDM16-GTF2IRD1 Complex Improves Systemic Glucose Homeostasis. *Cell Metab* (2018) 27:180–194.e6. doi: 10.1016/j.cmet.2017.12.005
146. Babaei R, Schuster M, Meln I, Lerch S, Ghandour RA, Pisani DF, et al. Jak-TGFbeta Cross-Talk Links Transient Adipose Tissue Inflammation to Beige Adipogenesis. *Sci Signal* (2018) 11:eaai7838. doi: 10.1126/scisignal.aai7838
147. Hill A, Waters L, Pozniak A. Are New Antiretroviral Treatments Increasing the Risks of Clinical Obesity? *J Virus Erad* (2019) 5:41–3. doi: 10.1016/S2055-6640(20)30277-6
148. Domingo P, Villarroya F, Giralt M, Domingo JC. Potential Role of the Melanocortin Signaling System Interference in the Excess Weight Gain Associated to Some Antiretroviral Drugs in People Living With HIV. *Int J Obes* (2020) 44:1970–3. doi: 10.1038/s41366-020-0551-5
149. McMahon C, Trevaskis JL, Carter C, Holsapple K, White K, Das M, et al. Lack of an Association Between Clinical INSTI-Related Body Weight Gain and Direct Interference With MC4 Receptor (MC4R), a Key Central Regulator of Body Weight. *PloS One* (2020) 15:e0229617. doi: 10.1371/journal.pone.0229617
150. Caron-Debarle M, Lagathu C, Boccara F, Vigouroux C, Capeau J. HIV-Associated Lipodystrophy: From Fat Injury to Premature Aging. *Trends Mol Med* (2010) 16:218–29. doi: 10.1016/j.molmed.2010.03.002
151. Vigouroux C, Maachi M, Nguyen TH, Coussieu C, Gharakhanian S, Funahashi T, et al. Serum Adipocytokines Are Related to Lipodystrophy and Metabolic Disorders in HIV-Infected Men Under Antiretroviral Therapy. *AIDS* (2003) 17:1503–11. doi: 10.1097/00002030-200307040-00011
152. Lihn AS, Pedersen SB, Richelsen B. Adiponectin: Action, Regulation and Association to Insulin Sensitivity. *Obes Rev* (2005) 6:13–21. doi: 10.1111/j.1467-789X.2005.00159.x
153. Fang H, Judd RL. Adiponectin Regulation and Function. *Compr Physiol* (2018) 8:1031–63. doi: 10.1002/cphy.c170046
154. Brennan AM, Mantzoros CS. Drug Insight: The Role of Leptin in Human Physiology and Pathophysiology–Emerging Clinical Applications. *Nat Clin Pract Endocrinol Metab* (2006) 2:318–27. doi: 10.1038/ncpendmet0196
155. Das S, Shahmanesh M, Stolinski M, Shojaee-Moradie F, Jefferson W, Jackson NC, et al. In Treatment-Naive and Antiretroviral-Treated Subjects With HIV, Reduced Plasma Adiponectin Is Associated With a Reduced Fractional Clearance Rate of VLDL, IDL and LDL Apolipoprotein B-100. *Diabetologia* (2006) 49:538–42. doi: 10.1007/s00125-005-0085-3
156. Dirajlal-Fargo S, Moser C, Brown TT, Kelesidis T, Dube MP, Stein JH, et al. Changes in Insulin Resistance After Initiation of Raltegravir or Protease Inhibitors With Tenofovir-Emtricitabine: AIDS Clinical Trials Group A5260s. *Open Forum Infect Dis* (2016) 3:ofw174. doi: 10.1093/ofid/ofw174
157. Katlama C, Assoumou L, Valantin MA, Soulié C, Martinez E, Béniguel L, et al. Dual Therapy Combining Raltegravir With Etravirine Maintains a High Level of Viral Suppression Over 96 Weeks in Long-Term Experienced HIV-Infected Individuals Over 45 Years on a PI-Based Regimen: Results From the Phase II ANRS 163 ETRAL Study. *J Antimicrob Chemother* (2019) 74:2742–51. doi: 10.1093/jac/dkz224
158. McComsey GA, Moser C, Currier J, Ribaudo HJ, Paczuski P, Dube MP, et al. Body Composition Changes After Initiation of Raltegravir or Protease Inhibitors: ACTG A5260s. *Clin Infect Dis* (2016) 62:853–62. doi: 10.1093/cid/ciw017
159. McLaughlin M, Walsh S, Galvin S. Dolutegravir-Induced Hyperglycaemia in a Patient Living With HIV. *J Antimicrob Chemother* (2018) 73:258–60. doi: 10.1093/jac/dkx365
160. Offor O, Utay N, Reynoso D, Somasunderam A, Currier J, Lake J. Adiponectin and the Steatosis Marker Chi3L1 Decrease Following Switch to Raltegravir Compared to Continued PI/NNRTI-based Antiretroviral Therapy. *PloS One* (2018) 13:e0196395. doi: 10.1371/journal.pone.0196395

161. Fruhbeck G, Catalan V, Rodriguez A, Gomez-Ambrosi J. Adiponectin-Leptin Ratio: A Promising Index to Estimate Adipose Tissue Dysfunction. Relation With Obesity-Associated Cardiometabolic Risk. *Adipocyte* (2018) 7:57–62. doi: 10.1080/21623945.2017.1402151
162. Vega GL, Grundy SM. Metabolic Risk Susceptibility in Men Is Partially Related to Adiponectin/Leptin Ratio. *J Obes* (2013) 2013:409679. doi: 10.1155/2013/409679
163. Cassol E, Misra V, Dutta A, Morgello S, Gabuzda D. Cerebrospinal Fluid Metabolomics Reveals Altered Waste Clearance and Accelerated Aging in HIV Patients With Neurocognitive Impairment. *AIDS* (2014) 28:1579–91. doi: 10.1097/QAD.0000000000000303
164. Shikuma CM, Gangcuangco LMA, Killebrew DA, Libutti DE, Chow DC, Nakamoto BK, et al. The Role of HIV and Monocytes/Macrophages in Adipose Tissue Biology. *J Acquir Immune Defic Syndr* (2014) 65:151–9. doi: 10.1097/01.qai.0000435599.27727.6c
165. Wanjalla CN, McDonnell WJ, Koethe JR. Adipose Tissue T Cells in HIV/SIV Infection. *Front Immunol* (2018) 9:2730. doi: 10.3389/fimmu.2018.02730
166. Damouche A, Pourcher G, Pourcher V, Benoist S, Busson E, Lataillade J-J, et al. High Proportion of PD-1-expressing CD4 $^{+}$ T Cells in Adipose Tissue Constitutes an Immunomodulatory Microenvironment That may Support HIV Persistence. *Eur J Immunol* (2017) 47:2113–23. doi: 10.1002/eji.201747060
167. Koethe JR, McDonnell W, Kennedy A, Abana CO, Pilkinton M, Setliff I, et al. Adipose Tissue Is Enriched for Activated and Late-differentiated CD8+ T Cells, and Shows Distinct CD8+ Receptor Usage, Compared to Blood in HIV-Infected Persons. *J Acquir Immune Defic Syndr* (2017) 77:e14–21. doi: 10.1097/QAI.0000000000001573
168. Laparra A, Tricot S, Le Van M, Damouche A, Gorwood J, Vaslin B, et al. The Frequencies of Immunosuppressive Cells in Adipose Tissue Differ in Human, Non-Human Primate, and Mouse Models. *Front Immunol* (2019) 10:117. doi: 10.3389/fimmu.2019.00117
169. Korencak M, Byrne M, Richter E, Schultz BT, Juszczak P, Ake JA, et al. Effect of HIV Infection and Antiretroviral Therapy on Immune Cellular Functions. *JCI Insight* (2019) 4(12):e126675. doi: 10.1172/jci.insight.126675
170. Masschelin PM, Cox AR, Chernis N, Hartig SM. The Impact of Oxidative Stress on Adipose Tissue Energy Balance. *Front Physiol* (2020) 10:1638. doi: 10.3389/fphys.2019.01638
171. Martínez-Martínez E, Souza-Neto FV, Jiménez-González S, Cachofeiro V. Oxidative Stress and Vascular Damage in the Context of Obesity: The Hidden Guest. *Antioxidants (Basel Switzerland)* (2021) 10:406. doi: 10.3390/antiox10030406
172. Apovian CM, Bigornia S, Mott M, Meyers MR, Ulloor J, Gagua M, et al. Adipose Macrophage Infiltration Is Associated With Insulin Resistance and Vascular Endothelial Dysfunction in Obese Subjects. *Arterioscler Thromb Vasc Biol* (2008) 28:1654–9. doi: 10.1161/ATVBAHA.108.170316
173. Frigolet ME, Torres N, Tovar AR. The Renin-Angiotensin System in Adipose Tissue and its Metabolic Consequences During Obesity. *J Nutr Biochem* (2013) 24:2003–15. doi: 10.1016/j.jnutbio.2013.07.002
174. Boccara F, Auclair M, Cohen A, Lefèvre C, Prot M, Bastard J-P, et al. HIV Protease Inhibitors Activate the Adipocyte Renin Angiotensin System. *Antivir Ther* (2010) 15:363–75. doi: 10.3851/IMP1533
175. Masenga SK, Elijovich F, Koethe JR, Hamooya BM, Heimburger DC, Munsaka SM, et al. Hypertension and Metabolic Syndrome in Persons With HIV. *Curr Hypertens Rep* (2020) 22:78. doi: 10.1007/s11906-020-01089-3
176. Srinivasa S, Fitch KV, Wong K, Torriani M, Mayhew C, Stanley T, et al. RAAS Activation Is Associated With Visceral Adiposity and Insulin Resistance Among HIV-Infected Patients. *J Clin Endocrinol Metab* (2015) 100:2873–82. doi: 10.1210/jc.2015-1461
177. da Silva Rosa SC, Nayak N, Caymo AM, Gordon JW. Mechanisms of Muscle Insulin Resistance and the Cross-Talk With Liver and Adipose Tissue. *Physiol Rep* (2020) 8:e14607. doi: 10.14814/phy2.14607
178. Bourgi K, Wanjalla C, Koethe JR. Inflammation and Metabolic Complications in HIV. *Curr HIV/AIDS Rep* (2018) 15:371–81. doi: 10.1007/s11904-018-0411-2
179. Giralt M, Díaz-Delfin J, Gallego-Escuredo JM, Villarroya J, Domingo P, Villarroya F. Lipotoxicity on the Basis of Metabolic Syndrome and Lipodystrophy in HIV-1-Infected Patients Under Antiretroviral Treatment. *Curr Pharm Des* (2010) 16:3371–8. doi: 10.2174/138161210793563527
180. Schouten J, Wit FW, Stolte IG, Kootstra NA, van der Valk M, Geerlings SE, et al. Group AGeCS. Cross-Sectional Comparison of the Prevalence of Age-Associated Comorbidities and Their Risk Factors Between HIV-Infected and Uninfected Individuals: The AGEhIV Cohort Study. *Clin Infect Dis* (2014) 59:1787–97. doi: 10.1093/cid/ciu701
181. Bastard J-PP, Fellahi S, Couffignal C, Raffi F, Gras G, Hardel L, et al. Increased Systemic Immune Activation and Inflammatory Profile of Long-Term HIV-Infected ART-Controlled Patients Is Related to Personal Factors, But Not to Markers of HIV Infection Severity. *J Antimicrob Chemother* (2015) 70:1816–24. doi: 10.1093/jac/dkv036
182. Gelpi M, Afzal S, Fuchs A, Lundgren J, Knudsen AD, Drivsholm N, et al. Prior Exposure to Thymidine Analogs and Didanosine Is Associated With Long-Lasting Alterations in Adipose Tissue Distribution and Cardiovascular Risk Factors. *AIDS* (2019) 33:675–83. doi: 10.1097/QAD.0000000000002119
183. Rosito GA, Massaro JM, Hoffmann U, Ruberg FL, Mahabadi AA, Vasan RS, et al. Pericardial Fat, Visceral Abdominal Fat, Cardiovascular Disease Risk Factors, and Vascular Calcification in a Community-Based Sample: The Framingham Heart Study. *Circulation* (2008) 117:605–13. doi: 10.1161/CIRCULATIONAHA.107.743062
184. Lee YJ, Wang CP, Hsu HL, Hung WC, Yu TH, Chen YH, et al. Increased Epicardial Adipose Tissue (EAT) Volume in Type 2 Diabetes Mellitus and Association With Metabolic Syndrome and Severity of Coronary Atherosclerosis. *Clin Endocrinol (Oxf)* (2009) 70:876–82. doi: 10.1111/j.1365-2265.2008.03411.x
185. Mazurek T, Zhang LF, Zalewski A, Mannion JD, Diehl JT, Arafat H, et al. Human Epicardial Adipose Tissue Is a Source of Inflammatory Mediators. *Circulation* (2003) 108:2460–6. doi: 10.1161/01.CIR.0000099542.57313.C5
186. Iacobellis G, Willens HJ. Echocardiographic Epicardial Fat: A Review of Research and Clinical Applications. *J Am Soc Echocardiogr* (2009) 22:1311–8. doi: 10.1016/j.echo.2009.10.013
187. Buggey J, Longenecker CT. Heart Fat in HIV: Marker or Mediator of Risk? *Curr Opin HIV AIDS* (2017) 12:572–8. doi: 10.1097/COH.0000000000000414
188. Iacobellis G, Pellicelli AM, Sharma AM, Grisorio B, Barbarini G, Barbaro G. Relation of Subepicardial Adipose Tissue to Carotid Intima-Media Thickness in Patients With Human Immunodeficiency Virus. *Am J Cardiol* (2007) 99:1470–2. doi: 10.1016/j.amjcard.2006.12.082
189. Iantorno M, Soleimanifard S, Schar M, Brown TT, Bonanno G, Barditch-Crovo P, et al. Regional Coronary Endothelial Dysfunction Is Related to the Degree of Local Epicardial Fat in People With HIV. *Atherosclerosis* (2018) 278:7–14. doi: 10.1016/j.atherosclerosis.2018.08.002
190. Maurice JB, Patel A, Scott AJ, Patel K, Thursz M, Lemoine M. Prevalence and Risk Factors of Nonalcoholic Fatty Liver Disease in HIV-Monoinfection. *AIDS* (2017) 31:1621–32. doi: 10.1097/QAD.0000000000001504
191. Lemoine M, Lacombe K, Bastard JP, Sebire M, Fonquernie L, Valin N, et al. Metabolic Syndrome and Obesity Are the Cornerstones of Liver Fibrosis in HIV-Monoinfected Patients. *AIDS* (2017) 31:1955–64. doi: 10.1097/QAD.0000000000001587
192. Morse CG, McLaughlin M, Matthews L, Proschan M, Thomas F, Gharib AM, et al. Nonalcoholic Steatohepatitis and Hepatic Fibrosis in HIV-1-Monoinfected Adults With Elevated Aminotransferase Levels on Antiretroviral Therapy. *Clin Infect Dis* (2015) 60:1569–78. doi: 10.1093/cid/civ101
193. Capeau J, Bouteloup V, Katlama C, Bastard J-P, Guiyedi V, Salmon-Ceron D, et al. Ten-Year Diabetes Incidence in 1046 HIV-Infected Patients Started on a Combination Antiretroviral Treatment. *AIDS* (2012) 26:303–14. doi: 10.1097/QAD.0b013e32834e8776
194. Bastard JP, Couffignal C, Fellahi S, Bard JM, Mentre F, Salmon D, et al. Diabetes and Dyslipidaemia Are Associated With Oxidative Stress Independently of Inflammation in Long-Term Antiretroviral-Treated HIV-Infected Patients. *Diabetes Metab* (2019) 45:573–81. doi: 10.1016/j.diabet.2019.02.008
195. Assoumou L, Racine C, Fellahi S, Lamaziere A, Farabos D, Beniguel L, et al. Fat Gain Differs by Sex and Hormonal Status in Persons Living With Suppressed HIV Switched to Raltegravir/Etravirine. *AIDS* (2020) 34:1859–62. doi: 10.1097/QAD.0000000000002644
196. Rebeiro PF, Jenkins CA, Bian A, Lake JE, Bourgi K, Moore RD, et al. Risk of Incident Diabetes Mellitus, Weight Gain, and Their Relationships With Integrase Inhibitor–Based Initial Antiretroviral Therapy Among Persons

With Human Immunodeficiency Virus in the United States and Canada. *Clin Infect Dis* (2020), ciaa1403. doi: 10.1093/cid/ciaa1403
197. Ursenbach A, Max V, Maurel M, Bani-Sadr F, Gagneux-Brunon A, Garraffo R, et al. Incidence of Diabetes in HIV-Infected Patients Treated With First-Line Integrase Strand Transfer Inhibitors: A French Multicentre Retrospective Study. *J Antimicrob Chemother* (2020) 75:3344–8. doi: 10.1093/jac/dkaa330
198. Bloch M, John M, Smith D, Rasmussen TA, Wright E. Managing HIV-Associated Inflammation and Ageing in the Era of Modern ART. *HIV Med* (2020) 21:2–16. doi: 10.1111/hiv.12952
199. Piché ME, Tchernof A, Després JP. Obesity Phenotypes, Diabetes, and Cardiovascular Diseases. *Circ Res* (2020) 126:1477–500. doi: 10.1161/CIRCRESAHA.120.316101
200. Ridker PM, Everett BM, Thuren T, MacFadyen JG, Chang WH, Ballantyne C, et al. Antiinflammatory Therapy With Canakinumab for Atherosclerotic Disease. *N Engl J Med* (2017) 377:1119–31. doi: 10.1056/nejmoa1707914
201. Hsue PY, Li D, Ma Y, Ishai A, Manion M, Nahrendorf M, et al. IL-1β Inhibition Reduces Atherosclerotic Inflammation in HIV Infection. *J Am Coll Cardiol* (2018) 72:2809–11. doi: 10.1016/j.jacc.2018.09.038
202. Hsue PY, Ribaudo HJ, Deeks SG, Bell T, Ridker PM, Fichtenbaum C, et al. Safety and Impact of Low-dose Methotrexate on Endothelial Function and Inflammation in Individuals With Treated Human Immunodeficiency Virus: AIDS Clinical Trials Group Study A5314. *Clin Infect Dis* (2019) 68:1877–86. doi: 10.1093/cid/ciy781
203. Antonopoulos A S, Margaritis M, Lee R, Channon K, Antoniades C. Statins as Anti-Inflammatory Agents in Atherogenesis: Molecular Mechanisms and Lessons From the Recent Clinical Trials. *Curr Pharm Des* (2012) 18:1519–30. doi: 10.2174/138161212799504803
204. Funderburg NT, Jiang Y, Debanne SM, Labbato D, Juchnowski S, Ferrari B, et al. Rosuvastatin Reduces Vascular Inflammation and T-Cell and Monocyte Activation in HIV-Infected Subjects on Antiretroviral Therapy. *J Acquir Immune Defic Syndr* (2015) 68:396–404. doi: 10.1097/QAI.0000000000000478
205. Toribio M, Fitch KV, Sanchez L, Burdo TH, Williams KC, Sponseller CA, et al. Effects of Pitavastatin and Pravastatin on Markers of Immune Activation and Arterial Inflammation in HIV. *AIDS* (2017) 31:797–806. doi: 10.1097/QAD.0000000000001427
206. Fichtenbaum CJ, Ribaudo HJ, Leon-Cruz J, Overton ET, Zanni MV, Malvestutto CD, et al. Patterns of Antiretroviral Therapy Use and Immunologic Profiles at Enrollment in the REPRIEVE Trial. *J Infect Dis* (2020) 222:S8–S19. doi: 10.1093/infdis/jiaa259

Conflict of Interest: The authors declare that the research was conducted in the absence of any commercial or financial relationships that could be construed as a potential conflict of interest.

Advantages of publishing in Frontiers

OPEN ACCESS
Articles are free to read for greatest visibility and readership

FAST PUBLICATION
Around 90 days from submission to decision

HIGH QUALITY PEER-REVIEW
Rigorous, collaborative, and constructive peer-review

TRANSPARENT PEER-REVIEW
Editors and reviewers acknowledged by name on published articles

Frontiers
Avenue du Tribunal-Fédéral 34
1005 Lausanne | Switzerland

Visit us: www.frontiersin.org
Contact us: frontiersin.org/about/contact

REPRODUCIBILITY OF RESEARCH
Support open data and methods to enhance research reproducibility

DIGITAL PUBLISHING
Articles designed for optimal readership across devices

FOLLOW US
@frontiersin

IMPACT METRICS
Advanced article metrics track visibility across digital media

EXTENSIVE PROMOTION
Marketing and promotion of impactful research

LOOP RESEARCH NETWORK
Our network increases your article's readership